INTERNATIONAL REVIEW OF CYTOLOGY

Kwang W. Jeon

International Review of Cytology

A Survey of Cell Biology

VOLUME 210

International Review of Cytology

A Survey of Cell Biology

Edited by

Kwang W. Jeon
Department of Biochemistry
University of Tennessee
Knoxville, Tennessee

VOLUME 210

CONTENTS

Structure and Function of Photoreceptor and Second-Order Cell Mosaics in the Retina of *Xenopus*

Robert Gábriel and Márta Wilhelm

Basement Membrane and β Amyloid Fibrillogenesis in Alzheimer's Disease

Sadayuki Inoue

Regulation of Microtubule-Associated Proteins

Lynne Cassimeris and Cynthia Spittle

Dynein Motors of the *Chlamydomonas* Flagellum

Linda M. DiBella and Stephen M. King

This Page Intentionally Left Blank

CONTRIBUTORS

Numbers in parentheses indicate the pages on which the authors' contributions begin.

Lynne Cassimeris (163), *Department of Biological Sciences, Lehigh University, Bethlehem, Pennsylvania 18015*

Linda M. DiBella (227), *Department of Biochemistry, University of Connecticut Health Center, Farmington, Connecticut 06032*

Robert Gábriel (77), *Department of General Zoology and Neurobiology, University of Pécs, H-7624 Pécs, Hungary*

Sadayuki Inoue (121), *Department of Anatomy and Cell Biology, McGill University, Montreal, Quebec, Canada H3A 2B2*

Stephen M. King (227), *Department of Biochemistry, University of Connecticut Health Center, Farmington, Connecticut 06032*

Stefan Lange (39), *Department of Clinical Bacteriology, Göteborg University, S-413 46 Göteborg, Sweden*

R. Levy (1), *Laboratoire de Biologie de la Reproduction du Pr. J. L. Laurent, Hôpital Nord, 42055 Saint Etienne, France*

Ivar Lönnroth (39), *Department of Medical Microbiology and Immunology, Göteborg University, S-413 46 Göteborg, Sweden*

Cynthia Spittle (163), *Department of Biological Sciences, Lehigh University, Bethlehem, Pennsylvania 18015*

Márta Wilhelm (77), *Institute for Physical Education and Sports Sciences, University of Pécs, H-7624 Pécs, Hungary*

This Page Intentionally Left Blank

Genetic Regulation of Preimplantation Embryo Survival

R. Levy

Laboratoire de Biologie de la Reproduction du Pr. J. L. Laurent, Hôpital Nord, 42055 Saint Etienne, France

Mammalian embryonic death is the most common outcome of fertilization. This review focuses on the recent advances concerning genetic regulation of preimplantation embryo survival. The predominant role of the *Ped* (preimplantation embryo development) gene, which regulates fast or slow cleavage of preimplantation mouse embryos, and its implication on embryo survival are discussed. Recent morphological and biochemical observations suggested that programmed cell death was an essential mechanism in preimplantation embryo fragmentation and survival, thus leading to original investigations on apoptosis and apoptosis-related genes. Other genes, transcripts, or proteins seem to be involved in embryo development and control of survival. In particular, the role of heat shock proteins (HSP), telomerase activity (human telomerase catalytic subunit hTCS), and the developmental significance of regulatory protein polarization (leptin, STAT 3) in preimplantation embryos are discussed.

KEY WORDS: Preimplantation embryo, Apoptosis, Genetic regulation, Embryo survival, *Ped* gene, Hsp.   © 2001 Academic Press.

I. Introduction

The preimplantation stage of mammalian development corresponds to the period between ovulation and implantation, where the fertilized embryo travels unattached through the reproductive tract while undergoing a series of cleavage divisions leading to the implanting blastocyst. The preimplantation time is crucial for reproductive success. Many mammalian embryos are unable to proceed through preimplantation development, often fragmenting, arresting, and dying within a few days postfertilization. Embryonic death is the most common outcome of fertilization.

In both mice and humans, 15–50% of preembryos die during the preimplantation period (Janny and Ménézo, 1996). Only 30–50% of human embryos cleave regularly to the blastocyst stage *in vitro*. The causes for the death of so many embryos have been intensively explored. If the overriding cause seems to be chromosome abnormality, genetic defects, immunological rejection, and a compromised uterine environment have also been implicated. However, many preimplantation deaths remain unexplained and the molecular process by which these anomalies result in pregnancy failure is not elucidated (Pergament and Fiddler, 1998).

This review analyzes recent data concerning genetic regulation of preimplantation embryo survival. The *Ped* (preimplantation embryo development) gene regulates fast or slow cleavage of preimplantation mouse embryos, influencing the rate of preimplantation embryonic development and subsequent embryonic survival in the mouse. Following the identification of the *Ped* gene, its characterization, its possible role, and its function in the mouse embryo development were recently established. Finally, the use of transgenic mouse allowed the strict analysis of the regulation of *Ped* gene expression.

Programmed cell death plays critical roles in a wide variety of physiological processes during development and in adult tissues. Recent data suggested that apoptosis may be a crucial process in early mammalian embryo survival. Morphological and biochemical hallmarks of apoptosis have been described in mammalian preimplantation embryos since the early cleavage stages. The possible causes for apoptosis in preimplantation embryo are discussed. Normal and apoptotic (i.e., fragmented) embryos express specific apoptosis-related genes during mammalian preimplantation embryo development, with severe changes when apoptosis is activated. These findings support a model in which mammalian preimplantation embryo development is continuously regulated by a balance of pro- and anti-apoptotic genes. Apoptosis may be a normal feature in human preimplantation development, both *in vivo* and *in vitro,* playing an active role in the developing embryo through the removal of supernumerary, misplaced, damaged, or genetically abnormal cells. Contrary to these beneficial effects, apoptosis may have detrimental effects if either the number of apoptotic cells or ratio of these cells to the normal cells is elevated. According to this value, embryos could either continue to develop or arrest.

II. The *Ped* Gene

A. Overview

1. Discovery of the Mouse *Ped* Gene

The *Ped* gene was discovered when it was observed that mouse embryos from some strains cleave faster than those from other strains during preimplantation

TABLE I

History of the Discovery and Identification of the *Ped* (Preimplantation Embryo Development) Gene

Observations	References
Mouse preembryos of some strains cleave faster than other strains: discovery of the mouse *Ped* gene with two functional alleles, fast and slow	Verbanac and Warner, 1981
The rate of development correlated with the major histocompatibility complex (MHC) haplotype of the mice	Goldbard *et al.,* 1982
Linkage of the *Ped* gene to the Q region in the mouse MHC using congenic mouse strains	Warner *et al.,* 1987a
Relationship of the Qa-2 antigen expression by preimplantation mouse embryos to the *Ped* gene product	Warner *et al.,* 1987b
Analysis of litter size and weight in mice differing in *Ped* gene phenotype and the Q region of the H-2 complex	Warner *et al.,* 1991
Removal of Qa-2 protein alters the *Ped* gene phenotype of preimplantation mouse embryos	Tian *et al.,* 1992
Preferential survival of mice expressing the Qa-2 protein	Warner *et al.,* 1993
Transgenic embryos and mice after microinjection showed that the PED phenotype is encoded by the Q7 and/or Q9 genes: (1) the Q9 MHC class I transgene converts the *Ped slow* to the *Ped fast* phenotype	Xu *et al.,* 1994
Mouse embryos that possess the Q7 and/or Q9 genes express Qa-2 protein and have a faster cleavage rate (*Ped fast*) than mouse embryos with a deletion of the Q7 and Q9 genes (*Ped slow*)	McElhinny *et al.,* 1998
Transgenic embryos and mice after microinjection showed that the PED phenotype is encoded by the Q7 and/or Q9 genes: (2) identification of the two MHC class Ib genes, Q7 and Q9, as the *Ped* gene in the mouse Q9, as the *Ped* gene in the mouse	Wu *et al.,* 1999
Ped fast embryos have a survival advantage over *Ped slow* embryos and the selection in favor of the *Ped fast* phenotype occurs between mid-gestation and birth	Exley *et al.,* 1999
TAP protein regulates Qa-2 expression on the cell surface of preimplantation embryos thereby influencing the PED phenotype	Ke *et al.,* 2000
Cross-linking of Qa-2 protein, the *Ped* gene product, increases the cleavage rate of C57BL/6 preimplantation mouse embryos	McElhinny *et al.,* 2000

development (Verbanac and Warner, 1981) (Table I). The *Ped* gene controls the rate of cleavage of preimplantation embryos, and the *Ped* gene phenotype is controlled by two alleles, *fast* and *slow,* which are defined by the number of cells in a given embryo at a specified time post-hCG administration. The *fast* allele of the *Ped* gene is dominant (Verbanac and Warner, 1981), with no influence of the uterine environment (Brownell and Warner, 1988) (i.e., same phenotype *in vivo* and *in vitro*) on *Ped* gene phenotype. The *Ped* gene does not influence the time of ovulation; the phenotype first manifests itself at the time of the first cleavage division (Golbard *et al.,* 1982). In fact, the embryonic *Ped* gene is inactive until

the two-cell stage (prior to zygotic gene activation), but maternally derived *Ped* transcripts can be detected in the zygote (Jin *et al.,* 1992).

2. Mapping the *Ped* Gene to the Mouse Major Histocompatibility Complex (MHC)

An association of the *Ped* gene phenotype with major histocompatibility complex (MHC) haplotype led to the hypothesis that the *Ped* gene maps to the mouse MHC, the *H-2* complex (Goldbard *et al.,* 1982). Analysis of congenic mouse strains and genetic linkage studies clearly demonstrated that the *Ped* gene was linked to the *H-2* complex and, more specifically, mapped the *Ped* gene to the Q region of the mouse MHC (Warner *et al.,* 1987a).

3. Identification of the *Ped* Gene at the Molecular Level and Its Protein Product

Additional observations demonstrated that the *Ped* gene protein product was the Qa-2 antigen, a class Ib MHC protein encoded in the Q region of the mouse MHC (Warner *et al.,* 1987b; Tian *et al.,* 1992; Warner *et al.,* 1993). Removal of Qa-2 antigen slows development rate (Tian *et al.,* 1992); increase of Qa-2 antigen speeds development rate (Warner *et al.,* 1993). Treatment of preimplantation embryos with antisense oligonucleotides to the genes encoding the Qa-2 antigen, Q6, Q7, Q8, and Q9, slows the development rate of embryos with the *fast Ped* allele (Xu *et al.,* 1993). Introduction of the Q9 transgene into a *Ped slow* mouse strain converts the *Ped* gene phenotype of the strain from *slow* to *fast* (Xu *et al.,* 1994).

Four similar genes encode the Qa-2 antigen, Q6, Q7, Q8, and Q9. The Q7 and Q9 genes are very similar (one nucleotide difference) and the Q6 and Q8 genes are almost identical, and therefore, these genes are referred to as the *Q6/Q8* gene pair and the *Q7/Q9* gene pair (Cai *et al.,* 1996; Stroynowski and Tabaczewski, 1996). Mouse strains expressing the *fast Ped* allele possess all four genes, whereas mouse strains expressing the *slow Ped* allele have a deletion for all four genes, making the *slow Ped* allele a "null" allele.

Further studies were focused on Q7 and Q9 genes as only the Q7/Q9 gene pair is transcribed in preimplantation mouse embryos (Cai *et al.,* 1996). Recent observations confirmed that mouse embryos that possess the *Q7* and/or *Q9* genes express Qa-2 protein and have a faster cleavage rate (*Ped fast*) than mouse embryos with a deletion of the *Q7* and *Q9* genes (*Ped slow*) (McElhinny, 1998; Wu *et al.,* 1998, 1999).

In addition to affecting rate of preimplantation embryonic cleavage, the Ped gene has pleiotropic effects: the fast Ped allele leads to larger litter sizes and higher pup weights, both at birth and at weaning. When a mixed population of embryos with the *fast* and *slow Ped* alleles is allowed to develop in a single uterine environment, there is preferential survival of *Ped fast* embryos, suggesting a survival advantage over *Ped slow* embryos (Warner *et al.,* 1991, 1993; Exley and Warner, 1999).

B. Mechanism of Action of the *Ped* Gene

1. Regulation of *Ped* Gene Expression

At the protein level, the *Ped fast* strains express Qa-2 antigen on the embryonic cell surface, whereas the *Ped slow* strains have the absence of Qa-2 antigen. The level of Qa-2 antigen on the surface of a single embryo from *Ped fast* mice can be detected in an immuno-PCR technique (Warner *et al.,* 1998a,b).

A recent study analyzing the molecular mechanism of Qa-2 protein in early mouse embryo development demonstrated a significant improvement in cleavage rate after immune manipulation (McElhinny and Warner, 2000). Qa-2 has been shown to be attached to the embryonic cell surface by a glycosylphosphatidylinositol (GPI) linkage and several GPI-linked proteins, including Qa-2, have been involved in signal transduction (Horejsi *et al.,* 1999). Cross-linking of Qa-2 protein not only induced T-cell activation but similarly affected preimplantation embryos. Treatment of C57BL/6 (both two-cell and eight-cell) embryos with anti-Qa-2 mAb followed by cross-linking with a second antibody, in the presence of 4/5-phorbol-12-myristate-13-acetate (PMA), resulted in a significant increase in cleavage rate. These results imply that the GPI-linked Qa-2 protein acts as a signal transduction molecule in response to cross-linking in preimplantation embryos (McElhinny and Warner, 2000). If cross-linking of Qa-2 protein on the C57BL/6 embryos would lead to similar effects *in vivo* is not known. However, one can hypothesize that molecules on the embryonic cells, on uterine epithelial cells or soluble molecules in the oviductal and/or uterine fluid, could recognize Qa-2 and mediate cross-linking in the early embryo. Identification of these molecules may be critical for determining the exact mode of action of Qa-2 and modify the signal transduction pathway leading to a rapid rate of cleavage.

Qa-2, similar to other MHC class I proteins, consists of three components: a heavy chain, a 2 microglobulin chain, and a small peptide. Peptides that bind to MHC class I molecules are primarily generated by the ubiquitin–proteasome pathway in the cytosol. These peptides are then transported by the transporter associated with antigen processing (TAP) protein from the cytosol into the endoplasmic reticulum (ER), where the peptides bind a nascent MHC class I heavy chain that is noncovalently associated with 2 microglobulin. The resulting class I MHC–peptide complex is then transported to the cell surface. In TAP-deficient cells, MHC class I molecules lack peptides and are consequently misfolded, unstable and retained in the endoplasmic reticulum. Consequently, in *Tap-1* knockout mice, the Qa-2 antigen is expressed internally but not on the cell surface (Ke and Warner, 2000). Importantly, the *Ped* gene phenotype of *Tap-1* knockout mice is *slow,* showing that Qa-2 antigen must be expressed on the cell surface to be functional. TAP protein regulates the expression of Qa-2 protein on the surface of preimplantation mouse embryos, thereby influencing the PED phenotype of the embryos and the subsequent cleavage rate and survival.

2. Selection in Favor of the *Ped Fast* Phenotype Occurs between Mid-gestation and Birth

As reported previously, *Ped slow* strains of mice have smaller litters and the pups weigh less at birth and weaning. Furthermore, in litters derived from *Ped fast/slow* F1 mice backcrossed to the *slow/slow* parent, significantly more *Ped fast* pups than the 50% expected could be observed at 2 months of age, suggesting a selection in favor of the *Ped fast* haplotype at some point during development. Recent data showed that selection in favor of the *Ped fast* haplotype occurs between day 14.5—mid-gestation—and birth (Exley and Warner, 1999).

3. *Ped* Phenotype, Fragmentation, and Apoptosis

A link between the rate of cleavage division (*Ped* phenotype), cellular fragmentation and apoptosis has recently been described. Applying the TdT-mediated dUTP nick-end labeling (TUNEL) assay to normal, slow developing, and fragmented mouse embryos, Warner *et al.* showed that fragmented embryos exhibit a very high degree of apoptosis (65.6%) compared with the normal embryos (1.1%) (with the *fast* Ped allele) (1998c). Moreover, the percentage of apoptotic cells in the slow developing embryos (with the *slow* Ped allele) was slightly increased (3.4%). These findings emphasize the previous observation that the *fast* allele is associated with higher reproductive success than the *slow* Ped allele.

C. A Human Homolog of the Mouse *Ped* Gene

Data from human *in vitro* fertilization (IVF) clinics suggest that the mouse *Ped* gene has a human homolog because embryos from pools of oocytes fertilized simultaneously have different cleavage rates, and those embryos that cleave at a faster rate are more likely to lead to a viable pregnancy. These observations suggest that the *Ped* phenotype is present in the human population. The phenotype may be derived from either parent (Janny and Ménézo, 1994). Candidates for the human homolog of the *Ped* gene include the three MHC class Ib genes, HLA-E, HLA-F, and HLA-G (Cao *et al.,* 1999). HLA-E mRNA is present in most day 3 human preimplantation embryos (84%), whereas half of them expressed HLA-G mRNA (44%). In contrast, none of them were positive for HLA-F (0%). As HLA-G shares many structural similarities with the *Q7* and *Q9* genes, it was first suggested to be the human homolog of the mouse Qa-2 protein (Jurisicova *et al.,* 1996a,b). However, recent evidence suggested that HLA-G and Qa-2 protein would differ from each other (Schmidt and Orr, 1993; LeBouteiller and Lenfant, 1996; Sipes *et al.,* 1996; O'Collaghan and Bell, 1998). Finally, HLA-G, unlike Qa-2, is not attached to the cell membrane via a GPI linkage. Many of the same evidence mitigating against HLA-G being the human *Ped* gene are similar for HLA-E.

Moreover, HLA-E has been recently found to be the human homolog of mouse Qa-1, not Qa-2 (Long, 1998). Finally, the MHC class Ia protein HLA-C has been reported to be linked to the cell membrane by a GPI anchor and to possibly be involved in reproduction (King *et al.,* 1997). Also, since two genes, *Q7* and *Q9,* have been identified as contributing to the *Ped* phenotype in mouse, more than one MHC class I gene would contribute to the Ped phenotype in humans (Brenner *et al.,* 1999).

III. Apoptosis and Apoptosis-Related Genes in Preimplantation Embryos

A. Programmed Cell Death (PCD) and Apoptosis

In a human, about 100,000 cells are produced every second by mitosis and a similar number die by a physiological suicide process known as *apoptosis*. Most of the cells produced during mammalian embryonic development undergo physiological cell death before the end of the perinatal period. During our life span, over 99.9% of our cells undergo the same fate (Vaux and Korsmeyer, 1999). That cell death that occurs in a predictable "programmed" fashion is defined as a cell death process following an intrinsic genetic program that is activated at a controlled time and is commonly used to control cell number, to maintain homeostasis, and as a defensive strategy, to remove mutated, damaged, or superfluous unwanted or useless cells. The physiological cell death process that is best understood at the molecular level is the process of apoptosis. Contrary to necrosis, apoptosis strictly affects individual cells. Apoptosis is a cell death with morphological, biochemical, and physiological characteristics. Main morphological features are condensation of chromatin at the nuclear membrane, membrane blebbing (without loss of integrity), shrinking of cytoplasm leading to the loss of intercellular connections, and formation of membrane bound vesicles (apoptotic bodies) (Wyllie *et al.,* 1980; Sanders and Wride, 1995). Apoptosis is also characterized by internucleosome cleavage of DNA, leading to the specific ladder pattern observed after agarose gel electrophoresis. In recent years, the molecular machinery responsible for apoptosis has been elucidated, revealing a family of intracellular proteases, the caspases, which are responsible directly or indirectly for the morphological changes that characterize the phenomenon of apoptosis (Reed, 2000). Mitochondria exert a decisive role in cell death control through the release of cytochrome C and AIF in the cytoplasm, leading to the activation of caspase cascade together with changes in membrane asymmetry and phosphatidylserine (PS) exposure. Finally, apoptotic cells with membrane alterations (i.e., PS translocation) are detected and removed through phagocytosis by adjacent cells or macrophages (Martin *et al.,* 1995).

B. Evidence for Apoptosis

1. Apoptosis in Blastocyst

The presence of dead cells in the preimplantation mammalian embryo has been well described in a number of species, including mouse, baboon, rhesus monkey, bovine embryos, pig, and human (reviewed by Hardy, 1997, 1999). Since Kerr *et al.* (1972), it has become apparent that these cells die by apoptosis, a form of programmed cell death. *In vivo,* over 80% of mouse blastocyst freshly flushed from the uterus on day 4 or 5 had one or more dead cells. Cell death was seen predominantly in the inner cell mass (ICM): the dead cell index in the ICM of mouse blastocyst freshly flushed from the reproductive tract is of the order of 10–20%, whereas in the trophectoderm is <3% (Hardy, 1997). The plateau in mouse ICM cell number seems not to be due to cessation of cell division but probably results from the high levels of cell death in this lineage. A first wave of cell death occurred 97 h post-HCG in 60–110 mouse cell embryos, during blastocyst expansion, with minimal levels of cell death at the late blastocyst stage, just before implantation (Handyside and Hunter, 1986). A relationship between dead cell index and total cell number can be observed at different times following fertilization, both *in vivo* and *in vitro.*

A similar observation was made in IVP bovine embryos: the majority of blastocysts possessed at least one apoptotic nucleus, with a negative correlation between the number of cells and the extent of apoptosis and the majority (but not all) of apoptotic nuclei located in the ICM region (Byrne *et al.,* 1999; Matwee *et al.,* 2000). Furthermore, faster cleaving zygotes had significantly more cells, significantly fewer apoptotic dead cells, and better rates of development at the blastocyst stage. About 75% of human blastocysts, which have been fertilized and cultured *in vitro,* had one or more dead cells on day 6: most of them had <10 dead cells, although some embryos had significant levels of cell death >15%. Unlike mouse blastocyst, dead cells seem to be present equally in the trophectoderm and the ICM (cell death index of 7–8%). As in the mouse, the incidence of cell death in human blastocyst seems to correlate with both cell number and embryo quality. Blastocysts with low cell numbers had variable rates of cell death from 0 to >30%, whereas blastocysts with >80 cells rarely reached levels of apoptosis of 10%. We can hypothesize that blastocysts with high levels of cell death and low cell number on day 6 presented a critical level of cell death and were in the process of arresting.

Thus, apoptosis can be observed in both *in vivo*- and *in vitro*-produced embryos; however, the extent of apoptosis is affected by *in vitro* culture conditions.

2. Apoptosis in Early Preimplantation Embryos

DNA fragmentation (as monitored by the terminal transferase-mediated DNA end labeling, TUNEL method) was observed in the nuclei of murine (Jurisicova, 1998a,b) and bovine (Byrne *et al.,* 1999; Matwee *et al.,* 2000) preembryos, in the

TABLE II

A Review of Recent Morphologic Evidence of Apoptosis in Mammalian Preimplantation Embryos

Observations	Materials and methods	References
Cell corpses and apoptotic bodies (electron microscopy) and degraded DNA (TUNEL) in arrested human embryos	229 Arrested human embryos (203 fragmented embryos)	Jurisicova *et al.,* 1996
Cellular fragments of variable size with a regular intact actin cortex; chromatin condensation and fragmentation	50 Arrested or fragmented human embryos	Levy *et al.,* 1998a
Direct relationship between increased H_2O_2 concentration in fragmented embryos, positive TUNEL assay, and electron microscopy (apoptotic bodies)	31 Fragmented and 15 nonfragmented human embryos	Yang *et al.,* 1998
Both arrested fragmented and nonfragmented embryos were annexin V-positive; 30% were TUNEL-positive (mostly fragmented)	50 Arrested or fragmented human embryos	Levy *et al.,* 1998b
Increased rate of embryo fragmentation in aged females during *in vivo* mating; A two-fold higher rate of fragmentation in IVF embryos compared with *in vivo* fertilized embryos	821 Murine embryos (*in vivo*); 230 murine embryos (*in vitro*)	Jurisicova *et al.,* 1998a
No evidence of apoptosis from the 2- to the 8-cell stage (before EGA); 30% of all 9- to 16-cell stage embryos had at least one dead cell; 50% of morula showed apoptotic cell death; fast cleaving embryos showed a lower rate of apoptosis compared with slower cleaving embryos	Bovine embryos (*in vitro* maturation and *in vitro* fertilization)	Byrne *et al.,* 1999
No evidence of apoptosis in zygotes and from the 2- to the 8-cell stage (before EGA); 50% of all 9- to 16-cell stage embryos had at least one dead cell; 79% of morulae/early blastocysts with death; 100% of expanded/hatched blastocysts had apoptotic cell at least one dead cell	449 Bovine embryos	Matwee *et al.,* 2000

very early cleavage stages, before the blastocyst stage. The presence of oligonu-cleosomal length DNA fragments (TUNEL) and apoptotic bodies (electron mi-croscopy) was first described in arrested fragmented human preimplantation em-bryos by Jurisicova *et al.* (1996c) (Table II). F-actin and chromatin DNA labeling of human arrested embryos allowed us to observe a few embryos that exhibited equally sized and uniformly shaped blastomeres with a regular actin cortex sur-rounding each cell, whereas, in fragmented embryos, numerous cellular fragments of unequal size and various localization were present (Fig. 1; see color insert). An intact actin cortex, without membrane disruption, surrounded each fragment (Levy *et al.,* 1998a,b). Most of the arrested embryos, regardless of the arrest stage or the morphology, displayed chromatin condensation and/or fragmentation. The

TUNEL procedure labeled apoptotic nuclei in about 30% of arrested human preimplantation embryos. TUNEL-positive cells were mainly observed in fragmented embryos (Fig. 3; see color insert). However, DNA fragmentation (as monitored by TUNEL assay) also occurs in necrosis and autolysis and TUNEL may fail to discriminate among these different cell deaths. Furthermore, key morphological features of apoptosis have been observed in the absence of internucleosomal DNA fragmentation (Cohen *et al.,* 1992). Thus, TUNEL detection of apoptosis in human preimplantation arrested embryos seemed to need additional investigation. During the early stages of apoptosis, changes also occur at the cell surface membrane. One of these plasma membrane alterations is the translocation of phosphatidylserine (PS) from the inner part to the outer layer of the membrane, thus exposing PS at the external surface of apoptotic cells, where it can be specifically recognized by macrophages. This has been observed in the early phases of apoptosis during which the cell membrane itself remains intact. Annexin V can bind PS with a high affinity. Annexin V staining could be observed in human arrested embryo from two cells to the morula stage, together with chromatin nuclear condensation or fragmentation, regardless of the embryo's grade. An irregular positive annexin V staining of plasma membrane PS could be observed on the surface membrane of the external blastomeres of nonfragmented embryos (Fig. 2a; see color insert). Fragmented embryos all showed positive staining that surrounded each cellular fragment, evoking apoptotic bodies (Fig. 2b; see color insert) (Levy *et al.,* 1998b).

C. Possible Causes of Apoptosis in Preimplantation Embryo

In vitro suboptimal culture conditions have been involved as well as the lack of growth or "survival" factors, the lack of (or overexposure to) hormones, chromosomal and nuclear abnormalities, excessive reactive oxygen species (ROS) production, or excessive spermatozoa.

1. Suboptimal Culture

The presence of apoptosis in mammalian preembryos *in vivo* does not mean that the *in vitro* environment has no effect on cell death. *In vitro*-produced embryos from several mammalian species typically exhibit lower cell numbers, altered ICM/TE ratios, blastomeres of irregular size, and cytoplasmic fragmentation (Hardy *et al.,* 1989). Embryos produced *in vitro* have increased sensitivity to cryopreservation and manipulation (Hasler *et al.,* 1995). When compared to *in vivo*-derived embryos, cultured embryos exhibit retarded developmental progress and reduced pregnancy rates upon transfer. In various species, levels of cell death *in vitro* were found to be significantly higher than *in vivo* (Papaioannou and Ebert, 1986; Brison and Schultz, 1997; Long *et al.,* 1998; Jurisicova *et al.,* 1998a).

Addition of serum to the culture medium has an effect on bovine and ovine embryo morphology (Gardner *et al.,* 1994), ultrastructure, metabolism, and postimplantation development. Serum has also been implicated in the enlarged offspring syndrome (Thompson *et al.,* 1995). Controversial observations exist concerning the effects of supplementation with fetal calf serum on the development of bovine embryos. Contrary to the findings of Van Langendonckt *et al.* (1997), Byrne *et al.* (1999) showed that the total number of cells decreased and the incidence of apoptosis increased with the presence of fetal bovine serum: in a recent TUNEL analysis of preimplantation bovine embryo, the apoptotic dead cell index was significantly higher ($P < 0.05$) in blastocysts cultured (from the two-cell stage) in the presence of 10% fetal bovine serum compared with those developed in serum-free medium.

The composition of the culture medium can influence embryo survival. Glutamine and taurine are reported to be beneficial for mouse embryo development *in vitro* and glutamine has been recently showed to improve human blastocyst formation *in vitro* (Devreker *et al.,* 1998). Glutamine—but not taurine—dramatically reduced cell number at the blastocyst stage, with particular increased levels of cell death in trophectoderm. Alternatively, culturing mouse embryos in KSOM medium lacking glutamine results in reduced levels of cell death, and cell numbers in blastocysts were higher and approached those found *in vivo* (Deverker and Hardy, 1997). Taurine was recently found to support the development of two- to four-cell human embryos to the blastocyst stage, although it does not further augment the beneficial effects of glutamine (Devreker *et al.,* 1999).

Glucose and insulin concentrations adversely affect rat blastocyst development (Table III). *In vivo* studies revealed and embryonic developmental delay as early as 48 h postfertilization (Diamond *et al.,* 1989). The authors also demonstrated that maternal diabetes delays oocyte maturation. This developmental delay was associated with a smaller number of blastocysts and a larger number of morulae recovered from diabetic rats (Vercheval *et al.,* 1990; Lea *et al.,* 1996). Blastocysts recovered from diabetic mothers contained 15–20% fewer cells with two-thirds of the loss located in the ICM (Pampfer *et al.,* 1990). Past the preimplantation stage, a marked impairment of trophoblast outgrowth has been observed (Pampfer *et al.,* 1994), with increased rates of congenital malformations such as neural tube defects (Otani *et al.,* 1991). *In vitro* studies confirmed the embryonic developmental delay in the progression to the blastocyst stage in hyperglycemic conditions (Diamond *et al.,* 1990; Moley *et al.,* 1994), with an additional direct degenerative effect on ICM cells of sera from diabetic rats (Ornoy and Zusman, 1991). Culturing rat embryos in increasing concentrations of glucose increases the incidence of cell death dramatically (de Hertogh *et al.,* 1991). TNF-α induces a decrease in the rate of development to blastocyst and in ICM cell number, similar to high glucose exposure, suggesting a hypothetical overexpression of this cytokine in diabetes (Pampfer *et al.,* 1995). A specific decrease in glucose transport at the two-cell and blastocyst stages, reflected by a decrease in glucose transporters at both the mRNA and

TABLE III

A Review of Recent Data Concerning Diabetes and Preimplantation Development

Data	References
A. *In vivo* studies	
Embryonic developmental delay as early as 48 h postfertilization	Diamond *et al.,* 1989
(1) Oocyte maturation delay; (2) Smaller number of	
blastocysts and larger number of morulae	Vercheval *et al.,* 1990,
recovered from diabetic rats	Lea *et al.,* 1996
Decreased inner cell mass ICM proportion—	Pampfer *et al.,* 1990
15–20%—in blastocysts from diabetic rats	
Impairment of trophoblast growth: 70%	Pampfer *et al.,* 1994
of control blastocyst implant versus 49% in the	
diabetic group (increased rate of fetal loss)	
Increased rates of congenital malformations—neural tube defects	Otani *et al.,* 1991
B. *In vitro* studies	
Embryonic developmental delay in the progression	Diamond *et al.,* 1990,
to the blastocyst stage under hyperglycemic conditions	Moley *et al.,* 1994
Developmental delay and direct degenerative effect on	Ornoy and Zusman, 1991
ICM cells of sera from diabetic rats (β-hydroxybutyrate	
and acetoacetate embryotoxicity)	
TNF-α induces a decrease in the rate of development to	Pampfer *et al.,* 1995
blastocyst and in ICM cell number, similar to that seen	
with high glucose exposure	
C. Specific genetic control of glucose transport and embryo survival	
Decrease in glucose transport at the two-cell and blastocyst	Moley *et al.,* 1999
stages is reflected by decrease in glucose transporters at both	
the mRNA and protein levels, suggesting downregulation of	
these transporters (GLUT1, -2, and -3)	
Increased cell death in rat blastocysts exposed to maternal	Pampfer *et al.,* 1997
diabetes *in utero* and to high glucose or TNF-α *in vitro*:	
cellular blebbing, nuclear condensation, DNA fragmentation	
predominantly in the ICM	
Increased cell loss in blastocysts from diabetic rats is due to	Moley *et al.,* 1998
glucose-induced apoptosis; a 2.5-fold higher expression of	
Bax mRNA in blastocysts from diabetic mice (RT PCR);	
6-fold higher Bax protein level in blastocysts from diabetic	
mice (CLSM); same effect on Bax with high-glucose	
conditions *in vitro;* correction after insulin administration	
to hyperglycemic mothers	

protein levels, suggests a genetic downregulation of these transporters (GLUT1, -2, and -3) (Moley, 1999). Increased morphological and biochemical hallmarks of cell death were noted in rat blastocysts exposed to maternal diabetes *in utero* and to high glucose or TNF *in vitro* (Pampfer *et al.,* 1997). Further analysis confirmed that increased cell loss in blastocysts from diabetic rats is due to glucose-induced apoptosis. Higher expression of Bax mRNA and higher Bax protein levels were

found in blastocysts from diabetic mice, mimicked in high-glucose conditions *in vitro,* and corrected after insuin administration to hyperglycemic mothers (Moley *et al.,* 1998). This data suggested that excessive cell death in the blastocyst, most probably resulting from the overstimulation of a basal suicidal program by various inducers such as glucose, might be a contributing factor of the early embryopathy associated with maternal diabetes (Pampfer, 2000). This hypothesis was discussed as further analysis of severely malformed and growth-retarded embryos of gestational day 12 from diabetic rates revealed pronounced DNA laddering on agarose gel, when no DNA laddering could be observed in any of the nonmalformed embryos from control and diabetic rats. This suggests that the widespread apoptosis observed in diabetic rats is not likely to play a major role in diabetes-induced dysmorphogenesis but rather in the early phases of resorption of severely malformed and developmentally retarded embryos (Forsberg *et al.,* 1998). However, a strict hyperglycemic control in diabetic women before and during the earliest stage after conception is recommended to prevent glucose-induced apoptosis *in vivo* (Moley, 1999).

Embryo density during culture was shown to influence preimplantation development: embryos cultured singly had a higher incidence of cell death than those cultured in groups. Alternatively, increasing the density of embryo culture accelerated development, increased final blastocyst cell number, and partially (50%) reduced the increase in cell death induced by culture *in vitro,* probably by secretion of growth factors (Brison and Schultz, 1997).

2. Lack of Survival Factors

Growth factors are known to regulate cell proliferation and differentiation during mammalian preimplantation development; embryos express functional growth factor receptors for ligands present in the maternal tract and those synthesized by the embryo itself. Although *in vitro* preimplantation embryo culture is possible, in the absence of maternal tract, embryo development is often retarded or compromised relative to *in vivo* development, suggesting roles for both embryo-derived and maternal growth factors.

Supplementation of culture medium with exogenous growth factors such as *transforming growth factor (TGF-α)* partially reduced excessive *in vitro* apoptotic cell death without accelrating development or increasing final cell number (Brison and Schultz, 1997). Moreover, the incidence of apoptosis is dramatically increased in the TGF-α-deficient mouse blastocysts; this increase is essentially restricted to the ICM when the embryos develop *in vivo* but extends to the trophectoderm cells for *in vitro* developing embryos (Brison and Schultz, 1998).

Insulin-like growth factor I (IGF-I) has been shown to increase the proportion of embryos forming blastocysts and the number of inner cell mass cells in human and other mammalian preimplantation embryos (Lighten *et al.,* 1998). A clear anti-apoptotic action of IGF-I during blastocyst development was recently

confirmed (Herrler *et al.,* 1998; Spanos *et al.,* 2000). The increased number of human blastocysts and reduced cell death in day 6 blastocysts after culture in IGF-I-supplemented medium suggest that IGF-I is rescuing *in vitro* embryos which would otherwise arrest and acts as a survival factor during preimplantation human development (Spanos *et al.,* 2000).

Platelet-activating factor (PAF; 1-*o*-alkyl-2-acetyl-*sn*-glycero-3-phosphocholine), a potent ether phospholipid, also acts as an autocrine growth/survival factor for the mammalian preimplantation embryo. Transcripts for the G protein-linked plasma membrane PAF receptor are present within unfertilized oocytes and newly fertilized zygotes, but only at low levels of expression, becoming quite inconsistent by the late zygote–early 32-cell stage, suggesting that, like many other gametic transcripts, it was degraded at this time. In contrast, a progressive increase of this message was observed past the 2-cell stage, with an amanitin-sensitive expression, indicating for the first time a new transcription from the zygotic genome (Stojanov and O'Neill, 1999). PAF supplementation of media enhances embryo metabolism, reduces the incidence of embryo cell death, improves development rates *in vitro,* and improves the pregnancy potential for embryos upon their transfer to the uterus (O'Neill, 1997). Careful timing studies revealed that the action of PAF to enhance embryo development and survival was not required until the late 2-cell stage, while exposure to PAF during only the 1-cell stage and early 2-cell stage had no obvious beneficial effect, suggesting an expression of a functional PAF receptor only from the late 2-cell stage onward during the normal preimplantation stage of development. Culture of zygotes (irrespective of their method of fertilization) caused expression from the zygotic genome to be retarded by more than 24 h. This retardation did not occur if culture commenced at the 2-cell stage, once PAF-receptor gene expression from the zygotic genome was initiated. These adverse effects of *in vitro* fertilization and embryo culture on the expression of this transcript may be a contributing factor for the poor viability of embryos produced in this manner. The reduced expression of PAF-receptor mRNA following IVF predicts that such embryos may have a deficiency in autocrine stimulation and also suggests that supplementation of growth media with exogenous PAF would be only patially beneficial. The effect of IVF and culture may also explain the conflicting literature.

Most mammalian cells express the machinery necessary to undergo programmed cell death; cells only survive if they are signaled to do so by themselves and other cells (Raff *et al.,* 1992). Culture of embryo in staurosporine, a protein kinase inhibitor that would be expected to inhibit extracellular signaling pathways, induces PCD (Weil *et al.,* 1996; Warner *et al.,* 1998c). Possible signals could consist of soluble "survival factors" produced by the embryo itself, other embryos, or maternal tract cells. Lack of survival factors has been found to contribute to cell death in *in vitro*-cultured embryos (Paria *et al.,* 1990). Thus, certain unexplained infertility could be due to inadequate production of growth factors or impaired cooperative interaction among preimplantation embryos and growth factors

(abnormal growth factor receptor, deficient signaling pathways), leading to *in vivo* excessive cell death. Human oviductal cells were recently shown to improve mouse embryo development by decreasing the incidence of apoptosis in mouse cocultured morula and blastocyst (Xu *et al.,* 2000). The beneficial effects of coculture—in particular, improved embryo quality, viability, and development with reduced cellular fragmentation—have yet not be fully elucidated. More likely, helper cells secrete some embryotrophic substances (such as growth factor receptors or ligands), reduce oxygen metabolite levels, or remove toxic compounds from culture medium (Wiemer *et al.,* 1998). Thus, helper cells reduce the *in vitro* cell death excessive levels observed by regulating the imbalance of certain constituents promoting transition of the maternally controlled zygote into an activated embryonic genome.

Nicotine and cotinine were found to inhibit apoptosis in different cell lines (Wright *et al.,* 1993; Marana *et al.,* 1998), suggesting that this inhibition confers survival advantage to neoplasic cells and contributes to the pathogenesis of tobacco-related cancer. Two different studies investigated whether fragmentation in human preimplantation embryos is associated with smoking (Zenzes and Reed, 1996, 1999). Morphological assessments in 1094 embryos (1996) and in 1682 embryos (1999) at the two- to eight-cell stage, graded for quality from 1 to 4, were analyzed in relation to follicular fluid nicotine. The proportion of good quality grades 1 and 2 embryos (with idem-size blastomeres and no fragments) increased with increasing cotinine concentrations ($P = 0.0001$), without age effect. These results suggest a cotinine-mediated inhibition of fragmentation (and apoptosis) in developing embryos of smokers and lead to the conclusion that smoking inhibits embryo fragmentation. Acquisition of resistance to fragmentation from smoking may confer survival advantage to genetically altered embryos (Zenzes, 2000).

Apoptosis may also result from unbalanced oxidative stress (Hockenbery *et al.,* 1993; Korsmeyer *et al.,* 1993, 1995). High concentrations of oxygen free radicals produced by prolonged exposure to a large number of excessive spermatozoa may contribute to an apparent depletion of glutathione and distrub the redox balance in preembryos (Jurisicova *et al.,* 1995). In preimplantation human embryos, the levels of both H_2O_2 concentration and DNA fragmentation in fragmented embryos were higher than that of nonfragmented embryos (Yang *et al.,* 1998). Shortly after intensive (1 mM H_2O_2 for 1.5 h) hydrogen peroxide treatment, mouse zygotes displayed PCD with cell shrinkage, cytochrome c release from mitochondria and caspase activation, and then terminal deoxynucleotidyl transferase mediated dUTP nick end labeling staining in condensed pronuclei (Liu *et al.,* 2000a,b). Mild oxidative stress (200 M for 15 min) induced a decline in mitochondrial membrane potential and disruption of the mitochondrial matrix, suggesting that mitochondria are involved in the early phase of oxidative stress-induced PCD. Furthermore, mitochondrial malfunction may contribute to cell cycle arrest, followed by cell death, triggered by mild oxidative stress.

3. Chromosomal and Nuclear Anomalies

High rates of multinucleation in arrested or poor quality human embryos have been well documented (Tesarik *et al.,* 1987; Balakier and Cadesky, 1997). This abnormality was described by several authors, with a frequency ranging from 17 to 69% and its presence in human embryos has been strongly correlated with chromosomal abnormalities (Kligman *et al.,* 1996). The substantially reduced viability of multinucleated embryos expressed by early cleavage arrest and the formation of abortive blastocysts during *in vitro* culture indicate the highly lethal nature of these embryos. A possible fate for multinucleated and genetically abnormal blastomeres may be that they undergo apoptosis (as demonstrated by the observation of fragmenting or condensing nuclei) and arrest. In spite of reduced viability, surprisingly, abnormal embryos containing multinucleated blastomeres may implant and give rise to healthy infants (Balakier and Cadesky, 1997). Healthy babies had most likely developed from normal mononucleated blastomeres, while their abnormal sibling became arrested and excluded from fetal development. Thus, embryo survival could depend on the ability of eliminating the aberrant cells.

4. Apoptosis in Follicular Fluids, Oocytes, and Cumulus Cells

Controlled ovarian stimulation, which is used to obtain a large number of oocytes, may lead to an abnormal follicular response to administered gonadotrophin, resulting in inadequate biochemical cytoplasmic maturation of the oocytes. Zygotes and embryos produced from such oocytes may not be able to proceed through fertilization and subsequent development if their PCD machinery is unbalanced.

DNA fragmentation in mouse gonadotrophin-stimulated atretic follicles and oocytes was reported (Perez *et al.,* 1999). Similar results were also observed in some human ovarian follicles obtained during oocyte retrieval from patients undergoing IVF. Expression of the apoptosis-related genes, caspase-1, caspase-3, DNA fragmentation factor, and apoptotic protease activating factor-1 in human granulosa cells indicates that granulosa cells from women undergoing IVF have intrinsic apoptotic machinery that could be activated (Izawa *et al.,* 1998). A relation between apoptosis in granulosa-lutein cells measured by flow cytometry and the outcome of IVF in patients with normal basal FSH levels was clearly demonstrated: women who become pregnant after IVF treatment have a significant lower percentage of apoptotic granulosa–lutein cells than those who do not become pregnant with a cutoff level of 13% apoptosis (Oosterhuis *et al.,* 1998). The incidence of apoptotic bodies in granulosa cells can also be used as an indicator of success of IVF (Nakahara *et al.,* 1998). Recent data underlined the relation between apoptosis in cumulus cells and the maturity of the corresponding oocytes (Host *et al.,* 2000). The incidence of apoptosis was significantly higher in cumulus cells from human immature germinal vesicle and metaphase I oocytes than in cumulus cells from mature metaphase II oocytes ($P < 0.0001$). Also, nonfertilized metaphase II

oocytes exhibited higher incidence of DNA fragmentation in cumulus cells than in fertilized metaphase II oocytes ($P = 0.0082$), suggesting a negative impact of apoptosis on the fertilization rate. Furthermore, DNA fragmentation detected in spermatozoa had an impact on the embryo score, suggesting that the degree of fragmentation in the embryo might be correlated to apoptosis in the spermatozoa (Host *et al.,* 2000).

Soluble forms of the Fas–FasL system can be detected in follicular fluids (FF) from gonadotropin-stimulated ovaries. The presence of significantly higher concentrations of soluble Fas (sFas) in FF containing immature oocytes and the detection of Fas ligand (sFasL) in FF containing atretic oocytes suggest that this system may play a role in preventing oocyte atresia during folliculogenesis. In contrast, levels of sFas in FF did not correlate with either fertilization, embryo quality resulting from mature fertilized oocytes, or apoptosis rate (DNA fragmentation) in cumulus cells. The Fas–FasL system is probably not essential for apoptotic events after fertilization failure. Following ovulation, apoptosis in cumulus cells and unfertilized oocytes may be facilitated by downregulation of bcl-2 rather than directly through the Fas–FasL system (De Los Santos *et al.,* 2000).

D. Genetic Regulation of Cell Death

The temporal expression patterns of several cell death regulatory genes was recently characterized during early avian (Muscarella *et al.,* 1998) and mammalian (Jurisicova *et al.,* 1998b) embryo development (Table IV). Several genes whose products have anti-apoptotic activity—bcl-2, bcl-xL, hsp70, grp78, and the glutathione *S* transferase—are expressed as early as the stage 1 embryo in the newly oviposited egg with a stress resistance pattern involving multiple anti-apoptotic genes at different regulatory points in the apoptotic cascade (Muscarella *et al.,* 1998). In mammals, transcript abundance of main cell death regulatory genes seemed to be altered in murine embryos undergoing fragmentation, so that the expression of genes involved in cell death (especially *Bad* and *Bcl-xS*) is elevated and the expression of genes involved in cell survival (*Bcl-2*) reduced (Jurisicova *et al.,* 1998b). Normal embryos exhibit detectable levels of *Bcl-2* transcription *de novo,* which may augment maternally derived stores of *Bcl-2, Bcl-x,* and *Bcl-w* mRNAs, thereby promoting survival. Surprisingly, normal embryos do not express the *Bcl-xS* transcript, but some fragmented embryos do. Differential expression of cell death-associated genes between the ICM and whole blastocysts was also observed, as ICM expressed proportionately larger amounts of the *Bcl-2* mRNA and lower amounts of *Bad* mRNA. This suggests that the expression of these two genes may play a role in controlling apoptosis withing the ICM.

Apoptosis may occur by default in embryos that fail to execute crucial developmental events during the first cell cycle including the integrity of maternal and paternal genomes, completion of S phase, correct recruitment of maternal mRNAs,

TABLE IV

Genetic Control of Apoptosis in Mammalian Preimplantation Embryos

Observation	Materials and methods	References
Bax mRNA and Bcl-2 mRNA were detected in mouse and human preimplantation embryos at all developmental stages	Human and murine preimplantation embryos	Warner *et al.,* 1998
Normal embryos expressed maternal RNA + *de novo* transcription of Bcl-2, Bcl-xL, Bcl-w (anti-apoptotic) with no Bcl-xS (pro-apoptotic); fragmented embryos expressed elevated Bad and Bcl-xS (pro-apoptotic) but reduced Bcl-2 (anti-apoptotic) mRNA	Mouse embryos: RT PCR analysis of caspases and BCL-2 family transcripts	Jurisicova *et al.,* 1998b
Caspases mRNA expression varied in a stage-specific manner; BCL-2 mRNAs could be detected at every stage of preimplantation development; enzymatic activity was observed in polar bodies, fragmented zygotes, and zygotes treated with staurosporine	Fragmented and normal mouse embryos: —TUNEL assay (blastocyst) —RT PCR analysis of caspases and BCL-2 family transcripts, caspase enzymatic activity	Exley *et al.,* 1999

and onset of the early phase of gene transcription. A hypothetical model of PCD regulation during mammalian early embryo development could be visualized by a delicate balance between cell death suppressors and inducers, which is established during oogenesis and persists through the whole course of embryo development. Healthy oocytes contain a passive cell death pathway that becomes activated upon fertilization. Once the killer program is triggered, it can be suppressed by an appropriate signal(s), possibly originating from the oocyte or generated by the early embryo itself. If this appropriate signal is not sent, cell death occurs. Alternatively, the oocyte may contain higher levels of cell death inducers, whereby even the correct signal emanating from the zygote would not be able to override the activated cell death pathway. Both of the last two scenarios would lead to embryo fragmentation and arrest.

Warner *et al.* (1998c) demonstrated that fragmented embryos exhibit a higher degree of apoptosis compared with the normal and slow developing embryos and examined the two major gene families which are involved in apoptosis, i.e., the caspase family and the Bcl-2 family (1998c). Two members of the Bcl-2 family, Bcl-2 (which promotes survival) and Bax (which promotes apoptosis) were analyzed in both mice and human preimplantation embryos. In mice, *Bax* mRNA were found to be present at all developmental stages, whereas *Bcl-2* mRNA was detected in zygotes and in preimplantation embryos, but not in the oocytes. When

BCL-2 and BAX protein levels were assessed using immunofluorescence, lower levels of BCL-2 were found in fragmented blastocysts compared to normal blastocyst. *Bax* and *Bcl-2* genes are also expressed in human preimplantation embryos with high expression of BCL-2 at cleavage stages and the blastocyst stage and low expression of BAX at cleavage stages and in blastocysts of good morphology. Interestingly, in a human blastocyst with extensive fragmentation, BAX expression was increased (Hardy, 1999). Expression of caspase mRNAs also varied in mouse preimplantation embryos in a stage-specific manner (Exley *et al.,* 1999): normal and apoptotic (i.e., fragmented) embryos express several apoptosis-related genes during preimplantation embryo development, with severe changes when apoptosis is activated. These findings support a model in which mammalian preimplantation embryo development may be regulated by the ratio of pro- and anti-apoptotic genes (BCL-2 to BAX for example) (Levy *et al.,* 2000). However, the precise genetic program controlling cell death in preimplantation embryos has not been elucidated fully and further investigations are needed to study such diverse regulators of cell death as harakiri (Inohara *et al.,* 1997).

IV. Heat Shock Proteins and Preembryo Development

Heat shock proteins (HSPs) are highly conserved cellular stress proteins present in every organism from prokaryotic bacteria to mammals, including man. HSP, which were first identified in cells after exposure to elevated temperature, represent a critical component of a very complex and highly conserved cellular defense mechanism to preserve cell survival under adverse environmental conditions.

HSP serve two major functions. First, under physiological conditions, they act as molecular chaperones (intracellular housekeeping proteins) which are involved in mediating the folding and transport of other intracellular proteins; HSPs also fulfill crucial roles in the maintenance of proteins in an inactive form and the prevention of protein degradation. Second, they are induced in response to cellular stresses, including hyperthermia, ischemia, free oxygen radicals, heavy metals, ethanol, amino acid analogs, inflammation and infection (Welch, 1992). Although heat shock proteins have long been known to protect cells from the effects of physical and chemical assaults, increasing evidence now indicates that they may have a more direct role in suppressing apoptosis in cells (Mosser *et al.,* 1997).

HSPs are classified into different families according to their molecular weight measured in kilodaltons. In the context of reproduction, HSP60 and HSP70 are most important. The HSP60 family consists of proteins that are highly expressed in a constitutive manner and are moderately stress inducible. The main localization of HSP60 is in the mitochondria, but its presence on the cell surface has been documented. The HSP70 family comprises several proteins that are localized in distinct cellular compartments. The constitutively synthesized HSC70 is found

in the cytosol and nuclei of cells and is only moderately stress inducible. The HSP70 family represents the most conserved group of proteins within the HSP superfamily.

A. Heat Shock Proteins and Preimplantation Embryos

A particular situation is noticed for hsp 70 genes in mammalian preimplantation embryos where HSP expression is directly linked to major events occurring during the preimplantation period and where embryonic cells express Hsp70s either constitutively, according to a developmental program, or in response to toxic stress (Luft and Dix, 1999). Bensaude *et al.* identified the spontaneous, constitutive Hsc70 and the heat- and sodium arsenite (NaAs)-induced Hsp70s (1983). First, the expression of hsc 70 mRNA is effective from one-cell stage onward, and the Hsc 70 protein is the predominant HSP expressed up to the blastocyst stage. The stress-inducible Hsp70s are referred to as Hsp70-1/3, because the 642-aa sequence of hsp70-1 is nearly identical to the 641-aa sequence of hsp70-3. The hsp70-1/3 mRNA is constitutively expressed as early as the one-cell stage, with a peak at the two-cell stage, and diminishes until becoming clearly heat-inducible by the blastocyst stage. A reasonable conclusion from the protein, mRNA, and transgene data is that there is an initial, constitutive burst of Hsp70-1/3 expression during activation of the zygotic genome which peaks during the two-cell stage; this initial burst continues through the second and third cleavages and overlaps with the developing potential for inducible Hsp70 synthesis, which is fully established by the blastocyst stage. Thus, a two-cell bovine embryo can undergo increased HSP70 synthesis in response to heat (Edwards *et al.,* 1997), indicating a capacity for changing its physiology in response to stress in an effort to stabilize cellular function and that this increase in HSP70 synthesis is the result of new transcription (Chandolia *et al.,* 1999).

Inducible expression is delayed until morula or early blastocyst stages. Since blastocyst formation marks the differentiation of the inner cell mass and the outer cell mass, progressive acquisition of HSP inducibility is associated with continuing embryonic differentiation. Thus, inducible HSP expression seems to be tightly developmentally regulated (Christians *et al.,* 1997).

B. HSP and IVF

1. IVF Culture and HSP Expression

Stressful manipulation—transfer, thawing, freezing—of embryos in culture is common in assisted reproductive technology where embryos have to cope with handling, oxidative stress, variation of light intensity or temperature and a complete

artificial *in vitro* environment. Premature transfer to the uterus at the four- to eight-cell stage may also lead to both nutritional and environmental stress. As a consequence, in the mouse, HSP70 expression is found to be 5- to 15-fold higher in *in vitro*-cultured embryos (Christians *et al.,* 1997).

Induced expression of HSP due to suboptimal culture conditions and defective environment and constitutive HSP expression may both represent an essential requirement for successful embryo growth in an adverse environment. Overexpression of HSP in this situation may be to the benefit of the developing embryo, whereas failed HSP induction could result in detrimental consequences for the growing embryo *in vitro.*

In certain IVF culture conditions, embryos are cultured in medium supplemented with maternal serum. Pre-existing HSP antibodies in these sera could be detrimental for the developing embryo. This was demonstrated in a recent study where two-cell mouse embryos were cultured in the presence or absence of monoclonal antibodies specific for mammalian HSP60, HSP70, and HSP90 (Neuer *et al.,* 1998). At day 3, only 29% of the embryos cultured with anti-HSP60 antibody developed to the blastocyst stage. By day 5, hatched embryos were present in 28% of the cultures containing anti-HSP70, with less than 10% of outgrown trophoblasts at day 7. Both anti-HSP60 and anti-HSP70 exerted a strong inhibitory effect on mouse embryo growth, but at unique developmental stages. An immune sensitization to heat shock proteins may be a cause of reproductive failure.

In the presence of HSP antibodies, embryos arrest with specific morphology including irregular sized blastomeres and multiple cellular fragments enclosed within the zonae pellucidae, suggesting apoptotic features. This is important to note as both the production of HSP and programmed cell death are closely related to each other. Both systems are considered as supporting programs responsible for the general well being of an organism and also as cellular response to environmental assaults. Importantly, there is a surprising overlap between stresses inducing stress response and assaults initiating apoptosis (Punyiczki and Fesus, 1998).

2. Disruption of Preimplantation Embryogenesis by the Inhibition of hsp70 Production

In order to elucidate the functions of constitutive and stress-inducible Hsp70 expression in mouse preimplantation embryos, the consequences of inhibiting expression with antisense oligonucleotides complementary to the mRNAs of hsp70-1 and hsp70-3 (A070-1/3) were evaluated. Transfection with 5 or 10 μM A070-1/3 reduced *in vitro* blastocyst formation to 30 and 0%, respectively (90% of control embryos developed to blastocyst) and heightened embryo sensitivity to arsenic (Dix *et al.,* 1998). These results indicate that some minimal amount of Hsp70-1 and/or hsp70-3 is required for preimplantation embryogenesis and that increasing the demand for hsp70s by toxicant exposure heightens this

requirement. Thus, constitutive expression of HSP70-1/3 appears crucial to preimplantation embryo development.

3. Mouse *in Vitro* Coculture Studies

Two-cell mouse embryos were grown under two conditions: half of the embryos were grown using 10% fetal calf serum (FCS) in RPMI and the rest were grown in an endometrial coculture (ECC) system. The effect of varying concentrations of monoclonal antibodies to HSP60 were analyzed under both conditions. Without ECC, embryo growth was significantly inhibited at a concentration of 100 μg/ml anti-HSP60 antibodies at each stage of development (blastocyst stage, 25%; hatching stage, 15%; and outgrowth stage, 15%; $P < 0.001$), whereas utilizing the ECC system, a slight toxicity appeared at a concentration of 100 μg/ml anti-HSP60 antibodies (blastocyst stage, 80%; not significant; hatching stage, 70%, $P = 0.02$; outgrowth stage, 60%, $P = 0.003$). In addition, TUNEL labeling was more frequent in embryos exposed to anti-HSP60 than in unexposed embryos (Neuer *et al.,* 2000). The endometrium coculture system appears to reduce the toxicity of heat shock protein antibodies. A possible mechanism of this toxicity may involve the induction of apoptosis. As HSPs are essential for successful completion of the single developmental stages of an embryo, one can hypothesize that the specific pattern of HSPs may play a crucial protective role against apoptosis (Mailhos *et al.,* 1993).

V. Telomerase Activity

The telomere is the end structure of the DNA molecule. Telomeres are repeats of DNA protecting the stability of chromosomes and are essential for chromosome end maintenance. The human telomerase catalytic subunit (hTCS), or human telomerase reverse transcriptase, is a ribonucleoprotein which synthesizes telomere repeats on the end of eukaryotic chromosomes. Telomerase activity is high in germ, embryonic, and cancer cells which are considered to be telomerase positive; in contrast, most somatic cells are telomerase negative.

Telomerase activity was detected in human testes and ovaries and human blastocysts, but not in mature spermatozoa or oocytes (Wright *et al.,* 1996). Telomerase activity was found in female rat germ cells with a level of enzyme activity in early antral and preovulatory follicles comparable to that of 293 cells, while levels in ovulated oocytes were 50-fold lower. Telomerase activity was present in even lower levels in pachytene spermatocytes and round spermatides, but no telomerase activity could be detected in spermatozoa from either the caput or the cauda epididymis (Eisenhauer *et al.,* 1997). These findings demonstrated that telomerase activity was present in female and male rat germ cells at several stages of

differentiation, with the exception of spermatozoa, and suggest that telomerase activity may be critical during meiosis.

Telomerase activity is also present in the early embryos (Eisenhauer *et al.,* 1997), but its level varies with the different developmental stages (Betts and King 1999; Xu and Yang, 2000). Relative telomerase activity appeared to decrease during oocyte maturation. It increased after *in vitro* fertilization and then decreased gradually until the bovine embryo reached the eight-cell stage (EGA). After the eight-cell stage, the telomerase activity significantly increased again at the morula and reached its highest level in the blastocyst stage, suggesting that telomerase activity is upregulated in morulae and blastocysts. This also provides evidence how telomerase activity and, possibly, the length of the telomere are reprogrammed during early embryo development.

Surprisingly, the dynamics of temolerase activity shares similarities with the dynamics of apoptosis during early bovine embryo development. No evidence of apoptosis could be detected from the 2- to the 8-cell stage (before EGA), but the number of dead cells increased after the 9- to 16-cell stage: 50 to 79% of morulae/early blastocysts displayed apoptotic cell death and 100% of expanded/hatched blastocysts had at least one dead cell.

Alternative mRNA splicing of *hTCS* may be important for regulation of telomerase activity. Interestingly, in unfertilized and immature gametes, as well as preimplantation embryos, hTCS expression revealed three different pattern PCR product sizes (Brenner *et al.,* 1999). Normal human oocytes and preimplantation embryos showed only the 457-bp PCR product—identical to the first identified *hTCS* gene. Surprisingly, in some compromised gametes and preimplantation embryos, hTCS expression revealed three different PCR product sizes: 457, 421, and 275 bp. It is important to note that certain tumors, cell lines, fetal tissues, and normal tissues, show similar splicing variants. It is unclear whether alternate splicing variants of *hTCS* in compromised embryos are important for the regulation of telomerase activity or whether they give rise to proteins with different biochemical functions. It is possible that alternative splicing patterns of *hTCS* in individual oocytes or embryos may serve as a marker for embryonic heath and survival.

Recent findings suggest that catalytic subunit of telomerase may protect against apoptosis. Suppression of the catalytic subunit of telomerase levels and function in embryonic mouse neurons in culture significantly increases their vulnerability to cell death with increased levels of oxidative stress and mitochondrial dysfunction; in contrast, overexpression of hTCS in pheochromocytoma cells resulted in decreased vulnerability to induced apoptosis (Zhu *et al.,* 2000). Thus, it may be hypothesized that the catalytic subunit of telomerase also protects the preembryo cells against apoptosis.

Whether alternate mRNA splicing patterns of telomerase activity in human embryos are associated with specific morphological abnormalities (e.g., cytoplasmic fragmentation, multinucleation, arrested embryos) and apoptosis needs further

investigations. More intriguing is the possibility of estimating an individual's life span by measuring the length of the telomeres in the unfertilized oocyte or an individual blastomere of a human embryo.

VI. Early Transcripts and Preimplantation Embryo Survival

Between fertilization and implantation, the human preembryo undergoes complex changes (Heikinheimo and Gibbons, 1998). The cytoplasmic mass of the preembryo is not increased prior to blastocyst stage. The advancing development is associated with reduced totipotency; thus, the developmental potential of individual blastomeres isolated from an eight-cell stage embryo is clearly reduced in comparison to that of a two-cell stage human embryo.

A. Developmental Significance of Regulatory Protein Polarization in Early Preimplantation Embryos

Recent evidence suggests that the differentiation of individual blastomeres may be initiated at these very early steps of embryo development. The regulatory protein leptin and the transcription factor STAT 3 displayed polarized distribution in both mouse and human oocytes. After fertilization, these polarized domains become differentially distributed between blastomeres in the cleavage stage embryo and between the inner cell mass and trophoblast of the blastocyst (Antczak and Van Blerkom, 1997). The pattern of inheritance of the polarized domains in daughter blastomeres appears to be associated with the manner in which successive equatorial or meridional planes of cell division interact with the polarized protein domains (Edwards and Beard, 1997). Similarly, considerable variation in the concentration of -actin and IL-1 mRNA between individual blastomeres originating from the same six- to eight-cell stage preembryo were noted (Krüssel *et al.,* 1988). This phenomenon of regulatory protein polarization during early human development also exists for the growth factors transforming growth factor 2 (TGF 2) and vascular endothelial growth factor (VEGF), the apoptosis-associated proteins Bcl-x and Bax, and the growth factor receptors c-kit and epidermal growth factor receptor EGF-R (Antczak and Van Blerkom, 1999). These findings might bear clinical significance to preimplantation genetic diagnosis: is the blastomere studied representative of the embryo as a whole, and does the biopsy procedure remove the essential blastomere for subsequent development?

It has been postulated that the localization of these polarized protein domains to the plasma membrane and subjacent cytoplasm makes them particularly exposed to the membrane extrusions which may occur during fragmentation. Loss of

nonpolarized proteins—E-cadherin—is less dramatic and without developmental consequence. In contrast, a spatial limited blastomere fragmentation may deeply alter embryo development as apoptosis proteins (Bcl-x and Bax) exist in a polarized domain. Indeed, the embryo development potential may rely on the particular pattern of fragmentation, the stage at which fragmentation occurs, and the particular blastomere(s) involved. This notion could explain why embryos with similar degrees of fragmentation can have very different developmental fates. Also, the study of fragmented embryos may provide critical insights into the potential roles of these regulatory proteins during the preimplantation period.

B. Regulatory Proteins

1. Cell Cycle and Tumor Suppressor Proteins

As shown by the high percentage of mosaicism in the preimplantation human embryo, the cell cycle control mechanisms are not fully developed at this early stage of development. Recent work has demonstrated that damaged chromatin does not prevent the exit from metaphase I and cell cycle progression in fused mouse oocytes (Fulka *et al.,* 1997). Suppressor p21 mRNA, one of the proteins involved in the control of chromatin integrity, is barely detectable in the oocyte and four-cell embryo, whereas increased concentrations of p21 mRNA are detectable in the blastocyst stage, p21 protein belongs to an enlarging family of tumor suppressor proteins and acts via inhibition of the activity of several cyclin–cdk complexes *in vitro;* also the expression of p21 is associated with cellular differentiation. This data suggests that additional levels of cell cycle regulation emerge as the embryonic development progresses. In line with this, particular attention must be paid to Wt1.

2. Wt1 as Required for Survival of the Preimplantation Embryo

Recent data suggested that the early preimplantation growth of the mammalian embryo during transport in the oviduct is dependent on an environment that is maintained through the coordinate action of *Wt1* and a modifier gene (Kreidberg *et al.,* 1999). The *Wt1* gene, originally identified as a tumor suppressor gene associated with Wilm's tumor, encodes a zinc-finger-containing transcription factor expressed during gonad and kidney development (Armstrong *et al.,* 1993) and in adult reproductive organs, including the testes, ovaries, oviduct, and uterus (Hsu *et al.,* 1995). Wt1 encodes a protein with four zinc fingers in the carboxy-terminus and an amino terminus that is enriched in proline and glutamine. A GC-rich cognate binding site for Wt1 is found in the promoter regions of several genes, and Wt1 has been demonstrated to either activate or repress transcription of these promoters. The complete early embryonic death in the oviduct observed for *Wt1*+/− females appeared to be due to the failure of one-cell embryos to undergo mitosis.

Neither levels of WT1 protein nor the ratio of WT1 spice forms were significantly altered in *Wt1+/−* reproductive organs, suggesting that the modifier effect acts downstream of WT1. Wt1 has been implicated in the regulation of growth factors present on preimplantation embryos such as insulin-like growth factor 2 and their receptors, or TGF-α, suggesting one possible route by which Wt1 may exert its effect on early embryogenesis. A possible link with embryo apoptosis remains to be determined. These results represent the first demonstration of a nonautonomously acting set of genes for preimplantation embryo survival. This model, where the growth and survival of the preimplantation embryo while transiting through the oviduct is dependent on WT1 function, offers a genetic approach to identifying a gene involved in maintaining the oviductal environment and competence that is likely to yield information relevant to human reproductive disorders.

3. *Oct-4* in the Preimplantation Embryo

The transcription factor *Oct-4* is a member of the POU domain family of octamer-binding proteins. Interestingly, all members of the class to which *Oct-4* belongs are expressed during early embryonic development. The Oct-4 has been found only in mammalian species. The presence of Oct-4 protein in the extracts of undifferentiated embryonic stem (ES) and embryonal carcinoma (EC) cells first suggested an association with the early stages of mouse embryogenesis. Subsequent analysis established that *Oct-4* is expressed throughout the preimplantation period. Oct-4 mRNA and protein are present in unfertilized oocytes, and the protein is localized to the pronuclei following fertilization. As is typical of most mRNAs, *Oct-4* mRNA levels drop dramatically after fertilization, although Oct-4 protein is detectable in the nuclei of two-cell embryos. Zygotic *Oct-4* expression is activated prior to the eight-cell stage. Expression of *Oct-4* mRNA and protein is abundant and uniform in all cells of the embryo through the morula stage. However, as the outer cells of the morula differentiate into trophectoderm, *Oct-4* is downregulated and becomes restricted to cells of the ICM in the blastocyst. Similarly, when ES or EC cells are induced to differentiate, *Oct-4* mRNA expression is also downregulated. Thus, the association of *Oct-4* with pluripotency is strengthened by its rapid downregulation during differentiation, both in the preimplantation embryo and in culture. *Oct-4* is both maternally and zygotically expressed in humans, and is present through the blastocyst stage (Abdel-Rahman *et al.,* 1995).

The restriction of Oct-4 to ICM, as TE differentiates, suggests that it is either required for maintenance of the pluripotent state, or prohibitive for differentiation. Recent investigations suggest that a continuous Oct-4 expression may be critical for maintenance the pluripotent state of the ICM. The phenotype resulting from inactivation of *Oct-4* in mouse embryo demonstrate how critical *Oct-4* is for early development. *Oct-4−/−* deficient embryos develop to the blastocyst stage, but the inner cell mass cells are not pluripotent; furthermore, in the absence of a true inner cell mass, trophoblast proliferation is not maintained. Interestingly, expansion of

trophoblast precursors is restored by an Oct4 target gene product, fibroblast growth factor-4. Therefore, Oct-4 also determines paracrine growth factor signaling from stem cells to the trophectoderm (Nichols *et al.,* 1998).

As a conclusion, numerous observations led to the conclusion that Oct-4 transcription factor may be an important embryonic regulator factor (Ovitt and Schöler, 1998). *Oct-4* is present as a maternal mRNA and subsequent expression of the gene occurs in every cell of the embryo until the first differentiation step. Thereafter, *Oct-4* expression is linked to pluripotent cells from which the germline is derived. Regulation of the *Oct-4* gene is accomplished by two enhancers linked to a single promoter. One of the enhancers is active only in undifferentiated cell types, while the second drives expression in the embryo following implantation. Downregulation of Oct-4 appears to be tightly controlled at several levels. The function of Oct-4 is presumed to involve the maintenance of an undifferentiated state, and also the determination or establishment of the germline. The putative targets identified for the Oct-4 transcription factor include a number of genes known to be vital to the preimplantation embryo, such as *E-codherin* and *HCG* in humans. Considering its expression pattern, its regulation, and its function, *Oct-4* clearly appears as a preeminent element within the regulatory hierarchy of genes controlling preimplantation development.

VII. Concluding Remarks

Progression of mammalian oocytes through maturation, ovulation, fertilization, and then early cleavages, blastocyst formation, and implantation depends on successful implementation of critical genetic and developmental programs and on successful interaction of the preimplantation embryo with its environment. Following ovulation, zygote survival depends on maternal mRNAs and proteins that accumulate during oocyte growth and maturation: maternal factors are thus responsible for the regulation of the earliest events of embryo formation. This stock will be used within the first few cleavage divisions, until the onset of zygotic gene activation, when the preimplantation embryo must take in charge its own development by transcriptional activation of its genome. Mechanisms and control of embryonic genome activation in mammalian embryos have been well described (review by Latham, 1999). Maternal transcripts are essential, promoting transition of the maternally controlled zygote into an activated embryonic genome.

In particular, a balance between cell death suppressors and inducers may exist, beginning with oogenesis and continuing throughout the preimplantation embryo period with successive checkpoints. Mature oocytes with appropriate mRNA stock will succeed through maturation and fertilization. However, the early embryo has to act to stop the activated cell death machinery in order to survive. Alternatively, poor-quality oocytes may contain higher levels of cell death inducers or lower

levels of cell death antagonists, leading to fertilization failure or poor-quality embryo that will fragment and/or arrest.

The first wave of apoptosis in the preimplantation embryo may take place during activation of the embryonic genome (EGA), which occurs at the two-cell stage in mice, the 4-cell stage in humans, and at the 9- to 16-cell stage in bovine embryos. As a matter of fact, there was no evidence of apoptosis before the first cell cycle in mice (Jurisicova *et al.,* 1998a,b; Warner *et al.,* 1998b,c), the second cell cycle in humans (Jurisicova *et al.,* 1996c; Levy *et al.* 1998b, 2000), and the 9- to 16-cell stage in bovine preimplantation embryo (Byrne *et al.,* 1999; Matwee *et al.,* 2000). This suggests that apoptosis may be present as early as EGA. In *Xenopus,* such a maternally regulated developmental checkpoint exists, at the stage of embryonic genome activation, which can trigger apoptosis (Sible *et al.,* 1997). In mammals, aberrant cell cycle checkpoint function and early embryonic cell death in the protein kinase Chk1(−/−) mice have been recently described; in culture, Chk1(−/−) blastocysts showed a severe defect in outgrowth of the ICM and died of apoptosis (Takai *et al.,* 2000).

Embryonic genome activation and transition to the blastocyst stage are two critical periods during human preimplantation embryo development where PCD has been observed. The second wave of apoptosis, occurring at the blastocyst stage, may be responsible for eliminating cells with inappropriate developmental potential, as one of the main functions of apoptosis during development is to suppress cells that are no longer required. Groups of ICM cells from early blastocysts are able to differentiate into TE cells while ICM cells from older expanded blastocysts are not able to do so, suggesting a loss of potential to form TE through blastocyst expansion (Handyside, 1978). Interestingly, the wave of cell death seen in mouse blastocyst coincides with this period, suggesting that cell death was the mechanism by which the expanding blastocyst eliminated ICM cells which retain the potential to form TE in order to prevent the formation of ectopic trophectoderm in the incipient germ layers (Handyside and Hunter, 1986; Pierce *et al.,* 1989; Parchment, 1993). However, cell death has also be observed in TE. Thus, it is likely that at blastocyst stage, apoptosis eliminates cells that are damaged, "in excess," aberrant, no longer required, or developmentally incompetent. Cellular quality and quantity control within the ICM is critical for subsequent development since this lineage is bound to form the fetus and it contains the germline.

The observation of apoptotic hallmarks in blastomeres before the blastocyst stage and the link between apoptosis, embryo survival, and cellular fragmentation still causes much controversy (Antczak and Van Blerkom, 1999). Can an imbalance between cell death suppressors and inductors in the preembryo cause blastomere fragmentation, or is the fragmentation itself the initiator of apoptosis if critical ratios or levels of developmentally important proteins are altered by partial or complete elimination of their polarized domains? The elucidation of this question needs further investigation. If apoptosis does occur in the very early cleavage

stages of embryo development, what function does it play? Apoptosis may be considered as a normal feature in human normal preimplantation development, *in vivo,* playing an active role in the developing embryo through the removal of genetically abnormal or mutated cells. Contrary to these beneficial effects and an embryo-protective role, apoptosis may have detrimental effects if either the number of apoptotic cells or ratio of these cells to the normal cells is elevated; according to this value, embryos could either continue to develop or arrest. This situation could occur both in *in vitro* suboptimal culture conditions and during *in vivo* abnormal development.

Apoptosis is present in very few cells in *in vivo* human normal developing pre-embryo and may be essential for further development. Excessive apoptosis described in some *in vitro*-produced preimplantation embryos raises the question of its possible consequences in the developing embryo. It is not very likely that excessive apoptosis in the preembryo leads to subsequent abnormal development. Nevertheless, at the later stages of development, the effects of most of chemical and physical teratogens are known to be associated with the induction of apoptosis in target organs (Brill *et al.,* 1999). Embryos of heat-shocked rodents exhibit anomalies such as exencephaly, microcephaly, microphtalmia, etc. In rat embryos exposed to a teratogenic dose of heat, a hallmark of apoptosis—DNA fragmentation—was found as early as 2.5 h after heat exposure. Finally, diabetes-induced teratogenesis has also been associated with perturbations in the regulation of apoptosis since the early embryo development and apoptosis has been involved in the resorption of severely malformed embryos.

Would it be possible to rescue some apoptotic embryos? Based on the hypothesis that excessive fragmentation is damaging to the embryo development, *in vitro*-assisted zona hatching procedure and fragment removal have been carried out with opposite results (Magli *et al.,* 1998; Warner *et al.,* 1998c). Recently, Morita *et al.* demostrated that a natural metabolite of ceramide, sphingosine-1-phosphate, protects mouse oocytes from chemotherapy and radiation-induced apoptosis (2000). This represents an innovative and exciting potential new treatment for preventing oocyte apoptosis after cancer therapy (Casper and Jurisicova, 2000). In line with this, could it be possible to prevent embryo apoptosis by regulating an imbalance of pro- and anti-apoptotic genes? Could a gene therapy on apoptosis-related genes (or other genes) be envisaged and certain genetic defects be corrected in the preembryo, or even in the gametes?

Increased understanding of the basic biology of the human oocyte and early embryo is likely to enhance the treatment of infertile patients. Biologists are just in the early stages of identifying critical factors or processes involved in the genetic control of preimplantation embryo survival. Knowledge of the molecular mechanisms of apoptosis in the preimplantation embryo will provide insight into the causes of certian infertility where aberrant cell death regulation may occur and is likely to help in the optimization of *in vitro* culture conditions and assisted reproductive techniques.

Acknowledgments

References

Abdel-Rahman, B., Fiddler, M., Rappolee, D., and Pergament, E. (1995). Expression of transcription regulating genes in human preimplantation embryos. *Hum. Reprod.* **10,** 2787–2792.

Antczak, M., and Van Blerkom, J. (1997). Oocyte influences on early development: The regulatory proteins leptin and STAT3 are polarized in mouse and human oocytes and differentially distributed within the cells of the preimplantation stage embryo. *Mol. Hum. Reprod.* **3**(12), 1067–1086.

Antczak, M., and Van Blerkom, J. (1999). Temporal and spatial aspects of fragmentation in early human embryos: Possible effects on developmental competence and association with the differential elimination of regulatory proteins from polarized domains. *Hum. Reprod.* **14,** 429–447.

Armstrong, J.F., Pritchard-Jones, K., Bickmore, W. A., Hastie, N. D., and Bard, J. B. (1993). The expression of the Wilms' tumor gene, *Wt1,* in the developing mammalian embryo. *Mech. Dev.* **40,** 5–97.

Balakier, H., and Cadesky, K. (1997). The frequency and developmental capability of human embryos containing multinucleated blastomeres. *Hum. Reprod.* **12,** 800–804.

Bensaude, O., Babinet, C., Morange, M., and Jacob, F. (1983). Heat shock proteins, first major products of zygotic gene activity in mouse embryo. *Nature* **305,** 331–333.

Betts, D. H., and Kinh, W. A. (1999). Temolerase activity and telomere detection during early bovine development. *Dev. Gent.* **25,** 397–403.

Brenner, C. A., Wolny, Y. M., Adler, R. R., and Cohen, J. (1999). Alternative splicing of the telomerase catalytic subunit in human oocytes and embryos. *Mol. Hum. Reprod.* **5,** 845–850.

Brill, A., Torchinsky, A., Howard, C., and Toder, V. (1999). The role of apoptosis in normal and abnormal embryonic development. *J. Assist. Reprod. Genet.* **16,** 512–519.

Brison, D. R., and Schultz, R. M. (1997). Apoptosis during mouse blastocyst formation: Evidence for a role for survival factors including transforming growth factor alpha. *Biol. Reprod.* **56,** 1088–1096.

Brison, D. R., and Schultz, R. M. (1998). Increased incidence of apoptosis in transforming growth factor alpha-deficient mouse blastocysts. *Biol. Reprod.* **59,** 136–144.

Brownell, M. S., and Warner, C. M. (1988). *Ped* gene expression by embryos cultured *in vitro. Biol. Reprod.* **39,** 806–811.

Byrne, A. T., Southgate, J., Brison, D. R., and Leese, H. J. (1999). Analysis of apoptosis in the preimplantation bovine embryo using TUNEL. *J. Reprod. Fertil.* **117,** 97–105.

Cai, W., Cao, W., Wu, L., Exley, G. E., Waneck, G. L., Karger, B. L., and Warner, C. M. (1996). Sequence and transcription of Qa-2 encoding genes in mouse lymphocytes and blastocysts. *Immunogenetics* **45,** 97–107.

Cao, W., Brenner, C. W., Alikani, M., Cohen, J., and Warner, C. M. (1999). Search for a human homologue of the mouse *Ped* gene. *Mol. Hum. Reprod.* **5,** 541–547.

Casper, R. F., and Jurisicova, A. (2000). Protecting the female germ line from cancer therapy. *Nat. Med.* **6,** 1100–1101.

Chandolia, R. K., Peltier, M. R., Tian, W., and Hansen, P. J. (1999). Transcriptional control of development, protein synthesis and heat-induced heat shock protein 70 synthesis in 2-cell bovine embryos. *Biol. Reprod.* **61,** 1644–1648.

Christians, E., Michel, E., and Renard, J. P. (1997). Developmental control of heat shock and chaperone gene expression. Hsp 70 genes and heat shock factors during preimplantation phase of mouse development. *Cell. Mol. Life Sci.* **53,** 168–178.

Cohen, G. M., Sun, X. M., Snowden, R. T., Dinsdale, D., and Skilleter, D. N. (1992). Key morphological features of apoptosis may occur in the absence of internucleosomal DNA fragmentation. *Biochem. J.* **286,** 331.

De Hertogh, R., Vanderheyden, I., and Pampfer, S. (1991). Maternal insulin treatment improves preimplantation embryo development in diabetic rats. *Diabetologica* **35,** 406–408.

Devreker, F., and Hardy, K. (1997). Effects of glutamine and taurine on preimplantation development and cleavage of mouse embryos *in vitro. Biol. Reprod.* **57,** 921–928.

Devreker, F., Van den Bergh, M., Biramane, J., Winston, R. L., Englert, Y., and Hardy, K. (1999). Effects of taurine on human embryo development *in vitro. Hum. Reprod.* **14,** 2350–2356.

Devreker, F., Winston, R. M., and Hardy, K. (1998). Glutamine improves human preimplantation development *in vitro. Fertil. Steril.* **69,** 293–299.

Diamond, M. P., Moley, K. H., Logan, J., *et al.* (1990). Manifestation of diabetes mellitus on mouse follicular and pre-embryo development: Effect of hyperglycemia per se. *Metabolism* **39,** 220–224.

Diamond, M. P., Moley, K. H., Pellicer, A., Vaughn, W. K., and DeCherney, A. H. (1989). Effects of streptozotocin-alloxan-induced diabetes mellitus on mouse follicular and early embryo development. *J. Reprod. Fertil.* **86,** 1–10.

Dix, D. J., Garges, J. B., and Hong, R. L. (1998). Inhibition of hsp70-1 and hsp70-3 expression disrupts preimplantation embryogenesis and heightens embryo sensitivity to arsenic. *Mol. Reprod. Dev.* **51,** 373–80.

Edwards, R., and Beard, H. (1997). Oocyte polarity and cell determination in early mammalian embryos. *Mol. Hum. Reprod.* **3,** 863–905.

Edwards, J. L., Ealy, A. D., Monterroso, V. H., and Hansen, P. J. (1997). Ontogeny of temperature-regulated heat shock protein 70 synthesis in preimplantation bovine embryos. *Mol. Reprod. Dev.* **48,** 25–33.

Eisenhauer, K. M., Gerstein, R. M., Chiu, C. P., Conti, M., and Hsueh, A. J. (1997). Telomerase activity in female and male rat germ cells undergoing meiosis and in early embryos. *Biol. Reprod.* **56,** 1120–1125.

Exley, G. E., Tang, C., McElhinny, A. S., and Warner, C. (1999). Expression of caspase and BCL-2 apoptotic family members in mouse preimplantation embryos. *Biol. Reprod.* **61,** 231–239.

Exley, G. E., and Warner, C. M. (1999). Selection in favor of the Ped fast haplotype occurs between midgestation and birth. *Immunogenetics* **49,** 653–659.

Forsberg, H., Eriksson, U. J., and Welsh, N. (1998). Apotosis in embryos of diabetic rats. *Pharmacol. Toxicol.* **83,** 104–111.

Fulka, J., Kalab, P., First, N. L., and Moor, R. M. (1997). Damaged chromatin does not prevent the exit from metaphase I in fused mouse oocytes. *Hum. Reprod.* **12,** 2473–2476.

Gardener, D. K., Lane, M., Spitzer, A., and Batt, P. A. (1994). Enhanced rates of cleavage and development for sheep zygotes cultured to the blastocyst stage *in vitro* in the absence of serum and somatic cells: Amino acids, vitamins and culturing embryos in groups stimulate development. *Biol. Reprod.* **50,** 390–400.

Goldbard, S. B., Verbanac, K. M., and Warner, C. M. (1982). Genetic analysis of H-2 linked gene(s) affecting early mouse embryo development. *J. Immunogenet.* **9,** 77–82.

Handyside, A. H. (1978). Time of commitment of inside cells isolated from preimplantation mouse embryos. *J. Embryol. Exp. Morphol.* **45,** 37–53.

Handyside, A. H., and Hunter, S. (1986). Cell division and death in the mouse blastocyst before implantation. *Roux's Arch. Dev. Biol.* **195,** 519–526.

Hardy, K. (1997). Cell death in the mammalian blastocyst. *Mol. Hum. Reprod.* **3,** 919–925.

Hardy, K. (1999). Apoptosis in the human embryo. *Rev. Reprod.* **4,** 125–134.

Hardy, K., Handyside, A. H., and Winston, R. M. (1989). The human blastocyst: Cell number, death and allocation during late preimplantation development *in vitro. Development* **107,** 597–604.

Hasler, J. F., Henderson, W. B., Hurtgen, P. J., Jin, Z. Q., McCauley, A. D., Mower, S. A., Neely, B.,

Shuey, L. S., Stokes, J. E., and Trimmer, S. A. (1995). Production, freezing, and transfer of bovine IVF embryos and subsequent calving results. *Therionology* **43,** 141–152.

Heikinheimo, O., and Gibbons, W. E. (1998). The molecular mechanisms of oocyte maturation and early embryonic development are unveiling new insights into reproductive medecine. *Mol. Hum. Reprod.* **4,** 745–756.

Herrler, A., Krusche, C. A., and Beier, H. M. (1998). Insulin and Insulin-like growth factor-I promote rabbit blastocyst development and prevent apoptosis. *Biol. Reprod.* **59,** 1302–1310.

Hockenbery, D. M., Oltvai, Z. N., Yin, X. M., Milliman, C. L., and Korsmeyer, S. J. (1993). Bcl-2 functions in an antioxidant pathway to prevent apoptosis. *Cell* **75,** 241–251.

Horejsi, V., Drbla, K., and Cebecauer, M., *et al.* (1999). GPI-domains: A role in signaling via immunoreceptors. *Immunol. Today* **20,** 22–26.

Host, E., Mikkelsen, A. L., Lindenberg, S., and Smidt-Jensen, S. (2000). Apoptosis in human cumulus cells in relation to maturation stage and cleavage of the corresponding oocyte. *Acta Obstet. Gynecol. Scand.* **79,** 936–940.

Hsu, S. Y., Kubo, M., Chun, S. Y., Haluska, F. G., Housman, D. E., and Hsueh, A. J. (1995). Wilms' tumor protein Wt1 as an overian transcription factor decreases in expression during follicle development and repression of inhibin-alpha gene promoter. *Mol. Endocrinol.* **9,** 1356–1366.

Inohara, N., Ding, L., Chen, S., and Nunez, G. (1997). Harakiri, a novel regulator of cell death, encodes a protein that activates apoptosis and interacts selectively with survival-promoting proteins Bcl-2 and Bcl-X(L). *EMBO J.* **16,** 1686–1694.

Izawa, M., Phuong, H. N., Kim, H. H., and Yeh, J. (1998). Expression of the apoptosis-related genes caspase-1, caspase-3, DNA fragmentation factor and apoptotic protease activating factor-1 in human granulosa cells. *Fertil. Steril.* **70,** 549–552.

Janny, L., and Ménézo, Y. (1994). Evidence for a strong paternal effect on human preimplantation embryo development and blastocyst formation. *Mol. Reprod. Dev.* **38,** 36–42.

Janny, L., and Ménézo, Y. J. R. (1996). Maternal age effect on early human embryonic development and blastocyst formation. *Mol. Reprod. Dev.* **45,** 31–37.

Jin, P., Meyer, T. E., and Warner, C. M. (1992). Control of embryo growth by the Ped gene: Use of reverse transcriptase polymerase chain reaction (RT-PCR) to measure mRNA in preimplantation embryos. *Assist. Reprod. Tech. Androl.* **3,** 377–383.

José De Los Santos, M., Anderson, D. J., Racowsky, C., and Hill, J. A. (2000). Presence of Fas-Fas ligand system and bcl-2 gene products in cells and fluids from gonadotropin-stimulated human ovaries (1). *Biol. Reprod.* **63,** 1811–1816.

Jurisicova, A. (1998b). Expression and regulation of genes associated with cell death during murine preimplantation embryo development. *Mol. Reprod. Dev.* **51**(3), 243–253.

Jurisicova, A., Casper, R. F., MacLusky, N. J., Gordon, B. M., and Librach, C. L. (1996a). HLA-G expression during preimplantation human embryo development. *Proc. Natl. Acad. Sci.* **93,** 161–165.

Jurisicova, A., Casper, R. F., MacLusky, N. J., Gordon, B. M., and Librach, C. L. (1996b). Embryonic human leukocyte antigen-G expression: Possible implications for human preimplantation development. *Fertil. Steril.* **65,** 997–1002.

Jurisicova, A., Rogers, I., Fasciani, A., Casper, R. F., and Varmuza, S. (1998a). Effect of maternal age and conditions of fertilization on programmed cell death during murine preimplantation embryo development. *Mol. Hum. Reprod.* **4,** 139–145.

Jurisicova, A., Varmuza, S., and Casper, R. F. (1995). Involvement of programmed cell death in preimplantation embryo demise. *Hum. Reprod. Update* **1,** 558–566.

Jurisicova, A., Varmuza, S., and Casper, R. F. (1996c). Programmed cell death and human embryo fragmentation. *Mol. Hum. Reprod.* **2,** 93–98.

Ke, X., and Warner, C. M. (2000). Regulation of *Ped* gene expression by TAP protein. *J. Reprod. Immunol.* **46,** 1–15.

Kerr, J. F. R., Wyllie, A. H., and Currie, A. R. (1972). Apoptosis: A basic biological phenomenon with wide-ranging implications in tissue kinetics. *Br. J. Cancer* **26,** 239–257.

King, A., Loke, Y. W., and Chaouat, G. (1997). NK cells and reproduction. *Immunol. Today,* **18,** 64–66.

Kligman, I., Benadiva, C., Alikani, M., and Munne, S. (1996). The presence of multinucleated blastomeres in human embryos is strongly correlated with chromosomal abnormalities. *Hum. Reprod.* **11,** 1492–1498.

Korsmeyer, S. J., Shutter, J. R., Veis, D. J., Merry, D. E., and Otvai, Z. N. (1993). Bcl-2/Bax: A rheostat that regulates an anti-oxidant pathway and cell death. *Cancer Biol.* **4,** 327–332.

Korsmeyer, S. J., Yin, X-M., Oltvai, Z. N., Veis-Novack, D. J., and Linette, G. P. (1995). Reactive oxygen species and the regulation of cell death by the Bcl-2 gene family. *Biochim. Biophys. Acta* **1271,** 63–66.

Kreidberg, J. A., Natoli, T. A., McGinnis, L., Donovan, M., Biggers, J. D., and Amstutz, A. (1999). Coordinate action of Wt1 and a modifier gene supports embryonic survival in the oviduct. *Mol. Reprod. Dev.* **52,** 366–375.

Krüssel, J. S., and Huang, H.-Y. Simon C., *et al.* (1998). Single blastomeres within human preimplantation embryos express different amounts of messenger ribonucleic acid for -actin and inbetrleukin-1 receptor type I. *J. Clin. Endocrinol. Metab.* **83,** 953–959.

Latham, K. E. (1999). Mechanisms and control of embryonic genome activation in mammalian embryos. *Int. Rev. Cytol.* **193,** 71–124.

Lea, R. G., McCraken, J. E., McIntyre, S. S., Smith, W., and Baird, J. D. (1996). Disturbed development of the preimplantation embryo in the insulin-dependent diabetic BB/E rat. *Diabetes* **45,** 1463–1470.

LeBouteiller, P. L., and Lenfant, F. (1996). Antigen-presenting function(s) of the non-classical HLA-E, -F and -G class I molecules: The beginning of a story. *Res. Immunol.* **147,** 301–313.

Levy, R., Benchaib, M., Cordonier, H., Souchier, C., and Guerin, J. F. (1998a). Lasser scanning confocal imaging of abnormal or arrested human preimplantation embryos. *J. Assist. Reprod. Genet.* **15,** 485–495.

Levy, R., Benchaib, M., Cordonier, H., Souchier, C., and Guerin, J. F. (1998b). Annexin V labeling and terminal transferase-mediated DNA end labeling (TUNEL) assay in human arrested embryos. *Mol. Hum. Reprod.* **4,** 775–783.

Levy, R., Cordonier, H., Czyba, J. C., and Guerin, J. F. (in press). Apoptosis in preimplantation mammalian embryo and genetics. Molecular, Cellular and Developmental Biology of Reproduction: Basic and clinical aspects.

Lighten, A. D., Moore, G. E., Winston, R. M., and Hardy, K. (1998). Routine addition of human insulinlike growth factor-I ligand could benefit clinical in-vitro fertilization culture. *Hum. Reprod.* **13,** 3144–3150.

Liu, L., and Keefe, D. L. (2000b). Cytoplasm mediates both development and oxidation-induced apoptosic cell death in mouse zygotes *Biol. Reprod.* **62,** 1828–1834.

Liu, L., Trimarchi, J. R., and Keefe, D. L. (2000a). Involvement of mitochondria in oxidative stress-induced cell death in mouse zygotes. *Biol. Reprod.* **62,** 1745–1753.

Long, E. O. (1998). Signal sequences stop killer cells. *Nature* **391,** 740–743.

Luft, J. C., and Dix, D. J. (1999). Hsp 70 expression and function during embryogenesis. *Cell Stress Chaperones* **4,** 162–170.

Magli, M. C., Gianaroli, L., Ferraretti, A. P., Fortini, D., Aicardi, G., and Montanaro, N. (1998). rescue of implantation potential in embryos with poor prognosis by assisted zona hatching. *Hum. Reprod.* **13,** 1331–1335.

Mailhos, C., Howard, M. K., and Latchman, D. S. (1993). Heat shock protects neuronal cells from programmed cell death by apoptosis. *Neuroscience* **55,** 621–627.

Marana, H. R. C., Andrade, J. M., and Martins, G. A., *et al.* (1998). Morphometric study of maternal smoking on apoptosis in the syncytiotrophoblast. *Int. J. Gynecol. Obstet.* **61,** 21–27.

Martin, S. J., Reutelingsperger, C. P., McGahon, A. J., Rader, J. A., van Schie, R. C., LaFace, D. M., and Green, D. R. (1995). Early redistribution of plasma membrane phosphatidylserine is a general feature of apoptosis regardless of the initiating stimulus: Inhibition by overexpression of Bcl-2 and Abl. *J. Exp. Med.* **182,** 1545–1556.

Matwee, C., Betts, D. H., and King, W. A. (2000). Apoptosis in the early bovine embryo. *Zygote* **8,** 57–68.

McElhinny, A. S. (1998). The expression pattern of the Qa-2 antigen in mouse preimplantation embryos and its correlation with the Ped gene phenotype. *Mol. Hum. Reprod.* **4,** 966–71.

McElhinny, A. S., and Warner, C. M. (2000). Cross-linking of Qa-2 protein, the Ped gene product, increases the cleavage rate of C57BL/6 preimplantation mouse embryos. *Mol. Hum. Reprod.* **6,** 517–522.

Moley, K. H. (1999). Diabetes and preimplantation events of embryogenesis. *Semin. Reprod. Endocrinol.* **17**(2), 137–151.

Moley, K. H., Chi, MM-Y., Knudson, C. M., Korsmeyer, S. J., and Mueckler, M. M. (1998). Hyperglycemia induces apoptosis in preimplantation embryos through cell death effector pathway. *Nat. Med.* **4,** 1421–1424.

Moley, K. H., Vaughn, W. K., and Diamond, M. P. (1994). Manifestation of diabetes mellitus on mouse preimplantation development: Effect of elevated concentration of metabolic intermediates. *Hum. Reprod.* **9,** 113–121.

Morota, Y., Perez, G. I., Paris, F., Miranda, S. R., Ehleiter, D., Haidmovitz-Friedman, A., Fuks, Z., Xie, Z., Reed, J. C., Schuchman, E. H., Kolesnick, R. N., and Tilly, J. L. (2000). Oocyte apoptosis is suppressed by disruption of the acid sphingomyelinase gene or by shingosine-1-phosphate therapy. *Nat. Med.* **6,** 1109–1114.

Mosser, D. D., Caron, A. W., Bourget, L., Denis-Larose, C., and Massie, B. (1997). Role of the human heat-shock protein hsp70 in protection against stress-induced apoptosis. *Mol. Cell. Biol.* **17,** 5317–5327.

Muscarella, D. E., Rachlinski, M. K., and Bloom, S. E. (1998). Expression of cell death regulatory genes and limited apoptosis induction in avian blastoderm cells. *Mol. Reprod. Dev.* **51,** 130–142.

Nakahara, K., Saito, H., Saito, T., Ito, M., Ohta, N., Sakai, N., Tezuka, N., Hiroi, M., and Watanabe, H. (1998). Incidence of apoptotic bodies in membrana granulosa of the patients participating in an in vitro fertilization program. *Fertil. Steril.* **67,** 302–308.

Neuer, A., Mele, C., and Liu, H. C., *et al.* (1998). Monoclonal antibodies to mammalian heat shock proteins impair mouse embryo development *in vitro. Hum. Reprod.* **13,** 987–990.

Neuer, A., Spandorfer, S. D., Giraldo, P., Dieterle, S., Rosenwaks, Z., and Witkin, S. S. (2000). The role of theat shock proteins in reproduction. *Hum. Reprod. Update* **6,** 149–159.

Nichols, J., Zevnik, B., Anastassiadis, K., Niwa, H., Klewe-Nebenius, D., Chambers, I., Scholer, H., and Smith, A. (1998). Formation of pluripotent stem cells in the mammalian embryo depends on the POU transcription factor Oct4. *Cell* **95,** 379–391.

O'Callaghan, C. A., and Bell, J. I. (1998). Structure and function of the human MHC class Ib molecules HLA-E, HLA-F and HLA-G. *Immunol. Rev.* **163,** 129–138.

O'Neill, C. (1997). Evidence for the requirement of autocrine growth factors for development of mouse preimplantation embryos *in vitro. Biol. Reprod.* **56,** 229–237.

Oosterhuis, G. J., Michgelsen, H. W., Cornelis, B. L., Schoemaker, J., and Vermes, I. (1998). Apoptotic cell death in human granulosa-lutein cells: A possible indicator of in vitro fertilization outcome. *Fertil. Steril.* **70,** 747–749.

Ornoy, A., and Zusman, I. (1991). Embryotoxic effect of diabetes on preimplantation embryos. *Isr. J. Med. Sci.* **27,** 487–492.

Otani, H., Tanaka, O., Tatewaki, R., Naora, H., and Yoneyama, T. (1991). Diabetic environment and genetic predisposition as causes of congenital malformations in NOD mouse embryos. *Diabetes* **40,** 1245–1250.

Ovitt, C. E., and Schöler, R. (1998). The molecular biology of Oct-4 in the early mouse embryo. *Mol. Hum. Reprod.* **4,** 1021–1031.

Paria, B. C., and Dey, S. K. (1990). Preimplantation embryo development *in vitro*: Cooperative interactions among embryos and role of growth factors. *Proc. Natl. Acad. Sci. USA* **87,** 4756–4760.

Pampfer, S. (2000). Peri-implantation embryopathy induced by maternal diabetes. *J. Reprod. Fertil. Suppl.* **55,** 129–139.

Pampfer, S., De Hertogh, R., Vanderheyden, I., Michiels, B., and Verchaval, M. (1990). Decreased inner cell mass proportion in blastocysts from diabetic rats. *Diabetes* **39,** 471–476.

Pampfer, S., De Hertogh, R., Vanderheyden, I., Michiels, B., and Verchaval, M. (1994). In vitro study of the carryover effect associated with early diabetic embryopathy in the rat. *Diabetologia* **37,** 855–862.

Pampfer, S., Vanderheyden, I., McCracken, J., Vesela, J., and DeHertogh, R. (1997). Increased cell death in rat blastocyst exposed to maternal diabetes in *utero* and to high glucose or tumor necrosis factor-(alpha) *in vitro*. *Development* **124,** 4827–4836.

Pampfer, S., Vanderheyden, I., Wuu, Y. D., Baufays, L., Maillet, O., and DeHertogh, R. (1995). A possible role for tumor necrosis-factor a in the early embryopathy associated with maternal diabetes in the rat. *Diabetes* **44,** 531–536.

Papaioannou, V. E., and Ebert, K. M. (1986). The preimplantation pig embryo: cell number and allocation to trophectoderm and inner cell mass of the blastocyst *in vivo* and *in vitro*. *Development* **102,** 793–803.

Parchment, R. E. (1993). The implications of a unified theory of programmed cell death, polyamines, oxyradicals and histogenesis in the embryo. *Int. J. Dev.* **37,** 75–83.

Perez, G. I., Tao, X.-J., and Tilly, J. L. (1999). Fragmentation and death (a. k. a. apoptosis) of ovulated oocytes. *Mol. Hum. Reprod.* **5,** 414–420.

Pergament, E., and Fiddler, M. (1998). The expression of genes in human preimplantation embryos. *Prenat. diagn.* **18,** 1366–1373.

Pierce, G. B., Lewellyn, A. L., and Parchment, R. E. (1989). Mechanism of programmed cell death in the blastocyst. *Proc. Natl. Acad. Sci. USA* **86,** 3654–3658.

Punyiczki, M., and Fesus, L. (1998). The two defense systems of the organism may have overlapping elements. *Ann. NY Acad. Sci.* **851,** 67–74.

Raff, M. C. (1992). Social controls on cell survival and cell death. *Nature* **356,** 379.

Reed, J. C. (2000). Mechanisms of apoptosis. *Am. J. Pathol.* **157,** 1415–1430.

Sanders, E. J., and Wride, M. A. (1995). Programmed cell death in development. *Int. Rev. Cytol.* **163,** 105–73.

Schmidt, C. M., and Orr, H. T. (1993). Maternal/Fetal intercation: The role of the MHC class I molecule HLA-G. *Crit. Rev. Immunol.* **13,** 207–224.

Sible, J. C., Anderson, J. A., Lewellyn, A. L., and Maller, J. L. (1997). Zygotic transcription is required to block a maternal programme of apoptosis in *Xenopus* embryos. *Dev. Biol.* **189,** 335–346.

Sipes, S. L., and Medaglia, M. V. Stabley D. L., *et al.* (1996). A new major histocompatibility complex Ib gene expressed in the mouse blastocyst and placenta. *Immunogenetics* **45,** 108–120.

Spanos, S., Becker, D. L., Winston, R. M., and Hardy, K. (2000). Anti-apoptotic action of insulin-growth factor I during human preimplantation embryo development. *Biol. Reprod.* **63,** 1413–1420.

Stojanov, T., and O'Neill, C. (1999). Ontogeny of expression of a receptor for platelet-activating factor in mouse preimplantation embryos and the effects of fertilization and culture in vitro on its expression. *Biol. Reprod.* **60,** 674–82.

Stroynowski, I., and Tabaczewski, P. (1996). Multiple products of class Ib Qa-2 genes—which are functional? *Res. Immunol.* **147,** 290–301.

Takai, H., Tominaga, K., Motoyama, N., Minamishima, Y. A., Nagahama, H., Tsukiyama, T., Ikeda, K., Nakayama, K., and Nakanishi, M. (2000). Aberrant cell cycle checkpoint function and early embryonic death in Chk1(-/-) mice. *Genes Dev.* **14,** 1439–1447.

Tesarik, J., Kopecny, V., Plachot, M., and Mandelbaum, J. (1987). Ultrastructural and autoradiographic observations on multinucleated blastomeres of human cleaving embryos obtained by in-vitro fertilization. *Hum. Reprod.* **2,** 127–136.

Thompson, J. G., Gardner, D. K., Pugh, P. A., McMillan, W. H., and Tervit, H. R. (1995). Lamb birth weight is affected by culture system utilised during in vitro pre-elongation development of ovine embryos. *Biol. Reprod.* **53,** 1385–1391.

Tian, Z., Xu, Y., and Warner, C. M. (1992). Removal of Qa-2 antigen alters the Ped gene phenotype of preimplantation mouse embryos. *Biol. Reprod.* **47,** 271–276.

Van Blerkom, J. (1997). Can the developmental competence of early human embryos be predicted effectively in the clinical IVF laboratory? *Hum. Reprod.* **12,** 1610–1614.

Van Langendonckt, A., Donnay, I., Schuurbiers, N., Auquier, P., Carolan, C., Massip, A., and Dessy, F. (1997). Effects of supplementation with fetal calf serum on development of bovine embryos in synthetic oviductal fluid medium. *J. Reprod. Fertil.* **109,** 87–93.

Vaux, D. L., and Korsmeyer, S. J. (1999). Cell death in development. *Cell* **96,** 245–254.

Verbanac, K. M., and Warner, C. M. (1981). Role of the major histocompatibility complex in the timing of early mammalian development. *In* "Cellular and Molecular Aspects of Implantation" (S. R. Glasser and D. W. Bullock, Eds.), pp. 467–470. Plenum New York.

Vercheval, M., De Hertogh, R., and Pampfer, S., *et al.* (1990). Experimental diabetes impairs rat embryo development during the preimplantation period. *Diabetologia* **33,** 187–191.

Warner, C. M., Brownell, M. S., and Rothschild, M. F. (1991). Analysis of litter size and weight in mice differing in *Ped* gene phenotype and the Q region of the H-2 complex. *J. Reprod. Immunol.* **19,** 303–313.

Warner, C. M., Cao, W., and Exley, G. E. (1998c). Genetic regulation of egg and embryo survival. *Hum. Reprod.* **13,** 178–190.

Warner, C. M., Exley, G. E., McElhinny, A. S., and Tang, C. (1998b). Genetic regulation of preimplantation mouse embryo survival. *J. Exp. Zool.* **282,** 272–279.

Warner, C. M., Gollnick, S. O., Flaherty, L., and Goldbard, S. B. (1987a). Analysis of Qa-2 antigen expression by preimplantation mouse embryos: Possible relationship to the preimplantation-embryo-development (Ped) gene product. *Biol. Reprod.* **36,** 611–616.

Warner, C. M., Gollnick, S. O., and Goldbard, S. B. (1987b). Linkage of the preimplantation-embryo-development (Ped) gene to the mouse major histocompatibility complex (MHC) Biol. *Reprod.* **36,** 606–610.

Warner, C. M., McElhinny, A. S., Wu, L., Cieluch, C., Ke, X., Cao, W., Tang, C., and Exley, G. E. (1998a). Role of the Ped gene and apoptosis genes in control of preimplantation development. *J. Assist. Reprod. Genet.* **15,** 331–337.

Warner, C. M., Panda, P., Almquist, C. D., and Xu, Y. (1993). Preferential survival of mice expressing the Qa-2 antigen. *J. Reprod. Fertil.* **99,** 145–147.

Weil, M., Jacobson, M. D., Coles, H. S. R., Davies, T. J., Gardner, R. L., Raff, K. D., and Raff, M. C. (1996). Constitutive expression of the machinery for programmed cell death. *J. Cell Biol.* **133,** 1053–1059.

Welch, W. J. (1992). Mammalian stress response: Cell physiology, structure/function of stress proteins, and its implications for medecine and disease. *Physiol. Rev.* **72,** 1063–1080.

Wiemer, K. E., Cohen, J., Tucker, M. J., and Godke, R. A. (1998). The application of co-culture in assisted reprdouction: 10 Years of experience with human embryos. *Hum. Reprod.* **13** (Suppl. 4), 226–238.

Wright, S. C., Zhong, G., Zheng, H., and Larrick, J. W. (1993). Nicotine inhibition of apoptosis suggests a role in tumor promotion. *FASEB J.* **7,** 1045–1051.

Wright, W. E., and Piatyszek, M. A. Rainey, W. E., *et al.* (1996) Telomerase activity in human germline and embryonic tissues and cells. *Dev. Genet.* **18,** 173–179.

Wu, L., Exley, G. E., and Warner, C. M. (1998). Differential expression of Ped gene candidates in preimplantation mouse embryos. *Biol. Reprod.* **59,** 941–952.

Wu, L., Feng, H., and Warner, C. M. (1999). Identification of two major histocompatibility complex class Ib genes, Q7 and Q9 as the Ped gene in the mouse. *Biol. Reprod.* **60,** 1114–1119.

Wyllie, A. H., Kerr, J. F. R., and Currie, A. R. (1980). Cell death: The significance of apoptosis. *Int. Rev. Cytol.* **68,** 251–306.

Xu, J., Cheung, T. M., Chan, S. T., Ho, P. C., and Yeung, W. S. (2000). Human oviductal cells reduce the incidence of apoptosis in cocultured mouse embryos. *Fertil. Steril.* **74,** 1215–1219.

Xu, Y., Jin, P., and Warner, C. M. (1993). Modulation of preimplantation embryonic development by antisense oligonucleotides to major histocompatibility complex genes. *Biol. Reprod.* **48,** 1042–1046.

Xu, Y., Jin, P., Mellor, A. L., and Warner, C. M. (1994). Identification of the *Ped* gene at the molecular level: The Q9 MHC class transgene converts the *Ped* slow to the *Ped* fast phenotype. *Biol. Reprod.* **51,** 695–699.

Xu, J., and Yang, X. (2000). Telomerase activity in bovine embryos during early development. *Biol. Reprod.* **63,** 1124–1128.

Yang, H. W., Hwang, K. J., Kwon, H. C., Kim, H. S., Choi, K. C., and Oh, K. S. (1998). Detection of reactive oxygen species (ROS) and apoptosis in human fragmented embryos. *Hum. Reprod.* **13,** 998–1002.

Zenzes, M. T. (2000). Smoking and reproduction: Gene damage to human gametes and embryos. *Hum. Reprod. Update* **6,** 122–131.

Zenzes, M. T., and Reed, T. E. (1996). Cigarette smoking may suppress apoptosis in human preembryos. *Hum. Reprod.* **11** (Abstract Book 1), 153. [Abstract D–128].

Zenzes, M. T., and Reed, T. E. (1999). Cigarette smoking inhibits apoptosis (programmed cell death) in early human embryos. *Fertil. Steril.* **72,** S132.

Zhu, H., Fu, W., and Mattson, M. P. (2000). The catalytic subunit of telomerase protects neurons against amyloid beta–peptide-induced apoptosis. *J. Neurochem.* **75,** 117–124.

This Page Intentionally Left Blank

The Antisecretory Factor: Synthesis, Anatomical and Cellular Distribution, and Biological Action in Experimental and Clinical Studies

Stefan Lange[1] and Ivar Lönnroth[2]

[1]Department of Clinical Bacteriology and [2]Department of Medical Microbiology and Immunology, Göteborg University, S-413 46 Göteborg, Sweden

The antisecretory factor (AF) is a 41-kDa protein that provides protection against diarrheal diseases and intestinal inflammation. Its cDNA has been cloned and sequenced. AF is highly potent, with 10^{-12} mol of recombinant AF being sufficient to counteract experimentally induced diarrhea in rat. The antisecretory activity is exerted by a peptide located between positions 35 and 50 of the AF sequence. Synthetic peptides based on this sequence are promising candidates for drugs to counteract intestinal hypersecretion, as well as imbalances of fluid transport in other body compartments. AF probably exerts its effects via nerves; AF immediately and potently inhibits ion transport across isolated nerve membranes from Deiters' cells. Immunocytochemistry has shown that AF is present in most tissues in the body, and *in situ* nucleic acid hybridization has shown that cells that store AF are also capable of AF synthesis. The endogenous plasma level of AF is increased by enterotoxins and by certain food constituents such as hydrothermally processed cereals. These cereals significantly improve clinical performance in patients suffering from inflammatory bowel diseases. AF-enhancing food also protects domestic animals against diarrheal diseases, and such feed has been used successfully in Swedish swine farming for the past 10 years. Increased understanding of AF action might result in expanded clinical applications and confirm that AF is an important regulator of homeostasis.

KEY WORDS: Antisecretory factor, Transport regulator, Endogenous stimulation, Functional food, Neuronal hormone, Membrane passage. © 2001 Academic Press.

I. Introduction

The transport of fluid and ions in the gut is controlled by the enteric nerve system. The gut sensory neurons include chemoreceptors, mechanoreceptors, and thermoreceptors, which react to the chemical composition, texture, and temperature of the intestinal contents, respectively (Goyal and Hirano, 1996; Pacha, 2000). Receptor signals are sorted by interneurons and then redirected to either excitatory or inhibitory motorsecretory neurons. Such neurons control intestinal motility, as well as transport across the mucosal epithelium (Booth, 1992; Cook, 1994). Gastrointestinal peptides modulate these excitatory and inhibitory nerve signals and induce either enhanced or reduced transport of ions, nutrients, and water. Peptides triggering secretion include vasoactive intestinal peptide, substance P, neurotensin, and atrial natriuretic factor. Peptides causing net absorption of fluid and ions include neuropeptide Y, peptide YY, angiotensin, sorbin, somatostatin, enkephalins, and other opioids (Hansen and Skadhauge, 1995; Vagne-Descroix *et al.,* 1991). The antisecretory drugs loperamide and octreotide act on opioid and somatostatin receptors, respectively.

We have used an animal model to study intestinal fluid secretion in rat ligated loops (Lange, 1982) with cholera toxin (CT) used as the secretagogue. By using this model as a bioassay, a new endogenous factor involved in intestinal resistance against cholera toxin and prostaglandin E1-induced fluid secretion (Lönnroth and Lange, 1981) was identified as an inducible antisecretory protein in the rat and pig (Lange and Lönnroth, 1984; Lange *et al.,* 1987a). This protein, called *antisecretory factor* (AF), accumulated in the gut and pituitary gland after challenge with enterotoxins such as cholera toxin, *Escherichia coli* LT, and *Clostridium difficile* toxin A (Lange and Lönnroth, 1984; Lönnroth and Lange, 1984, 1985; Lange and Lönnroth 1986; Torres *et al.,* 1991). AF is secreted into the blood, bile, and breast milk in response to intestinal enterotoxin challenge (Lange and Lönnroth, 1986), and the AF content in sows' milk probably is crucial for protection against neonatal diarrhea in suckling piglets (Lönnroth *et al.,* 1988a). AF purified from porcine pituitary is more potent than all of the previously described antisecretory peptides or drugs (Lönnroth and Lange, 1986). Enterotoxin-induced fluid secretion was inhibited in rats and pigs by 10^{-12} and 10^{-11} mol AF, respectively (Lönnroth and Lange, 1986; Lange *et al.,* 1987a). The sequences of the AF protein and cDNA have been determined by molecular cloning (Johansson *et al.,* 1995). Recombinant AF produced in *E. coli* was at least as potent as the purified native porcine AF. The action of AF on GABA-mediated chloride transport in isolated Deiters' nerve membranes suggests that most effects achieved by AF are nerve-mediated (Lange *et al.,* 1985, 1987b; Rapallino *et al.,* 1989). In addition, other groups have shown that an AF-like protein seems to regulate proteolytic degradation (Young *et al.,* 1998) and transcription (Anand *et al.,* 1998). The finding that certain carbohydrates and amino acids also are able to induce AF or AF-like proteins (Lönnroth and Lange, 1987) has had great therapeutic applications. Thus,

specially formulated AF-increasing feed has been used successfully in Swedish swine breeding for the past 10 years (Göransson *et al.,* 1993, 1995). Furthermore, a cost regime including AF-enhancing cereals had significant beneficial effects on clinical performance in patients suffering from inflammatory bowel disease (Björck *et al.,* 2000).

II. Basic Biology of the Antisecretory Factor (AF)

A. Molecular Biology

1. Chemical Purification of AF

The AF protein was originally characterized in extracts from intestinal mucosa and pituitary gland of mouse and rat. Whereas the intestinal protein was rapidly degraded, the pituitary protein was relatively stable due to lower proteolytic activity in this organ. The antisecretory activity of the purified products was measured in the rat jejunal ligated loop assay as percentage inhibition of cholera toxin-induced fluid secretion.

Our first successful purification of the AF protein occurred in 1986, at which time we were able to demonstrate the presence of AF with chemical methods. Protein extracted from more than 100 porcine pituitary glands was purified in three successive steps: (1) isoelectric focusing, (2) gel filtration, and (3) affinity chromatography in agarose gel. The purified protein was shown through SDS–PAGE to have an apparent molecular mass of 60 kDa and an isoelectric point (pI) of 4.8. Later preparations of porcine AF were made from blood plasma (Lönnroth *et al.,* 1988b) and purified by affinity chromatography, ultrafiltration, and isoelectric focusing. The AF protein obtained from plasma was polymeric in contrast to the AF obtained from pituitary glands which was monomeric. The plasma AF was used to raise polyclonal antibodies in rabbits which could be used to identify cloned AF protein.

2. Cloning of AF cDNA

AF was first cloned by screening a cDNA library from human pituitary glands (Johansson *et al.,* 1995). Out of >1,000,000 λ-GT11 clones, two expressing human AF were identified. The cDNA inserts of the clones were excised, purified, and subsequently recloned into a pGEX plasmid. After transfection into *E. coli,* plasmids were amplified and purified for sequencing of the cDNA. The two original clones contained most of the coding sequences, but both clones lacked the 5′-end coding for the N-terminal part of the AF protein. For obtaining the missing 5′-end, a PCR-based method called RACE (rapid amplification of cDNA ends) was performed. The missing sequence was amplified by PCR from cDNA obtained from the human brain. After inserting the missing 322 bp into the largest of the

original cDNA clones, a full-length construct of AF cDNA was inserted into a pGEX plasmid and sequenced. Further work has demonstrated that cDNA with more than 90% identity with the human cDNA has been cloned in rat (Tateishi *et al.,* 1999) and mouse (Pusch *et al.,* 1998). In contrast, Kawahara *et al.* (2000) recently have identified four variants of AF in mice which differ substantially in the 3′-end. These sequences are described below.

3. The AF Sequence

The full-length human AF cDNA contains 1309 bp, of which 1131 constitute the coding sequence. Both the DNA and the deduced protein sequence are unique in having essentially no resemblance to any other cDNA or protein, respectively. The only protein of significant homology was a hypothetical yeast protein (29% identity) of unknown function. The molecular weight of the human protein was 41,000 and the predicted pI 4.9. The isoelectric point was close to that expected (5.0), but the molecular weight was less than that predicted from our earlier experiments. In order to obtain more accurate physical chemical data on the protein, the pGex plasmid was transfected into *E. coli* and AF was expressed as a fusion protein with the enzyme glutathione *S*-transferase as the leading sequence. The glutathione enzyme permitted efficient isolation of the fusion protein on glutathione–agarose gel affinity columns. The AF-protein was released from the gel by treatment with the protease thrombin. The combined affinity chromatography and hydrolytic release gave an essentially pure preparation of recombinant AF (rAF) protein. The molecular mass of rAF, as defined by SDS–PAGE, was 55–60 kDa, which is similar to that of the natural protein. Thus the 41-kDa AF protein showed an abnormal migration in SDS–PAGE, probably due to the C-terminal sequence. Recently, five different AF proteins (Rpn10a–Rpn10e) were reported in mouse (Table I). The sequences of these proteins were 67–96% identical to AF1; the first 250 residues in each of the five proteins exactly matched those of AF-1, whereas the C-terminal sequence differed. The total number of amino acids was 376 for Rpn10a, 379 for Rpn10b, 368 for Rpn10c, 349 for Rpn10d, and 260 for Rpn10e. The protein with highest homology to AF-1, Rpn10a, has a molecular mass of 41 kDa and a pI of 4.9. The shortest mouse protein, Rpn10e, has a human analog that is identical until residue 258 and in addition has 8 extra amino acids (Table I).

4. The Antisecretory Part of the AF Peptide

The recombinant full-length AF becomes more active after treatment with trypsin, indicating that the activity of AF is achieved by fragments of the whole protein. To localize the active region of AF, truncated forms of AF were produced by recombinant techniques and tested for antisecretory activity in rat (Johansson *et al.,* 1997b). Many of the truncated peptides were active (Table II), and

TABLE I

AF (Rpn10) Proteins in Various Species

Species	Homology (% identity)	Molecular weight (kDa)	Isoelectric point (pI)
Man			
a	$(100)^a$	41	4.9
e	67	29	5.7
Rat			
a	97	41	4.5
Mouse			
a	96	41	4.9
b	95	41	4.5
c	82	40	4.8
d	79	38	5.1
e	67	28	5.5
Drosophila	45	43	4.5
Caenorhabditis	43	67	5.2

[a]Percentage of amino acids identical with human AF-1.

activity was dependent on the presence of a specific peptide between residues 35 and 50 in AF-1. Thus, AF-2 expressed by one of the clones lacked activity due to a deletion between residues 1 and 62. In contrast, AF-4 expressing the 105 N-terminal amino acids was active. Of the recombinant peptides expressed in *E. coli* AF-10, composed of residues 36–51, was the smallest; this 16-amino-acid peptide was also synthesized by organic solid phase synthesis.

TABLE II

Biological Effects of Peptides Made by Recombinant DNA Techniques or Solid Phase Synthesis

Code	Peptide	Effect
AF-1	————————————————————	+
AF-2	————————————	−
AF-4	——————	+
AF-6	———	+
AF-7	————	+
AF-9	—	−
AF-10	—— VCHSKTRSNPENNVGL	+
AF-12	— IVCHSKTR	+
AF-13	− VCHSKT	−

Both types of synthesis resulted in an active peptide having an ED_{50} value of about 5 pmol.

The organically synthesized octapeptide AF-12 (residues 35–42) had an ED_{50} value of 15 pmol, whereas the hexapeptide AF-13 (residues 35–42) lacked activity. These results suggest that the site of the antisecretory activity resides on a small region (I)VCHSKTR between residues 35 and 42 of the AF-1 molecule. Furthermore, AF-10 and AF-12 have been shown to reverse both intestinal inflammation and vascular permeability in the ligated jejunal loops of rats (see animal studies).

5. Antibodies Binding to Different Epitopes on the AF Molecule

Polyclonal antibodies were produced by immunizing rabbits with peptides derived from the AF sequence. These antibodies attach to different parts of the AF-molecule. Thus, the P8 and 105-antibody recognize the N-terminal portion of AF that is common to all five AF-proteins expressed in mouse. These antibodies react in Western blots with two different proteins expressed in lung, for example, and have an apparent molecular mass of 30 and 60 kDa, respectively. The H-3 antibody, which binds residues 250–278 in the AF-1 molecule, reacts with two proteins of approximate molecular mass of 50 and 60 kDa, respectively. The M2 antibody, which binds residues 316–340, recognized only the 60-kDa band. These results suggest that the 30-kDa band contains the N-terminal sequence but not the C-terminal sequences, i.e., those behind residue 250. This band might represent Rpn10e, which has a molecular weight of 28 kDa and a sequence that differs from Rpn10a after residue 250 (see Table I). The 60-kDa band containing residues 316–340 is probably either protein a and/or protein b, whereas the 50-kDa band, lacking residues 316–340 but containing residues 250–278, might represent either protein c or protein d (c residues 1–323, d residues 1–301 is identical to a). Antibodies specific for each of the five proteins are now being prepared. However, it will be difficult to produce antibodies capable of distinguishing between the a and b variants, because these proteins differ only in 3 amino acid residues. It should be easier to generate specific antibodies to proteins c and d, which have unique sequences in residues 323–368 and in residues 301–349, respectively.

6. AF-Binding Proteins: Possible AF Receptors

When the AF sequence was analyzed using bioinformatic models, residues 5–188 were predicted to contain a von Willenbrand-like motif (vWm). This is the only highly significant motif found in the AF structure and indicates that AF binds to other proteins via its N-terminal half. vWm proteins are frequently secreted extracellularly and tend to bind to other proteins (Edwards and Perkins, 1996). Indeed, three different AF-binding proteins have been identified: polyubiquitin and presinilins 1 and Id1. There are no homologies between the AF-binding sequences in these proteins, and different portions of the AF sequence bind to each protein.

Polyubiquitin, but not monomeric ubiquitin, binds with high affinity to AF. This binding seems to occur via two sites situated between residues 200 and 300 in AF (Young *et al.,* 1998; AF is called S5a by these authors) and thus does not involve the vWm. The mouse variants a and b contain these binding sites, whereas c, d, and e do not. The binding of the helix–loop–helix protein Id1 to a protein almost identical to AF was shown by Anand *et al.* (1997). The binding region in AF was identified as the N-terminal region containing the vWm motif. A third group has described binding between AF and the seven-loop membrane protein presinilin 1 (St. George-Hyslop *et al.,* 1996). As presenilin-1 occurs in nerve cell membranes, it might be a possible candidate for a receptor-mediating antisecretory activity. However, the published sequence did not include the N-terminal portion and therefore lacks the antisecretory portion of AF and also most of the vWm motif. Polyubiquitin and Id-l on the other hand are intracellular proteins and are therefore unlikely candidates as receptors mediating antisecretory activity. Identification of this receptor and the binding activities of each of the four new AF proteins (mouse Rpn10b, -c, -d, and -e) are urgently needed.

7. AF Genes in Mammalia

The human genome contains several potential *AF* genes. These gene loci are found on chromosomes 1, 19, and 23, the latter containing two potential AF-coding genes. In addition, chromosomes 10 and 15 contain processed pseudogenes of AF. In mouse, one *AF* gene (*Rpn10*) has been sequenced entirely (Kawahara *et al.,* 2000). This single gene seems to code for all five forms, Rpn10a, -b, -c, -d, and -e. This is achieved by a unique alternative splicing of the primary transcript. Of the 10 exons contained in *Rpn10*, only exons 7 to 10 undergo alternative splicing. Differential usage of the splice donor sites in intron 7 accounts for the presence or absence of a short segment coding for the amino Gly–Glu–Arg which is absent in Rpn10a and present in Rpn10b. The Rpn10c and -d cDNAs are generated because of a failure to splice out introns 9 and 8, respectively. The cDNA for Rpn10e is generated because intron 7 is not excised. This creates a stop codon 19 bp downstream from the 3′-end of exon 7, resulting in a smaller protein.

8. AF-Like RPN10 Genes in Nonmammalian Eukaryotes

Homologs of the *AF* gene have been identified in eukaryotic, but not in prokaryotic organisms. The corresponding proteins are called mcb1, p50, sun-1, or Rpn10, and they seem to function primarily as regulators of proteolytic degradation in the proteasome. The sequence responsible for antisecretory activity is present only in mammalian proteins. The yeast proteins have been most extensively studied. The bulk of the proteins occur free in the cytosol, but some are associated with the proteasome. Surprisingly, deletion of the *Rpn10* gene has no effect on the growth of yeast or the degradation of yeast proteins (Rubin *et al.,* 1997; Glickman *et al.,*

1999). Similarly, deletion of the corresponding gene in the moss *Physcomitrella* has no effect on the outgrowth of primary cells. However, in this multicellular organism the differentiation of secondary cells is altered, generating abnormal caulonema that are unable to form buds or gametophores (Girod *et al.,* 1999). Interestingly, treatment with the plant hormones auxin or cytokinin restored bud formation and subsequent partial development of gametophores.

B. Cellular Distribution and Expression of AF

1. Production of AF Antibodies and the AF mRNA Probe

In early studies, antisera against AF purified from pituitary gland were used. In later studies, well-defined antisera raised against either recombinant AF or synthetic AF peptides were used. Linear epitope(s) in AF were determined for each antibody by PepScan. Most of the antibodies have proven to be useful in immunohistochemistry, some of them also in ELISA, and some also in Western blots. These antibodies were used in AF immunoassays or in other forms of AF detection/visualization tests in various groups of healthy humans and patients, as well as in healthy and diseased animals. The AF sequence homology in man and animal suggests that the AF detection methods used in human medicine also will prove useful in veterinary medicine. The AF mRNA probe, suitable for *in situ* hybridization and Northern blots, was constructed using the 5′-end of the AF cDNA (bases 1–314 of the open reading frame).

   In the search for the *in vivo* regulatory function of AF, it was of importance to map out the cellular distribution of the AF protein in mammalian tissues. An initial study focusing on AF expression in mucosal membranes was done in pigs (Lange *et al.,* 1999). The pig was chosen primarily because we have collected most of our *in vivo* data on AF action from field studies of pigs. Secondly, the pig AF sequence is similar enough to that of human AF to allow use of the same antiserum, as well as the same mRNA probes in both species (Johansson, 1998).

   AF-expression in tissues was evaluated at the protein level by immunohisto-chemistry and at the mRNA level by *in situ* hybridization. By combining the two methods it was possible to discriminate between active synthesis of AF in the cell (*in situ* hybridization) and cellular uptake and storage of AF (immunohistochemistry). Northern blot performed on the same tissues used for histology revealed a single mRNA transcript with an estimated size of 1.4 kp in all of the tissues investigated. The histochemical results of the study are summarized below.

2. AF in Respiratory Organs

Expression of AF was observed in the epithelial lining of the nasal mucosa, in the trachea, and in the bronchial tree, suggesting a regulatory role for AF in the

lung clearance process, mediated via the pulsatory action of cilia. AF expression was also seen in mononuclear cells in the lamina propria. In alveoli, expression of AF mRNA and of AF protein was distinctly present in type II cells (also designated great alveolar cells), whereas no staining was seen in type I or squamous alveolar cells. Scattered lung macrophages were also positive for AF. The type II alveolar cells of the lung alveoli are thought to be responsible for production of the pulmonary surfactant, a substance of vital importance for total lung function (gas diffusion and immunological clearance of pathogens via the ciliar function). Impaired surfactant production (qualitatively or quantitatively) might precede the development of severe lung disease such as cystic fibrosis and chronic bronchitis. The colocalization of AF to type II alveolar cells tentatively suggests that AF might also play a regulatory role in the secretion of pulmonary surfactant (Kikkawa and Smith, 1983).

3. AF in the Gastrointestinal Tract and Gallbladder

In stomach, small intestine, and large intestine, AF and AF mRNA expression was evident in the surface epithelium, as well as in mononuclear cells in the underlying lamina propria. Double-labeling experiments indicate that these mononuclear cells represent a subgroup of T lymphocytes. Whether these cells can be further classified as a sort of dendritic cell correlated with the development of specific intestinal immune reactions remains to be evaluated (Banchereau and Steinman, 1998). We are presently performing immunoelectron microscopy to provide the information necessary for an unambiguous classification of the AF-positive cells in the intestinal submucosa tissue (Dr. Bengt Johansson, pers. commun.).

The ganglion cells in the myenteric and submucosal parasympathetic plexa along the intestinal tract were also AF-positive (Fig. 1), as was the epithelium of the gallbladder. Immunohistochemistry on sections from human intestinal biopsies showed an identical cellular distribution of AF-labeling as in pigs, i.e., in the epithelial cells as well as in the submucosal lymphocytes (Fig. 1).

In general, AF mRNA appeared to be expressed to the same degree in epithelial cells and in lymphocytes along the entire gastrointestinal tract including the gallbladder, whereas the AF protein appeared to be expressed preferentially in the subepithelial, lymphocyte-like cells. This difference in mRNA versus protein expression of AF could be due to differences in AF translation in the various cell types or a more rapid proteolytic degradation or secretion of AF in the epithelial cells.

4. AF in the Kidneys, Ureters, and Urinary Bladder

In the kidneys, identical staining results were obtained by using *in situ* hybridization or by applying the immunohistochemistry technique on selected sections. Thus, both methods distinctly revealed high AF expression in the thick
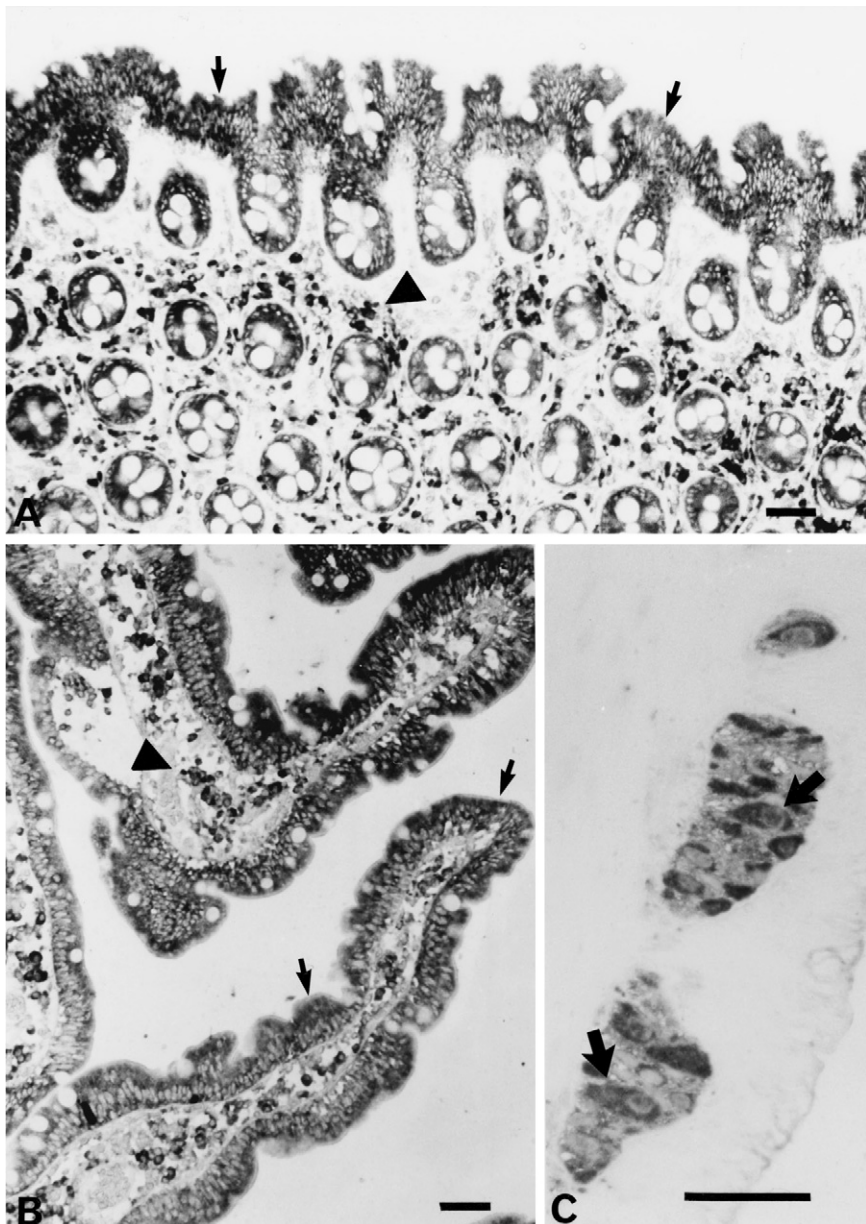
FIG. 1 Sections from human intestine processed to demonstrate AF-immunoreactivity. Alkaline phosphatase-conjugated secondary antibodies were used. Positive reactions appear dark. The sections are not counterstained. Bars, 50 μm. (A) Large intestine. AF-immunoreactivity is evident in epithelial cells lining the surface and the crypts (arrows) and in mononuclear cells in lamina propria (arrowhead). (B) Small intestine. AF-immunoreactivity in the epithelium lining the villi (arrows) and in cells in the lamina propria (arrowhead). (C) Myenteric plexus from the small intestine. AF-immunoreactivity is mainly seen in the neurons (arrows).

ascending limb of Henle. The remainder of the distal tubules showed weak staining, as did the collecting ducts and the thin limb of Henle. The proximal tubules and the glomeruli were not stained. The thick ascending limb of Henle is impermeable to water, chloride is actively transported out of the tubule, and the chloride ions are followed by passive sodium transport. The net result of this process is a gradient of hyperosmolarity in the kidney medullary interstitium, a prerequisite for urine concentration (Ganong, 1975). The specific localization of AF to this part of the nephron suggests that the AF protein participates in urine production, tentatively as a transport regulator. However, experiments related to urine production or other forms of kidney performance must be carried out before the biological significance of this most distinct localization of AF in the loop of Henle can be evaluated.

In the ureters and urinary bladder, AF expression was observed mainly in the epithelium, and also in solitary lymphocyte-like cells localized in the underlying submucosa.

5. AF in the Pituitary Gland

Immunohistochemical staining of sections from pig pituitary gland demonstrated AF-positive cells in the adenohypophysis, but no stained cells were seen in the pars intermedia or in the neurohypophysis. *In situ* hybridization showed that expression of AF mRNA in endocrine cells was strictly localized to the adeno part of the pituitary gland. These results confirm earlier observations of immunolabeling in sections of human pituitary tissue (Johansson *et al.,* 1995) and confirm that synthesis and storage of AF takes place in the very same cells, as occurs with several other pituitary hormones.

6. AF in the Central Nervous System

For practical reasons, rat and mouse were used for immunohistochemical AF mapping of the central nervous system. Preliminary data indicate that neurons in the central nervous system of rodents express AF at varying levels (Fig. 2). The most distinct and intense staining, however, was localized to the cortex and to the brain stem, where ependymal cells also were stained.

7. Cellular AF Distribution within Tissues: Concluding Remarks

In all tissues examined using immunohistochemistry, high AF expression is restricted to a specific and well defined cell population within the tissue investigated. Such cell types include certain types of epithelia, subgroups of leukocytes, certain endocrine cells, and neurons. All of these cell populations possess the capability to both synthesize and store AF. The function of AF in these cell types is not known. However, the anatomical localization of AF-expressing cells in mucous
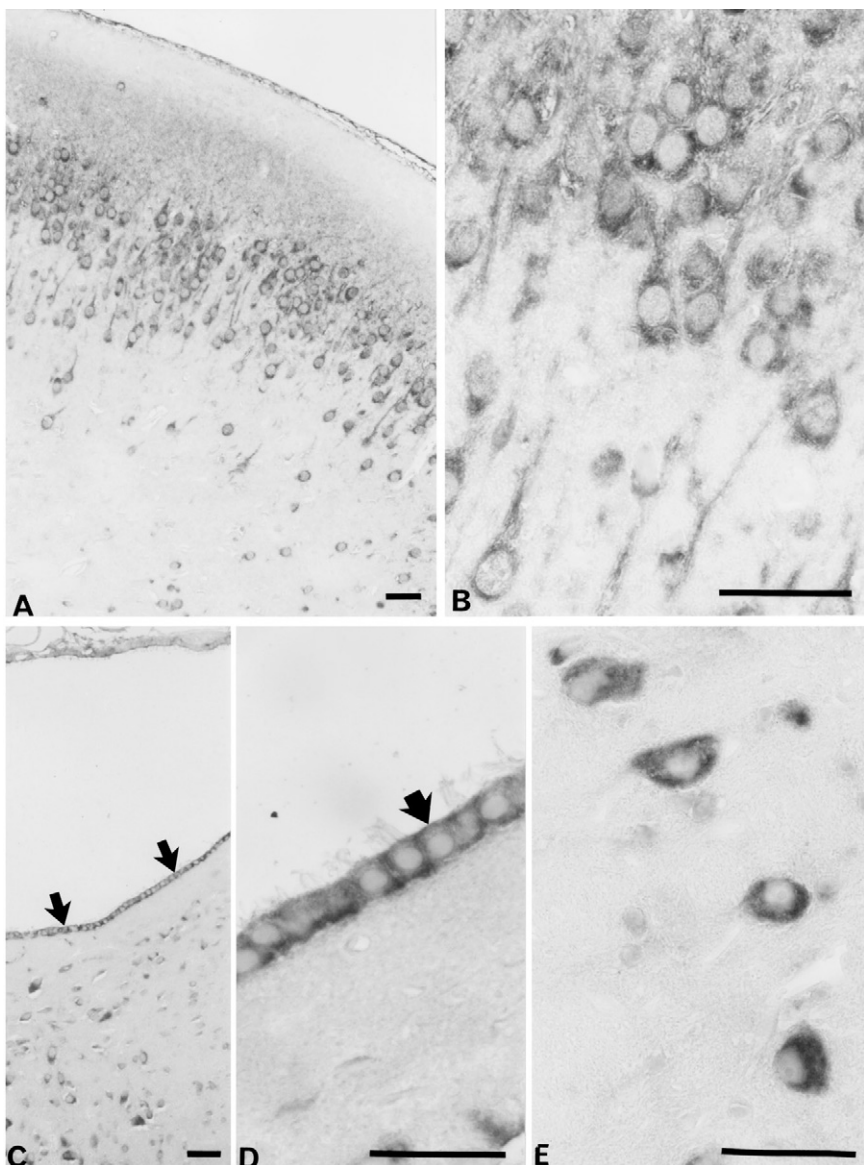
FIG. 2   Sections from rat brain processed to demonstrate AF-immunoreactivity. Alkaline phosphatase-conjugated secondary antibodies were used. Positive reactions appear dark. The sections are not counterstained. Bars, 50 μm. (A) Cortex showing intense staining in most neurons. (B) Larger magnification of A showing cytoplasmic staining of neurons. (C) Section from the brain stem showing staining of the ependymal cells making up the lining of the fourth ventricle (arrows) and of neurons. (D) Larger magnification of C. Cytoplasmic staining of the ependymal cells is seen, but cilia are not stained. (E) Section from medulla oblongata showing AF-positive neurons.

membranes is compatible with the postulated role of AF as a direct or indirect regulator of transport processes across cell membranes. This regulatory effect of AF is probably achieved by counteracting the pathophysiological imbalance in water and ion transport caused by chemical or infectious agents acting on all of the mucous membranes of mammalia.

III. Actions of AF

A. Effects of AF *In Vitro*

1. AF and Isolated Deiters' Membrane

We have demonstrated that AF inhibited small intestine pathological secretion of various etiologies *in vivo*. Our theory was that AF achieved its effect by influencing the reactivity of the intestinal neurons. It was therefore of interest to investigate the influence of AF on the passage of gamma-amino-butyric acid ([^{3}H]GABA) or ^{36}Cl$^-$ across isolated neuronal membranes of Deiters' cells (Hydén and Cupello, 1987). These *in vitro* experiments were possible to perform only after AF had been purified. The ability to manipulate isolated neuronal membrane *in vitro* provides mechanistic biological tools necessary for construction of experiments to elucidate detailed cellular effects of AF. These initial experiments have been verified by ongoing studies that confirm a specific direct and indirect action of AF, and peptide derivatives of AF, on the transport capabilities of membranes *in vitro* (Professor Aroldo Cupello, pers. commun.).

The techniques for Deiters' cell membrane isolation and for mounting the membrane between two small transport chambers have been developed and refined since the beginning of the 1960s at our university (Hydén and Cupello, 1987). The giant Deiters' cells, which are easily detected macroscopically, are located in the hindbrain as one of the four vestibular nuclei in the region of the sensory cranial nerves. These cells are among the largest of the central neurons; the volume of the cell body averages 90,400 μm^3. The size of these neurons in combination with the anatomical localization ensure the reproducibility of the membrane preparation as well as the performance of the general test procedure.

Functionally, Deiters' cells can be regarded as an integrative information center; their nerve endings terminate mainly in the four vestibular nuclei and in the cerebellum. GABA was chosen as a model substance for neuronal transport, because GABA is the main inhibitory neurotransmitter in mammalian brain (Enna and Gallager, 1983), and is consequently used as a model substance for neuronal transport. The postsynaptic action of GABA involves receptor complexes, i.e.,

the $GABA_A$ receptor, which upon interaction with the neurotransmitter activates a Cl^- channel. This, in turn, increases permeability of Cl^- ions across the plasma membrane of the target cell at the postsynaptic level.

2. AF versus [³H]GABA and ³⁶Cl⁻ Transport across Isolated Deiters' Membrane

The initial experiments demonstrated that AF inhibited [³H]GABA diffusion through the isolated membranes of Deiter's cells in a dose dependent fashion (Lange *et al.,* 1985). Furthermore, 10^{-13} M of AF was found to suppress the $^{36}Cl^-$ permeation across the Deiters' membrane, and this suppressive effect was further enhanced by the addition of 0.2 mM GABA (Lange *et al.,* 1987b).

Neutralization of AF by means of specific anti-AF immunoglobulins totally abolishes this inhibitory effect of AF. Preincubation of the Deiters' cell membranes with 10^{-6} M nipecotic acid or 10^{-3} M bicuculline abolished the AF effect, while preincubation with 10^{-4} M picrotoxin had no effect. These results consistently demonstrate that AF influences Cl^- transport via the $GABA_A$ receptor complex. Preincubation of the neuronal membrane with picrotoxin inhibited the $^{36}Cl^-$ permeation, and a subsequent incubation with AF further suppressed the already inhibited $^{36}Cl^-$ permeation. Probably, AF does not act via blockage of the very same Cl^- channels as those already affected by picrotoxin.

The interaction between AF/GABA/Cl^- might reflect a multiphasic AF action, which suggests that: (1) AF inhibits $^{36}Cl^-$ permeation via blockage of [³H]GABA transport, but this blockage includes only the GABA-regulated Cl^- channels (the rest of the Cl^- channels probably remain open), and (2) even in the absence of GABA, AF was found to inhibit $^{36}Cl^-$ passage (this suggests a direct effect of AF on Cl^- channels not under GABA control).

GABA acts as the main inhibitory neurotransmitter in the mammalian brain (Enna and Gallager, 1983) and in the enteric nervous system (Jessen, 1981). The regulatory action of AF on intestinal water and ion transport might be exerted via control of the permeability of enteric Cl^- channels, including those regulated by GABA. The results also suggest that AF is approximately 10^3 times more potent an inhibitor of GABA transport than met 5-enkephalin, the hitherto most potent inhibitor of GABA membrane permeation *in vitro*.

3. AF and Directed ³⁶Cl⁻ Transport

Further studies have demonstrated that the influence of AF on Cl^- passage was restricted to the out $\rightarrow$ in direction and that AF added to the chamber facing the inner side of the Deiters' membrane had no effect on $^{36}Cl^-$ permeability (Rapallino *et al.,* 1989). In fact, these results demonstrated that GABA, applied to the cytoplasmic side of the membrane, opens Cl^- channels, which is immediately followed by blocking by the AF molecule. The most probable explanation for this

effect is an electrostatic interaction between negative charges on these molecules vs the positive sites at the channel cytoplasmic mouth.

4. AF and Membrane Transport in General

The regulatory effect of AF on transport processes across Deiters' membranes is of interest because this system may extend to other forms of biological membranes. Thus, the influence of AF *in vivo* or *in vitro* on transport processes mediated across such membranes as the plexus choroideus of the brain and eye, membrana tympani of the inner ear, the nasal and lung mucosa membranes, and the epithelial lining of the salivary gland is of high priority for further studies.

B. Physiological Action of AF

1. General Effects of AF on the Small Intestine Secretory Process *In Vivo*

AF administered intravenously to rat at a dose of 10^{-12} mol inhibited CT-induced secretion (Lönnroth and Lange, 1986), whereas in the pig 10^{-11} mol of AF was found to reverse fluid secretion induced by CT or by the heat-labile toxin from *E. coli, E. coli* LT (Lange *et al.,* 1987a). Furthermore, AF has also been shown to inhibit fluid secretion induced by *C. difficile* toxin A (Torres *et al.,* 1991). The administration route for AF into the test animal has most frequently been injections via the penis or tongue vein, but the antisecretory effects of AF are also observed after intraintestinal injections in the upper part of the small intestine and after intranasal instillation. Using recombinant AF, the inhibitory effect on the secretory response has been demonstrated by injection of the protein both before and after toxin challenge into the loop. Surprisingly, AF emanating from the pituitary has been found effective for hypersecretion inhibition only when administered before toxin challenge. The reason for this discrepant action of AF obtained from different sources is unclear.

The most significant effects of AF on the secretory process were achieved when AF was administered close to the time of toxin challenge, suggesting a very rapid biological turnover rate of AF. In case of the overall effects mediated on the small intestinal mucosal architecture after challenge with okadaic acid (the toxin produced by blue mussels, a very potent phosphatase inhibitor), intravenously injected AF did not affect the rapid and exclusive epithelial losses from the villi; AF administration was found to selectively inhibit only the hypersecretion process initiated by this toxin (Lange *et al.,* 1990). Furthermore, it was demonstrated that repetitive, peroral CT treatment was followed by increased pituitary AF activity, which could also be effectively induced by repetitive, intranasal CT instillations.

A summary of these results suggests the following: (1) AF prepared from the pig pituitary source must be injected prior to toxin challenge to inhibit

enterotoxin-induced secretion, whereas recombinant AF can be injected either before or after intestinal toxin challenge and still remain effective in its inhibitory capacity. (2) The biological half-life of AF in rat is very short. No influence on the intestinal secretory process can be demonstrated 30 min after intravenous injection of AF. (3) Increase of endogenous AF activity is achieved in response to contact between CT and the intestinal or lung mucosal surface.

The *in vivo* inhibitory effect of AF in rats has been documented by others (Tateishi *et al.,* 1999), although with a discrepancy in AF bioactivity that cannot be explained by the data presented in their article. The use of recombinant His-tagged AF in a dose of $2.0-20$ μg in anesthetized rats of unknown strain makes it difficult to compare with our results. Skadhauge and coworkers (Gröndahl *et al.,* 2000; Hansen and Skadhauge, 1995), however, report the same inhibitory effect of AF given intravenously to rats as that reported earlier by us (Lönnroth *et al.,* 1988b).

Cholera toxin and toxin A from *C. difficile* have both been shown to mediate their effects via the enteric nervous system (Castagliuolo *et al.,* 1994; Goyal and Hirano, 1996). Cholera toxin activates the secretomotor reflexes via: (1) VIP-containing neurons (Jodal *et al.,* 1993), (2) motor neurons causing giant peristaltic contractions (Fan *et al.,* 1999), (3) interneurons (Nocerino *et al.,* 1995), and (4) direct action on secretomotor neurons to distal sites (Nocerino *et al.,* 1995).

Toxin A causes mast cell degranulation and secretion of multiple inflammatory mediators including prostaglandin, histamine, and serotonin (Castagliuolo *et al.,* 1994). These reactions probably trigger secretomotor reflexes and submucosal vasodilatation (Kurose *et al.,* 1994). Okadaic acid, which is the third enterotoxin inhibited by AF, causes nausea, vomiting and diarrhea, which suggests a neurogenic component in its action (Yasumoto *et al.,* 1985). The evidence for AF action by interference with the enteric nervous system includes the following: (1) AF is the hitherto most potent regulator of [^{3}H]GABA and ^{36}Cl$^-$ transport across isolated neuronal membranes of Deiters' cells (Lange *et al.,* 1985, 1987b; Rapallino *et al.,* 1989). (2) Vagotomy abolishes the antisecretory effect of AF (Lönnroth *et al.,* 1988b). (3) AF-positive neuronal cell bodies have been clearly demonstrated by immunohistochemistry in submucosal lymphoid cells in the gastrointestinal tract as well as in the central nervous system (Lange *et al.,* 1999).

It is therefore likely that AF exerts its antisecretory effects on enterotoxic secretion by influencing the activity of the nervous system, probably the interneurons or the secretomotor complex of the enteric nervous system.

2. AF and Intestinal Inflammation

Clostridium difficile is the most frequently identified pathogen in patients with antibiotic-associated diarrhea and colitis (Bartlett, 1994). This bacterium does not penetrate the intestinal epithelium and its pathogenicity has been ascribed to two similar enterotoxins designated toxin A and toxin B. Toxin A causes fluid

secretion, inflammation, and mucosal damage in experimental animals (Lyerly *et al.,* 1985; Torres *et al.,* 1990) and is probably the main cause of pseudomembranous colitis in man. Experiments in rats indicate that intestinal challenge with toxin A stimulates increased AF synthesis (Torres *et al.,* 1991). Furthermore, synthesis of AF was stimulated in patients suffering from acute colitis (Torres *et al.,* 1993). The effect of AF on toxin-induced inflammation and fluid secretion could be evaluated more accurately by use of recombinant AF (Johansson *et al.,* 1997b). Picomolar amounts of AF were sufficient to inhibit intestinal mucosal destruction as well as secretion caused by toxin A in rat small intestine (Johansson *et al.,* 1997a). AF potency was similar when measured after intravenous and intraluminar administration, and the protective effect of AF was equivalent when administered prior to or after the intestinal toxin challenge. Histological examination revealed that AF abolished the inflammation and bleeding in the small intestinal submucosa.

The intestinal anergy to the secretory and cytolytic action of *C. difficile* toxin A challenge might be explained by a form of desensitization of the small intestinal nervous system, probably mediated by the release of substance P from submucosal enteric mast cells. The enteric mast cells vesicular release is followed by a profound increase of chemical mediators into the intestinal tissue, stimulating the secretomotor neurons, followed by frequent intestinal peristaltic contractions and inflammatory reactions (Kelly and LaMont, 1998; Goyal and Hirano, 1996).

In order to investigate the correlation between AF and the process that makes the small intestine nonresponsive to inflammatory damage of various etiologies, we pretreated rats up to five times perorally with cholera toxin or with a solution of 5.5% sorbitol, followed by challenge with *C. difficile* toxin A in small intestinal ligated loops. Secretory and morphological observation of the loops after such challenge clearly demonstrated that this repetitive gastrointestinal treatment made the rat small intestine resistant to the hypersecretion, inflammation, and necrosis normally induced by *C. difficile* toxin A challenge (Lönnroth *et al.,* unpublished). Sorbitol triggers osmosensitive receptors in the enteric epithelium via vagal nerve fibers (Mei, 1978; Mei and Garnier, 1986). However, sorbitol, like the enterotoxins, might trigger secretomotor reflexes and cause diarrhea. The subsequent induction of AF after repetitive sorbitol treatment might depend on desensitized neuronal activity in the enteric nervous system (see above).

The *in vitro* impact of AF on neuronal tissue and neuronal reactivity suggests that AF plays an important role in regulating neuronal reactivity *in vivo*. Intestinal AF is synthesized and stored in the small intestinal epithelial cells, as well as in submucosal cells, probably belonging to the T-lymphocyte class (Lange *et al.,* 1999). Conclusively, the increased AF production in response to repetitive cholera toxin or sorbitol peroral treatments, respectively, might be directly or indirectly mediated via influences from the enteric nerves on these cells. Such a stimulatory signal might be mediated by VIP released from cholera toxin-activated secretomotor neurons (Jodal *et al.,* 1993). VIP also functions as a regulator of lymphocyte migration

in mesenteric lymph nodes and might in this way regulate the submucosal density of specific cells (Staniz *et al.,* 1986) and the localization of AF-positive cells.

3. AF and Intestinal Capillary Permeability

The influence of AF on epithelial *in vivo* transport may also include the effects of AF exerted on the epithelial cells of small intestinal capillaries situated in the intestinal submucosal tissue. Experiments were performed by CT challenge of the rat jejunal ligated loop, immediately followed by intravenous injection of the dye Evans blue. Subsequent microscopic examination of the localization of Evans blue within the intestinal tissue demonstrated that CT induced an increased transcapillary permeation of the dye in a heterogeneous fashion in the intestinal mucosa (Lange *et al.,* 1998). Extravasation of the dye was prominent in the top of the villi, while the crypts were spared. AF purified from pig plasma, as well as recombinant AF, were both capable of inhibiting the CT-induced alteration of transcapillary permeation. AF did not influence the recovery or the ability to detect extravasated Evans blue dye maker after luminal challenge with the buffer vehicle alone, i.e., during normophysiological intestinal mucosal transport procedures. This finding suggests that neither form of AF interferes with the physiological transport processes in the gut under normal conditions. The Evans blue dye method (LeVeen and Fishman, 1947), however, allows conclusions only about the CT effect on the transcapillary albumin flux (due to the binding between Evans blue and albumin), and the subsequent intestinal restitution after the intravenous administration of AF. Conclusively, any relationship between AF and CT and their effects on the mucosal microvasculature concerning water and ion transport/secretion remains to be investigated.

We have also observed a very significant *in vivo* effect of AF in rat brain. Thus, in the plexus choroideus of the brain fourth ventricle, we observed that the permeation of the dye Evans blue increased in response to challenge with CT. This increase of the dye permeation was significantly inhibited by an intravenous injection of AF prior to CT challenge. These results also suggest a general regulatory effect of AF on capillary permeation, irrespective of tissue localization.

4. AF Activity in Patients Suffering from Diarrhea: Studies in Mexico and Pakistan

The AF-activity in blood drawn from Mexican patients suffering from diarrhea ($N = 20$) and their matched controls ($N = 18$) were compared (Torres *et al.,* 1993). A significant increase in the AF level was noted between days 1 and 3 after the onset of diarrhea. The highest increase was noted in a patient suffering from *Giardia lamblia*. At day 9 the activity decreased to that found at day 1. Thus, the AF value peaked some days after the onset of the diarrhea, the peak coinciding with the time when the diarrhea decreased. The matched controls had an AF level

that was significantly higher than that day 1 in the patients. On the contrary, the activity in patients day 9 was significantly higher than that in the controls. Eight of the 18 healthy controls were infected with enteropatogenic microorganisms. The levels of circulating AF were equally low in subjects colonized or not colonized with enteropathogens. This finding suggest that the mere presence of pathogenic microorganisms in the gut is not enough to induce an increase in the AF concentration. Thus, it might be the intestinal secretion, rather than the mere presence of the pathogen, that triggers the AF production.

We recently demonstrated that AF is present in human milk as well. Relativly higher levels was found in milk from women in Pakistan than in milk from Swedish women (Hanson *et al.,* 2000). Presumably, mothers in poor countries have more frequently diarrhea due to enteric pathogens in the environment. The presence of AF in the milk may well protect their children from diarrhea.

IV. Studies on AF in Animals

A. Animal Models: The Ligated Loop Used as Bioassay

1. General Performance Requirements for the Study

Work performed in order to develop reproducible animal models for evaluation of experimental diarrhea was a prerequisite for determination of the *in vivo* clinical effects of AF in relation to health and disease in man and animal. The secretory response in the ligated jejunal loop served as the standardized bioassay for the determination of antisecretory potency in the tested AF preparations. Mice and rats are both usually susceptible to a variety of toxin challenges, these experimental animals are genetically defined, and are commercially available worldwide. Mice can also be genetically manipulated by the so-called "knockout" technique, which allows almost unlimited and specific modification of biological processes. However, mice made deficient in the AF gene (Kawahara *et al.,* 2000; in this article designated Rpn10) do not survive. These genetic deletions are embryonic lethal, suggesting an essential role for the *AF* gene in mouse development. The lethal effect of genetic AF knockout might also be true for other mammals because of the conserved structure of AF, and the frequent presence on various chromosomes of the AF gene from a phylogenetic point of view.

2. Animal Model, Historical Background, and Specific Requirements for the Present Study

The use of an *in vivo* secretion model was considered to be most important in continuously following the multitude of biochemical preparative procedures

necessary to achieve the pure form of AF. The defined hypersecretion in these animals was obtained after intraluminal challenge of graded doses of enterotoxins into one (mice and rats) or several (pigs) preparations of jejunal ligated loops. The selection of an *in vivo* secretion model, based on various rodent strains and pigs, with enterotoxins as the causative secretagogue, was chosen for several reasons. First, most biochemical and physiological studies focused on intestinal secretion have been carried out *in vitro,* ignoring the risk that such results might differ significantly from the biological conditions present *in vivo* (Diamond, 1995). The problems of performing relevant physiological studies of intestinal transport have, however, long been a subject of debate among scientists. Historically, the first experiment on epithelial transport employing modern biological analytical techniques dates from Munroe (1738), who described the "everted sac technique." This technique was further refined by several physiologists, as best described by Reid (1901) and Wilson and Wiseman (1954). Transport of water and ions across the vertical frog epithelium was also first described by Reid (1890), using the rabbit ileum as the discriminative, experimental tissue. All of these experimental techniques were again considered by Ussing and Zerahn (1951), who used the vertical frog epithelium as experimental tissue for studying transport, although the same investigators also used the guinea pig cecum for transport experiments (Ussing and Andersen, 1956). Another experimental design was presented by Lundgren (1984), where kinetics of the secretory response to enterotoxin challenge is studied in small intestinal ligated loops in anesthetized cats and rats (Cassuto *et al.,* 1982). The first experiments demonstrating CT-induced hypersecretion in ligated loops of conscious rabbits were performed in the mid 1950s (De and Chatterje, 1954; Dutta and Habbu, 1955). Cholera toxin has since been demonstrated to induce experimental diarrhea when injected intestinally in several animal species, including dogs (Sack and Carpenter, 1969), hamsters (Basu and Pickett, 1969), chinchillas (Blackman *et al.,* 1974), rats (Aziz *et al.,* 1968), and mice (Fujita and Finkelstein, 1972).

Since it has been demonstrated that all forms of anesthetic agents profoundly influence the secretory response to most forms of secretagogues (including all known forms of enterotoxins), the anaesthetic effects of anesthetics represent a serious obstacle to the use of all such methods (Lönnroth *et al.,* 1980; Lönnroth and Munck, 1980; Lönnroth and Jennische, 1982; Larsen, 1982; Uhing and Kimura, 1995). Furthermore, anesthetized animals also require accurately designed intravenous substitution in order to avoid metabolic acidosis as well as other forms of metabolic derangements depending on the length of the experimental time schedule. These facts indicate that the most reliable and easy-to-use model for studies of the *in vivo* secretory response to enterotoxin challenge is determination of the small intestinal secretory response to graded doses of toxin in conscious animals. Consequently, the ligated loop assay in conscious rats and pigs was used in our studies (Lange, 1982; Lange *et al.,* 1987a).

3. Animal Models and Intestinal Secretion: General Remarks

We elaborated and standardized an *in vivo* intestinal secretion model in conscious, nonanesthetized animals with the primary aim of using intestinal secretion in response to enterotoxin challenge as the bioassay in order to obtain the pure form of AF. This model was also elaborated in order to present suitable conditions for experimental studies of diarrheal diseases in general, with results that could rapidly be advanced to clinical tests with relevance to human and veterinary medicine.

B. Food Components Increasing Endogenous AF Synthesis

1. AF-Inducing Food

Intragastric injections with hyperosmolar solutions of D-mannose (0.91 Osm/kg), D-sorbitol (0.90 Osm/kg), L-alanine (1.52 Osm/kg), or L-glycine (1.75 Osm/kg) into rats were followed by a significant small intestinal hypersecretion. The secretion volume obtained following these injections was similar to the results achieved after 100 μg of CT challenge into nonligated small intestine. This osmotic hypersecretion induced increased pituitary AF synthesis without influencing the net weight of the pituitary (10.5 ± 0.1 mg per gland) or the concentrations of the extracted proteins (1.36 ± 0.11 mg per ml). All of the animals responding with increased pituitary AF synthesis to this intragastric challenge also displayed inhibited intestinal secretion to subsequent CT challenge. Chemical and immunological analyses of the AF protein produced in response to intestinal stimulation induced by sugars and amino acids demonstrated similarities and differences compared to AF isolated in response to intragastric CT challenge. The methods and measurements used to evaluate these differences included the isoelectric point, neutralization by specific antiserum (raised against CT-induced AF), determination of the molecular size (K_{av}), and the concentration of methyl-α-D-glucoside needed to release AF from an agarose gel. A retrospective evaluation of these results suggests that these differences in AF characteristics must be evaluated by several of the more refined chemical techniques presently used.

Experiments performed in rats and pigs suggested that the intake of certain carbohydrates and amino acids increased AF levels while simultaneously decreasing the incidence of diarrheal disease. These results encouraged further investigations concerning the influence of AF-inducing food in healthy volunteers. A positive result was noted when increased AF activity occurred in adult volunteers receiving a mixture of amino acids and carbohydrates. The routine clinical parameters, however, remained unaffected when analyzed along with the repetitive determinations of plasma AF activity. A second human study was then started in order to determine if an increase in AF activity could be achieved in response to intake of hydrothermally processed cereals (HPCs). The hydrothermally processed cereals were preferred over the previous use of sugars and amino acids, since a defined

hydrothermal treatment releases free sugars and amino acids to a desired concentration. The intake of HPC in healthy volunteers convincingly yielded an increase in endogenous plasma AF activity. This increased response in AF activity was found to be even more significant than the response to the carbohydrate/amino acid mixture previously tested. The biological mechanism behind this potent AF-inducing capacity of HPC-based food remains to be investigated. The most significant increase of AF activity occurred when HPC was administered three to four times daily in a dose of about 1 g per kg body weight. During the first HPC intake period, increased AF activity occurred after a period of 12–25 days of cereal eating. When increased plasma AF activity had been achieved and verified by at least three plasma analyses, HPC intake could be lowered to about 0.5 g per kg body weight without interfering with the stimulation of AF activity. When cereal intake was administered again after 10–20 days without HPC, increased AF activity was achieved after only 2–4 days of cereal intake. In conclusion, there exists some sort of "biological memory" for the human capacity to synthesize AF, and the first period of cereal intake seems to be responsible for "priming" the secondary, enhanced AF response.

2. Effect of AF-Inducing Food on Patients with Inflammatory Bowel Diseases (IBD)

Since the results on healthy subjects demonstrated the ability of HPC to induce increased AF activity without any side effects, the influence of HPC in diseased patients was investigated. A clinical trial was made with a group of patients suffering from chronic inflammatory bowel disease (IBD). The two most severe forms of this disease were included, namely *ulcerative colitis* and *Crohn's disease*. The main reason for the selection of this specific patient group was the severe impact of IBD registered in medical statistics in the entire industrialized world. In Europe, epidemiologic investigations performed during the past decades clearly demonstrate a continuous and ongoing increase in the number of patients diagnosed with IBD. This increase in IBD incidence has also occurred in Japan, where the number of IBD diagnoses has doubled during the past 10 years (Professor Leif Hultén pers. commun.). The etiological reason for the IBD increase in Western society is unclear (Hugot *et al.,* 1999; Sartor, 1995). Several hypotheses have been put forward, but none has provided a sufficient amount of relevant clinical data to be accepted by medical authorities. In Sweden, the prevalence of IBD is close to 1% in the population born in 1950 or later (Shivananda *et al.,* 1996). The nature of IBD is chronic and the onset of the disease often occurs early in life. Patients suffering from IBD require long-term medical surveillance in order to provide acceptable and relevant treatment for increasing the quality of life (Irvine *et al.,* 1996; Podolsky, 1995; Rabbett, 1996). The etiology behind the cyclic performance of the disease as well as of the intestinal tissue derangement leading to inflammation and/or diarrhea is unknown, but the colonic mucosal inflammation

disrupts both absorption and transit of fecal material (Sartor, 1995). The influence on bowel function in severe chronic cases often differs between total disease or distal disease of the colonic tissue. Despite intense research over the past three decades, it is commonly accepted that a definitive treatment for IBD (*ad intigum*) can seldom be achieved with the medications and surgical procedures currently available (Turnbull and Vallis, 1995). The need for additional treatment options in those patients is obvious.

A double blind study was constructed in order to evaluate the possible clinical effects of HPC on the outcome of the various forms of IBD disease (Björck *et al.,* 2000). Patients were randomized into an experimental group, receiving HPC diet, and into a control group, receiving conventionally processed cereals. Both active and placebo food had the same general nutritional value. All patients participating in the study had clinical conditions making outpatient treatment possible, and altogether 50 patients fulfilled the study period. All medication was kept unchanged during the diet period.

Plasma AF activity was not different between the two patient groups at the start of the experiment (day 0). After the 4-week diet period, AF activity in the HPC group was markedly increased and there was a significant difference between the HPC group and placebo group ($P < 0.001$). Plasma AF activity declined slowly after termination of HPC intake, but a significant ($P < 0.001$) difference between the active and placebo groups still persisted 4 weeks after termination of the HPC diet, i.e., 8 weeks after the start of the test. This slow kinetic decrease in the human AF response after ending HPC diet intake supports previous results obtained with the HPC diet in healthy man as well as the kinetics in AF responses of various etiology in pigs and rats (Lönnroth *et al.,* 1988b; Göransson *et al.,* 1995).

Clinical effects were evaluated as the patients' own registrations plotted together with the responsible clinician on a VAS scale. The registered increase in plasma AF activity correlated well with the patients' subjective assessment of clinical improvements in relation to HPC intake ($P < 0.05$ vs placebo diet). A similar response to the diet was observed in patients suffering from total and distal ulcerative colitis. Two patients with Crohn's disease were randomized to the active HPC diet, and both responded with significant improvements (VAS +100% and VAS +50%, respectively). This favorable response to HPC in patients suffering from Crohn's disease has been confirmed in our ongoing, clinical studies. The clinical significance of the HPC diet on Crohn's disease remains unclear. A more focused detailed study of patients suffering from this disease will hopefully begin in Spring 2001 and provide more specific information.

Routine blood analyses of both patient groups did not demonstrate any significant variation between the measured parameters during the time course of the experiments. No effects on blood lipids were observed with either diet. Rectal biopsies were taken in each patient before and after the diet period, and AF immunoreactivity was found in the epithelial lining of the intestine and in mononuclear cells in the lamina propria of all patients. This anatomical distribution of AF-positive

cells is in accordance both with the results from previous immunohistochemical studies performed in different experimental animals (Lange *et al.,* 1999) and also with the preliminary results from ongoing studies in man. There were no statistically significant changes in the AF staining pattern in biopsies obtained within the 4-week experimental interval in any patient group. A longer observation period may be required to verify histopathological improvements in the colonic mucosa in patients suffering from IBD.

3. AF in Patients with Chronic Diarrhea Due to Intestinal Resection

A group of patients with chronic diarrhea after intestinal resection was selected because they usually have an impairment of bowel function that is relatively stable over time. This intestinal stability makes it easier to assess the significance of an increase or decrease in intestinal output, and tests can be conducted without hospitalization of the patient. Furthermore, in this chronic stable situation, bowel function is unlikely to be affected or the mucosal tissue damaged by an inflammatory response.

Six patients were asked to participate in the study: three females and three males (47 ± 9 years old). All patients had long-standing diarrhea after extensive intestinal resection and attended an outpatient clinic. The patients' main clinical problems were related to high losses of intestinal secretion. At the time of the study, the patients were in a stable condition, without signs of active intestinal inflammation. Detailed clinical information and registrations of the patients, including their intestinal status, were available.

The patients were subjected to intake of 54 g of HPC daily during a 14-day test period. Intestinal output was measured during three periods: for 1 week just before treatment, during the 2 weeks of treatment, and for 1 week 4 weeks after the treatment with the HPC diet. AF activity was monitored continuously and was found to be insignificant in all of the patients before the test period. Thus, after intestinal resection, diarrhea per se does not seem to elicit an AF response, which is in contrast to diarrheal diseases of toxic etiology. Toxic peroral challenge in experimental models, as well as verified bacterial enterotoxin infections in man or animal, induce an AF response that may by itself contribute to the self-limiting nature of the disease (Göransson *et al.,* 1995; Torres *et al.,* 1993).

The AF plasma activity remained unaffected after HPC intake in all but two of the subjects. In these two patients responding with an increased AF activity after the HPC intake, however, a significant reduction of diarrheal secretion was registered. In the remaining four patients with constant insignificant plasma AF activity, no change in diarrhea was observed. Both patients with stimulated AF response had remaining small intestines that were about 300 cm longer than those of the other four patients. Thus, the length of the small bowel appears to be related to the ability

of humans to induce AF activity by dietary means. However, which part of the small intestine is the most important source for AF synthesis or regulation is unknown.

If the reduced length of the small bowel prevents patients from responding with increased AF synthesis to the HPC-diet, peroral administration of AF or its peptide derivatives should be considered.

C. AF-Inducing Animal Feed/Electrolyte Solutions versus Epidemic Diseases in Modern Farming

1. Feed Additives and Their Ecological Consequences: General Background

Fatal epidemic diseases caused by bacterial agents are real and continuous threats to modern farming. During the past four decades this highly competitive branch of agriculture has developed into a highly industrialized competitive production process, especially for meat-producing animals such as pigs, chickens, and cattle. The spread of various contagious epidemic infectious diseases in such biological production units is a very rapid process due to the close contact between animals. The interaction between the etiological mechanisms and the verified and mapped pandemic epidemic spread of such infectious diseases has been demonstrated to be multifactorial in nature. Consequently, in the preventive intervening work of infection prophylaxis, many different attempts have been made to overcome the various kinds of health problems affecting the general performance of animals. However, no single form of treatment, or combination of treatments, has proven to be "the gold standard" that is effective in preventing the variety of serious infectious diseases that threaten livestock. The lack of useful methods to inhibit or reduce incidence of infectious diseases has most often resulted in an increased use of antibiotics, coccidiostatics, and antihelminthics. However, most animals can only partly, or in some instances not at all, degrade the various antibiotic substances during their intestinal passage. This means that biologically active compounds are spread into the environment via urine and feces without any form of control or registration. The impact on the global ecological balance of these substances is of enormous and long-lasting importance. In the case of the nondegradable quinolones, commonly used as feed additives and excreted in quantities of thousands of tons, the present biological methods used do not offer any convenient method for calculating the multitude of ecological effects induced by the steadily increasing quinolone concentrations in the fauna (Endtz *et al.,* 1991, Hektoen *et al.,* 1995). Furthermore, metals are added in concentrations far higher than the nutritional requirements as prophylactics against postweaning diarrhea (Zn) or as growth promoters (Cu) in pigs. Zinc and copper are nondegradable during intestinal passage, and are consequently added to the fauna in a steadily increasing concentration. Nitrogen and phosphorus, also present in animal urine and feces,

both influence in various ways the surrounding fauna with a severe impact. The final outcome of the above facts, combined with the general, biological nature of this global and most complex problem, offered no other solution than a complete and total ban of antibiotics as a general additive in animal feed.

2. AF and Disease Prevention in Animal Farming

On January 1, 1986, the Swedish government outlawed the general addition of antibiotics to animal feed. The veterinary impact of this law was an increased incidence of diarrheal diseases among weaning piglets. Because of the increase in diarrhea, we were contacted in January 1986 by the Swedish farmers cooperative feed industry (SLR) who wanted research assistance to develop postweaning feeds for pigs, that were free from antibiotic additives. The research to be performed was not only focused on the problems caused by the prohibited use of antibiotic additives, but also on the claims that the developed feed should be economically and ecologically competitive when used practically in modern, industrialized pig production. Cooperative research was initiated between our group, The Swedish University of Agriculture in Uppsala, and The Research Unit of Lantmännens Foderutveckling AB at Svalöv. It was soon demonstrated that addition of specific sugars and amino acids capable of rat AF stimulation was also capable of stimulating pig AF. The concentrations of the amino acids and sugars were low, and not capable of inducing clinical or subclinical diarrhea. Pigs fed such a supplemented diet, or an electrolyte water solution supplemented with these specific sugars and amino acids, invariably demonstrated a significant increase of plasma AF activity. The stimulated increase of endogenous AF synthesis was significantly correlated to a reduction in the incidence of postweaning diarrhea, as well as to an increased daily weight gain (Göransson *et al.,* 1993). These results from the pig field experiments have been transferred and adopted to the breeding and production of cattle and chickens. The concept of adding sugars and amino acids in feed and also using electrolyte solutions can be extended for the commercial industrial development of feeds for the specific needs of horses, dogs, and cats.

The optimal pig feed composition was finally achieved by addition of sugars and amino acids within the limits usable for increasing the endogenous production of AF. The results of the piglets in the first field trials concerning diarrheal disease incidence are demonstrated in Table III.

The clinical effect of the AF-inducing diet is shown in Table III, and similar results have been obtained in numerous field trials performed thereafter. These results clearly show that high plasma AF activity in the postweaning period is correlated with reduced incidence of postweaning diarrhea and, subsequently, with an optimal increase in daily weight gain (Göransson *et al.,* 1995).

Experimentally induced stress, or increased corticoid plasma concentrations in response to ACTH injections, have proven to rapidly decrease plasma and

TABLE III

The Influence of an AF-Inducing Pig Weaning Diet, Based on the Concept of Adding Sugars and Amino Acids to a Low-Protein Diet

Group[a]	DWG[b]	AF units[c]	PWD[d]
C	251	0.52	41
AF	317*	0.94*	12*

Note: The daily weight gain, AF units in plasma, and frequency of postweaning diarrhea are shown (Göransson *et al.,* 1993).

[a]C, control groups given ordinary creep feed. AF, AF inducing diet.

[b]DWG, daily weight gain 0–35 days after weaning; total number of pigs = 891, located at five different farms.

[c]AF units/ml in plasma obtained 4 days after weaning.

[d]PWD, postweaning diarrhea, percentage of piglets with clinically measured diarrhea.

*Significant ($P < 0.05$) difference from control group.

pituitary levels of AF in rats (Lönnroth and Lange, 1988). This relationship between AF activity and blood corticosteroid levels in response to stress has also been observed in piglets. The most severe period of stress for the piglet occurs 1–4 days immediately after weaning, and the weaning period is commonly started around 35 days after partus in most Swedish herds. Consequently, 1–4 days after partus is the most common onset of postweaning diarrheal diseases. Clinical as well as subclinical diarrheal diseases are regularly followed by a decrease in daily weight gain. The onset of the diarrheal disease significantly correlates to low plasma AF activity. However, this decrease of AF activity can usually be inhibited, provided that the piglets consume an AF-inducing diet.

Stimulation of endogenous AF activity can also be achieved in piglets by mixing an appropriate amount of sugars and pure amino acids with what is commonly called an "electrolyte solution" in veterinary medicine, or in human medicine, an "oral rehydrate solution" (ORS). A piglet split litter experiment demonstrated a significant increase in plasma AF activity in response to drinking such an "electrolyte solution" (Table IV). Although no clinical signs of diarrhea were registered in this experiment, the daily weight gain during the first week after weaning in the control group was significantly lower compared to the electrolyte-drinking, AF-stimulated, experimental groups. These findings indicate beneficial effects of increased AF activity on subclinical forms of intestinal disorders.

The low-protein, AF-inducing diet experiments with piglets were verified by other researchers (Bolduan, 1997), demonstrating improved daily weight gain post weaning, which was significantly correlated to a reduced frequency of postweaning diarrhea, achieved by feeding the piglets an AF-inducing diet. The influence of increased endogenous stimulation of AF on the daily weight gain and incidence of diarrheal diseases were also evaluated in calves. Three herds were selected, and

TABLE IV

Feed Induced AF-Blood Concentrations and Production Performance for Piglets Weaned at 32 Days of Age

Group[a]	DWG[b]	AF units[c]
C	92	0.12
AF diet	155*	1.32*
AF drink	162*	1.20*

Note: The AF-stimulating electrolyte drink solution achieved this capacity by addition of sugars and amino acids (Lange and Göransson, 1999).

[a]Control groups given ordinary creep feed. AF diet, AF-inducing diet achieved by addition of sugars and amino acids to ordinary creep feed. AF drink, AF-inducing electrolyte solution. No. of piglets = 28 in each group.

[b]DWG, daily weight gain registered the final week postweaning, i.e., 32–39 days after birth.

[c]AF units/ml in plasma obtained 4 days after weaning.

*Significant ($P < 0.05$) difference from control group.

endogenous AF stimulation was achieved by giving a milk substitute supplemented with sugars and amino acids within the concentration limits previously found optimal for AF stimulation in piglets and rats (Table V).

The results in Table V demonstrate that in herd 1, the daily weight gain is about 70% higher in the AF-stimulated group, while in herd 2 the difference is reduced to 14%. This difference is further reduced to about 8% in herd 3. The most reasonable explanation for these large variations might be related to the different grades of hygiene in the herds. Thus, herd 1 demonstrated the lowest grade of sanitation while herds 2 and 3 displayed a good sanitation standard. This experiment shows that the AF-inducing milk substitute effectively counteracts the clinical as well

TABLE V

The Stimulatory Influence of an AF-Inducing Milk Substitute on Daily Weight Gain in Calves (Lange and Göransson, 1999)

Group[a]	Herd 1[b]	Herd 2[b]	Herd 3[b]
C	321	948	630
AF	548	1076	683

AF, experimental group given AF-inducing milk substitute made by addition of sugars and amino acids.

[a]C, control groups given ordinary milk substitute.

[b]Number of calves was from 9–33 in each group; the values represent daily weight gain per kg live weight relative value.

as the subclinical effects of a poor hygienic standard. This beneficial effect of an AF-stimulating milk substitute is of minor importance in herds with a high sanitation standard. The correlation between poor hygiene and beneficial effects of stimulated AF activity has been verified in all experiments and registrations performed so far. In healthy humans or animals (pigs, chickens, cattle, horses, dogs) living in an environment of optimal hygienic standards, we have so far been unable to detect any effect of the AF-stimulatory feeds or drinks on clinical or laboratory parameters. Thus, acknowledging the risk of oversimplification, the results described in the above experiments suggest that the intake of AF-stimulating food or drink can be used as insurance against the threat of intestinal imbalance causing diarrheal disease or intestinal inflammation. Such an imbalance is most commonly caused by an invasion of pathogenic parasites, bacteria or viruses, continuously and generously supplied by poor sanitation.

In humans as well as in animals (rats, pigs, cows), AF can commonly be detected in the milk (Lange and Lönnroth, 1986; Lönnroth *et al.,* 1988a; Hanson *et al.,* 2000). AF usually occurs in milk in a higher concentration than that found in plasma, suggesting an active transport of AF across the epithelial lining of the mammary gland. In pigs we have also succeeded in demonstrating that AF is transferred from the sow to the developing fetus via the placenta (Sigfridsson *et al.,* 1995). AF is also absorbed from the intestine of the newborn piglet, most probably *in toto* during the first 48 h of life, before the closing of the epithelial intercellular passage. The AF activity in the blood of suckling piglets is positively correlated with the AF level in the sow's milk. The clinical importance of high AF activity in sow's milk is demonstrated by the fact that piglets suckling milk with high AF activity are significantly better protected from neonatal diarrheal disease than piglets suckling milk with a low content of AF activity (Lönnroth *et al.,* 1988a). This finding has also been verified experimentally in rats (Lange and Lönnroth, 1986). The importance of stimulated plasma AF-activity in the piglet weaning period, achieved by an optimized AF-inducing diet or electrolyte drink, has also been observed in fattening calves during the postweaning period (see above). Thus, calves drinking an AF-inducing milk substitute during the first weeks in the fattening period after weaning gained weight significantly better than control animals.

D. Implications of the AF System Based on Experimental and Clinical Findings in Animals

The implications of the AF System are as follows: (1) Endogenous AF synthesis can be stimulated by addition of a proper mix of sugars and amino acids to low-protein creep feed. A diet stimulating endogenous AF synthesis in the piglet is correlated with protection against clinical or subclinical diarrheal diseases in the postweaning period and consequently by an increased daily weight gain. (2) AF

is transferred to the pig fetus via the placenta. AF is present in the colostrum as well as in the milk. AF is absorbed by suckling offspring, and a high level of AF in the milk is correlated with low levels of neonatal diarrheal disease in piglets. (3) A diet stimulating endogenous AF synthesis in the fattening calf is correlated with protection against diarrheal diseases in the postweaning period. Also in the calf, a reduction of intestinal diarrheal diseases is correlated with increased daily weight gain.

Despite our lack of knowledge of the exact mechanisms of action of AF at the cellular level, the experience obtained so far indicates at least two significant clinical effects of increased endogenous synthesis of AF in animals: (1) inhibition of pathological intestinal secretion, (2) normalization of small intestine secretion is commonly followed by an increase in daily weight gain in meat-producing animals.

V. Future Research: Clinical Studies

In an ongoing study, we have continuously selected patients with incapacitating *Mb. Ménière*. The clinical symptoms of this disease include attacks of fluctuating sensorineural hearing loss, rotatory vertigo, tinnitus, and a feeling of fullness in the affected ear. All of these patients are offered an HPC diet, and possible AF-stimulating effects are studied in the clinical outcome of *Mb. Ménière*. In total, 25 patients (12 women, 13 men) have so far been included in the study. The daily recommended intake of HPC follows that previously employed in the foregoing studies with 1 g per kg body weight, three times daily. The conventional medications for *Mb. Ménière* have not been altered in any of the patients. Increased plasma activity in response to HPC diet was demonstrated in 80% of the subjects. Among those patients reacting with increased plasma AF activity, about 15% showed normalized hearing in combination with a total recovery of the rotatory vertigo. Moreover, approximately half of the patients with attacks of rotatory vertigo had an alteration shown as persistent slight diffuse dizziness or total recovery. All patients responding with an insignificant AF induction (<0.5 plasma AF units) reported lack of clinical improvement, i.e., no effects on hearing or vertigo. The initial interpretation of these preliminary clinical data is that a simple addition of HPC might result in improvement for patients when conventional treatment fails. The etiological mechanism behind *Mb. Ménière* is related to impaired balance of fluids in the inner ear. Consequently, whether the clinical effects of AF are due to a direct influence on the peripheral receptors (cochlea and/or vestibulum), or if AF affects more centrally situated receptor mechanisms will be studied (Dr. Per Hanner, pers. commun.).

In Sweden, a total of 50–60 new cases of metastatic ileal carcinoid tumors are diagnosed each year (Wilander *et al.,* 1989). Carcinoid disease is often associated

with intestinal hypersecretion of varying severity, associated with diminished capacity for social activities and work. Surgery is the therapy of choice, but only 1 of 5 of patients with liver metastases can be cured. However, palliative surgery is worthwhile, e.g., debulking procedures or bypassing combined with medical treatment. The most frequently used drugs are somatostatin analogs and γ-interferon, although chemotherapy has limited effect. Persistent hypersecretory state in the small intestine after surgical and medical therapy may still impair social activities of individual patients. It was therefore of interest to evaluate a possible effect of an HPC diet in carcinoid patients with residual intestinal hypersecretion, despite surgical and medical treatment. Carcinoid patients were also offered a passive AF addition in the form of an egg drink containing high levels of AF. This study was designed as a double-blind crossover and has not reached the limit for breaking of the treatment code. Consequently, at this stage of the study, we can report only that most of the carcinoid patients tolerate the cereal intake as well as the egg drinks (Drs. Bo Wängberg and Anna Laurenius, pers. commun.).

Treatment of malignant diseases, with radiation therapy or cytotoxic drugs, causes unwanted side effects to most of the normal tissues of the patient. In case of the hematopoetic systems, the harmful effects are significantly reduced by the infusion of hematopoetic stem cells (allogeneic or autologous stem cell transplantation) or by the administration of hematopoetic growth factors. The dose-limiting side effects, however, are restricted to the gastrointestinal tract (the development of painful ulcerations in the oral cavity and in the esophagus, i.e., mucositis). Because of the damaged mucosa, food intake becomes difficult or impossible, and the mucosal injury in the small and large intestine elicits abdominal pain, diarrhea, dehydration, or even gastrointestinal perforation. Finally, since the mucosal barrier is disrupted, translocation of luminal microorganisms (bacteria and fungi) increases the risk of systemic infections and septicemia (Ruescher *et al.,* 1998). Clearly, in immunocompromised cancer patients undergoing intensive treatment with a curative intention, clinical failure due to mucositis is one of the major causes of morbidity and mortality (Snyder *et al.,* 1994). Despite these unwanted side effects, doses of cytotoxic drugs and/or radiation therapy have been escalated during the past 15 years in order to increase cure rates. Many prophylactic trials with agents to reduce mucositis have been performed, but no therapy has yet been proven effective. Thus, from a clinical point of view in hematology and oncology, the multitude of symptoms following mucositis causes morbidity and mortality and consequently obstructs further dose escalation (Saijo, 1997).

In order to counteract this mucosal destruction, we have elaborated animal models for evaluations of different forms of preventive treatment based on AF stimulation. The biological interaction between the AF-stimulating HPC diet or the AF-stimulating electrolyte solution in relation to radiation and/or cytostatic treatment are of major importance to develop treatment procedures of various forms of malignant diseases. Thus, clinical studies in tumor patients will be performed to investigate possible prophylactic effect of the HPC-diet on mucositis.

VI. Concluding Remarks

The AF protein regulates transport across biological membranes in the rodent, pig, and man. Five different forms of the AF protein have been sequenced and shown to have molecular masses between 28 and 41 kDa. A small part of the AF protein, a peptide situated between residues 35 and 50 in the AF sequence, is responsible for mediating the antisecretory activity, as determined by inhibition of experimentally induced hypersecretion in the small intestine. These peptides are promising as drugs for imbalance in fluid and ion transport. Expression of AF has been found in all tissues of mammals investigated hitherto. Histochemical techniques have revealed that all of the various cell types demonstrating presence of intracellular AF also possess the capacity to synthesize AF.

Enterotoxins induce stimulated AF production, followed by secretion of AF from an intracellular to an extracellular position in the tissue. Also, certain carbohydrates and amino acids are capable of stimulating increased synthesis of AF. Such food-induced stimulation of AF has been used to induce resistance to diarrheal diseases, as well as intestinal inflammation, in humans and animals.

Acknowledgments

References

Anand, G., Yin, X., Shahidi, A. K., Grove, L., and Prochownik, E. V. (1997). Novel regulation of the helix–loop–helix protein Id1 by S5a, a subunit of the 26 S proteasome. *J. Biol. Chem.* **272,** 19,140–19,151.

Aziz, K. M., Mohsin, A. K., Hase, W. K., and Phillips, R. A. (1968). Using the rat as a cholera "model." *Nature* **220,** 814–815.

Banchereau, J., and Steinman, R. M. (1998). Dendritic cells and the control of immunity. *Nature* **392,** 245–252.

Bartlett, J. G. (1994). *Clostridium difficile:* History of its role as an enteric pathogen and the current state of knowledge about the organism. *Clin. Infect. Dis.* **18**(Suppl. 4), S265–S272.

Basu, S., and Pickett, M. J. (1969). Reaction of Vibrio cholerae and choleragenic toxin in ileal loop of laboratory animals. *J. Bacteriol.* **100,** 1142–1143.

Björck, S., Bosaeus, I., Ek, E., Jennische, E., Lönnroth, I., Johansson, E., and Lange, S. (2000). Food-induced stimulation of the antisecretory factor can improve symptoms in human inflammatory bowel disease: A study of a concept. *Gut* **46,** 824–829.

Blackman, U. Z. Y., Goss, S. J., and Pickett, M. J. (1974). Experimental cholera in the chinchilla. *J. Infect. Dis.* **125,** 376–384.

Bolduan, G. (1997). Biofütterüng beim Abstzferkel. *Arch. Tierzucht A* **40,** 95–100.

Booth, I. W. (1992). Water and electrolyte handling in the small intestine. Current opinion in *Gastroenterology* **8,** 268–275.

Cassuto, J., Jodal, M., and Lundgren, O. (1982). The effect of nicotinic and muscarinic receptor blockade on cholera toxin induced intestinal secretion in rats and cats. *Acta Physiol. Scand.* **114,** 573–577.

Castagliuolo, I., LaMont, J. T., Letourneau, R., Kelly, C. P., O'Keane, J. C., Jaffer, A., Theoharides, T. C., and Pothoulakis, C. (1994). Neuronal involvement in the intestinal effects of *Clostridium difficile* toxin A and *Vibrio cholerae* enterotoxin in rat ileum. *Gastroenterology* **107,** 657–665.

Cooke, H. J. (1994). Neuroimmune signaling in regulation of intestinal ion transport. *Am. J. Physiol.* **266,** G167–G178.

De, S. N., and Chatterje, D. N. (1953). An experimental study of the mechanism of action of *Vibrio cholerae* on the intestinal mucous membrane. *J. Pathol. Bacteriol.* **46,** 559.

Diamond, J. M. (1995). Guts. How to be physiological. *Nature* **376,** 117–118.

DuPont, H. L., and Steele, J. H. (1987). Use of antimicrobial agents in animal feeds: Implications for human health. *Rev. Infect. Dis.* **9,** 447–460.

Dutta, N. K., and Habbu, M. K. (1955). Experimenal cholera in infants rabbits: a method for chemotherapeutic investigation. *J. Pharmacol.* **10,** 153–156.

Edwards, Y. J., and Perkins, S. J. (1996). Assessment of protein fold predictions from sequence information: The predicted alpha/beta double wound fold of the von Willebrand factor type A domain is similar to its crystal structure. *J. Mol. Biol.* **260,** 277–285.

Endtz, H. P., Ruijs, G. J., van Klingeren, B., Jansen, W. H., van der Reyden, T., and Mouton, R. P. (1991). Quinolone resistance in campylobacter isolated from man and poultry following the introduction of fluoroquinolones in veterinary medicine. *J. Antimicrob. Chemother.* **27,** 199–208.

Enna, S. J., and Gallager, J. P. (1983). Biochemical and electrophysiological characteristics of mammalian GABA receptors. *Int. Rev. Neurobiol.* **24,** 181–212.

Fan, Y. P., Chakder, S., and Rattan, S. (1999). Mechanism of action of cholera toxin on opossum internal anal sphincter smooth muscle. *Am. J. Physiol.* **277,** G152–G160.

Fujita, K., and Finkelstein, R. A. (1972). Antitoxic immunity in experimental cholera. Comparison of immunity induced perorally and parenterally in mice. *J. Infect. Dis.* **125,** 647–655.

Ganong, W. F. (1975). "Review of Medical Physiology," Chap. 38, 7th ed. Lange Medical, Los Altos.

Girod, P. A., Fu, H., Zryd, J. P., and Vierstra, R. D. (1999). Multiubiquitin chain binding subunit MCB1 (RPN10) of the 26S proteasome is essential for developmental progression in *Physcomitrella patens. Plant Cell* **11,** 1457–1472.

Glickman, M. H., Rubin, D. M., Fu, H., Larsen, C. N., Coux, O., Wefes, I., Pfeifer, G., Cjeka, Z., Vierstra, R., Baumeister, W., Fried, V., and Finley, D. (1999). Functional analysis of the proteasome regulatory particle. *Mol. Biol. Rep.* **26,** 21–28.

Göransson, L., Martinsson, K., Lange, S., and Lönnroth, I. (1993). Feed-induced lectins in piglets. Feed-induced lectins and their effect on post-weaning diarrhoea, daily weight gain and mortality. *J. Vet. Med. B* **40,** 478–484.

Göransson, L., Lange, S., and Lönnroth, I. (1995). Post weaning diarrhoea: Focus on diet. *Pigs News Inf.* **16,** 89N–91N.

Goyal, R. K., and Hirano, I. (1996). The enteric nervous system. *N. Engl. J. Med.* **334,** 1106–1115.

Gröndahl, M. L., Sörensen, H., Holm, A., and Skadhauge, E. (2000). "Effect of Antisecretory Factor-Derived Peptide on Induced Secretion in the Porcine Small Intestine *in Vivo* and *in Vitro.*" European 8th Symposium of Pig Physiology, Uppsala, June 19–23.

Hansen, M. B., and Skadhauge, E. (1995). New aspects of the pathophysiology and treatment of secretory diarrhoea. *Physiol. Res.* **44,** 61–78.

Hanson, L. Å., Lönnroth, I., Lange, S., Bjersing, J., and Dahlgren, U. (2000). Nutrition resistance to viral propagation. *Nutr. Rev.* **58,** S31–S37.

Hektoen, H., Berge, J. A., Hormazabal, V., and Yndestad, M. (1995). Persistence of antibacterial agents in marine sediments. *Aquaculture* **133,** 175–184.

Hugot, J. P., Zouali, H., Lesage, S., and Thomas, G. (1999). Etiology of the inflammatory bowel diseases. *Int. J. Colorectal Dis.* **14,** 2–9.

Hydén, H., and Cupello, A. (1987). Inhibition in the mammalian brain. A new theory of GABA mechanism of action. *Acta Physiol. Scan. Suppl.* **561,** 1–77.

Irvine, E. J., Zhou, Q., Thompson, A. K., and CCRPT Investigators (1996). The short inflammatory bowel disease questionnaire: A quality of life instrument for community physicians managing inflammatory bowel disease. *Am. J. Gastroenterol.* **91,** 1571–1578.

Jessen, K. R. (1981). GABA and the enteric nervous system—A neurotransmitter function? *Mol. Cell. Biochem.* **38,** 69–76.

Jodal, M., Holmgren, S., Lundgren, O., and Sjöqvist, A. (1993). Involvement of the myenteric plexus in the cholera toxin-induced net fluid secretion in the rat small intestine. *Gastroenterology* **105,** 1286–1293.

Johansson, E. (1998). "Cloning, Expression and Characterization of Antisecretory Factor." Thesis, Goteborg University, ISBN 91-628-2814-2.

Johansson, E., Jennische, E., Lange, S., and Lönnroth, I. (1997a). Antisecretory factor suppresses intestinal inflammation and hypersecretion. *Gut* **41,** 642–645.

Johansson, E., Lange, S., and Lönnroth, I. (1997b). Identification of an active site in the antisecretory factor protein. *Biochim. Biophys. Acta* **1362,** 177–182.

Johansson, E., Lönnroth, I., Lange, S., Jonson, I., Jennische, E., and Lönnroth, C. (1995). Molecular cloning and expression of a pituitary gland protein modulating intestinal fluid secretion. *J. Biol. Chem.* **270,** 20,615–20,620.

Kawahara, H., Kasahara, M., Nishiyama, A., Ohsumi, K., Goto, T., Kishimoto, T., Saeki, Y., Yokosawa, H., Shimbara, N., Murata, S., Chiba, T., Suzuki, K., and Tanaka, K. (2000). Developmentally regulated, alternative splicing of the Rpn10 gene generates multiple forms of 26S proteasomes. *EMBO J.* **19,** 4144–4153.

Kelly, C. P., and LaMont, J. T. (1998). *Clostridium difficile* infection. *Annu. Rev. Med.* **49,** 375–90.

Kikkawa, Y., and Smith, F. (1983). Cellular and biochemical aspects of pulmonary surfactant in health and disease. *Lab. Invest.* **49,** 122–139.

Kurose, I., Pothoulakis, C., LaMont, J. T., Anderson, D. C., Paulson, J. C., Miyasaka, M., Wolf, R., and Granger, D. N. (1994). *Clostridium difficile* toxin A-induced microvascular dysfunction. Role of histamine. *J. Clin. Invest.* **94,** 1919–1926.

Lange, S. (1982). A rat model for an *in vivo* assay of enterotoxic diarrhoea. *FEMS Microbiol. Lett.* **15,** 239–242.

Lange, S., Andersson, G. L., Jennische, E., Lönnroth, I., Li, X. P., and Edebo, L. (1990). Okadaic acid produces drastic histopathologic changes of the rat intestinal mucosa and with concomitant hypersecretion. *In* "Toxic Marine Phytoplankton" (E. Graneli, B. Sundström, L. Edler, D. M. Anderson, Eds.), pp. 356–361. Elsevier Science, New York.

Lange, S., Delbro, D., Jennische, E., Johansson, E., and Lönnroth, I. (1998). Recombinant or plasma-derived antisecretory factor inhibits cholera toxin-induced increase Evans blue permeation of rat intestinal capillaries. *Dig. Dis. Sci.* **43,** 2061–2070.

Lange, S., and Göransson, L. (1999). "Current Value of Alternatives to Antimicrobial Growth Promotors with Special Emphasis on Anti Secretory Factor, ASF." 50th Annual Meeting of the European Association for Animal Production (EAAP), Zurich, August 1999.

Lange, S., Jennische, E., Johansson, E., and Lönnroth, I. (1999). The antisecretory factor: Synthesis and intracellular localisation in porcine tissues. *Cell Tissue Res.* **296,** 607–617.

Lange, S., and Lönnroth, I. (1984). Passive transfer of protection against cholera toxin in the rat intestine. *FEMS Microbiol. Lett.* **24,** 165–168.

Lange, S., and Lönnroth, I. (1986). Bile and milk from cholera toxin treated rats contain a hormone-like factor which inhibits diarrhea induced by the toxin. *Int. Arch. Allergy Appl. Immunol.* **79,** 270–275.

Lange, S., Lönnroth, I., and Martinsson, K. (1994). Concentrations of antisecretory factor in eggs and in chicken blood plasma. *Br. Poult. Sci.* **35,** 615–620.

Lange, S., Lönnroth, I., Palm, A., and Hydén, H. (1985). An inhibitory protein of intestinal fluid secretion reverses neuronal GABA transport. *Biochem. Biophys. Res. Commun.* **130,** 1032–1036.

Lange, S., Lönnroth, I., Palm, A., and Hydén, H. (1987b). The effect of antisecretory factor on the permeability of nerve cell membrane to chloride ion. *Pflügers Arch.* **410,** 648–651.

Lange, S., Lönnroth, I., and Skadhauge, E. (1987a). Effects of the antisecretory factor in pigs. *Pflügers Arch.* **409,** 328–332.

Lange, S., Martinsson, K., Lönnroth, I., and Göransson, L. (1993). Plasma level of antisecretory factor (ASF) and its relation to post-weaning diarrhoea in piglets. *J. Vet. Med. B* **40,** 113–118.

Larsen, J. L. (1982). A study on inhibition of cholera toxin-induced intestinal hypersecretion by neuroleptics. *Acta Pharmacol. Toxicol.* **50,** 294–299.

LeVeen, H. H., and Fishman, W. H. (1947). Combination of Evans Blue with plasma protein: Its significance in capillary permeability studies, blood dye, disappearence curves, and its use as a protein tag. *Am. J. Physiol.* **151,** 26–33.

Lönnroth, I., and Jennische, E. (1982). Reversal of enterotoxic diarrhoea by anaesthetic and membrane-stabilizing agents. *Acta. Pharmacol. Toxicol.* **51,** 330–335.

Lönnroth, I., and Lange, S. (1981). A new principle for resistance to cholera: Desensitization to cyclic-AMP mediated diarrhoea induced by cholera toxin in the mouse intestine. *J. Cycl. Nucleotide Res.* **7,** 247–257.

Lönnroth, I., and Lange, S. (1984). Inhibition of cyclic AMP-mediated intestinal hypersecretion by pituitary extracts from rats pretreated with cholera toxin. *Med. Biol.* **62,** 290–294.

Lönnroth, I., and Lange, S. (1985). A hormone-like protein from the pituitary gland inhibits intestinal hypersecretion induced by cholera toxin. *Regul. Pept. Suppl.* **4,** 216–218.

Lönnroth, I., and Lange, S. (1986). Purification and characterization of the antisecretory factor—A protein in the central nervous system and in the gut which inhibits intestinal hypersecretion induced by cholera toxin. *Biochim. Biophys. Acta* **883,** 138–144.

Lönnroth, I., and Lange, S. (1987). Intake of monosaccharides or amino acids induces pituitary gland synthesis of proteins regulating intestinal fluid transport. *Biochim. Biophys. Acta* **925,** 117–123.

Lönnroth, I., and Lange, S. (1988). "Antisecretory Factor from the Pituitary Gland Regulate Intestinal Fluid Transport and Reverse Diarrhoea in Piglets." Symposium, Malmoe, May 31th, 1988.

Lönnroth, I., Lange, S., and Holmgren, J. (1980). Effect of phenothiazines, thioxanthenes and related drugs on experimental cholera. *In* "Phenothiazines and Structurally Related Drugs—Basic and Clinical Studies" (E. Usdin, H. Eckert, and J. S. Forrest, Eds.), pp. 303–306. Elsevier, New York.

Lönnroth, I., Lange, S., and Skadhauge, E. (1988b). The antisecretory factors: Inducible proteins which modulate secretion in the small intestine. *Comp. Biochem. Physiol. A* **90,** 611–617.

Lönnroth, I., Martinsson, K., and Lange, S. (1988a). Evidence of protection against diarrhoea in suckling piglets by a hormone-like protein in the sow's milk. *J. Vet. Med. B* **35,** 628–635.

Lönnroth, I., and Munck, B. (1980). Effect of chlorpromazine on ion transport induced by cholera toxin, cyclic AMP and cyclic GMP in isolated mucosa from hen intestine. *Acta Pharmacol. Toxicol.* **47,** 190–194.

Lundgren, O. (1984). Microcirculation of the gastrointestinal tract and pancreas. *In* "Handbook of Physiology" (E. M. Renkin and C. C. Michel, Eds.), Section 2, Vol. IV, pp. 799–863. American Physiological Society, Bethesda, MD.

Lyerly, D. M., Saum, K. E., MacDonald, D. K., and Wilkins, T. D. (1985). Effects of *Clostridium difficile* toxins given intragastrically to animals. *Infect. Immunol.* **47,** 349–352.

Mei, N. (1978). Vagal glucoreceptors in the small intestine of the cat. *J. Physiol.* **282,** 485–488.

Mei, N., and Garnier, L. (1986). Osmosensitive vagal receptors in the small intestine of the cat. *J. Auton. Nerv. Syst.* **16,** 159–170.

Munro, A. (1738). Miscellaneous remarks on the intestines. *In* "Medical Essays and Observations," 2nd ed., Vol. IV, pp. 76–92. Munro and Drummond, Edinburgh.

Nocerino, A., Iafusco, M., and Guandalini, S. (1995). Cholera toxin-induced small intestinal secretion has a secretory effect on the colon of the rat. *Gastroenterology* **108,** 34–39.

Pacha, J. (2000). Development of intestinal transport function in mammals. *Physiol Rev.* **80,** 1633–1667.

Podolsky, D. (1995). Inflammatory bowel disease. *N. Engl. J. Med.* **325,** 928–935.

Pusch, W., Jähner, D., and Ivell, R. (1998). Molecular cloning and testicular expression of the gene transcripts encoding the murine multiubiquitin-chain-binding protein (Mcb 1). *Gene* **207,** 19–24.

Rabbett, H., Elbadri, A., Thwaites, R., Northover, H., Dady, I., Firth, D., Hillier, V. F., Miller, V., and Thomas, A. G. (1996). Quality of life in children with Crohn's disease. *J. Pediatr. Gatsroenterol. Nutr.* **23,** 528–533.

Rapallino, M. V., Cupello, A., Lange, S., Lönnroth, I., and Hyden, H. (1989). Further studies on the effect of ASF factor on Cl-permeability across the Deiters' neurone plasma membrane. *Int. J. Neurosci* **46,** 93–95.

Reid, E. W. (1890). Osmosis experiments with living and dead membranes. *J. Physiol.* **11,** 312–314.

Reid, E. W. (1901). Transport of fluid by certain epithelia. *J. Physiol.* **26,** 436–438.

Rubin, D. M., van Nocker, S., Glickman, M., Coux, O., Wefes, I., Sadis, S., Fu, H., Goldberg, A., Vierstra, R., and Finley, D. (1997). ATPase and ubiquitin-binding proteins of the yeast proteasome. *Mol. Biol. Rep.* **24,** 17–26.

Ruescher, T. J., Sodeifi, A., Scrivani, S. J., Kaban, L. B., and Sonis, S. T. (1998). The impact of mucositis on alpha-haemolytic streptococcal infection in patients undergoing autologous bone marrow transplantation for haematologic malignancies. *Cancer* **82,** 2275–2281.

Sack, R. B., and Carpenter, C. C. J. (1969). Experimental canine cholera. I. Development of the model. *J. Infect. Dis.* **119,** 138–149.

Saijo, N. (1997). Chemotherapy: The more the better? Overview. *Cancer Chemother. Pharmacol. Suppl.* **40,** S100–S106.

Sartor, R. B. (1995). Current concepts of the etiology and pathogenesis of ulcerative colitis and Crohn's disease. *Gastroenterol. Clin. North Am.* **24,** 475–507.

Shivananda, S., Lennard-Jones, J., Logan, R., Fear, N., Price, A., Carpenter, L., and van Blankenstein, M. (1996). Incidence of inflammatory bowel disease across Europe: Is there a difference between north and south? Results of the European Collaborative Study on Inflammatory Bowel Disease (EC-IBD). *Gut* **39,** 690–697.

Sigfridsson, K., Lange, S., and Lönnroth, I. (1995). "Anti Secretory Factor (ASF) and Feed Induced Lectines (FIL) in Sow and Suckling Piglet." 46th Annual Meeting of the European Association for Animal Production (EAAP), Prague, September 1995.

Snyder, D. S., Negrin, R. S., O'Donnell, M. R., Chao, N. J., Amylon, M. D., Long, G. D., Nademanee, A. P., Stein, A. S., Parker, P. M., and Smith, E. P. (1994). Fractionated total-body irradiation and high-dose etoposide as a preparatory regimen for bone marrow transplantation for 94 patients with chronic myelogenous leukemia in chronic phase. *Blood* **84,** 1672–1679.

St. George-Hyslop, P. H., Rommens, J. M., and Fraser, P. E. (1996). "Method for Identifying Substances That Affect the Interaction of a Presenilin-1-Interacting Protein with a Mammalian Presenilin-1 Protein." U.S. Patent 6020143.

Stanisz, A. M., Befus, D., and Bienenstock, J. (1986). Differential effects of vasoactive intestinal peptide, substance P, and somatostatin on immunoglobulin synthesis and proliferations by lymphocytes from Peyer's patches, mesenteric lymph nodes, and spleen. *J. Immunol.* **136,** 152–156.

Tateishi, K., Misumim, Y., Ikehara, Y., Miyasaka, K., and Funakoshi, A. (1999). Molecular cloning and expression of rat antisecretory factor and its intracellular localization. *Biochem. Cell. Biol.* **77,** 223–228.

Torres, J., Jennische, E., Lange, S., and Lönnroth, I. (1990). Enterotoxins from *Clostridium difficile:* Diarrhoeogenic potency and morphological effects in the rat intenstine. *Gut* **31,** 781–785.

Torres, J., Jennische, E., Lange, S., and Lönnroth, I. (1991). *Clostridium difficile* toxin A induces a specific antisecretory factor which protects against intestinal mucosal damage. *Gut* **32,** 791–795.

Torres, J., Lönnroth, I., Lange, S., Camorlinga-Ponce, M., Gonzalez-Arroyo, S., and Munoz, O. (1993).

Antisecretory activity in a lectin fraction of plasma from patients with acute diarrhea. *Arch. Med. Res.* **24,** 7–11.

Turnbull, G. K., and Vallis, T. M. (1995). Quality of life in inflammatory bowel disease: The interaction of disease activity with psychosocial function. *Am. J. Gastroenterol.* **90,** 1450–1454.

Uhing, M. R., and Kimura, R. E. (1995). The effect of surgical bowel manipulation and anesthesia on intestinal glucose absorption in rats. *J. Clin. Invest.* **95,** 2790–2798.

Ussing, H. H., and Andersen, B. (1956). The relation between solvent drag and active transport of ions. *In* "Proceedings, 3rd International Congress of Biochemists, Brussels," p. 434. Academic Press, New York.

Ussing, H. H., and Zerahn, K. (1951). Active transport of sodium as the source of electric current in the short-cicuited isolated frog skin. *Acta Physiol. Scand.* **32,** 110–115.

Vagne-Descroix, M., Pansu, D., Jornvall, H., Carlquist, M., Guignard, H., Jourdan, G., Desvigne, A., Collinet, M., Caillet, C., and Mutt, V. (1991). Isolation and characterisation of porcine sorbin. *Eur. J. Biochem.* **201,** 53–59.

Wilander, E., Lundqvist, M. L., and Öberg, K. (1989). Gastrointestinal carcinoid tumours. *Prog. Histochem. Cytochem.* **19,** 1–88.

Wilson, T. H., and Wiseman, G. (1954). The use of sac of everted small intestine for the study of the transference of substances from the mucosal to the serosal surface. *J. Physiol.* **123,** 116–120.

Yasumoto, T., Murata, M., Oshima, Y., Matsumoto, G. K., and Clardy, J. (1985). Diarrhetic shellfish toxins. *Tetrahedron* **41,** 1019–1025.

Young, P., Deveraux, Q., Beal, R. E., Pickart, C. M., and Rechsteiner, M. (1998). Characterization of two polyubiquitin binding sites in the 26 S protease subunit 5a. *J. Biol. Chem.* **273,** 5461–5467.

This Page Intentionally Left Blank

Structure and Function of Photoreceptor and Second-Order Cell Mosaics in the Retina of *Xenopus*

Robert Gábriel[1] and Márta Wilhelm[3]

[1]Department of General Zoology and Neurobiology, and [3]Institute of Physical Education and Sports Sciences, University of Pécs, H-7624 Pécs, Hungary

The structure, physiology, synaptology, and neurochemistry of photoreceptors and second-order (horizontal and bipolar) cells of *Xenopus laevis* retina is reviewed. Rods represent 53% of the photoreceptors; the majority (97%) are green light-sensitive. Cones belong to large long-wavelength-sensitive (86%), large short-wavelength-sensitive (10%), and miniature ultraviolet wavelength-sensitive (4%) groups. Photoreceptors release glutamate tonically in darkness, hyperpolarize upon light stimulation and their transmitter release decreases. Photoreceptors form ribbon synapses with second-order cells where postsynaptic elements are organized into triads. Their overall adaptational status is regulated by ambient light conditions and set by the extracellular dopamine concentration. The activity of photorectors is under circadian control and is independent of the central body clock. Bipolar cell density is about 6000 cells/mm^2. They receive mixed inputs from rods and cones. Some bipolar cell types violate the rule of ON–OFF segregation, giving off terminal branches in both sublayers of the inner plexiform layer. The majority of them contain glutamate, a small fraction is GABA-positive and accumulates serotonin. Luminosity-type horizontal cells are more frequent ($\sim$1000 cells/mm^2) than chromaticity cells ($\sim$450 cells/mm^2). The dendritic field size of the latter type was threefold bigger than that of the former. Luminosity cells contact all photoreceptor types, whereas chromatic cells receive their inputs from the short-wavelength-sensitive cones and rods. Luminosity cells are involved in generating depolarizing responses in chromatic horizontal cells by red light stimulation which form multiple synapses with blue-light-sensitive cones. Calculations indicate that convergence ratios in *Xenopus* are similar to those in central retinal regions of mammals, predicting comparable spatial resolution.

I. Introduction

The retina of vertebrates is a sheath of nervous tissue in the back of the eye that translates light information into electrical signals and transmits it to the brain. On account of its accessibility and well-defined layered histological structure it has become one of the favorite experimental objects in neuroscience (Dowling, 1987). The retina, apart from the pigmented epithelium which joins it with the choroid tissue of the eye, consists of five major neuron types (photoreceptors, horizontal, bipolar, amacrine, and ganglion cells) and a radial glia (Müller cell). The cell bodies and the processes of the neurons form well-defined histological layers.

The cone-shaped outer segment of cones and the cylinder-like outer segments of rods mingle with the processes of the pigment epithelial cells. The cell bodies of the photoreceptors form the outer nuclear layer. They extend short axon-like processes (pedicles) toward the deeper layers of the retina, thus forming a synaptic layer (outer plexifrom layer), where they make synapses with the processes of horizontal and bipolar cells. The inner nuclear layer contains the cell bodies of retinal interneurons and the glial cells. Bipolar cells transmit the electrical signals into the inner plexiform layer, where they contact amacrine and ganglion cells. Ganglion cells provide the output of the retinal neural network toward the visual centers of the brain. The output signals code for contrast, color, and movement of the objects and in some species also provide directional information (Wässle and Boycott, 1991).

All the major cell types of he vertebrate retina form mosaics which cover the entire retinal surface (Wässle and Riemann, 1978; Wässle and Boycott, 1991; Cook and Chalupa, 2000). The mosaics of cells can be characterized by several parameters. In general, the most important question if a particular cell type provides full coverage of the retinal surface. Cells with horizontally extending dendrites and/or axons (horizontal, bipolar, amacrine, and ganglion cells) usually do so. The density and distribution of cells at different retinal locations are also often examined. It is generally accepted that convergence ratios should be calculated based on these parameters. It is also assumed that these parameters are useful in assessing the spatial resolution capacity of the retina of a given species (Wässle and Boycott, 1991; Cook and Chalupa, 2000).

Among vertabrates, cold-blooded animals, especially frogs offered a good model for neuroanatomists and neurophysiologists to study structure–function relationship in the central nervous system. Ramon y Cajal (1893) was instrumental in

defining intraretinal connection patterns and possible function of the main neuron classes. As one of the main objects of his study he chose the frog retina. Using optic fiber preparations, Hartline (1938) found that electrical activity was most pronounced at either light ON or light OFF. Some fibers reacted for both ON and OFF stimuli. Fifteen years later Barlow (1953a,b) discovered what we since came to recognize as the basic phenomenon of center-surround organization. A few years later complex receptive field properties were recognized (Maturana *et al.,* 1960).

With the considerable advance of experimental embryology and developmental biology frog retina and visual system fulfilled the role of a model of the developing eye. It was especially interesting, and unique for the same reason, since metamorphosis is unknown in other vertebrates and the eye grows throughout the whole life of animals (Straznicky and Gaze, 1971). Remarkably, retinal cell mosaics and the ratio of cell types are very similar at any eccentricity in the *Xenopus* retina. This implies a well-balanced cell generation and differentiation process (Straznicky, 1993).

Neurochemistry has also contributed enermously to a growing knowledge regarding retinal information processing. It was especially true in relation to volume transmission. There have been two major areas where *Xenopus* eye provided the first-and-best model in understanding the role of neuromodulation in adaptational processes. Besharshe and Iuvone (1983) demonstrated a circadian clock mechanism in the frog retina. This process later proved to be independent of the main circadian control center of the body, the suprachiasmatic nucleus, and was localized to the photoreceptors (Cahill and Besharshe, 1993). Like the circadian regulation, light and dark adaptation are also based on neurohumoral clues. By the early 1990s it had been established that dopamine was a key player in the light adaptational process. It has been measured accurately first in the *Xenopus* retina that extracellular dopamine concentration increased upon light stimulation and rapidly declined in darkness (Witkovsky *et al.,* 1993).

The above-mentioned data have opened a new era of investigations in every aspects of the retinal information processing. Several papers have been published on different aspects and model systems in retinal research (Sterling *et al.,* 1986; Sakai and Naka, 1987; Ammermüller and Kolb, 1996). None of the other model animals in retinal research, however, have the advantage of *Xenopus,* which is that so much is known about the genetic material of the species. Therefore, on one hand, we join the trend of summarizing the present knowledge on the structure and function of individual cell types of the retina in a model species, in this case in *Xenopus,* and attempt a synthesis regarding their role in retinal information processing by assessing their function in the retinal network. On the other hand, we wish to serve with this review the researchers who have started to analyze the molecular machinery underlying rhythmic processes, to study the expression pattern of certain proteins important in information processing and to reveal the steps of retinal development in *Xenopus*.

II. Formation of the Cell Mosaics in the Outer Retina

It was discovered in the early 1970s that the anuran retina produces new nerve cells throughout the whole life span of an animal (Straznicky and Gaze, 1971). Consequently one could consider the possibility that all nerve cell types, including the photoreceptors, are generated at all ages. Indeed, cellular determination proved to be independent of the lineage and birth date in *Xenopus* retina (Holt *et al.,* 1988) and it had also been shown that multipotent precursor cells give rise to all major cell types of the frog retina (Wetts and Fraser, 1988). The ratio of cell types generated at a given time point is largely dependent upon extrinsic factors. In mammals, these include inductive interactions with neighboring cells and extracellular signal molecules (Turner and Cepko, 1987; Turner *et al.,* 1990). We can only suppose that similar factors play pivotal roles in *Xenopus* retinal development. It has been shown recently that one of the factors profoundly influencing retinal photoreceptor cell fate maybe Delta, a factor that activates Notch-mediated inhibition in the late *Xenopus* gastrula (Dorsky *et al.,* 1995). Neuroepithelial progenitor cells that express high levels of Delta, inhibit the differentiation of their neighbors, but themselves become ganglion cells. If an additional photoreceptor-inducing signal (the exact nature of this is unknown to date) is present, the cells generated first become cones and then later rods (Dorsky *et al.,* 1997). Nevertheless, in larval development most of the retinal cell nuclei fail to accumulate [^{3}H]thymidine by stage 33/34 (for staging, see Nieuwkoop and Faber, 1956), suggesting that most of the neurons leave the mitotic cycle by this time (Stiemke and Hollyfiled, 1995). Another process in early development (stages 26 to 31) is the formation of a gap junction between stem cells (Fujisawa, 1982). Progenitors in the S and M phase but not in G1 phase of the cell cycle form transient gap junctions with each other. These gap junctions are abated at later stages and are again reformed during maturation at around stage 46 between horizonal cells (Nagy and Witkovsky, 1981).

A. Generation and Development of the Photoreceptor Cell Layer

Photoreceptor cells start to develop and differentiate in close connection with the pigment epithelium of the retina (Hollyfield and Witkovsky, 1974; Stiemke *et al.,* 1994). Early in development (from stage 31) photoreceptors can be discerned in the retina. Production of interphotorecptor retinoid-binding protein also starts early in embryonic development. It appears before the time of photoreceptor differentiation in the subretinal space and spreads from the central retina to the periphery. This protein may set the path for the photoreceptor precursors during their migration toward their final position (Hessler *et al.,* 1996). Interestingly, retinoic acid applied early in development (stage 11/12) completely

abated the formation of an eye or a retina. Its application at later stages led to the formation of microphthalmic eyes. It did not inhibit the formation of rods and cones, but altered the formation of ganglion cell projections (Manns and Fritzsch, 1991).

By stage 33/34 several cells in the central retina stain strongly with anti-calbindin (the 28-kDa D-vitamin dependent calcium-binding protein) antibodies. With this marker it is impossible to decide which photoreceptors appear first in the developing retina. Antibodies and riboprobes against photopigments provided the right tools for revealing the exact timing and sequence of photoreceptor generation.

1. Rods

The first cells immunoreactive to bovine rod opsin also appear at stage 33/34, at the time when immunostaining for calbindin turns strong in the photoreceptors (Chang and Harris, 1998). By stage 37/38 rod opsin immnureactivity spreads into the dorsal retina and clearly appeared in the presumed outer nuclear layer. However, calbindin immunreactive cells were always more numerous and spread further to the periphery than the rod opsin staining. This suggests that calbindin probably stains cones only and that cones are generated earlier than rods. This has been confirmed with double-labeling studies. Rods are generated later in embryonic life than cones (an increased rate of rod genesis was observed between stages 28 and 31; Chang and Harris, 1998).

2. Cones

The exact spatio-temporal pattern of cone photoreceptor generation has been de-scribed using mRNA probes and antibodies against red-sensitive cones. The expression of the red light-sensitive photopigment in the retina was observed first at stage 32 and became pronounced by stage 35/36. Bromodezoxyuridine and red opsin riboprobe double-labeling showed that red-light-sensitive cones become postmitotic very early in development (at stage 23; Chang and Harris, 1998). No information is available on other cone types. However, on the basis of calbindin distribution studies it seems possible that the timetable of generating other cone types is identical with that of the red-sensitive cones.

B. Generation and Development of the Second-Order Cells

Second-order cells include two major classes of neurons in the retina: bipolar and horizontal cells. These classes can be divided into further neuron types (see below). The generation and differentiation process of these cells start later than those of the photoreceptors (Witkovsky, 2000). From a developmental point of view, however, the time of generation of these cells is critical, since without them the transmission

from photoreceptors to third-order cells (including ganglion cells) cannot happen. As a consequence, visual signals even if processed by the photoreceptors, cannot reach the ganglion cells and cannot be expedited toward the brain. Therefore, formation of synapses between photoreceptors and second-order cells is crucial regarding retinal function. As the dendrites of the bipolar and horizontal cells grow toward the photoreceptors they create a perceptible outer plexiform layer by stage 37/38 (Chen and Witkovsky, 1978). This layer continues to grow in thickness until metamorphosis. However, lack of suitable neurochemical markers hindered the identification of cell types in the outer portion of the inner nuclear layer.

1. Bipolar Cells

To date, bipolar cells could not be selectively identified in early stages of the development. Calretinin labels bipolar cells in fully developed frog retina (Gábriel *et al.,* 1998; Gábriel, 2000); however, at present we do not know if this marker is suitable for early identification of this cell type, especially because many amacrine and ganglion cells are also calretinin-positive in adult animals. Bipolar cells nevertheless form characteristic basal junctions with the photoreceptors as early as stage 40 (Chen and Witkovsky, 1978). Although direct evidence is not available, intracellular recordings from tadpole ganglion cells indicate that bipolar cells are fully functional at stage 43 (Chung *et al.,*1975). By this time most of the amacrine cells express their final neurochemical markers (Rayborn *et al.,* 1981; Frederick *et al.,* 1989; Hiscock and Straznicky, 1990; Zhu and Straznicky, 1991, 1992), thus providing guidance for bipolar cell terminals and laying the foundation of selective synaptogenesis in the inner retina. The bipolar cell synapses in the inner retina continue to mature up until metamorphosis (stages 62–66), which brings about a reorganization: basal junctions decline in number and invaginating bipolar cell synapses appear at photoreceptor bases (Witkovsky and Powell, 1981).

2. Horizontal Cells

No distinctive markers are available to fully identify horizontal cells in adult anurans, and this is true for the developing animals too. All we know at present regarding their development comes from electronmicroscopic studies. Horizontal cells start to develop at about the same time as bipolar cells. By stage 46 the horizontal cell dendrites contain synaptic thickenings adjacent to the arciform densities of the photoreceptor cells. In freeze–fracture images multiple rows of particles could be discerned on the P-face of horizontal cell dendrites, which distinguishes them from the bipolar cell processes (Nagy and Witkovsky, 1981). Gap junctions between homologous horizontal cells start to develop at about this age and are continued to be present throughout life.

III. Anatomy and Physiology of the Photoreceptors

The *Xenopus* retina, depending on size, contains 200,000–300,000 photoreceptor cells (Wilhelm and Gábriel, 1999). As is mentioned in the preceeding section, the different cell mosaics of the *Xenopus* retina have rather uniform distribution (Saxén, 1954; Wilhelm and Gábriel, 1999). The photoreceptors are no exception to the rule. Photoreceptor cell types share some of their remarkable morphological and physiological characteristics. Other features differ from type to type.

A. Types, Density, and Distribution of Photoreceptors

In most anuran retina, the spectral sensitivity of visual pigments fall into five categories. One pigment type maximally absorbs ultraviolet light (exact absorption maximum is not known), the second and third blue light of almost identical wavelength (440 and 445 nm), the fourth has its absorbtion maximum in the green (523 nm) range, while the fifth in the red portion (611 nm) of the spectrum (Witkovsky *et al.,* 1981; Hárosi, 1982; Röhlich *et al.,* 1989; Röhlich and Szél, 2000; Witkovsky, 2000). In *Xenopus* the situation conforms well with this general anuran pattern, although the cell types which contain one or the other pigment may be different from those in other anurans.

The combined density of photoreceptors was found to be about 14,000 cells/mm^2. Photoreceptors can easily be classified as rods and cones on the basis of their anatomical features (Fig. 1a). Rods have long and cylindrical outer segments while cones bear short outer segments but contain a colorless oil droplet (Saxén, 1954). Also, cell bodies of the cones are shifted toward the outer plexiform layer compared to rods. The pedicles of rods and cones can be distinguished at the ultrastructural level (Fig. 1b) and both enclose several processes deriving from bipolar and horizontal cells. Photoreceptors emit filopodia, the function of which is unknown at present.

Rods represented 53% of all photoreceptors; the remaining 47% are cones. The rod/cone ratio (overall 1.13:1) did not change significantly from center to periphery (Wilhelm and Gábriel, 1999). Similar ratios have been described earlier; however, the cell density was then estimated much higher (almost double; Saxén, 1954). This could be due to the fact that those cell counts were taken from dehydrated preparations where the linear shrinkage may be up to 25%. The outer segments of rods change substantially with their retinal location. The superior retina contains rods with long (over 40 μm) outer segments, while inferior retinal rods are shorter (Zhu *et al.,* 1990).

The distribution of cone photoreceptors showed that the photoreceptor mosaic organization is imprecise in *Xenopus:* although most of the cones are arranged by some degree of minimal spacing. Occasional grouping of cones of the same types
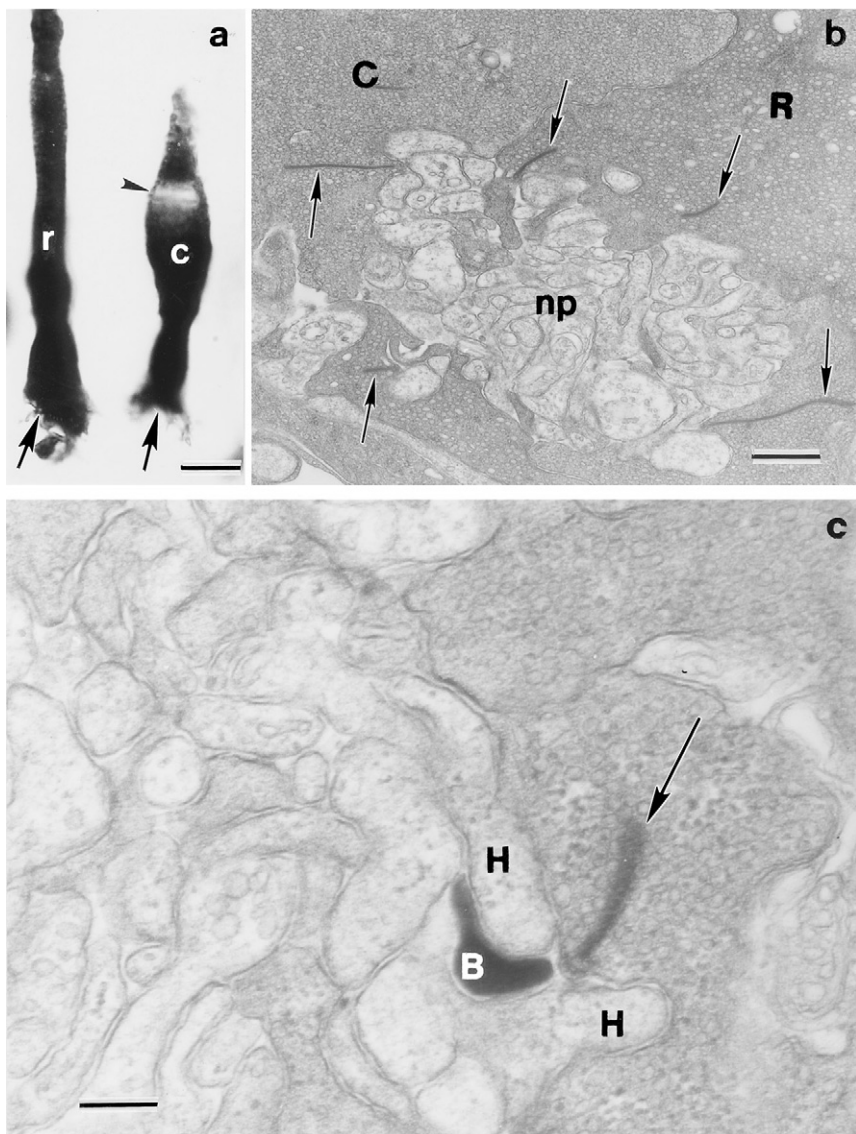
FIG. 1 Photomicrographs of photoreceptor cells. (a) Golgi-impregnated photoreceptors (r, rod; c, cone). Arrowhead labels the oil droplet of the cone; arrows point to the synaptic terminals. Bar = 10 μm. Courtesy of Dr. P. Witkovsky. (b) Rod and cone pedicles (labeled with R and C, respectively) surround a neuropil (np) area. Synaptic ribbons are marked with arrows. Bar = 500 nm. (c) Dendritic tip of an intracellularly filled bipolar cell (B) in central position of a postsynaptic triad at a photoreceptor synaptic ribbon (arrow). H, horizontal cell dendrites as lateral elements of the triad. Bar = 100 nm.

(especially those of the presumed blue-light-sensitive cones) has been observed (Chang and Harris, 1998; Wilhelm and Gábriel, 1999; Röhlich and Szél, 2000). No governing rules for the rod (including the minor rod) population could be found so far.

The basic phototransduction mechanism is identical in rods and cones and is not reviewed here. In essence, light captured by a photoreceptor outer segment closes nonselective cation channels in the cell membrane, which causes the photoreceptors to hyperpolarize. In turn, the photoreceptor reduces the tonic release of its neurotransmitter (Pugh and Cobbs, 1986; Baylor, 1987). The light-sensitive cation channel is regulated by the concentration of cGMP. The cGMP level, on one hand, is dependent on the kinetics of the phototransduction cascade while on the other also depends on the activity of nitric oxide synthase that is present in rod ellipsoids (Kurenny *et al.,* 1994; Nöll *et al.,* 1994). Nitric oxide activates the guanylate cyclase under physiological Ca^{2+} concentrations and increases the cGMP level in the rod outer segments. Nitric oxide may also reach the photoreceptors from the inner retina where it is found predominantly in amacrine cells in frogs (Sato, 1990; Gábriel, 1991; Straznicky and Gábriel, 1991), and apart from the cGMP level it may also influence voltage-gated ionic currents (Kurenny *et al.,* 1994).

A number of factors significantly influence the actual synaptic output of the photoreceptors. This ensemble of modulatory influences is able to "retransduce" the electrical signals generated at the outer segment into a chemical one (Barnes, 1994). Some details of the latter process will be discussed in more detail later in section III.

1. Rods

Morphologically, rods are quite uniform across the retina. The majority (97%) of them are green-sensitive (Witkovsky *et al.,* 1981). The pigment has recently been cloned and tied firmly to the principal rod population of the *Xenopus* retina (Saha and Grainger, 1993). There is a minor blue-sensitive rod population (Witkovsky *et al.,* 1981), which was distinguished on the basis of its elevated fucose uptake capacity of their thinner outer segments compared to that seen in the green-sensitive rods (Hollyfield *et al.,* 1984). For a long time no other markers were found for this cell. However, most recently they were found to be labeled with C-terminal specific anti-rhodopsin monoclonal antibodies against bovine opsin (Röhlich and Szél, 2000). Molecular biological manipulations made it possible to generate transgenic embryos by using a 5.5-kb upstream fragment from the principal rod opsin gene which controlled a reporter gene, green fluorescent protein (Knox *et al.,* 1998). This construct drives expression only in the retina and the pineal gland. This model may be used to study rod function in the retina under normal and pathological conditions.

Although the absorption spectrum of the minor rod photopigment is remarkably similar to the blue light-sensitive cone photopigment (Starace and Knox,

1998), these rods show similar visual pigment kinetics to that of the principal rods (Matthews, 1983). The rods function, as in all other species, to subserve scotopic vision (Crescitelli, 1991). The role of the minor rods in vision is not known at present.

2. Cones

Morphologically, large single cones, small single cones, and double cones with one principal and one small accessory member can be distinguished. The visual pigment content and the distribution of different spectral cone types were studied with anti-visual pigment antibodies (Röhlich *et al.,* 1989; Zhang *et al.,* 1994) and lectin labeling (Zhang *et al.,* 1994 ,Wilhelm and Gábriel, 1999).

Large cones (oil droplet diameter >6 μm) fall into two categories: one stains with antibodies against the red visual pigment and binds peanut-agglutinin while the other does not (Röhlich *et al.,* 1989; Zhang *et al.,* 1994; Chang and Harris, 1998). Cones containing the red-light-sensitive visual pigment represent the majority of the cone population (85.7%), and dominate the light response of the *Xenopus* retina (see below). This is the component of the light that reaches farthest down in the water without scatter and absorption; therefore, it can be used best for object detection in murky waters where *Xenopus* lives.

Blue-light-sensitive cones represent 10.2% of all cones. These cells have an oil droplet with a diameter of less than 6 μm. They tend to gather into groups of two to six cells while in the case of other cone cell types spatial pattern formation could not be observed (Wilhelm and Gábriel, 1999). An opsin belonging to the S-class of photopigments has been cloned. The probable absorption maximum of this pigment *in vivo* could be around 440–445 nm (Starace and Knox, 1998). Photoreceptors containing this pigment may serve as sky detectors in aquatic amphibians like *Xenopus*.

Photoreceptors with small oil droplet diameter (<4 μm) bind peanut-agglutinin and the stilbene dye DIDS, but cannot be labeled with COS-1 monoclonal antibodies (Röhlich *et al.,* 1989; Zhang *et al.,* 1994). The presumed pigment of this cone type has been cloned recently and shown to be UV-sensitive (Starace and Knox, 1997). The exact *in vivo* absorption maximum of this pigment is unknown. The UV-sensitive miniature cone population amounts to 4.1% of all cones. Since the UV light scatters on little particles in the surface waters, it can be used to detect small floating objects (like the zooplankton) and may be potentially useful in locating prey.

Both the large and small accessory members of the double cones can be labeled with the COS-1 monoclonal antibody. The small accessory member does not have an oil droplet but possesses a long, slowly tapering outer segment. It seems that in agreement with results obtained in other species, members of the double cones are spectrally identical in *Xenopus* (Röhlich and Szél, 2000). It is not known how the colorless oil droplets influence spectral sensitivity in cones and if the presence or absence of this structure changes anything related to color processing in this species.

B. Characteristics of the Photoreceptor Output to Second-Order Cells

The organization of the vertebrate retina shows several features that can be considered standard in phylogenetic development. The layered structure of the nervous tissue is practically identical in all major phylogenetic groups in vertebrates, as well as the basic cell types. This applies also to the organization of the photoreceptor synapse with second-order cells. One striking feature of this latter is that a postsynaptic triad consisting of a bipolar cell dendrite and two horizontal cell processes can be found at all synaptic sites. Another is that the presynaptic photoreceptor terminals contain synaptic ribbons. However, several details of this intricate structure are characteristic to amphibian species only. For example, both rods and cones have a central invagination, contacting several bipolar and horizontal cell processes. This means that all second-order cells receive mixed rod and cone signals (Dowling, 1968) and invites several functional consequences which will be discussed below.

1. Ultrastructure of the Photoreceptor Synapse

The photoreceptor terminals bear a large central invagination. The rods and cones can be distinguished on ultrastructural basis: rods have darker cytoplasm and contain less glycogen granules than cones in normal electron microscopic preparations. In the central invaginations of both rods and cones a neuropil area can be found. The photoreceptor terminal itself contains electron-dense synaptic ribbons, often more than 1 μm long (Fig. 1b). Round clear synaptic vesicles usually line up close to the ribbon. Occasionally dense-cored vesicles can also be seen here, the presence of which is regulated by lighting conditions (Osborne and Monaghan, 1976). We found that application of D2 dopamine receptor agonist induces the appearance of these dense cores, while D2 antagonists supress them.

The ribbon faces a membrane thickening within the terminal, the so-called arciform density. Vesicles are often seen in the process of exocytosis at this area. It has been shown that in retinal bipolar cells which contain similar ribbons, this part is the transmitter release site (von Gersdorff and Matthews, 1994), and this seems to hold true for photoreceptors too. The photoreceptor pedicles are usually laden with synaptic vesicles in their entire extent (Fig. 1b). This means that a large transmitter pool is readily available for release. Since photoreceptors release their transmitter tonically, a large transmitter pool is indeed required in order to be able to maintain this process. Among the synaptic vesicles, glycogen granules and small cysterns of smooth endoplasmic reticulum can be seen in some cases. The latter may be the site of the internal calcium stores which may release calcium upon stimulation of inositol-trisphosphate receptors (Peng *et al.,* 1991; Krizaj and Copenhagen, 1998). The number of ribbons in one photoreceptor terminal has been estimated to be around 15. In serial section reconstructions (R. Gábriel,

unpublished observations) the number of ribbons in rods is somewhat less (13 to 15) than in cones (16–22).

On the postsynaptic site, the triadic arrangement of the elements is clearly visible. Horizontal cell processes occupy the lateral positions in the triad, while a bipolar cell dendrite can be found in the middle (Fig. 1c). All three elements bear prominent postsynaptic densities. The horizontal cell processes may contain a few synaptic vesicles. Morphologically differentiated synaptic output sites, however, could not be identified in any part of the horizontal cells.

2. The Transmitter Substance

It has long been suggested that photoreceptors in all vertebrate species contain glutamate as a transmitter (Massey and Redburn, 1987; Copenhagen and Jahr, 1989; Marc *et al.,* 1990; Massey, 1990; Thoreson and Witkovsky, 1999). This has recently been proven unequivocally in *Xenopus* by biochemical measurement using a reduced retina preparation where only the photoreceptor layer has been left intact (Schmitz and Witkovsky, 1996). However, it still can be questioned if all the photoreceptor types contain and release glutamate as a transmitter. To data all evidence points to this direction. Light stimulation of rods and red-light-sensitive cones results in hyperpolarization in horizontal cells which can be blocked by non-NMDA ionotropic glutamate receptor blockers (Krizaj *et al.,* 1994). There is indirect evidence that blue-sensitive cones release glutamate. The chromatic horizontal cells receive inputs from rods and blue-sensitive cones only. Isolated chromatic horizontal cells respond only to exogenously applied glutamate agonists, but not for GABA or glycine (Witkovsky *et al.,* 1995). Nothing is known about the minor rods and miniature cones in this respect.

There has been one further transmitter candidate substance localized to the photoreceptors of the *Xenopus* retina. Carnosine (β-alanil-L-histidine dipeptide) has been found to colocalize with glutamate (Panzanelli *et al.,* 1997) and implied to be acting as a neuromodulator at GABA and glutamate receptors by virtue of its ability chelate Zn^{2+} ions. It is probable that carnosine is released from the photoreceptor terminals since it was localized to the synaptic vesicles (Pognetto *et al.,* 1992). It is also interesting to note that bipolar cells colocalize glutamate and carnosine (Panzanelli *et al.,* 1997); thus a similar situation can be supposed at the bipolar cell terminals.

3. Electrical Events at the Photoreceptor Terminal

The photoreceptors of the retina operate with a surprising twist in their physiology: they are continuosly depolarized in darkness, due to the fact that a cGMP-gated nonspecific cation channel is open and carries Na^+ and Ca^{2+} ions into the cell. When light is flashed on the cells, a number of enzymatic processes lead to the destruction of cGMP, the channel closes, and this leads to the hyperpolarization of

the photoreceptor cells. They, in turn decrease the rate of their transmitter release (Yau and Baylor, 1989). However, shaping of electric activity of the photoreceptors is not entirely dependent only on the phototransduction process. There are several further electrically active elements present in the photoreceptor cell. Therefore (i) the photoreceptor voltage response measured in the innner segment barely resembles to the transduction current and consequently (ii) transmitter release from the photoreceptor terminal is not necesserily identical to every identical photic stimuli. Paracrine effects and second messenger interactions have to be taken into account when one examines the transmitter release from the photoreceptor terminals. Some of these will be discussed further in section VI. The most important ion channels participating in this process belong to the family of K^+, Cl^-, and Ca^{2+} channels (Barnes, 1994).

Normally, photoreceptor resting potential is near -40 mV in the dark in cold-blooded vertebrates. Bright light may hyperpolarize this membrane potential to -70 mV, but the membrane potential bounces back to -50 mV within a few hundred milliseconds. This is due to the activation of voltage-dependent ion channels. The I_h current of rods and cones was characterized as a slow, monovalent cation current activated by hyperpolarization between -50 and -90 mV (Attwell *et al.,* 1982; Hestrin, 1987). The same current is present in *Xenopus* photoreceptors and has been shown to be prone to neuromodulation (Akopian and Witkovsky, 1996; Akopian, 2000). Another slow potassium current is able to shape the photoreceptor response when its amplitude is small. This current plays a crucial role in rod function since it is active between -30 and -70 mV and does not inactivate. It was termed K_x and seems to be essential in setting the rod resting potential (Hestrin, 1987). During mild hyperpolarization these channels deactivate, thus speeding up the rod voltage response by more than 10% (Beech and Barnes, 1989). The two currents are complimentary and the channels that mediate them operate throughout the photoreceptor range. All in all, cooperative action of these channels provide the basis for fine tuning the membrane potential of the cell to best suit the transmitter release machinery. Cloride channels also play some role in shaping photoreceptor light responses. Depletion of intracellular Cl^- leads to a decrease in L-type Ca-channel conductance which may lead to a decrease in transmitter release (Thoreson *et al.,* 2000). Cloride ions seem to interact directly with the intracellular surface of the Ca-channel. It can be calculated that transmitter release may be reduced by as much as 40% (Thoreson *et al.,* 2000). Nevertheless, cloride ions seem to contribute to the so-called prolonged depolarization *in vivo.* Prolonged depolarization can be induced in photoreceptors by surround illumination and thus it is related to the activation of the negative feedback system (Thoreson and Burkhardt, 1990, 1991). Whole cell patch-clamped cones under prolonged depolarization showed a robust activation of Ca-activated Cl-conductance. The initial calcium spikes seem to be essential to the activation of this conductance (Barnes and Deschnes, 1992). This process contributes to the complete repolarization of the photoreceptor cell membrane (Barnes, 1994). A metabolic factor that may influence the photoreceptor

output synapse is the pH of the extracellular space. The pH changes (up to 0.2 pH unit) are known to occur as a result of reduced metabolic activity of the outer segment upon light stimulation. External alkalinization from pH 7 to pH 8 shifted the voltage dependence of the calcium channel activation negative by 12 mV (Barnes *et al.,* 1993). This results in larger Ca-current and increased transmitter release.

Homologous photoreceptors (at least principal rods and red cones) in anuran retinas are coupled into networks (Gold, 1979; Gold and Dowling, 1979; Krizaj *et al.,* 1998). Signal from one cell to the neighboring photoreceptors spreads via gap juctions. This couples the adaptational state of the cells and also the response to light itself. Increasing the diameter of the light spot shone onto the photoreceptors up to 50 μm resulted in a continously larger response. With large spots (above 500 μm), however, less hyperpolarization was produced (Baylor *et al.,* 1971). This latter fenomenon, at least in the case of cones, is due to feed-back from horizontal cells (see section IV).

4. Ion Channels Involved in Transmitter Release

It is generally accepted that synaptic release of neurotransmitters requires increased Ca^{2+} concentration at the release site. In most cases voltage-gated Ca^{2+} channels provide the means of entry into the terminal from the extracellular space. Both rod and cone terminals seem to bear L-type calcium channels as was defined indirectly in pharmacological experiments (Barnes and Hille, 1989). Later this finding was confirmed in *Xenopus* utilizing reduced retina preparations and bioluminescence measuerement of glutamate (Schmitz and Witkovsky, 1997; Witkovsky, 2000). Glutamate release is in linear relation with the activation of L-type Ca-channels and the internal Ca^{2+} concentration (Witkovsky *et al.,* 1997). It is also possible that calcium released from intracellular stores may contribute to regulation of transmitter release. Ca-induced Ca^{2+} release may act as a negative feedback and reduce glutamate release (Krizaj *et al.,* 1999).

IV. Anatomy and Physiology of the Second-Order Cells

The second-order cells of the retina are the bipolar and horizontal cells. Bipolar cells of the vertebrate retina come approximately in 10 subtypes (Kolb *et al.,* 1981; Martin and Grünert, 1991; Euler and Wässle 1995), while the horizontal cells may be divided into one to four subtypes based on morphological criteria (Stell and Lightfoot, 1975; Leeper, 1978; Röhrenbeck *et al.,* 1987; Peichl and Gonzalez-Soriano, 1994). Bipolar cells of the vertebrate retina mostly contain glutamate as a transmitter regardless of their physiological nature (Ehinger *et al.,* 1988; Marc *et al.,* 1990). Certain bipolar cell types may contain distinguishing neurochemical markers.

Both the bipolar and the horizontal cells are placed preferentially in the outer half of the IPL, and in frogs they are mostly supposed to be present in the outer row of cells (Zhu *et al.,* 1990). Some bipolar cells may be displaced into the photoreceptor layer, but displacement of these cells is rare in frogs.

A. Bipolar Cells

Surprisingly, there have been very few studies published in the literature regarding bipolar cells of the anuran retina. Morphological descriptions of 10 bipolar cell subtypes have been published for *Rana* species (Shkolnik-Yarros and Podugolnikova, 1979), but no comprehensive studies have been carried out in *Xenopus* to date. We know only that they contain calretinin (Fig. 2a) and their total number is about 6000/mm^2 (Wilhelm and Gábriel, 1999). Some bipolar cells in the anuran retina immunoreactive for GABA (Mosinger *et al.,* 1986; Gábriel *et al.,* 1992) and/or its synthesizing enzyme, glutamic acid decarboxylase (Agardh *et al.,* 1987). GABA-positive bipolar cells in *Xenopus* are able to accumulate, but not synthesize, serotonin (Zhu *et al.,* 1992; Zhu and Straznicky, 1993).
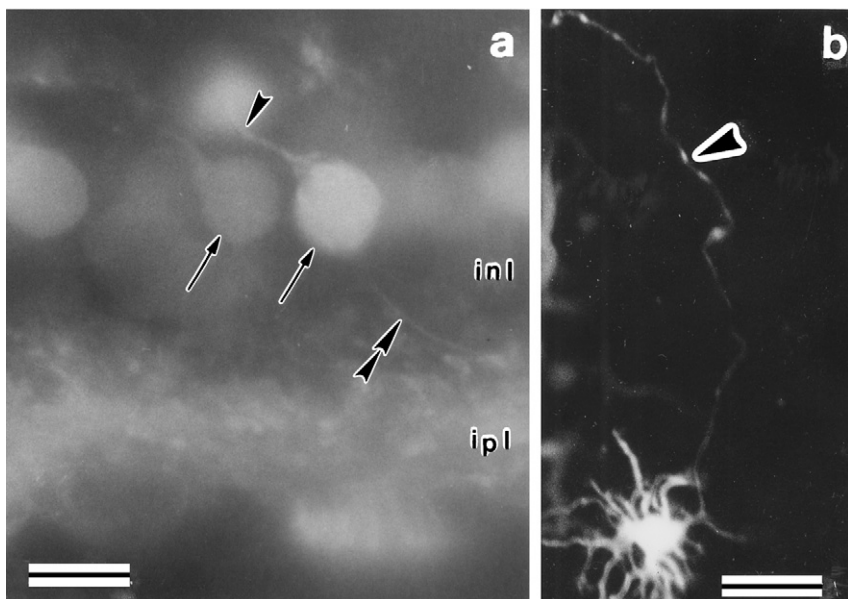
FIG. 2 Photomicrographs of second-order cells. (a) Bipolar cells (arrows) in the inner nuclear layer (INL) labeled with calretinin immunocytochemistry. Arrowhead, dendritic process running toward the outer retina; double arrowhead, axonal process which enters the inner plexiform layer (IPL). Bar = 15 μm. (b) Luminosity-type horizontal cell filled with Lucifer Yellow. Arrowhead, the long, thin and varicose initial part of the axon. Bar = 20 μm. Courtesy of Dr. J. Vígh.

Bipolar cells of the vertebrate retina come in two major physiological varieties: hyperpolarizing and depolarizing cells. Besides, most of them show center-surround organization, hyperpolarizing bipolars being OFF-center while depolarizing ones are ON-center cells (Famiglietti and Kolb, 1976). In the next paragraph we have collected all the available information on *Xenopus* retinal bipolar cells. The most complete physiological description derives from Stone and Schütte (1991). Unless indicated otherwise, description of physiology and pharmacology of these cells is made on the basis of their study.

1. Hyperpolarizing (OFF-Center) Bipolar Cells

Red flashes evoked more and more transient responses from these cells as the diameter of the light spot was increased. The same cells produced depolarizing responses when they were illuminated with annuli with an inner diameter larger than 0.25 mm. The depolarizing responses were followed by afterhyperpolarization.

Glycine consistently suppressed the depolarizing surround response in OFF-center bipolar cells, and reduced the amplitude of the center response. GABA caused a substantial reduction of the hyperpolarizing response and only a slight reduction in the depolarizing surround response in these cells. Clearly, the physiological observations and the results of pharmacological experiments indicate a strong center-surround antagonism which is mediated through amacrine cells of the inner retina.

OFF-center bipolar cells had their major axonal branches in sublaminas 1 and 2 in the inner plexiform layer. One type is almost certainly the GABA-containing serotonin-accumulating bipolar cell (Schütte and Witkovsky, 1990; Zhu and Straznicky, 1993). The neurochemical signature of the other OFF-center bipolar cells is not known. Occasionally, additional fine branches of these cells descended into the deeper sublaminas of the inner plexiform layer. Golgi impregnation confirmed this finding (Witkovsky *et al.,* 1994). Out of the seven bipolar cells types shown in this paper only three showed branches confined to either the OFF or the ON sublayer of the inner plexiform layer; the other four violated the rule of the morphological segregation of ON and OFF channels at the bipolar cell level as described for mammals (Famiglietti and Kolb, 1976; Miller and Dacheux, 1976). Therefore physiology and morphology of bipolar cells in *Xenopus* cannot be reconciled in the same fashion as in mammals.

Bipolar cells of the *Xenopus* retina receive inputs from both rods and cones in the outer plexiform layer as evidenced by both anatomical and physiological methods (Gábriel *et al.,* 1993; Krizaj, 1995). This is in contrast with the mammalian retina where rod and cone signal reaches the ganglion cells through a separate neural network (Sterling *et al.,* 1988). They were found to synapse preferentially with amacrine cell dendrites in the inner plexiform layer (Dubin, 1970; Gábriel and Straznicky, 1993; Buzás *et al.,* 1996). However, a significant proportion of bipolar cell axons formed direct contacts with retrogradely filled ganglion cell

dendrites, indicating that OFF-center bipolar cells may have a more direct influence on the retinal output to the visual centers than their ON-center counterparts (Buzás *et al.,* 1996). This finding is further substantiated by the fact that in *Xenopus* more types of OFF- than ON-center ganglion cells could be identified morphologically (Straznicky and Straznicky, 1988).

2. Depolarizing Bipolar Cells

Small spots with fixed intensity evoked sustained responses in ON-bipolar cells. The larger the spot size was increased, the more transient the response grew. The effect of antagonistic surround could similarly be observed as in the case of the OFF-center cells. A permanent feature of these cells was the delayed afterhyperpolarization, which peaked 125–300 ms after light OFF, and it took 1.1–2.2 s for the cells to recover. The largest amplitude and the fastest times to peak were observed in the presence of background illumination. Glycine decreased the center response by about 30–70% and also eliminated the afterhyperpolarization as well as the hyperpolarizing surround response. GABA did not change the center response significantly, only decreased the surround hyperpolarization dramatically.

Neither the exact morphology nor the neurochemical signatures of the ON-center cells are known in *Xenopus*. However, recently we have managed to record and fill intracellularly (Fig. 3) a wide-field ON bipolar cell (D. Krizaj, R. Gábriel, and P. Witkovsky, unpublished results), which morphologically resembles the blue ON bipolar cells of mammals (Mariani, 1984). This cell had wider dendritic than
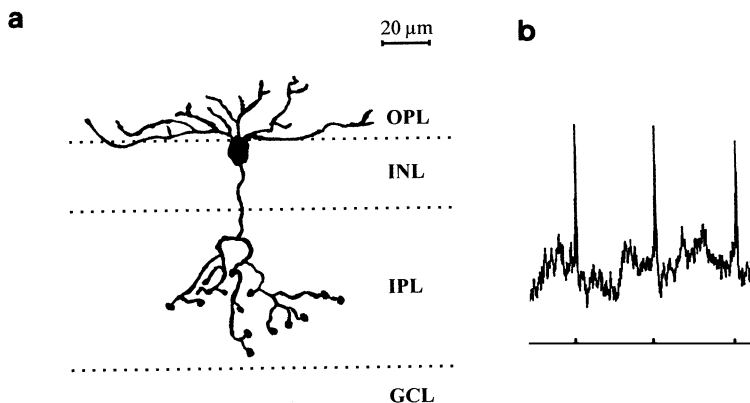
FIG. 3   Wide-field bipolar cell. (a) Drawing of a wide-field depolarizing (ON) bipolar cell filled with neurobiotin. OPL, outer plexiform layer: INL, inner nuclear layer: IPL, inner plexiform layer: GCL, ganglion cell layer. (b) Light response of the same cell for red flashes at 90% of saturating light intesity. OPL, outer plexiform layer; INL, inner nuclear layer; IPL, inner plexiform layer; GCL, ganglion cell layer. Flashes were for 20 ms in 1-s intervals, the maximum voltage response of the bipolar cell is 15 mV.

axonal field and did not show clear color opponency but instead seemed to respond nearly equally well to all visible wavelengths; therefore it most probably is not in the service of processing color information.

B. Horizontal Cells

Horizontal cells of the frog retina have been classified into two major classes: axon-bearing and axonless horizontal cells (Stephan and Weiler, 1981). This classification seems to be standing true for all amphibians. Morphology correlates well with physiology and neurochemistry: the two kinds of horizontal cells bear distinct physiological characteristics and neurochemical composition. Here below we used the physiological classification for introducing these cells.

1. Luminosity Cells

Luminosity cells hyperpolarize to stimuli of all wavelengths (Witkovsky and Stone, 1983; Witkovsky *et al.,* 1988a). The hyperpolarization is due to a glutamate-induced AMPA-type conductance (Krizaj *et al.,* 1994). These cells have been identified as oval-shaped, slightly flattened cells in the outer row of cells in the INL, bearing long axonal processes (Witkovsky *et al.,* 1988a). They show substantial tracer coupling if injected with neurobiotin (Wilhelm and Gábriel, 1999), but none when injected with Lucifer Yellow (Fig. 2b). The axons of these cells run in the OPL, although occasionally they can be seen among the cells of the INL. These processes can be up to about 1 mm long, and electrically they are isolated from the cell body, forming independent information processing units. The axon terminals enter the photoreceptor pedicles and interact directly with different photoreceptor cell types (see in section V).

   As morphology suggests, the luminosity cells are composed of two functional units. The cell body region has a mean length constant of 170 μm while the axonal arbor 450 μm (Stone and Witkovsky, 1987). The two anatomical and functional units are connected with a small diameter single axonal process (Witkovsky *et al.,* 1988a) which effectively isolates the cell body from the axon terminal.

   Luminosity cells form a slightly irregular mosaic with a dendritic coverage factor of 3.3 and an average density of about 1000 cells/mm^2. The cells bear short dendrites emerging directly from the cell body and reaching directly toward the photoreceptors. They seem to contact all the photoreceptor cells within their dendritic field.

2. Chromacity Cells

Horizontal cells that respond differentially to different wavelength of the spectrum are called chromacity cells or chromatic horizontal cells. There is one such cell

type in *Xenopus,* the green–red chromatic cell. This cell hyperpolarizes to blue and green light but depolarizes to red light and shows the typical morphology of axonless horizontal cells (Stone *et al.,* 1990). They are flattened cells located in the outer row of the INL, possessing three to five main dendritic branches which are smooth and bear short club-like or claw-like terminals (Stone *et al.,* 1990; Wilhelm and Gábriel, 1999) which contact selected photoreceptors or receptor clusters. They form a slightly irregular mosaic with a coverage factor of 5.2 and an average density of about 400 cells/mm^2. If injected intracellularly with neurobiotin, these cells show tracer coupling, whereas Lucifer Yellow or horseradish peroxidase are unable to pass from one cell to the other (Wilhelm and Gábriel, 1999).

The hyperpolarizing response is mediated by glutamate released from the photoreceptors they contact (Stone *et al.,* 1990) while the depolarizing response is due to a GABAergic feedback from luminosity horizontal cells to the red cones (Witkovsky *et al.,* 1995). GABA did not affect the response properties of these cells. In contrast, glycine consistently eliminated the depolarizing component of the response (Stone *et al.,* 1990). It has been shown later that glycine achieves this effect indirectly, acting through the luminosity horizontal cells possibly by inhibiting their feedback to the red-sensitive cones (Witkovsky *et al.,* 1995). Indeed, there was little if any interaction of the red- and blue-evoked responses of these cells revealed in white noise analysis (Stone, 1994). Currently we do not know the transmitter(s) present in this cell type.

V. Synaptic Connectivity in the Outer Retina

Synaptic connections are subdivided into two major categories: electrical contacts and chemical contacts. The place of synapses in the outer retina is the outer plexiform layer, although as we will see in this section, electrical contacts and possible nonsynaptic interactions may also occur elsewhere. Both types of contacts are seen in the outer retina. Here we describe first the electrical connections and later the chemical synapses.

A. Electrical Synapses

Electrical synapses are present in higher number in the retinas of vertebrates than in other parts of the central nervous system. Therefore their importance in retinal information processing has been considered substantial (Wässle and Boycott, 1991; Cook and Becker, 1995).

It has been known for some time that the major types of anuran photoreceptors, principal rods and red cones (Gold and Dowling, 1979), and the horizontal cells (Stone and Witkovsky, 1987; Krizaj, 1995; Witkovsky *et al.,* 1995) are connected

with homologous gap junctions. These junctions are frequent, enabling the receptors to reduce inherent electrical noise associated with the phototransduction machinery and the horizontal cells to average their input over the entire retinal network. The connexins that are involved in the formation of gap junctions in the amphibian retina are largely unknown.

1. Homologous Junctions

Red cones and the principal rods are coupled to each other with homologous junctions. Rods interact with one another by pooling their signals, so that in dark-adapted rods at least 85% of the response recorded from a single rod is generated by pigment molecules bleached in other receptors (Fain, 1975). The red cone network probably works along the same principles. The homologous junctions between photoreceptors cannot be modified by dopaminergic ligands.

Both luminosity and chromatic horizontal cells are also coupled among themselves with homologous gap junctions of rather big size. These junctions are easily identifiable under an electron microscope; therefore it is surprising that Lucifer Yellow does not penetrate these junctions. However, neurobiotin, a low-molecular-weight tracer that routinely passes most of the retinal gap junctions (Vaney, 1991), does (Wilhelm and Gábriel, 1999). These junctions are modifiable with D1 receptor ligands and gap junctions can be uncoupled with intracellular injection of cAMP in *Xenopus* (Krizaj, 1995, 2000).

Homologous coupling of any type of bipolar cell has not been reported in the literature to date.

2. Heterologous Junctions

As was first pointed out by Raviola and Gilula (1973), gap junctions can be present between heterologous photoreceptors. While homologous junctions are usually not regulated by endogenous retinal neurotransmitters, the heterologous coupling is prone to regulation through D2 dopamine receptors (Krizaj *et al.,* 1998; Krizaj, 2000). It has also been shown recently, that rod–cone gap junctions, though fewer in number and smaller in size, can be localized to the inner segment of the photoreceptors in *Xenopus*. Since heterologous junctions are not formed between all cones and rods, coupled rods and cones serve as "hot spots" during photoreceptor signaling in the mesopic state when both systems are active (Krizaj, 2000). However, the fairly small size of these junctions limits their capability of spreading signals into the network (Krizaj *et al.,* 1998). Therefore regularly spaced hot spots are required to maintain even information flow from the rod system to cones, and maybe vice versa.

Heterologous junctions between horizontal cells were not observed in the *Xenopus* retina. Similarly, coupling of bipolar cell types either to each other or to other cell types is unknown at present.

B. Chemical Synapses

As has been described formerly a major synaptic conglomerate is found at the photoreceptor bases (both rods and cones) in the *Xenopus* retina. The most conspicuous element of this complex is the synaptic triad found at the ribbons of the photoreceptor cells. The postsynaptic triad contains dendrites of bipolar and horizontal cells.

Less numerous are the other chemical synapses of the outer plexiform layer. These are formed by horizontal and interplexiform cells as presynaptic elements. Besides morphologically specialized synapses nonsynaptic interaction also takes place here: short-range interactions between horizontal cells, interplexiform cell axon terminals and photoreceptors, and long-range interactions by way of substances that diffuse from the inner to the outer retina. Short-range interactions will be discussed in this section, while the long-range ones will be discussed in section VI.

1. Photoreceptor to Bipolar Cell Synapses

Bipolar cells receive their inputs at the ribbon synapses in both rod and cone pedicles (Fig. 1c). They invaginate deeply into the photoreceptor terminals and occupy mostly central position in the postsynaptic triad (Dowling, 1968; Gábriel *et al.,* 1993). It is assumed that all anuran retinal bipolar cells seem to receive mixed rod and cone input, and this has been unequivocally demonstrated in the case of serotonin-accumulating bipolar cells in *Xenopus* (Gábriel *et al.,* 1993). One bipolar cell may receive more than one synapse in one photoreceptor terminal. Physiological evidence for the mixed photoreceptor input is also available in anuran species (Belgum and Copenhagen, 1988; Krizaj, 1995).

Bipolar cells exhibit linear scaling properties and temporal filtering and saturate at high light intensities. Cone inputs tonically suppress rod inputs; however, in dark-adapted bipolar cells cone signals are not suppressed. Hyperpolarizing cells bear AMPA/kainate type receptors while depolarizing cells transduce the glutamatergic signals with metabotropic glutamate receptor 6 (Krizaj, 1995; Thoreson and Witkovsky, 1999). Currently we do not know if GABA-containing bipolar cells differ in their receptors from the other bipolar cell types.

It has been shown that biplexiform ganglion cells exist in the retina of *Xenopus* (Tóth and Straznicky, 1989) and that they extend their processes into the outer plexiform layer and invade the photoreceptor terminals, synapsing with both rods and cones. These dendrites occupy central positions at the photoreceptor ribbon; thus regarding their connectivity they seem to behave like bipolar cells (Straznicky and Gábriel, 1995). Biplexiform ganglion cells have been inferred to be involved in a fast feed-forward pathway that could circumvent the complicated and slow retinal information processing pathway and would transfer information to the brain with a minimal time delay.

2. Photoreceptor to Horizontal Cell Synapses

Horizontal cells dendrites usually occupy lateral positions in the postsynaptic triad. Both luminosity type and chromatic cells contact the photoreceptors, although in slightly different fashion.

Luminosity cells contact all photoreceptors within their dendritic field (Wilhelm and Gábriel, 1999). They seem to extend only few dendritic branches into one photoreceptor pedicle. The axons of these cells travel to considerable distance (up to 1 mm) and form specialized junctions with photoreceptors (Witkovsky *et al.,* 1988a). Both rods and cones contact the head of the spine-like protrusions of horizontal cell axons.

Luminosity cells posses ionotropic glutamate receptors of the AMPA/kainate type. These have been shown by electrophysiological methods (Krizaj *et al.,* 1994). Despite all of our efforts we could not label these proteins with immunocyto-chemical methods (R. Gábriel and P. Witkovsky, unpublished results), although their presence could be verified in Western blots (R. Wenthold, pers. commun.). Since horizontal cells receive inputs from both rods and cones, the question arises if both synapses use the same receptor complexes. To date, compelling evidence has not been gathered in this respect. However, results indicate that both rod and cone responses can be blocked with the same drugs, suggesting the presence of a single type of glutamate receptors. The subunit compositions of this receptor complex, however, is unknown at present. However, the linear voltage/current relationship suggests the involvement of the low affinity gluta-mate receptor type 2 subunit in the receptor complex (Thoreson and Witkovsky, 1999).

Another major transmitter receptor family present in luminosity horizontal cells is the GABA receptors. Luminosity cells seem to posses both $GABA_A$ and $GABA_C$ receptors; the latter type may be serving as autoreceptor by regulating GABA release (Djamgoz, 1995). Since most of the distal retinal neurons typically respond tonically to prolonged stimuli, it may be of advantage to have such receptors on the horizontal cells (Qian and Dowling, 1993).

Apart from the ligand-gated channels that drive the horizontal cell membrane potential, voltage-gated channels also play a significant part in shaping the mem-brane properties of horizontal cells. Both L- and T-type calcium currents could be identified. The transient A-type potassium current in these cells was found to be calcium-dependent in *Xenopus* horizontal cells (Akopian and Witkovsky, 1992; Akopian, 2000).

Chromatic cells seem to be selective in forming their synaptic contacts. They preferentially contact blue cones (Witkovsky *et al.,* 1995); however, about one-quarter of their contacts are made with rods (Wilhelm and Gábriel, 1999). They seem not to provide any specialized synaptic outputs in the outer plexiform layer. At the same time, they form multiple synapses within one photoreceptor base and contact all the blue cones within their dendritic field (Wilhelm and Gábriel,

1999), resembling the blue-cone horizontal cells of Equids (Sandmann *et al.,* 1996) to some extent. Chromatic cells respond to glutamate and seem to posses similar glutamate receptors and intrinsic channels to those described on luminosity cells. However, it does not respond for glycine and GABA (Witkovsky *et al.,* 1995). The transmitter content of the cell is not known, nor its potential targets.

Horizontal cells receive numerous inputs but seem to provide very few output synapses in the *Xenopus* retina. Indeed, release of its transmitter, GABA, seems to be nonsynaptic, depending rather on ligand-gated channel-mediated sodium influx than on the membrane potential of the cell (Cunningham *et al.,* 1988). Infrequent, small synaptic contacts (or rather presynaptic vesicle accumulation without prominent postsynaptic specializations) were observed from luminosity type horizontal cells to bipolar cell dendrites (Gábriel *et al.,* 1993). Although there are no specialized synaptic contacts found between horizontal cells and cone photoreceptors where horizontal cells would occupy presynaptic positions, there is evidence for feedback. The existence of this mechanism was originally observed in turtle (Baylor *et al.,* 1971) and subsequently shown indirecty in *Xenopus* (Stone *et al.,* 1990). The fundamental electrical manifestation of the feedback is a maintained, depolarizing potential that is graded with the intensity and/or spatial extent of illumination in the receptive field surround (Burkhardt, 1993). Later direct evidence has been provided by showing that the depolarizing response of the chromatic horizontal cell arises as a consequence of GABAergic feedback from luminosity cells to the red cones (Witkovsky *et al.,* 1995). The site of feedback could not be determined in *Xenopus*. There is some evidence that the feedback maybe mediated at the spinules of the horizontal cells in fish (Wagner and Djamgoz, 1993), but these structures, despite all of our efforts (R. Gábriel and P. Witkovsky, unpublished) could not be found in frog. The feedback is mediated largely through $GABA_A$ and in smaller part $GABA_C$ receptors (Djamgoz, 1995; Lukasiewicz, 1996).

GABA released from the horizontal cells may also affect other luminosity-type horizontal cells but not the chromatic cells (Witkovsky *et al.,* 1995). The effect of GABA on bipolar cell dendrites has not been studied to date in *Xenopus,* and could neither be found in other amphibians (Djamgoz, 1995; Lukasiewicz, 1996). In contrast, pharmacological evidence for the presence of all the three GABA receptor subtypes on the bipolar cell axon terminal could be furnished (Tachibana and Kaneko, 1987; Slaughter, 1995; Lukasiewicz, 1996). This is likely to be the case in *Xenopus,* too.

3. Feedback from the Inner Retina to the Outer Plexiform Layer

Information from the outer to the inner plexiform layer is carried by the bipolar cells. However, this process is influenced by the interplexiform cells. Interplexiform

cells are a class of neurons that have dendritic branches in the inner plexiform layer and receive inputs from bipolar and amacrine cells and emit axonal processes toward the outer retina. In the amphibian retina two neurochemically identified cell types have been classified as interplexiform cells.

Some of the dopaminergic cells have been shown to emit processes toward the outer plexiform layer either from the cell body or from the horizontal processes in sublamina 1 of the inner plexiform layer (Gábriel *et al.,* 1991; Schütte and Witkovsky 1991; Witkovsky *et al.,* 1994). The processes directed toward the outer plexiform layer do not form synapses with any of the other elements but seem to release their dopamine content nonsynaptically (Gábriel *et al.,* 1991). The effect of dopamine will be discussed in detail in section VI.

The second type of interplexiform cell in the anuran retina is the glycinergic cell. First these were identified on the basis of their glycine uptake (Voaden *et al.,* 1974) and 14 years later somatostatin could be colocalized in these cells (Smiley and Basinger, 1988). The processes of these cells which ramify in the outer plexiform layer could not be found in contact with those of the luminosity horizontal cells (Kleinschmidt and Yazulla, 1984) in spite of the fact that luminosity cells posses functional glycine receptors (Witkovsky and Stone, 1987; Witkovsky *et al.,* 1995). Profiles with ultrastructure identical to those that accumulate glycine were seen to contact dendritic processes in the outer plexiform layer near the bases of the photoreceptors (R. Gábriel and P. Witkovsky, unpublished observations) and somatostatin-immunoreactive fibers were seen to form pericellular baskets around cell bodies in the outermost row of the inner nuclear layer (Vígh *et al.,* 2000). The neuromodulatory role of somatostatin will be described and discussed in detail in section VI.

Although the results of neurochemical and ultrastructural studies are somewhat contraversial, physiological evidence, however, points to the direction that glycine released from the glycinergic interplexiform cell may have influence on both horizontal and bipolar cell function. Glycine application depolarized the dark membrane potential of luminosity horizontal cells to the level of E_{Cl} and also drastically reduced the light responsiveness for all wavelengths. Glycine seems to supress cone input more than rod input in these cells (Witkovsky and Stone, 1987). Glycine consistently suppressed the depolarizing surround response in OFF-center bipolar cells. In both ON and OFF bipolar cells it reduced the amplitude of the center response. It also eliminated the center afterhyperpolarization as well as the hyperpolarizing surround response in ON bipolar cells (Stone and Schütte, 1991). Whether all these responses originated in the inner retina or at least some of them partially were mediated in the outer retina remains to be examined. All in all, the topic of interplexiform cell function in retinal information processing is far from being settled. The main obstacle of research into this problem seems to be the scarcity of these cells, may they belong to any one of the above-mentioned neurochemically identified cell types.

VI. Neuromodulation of the Outer Retinal Synapses

Neuromodulation is defined as "...the ability of neurons to alter their eletrical properties in response to intracellularbiochemical changes resulting from synaptic or hormonal stimulation" (Kaczmarek and Levitan, 1987). Many if not most receptors and ion channels are dynamic and have more than one conformational state. The integrative aspect of neuromodulation involves the interaction between ligand- and voltage-gated channels, protein kinases, and phosphatases and the effect of small second messenger molecules or ions. The list of potential neuromodulators in the *Xenopus* retina is long (dopamine, serotonin, at least half a dozen or so neuropeptides, NO), and most of the neurons which contain these substances are localized to the amacrine cell layer and their processes ramify in the inner retina (Vígh *et al.,* 2000). Therefore volume transmission must play a substantial role if these substances are to act in the outer retinal layers too. Indeed, there is mismatch between the site of release and the receptor location regarding at least three substances (see below).

The effects of two such neuromodulators, dopamine and somatostatin, have been been studied to date in detail. Although some of the result described below derives from experiments done in tiger salamander retina, we believe that most of the processes discussed are fundamentally identical in all terrestrial cold-blooded vertebrates.

A. Dopamine

The first precise anatomical description of dopaminergic neurons of the vertebrate retina appeared quite late in the literature (Török and Stone, 1979). Since then it became clear that the dopaminergic neuron is one of the most conserved cell types in the vertebrate retina (Dacey, 1990; Vaney, 1990; Witkovsky and Dearry 1991). It has been shown that these cells have a bi- or tristratified dendritic tree, form a rare but regular mosaic, and bear axon-like processes. All these features were found to be true in *Xenopus* (Schütte and Witkovsky, 1991; Zhu and Straznicky, 1991). It has also been found that about 20% of the dopaminergic cells send processes toward the outer retina but some of these axons never reach the outermost retinal layes (Witkovsky *et al.,* 1994). These cells release dopamine by light stimulation and maintain a high (up to 1 μm) extracellular concentration during illumination (Boatright *et al.,* 1989; Witkovsky *et al.,* 1993) and this substance exerts a powerful effect on photoreceptor to second-order cell communication (Krizaj and Witkovsky, 1993). Dopamine appears to function as a classic neuromodulator in the retina: (i) not dependent on point-to-point anatomical connection in every case, (ii) does not open or close ion channels directly, but rather works through second messengers, and (iii) acts slowly and diffusely and its actions are

long lasting, on the time scale of minutes to hours (Witkovsky and Dearry, 1991). These statements are particularly true for the outer retina, as we shall describe here below.

1. Effect on Photoreceptors

The effect of dopamine on photoreceptors can be discussed in the following contexts: (i) influence on retinomotor movements, (ii) effect on voltage-gated channels, (iii) rod-cone communication, and (iv) relation to the circadian cycle. While the first three of the four aspects are directly related to light adaptation and will be discussed here, the fourth one belongs more to the general concept of cyclic processes and will be briefly discussed in section VI. D of this chapter.

Retinomotor movements are more prominent in cones than in rods in *Xenopus* (Besharshe and Witkovsky, 1992). Cones usually contract while rods elongate in constant light thus providing optimal geometry for photon capturing of the former photoreceptor type and minimize damage to the sensitive pigment system of rods (Currie *et al.,* 1978).

As has been described in section IV, intrinsic currents of the photoreceptor inner segments modify the output properties rods and cones, out of which one of the most prominents is I_h, a hyperpolarization-activated Na^+/K^+ current. In *Xenopus* retinal rods dopamine reversibly reduced I_h through a D2 receptor-mediated mechanism (Akopian and Witkovsky, 1996). This means that in the presence of dopamine rod synaptic transmission will be impaired, since the plateau phase of the rod response will occur at a more hyperpolarized voltage than without, at which level synaptic transmission is reduced. This goes well with the fact that dopamine promotes cone to second-order neuron transmission but reduces rod to second-order cell information transfer (Witkovsky *et al.,* 1988b; Akopian, 2000). It is not known, however, what if any effect dopamine has on I_h of cones.

Another issue to be considered here is the modification of heterologous rod/cone gap junctions. The existence of these junctions and their functional modification by light have been first proposed on the basis of electrophysiological experiments by Yang and Wu (1989) in tiger salamander retina. Similar junctions have been identified between rods and cones in *Xenopus*. They were localized to the inner segments of the photoreceptors slightly distal to the fins (Krizaj *et al.,* 1998). The flicker response of rods increased if the retinas became light-adapted or were treated with D2 receptor agonists. Injection of neurobiotin in the presence of D2 receptor agonists and antagonists confirmed the involvement of this receptor in the modulation of gap junction permeability. On average, every sixth rod couples directly to a cone. Mathematical modeling showed that at least the next three neighbors of the rods which are connected with gap junction to a cone receive substantial electrical input (Krizaj *et al.,* 1998). This arrangement provides means for the rod and cone signals to mix presynaptically and thus enables effective visual

signal processing in the mesopic state where both rods and cones are active. The balance of rod and cone output signals, therefore, is set at least partially already at the level of the photoreceptors.

2. Effect on Bipolar Cells

Bipolar cells are crucial elements in retinal information processing, since this is the cell type that carries the signals from the outer to the inner retina. Yet, we have comparatively the least information on how dopamine influences their functional states. Dopamine depolarized the OFF-center and hyperpolarized the ON-center cells and enhanced the center responses in goldfish (Hedden and Dowling, 1978) and a similar effect could be observed at the ganglion cell level in rabbit (Jensen and Daw, 1984). Application of both D1 and D2 dopaminergic agonists seem to enhance both the flash and the flicker responses of bipolar cells in *Xenopus*. Additionally, D1 receptor-mediated mechanisms participate in preserving responsiveness of bipolar cells when background light is applied (Krizaj, 1995). It is unknown at present exactly which intracellular mechanisms act this way, although it can be inferred that dopamine may have multiple sites of action.

Dopamine also seems to enhance the glutamate-gated currents of hyperpolarizing (OFF) bipolar cells by a cAMP-activated mechanism in tiger salamander. It was also verified that it did not enhance the amplitude of unitary events but increased the frequency and duration of channel openings. Bipolar cells receive inputs from rods and cones, but it must be noted that dopamine may regulate only those cells that are associated with cone input (Maguire and Werblin, 1994). This implies that ionotropic glutamate receptor complexes in bipolar cells may have different subunit composition at the site of rod and cone inputs (Thoreson and Witkovsky, 1999).

3. Effect on Horizontal Cells

Several groups have provided solid data that application of dopamine and D1 receptor agonists lead to reduction of both electrical and dye coupling between horizontal cells in almost all vertebrate retinas (Witkovsky and Dearry, 1991). The situation is quite similar in *Xenopus*. Injection of cAMP into the cells uncouples the horizontal cell network. The drugs that activate D1 receptors also have other profound effects on the physiology of the horizontal cells. The responses of the horizontal cells become cone-dominated and resemble those of the light-adapted horizontal cells in the following properties: (i) the rod component could not be detected, (ii) red flicker responses are potentiated, and (iii) the green flicker response is abolished. Dopamine also augments the inward currents elicited by glutamate and kainate (Krizaj *et al.,* 1994). Depletion of dopamine resulted in a horizontal cell response resembling those derived from dark-adapted retinas (Witkovsky and Shi, 1990).

Both D1 and D2 receptors were localized in the outer plexiform layer of the frog retina. Dopamine D2 receptors were mostly found on photorecepors while D1 receptors on horizontal cells (Wagner *et al.,*1993; Behrens and Wagner, 1995). Although both D1 and D2 agonists elicited qualitatively similar effects, the D1 agonists produced a quantitatively greater increase in the amplitude and accelerated the kinetics of the cone input (Witkovsky *et al.,* 1989). These findings indicate that dopamine and related ligands act primarily through the cone pathway. It seems that dopamine is both necessery and sufficient to mimic the light adaptation process in the *Xenopus* retina (Krizaj, 2000), and one critical component of this adapatation, the efficacy of the photoreceptor to horizontal cell synaptic transfer is almost entirely controlled by the dopaminergic system in the retina. Since horizontal cells contribute to the surround organization of the bipolar cells, it is obvious that apart from the direct effect of dopamine on the bipolar cells themselves, indirect effects of dopamine through the horizontal cell network can also be expected on the signal that is carried into the inner plexiform layer.

Recently, however, another monoamine, serotonin came into consideration as potential presynaptic modulator of the transmitter release at the photoreceptor synapse. Serotonin 2a receptors were localized to photoreceptor cell terminals in rabbit (Pootnakit *et al.,* 1999), which could control intracellular Ca^{2+} level through release from intracellular stores. This would modify transmitter release and this change may affect both the membrane potential and the response properties of the second-order cells, including the horizontal cells. Endogenous serotonin levels were found to be high in the frog retina (Tornquist *et al.,* 1983) and this substance has been localized to numerous amacrine cells in *Xenopus* (Schütte and Witkovsky, 1990; Zhu *et al.,* 1992); therefore, it cannot be excluded that this substance, similarly to dopamine, may reach the outer plexiform layer by diffusion to exert its effect.

B. Somatostatin

There has been a long search for the role of somatostatin in retinal information processing. It has been localized first in the mammalian retina to amacrine cells (Yamada *et al.,* 1980) and shown later in rabbit that it affects the firing pattern of the ganglion cells (Zalutsky and Miller, 1990). In frogs, Smiley and Basinger (1988) found that glycinergic interplexiform cells contain somatostatin. The anatomy of this cell type and the effect of glycine on horizontal cell function has been described in section V. The morphology and synaptology of this cell suggested that somatostatin could exert its main effect on neurons of the outer retina.

Intracellular recording from horizontal cells in *Xenopus* eyecups, in the presence of somatostatin or its short peptide analog Sandostatin produced no changes in membrane potential or response amlitude and kinetics (P. Witkovsky, pers. commun.) and neither could researchers find a consistent effect on rods (T. Szikra and

P. Witkovsky, pers. commun.). This negative result, however, may have been due to the lack of penetration of this large molecular weight substance into the retina in eyecups.

Former studies in rabbit and rat have shown that somatostatin 2A receptors are widely distributed in both plexiform layers of the retina (Johnson *et al.,* 1998, 1999). Next, therefore, we performed immunocytochemical stainings for the presence of somatostatin 2A receptors both in *Xenopus* and tiger salamander and found the preferential localization of this receptor subtype to the photoreceptor terminals (Akopian *et al.,* 2000).

The cellular actions of somatostatin are mediated via five distinct G-protein coupled receptor types (Hoyer *et al.,* 1995), out of which somatostatin 2 receptors come in two isoforms resulting from alternative mRNA splicing (Vanetti *et al.,* 1992). Somatostatin 2A receptors may modulate many kinds of K^+ and the L- and N-type Ca^{2+} currents in neurons, endocrine cells, and cell lines (Rosenthal *et al.,* 1988; Wang *et al.,* 1989; White *et al.,* 1991; Shapiro and Hille, 1993; Takano *et al.,* 1997). In addition, the action of somatostatin resulted in a reduction of transmitter release (Boehm and Betz, 1997). In the light of these findings somatostatin was expected to be a prime regulator of transmitter release from photoreceptor cells. The experiments described below were mostly done in tiger salamander (Akopian *et al.,* 2000), and several of them were repeated with identical results in *Xenopus*.

1. Effect on Photoreceptors

Application of somatostatin resulted in a strong enhancement of the delayed outward potassium currents of both rods and cones. The hyperpolarization-activated current (I_h), which is strongly regulated by dopamine, however, was not affected. Therefore, dopamine and somatostatin seem to regulate two different potassium currents in photoreceptors.

Interestingly, somatostatin has opposite effects on the Ca^{2+} currents of the two photoreceptor types. Calcium currents are mediated through L-type channels in photoreceptors (Schmitz and Witkovsky, 1997) Voltage-gated Ca^{2+} currents were markedly reduced in rods while increased in cones by about 40%. This enhancement is due to a shift toward negative voltage of activation function (Akopian *et al.,* 2000). The higher Ca^{2+} levels that may result in after the action of somatostatin on cone terminals would facilitate transmitter release. Transmitter release is under multiple neuromodulatory control which include pH (Barnes *et al.,* 1993), dopamine (Stella and Thoreson, 1998), Ca^{2+} release from intracellular stores (Krizaj *et al.,* 1999), and GABA release from horizontal cells (Verweij *et al.,* 1996). Somatostatin seems to fit into the row of substances that could facilitate transmitter release from cones and suppress the rod system. This is of great importance since all second-order cells in the amphibian retina receive mixed rod and cone signals. Augmentation of the cone system favors the photopic vision, results in better spatial resolution and enhanced color processing (Krizaj, 2000).

2. Effect on Second-Order Cells: Direct or Indirect?

As described above, intracellular signals recorded from horizontal cells showed consistent changes in neither the resting potential nor the amplitude of responses. Somatostatin 2A receptors were not concentrated in cell bodies at the outer edge of the inner plexiform layer. In salamander retinal slices horizontal and bipolar cells seemed to be inresponsive to somatostatin (A. Akopian, pers. commun.). Interestingly, however, somatostatin abolished light-induced excitatory responses in ganglion cells (Akopian, 2000). Unfortunately we do not have any knowledge of the retinal distribution of any other somatostatin receptors than somatostatin receptor 2A. It can be inferred on the basis of these results that somatostatin exerts its major effects on the photoreceptors.

C. Self-Regulation of Glutamate Release from Photoreceptors

There is no compelling evidence to date for the presence of ionotropic glutamate receptors on photoreceptor cells (Thoreson and Witkovsky, 1999). Among the eight types of metabotropic glutamate receptors, however, seems to be one, the metabotropic glutamate receptor 8 to be present in photoreceptor terminals in rat (Koulen *et al.,* 1999). Application of agonists of this receptor led to a decrease of intracellular Ca^{2+} concentration. It has also been proved that the cAMP signaling pathway does not play a role in generating this response. The effect of this autofeedback will be reduction in transmitter release through downregulating intracellular Ca^{2+}. In other systems group III metabotropic glutamate receptors are also involved in regulating transmitter release. Possible mechanisms are downregulation of presynaptic voltage-gated calcium channels through G-proteins, an increase of a potassium conductance leading to hyperpolarization of the cell or a direct presynaptic receptor action on the exocytotic machinery downstream of calcium (Wu and Saggau, 1997).

Apart from iontropic and metabotropic receptors, transporter molecules may also serve as autoregulators of transmitter release. Their activation can lead to net current flow through the cell membrane. Since glutamate is released tonically from photoreceptors, their reuptake may generate substantial current and cause changes in the membrane potential.

Action of glutamate is terminated by reuptake and it is clear now that glutamate transporters are coupled to Cl^- channels (Lester *et al.,* 1996). Molecular cloning studies have recently confirmed the presence of a family of glutamate uptake proteins in retina. The retinal members of this family all show Na-dependence and saturating kinetics (Eliasof *et al.,* 1998). There are five major isoforms present in the central nervous system out of which excitatory amino acid transporters 1, 2, and 5 are present in the retina, the last one being retina-specific (Arriza *et al.,* 1997).

Transporters 1 and 5 may be present in all photoreceptors, while 2 is cone-specific (Eliasof *et al.,* 1998). Consistent with cell-specific differences in transporter distribution there also appear to be differences between photoreceptor types and species (Thoreson and Witkovsky, 1999). It has been suggested that the cloride channel is an integral part of the transporter protein and Cl^- flux occurs when the glutamate and Na^+ binding sites face the cell interior (Larsson *et al.,* 1996). Glutamate binding to the transporter may cause currents which are big enough so that they make photoreceptors to respond to their own glutamate or glutamate released by their neighbors (Tachibana and Kaneko, 1988). Thereby, altering the presynaptic membrane potential, glutamate-evoked cloride currents can act as a feedback mechanism to adjust Ca-dependent glutamate release (Thoreson and Witkovsky, 1999).

Although the presence of metabotropic glutamate receptor 8 has not been verified in amphibian retinas, it is tempting to speculate that there are at least two autofeedback mechanisms that are able to regulate glutamate release from retinal photoreceptors exist in all vertebrate species.

D. Circadian Events

One of the most intriguing questions in retinal research how short- and long-term light adaptation occur and interact. As we have shown above, the major short-term light adaptation factor is dopamine. Nonetheless, sensitivity of the visual system is not uniform throughout the day. Visual acuity must be adapted for better survival chances.

While light adaptation systems only perceive the light intensity changes the circadian system enables the retinas to prepare for them (Anderson and Green, 2000). This means that the biochemistry, physiology, and morphology of the retina must be reorganized every 24 h. Evidence can be obtained from animals entrained to a constant 12-h light/12-h dark cycle and then maintained in constant darkness. This way the clock-regulated (and not the light-dependent) adaptational responses can be selectively studied. Under these conditions ERG b-wave amplitudes show highly rhythmic behavior, increasing during the subjective day and decreasing during the subjective night (Manglapus *et al.,* 1999). Rod disc shedding and cone contraction happens during both light adaptation and circadian adaptation (Cahill and Besharshe, 1995). Melatonin seems to be the circadian dark signal to the retinal network (Besharshe and Iuvone, 1983), and it also inhibits dopamine release (Dubocovich, 1983). Not only the synthesis (Green *et al.,* 1995) but the release of melatonin is also highly rhythmic (Cahill and Besharshe, 1990) and is maintained in reduced retina preparations where only the photoreceptor layer has been left intact (Cahill and Besharshe, 1992). In addition, the retinal clock can be entrained, demonstrating that it is able to respond to the change in the Zeitgeber (Besharshe and Iuvone, 1983). It was also shown that the clock is independent from the central circadian control center of the body, the suprachiasmatic nucleus, since
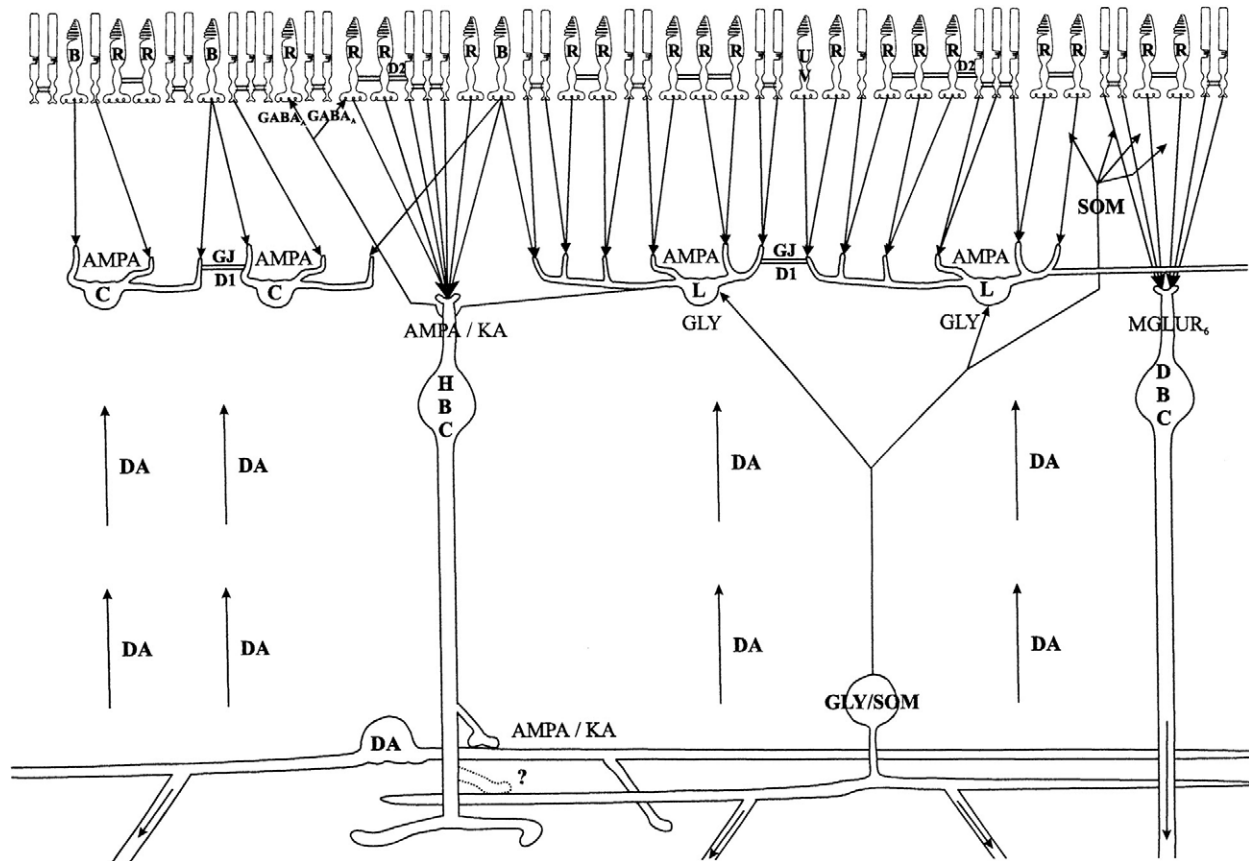
in vitro eyecup and isolated retina preparations maintain their rhythmic melatonin production (Cahill and Besharshe, 1993). Thus the retinal clockwork complies with all the requirements of an independent circadian system.

Circadian regulation requires enormous transcriptional and translational activity. A thorough search for rhythmically expressed genes in *Xenopus* retina was recently undertaken (Green and Besharse, 1996a). Several gene products were identified, most of them (*period 2, crytochromes 1, 2a, and 2b*) homologous to those described in flies and/or mice (Zhu and Green, 1999; Zhuang *et al.,* 1999; Zhu *et al.,* 2000) and localized to the photoreceptor layer. The *Xenopus* homolog of *Clock* is also expressed but it does not show rhythmicity (Zhu *et al.,* 2000). Nocturnin, however, seems to be unique to *Xenopus* (Green and Besharse, 1996b). With recent advances in transgene technology stable green fluorescent protein expression could be achieved by inserting this gene into the opsin gene (Knox *et al.,* 1998). The *Xenopus* opsin promoter is highly specific to retinal rods and pinal photoreceptor cells; therefore, it is an extremely promising tool in studying rod circadian function.

VII. Concluding Remarks

The term *retina* originally comes from an arabic word which means "small net." Indeed, processes of retinal neurons form a network-like structure at the levels of the plexiform layers. Although the general structure of the outer plexiform layer is relatively simple, our summary diagram (Fig. 4) shows how intricate is the relation of the individual cell types with each other. All three communication types of the

---

FIG. 4 Summary diagram of synaptic and nonsynaptic connections in the outer plexiform layer of *Xenopus* retina. Photoreceptors (empty, rods; B, blue-light-sensitive; R, red-light-sensitive; UV, ultraviolet-light-sensitive cones) form synaptic contacts (arrows) with horizontal cells with AMPA receptors. Axon-bearing luminosity (L) type horizontal cells feed back to red cones through GABA$_A$ receptors. Both L-type and chromatic (C) horizontal cells are connected with gap junctions (GJ, double lines) which can be modulated through D1 dopamine receptors (D1). Hyperpolarizing bipolar cells (HBC) receive photoreceptor inputs through AMPA and/or kainate (KA) receptors and activate the dopaminergic (DA) and possibly the glicin/somatostatin (GLY/SOM)-containing interplexiform cells. Depolarizing bipolar cells (DBC) employ sign-inverting metabotropic glutamate receptor 6 (MGLUR6). The interplexiform cell forms glycinergic synapses (GLY) on the L-cells while somatostatin (SOM) released from the varicose axon-like processes reach the photoreceptors terminals with diffusion (branching freely ending arrows at the photoreceptor bases) where they activate somatostation 2A receptors. Dopamine (DA) released tonically from the processes of the dopaminergic interplexiform cell diffuses through the entire inner nuclear layer (upward pointing parallel arrows). Upon reaching the photoreceptors they regulate selectively the rod–cone gap junctions (double lines) through D2 dopamine receptors, while the gap junctions between homologous photoreceptors are not regulated by dopamine.

nervous system plays a substantial role of setting the function of the outer retinal circuits. Chemical synapses drive the system of the second-order cells. This hardwired circuit carries out the basic functions of the outer retina, namely the first step in color processing and formation of bipolar cell center-surround organization. Electrical connections provide means for signal averaging and synchronization, mainly for homologous neurons in the horizontal pathway. Intertype electrical interactions are rare; however, they play an important role in system adaptation. Adaptation is also strongly influenced by neurohumoral clues that derive from the inner retina. Both dopamine and somatostatin reach their targets by diffusion. It may be expected that the number of substances with proven neuromodulatory effects on outer retinal elements will increase in the near future. One candidate for this role is serotonin. The neurohumoral clues that play roles in short-term light adaptation are further supplemented by a long-term adaptational (circadian) signal, melatonin. All these substances seem to modify the functional state of the second messenger systems. "What we need to know is by what arrangement can several types of photoreceptors converge upon a ganglion cell and exhibit at the same time the characteristics and the very different properties seen in the mesopic state" wrote Rushton (1959). We have shown in this paper that most of the processes that make possible such a versatility of visual function can be tied to the outer plexiform layer in frog.

Functional adaptation enables the retinal network to work with maximal spatial resolution in order to achieve the highest possible visual acuity under all environmental lighting conditions. Visual acuity depends on the convergence ratios of first-, second-, and third-order cells and the sampling aperture (Wässle and Boycott, 1991). This latter parameter depends on the ganglion cell dendritic field, namely, it is identical with the center component of the receptive field. The spacing between neighboring ganglion cells defines the sampling distance, that is which spatial frequency is unambigously available within the visual system (the Nyquist limit: Snyder and Miller, 1977). Convergence ratios are low in the *Xenopus* retina. About 15,000/mm^2 photoreceptor cells (Wilhelm and Gábriel, 1999) are connected with 6000/mm^2 (Wilhelm and Gábriel, 1999), which finally converge on about 3000/mm^2 ganglion cells (Dunlop and Beazley, 1984). This is an overall photoreceptor to ganglion cell ratio of 5:1. These ratios are applicable to the entire extent of the retina since there is no marked center to periphery cell density gradient can be found in *Xenopus*.

About 90% of the ganglion cells belong to the category of small neurons with a dendritic field diameter of around 100 μm (Straznicky and Straznicky, 1988). If all these subserve acute vision and their dendritic tree overlaps minimally, one cell covers about 400 μm^2 area. This same area contans six photoreceptors (three rods and three cones). The theoretical Nyquist limit (1.73a, where a is the intercell spacing) for this cell mosaic is about 150 μm, which is about 1/10 of the primate foveal resolution power (Wässle and Boycott, 1991). However, resolution power decreases sharply from center to periphery in primates

with the decreasing cell densities, but remains almost identical in *Xenopus* due to the uniform distribution of cells in the retina.

Acknowledgments

References

Agardh, E., Bruun, A., Ehinger, B., Ekström, P., van Veen, T., and Wu, J.-Y. (1987). Gamma-aminobutyric acid and glutamic acid decarboxylase immunoreactive neurons in the retina of different vertebrates. *J. Comp. Neurol.* **258,** 622–630.

Akopian, A. (2000). Neuromodulation of ligand- and voltage-gated channels in the amphibian retina. *Microsc. Res. Technol.* **50,** 403–410.

Akopian, A., Johnson, J., Gabriel, R., Brecha, N., and Witkovsky, P. (2000). Somatostatin modulates voltage-gated K^+ and Ca^{2+} currents in rod and cone photoreceptors of the salamander retina. *J. Neurosci.* **20,** 929–936.

Akopian, A., and Witkovsky, P. (1992). Modulation of transient outward potassium current by GTP, calcium and glutamate in horizontal cells of the *Xenopus* retina. *J. Neurophysiol.* **71,** 1661–1671.

Akopian, A., and Witkovsky, P. (1996). D2 dopamine receptor-mediated inhibition of a hyperpolarization-activated current in rod photoreceptors. *J. Neurophysiol.* **76,** 1828–1835.

Ammermüller, J., and Kolb, H. (1996). Functional architecture of the turtle retina. *Prog. Retinal Res.* **15,** 393–433.

Anderson, F. A., and Green, C. B. (2000). Symphony of rhythms in the *Xenopus laevis* retina. *Microsc. Res. Technol.* **50,** 360–372.

Arriza, J. L., Eliasof, S., Kavanaugh, M. P., and Amara, S. G. (1997). Excitatory amino acid transporter 5, a retinal glutamate transporter coupled to a cloride conductance. *Proc. Natl. Acad. Sci. USA* **94,** 4155–4160.

Attwell, D., Werblin, F. S., and Wilson, M. (1982). The properties of single cones isolated from tiger salamander retina. *J. Physiol. (London)* **328,** 259–283.

Barlow, H. B. (1953a). Action potentials from the frog's retina. *J. Physiol.* **119,** 58–68.

Barlow, H. B. (1953b). Summation and inhibition in the frog's retina. *J. Physiol,* 119, 69–88.

Barnes, S. (1994). After transduction: Response shaping and control of transmission by ion channels of the photoreceptor inner segment. *Neuroscience* **58,** 447–459.

Barnes, S., and Deschnes, M. C. (1992). Ionic basis of regenerative depolarization and membrane bistability in cone photoreceptors. *J. Neurophysiol.* **68,** 745–755.

Barnes, S., and Hille, B. (1989). Ionic channels of the inner segments of tiger salamander cone photoreceptors. *J. Gen. Physiol.* **94,** 919–743.

Barnes, S., Merchant, V., and Mahmud, F. (1993). Modulation of transmission gain by protons at the photoreceptor output synapse. *Proc. Natl. Acad. Sci. USA* **90,** 10,081–10,085.

Baylor, D. A. (1987). Photoreceptor signals and vision. *Invest. Ophthalmol. Vis. Sci.* **28,** 34–49.

Baylor, D. A., Fuortes, M. G. F., and Nunn, B. J. (1971). Receptive field of cones in the retina of turtle. *J. Physiol.* **214,** 265–294.

Beech, D. J., and Barnes, S. (1989). Characterization of voltage-gated K+ channel that accelerates the rod response. *Neuron* **3,** 573–581.

Beherns, U. D., and Wagner, H.-J. (1995). Localization of dopamine D1-receptors in vertebrate retinae. *Neurochem. Int.* **27,** 497–507.

Belgum, J. H., and Copenhagen, D. R. (1988). Synaptic transfer of rod signals to horizontal and bipolar cells in the retina of the toad (*Bufo marinus*). *J. Physiol.* **396,** 225–245.

Besharshe, J. C., and Iuvone, P. M. (1983). Circadian clock in *Xenopus* eye controlling retinal serotonin N-acetyltransferase. *Nature* **305,** 133–135.

Besharshe, J. C., and Witkovsky, P. (1992). Light-evoked contraction of red-absorbing cones in the *Xenopus* retina is maximally sensitive to green light. *Visual Neurosci.* **8,** 243–249.

Boatright, J. H., Hoel, M. J., and Iuvone, P. M. (1989). Stimulation of endogenous dopamine release and metabolism in amphibian retina by light- and K$^+$-evoked depolarization. *Brain Res.* **482,** 164–168.

Boehm, S., and Betz, H. (1997). Somatostatin inhibits excitatory transmission at rat hippocampal synapses via presynaptic receptors. *J. Neurosci.* **17,** 4066–4075.

Burkhardt, D. A. (1993). Synaptic feedback, depolarization, and color opponency in cone photoreceptors. *Visual Neurosci.* **10,** 981–989.

Buzás, P., Jeges, S., and Gábriel, R. (1996). The number and distribution of bipolar to ganglion cell synapses in the inner plexiform layer of the anuran retina. *Visual Neurosci.* **13,** 1099–1107.

Cahill, G. M., and Beshrshe, J. C. (1990). Circadian regulation of melatonijn in the retina of *Xenopus laevis:* Limitation by serotonin availablity. *J. Neurochem.* **54,** 716–719.

Cahill, G. M., and Beshrshe, J. C. (1992). Light-sensitive melatonin synthesis after destruction of inner retina. *Visual Neurosci.* **8,** 487–490.

Cahill, G. B., and Besharshe, J. C. (1993). Circadian clock function localized in *Xenopus* retinal photoreceptors. *Neuron* **10,** 573–577.

Cahill, G. M., and Besharshe, J. C. (1995). Circadian rhythmicity in vertebrate retinas: regulation by photoreceptor oscillation. *Prog. Retinal Res.* **14,** 267–291.

Cajal, S. R. y (1893). La retine des vertebrates. *La Cellule* **9,** 119–257.

Chang, W. S., and Harris, W. A. (1998). Sequential genesis and determination of cone and rod photoreceptors in *Xenopus*. *J. Neurobiol.* **35,** 227–244.

Chen, F., and Witkovsky, P. (1978). The formation of photoreceptor synapses in the retina of larval *Xenopus*. *J. Neurocytol.* **7,** 721–740.

Chung, S. H., Stirling, R. V., and Gaze, R. M. (1975). The structural and functional development of the retina in larval *Xenopus*. *J. Embryol. Exp. Morphol.* **33,** 915–940.

Cook, J. E., and Becker, D. L. (1995). Gap junctions in the vertebrate retina. *Microsc. Res. Technol* **31,** 408–419.

Cook, J. E., and Chalupa, L. (2000). Retinal mosaics: New insights into an old concept. *Trends Neurosci.* **23,** 26–34.

Copenhagen, D. R., and Jahr, C. E. (1989). Release of endogenous excitatory amino acids from turtle photoreceptors. *Nature* **341,** 536–539.

Crestcitelli, F. (1991). The natural history of visual pigments: 1990. *Prog. Retinal Res.* **11,** 1–32.

Cunningham, J. R., Neal, M. J., Stone, S., and Witkovsky, P. (1988). GABA release from *Xenopus* retina does not correlate with horizontal cell membrane potential. *Neuroscience* **24,** 39–48.

Currie, J. R., Hollyfield, J. G., and Rayborn, M. E. (1978). Rod outer segments elongate in constant light: Darkness is required for normal shedding. *Vision Res.* **18,** 995–1003.

Dacey, D. M. (1990). The dopaminergic amacrine cell. *J. Comp. Neurol.* **301,** 461–489.

Djamgoz, M. B. A. (1995). Diversity of GABA receptors in the vertebrate outer retina. *Trends Neurosci.* **18,** 118–120.

Dorsky, R. I., Chang, W. S., Rapaport, D. H., and Harris, W. A. (1997). Regulation of neuronal diversity in the *Xenopus* retina by Delta signalling. *Nature* **385,** 67–70.

Dorsky, R. I., Rapaport, D. H., and Harris, W. A. (1995). Xotch inhibits cell differentiation in the *Xenopus* retina. *Neuron* **14,** 487–496.

Dowling, J. E. (1968). Synaptic organization of the frog retina: An electron microscopic analysis comparing retinas of frogs and primates. *Proc. R. Soc. London B* **170,** 205–228.

Dowling, J. E. (1987). "The Retina. An Approachable Part of the Brain." Belknap Press of Harvard University Press, Cambridge.

Dubin, M. W. (1970). The inner plexiform layer of the vertebrate retina: A quantitative and comparative electron microscopic analysis. *J. Comp. Neurol.* **140,** 479–506.

Dubocovich, M. L. (1983). Melatonin is a potent modulator of dopamine release in the retina. *Nature* **306,** 782–784.

Dunlop, S. A., and Beazley, L. D. (1984). A morphometric study of the retinal ganglion cell layer and optic nerve from metamorphosis in *Xenopus laevis*. *Vision Res.* **24,** 417–427.

Ehinger, B., Ottersen, O. P., and Storm-Mathisen, J. (1988). Bipolar cells in the turtle retina are strongly immunoreactive for glutamate. *Proc. Natl. Acad. Sci. USA* **85,** 8321–8325.

Eliasof, S., Arriza, J. L., Leighton, B. H., Kavanaugh, M. P., and Amara, S. G. (1998). Excitatory amino acid transporters of the salamander retina: Identification, localization and function. *J. Neurosci.* **18,** 698–712.

Euler, T., and Wässle, H. (1995). Immunocytochemical identification of cone bipolar cells in the rat retina. *J. Comp. Neurol.* **361,** 461–478.

Fain, G. L. (1975). Quantum sensitivity of rods in the toad retina. *Science* **187,** 838–841.

Famiglietti, E. V., and Kolb, H. (1976). Structural basis for ON- and OFF-center responses in retinal ganglion cells. *Science* **194,** 193–195.

Frederick, M. J., Rayborn, M. E., and Hollyfield, J. G. (1989). Serotoninergic neurons in the retina of *Xenopus laevis:* Selective staining, identification development and content. *J. Comp. Neurol.* **281,** 516–531.

Fujisawa, H. (1982). Formation of gap junctions by stem cells in the developing retina of the clawed frog (*Xenopus laevis*). *Anat. Embryol.* **165,** 141–149.

Gábriel, R. (1991). A method for the demonstration of NADPH-diaphorase avtivity in anuran species using unfixed retinal wholemounts. *Arch. Histol. Cytol.* **54,** 207–211.

Gábriel, R. (2000). Calretinin is present in serotonin- and GABA-positive amacrine cell populations in the retina of *Xenopus laevis*. *Neurosci. Lett.* **285,** 9–12.

Gábriel, R., and Straznicky, C. (1993). Quantitative analysis of GABA-immunoreactive synapses in the retina of *Bufo marinus:* Identification of direct output to ganglion cells and contacts with dopaminergic amacrine cells. *J. Neurocytol.* **22,** 26–38.

Gábriel, R., Straznicky, C., and Wye-Dvorak, J. (1992). GABA-like immunoreactive neurons in the retina of *Bufo marinus:* Evidence for the presence of GABA-containing ganglion cells. *Brain Res.* **571,** 175–179.

Gábriel, R., Völgyi, B., and Pollák, E. (1998). Calretinin-immunoreactive elements in the retina and optic tectum of the frog, *Rana esculenta. Brain Res.* **782,** 53–62.

Gábriel, R., Zhu, B. S., and Straznicky, C. (1991). Tyrosine hydroxilase-immunoreactive elements in the distal retina of *Bufo marinus:* A light and electron microscopic study. *Brain Res.* **559,** 225–232.

Gábriel, R., Zhu, B. S., and Straznicky, C. (1993). Synaptic contacts of serotonin-like immunoreactive and 5,7-dihydroxytryptamine-accumulating neurons in the anuran retina. *Neuroscience* **54,** 1103–1114.

Gold, G. H. (1979). Photoreceptor coupling in retina of the toad, *Bufo marinus*. II. Physiology. *J. Neurophysiol.* **42,** 292–310.

Gold, G. H., and Dowling, J. E. (1979). Photoreceptor coupling in retina of the toad, *Bufo marinus*. I. Anatomy. *J. Neurophysiol.* **42,** 292–310.

Green, C. B., and Besharshe, J. C. (1996a). Identification of a novel vertebrate cicadian clock-regulated gene enoding the protein nocturnin. *Proc Natl. Acad. Sci USA* **93,** 14,884–14,888.

Green, C. B., and Besharshe, J. C. (1996b). Use of a high stringency differential display screen for identification of retinal mRNAs that are regulated by a circadian clock. *Mol. Brain Res.* **37,** 157–165.

Green, C. B., Cahill, G. M., and Besharse, J. C. (1995). Regulation of tryptophane hydroxylase expression by a retinal cicadian oscillator *in vitro. Brain Res.* **677,** 283–290.

Hárosi, F. I. (1982). Recent results from single-cell spectrophotometry: Cone pigments in frog, fish and monkey. *Color Res. Appl.* **7,** 135–141.

Hartline, H. K. (1938). The response of single optic fibers of the vertebrate eye to illumination of the retina. *Am. J. Physiol.* **121,** 400–415.

Hedden, W. L., and Dowling, J. E. (1978). The interplexiform cell system. II. Effects of dopamine on goldfish retinal neurones. *Proc. R. Soc. London B.* **201,** 27–51.

Hessler, R. B., Baer, C. A., Bukelman, A., Kitteridge, K. I., and Gozalez-Fernandez, F. (1996). Interphotoreceptor retinoid binding protein (IRBP): Expression in the adult and developing *Xenopus* retina. *J. Comp. Neurol.* **367,** 329–341.

Hestrin, S. (1987). The properties and function of inward rectification in rod photoreceptors of the tiger salamander retina. *J. Physiol.* **390,** 319–333.

Hiscock, J., and Straznicky, C. (1990). Neuropeptide Y- and substance P-like immunoreactive amacrine cells in the retina of developing *Xenopus laevis. Dev. Brain Res.* **54,** 105–113.

Hollyfield, J. G., Rayborn, M. E., and Rosenthal, J. (1984). Two populations of rod photoreceptors in the retina of *Xenopus laevis* identified with ^{3}H-fucose autoradiography. *Vision Res.* **24,** 777–782.

Hollyfield, J. G., and Witkovsky, P. (1974). Pigmented retina epithelium involvement in photoreceptor development and function. *J. Exp. Zool.* **189,** 357–378.

Holt, H. E., Bertsch, T. W., Ellis, H. M., and Harris, W. A. (1988). Cellular determination in the *Xenopus* retina is independent of lineage and birth date. *Neuron* **1,** 15–26.

Hoyer, D., Bell, G. I., Berelowitz, M., Epelbaum, J., Feniuk, W., Humprey, P. P., O'Carroll, A. M., Patel, Y. C., Schonbrunn, A., and Taylor, J. E. *et al.* (1995). Classification and nomenclature of somatostatin receptors. *Trends Pharmacol. Sci.* **16,** 86–88.

Jensen, R., and Daw, N. W. (1984). Effect of dopamine antagonists on receptive fields of brisk cells and directionally selective cells in rabbit retina. *J. Neurosci.* **4,** 2979–2985.

Johnson, J, Wong, H., Walsh, J., and Brecha, N. (1998). Expression of the somatostatin subtype 2a receptor in the rabbit retina. *J. Comp. Neurol.* **392,** 1–9.

Johnson, J., Wu, V., Wong, H., Walsh, J., and Brecha, N. (1999). Somatostatin receptor subtype 2A in the rat retina. *Neuroscience* **94,** 675–683.

Kaczmarek, L. K., and Levitan, I. B. (1987). "Neuromodulation—The Biochemical Control of Neuronal Excitability." Oxford University Press, London.

Kleinschmidt, J., and Yazulla, S. (1984). Uptake of 3H-glycine in the outer plexiform layer of the retina of the toad, *Bufo marinus. J. Comp. Neurol.* **230,** 352–360.

Kolb, H., Nelson, R., and Mariani, A. P. (1981). Amacrine cells, bipolar cells and ganglion cells of the cat retina: A Golgi study. *Vision Res.* **21,** 1081–1114.

Koulen, P., Kuhn, R., Wässle, H., and Brandstätter, J. H. (1999). Modulation of intracellular calcium concentration in photoreceptor terminals by a presynaptic metabotropic glutamate receptor. *Proc. Natl. Acad. Sci. USA* **96,** 9909–9914.

Knox, B., Schlueter, C., Sanger, B. M., Green, C. B., and Besharshe, J. C. (1998). Transgene expression in *Xenopus* rods. *FEBS Lett.* **20,** 117–121.

Krizaj, D. (1995). "Synaptic Integration and Neuromodulation at the Photoreceptor Synapse: Mechanisms and Functional Significance." Ph. D. thesis, New York University, New York. UMI Dissertation Services, Ann Arbor.

Krizaj, D. (2000). Mesopic state: Cellular mechanisms involved in pre- and postsynaptic mixing of rod and cone signals. *Microsc. Res. Technol.* **50,** 347–359.

Krizaj, D., Akopian, A., and Witkovsky, P. (1994). The effect of L-glutamate, AMPA, quisqualate and kainate on retinal horizontal cells depend on adaptational state: Implications for rod–cone interactions. *J. Neurosci.* **14,** 5661–5671.

Krizaj, D., Bao, J. X., Schmitz, Y., Witkovsky, P., and Copenhagen, D. (1999). Caffeine-sensitive calcium stores regulate synaptic transmission from retinal rod photoreceptors. *J. Neurosci.* **19,** 7249–7261.

Krizaj, D., and Copenhagen, D. R. (1998). Compartmentalization of calcium extrusion mechanisms in the outer and inner segments of photoreceptors. *Neuron* **21,** 249–256.

Krizaj, D., Gábriel, R., Owen, G. W., and Witkovsky, P. (1998). Dopamine D2 receptor modulation of rod–cone coupling in the *Xenopus* retina. *J. Comp. Neurol.* **398,** 529–538.

Krizaj, D., and Witkovsky, P. (1993). Effects of submicromolar concentrations of dopamine on photoreceptor to horizontal cell communication. *Brain Res.* **627,** 122–128.

Kurenny, D. E., Moroz, L., Turner, R. W., Sharkey, K. A., and Barnes, S. (1994). Modulation of ion channels in rod photoreceptors by nitric oxide. *Neuron* **13,** 315–324.

Larsson, H. P., Picaud, S. A., Werblin, F. S., and Lecar, H. (1996). Noise analysis of the glutamate-activated current in photoreceptors. *Biophys. J.* **70,** 733–742.

Leeper, H. F. (1978). Horizontal cells of the turtle retina I. Light microscopy of Golgi preparations. *J. Comp. Neurol.* **182,** 777–794.

Lester, H. A., Cao, Y., and Mager, S. (1996). Listening to neurotransmitter transporters. *Neuron* **17,** 807–810.

Lukasiewicz, P. D. (1996). GABA$_C$ receptors in the vertebrate retina. *Mol. Neurobiol.* **12,** 181–194.

Maguire, G., and Werblin, F. (1994). Dopamine enhances a glutamate-gated ionic current in OFF bipolar cells of the tiger salamander retina. *J. Neurosci.* **14,** 6094–9101.

Manglapus, M., Parshley, M., Stewart, K., Engbretson, G., Knox, B., and Barlow, R. (1999). Circadian changes of ERG responses in the *Xenopus laevis*. *Invest. Ophthalmol. Vis. Sci.* **40,** S610.

Manns, M., and Fritzsch, B. (1991). The eye in the brain: Retinoic acid effects morphogenesis of the eye and pathway selection of axons but not the differentiation of the retina in *Xenopus laevis*. *Neurosci. Lett.* **127,** 150–154.

Marc, R., Liu, W. L. S., Kalloniatis, M., Raiguel, S. F., and van Hasendonck, E. (1990). Patterns of glutamate immunoreactiviy in the goldfish retina. *J. Neurosci.* **10,** 4006–4034.

Mariani, A. P. (1984). Bipolar cells in the monkey retina selective for the cones likely to be blue-sensitive. *Nature* **308,** 184–186.

Martin, P. R., and Grünert, U. (1991). Spatial density and immunoreactivity of bipolar cells in the macaque monkey retina. *J. Comp. Neurol.* **323,** 269–287.

Massey, S. C. (1990). Cell types using glutamate as a neurotransmitter in the vertebrate retina. *Prog. Retinal Res.* **9,** 399–425.

Massey, S. C., and Redburn, D. A. (1987). Transmitter circuits in the vertebrate retina. *Prog. Neurobiol.* **28,** 55–96.

Matthews, G. (1983). Physiological characteristics of single green rod photoreceptors from toad retina. *J. Physiol.* **342,** 347–359.

Maturana, H. R., Lettwin, J. Y., McCulloch, W. S., and Pitts, W. H. (1960). Anatomy and physiology of vision in the frog (*Rana pipiens*). *J. Gen. Physiol.* **43,** 129–175.

Miller, R. F., and Dacheux, R. F. (1976). Synaptic organization and ionic basis of on and off channels in mudpuppy retina. II. Chloride-dependent ganglion cell mechanisms. *J. Gen. Physiol.* **67,** 639–659.

Mosinger, J. L., Yazulla, S., and Studholme, K. (1986). GABA-like immunoreactivity in the vertebrate retina: A species comparison. *Exp. Eye Res.* **42,** 631–644.

Nagy, A. R., and Witkovsky, P. (1981). A freeze–fracture study of synaptogenesis in the distal retina of larval *Xenopus*. *J. Neurocytol.* **10,** 897–919.

Nieuwkoop, P. D., and Faber, J. (1956). "Normal table of *Xenopus laevis* (Daudin)." North Holland Publishing, Amsterdam.

Nöll, G. N., Billek, M., Pietruck, C., and Schmidt, K.-F. (1994). Inhibition of nitric oxyde synthase alters light responses and dark voltage of amphibian photoreceptors. *Neuropharmacology* **33,** 1407–1412.

Osborne, M. P., and Monaghan, P. (1976). Effects of light and dark upon photoreceptor synapses in the retina of *Xenopus laevis*. *Cell Tissue Res.* **173,** 211–220.

Panzanelli, P., Cantino, D., and Sassoe-Pognetto, M. (1997). Co-localization of carnosine and glutamate in photoreceptors and bipolar cells of the frog retina. *Brain Res.* **758,** 143–152.

Peichl, L., and González-Soriano, J. (1994). Morphological types of horizontal cells in rodent retinae: A comparison of rat, mouse, gerbil and guinea-pig. *Visual Neurosci.* **11,** 501–517.

Peng, Y.-W., Sharp, A. H., Snyder, S. H., and Yau, K.-W. (1991). Localization of the inositol 1,4,5,-trisphosphate receptor in synaptic terminals of the vertebrate retina. *Neuron* **6,** 525–531.

Pognetto, M. S., Cantino, D., and Fasolo, A. (1992). Carnosine-like immunoreactivity is associated with synaptic vesicles in photoreceptors of the frog retina. *Brain Res.* **578,** 261–268.

Pootanakit, K., Prior, K. J., Hunter, D. D., and Brunken, W. J. (1999). 5-HT2a receptors in the rabbit retina: Potential presynaptic modulators. *Visual Neurosci.* **16,** 221–230.

Pugh, E. N., and Cobbs, W. H. (1986). Visual transduction in vertebrate rods and cones: A tale of two transmitters, calcium and cyclic GMP. *Vision Res.* **26,** 1613–1643.

Qian, H., and Dowling, J. E. (1993). Novel GABA responses from rod-driven retinal horizontal cells. *Nature* **361,** 162–164.

Raviola, E., and Gilula, N. B. (1973). Gap junctions between photoreceptor cells in the vertebrate retina. *Proc. Natl. Acad. Sci. USA* **70,** 1677–1681.

Rayborn, M. E., Sarthy, P. V., Lam, D. M. K., and Hollyfield, J. G. (1981). The emergence, localization, and maturation of neurotransmitter systems during development of the retina in *Xenopus laevis*. II. Glycine. *J. Comp. Neurol.* **195,** 585–593.

Röhlich, P., and Szél, Á. (2000). Photoreceptor cells in the *Xenopus* retina. *Microsc. Res. Techn.* **50,** 327–337.

Röhlich, P., Szél, A., and Papermaster, D. S. (1989). Immunocytochemical reactivity of *Xenopus laevis* retinal rods and cones with several monoclonal antibodies to visual pigments. *J. Comp. Neurol.* **290,** 105–117.

Röhrenbeck, J., Wässle, H., and Heizmann, C. W. (1987). Immunocytochemical labeling of horizontal cells in the mammalian retina using antibodies against calcium-binding proteins. *Neurosci. Lett.* **77,** 255–260.

Rosenthal, W., Hescheler, J., Klaus-Dieter, H., Spicher, K., Trautwei, W., and Schultz, G. (1988). Cyclic AMP-independent dual regulation of voltage-dependent Ca currents by LHRH and somatostatin in pituitary cell line. *EMBO J.* **7,** 1627–1633.

Rushton, W. A. H. (1959). Excitation pools in the frog retina. *J. Physiol.* **149,** 327–345.

Saha, M. S., and Grainger, R. M. (1993). Early opsin expression in *Xenopus* embryos preceeds photoreceptor differentiation. *Mol. Brain Res.* **17,** 307–318.

Sandmann, D., Boycott, B. B., and Peichl, L. (1996). Blue cone horizontal cells in the retinae of horses and other *Equidae*. *J. Neurosci.* **16,** 3381–3396.

Sakai, H., and Naka, K. (1987). Neuron network in the catfish retina. *Prog. Retinal Res.* **9,** 149–208.

Sato, T. (1990). NADPH-diaphorase positive amacrine cells in the retinae of the frog (*Rana esculenta*) and pigeon (*Columba livia*). *Arch. Histol. Cytol.* **53,** 63–69.

Saxén, L. (1954). The development of the visual cells. Embryological and physiological investigations on amphibia. *Ann. Acad. Sci. Fenn. Ser. A* **23,** 1–93.

Schmitz, Y., and Witkovsky, P. (1996). Glutamate release by the intact light-responsive photoreceptor layer of the *Xenopus* retina. *J. Neurosci. Meth.* **68,** 55–60.

Schmitz, Y., and Witkovsky, P. (1997). Dependence of photoreceptor glutamate release on a dihydropyridine-sensitive calcium channel. *Neuroscience* **78,** 1209–1216.

Schütte, M., and Witkovsky, P. (1990). Serotonin-like immunoreactivity in the retina of clawed frog, *Xenopus laevis*. *J. Neurocytol.* **19,** 504–518.

Schütte, M., and Witkovsky, P. (1991). Dopaminergic interplexiform cells and centrifugal fibers in the *Xenopus* retina. *J. Neurocytol.* **20,** 195–207.

Shapiro, M. S., and Hille, B. (1993). Substance P and somatostatin inhibit calcium channels in rat sympathetic neurons via different G-protein pathways. *Neuron* **10,** 11–20.

Shkolnik-Yarros, E. G., and Podugolnikova, T. A. (1979). Bipolar cells of the frog retina: A Golgi study. *Vision Res.* **18,** 301–310.

Slaughter, M. M. (1995). GABAb receptors in the vertebrate retina. *Prog. Retinal Res.* **14,** 293–311.

Smiley, J. F., and Basinger, S. F. (1988). Somatostatin-like immunoreactivity and glycine high-affinity uptake colocalize to an interplexiform cell type of the *Xenopus laevis* retina. *J. Comp. Neurol.* **274,** 608–618.

Snyder, A. W., and Miller, W. H. (1977). Photoreceptor diameter and spacing for highest resolving power. *J. Opt. Soc. Am.* **67,** 696–698.

Starace, D. M., and Knox, B. E. (1997). Activation of transducin by a *Xenopus* short wavelength visual pigment. *J. Biol. Chem.* **272,** 1095–1100.

Starace, D. M., and Knox, B. E. (1998). Cloning and expression of a *Xenopus* short wavelength cone pigment. *Exp. Eye Res.* **67,** 209–220.

Stell, W. K., and Lightfoot, D. O. (1975). Color-specific interconnections of cones and horizontal cells in the retina of the goldfish. *J. Comp. Neurol.* **159,** 473–502.

Stella, S., and Thoreson, W. B. (1998). Differential modulation of rod and cone calcium currents by cAMP and a D2 dopamine receptor agonist. *Invest. Ophthalmol. Vis. Sci.* **39,** S983.

Stephan, P., and Weiler, R. (1981). Morphology of horizontal cells in the frog retina. *Cell Tissue Res.* **221,** 443–449.

Sterling, P., Freed, M. A., and Smith, R. G. (1986). Microcircuitry and functional architecture of the cat retina. *Trends Neurosci.* **9,** 186–192.

Sterling, P., Freed, M. A., and Smith, R. G. (1988). Architecture of rod and cone circuits to the on-beta ganglion cell. *J. Neurosci.* **8,** 623–642.

Stiemke, M. M., Landers, R. A., Al-Ubaidi, M. R., and Hollyfield, J. G. (1994). Photoreceptor outer segment development in *Xenopus laevis:* Influence of the pigment epithelium. *Dev. Biol.* **162,** 169–180.

Stiemke, M. M., and Hollyfield, J. G. (1995). Cell birthdays in *Xenopus laevis* retina. *Differentiation* **58,** 189–193.

Stone, S. L. (1994). White noise analysis of a chromatic type horizontal cell in the *Xenopus* retina. *J. Gen. Physiol.* **103,** 991–1017.

Stone, S., and Schütte, M. (1991). Physiological and morphological properties of OFF- and ON-center bipolar cells in *Xenopus* retina: Effects of glycine and GABA. *Vis. Neurosci.* **7,** 363–376.

Stone, S., and Witkovsky, P. (1987). Center-surround orgaization of *Xenopus* horizontal cells and its modification by γ-aminobutyric acid. *Exp. Biol.* **47,** 1–12.

Stone, S., Witkovsky, P., and Schütte, M. (1990). A chromatic horizontal cell in *Xenopus* retina: Intracellular staining and synaptic pharmacology. *J. Neurophysiol.* **64,** 1683–1694.

Straznicky, C. (1993). Development of the Anuran Retina: Past and present. *In* "Formation and Re-generation of Nerve Connections" (J. W. Fawcett and S. C. Sharma, Eds.), pp. 162–184. Birkhauser, Boston.

Straznicky, C., and Gábriel, R. (1991). NADPH-diaphorase positive neuron in the retina of *Bufo marinus:* Selective staining of bipolar and amacrine cells. *Arch. Histol. Cytol.* **54,** 213–220.

Straznicky, C., and Gábriel, R. (1995). Synapses of biplexiform ganglion cells in the outer plexiform layer of the retina of *Xenopus laevis*. *J. Brain Res.* **36,** 135–141.

Straznicky, K., and Gaze, M. (1971). The growth of the retina in *Xenopus laevis*: An autoradiographic study. *J. Embryol. Exp. Morphol.* **26,** 67–79.

Straznicky, C., and Straznicky, I. T. (1988). Morphological classification of retinal ganglion cells in adult *Xenopus laevis*. *Anat. Embryol.* **178,** 143–153.

Tachibana, M., and Kaneko, A. (1987). γ-Aminobutyric acid exerts a local inhibitory action on the axon terminal of bipolar cells: Evidence for negative feedback from amacrine cells. *Proc. Natl. Acad. Sci. USA* **84,** 3501–3505.

Tachibana, M., and Kaneko, A. (1988). L-Glutamate-induced depolarization in solitary photoreceptors: A process that may contribute to the interaction between photoreceptors *in situ. Proc. Natl. Acad. Sci. USA* **85,** 5315–5319.

Takano, K., Yasufuku-Takano, J., Kozasa, T., Nakajima, S., and Nakajima, Y. (1997). Different

G-proteins mediate somatostatin-induced inward rectifier K+ currents in murine brain and endocrine cells. *J. Physiol.* **502,** 559–567.

Thoreson, W. B., and Burkhardt, D. A. (1990). Effect of synaptic blocking agents on the depolarizing responsees of turtle cones evoked by surround illumination. *Vis. Neurosci.* **5,** 571–583.

Thoreson, W. B., and Burkhardt, D. A. (1991). Ionic influences on the prolonged depolarization of turtle cones *in situ. J. Neurophysiol.* **65,** 96–110.

Thoreson, W. B., Nitzan, R., and Miller, R. F. (2000). Chloride efflux inhibits single calcium channel open probability in vertebrate photoreceptors: Chloride imaging and cell-attached patch-clamp recording. *Visual Neurosci.* **17,** 197–206.

Thoreson, W. B., and Witkovsky, P. (1999). Glutamate circuits and receptors in the retina. *Prog. Retinal Res.* **18,** 765–810.

Törk, I., and Stone, J. (1979). Morphology of catecholamine-containing amacrine cells in the cat retinas seen in retina wholemounts. *Brain Res.* **169,** 261–273.

Tornquist, K., Hansson, C., and Ehinger, B. (1983). Immunohistochemical and quantitative analysis of 5-hydrohytryptamine in the retina of some vertebrates. *Neurochem. Int.* **5,** 299–308.

Tóth, P., and Straznicky, C. (1989). Biplexiform ganglion cells in the retina of *Xenopus laevis. Brain Res.* **499,** 378–382.

Turner, D. L., and Cepko, C. L. (1987). A common progenitor for neurons and glia persists in rat retina late in development. *Nature* **328,** 131–136.

Turner, D. L., Snyder, E. Y., and Cepko, C. L. (1990). Lineage-independent determination of cell type in the embryonic mouse retina. *Neuron* **4,** 833–845.

Vaney, D. I. (1990). The mosaic of amacrine cells in the mammalian retina. *Prog. Retinal Res.* **9,** 49–100.

Vaney, D. I. (1991). Many diverse types of retinal neurons show tracer coupling when injected with biocytin or neurobiotin. *Neurosci. Lett.* **125,** 187–190.

Vanetti, M, Kouba, M., Wang, X., Vogt, G., and Hollt, V. (1992). Cloning and expression of a novel mouse somatostatin receptor (SSTR2B). *FEBS Lett.* **311,** 290–294.

Verweij, J., Kammermans, M., and Spekreijse, H. (1996). Horizontal cells feed back to cones by shifting the cone calcium current activation range. *Vision Res.* **36,** 3943–3953.

Vígh, J., Bánvölgyi, T., and Wilhelm, M. (2000). Amacrine cells of the anuran retina: Morphology, chemical neuroanatomy and physiology. *Microsc. Res. Technol.* **50,** 373–383.

Voaden, M. J., Marshall, J., and Murani, N. (1974). The uptake of (3H)γ-aminobutyric acid and (3H)glycine by the isolated retina of frog. *Brain Res.* **67,** 115–132.

Von Gersdorff, H., and Matthews, G. (1994). Dynamics of vesicle fusion and membrane retrieval in synaptic terminals. *Nature* **637,** 735–739.

Wagner, H.-J., and Djamgoz, M. B. A. (1993). Spinules: A case for retinal synaptic plasticity. *Trends Neurosci.* **16,** 201–206.

Wagner, H.-J., Luo, B. G., Ariano, M. A., Sibley, D. R., and Stell, W. K. (1993). Localization of D2 dopamine receptors in vertebrate retinae with anti-peptide antibodies. *J. Comp. Neurol.* **331,** 469–481.

Wang, H. L., Bogen, G., Reisine, T., and Dichter, M. (1989). Somatostatin-14 and somatostatin-28 induce opposite effects on rat neocortical neurons. *Proc. Natl. Acad. Sci. USA* **86,** 9616–9620.

Wässle, H., and Boycott, B. B. (1991). Functional arhitecture of the mammalian retina. *Physiol. Rev.* **71,** 447–480.

Wässle, H., and Riemann, H. J. (1978). The mosaic of nerve cells in the mammalian retina. *Proc. R. Soc. Biol. London B* **200,** 441–461.

Wetts, R., and Fraser, S. E. (1988). Multipotent precursors can give rise to all major cell types of the frog retina. *Science* **239,** 1142–1145.

White, R. E., Schonbrunn, A., and Armstrong, D. (1991). Somatostatin stimulates Ca-activated K channels through protein dephosphorylation. *Nature* **351,** 570–573.

Wilhelm, M., and Gábriel, R. (1999). Functional anatomy of the photoreceptor and second-order cell mosaics in the retina of *Xenopus laevis. Cell Tissue Res.* **297,** 35–46.

Witkovsky, P. (2000). Photoreceptor classes and transmission at the photorecepptro synapse in the retina of clawed frog, *Xenopus laevis. Microsc. Res. Technol.* **50,** 338–346.

Witkovsky, P., and Dearry, A. (1991). Functional roles of dopamine in the vertebrate retina. *Prog. Retinal Res.* **10,** 247–292.

Witkovsky, P., and Powell, C. C. (1981). Synapse formation and modification between distal retinal neurons in larval and juvenile *Xenopus. Proc. R. Soc. London B* **211,** 373–389.

Witkovsky, P., Gábriel, R., Krizaj, D., and Akopian, A. (1995). Feedback from luminosity horizontal cells mediates depolarizing responses of chromacity horizontal cells in the *Xenopus* retina. *Proc. Natl. Acad. Sci. USA* **92,** 3556–3560.

Witkovsky, P., Levine, J. S., Engbretson, G. A., Hassin, G., and MacNichol, E. F. (1981). A microspectrophotometric study of normal and artificial visual pigments in the photoreceptors of *Xenopus laevis. Vision Res.* **26,** 867–873.

Witkovsky, P., Nicholson, C., Rice, M. E., Bohmaker, K., and Meller, M. E. (1993). Extracellular dopamine concentration in the retina of the clawed frog, *Xenopus laevis. Proc. Natl. Acad. Sci. USA* **90,** 5667–5671.

Witkovsky, P., Schmitz, Y., Akopian, A., Krizaj, D., and Tranchina, D. (1997). Gain of rod to horizontal cell synaptic transfer: Relation to glutamate release and a dihydropiridine-sensitive calcium current. *J. Neuroci.* **17,** 7297–7306.

Witkovsky, P., and Shi, X.-P. (1990). Slow light and dark adaptation of horizontal cells in the *Xenopus* retina: A role for endogenous dopamine. *Visual Neurosci.* **5,** 405–413.

Witkovsky, P., and Stone, S. (1983). Rod and cone inputs to bipolar and horizontal cells of the *Xenopus* retina. *Vision Res.* **23,** 1251–1258.

Witkovsky, P., and Stone, S. (1987). GABA and glycine modify the balance of rod and cone inputs horizontal cells in the *Xenopus* retina. *Exp. Biol.* **47,** 12–22.

Witkovsky, P., Stobe, S., and Besharse, J. C. (1988b). Dopamine modifies the balance of rod and cone inputs to horizontal cells of the *Xenopus* retina. *Brain Res.* **449,** 332–336.

Witkovsky, P., Stone, S. L., and MacDonald, E. D. (1988a). Morphology and synaptic connections of HRP-filled, axon-bearing horizontal cells in the *Xenopus* retina. *J. Comp. Neurol.* **275,** 29–38.

Witkovsky, P., Stone, S., and Tranchina, D. (1989). Photoreceptor to horizontal cell synaptic transfer in the *Xenopus* retina: Modulation by dopamine ligands and a circuit model for interactions of rod and cone inputs. *J. Neurophysiol.* **62,** 864–881.

Witkovsky, P., Zhang, J., and Blam, O. (1994). Dopaminergic neurons in the retina of *laevis: Xenopus laevis:* Amacrine vs. interplexiform subtypes and relation to bipolar cells. *Cell Tissue Res.* **278,** 45–56.

Wu, L.-G., and Saggau, P. (1997). Presynaptic inhibition of elicited neurotransmitter release. *Trends Neurosci.* **20,** 204–212.

Yamada, T., Marshak, D., Basinger, S., Walsh, J., Moreley, J., and Stell, W. (1980). Somatostatin-like immunoreactivity in the retina. *Proc. Natl. Acad. Sci. USA* **77,** 1691–1695.

Yang, X.-L., and Wu, S. M. (1989). Modulation of rod-cone coupling by light. *Science* **224,** 352–354.

Yau, K.-W., and Baylor, D. A. (1989). Cyclic GMP-activated conductance of retinal photoreceptor cells. *Annu. Rev. Neurosci.* **12,** 289–327.

Zalutsky, R. A., and Miller, R. F. (1990). The physiology of somatostatin in the rabbit retina. *J. Neurosci.* **10,** 383–393.

Zhang, J., Kleinschmidt, J., Sun, P., and Witkovsky, P. (1994). Identification of cone classes in *Xenopus* retina by immunocytochemistry and staining with lectins and vital dyes. *Visual Neurosci.* **11,** 1185–1192.

Zhu, B. S., Gábriel, R., and Straznicky, C. (1992). Serotonin synthesis and accumulation by neurons of the anuran retina. *Visual Neurosci.* **9,** 377–388.

Zhu, B. S., Hiscock, J., and Straznicky, C. (1990). The changing distribution of neurons in the inner nuclear layer from metamorphosis to adult: A morphometric analysis of the anuran retina. *Anat. Embryol.* **181,** 585–594.

Zhu, B. S., and Straznicky, C. (1991). Morphology and retinal distribution of tyrosine hydroxylase-like immunoreactive amacrine cells in the retina of developing *Xenopus laevis*. *Anat. Embryol.* **184,** 33–45.

Zhu, B. S., and Straznicky, C. (1992). Large serotonin-like immunoreactive amacrine cells in the retina of developing *Xenopus laevis*. *Dev. Brain Res.* **69,** 109–116.

Zhu, B. S., and Straznicky, C. (1993). Co-localisation of serotonin and GABA in neurons of the *Xenopus laevis* retina. *Anat. Embryol.* **187,** 549–555.

Zhu, H., and Green, C. B. (1999). Identification and characterizetion of *Xenopus laevis* cryptochromes. *Invest. Ophthalmol. Vis. Sci.* **40,** S609.

Zhu, H., LaRue, S, Whiteley, A., Steeves, T. D., Takahashi, J. S., and Green, C. B. (2000). The *Xenopus Clock* gene is constitutively expressed in retinal photoreceptors. *Mol. Brain Res.* **75,** 303–308.

Zhuang, M., Wang, Y, Baker, S. A., Steenhard, B. M., and Besharse, J. C. (1999). Cloning and characterization of a *Xenopus* homolog of the *Drosophila* clock gene period. *Invest. Ophthalmol. Vis. Sci.* **40,** S609.

Basement Membrane and β Amyloid Fibrillogenesis in Alzheimer's Disease

Sadayuki Inoue

Department of Anatomy and Cell Biology, McGill University,
Montreal, Quebec, Canada H3A 2B2

High-resolution ultrastructural and immunohistochemical studies revealed that *in situ* β amyloid fibrils of Alzheimer's disease were made up of a core consisting of a solid column of amyloid P component (AP) and associated chondroitin sulfate proteoglycan, and a heparan sulfate proteoglycan surface layer with externally associated fine filaments of β protein. The main body of β amyloid fibrils closely resembled that of microfibrils. Abundant microfibrils were reported to be present at the basement membrane of capillaries with "leaky" blood–urine or blood–air barriers. Similarly, abundant microfibril-like β amyloid fibrils are formed at the microvascular basement membrane in cerebrovascular amyloid angiopathy with altered blood–brain barrier. Since AP is an indispensable major component of microfibrils and microfibril-like structures, the formation of microfibrils may depend on, among other factors, the availability of AP. Thus, in β amyloid fibrillogenesis fibrils may be built around AP which continuously leaks out from circulation into vascular basement membrane, and β amyloid fibrils may be regarded as pathologically altered basement membrane-associated microfibrils. With no source of AP around them, senile plaque fibrils may also be derived from perivascular amyloid.

KEY WORDS: Alzheimer's disease, β Amyloid fibrils, Cerebrovascular amyloid angiopathy, Blood–brain barrier, Vascular basement membrane, Amyloid P component, Microfibrils.   © 2001 Academic Press.

I. Introduction

Alzheimer's disease is a neurologic disorder and the most common form of human amyloidosis that leads to dementia (Castaño and Frangione, 1988). In the cerebral cortex of the brain this disorder is characterized by the occurrence of neuritic, or senile, plaques, microvascular amyloid angiopathy, and neurofibrillary tangles. The core of the plaques (Wisniewski and Wegiel, 1994) and perivascular amyloid deposits in amyloid angiopathy (Miyakawa *et al.,* 1988; Perlmutter and Chui, 1990) are composed of β amyloid fibrils. The fibrils, in turn, are known to contain the β protein (Aβ) (Glenner and Wong, 1984; Wong *et al.,* 1985).

In recent detailed ultrastructural and immunohistochemical studies, β amyloid fibrils *in situ* in the brain of patients with Alzheimer's disease were found to resemble connective tissue microfibrils (Inoue *et al.,* 1999). They had a solid core containing amyloid P component (AP), and Aβ was localized in the form of 1-nm-wide flexible filaments at the surface of the microfibril-like main body of the fibril.

In this article the close similarity of β amyloid fibrils with connective tissue microfibrils is first discussed in detail. Then, the association, under normal and pathological conditions, of large amounts of microfibrils with basement membranes, particularly with vascular basement membranes is reviewed. A possible pathological mechanism for the generation of these abundant perivascular microfibrils is examined with the possibility that AP, leaked out from the circulation through an altered vascular wall, is related to the production of these abundant microfibrils. Similarly, a possible mechanism for the production of abundant microfibril-like β amyloid fibrils at the basement membrane of cerebrocortical microvasculature with an altered blood–brain barrier in the brain with Alzheimer's disease is presented.

II. Ultrastructure and Composition of Isolated and *in Situ* β Amyloid Fibrils

A. Isolated Fibrils and Fibrils Formed from Aβ Analogs

Observations with negative staining of β amyloid fibrils isolated from the brain of patients with senile dementia of the Alzheimer type showed that the fibrils were unbranched, straight rods 4–8 nm in width (Merz *et al.,* 1983). They showed a slow twisting conformation with the presence of repeating narrowings (2–4 nm) with a periodicity of 30–40 nm. The fibrils were apparently made up of two laterally

associated "filaments" 2–4 nm in diameter. This specific conformation of isolated β amyloid fibrils was also confirmed after embedding and thin sectioning (Merz *et al.,* 1983).

In a more recent study β amyloid fibrils were reconstituted from β amyloid protein (β-amyloid$_{1-40}$) isolated from amyloid plaques in the brain of patients with Alzheimer's disease (Roher *et al.,* 1993). These 10-nm-wide reconstituted fibrils were composed of two intertwined strands each 5 nm in width.

Synthetic Aβ analogs, β_{1-42} as well as those with 30, 33, 36, and 39 residues, were incubated in various media and resultant fibrillar structures were examined ultrastructurally with either negative staining or thin sectioning (Burdick *et al.,* 1992). These authors reported that these fibrils produced *in vitro* were similar to the fibrils isolated from senile plaques and cerebrovascular amyloid angiopathy. Aβ_{1-40} was synthesized and incubated with or without the presence of apoE (Castaño *et al.,* 1995). Fibrils were formed and their formation was enhanced by coincubation with apoE. Again, these *in vitro*-formed, approximately 10-nm-wide fibrils were reported, after observation with negative staining, to be similar to isolated fibrils.

B. *In Situ* Fibrils

1. Previous Results

β Amyloid fibrils *in situ* in the brain of patients with Alzheimer's disease and Down's syndrome were examined after embedding and thin sectioning (Miyakawa *et al.,* 1986a, 1988). They were found to be 7- to 10-nm-wide rod-like tubular structures and longitudinal sections showed that they were made up of two parallel dark lines separated by a lucent space, as also reported earlier (Terry *et al.,* 1964). In transverse sections each fibril was composed of a ring-like structure which appeared to be composed of globular subunits. With the use of the method of quick freezing followed by surface replication, Miyakawa *et al.* (1986a) observed that each of 13- to 15-nm-wide fibrils was a hollow rod in which the wall was composed of 3- to 5-nm-wide globular subunits. The subunits were arranged in a tight helix, each turn of which consisted of five closely attached subunits.

2. Recent Systematic High-Resolution Examinations

Recently detailed ultrastructural organization of β amyloid fibrils *in situ* in the brain of patients with Alzheimer's disease was studied in our laboratories (Inoue *et al.,* 1999). For systematic high-resolution, thin-section electron microscopy and immunolabeling, a method developed in our laboratories in recent years for examinations of microfibril-related structures, and described in detail for the examination of *in situ* fibrils of experimental murine AA amyloid (Inoue and Kisilevsky, 1999),

was mainly used. A "systematic microdissection" of β amyloid fibrils was done on thin sections by selecting fibrils sectioned parallel to their axis at different levels of depth. Slightly obliquely sectioned fibrils were utilized for identification of successive levels by observing gradual transition of one layer to the next.

Thus, the outermost surface (outer layer) of the β amyloid fibril was observed to be a layer of random assemblies of 4.5- to 5-nm-wide ribbon-like "double tracks" previously identified (Inoue *et al.,* 1989a) by immunogold labeling as basement membrane-type heparan sulfate proteoglycan (HSPG, perlecan) (Table I). On the outer surface of this layer numerous flexible filaments approximately 1 nm in width and immunohistochemically identified as Aβ were associated (see schematic drawing in Fig. 1). Underneath the HSPG surface layer was the core of the fibril. This rigid core, 9 nm in diameter, was composed of a helically wound second type of ribbon-like double track 3 nm in width. This helical structure enclosed a poorly stained material at its center. Double tracks 3 nm in width were previously identified as chondroitin sulfate proteoglycan (CSPG) with immunogold labeling (Inoue, 1995a). Sections longitudinally cut through the center of the core showed three characteristic parallel dark lines with the middle one often being a string of dark dots. Transverse sections of the core revealed a round or often pentagonal frame with a clear "lumen" containing a central dark dot. In variably loosened cores, a central poorly stained material was often recognized as irregular assemblies of individual 3.5-nm-wide pentagonal frames known to be "pentosomes," the subunits of AP (Inoue, 1991). It was shown that individual pentosomes were intensely stained while after assembly into 8.5-nm-wide disk-like pentagonal AP units they become unstainable (see Figs. 4a–e of Inoue, 1995a) and can be visualized

TABLE I

Components of β Amyloid Fibrils and Their Ultrastructure Identified by ImmunostainingLabeling and *in Vitro* Reconstitution Experiments

Component	Ultrastructure	References
HSPG[a] (perlecan)	4.5- to 5-nm-wide ribbon-like "double tracks"	Inoue *et al.,* 1989a, 1999; Sawada and Inoue, 1994
CSPG	3-nm-wide ribbon-like "double tracks"	Inoue *et al.,* 1997, 1999; Inoue, 1995a
AP subunits ("pentosomes")	3.5-nm-wide pentagonal frames (among other conformations depending on their orientation)	Inoue, 1991
Aβ	1-nm-wide flexible filaments (with tendency to form 3-nm-wide tight helices)	Inoue *et al.,* 1999

[a]HSPG, heparan sulfate proteoglycan; CSPG, chondroitin sulfate proteoglycan; AP, amyloid P component; Aβ, β amyloid protein.
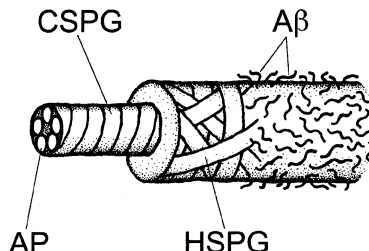
FIG. 1 Schematic representation (cut-out model) of β amyloid fibril *in situ*. The core is made up of a central assembly of pentosomes (AP subunits) which is wrapped in helically wound 3-nm-wide CSPG double tracks. The surface layer of the fibril is composed of a random assembly of 4.5- to 5-nm-wide HSPG double tracks onto which 1-nm-wide flexible filaments of Aβ are associated. See text for detailed explanations. The prototype of this model was proposed by Inoue *et al.* (1999).

only by negative staining. Therefore, the previously reported "tubular" appearance (Miyakawa *et al.,* 1986a, 1988; Terry *et al.,* 1964) of β amyloid fibrils was in fact likely to be due to the presence of the poorly stained pentameric assembly of pentosomes at the core of the fibril.

3. Comparison with Fibrils of Other Types of Amyloid

In situ fibrils of various other types of amyloid were characterized ultrastructurally and immunohistochemically in detail with the method described for the study of the fibrils of experimental murine AA amyloid (Inoue and Kisilevsky, 1999) and also used for examination of β amyloid fibrils as described above. Amyloids so far examined in our laboratories include experimental murine AA amyloid (Inoue and Kisilevsky, 1996), hemodialysis-associated β2-microglobulin amyloid (Inoue *et al.,* 1997), familial amyloid polyneuropathy amyloid (Inoue *et al.,* 1998a), and AL amyloid (S. Inoue, M. Kuroiwa, and R. Kisilevsky, unpublished data).

Fibrils of experimental murine AA amyloid were straight rod-like structures varying from 9 to 16 nm in width (Inoue and Kisilevsky, 1996). They were composed of a core and surface layer which was externally associated with numerous 1- to 2-nm-wide flexible filaments. The core, with a uniform and solid appearance, was made up of a rod-like assembly of pentosomes and was helically wrapped by 3-nm-wide ribbon-like CSPG double tracks. The surface layer was more irregular in its thickness and was made up of random assemblies of 4.5- to 5-nm-wide ribbon-like HSPG double tracks. Finally, fine flexible filaments localized at the surface of the HSPG layer were identified as AA protein with immunogold labeling by the use of 1-nm and 5-nm gold particles. The areas of deposit of the amyloid also contained, in addition to the above-described "mature" fibrils, what appeared to be AA amyloid fibrils in intermediate stages of formation. They were individual 3-nm-wide CSPG double tracks associated

with numerous pentosomes and these CSPG double track–pentosome complexes were in various stages from loose irregular to tighter coiling.

In summary, experimental murine AA amyloid fibrils were made up of a solid core of CSPG and AP, covered by a surface layer of HSPG. AA protein, a protein specific to this amyloid, was associated with the outermost surface of the fibril in the form of loose assemblies of 1- to 2-nm-wide flexible filaments (Inoue and Kisilevsky, 1996).

Hemodialysis-associated β2-microglobulin amyloid fibrils were intensely curved rod-like structures (Inoue *et al.,* 1997). They were made up of a core that was identical to that of the fibrils of experimental AA amyloid and a surface layer which was externally associated with numerous 1-nm-wide flexible filaments. The surface layer of the fibrils of this type of amyloid was composed of random assemblies of 3-nm-wide CSPG double tracks instead of 4.5- to 5-nm-wide HSPG double tracks. External 1-nm-wide filaments were identified as β2-microglobulin. Thus, an unusual feature of β2-microglobulin amyloid fibrils was their CSPG surface layer in which chondroitin sulfate chains may be less effective in providing a rigidity to the fibril core resulting in the curved conformation of the fibrils. Nevertheless, the overall structure of the fibril of this type of amyloid was found to be similar to that of experimental AA amyloid; that is, a protein specific to each type of amyloid was localized in the form of fine filaments at the surface of the main body of the fibril made up of a core and surface layer.

Fibrils of familial amyloid polyneuropathy (FAP) amyloid observed in sural nerve biopsies from FAP(Met 30) patients were straight rod-like structures composed of a core and a surface layer externally associated with 0.5- to 1-nm-wide flexible filaments (Inoue *et al.,* 1998a). The core was found to be identical to that in the fibrils of both experimental AA amyloid and β2-microglobulin amyloid and was made up of AP and CSPG. The surface layer was composed of random assemblies of 4.5- to 5-nm-wide HSPG double tracks. Fine filaments were identified with immunogold labeling as transthyretin. In addition to these fibrils, deposits of an "amorphous" material were also observed and it was a mixture of individual components of the fibril. Again a protein specific to this particular amyloid was present at the surface of the fibril in the form of fine flexible filaments.

Deposits of AL amyloid in the liver and spleen of a patient with AL amyloidosis were composed of coalesced round structures approximately 2 μm in diameter (S. Inoue, M. Kuroiwa, and R. Kisilevsky, unpublished data). The periphery of the round structures was made up of a random mixture of HSPG and CSPG double tracks, 1-nm-wide flexible filaments and a limited amount of pentosomes. Toward the center of the structure, assemblies of irregular fibrils were observed. The fibrils were composed of a surface layer and a core. The surface layer was a random assembly of 4.5- to 5-nm-wide HSPG double tracks, onto which 1-nm-wide flexible filaments of possibly immunoglobulin light chains were attached. unlike the fibrils of other types of amyloid, however, the core of AL amyloid fibrils was not a uniform structure, but rather an irregular one which contained an apparently

insufficient amount of pentosomes to form a solid core. In spite of this irregularity the fibrils of AL amyloid had a structure common to the fibrils of all other types of amyloid so far examined; that is, the main body of the fibril was peripherally associated with a protein specific to the given type of amyloid, in this case possibly immunoglobulin light chains, in the form of approximately 1-nm-wide flexible filaments.

Thus, there is a distinct pattern of organization of amyloid fibrils common to all types of amyloid so far examined including β amyloid of Alzheimer's disease, with only minor exceptions. The main body of the fibril is composed of a surface layer containing HSPG, with the exception of β2-microglobulin amyloid fibrils in which HSPG is replaced by CSPG, and a uniform and solid core made up of CSPG and AP with the exception that the core of AL amyloid fibrils is irregular due to an insufficient amount of available pentosomes for the formation of a rigid core. A protein specific to each type of amyloid is associated with the outermost surface of the main body of the fibril in the form of fine (approximately 1-nm-wide) flexible filaments. The main body of the amyloid fibril is also found to be identical to connective tissue microfibrils as well as to basement membrane-associated microfibrils ("bastotubules") as described below (Section III.B).

4. Conformation and Arrangement of Aβ in the β Amyloid Fibrils

As described above the β amyloid fibril is composed of a main fibrillar structure containing CSPG, HSPG, and AP onto the surface of which Aβ is associated in the form of 1-nm-wide flexible filaments (Inoue *et al.*, 1999). However, recent evidence indicates the possibility that Aβ filaments, and filaments of other types of amyloid as well, may be localized at the surface of the main body of the fibril in a more organized manner.

As described above, in the fibril of experimental murine AA amyloid, AA protein was found to be localized, as in the case of β amyloid, at the surface of the main body of the fibril in the form of 1-nm-wide flexible filaments in tissue samples prepared by the use of glutaraldehyde as the primary fixative (Inoue and Kisilevsky, 1996). However, following the use of formaldehyde instead of glutaraldehyde, a significant proportion, but not all, of the AA amyloid fibrils showed the AA protein in a more organized arrangement. AA protein filaments 1 nm in width were coiled into 3-nm-wide tight helices, and at the surface of the main body of the fibril the helices were arranged parallel to the axis of the fibril and also to one another with a uniform center-to-center distance of approximately 5 nm. Therefore, there was the possibility that this well organized structure was the original, unaltered conformation of the AA protein in AA amyloid fibrils in the living state, in view of the known faster tissue penetration, and resulting quicker fixation, of formaldehyde as compared with glutaraldehyde.

In order to examine this possibility, recent, more advanced methods of tissue preparation, that is, fixation with cryofixation and dehydration with freeze

substitution, were used. These methods are believed to allow preservation of tissues in a state closest to that found in the living condition (Elder, 1989; Harvey, 1981). The result showed that the AA protein in the form of regular parallel 3-nm-wide helices, which was observed in a part of formaldehyde-fixed fibrils but not in glutaraldehyde-fixed fibrils, was observed virtually in all fibrils of experimental murine AA amyloid (S. Inoue, M. Kuroiwa, R. Kisilevsky, unpublished data) (Fig. 2). Therefore, it is demonstrated, at least in one type of amyloid, that a protein specific to the given type of amyloid is present at the surface of the main body of the fibril in an arrangement more elaborate than that originally thought. It is not yet certain whether amyloid proteins in other types of amyloid including Aβ of Alzheimer's disease are also present with this characteristic conformation and arrangement. Evidence that may be in favor of such a specific arrangement of the amyloid protein is a published electron micrograph of β amyloid fibrils (Fig. 5A in Miyakawa *et al.,* 1986b). This micrograph shows groups of approximately 3-nm-wide parallel straight strands with a pattern indicative of helical structure in a thin section preparation of β amyloid fibrils. This arrangement resembles that of the AA protein in cryofixed fibrils of experimental AA amyloid described above, although the authors of this article interpreted the arrangement otherwise. Therefore, there is a possibility that Aβ is also present at the surface of the main body of the fibril in the form of parallel 3-nm-wide tight helices.

C. Possible Reasons for Disagreement in the Structure of β Amyloid Fibrils as Observed *in Situ* and after Isolation

As discussed above, β amyloid fibrils isolated from the brain of patients with Alzheimer's disease are 8- to 10-nm-wide slowly twisting structures, and they are composed of two laterally associated strands 2–5 nm in width (for example, Merz *et al.,* 1983; Roher *et al.,* 1993). The fibrils reconsituted from synthetic Aβ analogs were also reported to take a similar conformation. On the other hand, in β amyloid fibrils observed *in situ,* Aβ is localized in the form of 1-nm-wide flexible filaments at the surface of the main body of the fibril made up of HSPG, CSPG, and AP (Inoue *et al.,* 1999).

Thus, there is a significant different in the structure of β amyloid fibrils *in situ* and after isolation. The reason for this disagreement has not yet been fully investigated. However, the results of the following study with the fibrils of experimental murine AA amyloid may offer some clues which will be helpful in the clarification of this crucial problem.

There is a question in the adequacy of the procedures of isolation in satisfactorily preserving the detailed original ultrastructural arrangements of often delicate and frail biological structures such as amyloid fibrils. To examine this problem, the fibrils of experimental murine AA amyloid were observed in detail at high resolution before and after their isolation (Inoue *et al.,* 1998b). Fibrils of experimental
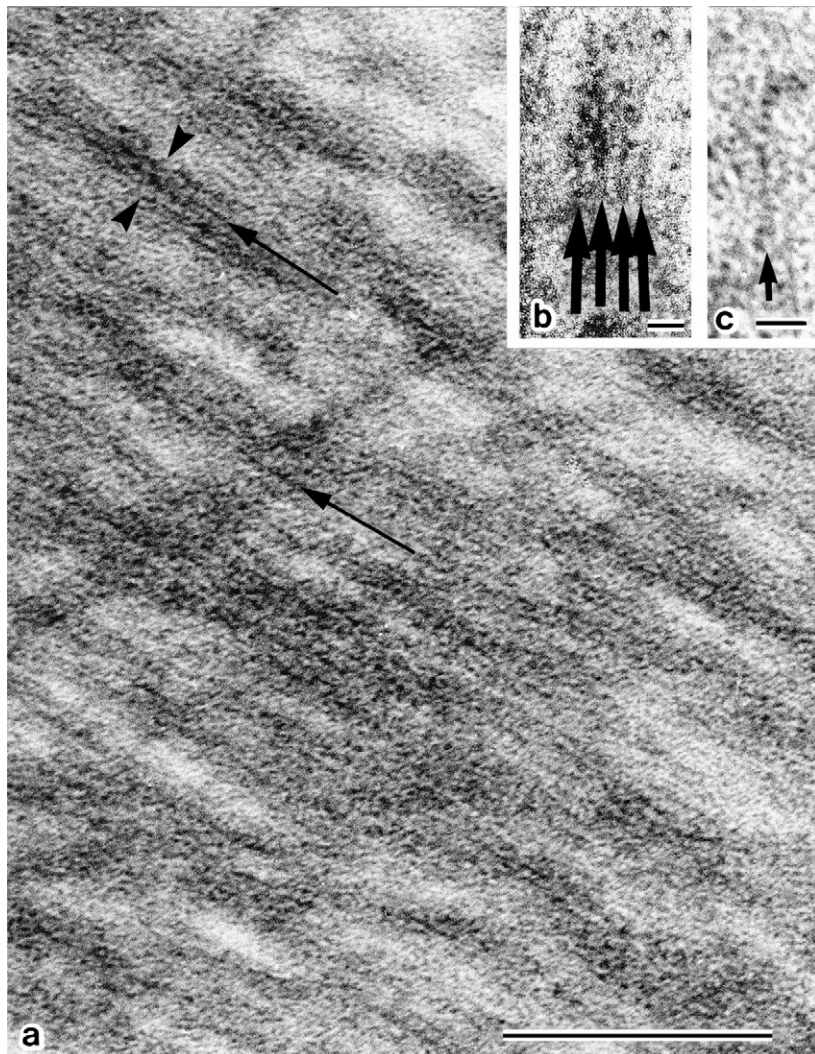
FIG. 2   Tissue of experimental mouse AA amyloid fixed with immersion cryofixation followed by dehydration with freeze substitution. (a) General view of parallel assembly of AA amyloid fibrils (width of a fibril is indicated by arrowheads). It is characterized by the presence of fine straight strands (arrows) which are parallel to the axis of the fibril and also to one another. These strands are localized at the surface of the fibril as also confirmed by the observation of transversely sectioned fibrils. (b) Up to four parallel strands (arrows) are seen over each fibril with a uniform center-to-center distance of 5 nm (the total number of strands around the circumference of the fibril is estimated to be six). (c) The strand, which was positively immunolabeled for AA protein, was resolved, when staining was optimum, to be a 3-nm-wide rod made up of 1-nm-wide filaments in a tight helix. (a) $\times$ 353,600, bar = 100 nm; (b) $\times$ 503,200, bar = 10 nm; (c) $\times$ 646,000, bar = 10 nm (all original magnifications).

murine AA amyloid were isolated with the standard distilled water washing method (Pras *et al.,* 1968). Isolated fibrils were composed of variously loosened cores of the above-described *in situ* fibrils after their HSPG surface layer as well as AA protein filaments became detached from the fibril and dispersed into the distilled water. These denuded fibrils (cores) appeared less rigid and often lost their linearity and typical fibrillar appearance to various extents. The freed 1-nm-wide AA protein filaments in the distilled water then became coiled into 3-nm-wide tight helices. These helices, in turn, formed pairs by lateral association and became characteristic slowly twisting structures resembling the reported "isolated amyloid fibrils." The latter were much more conspicuous due to their characteristic clear cut conformation as compared with the denuded fibrils which variously lost their consistency (Inoue *et al.,* 1998b).

It is also probable that in the case of the β amyloid fibrils of Alzheimer's disease isolated fibrils with the reported slowly twisting conformation were similarly and artifactually formed during the procedure of isolation with the distilled water washing method.

III. Close Similarity of β Amyloid Fibrils *in Situ* with Connective Tissue Microfibrils

A. Ultrastructure and Composition of Microfibrils

Microfibrils, the name coined by Low (1961a,b, 1962), are a major fibrous component of the connective tissue. They are straight rod-like structures approximately 10 nm in width, and have been best known as the peripheral component of elastic fibers (Cleary and Gibson, 1983). They are also localized free within tissue space as, for example, the main constituent of the suspensory ligament (Raviola, 1971). Microfibrils are abundant in areas of tissues known to be subjected to severe mechanical stress and have an important role as the connecting rods interlinking various connective tissue components and cells for a unified efficient functioning of the tissue as a whole (Essner and Gordon, 1984; Goldfischer *et al.,* 1983; Krauhs, 1983; Leak and Burke, 1968).

The biochemical composition of microfibrils has been intensely studied in the past few decades (Cleary and Gibson, 1983; also see Discussion in Inoue, 1995b) and the presence of various components including fibrillin (Sakai *et al.,* 1986) and HSPG (Volker *et al.,* 1987) has been reported. However, detailed ultrastructural studies of microfibrils have been scarce and often fragmentary. The results of more systematic ultrastructural studies showed that the microfibril proper was composed of a "tubule" and 3-nm-wide ribbon-like structures which were helically wrapped around the former (Inoue and Leblond, 1986). With positive immunodetection of AP in the microfibrils (Inoue *et al.,* 1986) it was concluded that the

tubule was made up of a column of successive flat disk-like pentagonal AP units (Inoue and Leblond, 1986) (Figs. 3 and 4).

More recent studies showed that microfibrils were composed of a microfibril proper (Inoue, 1995a), which was previously thought to be an intact microfibril ("classical" microfibrils), and externally associated components (Inoue, 1995b).
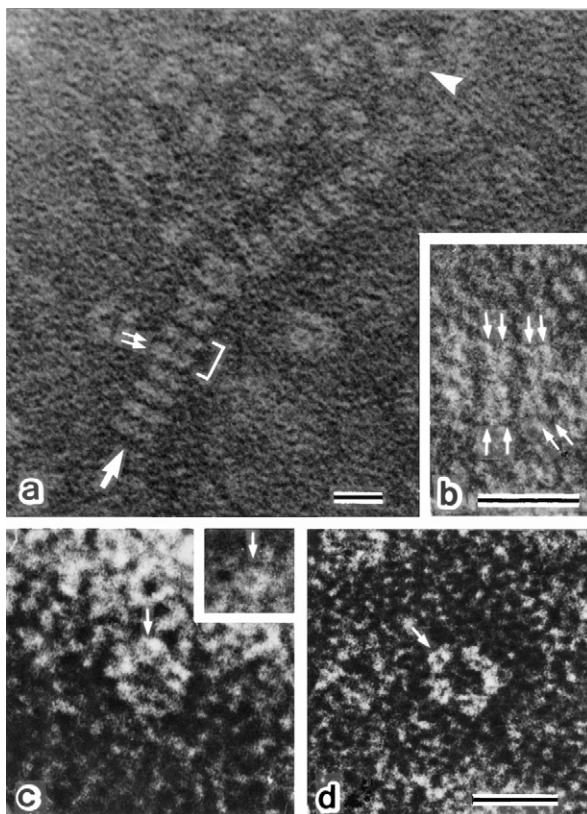
FIG. 3 High-resolution observations of AP with negative staining (see also Fig. 4). (a) Individual 8- to 9-nm-wide disk-like pentagonal units (face-on view, arrowhead) as well as their rod-like assembly (large arrow) are present. Bracket indicates side view of an AP molecule composed of face-to-face attachment of two units containing a total of 10 subunits. Each subunit in its side view is a U-shaped structure (paired tiny arrows). (b) High-magnification view of AP molecule (side view) composed of U-shaped subunits (paired arrows). (c) Commonly seen face-on view of a unit composed of five subunits (arrow). (Inset) The subunit shows the conformation of a minipentagonal frame 3.5 nm in width (arrow). (d) Rarely seen face-on view of the unit composed of five smaller pentagonal frames (arrow). A central "hole" surrounded by subunits is much larger than that in (c). (a) $\times 664,700$, bar $= 10$ nm; (b) $\times 1,280,000$, bar $= 10$ nm; (c, inset, d) $\times 1,100,000$, bar $= 10$ nm (all original magnifications). (Reproduced with permission from *Cell Tissue Research*. Pentosome—a new connective tissue component—is a subunit of amyloid P. S. Inoue, Vol. 263, pp. 431–438, Fig. 7a–d, 1991. Copyright © 1991 by Springer–Verlag.)
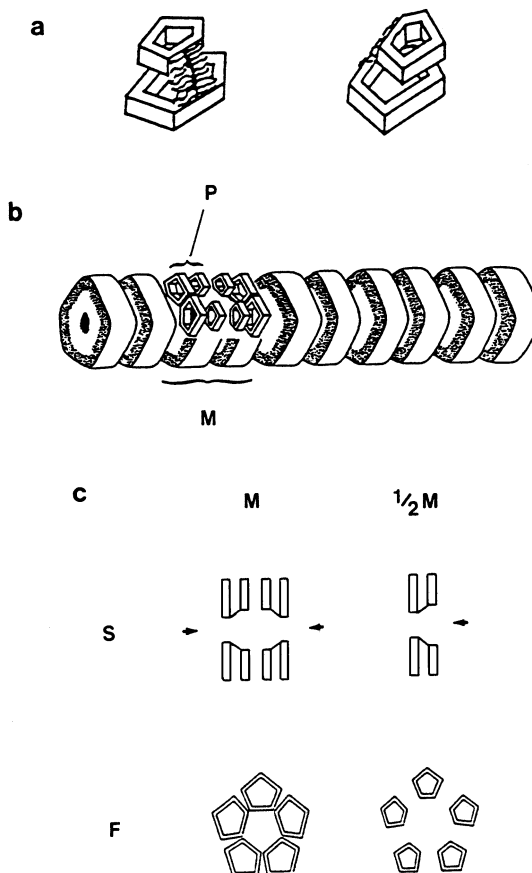
FIG. 4   Schematic drawing of AP subunits (pentosomes) and their assemblies. (a) Pentosomes seen from two directions. (b) Assembly of pentosomes (P) into a rod-like structure. M, a molecule of AP. (c) Side (S) and face-on view (F) of AP molecule (M) and "half-molecule" (12 M). Face-on views are those seen from the directions indicated by arrows in S. Half-molecules of AP are only rarely present in the preparation. (Modified with permission from *Cell Tissue Research*. Pentosome—a new connective tissue component—is a subunit of amyloid P. S. Inoue, Vol. 263, pp. 431–438, Fig. 8a–f, 1991. Copyright © 1991 by Springer–Verlag.)

The former were microfibrils identifiable after preparation of the tissue with conventional methods, in which externally associated materials were usually lost during the course of the preparation. For the study of the ultrastructure of microfibrils proper, tissue containing areas in the vicinity of "mature" microfibrils proper in the posterior chamber of the mouse eye was prepared with nonconventional methods which included embedding in a water-soluble resin. In these areas various stages of the formation of microfibrils proper were observed. Free individual ribbon-like 3-nm-wide double tracks made up of CSPG were seen associated on both sides

with 3.5-nm-wide particulate AP subunits, or "pentosomes" (Inoue, 1991). These CSPG double track–pentosome complexes were also seen as being coiled to various degrees from loose to tight, and in the tighter helices all associated pentosomes were wrapped and enclosed within the center of the helix. As the helix became increasingly tighter enclosed pentosomes combined with one another to form successive 8- to 9-nm-wide disk-like AP units (Figs. 3 and 4), and, together with the helically applied CSPG double tracks, it resulted in the formation of straight rod-like structures indistinguishable from microfibrils proper. The intact microfibril proper was characterized by cross-striations at its surface due to the presence of the helically wound 3-nm-wide CSPG double tracks. The transverse section of a microfibril proper shows a round or often pentagonal frame with a lucent lumen containing a tiny central dot. Individual pentosomes could be stained intensely but when they assembled, as described above, into pentagonal AP units they became virtually unstainable (Inoue, 1995a) and these AP units could be visualized only by negative staining. Therefore, the microfibril proper with its center occupied by a column of AP, appeared "tubular" with a "lucent lumen," as has long been reported. A tiny dark dot at the center of the "lumen" in transversely sectioned microfibrils proper was in fact a stain-filled tiny hole left at the center of a 8- to 9-nm-wide disk-like AP unit in which five pentosomes were assembled.

Disorganization (Fig. 5) and reorganization (Fig. 6) of microfibrils proper, which are composed of CSPG double tracks and pentosomes as described above, could be demonstrated. When intact microfibrils proper *in situ,* as shown at medium (Fig. 5a) and high magnification (Fig. 5b), were treated with a deaminating agent, nitrous acid, they lost their integrity with the release of abundant pentosomes (Fig. 5c). At higher magnification the crumbling remain of a microfibril proper composed of entangled CSPG double tracks were seen along with the presence of freshly released pentosomes (Fig. 5d). For *in vitro* reorganization, or reconsitution, of microfibrils proper, pentosomes (Fig. 6a) and a preparation of CSPG were coincubated at 35°C. The resultant precipitate contained parallel assemblies of reconsituted microfibrils proper (Fig. 6c) and their ultrastructure and composition were very similar to those of microfibrils proper observed in the tissue (Inoue, 1995a). Incubation of CSPG alone resulted in the formation of aggregates of 3-nm-wide ribbon-like double tracks (Fig. 6b).

Components externally associated with the microfibril proper are usually lost following preparation of tissues for ultrastructural examinations with conventional methods. The only exception was fibronectin, which was observed to be associated at the surface of microfibrils proper in the form of, on the average, 1.5-nm wide flexible filaments even after preparation of the tissue with conventional methods (Inoue *et al.,* 1989b). The other external components were shown to be preserved by the use of preparative methods known to minimize the loss of tissue components which included dehydration with freeze substitution, embedding in water-miscible resin without dehydration and the use of potassium permanganate or uranyl acetate as fixatives (Inoue, 1995b). Small clusters of fibrillin were periodically associated
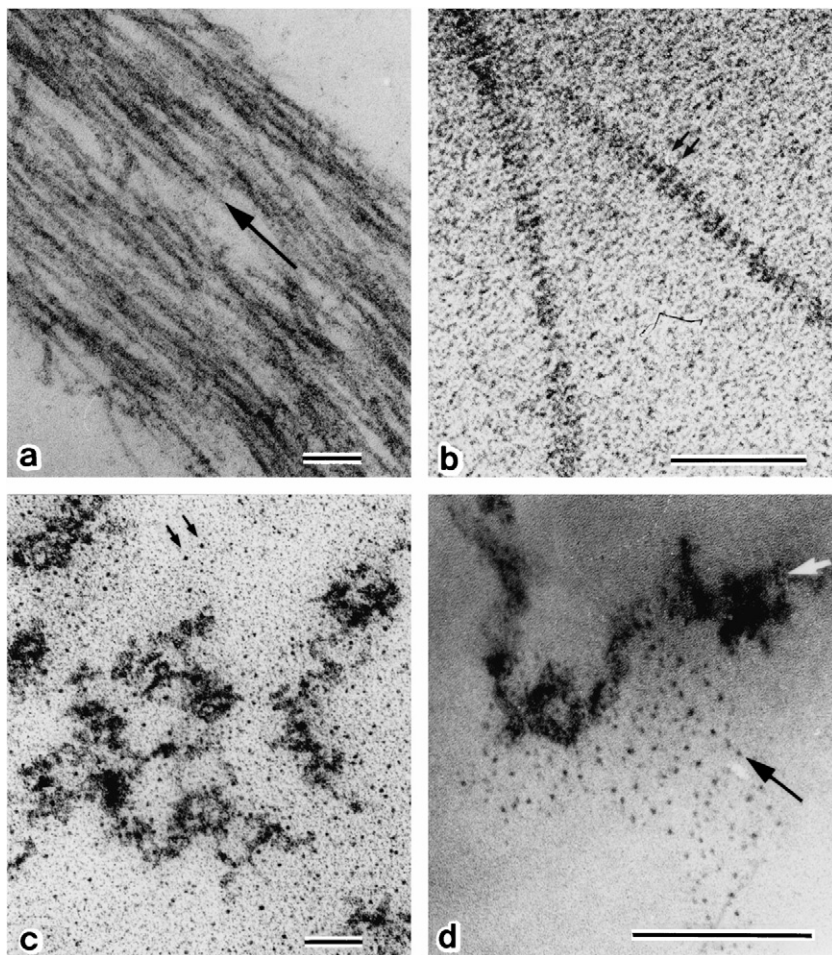
FIG. 5   Disorganization of the main body of the microfibril ("classic" microfibril). (a) Intact classic microfibrils (zonular microfibrils of the mouse eye) are unbranched, straight rods approximately 10 nm in diameter (arrow). (b) Their surface is characterized by the presence of cross-striations (tiny arrows) due to the presence of helically wound 3-nm-wide CSPG "double tracks." (c) After treatment with a deaminating agent, nitrous acid, classic microfibrils lost linearity and integrity with the release of abundant pentosomes (AP subunits) (tiny arrows). (d) At high magnification it was apparent that the degradation of classic microfibrils coincided with the release of pentosomes. A disorganizing microfibril (white arrow) is seen still attached by pentosomes in the form of parallel strings (dark arrow) immediately after their release. (a) $\times$ 77,700, (b) $\times$ 179,100, (c) $\times$ 77,700, (d) $\times$ 238,000; bars = 100 nm (all original magnifications).
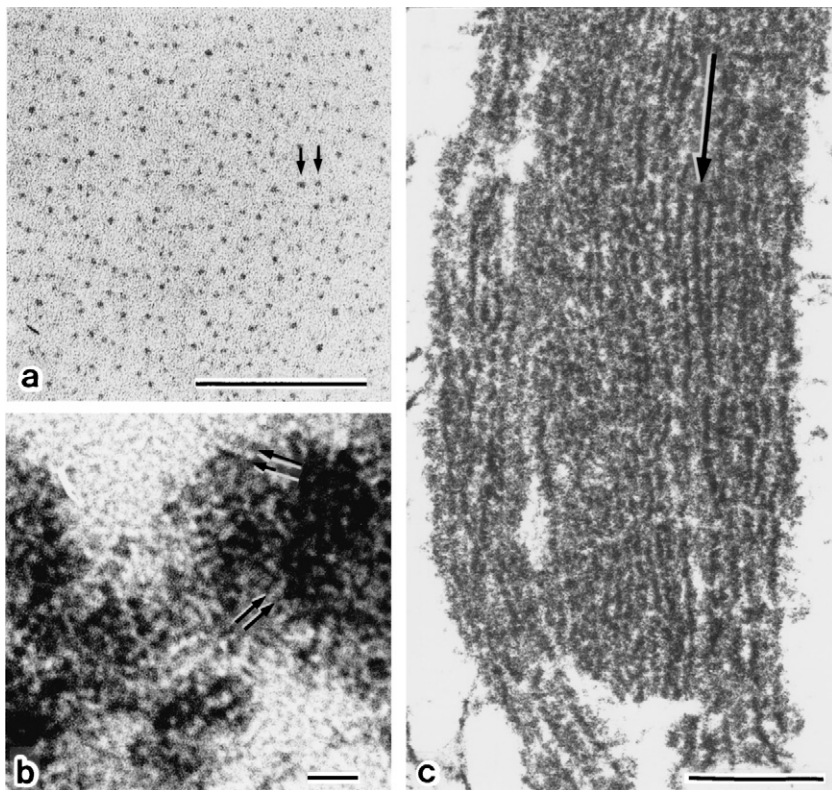
FIG. 6 Reorganization of classic microfibrils. For *in vitro* reorganization, or reconstitution, a preparation of pentosomes (a, arrows) was coincubated with purified CSPG at 35°C for 1 h. The resultant precipitate was composed of parallel assemblies of reconstituted classic microfibrils (c, arrow). Incubation of CSPG alone produced random aggregates of 3-nm-wide CSPG double tracks (b, paired arrows). (a) × 229,500, bar = 100 nm; (b) × 641,900, bar = 10 nm; (c) × 17,700, bar = 1 μm. [(c) Modified with permission from *Cell Tissue Research*. Ultrastructural organization of connective tissue microfibrils in the posterior chamber of the eye *in vivo* and *in vitro*. S. Inoue, Vol. 279, pp. 291–302, Fig. 11b, 1995. Copyright © 1995 by Springer–Verlag.]

at the surface with a uniform interval of 45 to 65 nm along the length of microfibrils proper. In addition, these whole microfibrils proper were enclosed in large random assemblies of 4.5- to 5-nm-wide ribbon-like HSPG double tracks. Periodically associated fibrillin may mediate the association of HSPG with the microfibril proper because when some HSPG was lost during preparation, remaining HSPG double tracks were still attached to the microfibril proper in the form of small clusters localized at periodical sites where fibrillin was associated (Inoue, 1995b).

B. Comparison of β Amyloid Fibrils *in Situ* with Microfibrils

There is a close similarity between β amyloid fibrils *in situ* (Inoue *et al.,* 1999) and connective tissue microfibrils (Inoue, 1995a,b). They have a common core made up of helically wound 3-nm-wide ribbon-like double tracks which enclose a column of assemblies of pentosomes, the subunit of AP. The core of both β amyloid fibrils and microfibrils is enclosed within the surface layer of HSPG although it is much thicker in the case of microfibrils in which the association is probably mediated by periodically localized fibrillin. β Amyloid fibrils are associated at their surface with 1-nm-wide flexible Aβ filaments while 1.5-nm-wide flexible fibronectin filaments are similarly associated with the surface of microfibrils. From these observations β amyloid fibrils, as well as the fibrils of other types of amyloid so far examined (Inoue and Kisilevsky, 1996; Inoue *et al.,* 1997, 1998a; S. Inoue, M. Kuroiwa, and R. Kisilevsky, unpublished data), resemble microfibrils, and β amyloid fibrils may be regarded as a pathologically modified form of microfibrils as described below.

IV. Association of Microfibrils with Normal and Pathological Basement Membranes

A. Ultrastructure and Composition of Common Basement Membranes

The most commonly and widely occurring basement membrane is a characteristic laminated structure with the total thickness of less than 200 nm, which is in association with the epithelia (Fig. 7a), endothelia, and muscle fibers, and which also surrounds the central nervous system. It has generally been known to be composed of three layers (Kefalides *et al.,* 1979; Laurie and Leblond, 1985; Inoue and Leblond, 1988; Inoue, 1989). The main dense layer is referred to as the lamina densa (Fig. 7a,D) with a thickness varying from 25 to 125 nm depending on the location. A 15- to 65-nm-wide lucent layer, or space, the lamina lucida, is localized between the surface of the cell and the lamina densa. This narrow space has been shown to be artifactually produced during preparation of tissues with conventional methods for ultrastructural studies (Goldberg and Escaig-Haye, 1986; Chan and Inoue, 1994). The third layer of common basement membranes is a poorly delimited transitional zone between the lamina densa and underlying connective tissue. It is known as the lamina or pars fibroreticularis and contains specialized structures such as anchoring fibrils.

At the ultrastructural level the whole lamina densa of common basement membranes is composed of a fine network of irregular anastomosing strands referred to as "cords" (Inoue and Leblond, 1988; Inoue, 1989, 1994). The thickness of the
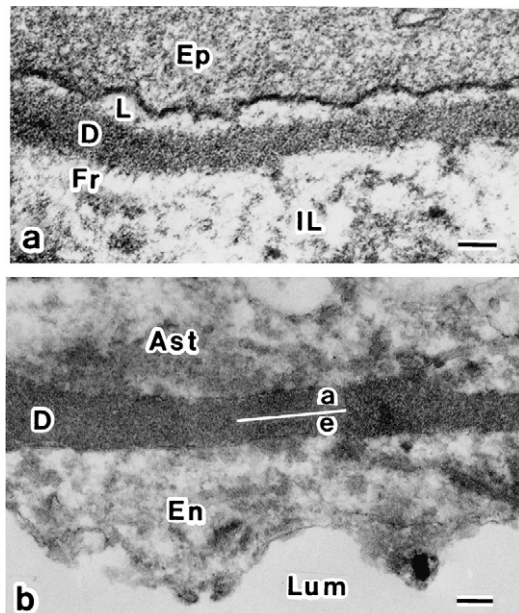
FIG. 7 Common basement membrane (a) and "double" basement membrane (b). (a) A typical common basement membrane (basement membrane of monkey seminiferous epithelium) is composed of a dense main layer referred to as the lamina densa (D); a lucent layer (space) between the surface of an epithelial cell (Ep) and the lamina densa is the lamina lucida (L), which was shown to be an artifact produced during preparation of tissues with conventional methods. The transition zone between the lamina densa and connective tissue (internal lamina, IL) is referred to as the pars or lamina fibroreticularis (Fr). (b) Double basement membrane. The basement membrane of the capillary wall of the normal human cerebral cortex is shown as an example. The lamina densa (D) of this basement membrane is formed by the fusion of the lamina densa (a) of the basement membrane of an astrocyte and that (e) of the basement membrane of the capillary endothelium. With the method used for the preparation of this specimen the artifactual laminae lucidae were not produced along both sides of the fused lamina densa. Ast, endfoot of astrocyte; En, endothelial cell; Lum, lumen of capillary. (a) $\times$ 48,000, (b) $\times$ 44,500; bars = 100 nm (all original magnifications).

cords varies from 3.2 to 4.8 nm in routinely processed and thin sectioned murine tissues (Inoue, 1994) and in tissues after cryofixation and freeze–drying or substitution (Chan *et al.,* 1993a,b). The size of the openings of the cord network, or the "intercordal space diameter index" (ICSDI, see Inoue and Leblond, 1988) of the cord network, varies from 11.1 to 14.2 nm (Inoue, 1994). As to the ultrastructure and biochemical composition of the cord itself all basement membrane components are integrated within the cord since all of the components were immunodetected within the cords (Laurie *et al.,* 1982, 1984). Following the treatment of the cord network with a proteolytic enzyme, plasmin, all of the components of the cord were digested away leaving behind a network of fine filaments which

were positively immunostained for type IV collagen (Inoue *et al.,* 1983). These results indicate that the basement membrane cord is composed of a core of a type IV collagen filament which is covered by and integrated with other components of the basement membrane including laminin, HSPG, entactin, and others (Inoue and Leblond, 1988; Inoue, 1989).

B. Vascular (``Double") Basement Membranes

An unusual specialization of common basement membranes is the formation of "double" basement membranes by the fusion of two common basement membranes. Thus, the basement membrane of the vascular endothelium fuses with that of the epithelium in such a way that the laminae densae of both endothelial and epithelial basement membranes fuse to one another to form a compound lamina densa while the two laminae fibroreticulares are lost. Two laminae lucidae persist on both sides of the compound lamina densa and are referred to as the lamina lucida interna (facing the endothelium) and externa (facing the epithelium). As described above, however, these lucent spaces are known to be produced artifactually and if the tissue is processed in a way which is known not to produce such an artifact, the surfaces of the compound lamina densa are directly in contact with an epithelium on the one side and the capillary endothelium on the other without the presence of intervening laminae lucidae. Thus, as shown in Fig. 7b with the basement membrane of the cerebrocortical microvasculature as an example, the astrocyte half of this double basement membrane is closely applied to the astrocyte and the endothelial half is directly associated with the endothelial cell.

This type of specialized basement membrane is observed in diverse locations within the body. The glomerular basement membrane of the kidney occurs by the fusion of the basement membrane of the visceral epithelium of the glomerulus and that of the glomerular capillary endothelium (Farquhar, 1991). In the lung, the alveolar–capillary basement membrane is formed as a result of the fusion of the basement membrane of the alveolar epithelium and that of the pulmonary capillary endothelium at areas where the narrow connective tissue space between these two common basement membranes is abolished (Low, 1961a). Finally, the wall of the cerebromicrovasculature of the brain contains a double basement membrane, as shown above (Fig. 7b), formed by the fusion of the basement membrane of the astrocyte and that of the vascular endothelial basement membrane (Buée *et al.,* 1997).

At the ultrastructural level double basement membranes resemble common basement membranes (Laurie *et al.,* 1984). The glomerular basement membrane of the rat kidney is composed of a fine network of cords of a thickness comparable to that of the cords of common basement membranes. The size of the openings of the cord network (ICSDI, see above), however, was slightly smaller (8 nm) due to the well known role of this particular basement membrane as a filtration barrier (Farquhar, 1991).

C. Abundant Basotubules in Vascular Basement Membranes in Health and Disease

Incorporation of small numbers of microfibrils into normal basement membranes which include the glomerular basement membrane of the kidney, has long been known (Farquhar, 1991; Farquhar *et al.,* 1961; Hsu and Churg, 1979; Latta, 1970) under the name of either "distinct fibrils," "large straight fibrils," or, more recently, "basotubules" (Inoue *et al.,* 1983; Laurie *et al.,* 1984). In the normal glomerular basement membrane small numbers of basotubules were localized preferentially at the lamina lucida interna or the lamina densa at its endothelial half, that is, at sites closer to the capillary lumen (Farquhar *et al.,* 1961; Laurie *et al.,* 1984).

In disease conditions the amount of basotubules was reported to increase considerably (Hsu and Churg, 1979; Hsu *et al.,* 1980; Olsen, 1979; Inoue and Bendayan, 1995). In various glomerular diseases which include transplant glomerulopathy caused by chronic renal allograft rejection (particularly when it was associated with focal sclerotic legions), preecclamptic nephropathy, and focal segmental glomerulosclerosis, abundant basotubules were localized within the specific area of a widened subendothelial space, that is, the lamina lucida interna, of the glomerular basement membrane (Hsu and Churg, 1979; Olsen, 1979; Hsu *et al.,* 1980). In these diseases loosening or breakdown of the blood–urine barrier (Table II) to various extents has been known to occur as a result of vascular damage including partial or complete detachment of the endothelium as seen, for example, in transplant glomerulopathy, and proteinuria was always associated with these diseases (Hsu and Churg, 1979). The specific site where these abundant basotubules were present coincided with the structure (vascular basement membrane) which leaked out plasma may first encounter.

Detailed high-resolution ultrastructural studies in our laboratories (Inoue and Bendayan, 1995) showed that the lamina densa of the basement membrane split into epithelial and endothelial halves in the rat glomerular basement membrane with long-term experimental diabetes. Drastic changes occurred in the endothelial half where the basic structure of the lamina densa, that is, the cord network, was mostly lost and bundles of basotubules appeared within the resultant vacant spaces (Figs. 8a and 8b). The amount of these basotubules varied and in certain cases were extremely abundant, and the bundles of basotubules reached widths of as much as 400 to 450 nm, in comparison with the smaller width of the whole lamina densa in age-matched control animals (approximately 200 nm). These large bundles had a tendency to "grow" (extend) out of the basement membrane into the lumen of the capillary (Fig. 8c). Again, this specific site of abundant basotubules is also the site into where plasma may first leak after breakdown of blood–urine barrier with resultant major proteinuria.

In an unusual circumstance an association of abundant basotubules with the vascular basement membrane is also known to occur in normal tissues. The

TABLE II

Incomplete or Impaired Barriers around Capillaries and Localization of Abundant Microfibril-Related Structures

Barrier	Blood–air	Blood–urine	Blood–brain
Tissue condition	Normal	Pathological	Pathological
State of barrier	Incomplete barrier with "loose" endothelial junction	Impaired barrier with proteinurea	Compromise of barrier with leakage of plasma
Abundant presence of	Microfibrils (basotubules)	Microfibrils (basotubules)	Microfibril-like β amyloid fibrils
Basement membrane (BM) involved	Alviolar and capillary BM of lung	Glomerular BM of kidney	Cerebrovascular BM of brain
Disease	—	For example: transplant glomerulopathy, long-term experimental murine diabetes	Cerebral amyloid angiopathy of Alzheimer's disease

alveolar–capillary wall of the lung is made up of a thin layer of the alveolar epithelium with an associated basement membrane and, across an intervening thin layer of connective tissue, the pulmonary capillary endothelium with its basement membrane. The width of this intervening layer of connective tissue varies and, in places, it is obliterated. Thus, a double basement membrane is formed in such areas as a result of fusion of the epithelial and endothelial basement membranes. In the normal human lung, in areas where the alveolar–capillary wall contains a narrow connective tissue space, both epithelial and endothelial basement membranes were reported to be associated with unusually abundant basotubules (Low, 1961a,b, 1962) (Table II). The lamina densa of both basement membranes was shown to be rich in basotubules running approximately parallel to the direction of the lamina

FIG. 8   Rat glomerular basement membrane with long-term experimental diabetes. (a) Degradation and loss of endothelial half (en) of the lamina densa (D). ep, epithelial half of the lamina densa; Ep, foot process of podocyte of visceral epithelium; En, endothelial cell. (b) Presence of numerous irregular microfibrils (arrow) which fill the space of the endothelial half of the lamina densa. The epithelial half (ep) of the lamina densa is relatively unchanged. (c) Abundant microfibrils are extending away from the basement membrane in the direction (arrow) toward the lumen of the capillary. (a) × 38,900, (b,c) × 62,900; bars = 100 nm (all original magnifications).
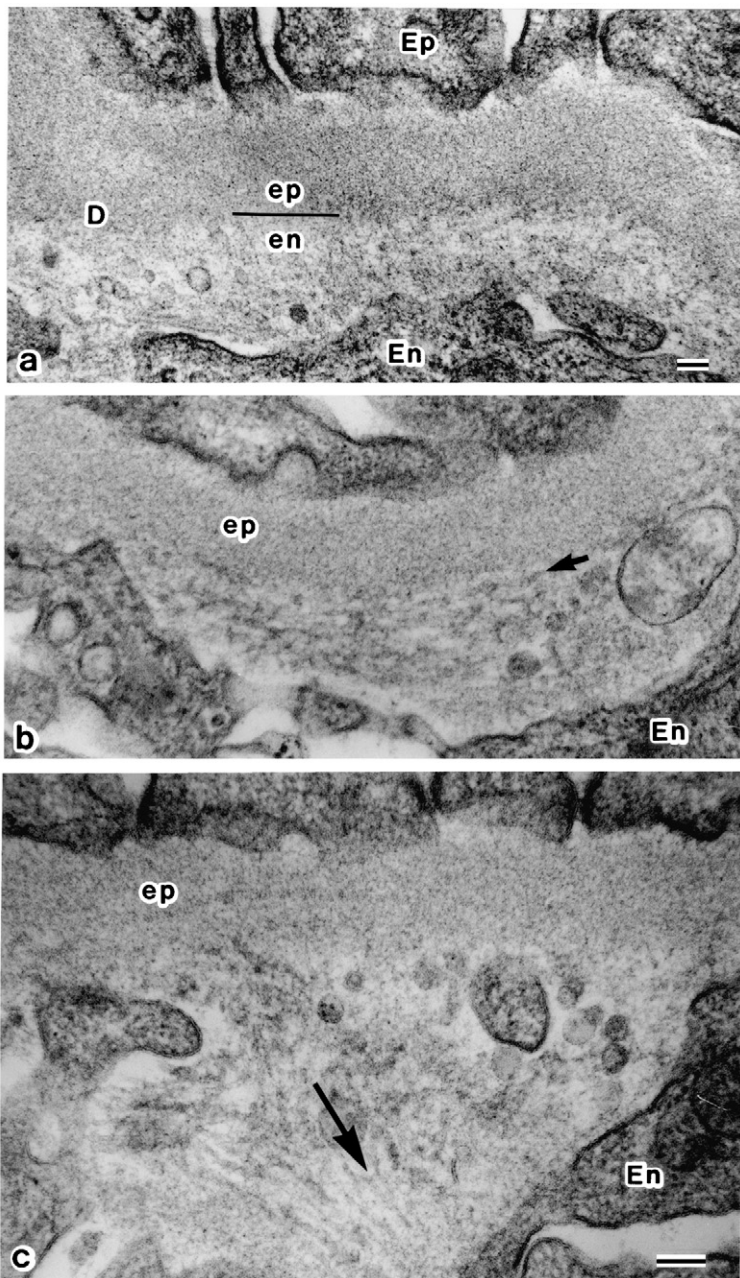
densa and giving the impression that the lamina densa was largely made up of basotubules. In addition many of them were seen fraying toward the connective tissue space to form extensive "zona diffusa" (lamina fibroreticularis) exclusively made up of microfibrils. In the narrow connective tissue space between these two types of basement membranes, microfibrils were also unusually numerous. The double basement membrane of the alveolar–capillary wall formed by the fusion of epithelial and endothelial basement membranes was also examined in the normal mouse lung (Fig. 9a). It contained a number of
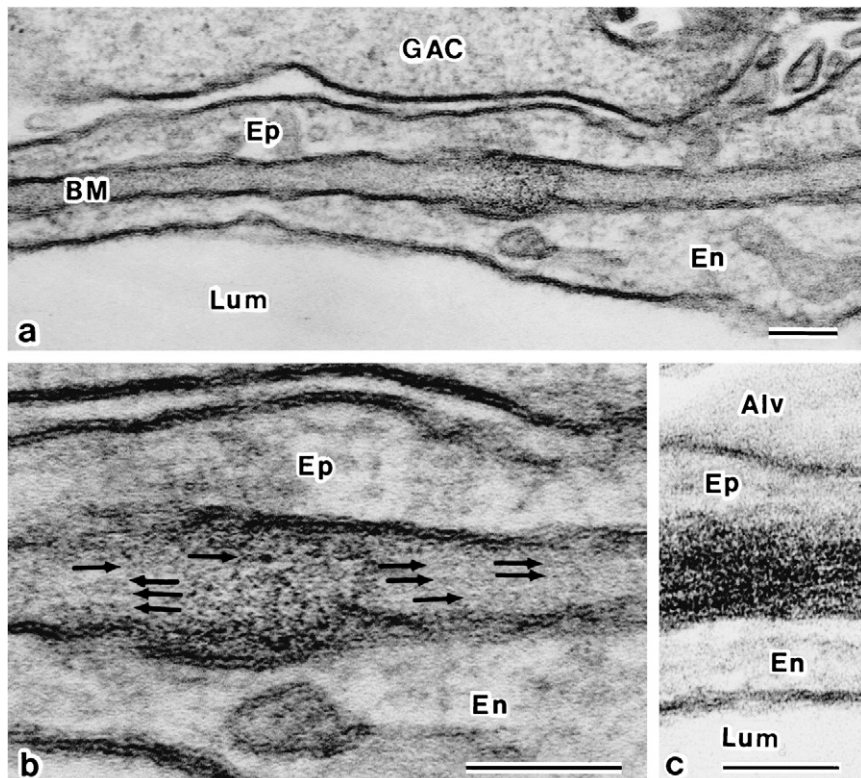
FIG. 9   Alveolar–capillary wall of the mouse lung. (a) The basement membrane (double basement membrane) is localized between the alveolar epithelium (Ep) and pulmonary capillary endothelium (En). GAC, great alveolar cell; Lum, capillary lumen. (b) High-magnification view of a part of (a) in which the basement membrane contains many parallel basotubules (arrows). Ep, alveolar epithelium; En, capillary endothelium. (c) An area of the basement membrane which is filled and tightly packed with more abundant basotubules. Alv, alveolus; Ep, alveolar epithelium; En, capillary endothelium; Lum, capillary lumen. (a) × 88,400, (b) × 204,700, (c) × 150,500; bars = 100 nm (all original magnifications).

basotubules running parallel to the surface of the basement membrane as visualized where their orientation was favorable, that is, where they were parallel to the plane of the section (Fig. 9b). In areas where basotubules were more densely packed, the whole lamina densa of the basement membrane appeared as a finely striped structure (Fig. 9c).

As to the relative permeability of the alveolar epithelium and pulmonary capillary endothelium of the alveolar-capillary wall of the normal lung, earlier tracer experiments showed that the ultrastructural cytological tracer horseradish peroxidase was able to penetrate through the intercellular spaces of the capillary endothelium of the rat while the alveolar epithelium was impermeable because of the presence of the "tight" zonula occludens (tight junction) as observed with thin section electron microscopy (Schneeberger-Keeley and Karnovsky, 1968; Schneeberger and Karnovsky, 1971). The results of physiological experiments also indicated that pulmonary capillaries of the normal lung were a highly permeable, "porous" structure (Taylor and Gaar, 1970). This "leakiness" of the mouse pulmonary capillary endothelium (Table II) and detailed nature of the endothelial junction was further studied with a freeze–fracture technique (Schneeberger and Karnovsky, 1976) which showed that the vascular junction resembled "leaky" junctions. A detailed study with dog lung (Inoue *et al.,* 1976) showed that while the zonula occludens of the alveolar epithelium was made up of a well developed network of junctional strands typical of tight junctions, the endothelial zonula occuludens was poorly organized and composed of a few staggered parallel strands often with free ends. In this arrangement, strand-free areas were likely to pass through the zone of this "loose" zonula occludens.

The presence of unusually abundant basotubules was also observed in a nonvascular basement membrane. The cells of the mouse Engelbreth–Holm–Swarm tumor produce a large amount of basement membrane matrix. The region of the matrix distal to the cells contained unusually abundant basotubules which were arranged regularly and parallel to one another as the major constituent of the matrix (Fig. 10a), whereas the proximal region contained only a few of them (Inoue and Leblond, 1985a). A prominent ultrastructural feature of this tumor is that the whole matrix is filled with abundant AP (free pentosomes) (Figs. 10b and 10c) and the proximal and distal regions contained similar amounts of AP as measured with immunohistochemical quantitation (Grant *et al.,* 1985). In this tumor, as new matrix is continuously produced by the cells, old matrix is gradually displaced outwardly, and during this process freely and abundantly available pentosomes in the matrix are gradually utilized for the formation of basotubules as the matrix moves outwardly (Inoue and Leblond, 1985b).

These observations may suggest that the unrestricted, continuous availability of AP (pentosomes) in the basement membrane is directly related to the emergence of large amounts of basotubules.
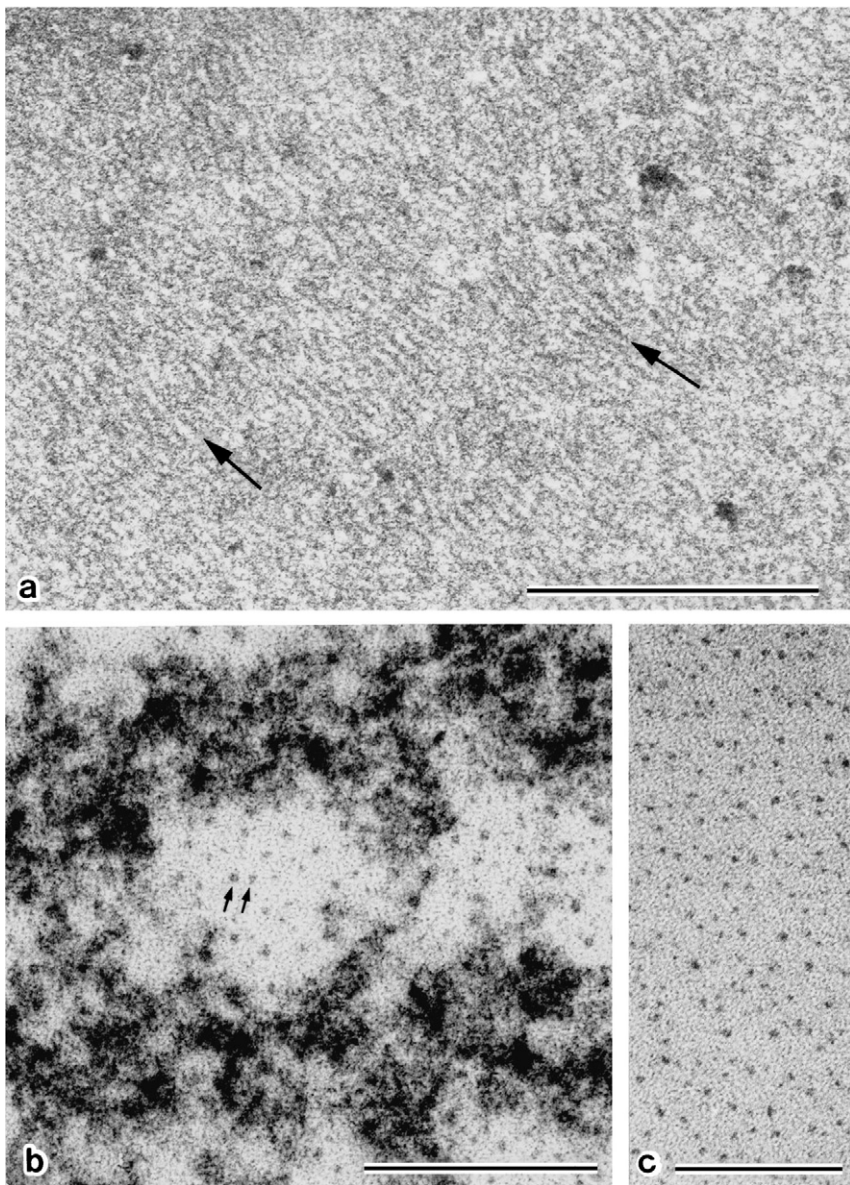
FIG. 10 Basement membrane matrix of the mouse Engelbreth–Holm–Swarm tumor. (a) Face-on view of a layer of the matrix which is distal to tumor cells. The matrix is filled with abundant microfibrils (arrows) which are arranged approximately parallel to one another. The presence of an excess amount of microfibrils caused disruption of the basic structure of the basement membrane, that is, the cord network, which became obscure. (b) At high magnification the whole basement membrane matrix is seen being "immersed" in unusually dense accumulations of pentosomes (tiny arrows) as shown at the distal region where two transversely sectioned parallel layers of the matrix are seen. (c) Numerous pentosomes flowed out of the matrix at its edge of incision. (a) $\times$ 39,100, bar = 1 μm; (b) $\times$ 311,000, bar = 100 nm; (c) $\times$ 226,300, bar = 100 nm (all original magnifications).

V. β Amyloid Fibrils as Pathologically Altered, Vascular Basement Membrane-Associated Microfibrils: A Hypothesis

A. Spatial Relationship between β Amyloid Fibrils and Vascular Basement Membrane in Cerebrovascular Amyloid Angiopathy

1. Previous Results

β Amyloid fibrils were reported to arise at the wall of degenerating microvasculature in cerebrovascular amyloid angiopathy (Miyakawa *et al.,* 1986a,b, 1990). They were likely to be formed at, and emanating from, the abluminal half of the vascular basement membrane (Miyakawa *et al.,* 1982, 1988), and the microvascular basement membrane, among other constituents of the vascular wall, may serve as the nidus for the formation of the β amyloid deposits (Perlmutter *et al.,* 1990). In another detailed study (Yamaguchi *et al.,* 1992) vascular amyloid fibrils were at first formed within the abluminal side, rather than the subendothelial side, of the vascular basement membrane and then extended out of the vasculature into the adjacent neuropil.

2. High-Resolution Observations

Recently, the relationship between the basement membrane of the cerebromicrovasculature and perivascular deposits of β amyloid fibrils (Fig. 11a) in the brain of patients with Alzheimer's disease has been examined in our laboratories in detail with high-resolution ultrastructural studies. Moderately stained, small round masses were observed to be in close association with the abluminal surface of the whole or separated astrocyte half of the vascular basement membrane (Figs. 11a and 11c), where previously associated cells were already lost. These masses were 80 to 100 nm in diameter and approximately spherical in shape as observed in sections cut perpendicular (Fig. 11c) as well as parallel to the surface of the basement membrane. Similar masses with a dome or hemispherical shape were also observed and were closely applied onto the surface of the basement membrane (Fig. 11b). In the normal control brain these masses were not observed.

High-resolution observations showed that both the spherical and the dome-shaped masses were composed of random assemblies of a few, ultrastructurally distinct, components. First, a prominent characteristic of the spherical mass was the presence of unusually abundant pentosomes (3.5-nm-wide AP subunits) (Fig. 11d, circled). Other components of the spherical mass included 3-nm-wide ribbon-like CSPG "double tracks" (Fig. 11d, paired arrows), 4.5- to 5-nm-wide HSPG double tracks, and 1-nm-wide flexible filaments which resembled 1-nm-wide filaments
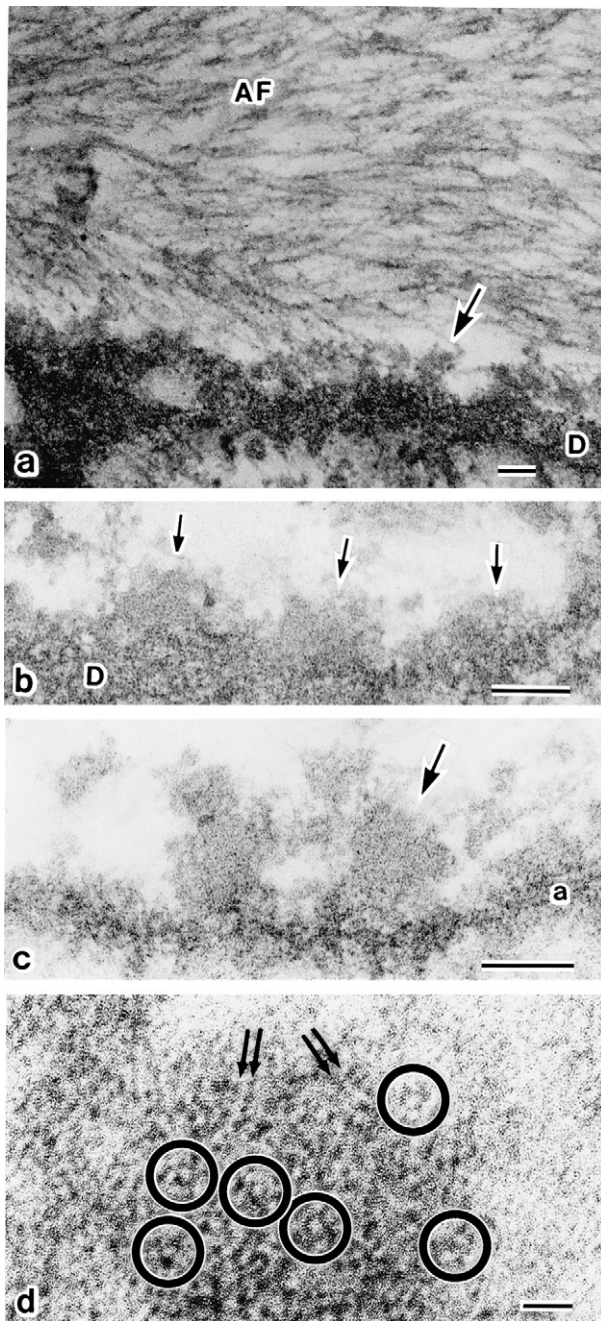
recently observed at the surface of β amyloid fibrils and immunohistochemically identified as Aβ (Inoue *et al.,* 1999). The whole basement membrane, or its astrocyte-half, onto which these masses were adhered, also contained unusually abundant pentosomes and 1-nm-wide flexible filaments among the cord network.

In other areas, a group of a few parallel β amyloid fibrils was seen emerging from each of the spherical masses and extended, always obliquely against the surface of the basement membrane for unknown reasons, toward the perivascular space (Fig. 12a). In places the content of the whole mass appeared to be converted into a group of parallel fibrils (Fig. 12b). The latter arrangement gave an impression as if these parallel β amyloid fibrils were directly emanating from the surface of the basement membrane (Fig. 12b). In areas where most of the spherical masses appeared to be converted into groups of fibrils, these groups merged with one another to form large parallel assemblies of fibrils which were oriented obliquely at first (Fig. 12c) and then parallel to the surface of the basement membrane, and finally formed into a well known large "perivascular amyloid star" (Fig. 11a).

This ultrastructure of fibrillogenesis observed in our laboratories is different from results reported previously. The latter suggested that β amyloid fibrils were formed within the vascular basement membrane while our observations indicate that the formation of the fibrils in fact takes place within the adjoining extra-basement membrane space. The reason for this disagreement is currently not clear.

B. β Amyloid Fibrillogenesis and Relationship between Perivascular Amyloid and Senile Plaques in Alzheimer's Disease

1. "Pentosomes" as Major Building Material of Microfibrils and Microfibril-like β Amyloid Fibrils

As described above, the greater part of the core which is common to both microfibrils (Inoue, 1995a) and β amyloid fibrils (Inoue *et al.,* 1999) is made up of AP in

---

FIG. 11 Capillary basement membrane of cerebral cortex of the brain with Alzheimer's disease. (a) Lower magnification view in which the lamina densa (D) of the basement membrane is associated with small round masses (arrow) at its denuded outer surface. AF, dense assembly of β amyloid fibrils which is a part of a large perivascular amyloid star. (b) Higher magnification view of moderately stained dome-shaped, or hemispherical masses (arrows) closely associated with the surface of the lamina densa (D) of the basement membrane. (c) Moderately stained round or spherical masses approximately 100 nm in diameter (arrow) are attached to the surface of the split astrocyte half (a) of the lamina densa of the basement membrane. (d) High magnification view of a spherical mass in which abundant AP subunits in the form of 3.5-nm-wide pentagonal frames (Inoue, 1991) are present (circled). CSPG in the form of 3-nm-wide ribbon-like "double tracks" (Inoue, 1995a), among other structures, are indicated by paired arrows. (a) $\times$ 48,500, (b) $\times$ 96,900, (c) $\times$ 118,700, (d) $\times$ 644,300; bars = 100 nm (a–c) and 10 nm (d) (all original magnifications).
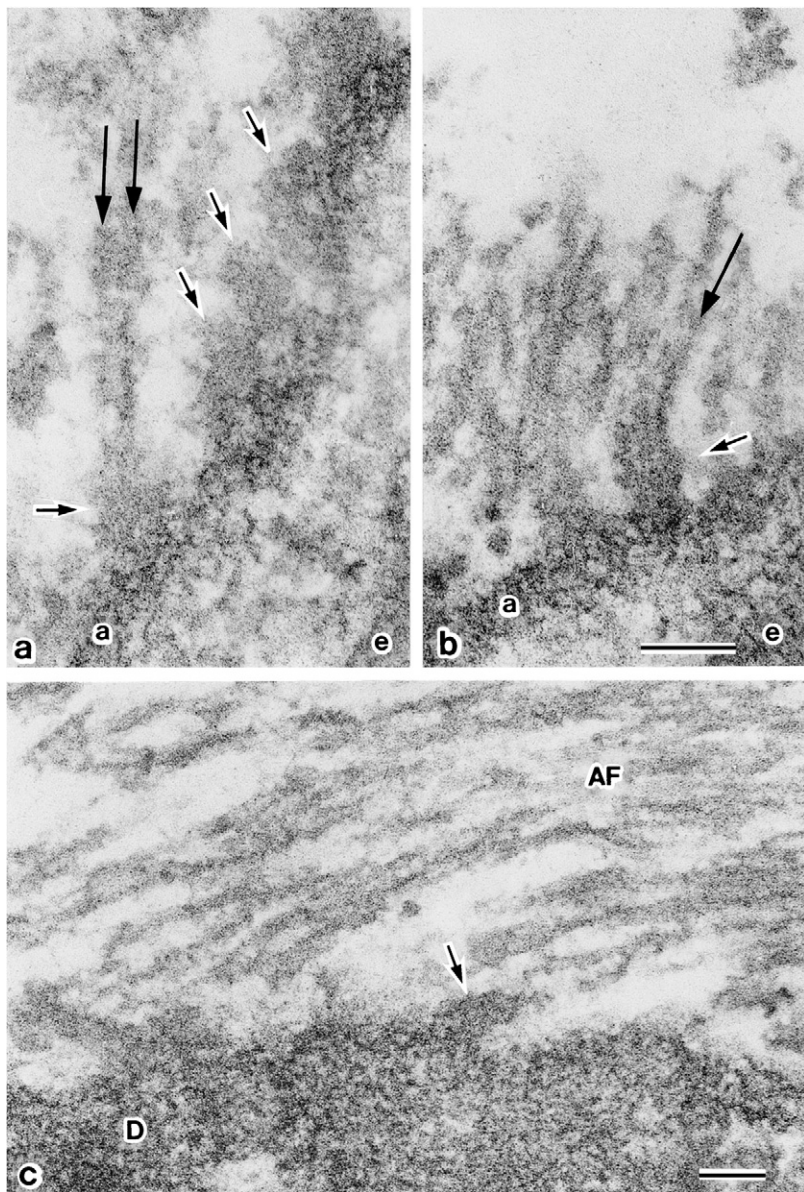
FIG. 12   Transformation of spherical masses into β amyloid fibrils at the surface of a whole or split astrocyte half (a) of the lamina densa of the basement membrane. (a) Two fibrils (long arrows) are seen extending out of one of the spherical masses (small arrows). Note that a split half of the basement membrane is running diagonally in this micrograph and therefore fibrils are extending obliquely against the surface of the split basement membrane. e, split endothelial half of the basement membrane. (b) Almost the entire content of the spherical masses (small arrow) is converted into the fibrils (long

such a way that five pentosomes assemble at first into 8.5-nm-wide disk-like pentagonal units, and then two units associate face-to-face to form an AP molecule. The molecules are further assembled into elongated rod-like assemblies (Figs. 3 and 4). Thus, this characteristic assembly of pentosomes is likely to constitute the backbone of β amyloid fibrils. It was clearly demonstrated that the release of pentosomes from the common core, "classic" microfibrils (Inoue, 1995a), resulted in the immediate and complete loss of their linear integrity (Figs. 5c and 5d). Therefore, for the continous production of β amyloid fibrils in the brain with Alzheimer's disease, a steady supply of pentosomes may be essential.

2. Blood Plasma Released from the Circulation as a Chronic, Steady Source of Pentosomes

As described in detail in Section IV.C, breakdown of the blood–urine barrier occurs in various glomerular diseases at the capillary wall of the glomerulus. In the normal lung, the blood–air barrier has been shown to be a leaky one. An observation common to these two cases is that the basement membranes, that is, the glomerular basement membrane in disease, and the alveolar and capillary basement membranes of the normal lung, are unusually rich in basotubules (Table II). Since AP is a major component of the basotubule and which forms their backbone structure, it is highly possible that circulating AP which has leaked out through the altered barrier into the basement membrane in the form of its subunits (pentosomes) become the nidus for the formation of basotubules within this immediate site (basement membrane) which is first reached following their release from the circulation.

In the case of Alzheimer's disease, compromise of the blood–brain barrier (Table II) at the wall of the cerebromicrovasculature has long been proposed to be the initiating mechanism of the pathogenesis of Alzheimer's disease (Glenner, 1979). Indeed, the presence of endogenous albumin was immunohistochemically demonstrated in the walls of certain microvasculatures with abnormalities unique to Alzheimer's disease, as well as within the adjacent neuropil in brain tissues obtained through biopsies (rather than autopsies). On the other hand, in vasculature with normal appearance, albumin was confined within the lumen (Wisniewski *et al.,* 1997). These results appear to be direct proof for the occurrence of the focal disruption of the blood–brain barrier in certain microvasculatures in the brain of patients with Alzheimer's disease (Wisniewski *et al.,* 1997). Based on such

arrow). a, e, split astrocyte and endothelial halves of the basement membrane, respectively. (c) At the surface of a pathologically altered lamina densa (D) with many irregular holes, most spherical masses are seen converted into numerous parallel fibrils (AF) running obliquely against the surface of the lamina densa. Small arrow indicates a rare remnant of a spherical mass. (a, b) $\times$ 124,100, (c) $\times$ 89,300; bars = 100 nm (all original magnifications).

focal alterations of the barrier, leakage of neurotoxic plasma substances (Glenner, 1979) or circulating βAPP (Selkoe, 1986, 1989a) were proposed to trigger β amyloidogenesis.

In relation to the microrelease of plasma components through an altered blood–brain barrier, recent high-resolution observations in our laboratories (Section V.A.2) showed that the basement membrane of the cerebrocortical microvasculature in the brain with Alzheimer's disease was unusually rich in pentosomes. These abundant, 3.5-nm-wide pentosomes as well as numerous flexible filaments approximately 1 nm in width, which were not seen in the normal basement membrane, were present within the cord network of a whole, or split astrocyte half of the vascular basement membrane. Among these two types of structures, the most likely source of pentosomes is the circulating AP which has leaked out through the altered blood–brain barrier and spread within the basement membrane, the structure directly in contact with the endothelium which constitutes the barrier. Incidentally, the observation of individual pentosomes rather than their decameric assemblies (AP molecules) (Osmand *et al.,* 1977) in the vascular basement membrane may suggest that AP is released from the circulation in the subunit form (pentosomes). The results of previous reports are also in favor of the intracerebral influx of circulating AP. In amyloid angiopathy the presence of AP in the cerebral vasculature was demonstrated by a number of authors (Coria *et al.,* 1988; Kalyan-Ranan and Kalyan-Ranan, 1984; Rowe *et al.,* 1984; Vinters, 1987), and since there is no evidence for the intracerebral production of AP (Kalaria *et al.,* 1991) it is likely that it originates from circulating AP which has leaked out of the microvasculature.

The biochemical nature as well as the origin of the second type of structure observed in the vascular basement membrane, that is, the 1-nm-wide flexible filaments, were not clear but it is highly possible that these filaments, which resemble Aβ filaments recently observed at the surface of β amyloid fibrils (Inoue *et al.,* 1999), are made up of Aβ as discussed below.

3. Possible Process of *in Vivo* Formation of β Amyloid Fibrils

The two above-described types of structures, that is, pentosomes and 1-nm-wide flexible filaments which were abundantly present within the cord network of the basement membrane of the microvasculature with cerebrovascular amyloid angiopathy, appeared to diffuse, or "seep," out of the basement membrane, together with other materials (see below). At the surface of the basement membrane where vascular cells were already lost, they may then assemble at first in the form of dome-shaped masses which then become spherical ones.

Incidentally, it is not certain whether all of the pentosomes which have diffused out of the basement membrane are incorporated into the spherical masses and consequently (see below) contribute to the formation of β amyloid fibrils. It is possible that a portion of them further penetrates deep into the cortical tissue. If this is the case, then these more deeply penetrating pentosomes may cause damages

to brain cells. Cell death induced by AP in cultures of rat cerebral cortex (Urbányi *et al.,* 1994) as well as cellular uptake of AP and marked toxicity to neurons in a human-derived neuronal cell line (Duong *et al.,* 1998), were reported.

In addition to pentosomes and 1-nm-wide filaments, the remaining components of the spherical masses at the surface of the basement membrane were mainly the same as the rest of the components of β amyloid fibrils, that is, 3-nm-wide CSPG double tracks and 4.5- to 5-nm-wide HSPG double tracks, as well as possible additional components which could not be positively identified based on their ultrastructure alone (Section V.A.2). One of the most remarkable observations was the emergence of β amyloid fibrils directly from these 100-nm-wide spherical masses, and conversion of the material of the entire mass into the fibrils which extended away obliquely from the surface of the basement membrane. It is interesting to note that while basotubules were reported to be formed within other vascular basement membranes in different locations such as the glomerular basement membrane in disease and the alveolar–capillary basement membrane of the normal lung, the basotubule-like β amyloid fibrils were formed at immediate periphery of, instead of within, the basement membrane of the cerebromicrovasculature. The reason for this difference is not clear. Although an apparent major difference between basotubules (microfibrils) and β amyloid fibrils is the addition of Aβ at the surface in the case of the latter, it is not certain whether this difference gives rise to a change in the location of the formation of the fibrils.

HSPG is a major component of the basement membrane and it is known to have a significant role in maintaining the integrity of the basement membrane (Hassell *et al.,* 1985; Fujiwara *et al.,* 1984; Laurie, 1985). In amyloid angiopathy, HSPG in the vascular basement membrane is known to be lost (Snow *et al.,* 1988). In addition, newly synthesized HSPG may be prevented from being incorporated into the basement membrane. HSPG, as well as laminin, were reported to have a high affinity with βAPP (Narindrasorasak *et al.,* 1991, 1992; Multhaup *et al.,* 1992, 1993), and therefore these components may be prevented, in the presence of βAPP, from being incorporated into the basement membrane because of a disturbance in the normal interactions between individual basement membrane components (Kisilevsky, 1994; Narindrasorasak *et al.,* 1995). If this is the case, the vascular basement membrane may become deteriolated because of the difficulty in maintaining the normal cord network due to the lack of HSPG as amyloid angiopathy progresses. This preexisting and newly synthesized HSPG may possibly be utilized for the formation of the surface layer of β amyloid fibrils.

The exact origin of the other components of β amyloid fibrils in amyloid angiopathy is not very clear. CSPG was reported to be present in the cerebral vasculature with amyloid angiopathy (DeWitt *et al.,* 1993), and astrocytes are known to accumulate CSPG in the presence of Aβ (Canning *et al.,* 1993). This component is also produced by endothelial and smooth muscle cells (Kinsella and Wight, 1986; Schönherr *et al.,* 1991; Yao *et al.,* 1994). CSPG produced as above may

be utilized, together with available pentosomes (AP) as described above, for the formation of the core of β amyloid fibrils.

As to the nature of the 1-nm-wide flexible filaments found to be abundant in the vascular basement membrane as well as within the spherical masses, they are not likely to be the components of the basement membrane such as the filaments of fibronectin or type IV collagen because of their known distinctly larger width. Fibronectin, an extrinsic component of the basement membrane, is known to take the form of 1.2- to 3-nm-wide filaments (Inoue *et al.,* 1989b), and the width of type IV collagen filaments, the core filament of the basement membrane cords, is 1.5, 2–2.5, and 3 nm depending on whether they are composed of a single, or two to three laterally associated molecules (Inoue and Leblond, 1988; Inoue *et al.,* 1983). On the other hand, there is a report of the localization of Aβ specifically within the cortical vascular basement membrane. Degradative intermediates of βAPP produced by a variety of cell types are probably trapped within the vascular basement membrane and are cleaved with proteases at this location to produce Aβ (Yamaguchi *et al.,* 1992). Therefore, it is highly likely that these 1-nm-wide filaments, which resemble the 1-nm-wide flexible Aβ filaments at the surface of β amyloid fibrils (Inoue *et al.,* 1999), are indeed made up of Aβ.

As expected from the reported severe alterations and degradation of the vascular basement membrane in amyloid angiopathy (Perlmutter and Chui, 1990) and also from the results of our ultrastructural studies, it is possible that the cord network of the basement membrane deteriorates and the resulting fragments of the cords as well as possible detached individual components of the basement membrane such as laminin may be released from the degrading basement membrane. Various newly synthesized basement membrane components may be prevented, as discussed above for HSPG, from being incorporated into the basement membrane because of a disturbance to interactions among individual basement membrane components themselves with the presence of βAPP. Thus, there is a possibility that various preexisting and newly synthesized components of the basement membrane may be turned away from the basement membrane and are instead incorporated into the spherical masses. However, our observations showed that filaments with a thickness ranging from 1.5 to 3 nm, which may correspond to type IV collagen filaments, were not present in the masses. It indicated that all components of the basement membrane, with the possible exception of HSPG, are not necessarily included in the spherical masses. They may, instead, directly diffuse into the perivascular spaces and then become associated with and adhere to individual or bundles of "mature" β amyloid fibrils since colocalization of laminin and type IV collagen in addition to HSPG with plaque-like accumulations of amyloid in the close vicinity of capillaries in Alzheimer's disease was immunohistochemically demonstrated (Perlmutter and Chui, 1990).

The mechanism for the formation of β amyloid fibrils within the spherical masses at the surface of the denuded vascular basement membrane is not clear. However, a possibility is that the core of the fibril is at first formed from AP

(pentosomes) and 3-nm-wide ribbon-like CSPG double tracks in a manner similar to that seen in our *in vitro* reconstitution experiment (Inoue, 1995a) (Figs. 6a– 6c). HSPG double tracks 4.5–5 nm in width may then be randomly applied onto the surface of the core to form the surface layer of the fibril. Finally, 1-nm-wide Aβ filaments may be associated with the outermost surface to complete the fibril. As new fibrils are continuously formed from successively formed spherical masses, older fibrils, probably attached by additional substances such as basement membrane components, may gradually be displaced outwardly and accumulate into perivascular amyloid deposits of ever increasing size in amyloid angiopathy.

4. Relationship between Amyloid Angiopathy and Senile Plaque

The relationship between the above described perivascular amyloid deposits in cerebrovascular amyloid angiopathy and the core of senile plaques has been the subject of much concern (for example, see reviews of Selkoe, 1986, 1987, 1989a,b). Although earlier reports were in favor of a close relationship between the two (Scholz, 1938; Corsellis and Brierlery, 1954; Mandybur, 1975; Ishii, 1969) the problem has remained to be settled.

Miyakawa *et al.* (1982) thought that amyloid fibrils at the core of senile plaques were originally produced at the microvasculature with amyloid angiopathy. These authors, by means of examinations of serial sections with the electron microscope, found within the senile plaque at least one capillary severely damaged or destroyed with amyloid angiopathy. A more recent report from the same group (Miyakawa, 1997) again confirmed, by observations of a large number of serial sections, their previous results of the invariable presence of a variously destroyed microvessel within the plaque. Based on these observations these authors concluded that the core of senile plaques is continuous with perivascular amyloid deposits, and without the use of serial sections they appeared as independent structures due to the three-dimensionally elongated shapes of amyloid deposits.

However, the results of light microscopic observations by other investigators (Kawai *et al.,* 1992), also with the use of serial sections, indicated that the association of amyloid plaques with microvessels may merely be the result of chance contact, and the deposition of amyloid in senile plaques and the perivascular space was thought to occurs through two distinct mechanisms (Kawai *et al.,* 1990).

The concept of the continuity of perivascular amyloid deposits with senile plaques may be supported by the result of observations of tissues with Dutch-type hereditary cerebral hemorrhage with amyloidosis (HCHWA-D) (van Duinen *et al.,* 1987). This disorder is pathologically related to Alzheimer's disease and is charcterized by vascular amyloid deposits, Aβ immunostainable "senile plaque-like" structures with no typical core, and no neurofibrillary tangles. The presence of these structures appears to support the concept that the deposition of β amyloid is at first initiated in the vessel wall before spreading into the parenchyma of the brain. However, there is a difficulty in explaining the presence of senile plaque-like

structures in HCHWA-D. If senile plaques represent transversely sectioned extensions of perivascular amyloid deposits, these plaque-like structures should contain "mature" β amyloid fibrils instead of nonfibrillar Aβ.

In senile plaques colocalization of major components of the basement membrane including HSPG (Perlmutter, 1994; Perlmutter *et al.,* 1990, 1991; Snow *et al.,* 1988, 1990; Narindrasorasak *et al.,* 1991), laminin (Murtomäki *et al.,* 1992; Perlmutter, 1994) and type IV collagen (Perlmutter *et al.,* 1991) as well as fibronectin (Howard and Pilkington, 1990) has been reported. It was suggested that this colocalization may indicate direct involvement of the basement membrane of the cerebromicrovasculature or its components in the pathogenesis of Alzheimer's disease (Perlmutter *et al.,* 1991).

Thus, the relationship between the perivascular amyloid deposits in amyloid angiopathy and the core of senile plaques is still not very clear, but these structures are possibly related because of the following two reasons. First, AP (pentosomes) forms the backbone of β amyloid fibrils as described above, and a source for the continuous supply of AP, an unavoidable prerequisite for the formation of microfibril-like β amyloid fibrils, is not apparent within the direct vicinity of the plaques in the brain with Alzheimer's disease. Second, because of the lack of an alternate, more convincing reason for the presence of basement membrane components within senile plaques, it seems reasonable to suppose that these components are originating from the basement membrane of the cerebrocortical microvasculature with amyloid angiopathy and were carried by outwardly displaced deposits of abundant β amyloid fibrils.

VI. Concluding Remarks

A recent finding that the main body of β amyloid fibrils *in situ* is very similar or identical to that of connective tissue microfibrils has prompted us to examine possible mechanisms for β amyloid fibrillogenesis in the brain of patients with Alzheimer's disease. A β amyloid fibril is composed of a core made up of a column of AP and surrounding CSPG and a surface layer of HSPG. β Amyloid protein is associated with the outermost surface of the fibril in the form of fine flexible filaments. Thus, in summary of the above discussions, AP is one of the major constituents of β amyloid fibrils, and it constitutes the backbone of the fibrils. Therefore, there would seem to be no way of producing intact β amyloid fibrils in the absence of this component even if all other components of the fibril including Aβ are available.

Thus, the source of a steady supply of AP in the cerebral cortex of the brain appears to be critically important in β amyloid fibrillogenesis. Since AP is known not to be produced in the brain, the only available source for this component may be circulating AP. The modification, or breakdown, of the blood–brain barrier at the degrading cerebral microvasculature has been reported in Alzheimer's disease

and the AP contained in plasma which has leaked out is likely to be the only available source of AP for the formation of the β amyloid fibrils. There is a close similarity between this rather unique way of supplying AP in the brain with Alzheimer's disease and the supply of AP in the glomerulus of the kidney in disease or the alveolar–capillary wall of normal lungs in which circulating AP is likely to be made available through a damaged blood–urine barrier and loose blood–air barrier, respectively, for the formation of abundant microfibrils (basotubules). The importance of the availability of AP for the formation of microfibrils is also demonstrated in the AP-rich basement membrane matrix of the mouse Engelbreth–Holm–Swarm tumor.

Thus, in cerebrovascular amyloid angiopathy, abundant β amyloid fibrils are produced at the basement membrane of the cerebrocortical microvasculature, the first structure which the leaked-out AP is likely to encounter. HSPG is a major component of the basement membrane with its well known role of maintaining the integrity of the basement membrane. It is possible that HSPG already within the vascular basement membrane or newly synthesized HSPG destined for the basement membrane may be utilized for the formation of the surface layer of newly and continuously forming β amyloid fibrils. This may, in turn, accelerate the degradation of the vascular basement membrane and the release of its components including laminin and type IV collagen which may accompany the outwardly moving bundles of continuously forming β amyloid fibrils. Together with other components of the fibril including Aβ which are likely to be available at this specific site (vascular basement membrane), β amyloid fibrils may continuously be formed. However, the origin of the β amyloid fibrils which form the core of senile plaques is not clear. Nevertheless, since a continuous supply of AP is apparently not available around the site of the plaques it is possible that these plaque fibrils are also derived from perivascular amyloid deposits.

Acknowledgments

References

Buée, L., Hof, A. R., and Delacourte, A. (1997). Brain microvascular changes in Alzheimer's disease and other dementias. *Ann. NY Acad. Sci.* **826,** 7–24.
Burdick, D., Soreghan, B., Kwon, M., Kosmoski, J., Knauer, M., Henschen, A., Yates, J., Cotman, C.,

and Glabe, C. (1992). Assembly and aggregation properties of synthetic Alzheimer's A4β amyloid peptide analogs. *J. Biol. Chem.* **267,** 546–554.

Canning, D. R., McKeon, R. J., DeWitt, D. A., Perry, G., Wujek, J., Fredrickson, R. C. A., and Silver, J. (1993). β-Amyloid of Alzheimer's disease induces reactive glliosis that inhibits axonal outgrowth. *Exp. Neurol.* **124,** 289–298.

Castaño, E. M., and Frangione, B. (1988). Human amyloidosis, Alzheimer's disease and related disorders. *Lab. Invest.* **58,** 122–132.

Castaño, E. M., Prelli, F., Wisniewski, T., Golabek, A., Kumar, R. A., Soto, C., and Frangione, B. (1995). Fibrillogenesis in Alzheimer's disease of amyloid β peptides and apolipoprotein E. *Biochem. J.* **306,** 599–604.

Chan, F. L., and Inoue, S. (1994). Lamina lucida of basement membrane: An artefact. *Microsc. Res. Technol.* **28,** 48–59.

Chan, F. L., Inoue, S., and Leblond, C. P. (1993a). Cryofixation of basement membrane followed by freeze substitution or freeze drying demonstrates that they are composed of a tridimensional network of irregular cords. *Anat. Rec.* **235,** 191–205.

Chan, F. L., Inoue, S., and Leblond, C. P. (1993b). The basement membranes of cryofixed or aldehyde-fixed, freeze substituted tissues are composed of a lamina densa and do not contain a lamina lucida. *Cell Tissue Res.* **273,** 41–52.

Cleary, E. G., and Gibson, M. A. (1983). Elastin-associated microfibrils and microfibrillar proteins. *Int. Rev. Connect. Tissue Res.* **10,** 97–209.

Coria, F., Castaño, E., Prelli, F., Larrondo-Lillo, M., van Duinen, S., Shelanski, M. L., and Frangione, B. (1988). Isolation and characterization of amyloid P component from Alzheimer's disease and other types of cerebral amyloidosis. *Lab. Invest.* **58,** 454–458.

Corsellis, J. A. N., and Brierlery, J. B. (1954). An unusual type of presenile dementia. *Brain* **77,** 571–587.

DeWitt, D. A., Silver, J., Canning, D. R., and Perry, G. (1993). Chondroitin sulfate proteoglycans are associated with the lesions of Alzheimer's disease. *Exp. Neurol.* **121,** 149–152.

Duong, T., Acton, P. J., and Johnson, R. A. (1998). The in vitro neuronal toxicity of pentraxins associated with Alzheimer's disease brain lesions. *Brain Res.* **813,** 303–312.

Elder, H. Y. (1989). Cryofixation. *Tech. Immunocytochem.* **4,** 1–28.

Essner, E., and Gordon, S. R. (1984). Demonstration of microfibrils in Bruch's membrane of the eye. *Tissue Cell* **16,** 779–788.

Farquhar, M. G. (1991). The glomerular basement membrane. A selective macromolecular filter. *In* "Cell Biology of Extracellular Matrix" (E. D. Hay, Ed.), pp. 365–418. Plenum Press, New York,

Farquhar, M. G., Wissig, S. L., and Palade, G. E. (1961). Glomerular permeability. I. Ferritin transfer across the normal glomerular capillary wall. *J. Exp. Med.* **113,** 47–66.

Fujiwara, S., Wiedemann, H., Timpl, R., Lustig, A., and Engel, J. (1984). Structure and interactions of heparan sulfate proteoglycans from a mouse tumor basement membrane. *Eur. J. Biochem.* **143,** 145–157.

Glenner, G. G. (1979). Congophilic microangiopathy in the pathogenesis of Alzheimer's disease (presenile dementia). *Med. Hypotheses* **5,** 1231–1236.

Glenner, G. G., and Wong, C. W. (1984). Alzheimer's disease: Initial report of the purification and characterization of a novel cerebrovascular amyloid protein. *Biochem. Biophys. Res. Commun.* **120,** 885–890.

Goldberg, M., and Escaig-Haye, F. (1986). Is the lamina lucida of the basement membrane a fixation artefact?. *Eur. J. Cell Biol.* **42,** 365–368.

Goldfischer, S., Coltoff-Schiller, B., Schwartz, E., and Blumenfeld, O. O. (1983). Ultrastructure and staining properties of aortic microfibrils (Oxytalan). *J. Histochem. Cytochem.* **31,** 382–390.

Grant, D. S., Kleinman, H. K., Leblond, C. P., Inoue, S., Chung, A. E., and Martin, G. R. (1985). The basement-membrane-like matrix of the mouse EHS tumor. II. Immunohistochemical quantitation of six of its components. *Am. J. Anat.* **174,** 387–398.

Harvey, D. M. R. (1981). Freeze substitution. *J. Microsc.* **127,** 209–221.

Hassell, J. R., Layshon, W. C., Ledbetter, S. R., Tyree, B., Suzuki, S., Kato, M., Kimata, K., and Kleinman, H. K. (1985). Isolation of two forms of basement membrane proteoglycans. *J. Biol. Chem.* **260,** 8098–8105.

Howard, J., and Pilkington, G. J. (1990). Antibodies to fibronectin bind to plaques and other structures in Alzheimer's disease and control brain. *Neurosci. Lett.* **118,** 71–76.

Hsu, H.-C., and Churg, J. (1979). Glomerular microfibrils in renal disease: A comparative electron microscopy study. *Kidney Int.* **16,** 497–504.

Hsu, H.-C., Suzuki, Y., Churg, J., and Grishman, E. (1980). Ultrastructure of transplant glomerulopathy. *Histopathology (Oxford)* **4,** 351–367.

Inoue, S. (1989). Ultrastructure of basement membranes. *Int. Rev. Cytol.* **117,** 57–98.

Inoue, S. (1991). Pentosome—a new connective tissue component—is a subunit of amyloid P. *Cell Tissue Res.* **263,** 431–438.

Inoue, S. (1994). Basic structure of basement membranes is a fine network of "cords," irregular anastomosing strands. *Microsc. Res. Technol.* 28, 29–47.

Inoue, S. (1995a). Ultrastructural organization of connective tissue microfibrils in the posterior chamber of the eye *in vivo* and *in vitro. Cell Tissue Res.* **279,** 291–302.

Inoue, S. (1995b). Ultrastructural and immunohistochemical studies of microfibril-associated components in the posterior chamber of the eye. *Cell Tissue Res.* **279,** 303–313.

Inoue, S., and Bendayan, M. (1995). High-resolution ultrastructural study of the rat glomerular basement membrane in long term experimental diabetes. *Ultrastruct. Pathol.* **19,** 175–185.

Inoue, S., Grant, D., and Leblond, C. P. (1989a). Heparan sulfate proteoglycan is present in basement membrane as a double-tracked structure. *J. Histochem. Cytochem.* **37,** 597–602.

Inoue, S., and Kisilevsky, R. (1996). A high resolution ultrastructural study of experimental murine AA amyloid. *Lab. Invest.* **74,** 670–683.

Inoue, S., and Kisilevsky, R. (1999). *In situ* electron microscopy of amyloid deposits in tissues. *Methods Enzymol.* **309,** 496–509.

Inoue, S., Kuroiwa, M., and Kisilevsky, R. (1999). Basement membranes, microfibrils and β amyloid fibrillogenesis in Alzheimer's disease: High resolution ultrastructural findings. *Brain Res. Rev.* **29,** 218–231.

Inoue, S., Kuroiwa, M., Ohashi, K., Hara, M., and Kisilevsky, R. (1997). Ultrastructural organization of hemodialysis-associated β_2-microglobulin amyloid fibrils. *Kidney Int.* **52,** 1543–1549.

Inoue, S., Kuroiwa, M., Saraiva, M. J., Guimarães, A., and Kisilevsky, R. (1998a). Ultrastructure of familial amyloid polyneuropathy amyloid fibrils: Examination with high-resolution electron microscopy. *J. Struct. Biol.* **124,** 1–12.

Inoue, S., Kuroiwa, M., Tan, R., and Kisilevsky, R. (1998b). A high resolution ultrastructural comparison of isolated and *in situ* murine AA amyloid fibrils. *Amyloid: Int. J. Exp. Clin. Invest.* **5,** 99–110.

Inoue, S., and Leblond, C. P. (1985a). The basement-membrane-like matrix of the mouse EHS tumor. I. Ultrastructure. *Am. J. Anat.* **174,** 373–386.

Inoue, S., and Leblond, C. P. (1985b). The basement-membrane-like matrix of the mouse EHS tumor. III. Immunodetection of the amyloid P component in basotubules. *Am. J. Anat.* **174,** 399–407.

Inoue, S., and Leblond, C. P. (1986). The microfibrils of connective tissue. I. Ultrastructure. *Am. J. Anat.* **176,** 121–138.

Inoue, S., and Leblond, C. P. (1988). Three-dimensional network of cords: the main component of basement membranes. *Am. J. Anat.* **181,** 341–358.

Inoue, S., Leblond, C. P., and Laurie, G. W. (1983). Ultrastructure of Reichert's membrane, a multilayered basement membrane in the parietal wall of the rat yolk sac. *J. Cell Biol.* **97,** 1524–1537.

Inoue, S., Leblond, C. P., Grant, D. S., and Rico, P. (1986). The microfibrils of connective tissue. II. Immunohistochemical detection of the amyloid P component. *Am. J. Anat.* **176,** 139–152.

Inoue, S., Leblond, C. P., Rico, P., and Grant, D. (1989b). Association of fibronectin with the microfibrils of connective tissue. *Am. J. Anat.* **186,** 43–54.

Inoue, S., Michel, R. P., and Hogg, J. C. (1976). Zonulae occludentes in alveolar epithelium and capillary endothelium of dog lungs studied with the freeze–fracture technique. *J. Ultrastruct. Res.* **56,** 215–225.

Ishii, T. (1969). Enzyme histochemical studies of senile plaques and the plaque-like degeneration of arteries and capillaries (Scholz). *Acta Neuropathol.* **14,** 250–260.

Kalaria, R. N., Golde, T. E., Cohen, M. L., and Younkin, S. G. (1991). Serum amyloid P in Alzheimer's disease. Implications for dysfunction of the blood–brain barrier. *Ann. NY Acad. Sci.* **640,** 145–148.

Kalayan-Ranan, U. P., and Kalayan-Ranan, K. (1984). Cerebral amyloid angiopathy causing intracranial hemorrhage. *Ann. Neurol.* **16,** 321–329.

Kawai, M., Cras, P., and Perry, G. (1992). Serial reconstitution of β-protein amyloid plaques: Relationship to microvessels and size distribution. *Brain Res.* **592,** 278–282.

Kawai, M., Kalaria, R. N., Harik, S. I., and Perry, G. (1990). The relationship of amyloid plaques to cerebral capillaries in Alzheimer's disease. *Am. J. Pathol.* **137,** 1435–1446.

Kefalides, N. A., Alper, R., and Clark, C. C. (1979). Biochemistry and metabolism of basement membrane. *Int. Rev. Cytol.* **61,** 167–228.

Kinsella, M. G., and Wight, T. N. (1986). Modulation of sulfated proteoglycan synthesis by bovine aortic endothelial cells during migration. *J. Cell Biol.* **102,** 679–687.

Kisilevsky, R. (1994). Proteoglycans and other basement membrane proteins in amyloidoses. *Mol. Neurobiol.* **9,** 23–24.

Krauhs, J. M. (1983). Microfibrils in the aorta. *Connect. Tissue Res.* **11,** 153–167.

Latta, H. (1970). The glomerular capillary wall. *J. Ultrastruct. Res.* **32,** 526–544.

Laurie, G. W. (1985). Lack of heparan sulfate proteoglycan in a discontinuous and irregular placental basement membrane. *Dev. Biol.* **108,** 299–309.

Laurie, G. W., and Leblond, C. P. (1985). Basement membrane nomenclature. *Nature* **313,** 272.

Laurie, G. W., Leblond, C. P., Inoue, S., Martin, G. R., and Chung, A. (1984). Fine structure of glomerular basement membrane and immunolocalization of five basement membrane components to the lamina densa (basal lamina) and its extensions in both glomeruli and tubules of the rat kidney. *Am. J. Anat.* **169,** 463–481.

Laurie, G. W., Leblond, C. P., and Martin, G. R. (1982). Localization of type IV collagen, laminin, heparan sulfate proteoglycan, and fibronectin to the basal lamina of basement membranes. *J. Cell Biol.* **95,** 340–344.

Leak, L. V., and Burke, J. F. (1968). Ultrastructural studies on the lymphatic anchoring filaments. *J. Cell Biol.* **36,** 129–149.

Low, F. N. (1961a). The extracellular portion of the human blood–air barrier and its relation to tissue space. *Anat. Rec.* **139,** 105–124.

Low, F. N. (1961b). Microfibrils, a small extracellular component of connective tissue. *Anat. Rec.* **139,** 250.

Low, F. N. (1962). Microfibrils, fine filamentous components of the tissue space. *Anat. Rec.* **142,** 131–137.

Mandybur, T. I. (1975). The incidence of cerebral amyloid angiopathy in Alzheimer's disease. *Neurology (Minneapolis)* **25,** 120–126.

Merz, P. A., Wisniewski, H. M., Somerville, R. A., Bobin, S. A., Masters, C. L., and Iqbal, K. (1983). Ultrastructural morphology of amyloid fibrils from neuritic and amyloid plaques. *Acta Neuropathol.* **60,** 113–124.

Miyakawa, T. (1997). Electron microscopy of amyloid fibrils and microvessels. *Ann. NY Acad. Sci.* **826,** 25–34.

Miyakawa, T., Katsuragi, S., and Kumamoto, R. (1988). Ultrastructure of perivascular amyloid fibrils in Alzheimer's disease. *Virchows Arch. [Cell. Pathol.]* **56,** 21–24.

Miyakawa, T., Katsuragi, S., and Watanabe, K. (1990). Ultrastructure of amyloid fibrils in Alzheimer's disease and down's syndrome. *In* "Amyloid and Amyloidosis: Proceedings of 5th Int. Symp. on Amyloidosis, Hakone, Japan" (T. Isobe, S. Araki, F. Uchino, S Kato, and E. Tsubura, Eds.), pp. 573–578. Prenum Press, New York.

Miyakawa, T., Katsuragi, S., Watanabe, K., Simoji, A., and Ikeuchi, Y. (1986b). Ultrastructural studies of amyloid fibrils and senile plaques in human brain. *Acta Neuropathol. (Berlin)* **70,** 202–208.

Miyakawa, T., Shimoji, A., Kuramoto, R., and Higuchi, Y. (1982). The relationship between senile plaques and cerebral blood vessels in Alzheimer's disease and senile dementia. *Virchows Arch. [Cell. Pathol.]* **40,** 121–129.

Miyakawa, T., Watanabe, K., and Katsurgi, S. (1986a). Ultrastructure of amyloid fibrils in Alzheimer's disease and Down's syndrome. *Virchows Arch. [Cell. Pathol.]* **52,** 99–106.

Multhaup, G., Bush, A. I., Pollwein, P., Masters, C. L., and Beyreuther, K. (1992). Specific binding of the Alsheimer beta-A4 amyloid precursor to collagen, laminin, and heparin. *J. Prot. Chem.* **11,** 398–399.

Multhaup, G., Masters, C. L., and Beyreuther, K. (1993). A molecular approach to Alzheimer's disease. *Biol. Chem. Hoppe-Seyler* **374,** 1–8.

Murtomäki, S., Risteli, J., Risteli, L., Koivisto, U-. M., Johansson, S., and Liesi, P. (1992). Laminin and its neurite outgrowth-promoting domain in the brain in Alzheimer's disease and Down's syndrome patients. *J. Neurosci. Res.* **32,** 261–273.

Narindrasorasak, S., Altman, A., Gonzalez-DeWhitt, P., Greenberg, B. D., and Kisilevsky, R. (1995). An interaction between basement membrane and Alzheimer amyloid precursor proteins suggests a role in the pathogenesis of Alzheimer's disease. *Lab. Invest.* **72,** 272–282.

Narindrasorasak, S., Lowery, D. E., Altman, R. A., Gonzalez-DeWhitt, P. A., Greenberg, B. D., and Kisilevsky, R. (1992). Characterization of high affinity binding between laminin and the Alzheimer's disease amyloid precursor proteins. *Lab. Invest.* **67,** 643–652.

Narindrasorasak, S., Lowery, D., Gonzalez-DeWhitt, P., Poorman, R. A., Greenberg, B., and Kisilevsky, R. (1991). High affinity interactions between the Alzheimer's β-amyloid precursor proteins and the basement membrane form of heparan sulfate proteoglycan. *J. Biol. Chem.* **266,** 12,878–12,883.

Narindrasorasak, S., Young, I., Aubin, S., Ludwin, S. K., and Kisilevsky, R. (1991). Basement membrane heparan sulfate proteoglycan is part of isolated Alzheimer's amyloid plaques. *In* "Alzheimer's Disease: Basic Mechanisms, Diagnosis and Therapeutic Strategies" (K. Iqbal, D. R. C. McLachlan, B. Winblad, H. M. Wisniewski, Eds.), pp. 289–296. Wiley, New York.

Olsen, S. (1979). Pathology of the renal allograft rejection. *Monogr. Pathol.* **20,** 327–355.

Osmand, A. P., Friedenson, B., Gewurz, H., Painter, R. H., Hofmann, T., and Shelton, E. (1977). Characterization of C-reactive protein and the complement subcomponent Clt and homologous protein displaying cyclic pentameric synmetry (pentraxins). *Proc. Natl. Acad. Sci. USA* **74,** 739–743.

Perlmutter, L. S. (1994). Microvascular pathology and vascular basement membrane components in Alzheimer's disease. *Mol. Neurobiol.* **9,** 33–40.

Perlmutter, L. S., Barrón, E., Saperia, D., and Chui, H. C. (1991). Association between vascular basement membrane components and the lesions of Alzheimer's disease. *J. Neurosci. Res.* **30,** 673–681.

Perlmutter, L. S., and Chui, H. C. (1990). Microangiopathy, a vascular basement membrane and Alzheimer's disease: A review. *Brain Res. Bull.* **24,** 677–686.

Perlmutter, L. S., Chui, H. C., Saperia, D., and Athanikar, J. (1990). Microangiopathy and the colocalization of heparan sulfate proteoglycan with amyloid in senile plaques of Alzheimer's disease. *Brain Res.* **508,** 13–19.

Pras, M., Schubert, M., Zucker-Franklin, D., Rimon, A., and Franklin, E. C. (1968). The characterization of soluble amyloid prepared in water. *J. Clin. Invest.* **47,** 924–933.

Raviola, G. (1971). The fine structure of the ciliary zonule and ciliary epithelium. With special regard to the organization and insertion of the zonular fibrils. *Invest. Ophthalmol.* **10,** 851–869.

Roher, A. E., Palmer, K. C., Yurewicz, E. C., Ball, M. J., and Greenberg, B. D. (1993). Morphological and biochemical analyses of amyloid plaque core proteins purified from Alzheimer disease brain tissue. *J. Neurochem.* **61,** 1916–1926.

Rowe, I. F., Jensson, O., Lewis, P. D., Candy, J., Tennent, G. A., and Peppys, M. B. (1984). Immuno-histochemical demonstration of amyloid P component in cerebrovascular amyloidosis. *Neuropathol. Appl. Neurobiol.* **10,** 53–61.

Sakai, L. Y., Keene, D. R., and Engvall, E. (1986). Fibrillin, a new 350-kD glycoprotein, is a component of extracellular microfibrils. *J. Cell Biol.* **103,** 2499–2509.

Sawada, T., and Inoue, S. (1994). Characterization of the fibrillar layer at the epithelial–mesenchymal junction in tooth germs. *Cell Tissue Res.* **278,** 563–571.

Schneeberger, E. E., and Karnovsky, M. J. (1971). The influence of intravascular fluid volume on the permeability of newborn and adult mouse lungs to ultrastructural protein tracers. *J. Cell Biol.* **49,** 319–334.

Schneeberger, E. E., and Karnovsky, M. J. (1976). Substructure of intercellular junctions in freeze-fractured alveolar-capillary membranes of mouse lung. *Circulation Res.* **38,** 404–411.

Schneeberger-Keeley, E. E., and Karnovsky, M. J. (1968). The ultrastructural basis of alveolar-capillary membrane permeability to peroxidase used as a tracer. *J. Cell Biol.* **37,** 781–793.

Sholz, W. (1938). Studien zur pathologie der Hirngefässe. II. Die drüsige Enlartung der Hirnarterien und Capillaren. *Z. Neurol.* **162,** 694–715.

Schönherr, E., Jarvelainen, H. T., Sandell, L. J., and Wight, T. N. (1991). Effects of platelet-derived growth factor and transferring growth factor-β1 on the synthesis of a large versican-like chondroitin-sulfate proteoglycan by arterial smooth muscle cells. *J. Biol. Chem.* **266,** 17640–17647.

Selkoe, D. J. (1986). Altered structural proteins in plaques and tangles: What do they tell us about the biology of Alzheimer's disease?. *Neurobiol. Aging* **7,** 425–432.

Selkoe, D. J. (1987). Deciphering Alzheimer's disease: The pace quickens. *Trends Neurosci.* **10,** 181–184.

Selkoe, D. J. (1989a). Molecular pathology of amyloidogenic proteins and the role of vascular amyloidosis in Alzheimer's disease. *Neurobiol. Aging* **10,** 387–395.

Selkoe, D. J. (1989b). Biochemistry of altered brain proteins in Alzheimer's disease. *Ann. Rev. Neurosci.* **12,** 463–490.

Snow, A. D., Mar, H., Nochlin, D., Kimata, K., Kato, M., Suzuki, S., Hassell, J., and Wight, T. N. (1988). The presence of heparan sulfate proteoglycans in the neuritic plaques and congophilic angiopathy in Alzheimer's disease. *Am. J. Pathol.* **133,** 456–463.

Snow, A. D., Mar, H., Nochlin, D., Sekiguchi, R. T., Kimata, K., Koide, Y., and Wight, T. N. (1990). Early accumulation of heparan sulfate in neurons and in the beta-amyloid protein-containing lesions of Alzheimer's disease and Down's syndrome. *Am. J. Pathol.* **137,** 1253–1270.

Taylor, A. E., and Gaar, K. A., Jr. (1970). Estimation of equivalent pore radii of pulmonary capillary and alveolar membranes. *Am. J. Physiol.* **218,** 1133–1140.

Terry, R. D., Gonatas, N. K., and Weiss, M. (1964). Ultrastructural studies in Alzheimer's presenile dementia. *Am. J. Pathol.* **44,** 269–283.

Urbányi, Z., Lakics, V., and Erdö, S. L. (1994). Serum amyloid P component-induced cell death in primary cultures of rat cerebral cortex. *Eur. J. Pharmacol.* **270,** 375–378.

van Duinen, S. G., Castaño, E. M., Prelli, F., Bots, G. T. A. B., Luyendijk, W., and Frangione, B. (1987). Hereditary cerebral hemorrhage with amyloidosis in patients of Dutch origin is related to Alzheimer's disease. *Proc. Natl. Acad. Sci. USA* **84,** 5991–5994.

Vinters, H. V. (1987). Cerebral amyloid angiopathy: A critical reaview. *Stroke* **18,** 311–324.

Volker, W., Schmidt, A., and Buddecke, E. (1987). Mapping of proteoglycans in human arterial tissue. *Eur. J. Cell Biol.* **45,** 72–79.

Wisniewski, H. M., Vorbrodt, A. W., and Wegial, J. (1997). Amyloid angiopathy and blood-brain changes in Alzheimer's disease. *Ann. NY Acad. Sci.* **826,** 161–172.

Wisniewski, H. M., and Wegiel, J. (1994). Beta-protein fibrillogenesis and neuritic plaques. *In* "Neurodegenerative Diseases" (D. B. Calne, Ed.), pp. 83–95. Saunders Philadelphia,

Wong, C. W., Quavanta, V., and Glenner, G. G. (1985). Neuritic plaques and cerebrovascular amyloid in Alzheimer's disease are antigenically related. *Proc. Natl. Acad. Sci. USA* **82,** 8729–8732.

Yamaguchi, H., Yamazaki, T., Lemere, C. A., Frosch, M. P., and Selkoe, D. J. (1992). Beta amyloid is focally deposited within the outer basement membrane in the amyloid angiopathy of Alzheimer's disease. *Am. J. Pathol.* **141,** 249–259.

Yao, L. Y., Moody, C., Schönherr, E., Wight, T. N., and Sandell, L. J. (1994). Identification of the proteoglycan versican in aorta and smooth-muscle cells by DNA-sequence analysis, in situ hybridization and immunohistochemistry. *Matrix Biol.* **14,** 213–225.

This Page Intentionally Left Blank

Regulation of Microtubule-Associated Proteins

Lynne Cassimeris and Cynthia Spittle
Department of Biological Sciences, Lehigh University
Bethlehem, Pennsylvania 18015

Microtubule-associated proteins (MAPs) function to regulate the assembly dynamics and organization of microtubule polymers. Upstream regulation of MAP activities is the major mechanism used by cells to modify and control microtubule assembly and organization. This review summarizes the functional activities of MAPs found in animal cells and discusses how these MAPs are regulated. Mechanisms controlling gene expression, isoform-specific expression, protein localization, phosphorylation, and degradation are discussed. Additional regulatory mechanisms include synergy or competition between MAPs and the activities of cofactors or binding partners. For each MAP it is likely that regulation *in vivo* reflects a composite of multiple regulatory mechanisms.

KEY WORDS: MAPs, Tau, Oncoprotein 18/Stathmin, Phosphorylation, Microtubules, Dynamic instability, Tubulin. © 2001 Academic Press.

I. Introduction

Microtubule (MT) polymers participate in a number of functions within cells including chromosome movement in mitosis, vesicle and organelle motility, cell polarity, and flagellar-based motility. In many cases these polymers are also dynamic and continually turn over by processes of dynamic instability and/or treadmilling. The ability of a single polymer to participate in different cellular processes and to show a variety of polymer stabilities and turnover mechanisms is thought to be due primarily to a broad class of tubulin/MT-interacting proteins—the MT-associated proteins (MAPs).

MAPs were originally defined as proteins able to fractionate stoichiometrically with MTs through rounds of polymer assembly and disassembly and to stimulate

MT assembly and nucleation, suggesting a specific affinity for MTs and function in stimulating MT assembly (Stebbings and Hyams, 1979). This original definition placed fairly strict limits on what consituted a MAP and did not describe many proteins now known to regulate specific steps in MT assembly or proteins that associate transiently with MTs. To broaden this definition, Solomon *et al.* (1979) suggested that MAPs be defined as proteins bound to MTs *in vivo.* Since many proteins bind MTs transiently, this definition is also restrictive. How then do we define a MAP? For the purposes of this review, we will consider MAPs as nonmotor proteins that modify MT assembly. We will also make exceptions to this definition and include: (a) proteins with homology to motor proteins but which appear to function primarily in regulating assembly (i.e., Kin I kinesin family; Desai *et al.,* 1999), (b) soluble proteins that interact with tubulin dimers to modify assembly, and (c) proteins that bind MTs and alter polymer organization, rather than assembly. Additional functions of MAPs may include roles as scaffold proteins to localize other molecules to the MT lattice (e.g., kinases and phosphatases; Morishima-Kawashima and Kosik, 1996; Andreassen *et al.,* 1998; Sontag *et al.,* 1995; Ookata *et al.,* 1995; Charasse *et al.,* 2000), to modify or regulate organelle motility (Lopez and Sheetz, 1993), or to define the spacings between MTs (Stebbings and Hyams, 1979; Chen *et al.,* 1992).

The focus of this review is to examine what is known about regulation of MAP functions. If MAPs dictate the different MT-based functions, then it is the upstream regulators that determine when and where these MAPs are active, thus integrating signals to form and reorganize the MT cytoskeleton. It should be noted that tubulin itself is also modified by posttranslational modifications and expressed as a number of different isoforms. These modifications to the tubulin subunits may contribute to changes in MT assembly properties or the abilities of different proteins to bind the polymer (Luduena, 1998; Xia *et al.,* 2000; Panda *et al.,* 1994). Conventional motor proteins may also function to modify MT assembly and this area has been reviewed recently (Hunter and Wordeman, 2000).

We will first review MT polymer structure and assembly mechanisms. We will then briefly review the different families of MAPs and their functions. Last, we will consider a number of different regulatory mechanisms and describe how MAPs are regulated by these mechanisms. In this review we focus on MAPs present in animal cells. Studies of plant MTs and MAPs have been reviewed recently (Smertenko *et al.,* 2000; Wick, 2000).

II. Overview

A. A Review of Microtubule Polymer and Assembly Dynamics

Microtubules are linear polymers which self-assemble from tubulin heterodimers. Each heterodimer is composed of α and β tubulin subunits. The heterodimers are

arranged in a linear array of alternating α and β tubulin subunits; this linear array forms a protofilament. Typically 13 protofilaments form the cylindrical wall of a MT, resulting in a tubular structure where adjacent monomers interact laterally with monomers of the same type (e.g., $\alpha-\alpha$ or $\beta-\beta$ interactions; Fig. 1; see color insert). For a 13-protofilament MT, this structure includes in a discontinuity, or seam, where the α tubulin of one protofilament binds laterally to the β tubulin of the adjacent protofilament (Fig. 1; see color insert).

Given the polarity inherent in the heterodimer and the head-to-tail association of heterodimers in the protofilaments, the resulting MT polymer is structurally polarized with one end described as the "plus end" and the other as the "minus end." Microtubules self-assemble from tubulin subunits when above a critical subunit concentration through the addition of heterodimers to the ends of the polymer. The structural polarity is accompanied by a kinetic polarity demonstrated by the faster addition of subunits onto the plus end compared to the minus end (Allen and Borisy, 1974). Microtubules elongate along individual protofilaments that can generate sheets of protofilaments, the ends which can close to form a tube (Fig. 1).

The assembly of purified tubulin *in vitro,* and MT assembly at the periphery of cells, is best described by the dynamic instability model (Mitchison and Kirschner, 1984; Cassimeris *et al.,* 1988; Sammak and Borisy, 1988; Schulze and Kirschner, 1988; Walker *et al.,* 1988; Waterman-Storer and Salmon, 1997). In this model, MTs exist in persistent phases of elongation or rapid shortening, where subunits add or subtract from filament ends, with abrupt transitions between these two states. The switch from elongation to shortening is termed catastrophe, and the switch from shortening to elongation, rescue (Fig. 2; Walker *et al.,* 1988).

The molecular mechanisms regulating the abrupt transitions of dynamic instability for pure tubulin are not completely understood, but it is likely that MTs are inherently unstable and that they are stabilized by a cap of more stable subunits (Mitchison and Kirschner, 1984). Original models of dynamic instability proposed that the stabilizing cap was composed of GTP-tubulin subunits on an unstable core of GDP-tubulin subunits (Carlier *et al.,* 1987; Mitchison and Kirschner, 1984; GDP- and GTP-tubulin refer to the nucleotide bound at an exchangeable site on β tubulin). Recent estimates suggest that the cap is $\sim$1 subunit deep (Drechsel and Kirschner, 1994; Caplow and Shanks, 1996) since subunit addition should stimulate hydrolysis of the penultimate dimer, at least at the plus end (Nogales *et al.,* 1999). GTP hydrolysis causes a structural change in the MT lattice and these structural changes are likely responsible for the two state behavior of dynamic instability. Protofilaments composed of GTP-tubulin have a straight conformation, while GDP-tubulins form curved protofilaments (Hyman *et al.,* 1992; Mandelkow *et al.,* 1991). Loss of a stabilizing cap thus allows the GDP-protofilaments to curve outward from the MT lattice prior to, or concurrent with, depolymerization. These curving protofilaments ("ram's horns") have been observed by electron microscopy (Chretien *et al.,* 1995; Mandelkow

A. Dynamic Instability
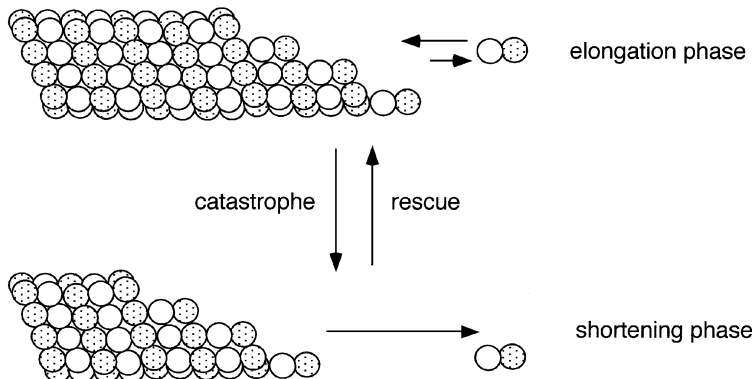
B. Treadmilling
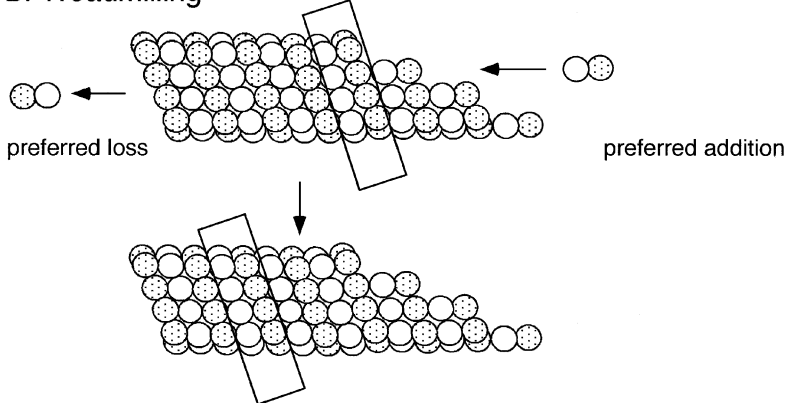
FIG. 2   Microtubule assembly mechanisms. (A) Dynamic instability of microtubules. In the elongation phase, subunits add to filament ends, but there is also an appreciable dissociation of tubulin subunits during this phase. In the shortening phase, protofilaments peel away from the lattice (not shown) and subunit loss is considerably faster than the relatively slow dissociation rate measured during the elongation phase. The abrupt transitions between these two phases are termed catastrophe and rescue. (B) Treadmilling of microtubules by preferential subunit addition and loss from opposite ends of the filament. Over time, subunits are transported down the lattice based on the biased addition and loss of subunits from the ends (shown by the boxes).

et al., 1991; Simon and Salmon, 1990). Further evidence for structural differences between growing and shortening MT ends has been demonstrated by the structure of growing ends. These growing ends are formed from extensions of protofilaments; initially these extensions take the form of an open sheet that subsequently closes to form the hollow MT (Chretien *et al.,* 1995; Simon and Salmon,

1990). Sheet closure at the MT tip may stimulate catastrophe, perhaps by forcing GTP hydrolysis (Chretien *et al.,* 1995; Hyman and Karsenti, 1996; Arnal *et al.,* 2000).

Studies both *in vitro* and *in vivo* have demonstrated that MTs can also turn over by a process termed treadmilling whereby subunit addition is favored at one end of the polymer and subunit disassembly is favored at the opposite end of the polymer (Fig. 2). Treadmilling generates a flux of tubulin subunits toward the polymer end where subunit loss occurs (Margolis and Wilson, 1981). This treadmilling process also requires GTP hydrolysis since both treadmilling and dynamic instability represent nonequilibrium assembly dynamics. Microtubule treadmilling has been observed for purified tubulin (Panda *et al.,* 1999; Hotani and Horio, 1988) and in living cells, where treadmilling may contribute significantly to polymer turnover (Waterman-Storer and Salmon, 1997; Rodionov and Borisy, 1997).

B. A Survey of MAPs and Their Functions

Below we present a survey of a number of MAPs and brief descriptions of their functions *in vitro* and *in vivo*. We have divided the MAPs into two broad classes of regulatory proteins: those that stabilize MTs and those that destabilize MTs. In some cases we have assigned a MAP to one of these categories based on phenotypes observed *in vivo* after over- or underexpression, rather than on direct observation of MT assembly dynamics *in vitro.*

MAP regulation of MT assembly dynamics has been studied primarily for MTs undergoing dynamic instability. Given the recent observations of MT treadmilling in cells, it will be important to learn how MAPs also regulate the treadmilling process.

1. Microtubule Stabilizers

This section will describe proteins that stabilize MT polymers. Stabilization is a general classification where any molecular mechanism that favors subunit addition, inhibits subunit loss from the MT lattice, or stimulates nucleation will generate an increase in polymer. For MTs undergoing turnover by dynamic instability, increased stabilization could result through: (1) slowing dissociation, or stimulating addition, of tubulin subunits during the elongation phase; (2) blocking catastrophes; (3) stimulating rescues; or (4) slowing the rapid shortening phase. Likewise for treadmilling MTs stabilizing proteins could act to enhance subunit addition or slow subunit loss.

Molecular mechanisms to generate these stabilizing effects could occur if MAPs were able to cross-link adjacent protofilaments (e.g., Gustke *et al.,* 1994; Fig. 3). This type of cross-linking could block the splaying of protofilaments observed during MT shortening. Stabilization could also occur through cross-linking dimers along the length of a protofilament (Fig. 3). In this case binding along a protofilament
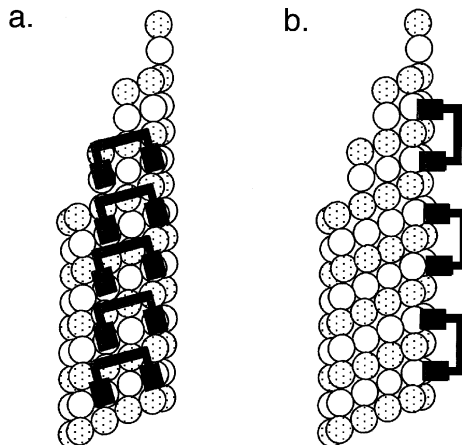
FIG. 3 Models for MAP stabilization of microtubules. Each model shows a hypothetical MAP with two microtubule-binding domains (thicker black boxes) connected by a nonbinding region (thinner black boxes). In (a) the MAP cross-links protofilaments laterally. In (b) the MAP cross-links dimers along the protofilament axis. See text for further discussion.

would stabilize the protofilament and form a stable base for lateral interactions with adjacent protofilaments. The cross-linking of tubulin subunits within the MT lattice is consistent with the identification of repeated sequences within the MT-binding domain of a number of stabilizing MAPs (discussed below for individual MAPs; see also Chapin and Bulinski, 1992). Hypothetically it is also possible that MAPs could stabilize MTs by preserving the GTP cap at the MT end, perhaps by slowing GTP hydrolysis. Finally, MAP binding could alter the conformation of tubulin subunits within the protofilament lattice (Amos, 2000; Pedrotti *et al.,* 1996).

When expressed experimentally at high levels in cells, MAPs may also induce bundling of MTs (e.g., Lewis *et al.,* 1989; Kanai *et al.,* 1992; Barlow *et al.,* 1994; Masson and Kreis, 1993; Andersen and Karsenti, 1997). Bundles are very stable structures (Barlow *et al.,* 1994; Masson and Kreis, 1993). Most researchers have proposed that bundles arise through MAP domains projecting out from the MT acting to cross-link adjacent polymers (Lewis *et al.,* 1989; Kanai *et al.,* 1992), but Preuss *et al.* (1997) suggested that bundles arise through the pronounced nucleating activity of these MAPs which would generate rapid assembly within the confined cytoplasm, generating alignment of the assembling MTs.

a. Mammalian MAP1   Originally described as the highest molecular weight band cofractionating with brain MTs MAP1 actually comprises three polypeptides, MAP1A, -1B, and -1C. MAP1C was subsequently identified as the motor protein cytoplasmic dynein and will not be considered here.

MAP1A and -1B are large proteins encoded on two separate genes (Bloom *et al.,* 1984; Garner *et al.,* 1990; Schoenfeld *et al.,* 1989; Langkopf *et al.,* 1992). Each protein consists of a unique, but similar, heavy chain which may associate noncovalently with the same set of three light chains: LC1, LC2, and LC3 (Hammarback *et al.,* 1991; Langkopf *et al.,* 1992). MAP1A heavy chain and LC2 are translated as a single large polyprotein which is subsequently cleaved by a protease to release LC2 (Langkopf *et al.,* 1992; Fink *et al.,* 1996). Likewise, MAP1B heavy chain and LC1 are synthesized as a polyprotein and subsequently cleaved (Hammarback *et al.,* 1991). The MT-binding domain is found within the amino terminus of each heavy chain and has been characterized as a basic region containing repeated KKE(E/I/V) motifs (Noble *et al.,* 1989; Vaillant *et al.,* 1998). The light chains LC1 and LC3 may also bind independently to MTs (Mann and Hammarback, 1994; Togel *et al.,* 1998; Zauner *et al.,* 1992).

MAP1A is found throughout the nerve cell, but particularly in dendrites, and expression levels are highest in the adult brain, but lower levels of MAP1A are found in other tissues (Schoenfeld *et al.,* 1989; Riederer and Matus, 1985; Garner *et al.,* 1990; Bloom *et al.,* 1984). Interestingly, MAP1A may also bind actin filaments (Pedrotti *et al.,* 1994), may help localize a membrane-associated guanylate kinase, postsynaptic density-93 protein, to specific synaptic sites (Brenman *et al.,* 1998), and may bind RNA/protein complexes (DeFranco *et al.,* 1998). *In vitro* MAP1A stabilizes MTs by increasing nucleation and stimulating elongation of tubulin subunits from MT ends (Pedrotti and Islam, 1994) but is a less potent MT stabilizer than MAP2 (Vaillant *et al.,* 1998).

MAP1B is the first MAP detected during neurogenesis (Muller *et al.,* 1994) and is found throughout the nerve cell but is more concentrated at the distal end of the axon (DiTella *et al.,* 1996; Bush *et al.,* 1996; Boyne *et al.,* 1995; Black *et al.,* 1994; Sato-Yoshitake *et al.,* 1989). In *in vitro* MT assembly assays, MAP1B promotes nucleation and weakly stabilizes MT polymer, but MAP1B does not suppress dynamic instability to the extent observed with the other neuronal MAPs, MAP2 and tau (Vandecandelaere *et al.,* 1996). MAP1B has also been reported to specifically link GABAc receptors to the cytoskeleton at synaptic sites (Hanley *et al.,* 1999; Pattnaik *et al.,* 2000) and can also bind actin filaments (Pedrotti and Islam, 1996; Togel *et al.,* 1998). MAP1B is required for nervous system development in the mouse as demonstrated by knockout of the MAP1B gene (Edelmann *et al.,* 1996; Takei *et al.,* 1997; Meixner *et al.,* 2000; Takei *et al.,* 2000).

b. MAP2 This heat-stable mammalian MAP is found specifically in dendrites of neuronal cells (Bernhardt and Matus, 1984). MAP2 is encoded by a single gene; differential mRNA splicing gives rise to at least three major MAP2 isoforms (Kalcheva *et al.,* 1995; reviewed byShafit-Zagardo and Kalcheva, 1998). MAP2a and MAP2b are high-molecular-weight isoforms, while MAP2c is significantly smaller (∼200 kDa vs 47 kDa). The N-terminus of MAP2 contains a projection

domain which affects the arrangement of MTs within the neurite extension (Vallee, 1980; LeClerc *et al.,* 1996) while the C-terminus contains a MT-binding motif also found in tau and MAP4 (Chapin and Bulinski, 1991). This binding motif consists of a repeated 18-amino-acid sequence separated by less conserved proline-rich spacer segments (Lewis *et al.,* 1989; Lee *et al.,* 1989; Himmler *et al.,* 1989; Chapin and Bulinski, 1991; Aizawa *et al.,* 1991).

In *in vitro* MT assembly assays, MAP2 (most likely a combination of MAP2a and -2b) promotes nucleation and reduces the critical concentration for assembly (Sloboda *et al.,* 1976; Murphy *et al.,* 1977; Vandecandelaere *et al.,* 1996), increases elongation velocity ∼2-fold, slows shortening velocity and suppresses MT turnover by decreasing catastrophes (∼2-fold) and increasing rescues (∼5-fold; Pryer *et al.,* 1992; Kowalski and Williams, 1993). MAP2c also stabilizes MTs by lowering the critical concentration for assembly and dramatically reducing catastrophes (Ludin *et al.,* 1996; Gamblin *et al.,* 1996). Consistent with the *in vitro* studies, microinjection of MAP2 into living cells also increases MT stability (Dhamodharan and Wadsworth, 1995).

MAP2 can also bind to actin filaments *in vitro* (Seldon and Pollard, 1983) and MAP2c can associate with actin filaments in the lamella region of cells (Cunningham *et al.,* 1987; Ozer and Halpain, 2000). MAP2c also binds to the SH3 domains of c-Src and Grb2, suggesting that MAP2 can act as a scaffold for signaling molecules (Lim and Halpain, 2000). MAP2 may also bind to neurofilaments (Miyata *et al.,* 1986).

c. Tau   Tau was one of the first proteins identified which stimulated MT assembly *in vitro* (Cleveland *et al.,* 1977; Weingarten *et al.,* 1975). Alternative splicing of a single tau gene produces six tau protein isoforms (Neve, 1986; Himmler, 1989; reviewed by Buee *et al.,* 2000). All tau forms are localized in axons (Brion *et al.,* 1988; Hirokawa, 1994) where they are concentrated at the growth cone (Black *et al.,* 1996).

The MT-binding domain of tau is located within the C-terminal half of the protein (Lee *et al.,* 1989; Himmler *et al.,* 1989) and consists of a series of repeats with homology to the MT-binding repeats found in MAP2 and MAP4 (Chapin and Bulinski, 1991; Ennulat *et al.,* 1989; Joly *et al.,* 1989). Isoforms differ in the number of repeats, having either three or four MT binding repeats (Goedert *et al.,* 1989a; Himmler *et al.,* 1989; Lee *et al.,* 1989), but the organization of the repeats does not alter MT binding (Trinczek *et al.,* 1995).

Regions flanking the MT-binding domain are also necessary for MT binding and are thought to target the binding domain to the MT lattice (Goode and Feinstein, 1994; Goode *et al.,* 1997; Kanai *et al.,* 1992; Lee and Rook, 1992; Gustke *et al.,* 1994), consistent with a model where tau binds MTs through multiple sites on tau (Butner and Kirschner, 1991). Binding to MTs likely cross-links adjacent protofilaments (Gustke *et al.,* 1994) which would explain the increased MT rigidity observed after tau binding to MTs (Dye *et al.,* 1993; Felgner *et al.,* 1993).

Studies *in vitro* demonstrated that tau promoted assembly through increased nucleation and increased stabilization of MT polymer. Tau alters dynamic instability by decreasing catastrophes and slowing shortening rates (Horio and Hotani, 1986; Bre and Karsenti, 1990; Pryer *et al.,* 1992; Drechsel *et al.,* 1992). Tau also increases the rate of MT polymerization (Drechsel *et al.,* 1992). When examined under *in vitro* conditions favoring MT treadmilling, tau protein suppresses treadmilling (Panda *et al.,* 1999).

The MT stabilizing effects of tau have also been demonstrated *in vivo* (Drubin and Kirschner, 1986; Lewis *et al.,* 1989; Kanai *et al.,* 1989). When expressed in nonneuronal cells, tau overexpression is sufficient to generate axon-like extensions (Esmaeli-Azad *et al.,* 1994; Knops *et al.,* 1991; Baas *et al.,* 1991; Harada *et al.,* 1994; Kosik and Caceres, 1991), suggesting that MT stabilization by tau contributes significantly to axon formation. Microtubule bundling and perhaps other undefined activities may also be required for axonal formation (Drubin and Kirschner, 1986).

Experiments to decrease tau expression also support a role of tau in axon formation and maintenance. Treatment of cultured neurons with antisense oligonucleotides to tau mRNA resulted in cells that were unable to extend axons (Caceres and Kosik, 1990). Rapid inactivation of tau through chromophore-assisted laser inactivation also resulted in a slowing of growth cone motility and a general decrease in neurite extension (Liu *et al.,* 1999). Mice deficient in tau protein develop to adulthood but contain defects in small-caliber axons (Harada *et al.,* 1994).

Tau protein is also associated with the plasma membrane in nerve cells (Brandt *et al.,* 1995) and may also bind to neurofilaments (Miyata *et al.,* 1986). Binding to the cortex requires actin filaments in the cortex (Maas *et al.,* 2000), but is unlikely through a direct interaction with actin filaments since tau constructs lacking the actin binding domain are still able to localize to the cell cortex (Brandt *et al.,* 1995).

During several disease processes tau protein aggregates into filaments. These diseases include Alzheimer's disease (Kosik and Greenberg, 1994), Down's syndrome (Flament *et al.,* 1990), progressive supranuclear palsy (Hof *et al.,* 1992), corticobasal degeneration (Feany and Dickson, 1995), Pick's disease (Feany *et al.,* 1996), and frontotemporal dementia with parkinsonism linked to chromosome 17 (FTDP-17; Poorkaj *et al.,* 1998).

Nonmammalian cells also express proteins with sequence homology to tau protein. For example, DMAP-85 of Drosophila also functions to stabilize MTs *in vitro* (Camiazo *et al.,* 1995).

d. MAP4/XMAP230   The best characterized MAP in nonneuronal mammalian cells is MAP4, a MAP originally identified in a human cell line as a protein that stimulated MT assembly (Bulinski and Borisy, 1980a; Bulinski, 1994). MAP4 is expressed in many tissues (Bulinski and Borisy, 1980b). MAP4 contains a unique N-terminal projection domain with multiple KDM repeats and a MT-binding

domain within the C-terminus that is related to that found in tau and MAP2 (Aizawa *et al.,* 1990; Chapin and Bulinski, 1992; West *et al.,* 1991). Although MAP4 shares this MT-binding domain with other MAPs, it affects assembly differently: when added to purified tubulin, MAP4 stabilizes microtubules by an ~30-fold increase in rescue frequency (Ookata *et al.,* 1995; Itoh and Hotani, 1994). The unique activity of MAP4, compared to MAP2 and tau, is consistent with the results of several studies suggesting that sequences outside the 18-amino-acid repeats are required for MT binding and that these additional sequences may significantly dictate MT-binding properties (Kanai *et al.,* 1992; Lee and Rook, 1992; Gustke *et al.,* 1994; Goode and Feinstein, 1994; Goode *et al.,* 1997).

Several alternatively spliced isoforms of MAP4 have been identified which contain three to five MT binding repeats (Chapin *et al.,* 1995). Tissue and developmental variations in isoform expression may alter the effects of MAP4 on MT stabilization (Chapin *et al.,* 1995).

Increased MAP4 levels in cells, through overexpression or microinjection of the protein, resulted in MTs with greater stability to the drug nocodazole (Nguyen *et al.,* 1997; Yoshida *et al.,* 1996; Olson *et al.,* 1995), a slowing in cell growth (Nguyen *et al.,* 1997), and a reduction in MT-dependent movement of vesicles and organelles (Bulinski *et al.,* 1997). A muscle-specific isoform of MAP4 is also required for myogenesis (Mangan and Olmsted, 1996). Decreased levels of MAP4 caused a reduction in MT polymer and a slowing of MT recovery from drug-induced depolymerization (Nguyen *et al.,* 1999). Not all studies have identified phenotypes after MAP4 reduction (Barlow *et al.,* 1994; Wang *et al.,* 1996), suggesting that molecules with functions similar to MAP4 exist in mammalian cells (Wang *et al.,* 1996).

The *Xenopus* protein XMAP230 is related to MAP4 (~30% identity) and may be the frog homolog of MAP4 since it contains the same sequence motifs and protein domains found in mammalian MAP4 (Shiina and Tsukita, 1999). Although MAP4 and XMAP230 appear related based on sequence, these proteins differ in their mechanisms of MT stabilization. XMAP230 increases MT elongation rate and greatly suppresses catastrophes *in vitro* (Andersen *et al.,* 1994). Depletion of XMAP230 from *Xenopus* egg extracts did not change MT growth rate but did result in reduced MT density within spindles and a resultant loss of chromosomes from the spindle, suggesting that XMAP230 is required to stabilize spindle MTs (Cha *et al.,* 1999).

e. TOGp/XMAP215 Family   A second *Xenopus* MAP, XMAP215, was initially isolated based on its ability to stimulate rapid MT assembly (Gard and Kirschner, 1987). Subsequent *in vitro* studies demonstrated that XMAP215 stimulates MT plus end growth by ~7- to 10-fold with little effect on MT minus ends (Vasquez *et al.,* 1994). These rapidly growing plus ends remain dynamic and thus XMAP215 generates the assembly of long, highly dynamic MTs (Vasquez *et al.,* 1994).

Depletion of XMAP215 from *Xenopus* egg extracts results in reduced MT elongation rates in interphase, increased catastrophes throughout the cell cycle, and defects in spindle assembly (Tournebize *et al.,* 2000).

Homologs of XMAP215 have been identified in a wide range of species, including a sequence found in the plant, *Arabadopsis thaliana.* These homologs include TOGp in humans (Charrasse *et al.,* 1998), mini-spindles in *Drosophila* (Cullen *et al.,* 1999), Zyg-9 in *Caenorhabditis elegans* (Matthews *et al.,* 1998), Stu2p in *Saccharomyces cerevisiae* (Wang and Huffacker, 1997), p93[dis1] in *Schizosaccharomyces pombe* (Nabeshima *et al.,* 1995), and DdCP224 in *Dictyostelium* (Graf *et al.,* 2000). The *S. cerevisiae* and *S. pombe* proteins are approximately half the size the other family members and have homology to the amino terminal half of XMAP215/TOGp. Mutations in genes encoding mini-spindles, zyg-9, or p93[dis1] resulted in defective spindle assembly and short MTs (Cullen *et al.,* 1999; Matthews *et al.,* 1998; Nabeshima *et al.,* 1995). Consistent with these observations, depletion of XMAP215 or TOGp from cell extracts resulted in reduced spindle/aster assembly (Tournebize *et al.,* 2000; Dionne *et al.,* 2000).

Analysis of MT-binding domains in Stu2p, p93[dis1], and TOGp showed that a region in the N-terminus is required (Wang and Huffacker, 1997; Nabeshima *et al.,* 1995; Spittle *et al.,* 2000). TOGp also has a region in the C-terminal half of the molecule which binds tubulin dimers/oligomers and this domain may function to promote MT elongation (Spittle *et al.,* 2000). Binding studies suggest that TOGp binds along a protofilament rather than cross-linking adjacent protofilaments (Spittle *et al.,* 2000).

f. XMAP310 This *Xenopus* protein stabilizes MTs by increasing rescues (5- to 10-fold) and slowing shortening by about 2-fold (Andersen and Karsenti, 1997). XMAP310 also bundles MTs (Andersen and Karsenti, 1997).

g. CLIPs Cytoplasmic linker proteins, CLIPs, are thought to link structures such as endosomes to MTs. The first described CLIP was CLIP170, a protein that binds specifically to growing MT plus ends (Pierre *et al.,* 1992; Diamantopoulos *et al.,* 1999; Perez *et al.,* 1999). CLIP170 has a 69-amino-acid MT binding motif repeated twice near its N-terminus (Pierre *et al.,* 1992). A similar MT-binding motif has been identified in p150 (a subunit of the dynactin complex), CLIP115 (a neuronal specific CLIP), two of the cofactors required for tubulin folding and Bik1p from *S. cerevisiae* (reviewed in Rickard, 1999). Additional serine-rich regions in CLIP115 found adjacent to the MT-binding motifs are also required for MT-binding in this protein (Hoogenraad *et al.,* 2000). Studies *in vitro* showed that CLIP170 can stimulate MT nucleation (Diamantopoulos *et al.,* 1999), suggesting that CLIP170, and perhaps CLIP115, may play a role in regulating MT assembly dynamics and/or nucleation *in vivo.* The *Drosophila* homolog of CLIP170 (D-CLIP-190) also binds myosin (Lantz and Miller, 1998), but it is not known whether this is a general property of CLIPs.

h. Stable Tubule-Only Polypeptides   STOPs (stable tubule-only polypeptides) were initially isolated from rat brain. This 100-kDa protein contains a central domain consisting of five 46-amino-acid repeats and a C-terminal domain containing 28 repeats of approximately 11 amino acids (Bosc *et al.,* 1996). A smaller isoform of 47 kDa is expressed in fibroblasts and has been named F-STOP (Denarier *et al.,* 1998). STOPs stabilize MTs against depolymerization by cold temperature or Ca^{2+} ions (reviewed by Margolis and Job, 1999). In fibroblasts, F-STOP is soluble in interphase but bound to kinetochore and midbody MTs (Margolis *et al.,* 1990; Denarier *et al.,* 1998).

i. APC   The adenomatous polyposis coli (APC) gene encodes a tumor suppressor which is mutated in both sporadic and some inherited forms of colon cancer (for reviews see Kinzler and Vogelstein, 1996; Polakis, 1997; Nathke, 1999; McCartney and Peifer, 2000). Wild-type APC protein (310 kDa) can be found in both the nucleus (Neufeld *et al.,* 2000) and localized at the distal ends of interphase MTs (Nathke *et al.,* 1996; Mimori-Kiyosue *et al.,* 2000a). The MT-binding domain is found in the C-terminus, which is frequently deleted in APC-related cancers (Munemitsu *et al.,* 1994; Smith *et al.,* 1994; Kintzer and Volgelstein, 1996). Biochemical analysis of the MT-binding domain has shown that it is a basic region with a pI similar to the MT-binding domain in tau (Deka *et al.,* 1998). The APC MT-binding domain promotes MT assembly *in vitro* (Munemitsu *et al.,* 1994). APC binds to EB1 (Su *et al.,* 1995) which also binds MTs (Mimori-Kiyosue *et al.,* 2000b). The EB1-interacting domain is also in the C-terminus of APC (Su *et al.,* 1995). Several *in vivo* studies in which normal APC levels were altered or mutant APC was expressed support a role for this protein in cell migration (Mahmoud *et al.,* 1997; Wong *et al.,* 1996; Frohli Hoier *et al.,* 2000) but it is not known whether this is mediated via microtubules.

   APC may regulate cell migration through its interaction with cell adhesion complex molecules like β-catenin, α-catenin, and/or plakoglobin (Rubinfeld *et al.,* 1993, 1995; Su *et al.,* 1995; Pollack *et al.,* 1997; Pollack *et al.,* 1997), either by regulating β-catenin turnover (Munemitsu *et al.,* 1995) or through a signaling cascade that includes β-catenin (reviewed by Barth *et al.,* 1997; Vleminckx *et al.,* 1997; Peiffer, 1995; Hinck *et al.,* 1994). Additional functions for APC in regulating the balance of cell proliferation/apoptosis have also been proposed based on its interactions with β-catenin and EB1 and other molecules such as the human homolog of the disc large protein of *Drosophila* and GSK3β (Peifer, 1996; Rubinfeld *et al.,* 1996; Matsumine *et al.,* 1996; reviewed by Peifer and Polakis, 2000).

j. EB1 Family   The EB1 family is a highly conserved group of proteins which are found in all eukaryotic organisms and various cell types (reviewed by Tirnauer and Bierer, 2000). The budding yeast homolog, Bim1p, was identified through a yeast two-hybrid screen for α-tubulin interacting proteins (Schwartz *et al.,* 1997).

Deletion of the BIM1 gene resulted in cells with shorter MTs which show less frequent rescues (Tirnauer *et al.,* 1999), suggesting that Bim1p may act as a MT stabilizer in this general classification scheme. However, cells deleted of BIM1 also show changes in MT dynamics consistent with Bim1p functioning to destabilize microtubules. These mutant cells show slower shortening, decreased catastrophes and decreased turnover (Tirnauer *et al.,* 1999).

The changes in MT dynamics observed after BIM1 deletion occur during the G1 phase of the cell cycle. Bim1p also functions during mitosis since cells lacking this protein contain misaligned spindles (Tirnauer *et al.,* 1999). Spindle positioning has been shown to be a two-step process that likely involves the interaction of Bim1p with Kar9p (Lee *et al.,* 2000; Korinek *et al.,* 2000; Bloom, 2000) and the dynein/dynactin complex (Adams and Cooper, 2000; Yeh *et al.,* 1995; Muhua *et al.,* 1998).

The fission yeast homolog, Mal3p, was isolated in a screen for defects in chromosome segregation (Beinhaurer *et al.,* 1997). Mutations in the MAL3 protein resulted in short interphase MTs, suggesting that the wild-type protein contributes to MT assembly or stability (Beinhauer *et al.,* 1997). However, overexpression of *Mal3* disrupted spindle formation, suggesting that this family of proteins can also destabilize MTs (Beinhauer *et al.,* 1997). Therefore, results with Bim1p and Mal3p each suggest that this family of proteins can contribute to either MT stabilization or destabilization, but it is not yet clear how they function.

The human homolog, EB1, is a small (30- to 35-kDa) protein that was identified in a yeast two-hybrid screen for proteins interacting with APC (Su *et al.,* 1995). Human EB1 was subsequently shown to bind MTs in cells (Berrueta *et al.,* 1998; Morrison *et al.,* 1998) where it concentrates at MT plus ends (Morrison *et al.,* 1998; Juwana *et al.,* 1999). The MT-binding domain is a basic region within the highly conserved N-terminus (Juwana *et al.,* 1999).

k. Doublecortin   Mutations in the gene encoding doublecortin are responsible for X-linked lissencephaly which results from failure of neurons to properly migrate into the cerebral cortex (Gleeson *et al.,* 1999; Francis *et al.,* 1999). Doublecortin binds and stabilizes microtubules in *in vitro* assays (Horesh *et al.,* 1999; Gleeson *et al.,* 1999; Francis *et al.,* 1999). The MT-binding domain of doublecortin was identified recently as a pair of internal repeats (Taylor *et al.,* 2000). These sequence repeats coincide with clusters of observed mutations in patients with X-linked lissencephaly; these correlations support the idea that the interaction of doublecortin with MTs functions in neuronal migration (Taylor *et al.,* 2000).

Other mutations giving rise to lissencephaly result from mutations in the LIS1 gene. At this time it is not clear whether LIS1 regulates MT assembly (Sapir *et al.,* 1997) or dynein-based motility (Faulkner *et al.,* 2000). Since the function and potential regulation of LIS1 are not known, it will not be considered further in this review.

l. E-MAP-115/Ensconsin   This MAP was isolated from epithelial cells and when overexpressed could cause MT bundling and resistance to MT depolymerization by nocodazole treatment (Masson and Kreis, 1993). Recent studies have questioned the role of E-MAP-115/ensconsin in regulating MT dynamics since assembly dynamics were unchanged in cells expressing a 10-fold excess of GFP-ensconsin compared to the dynamics in nontransfected cells (Faire *et al.,* 1999). Alternatively, E-MAP-115 function may be critical in some differentiated cells since E-MAP-115 is required for spermatogenesis in mice (Komada *et al.,* 2000).

m. NuMA   Nuclear mitotic apparatus protein (NuMA) was originally identified because of its unique cell cycle-specific localization pattern: NuMA is located within the nucleus during interphase and bound to spindle poles during mitosis (Lyderson and Pettijohn, 1980; Price and Pettijohn, 1986). This 200- to 230-kDa phosphoprotein was simultaneously identified in several other studies using centrosome-specific human autoimmune sera or monoclonal antibodies and named centrophilin (Tousson *et al.,* 1991), SP-H (Maekawa *et al.,* 1991), and SPN (Kallajoki *et al.,* 1991). The predicted secondary structure of NuMA is a protein with globular–helical–globular organization (Yang *et al.,* 1992; Compton *et al.,* 1992), which has the MT binding domain located in the globular C-terminus (Maekawa and Kuriyama, 1993).

NuMA is proposed to function as a nuclear-scaffold during interphase as suggested by results from overexpression of various constructs of the NuMA protein (reviewed by Harborth and Osborn, 1999; Gueth-Hallonet *et al.,* 1998). A recent electron microscopy study has shown that NuMA is also part of a mitotic spindle matrix (Dionne *et al.,* 1999). Many studies have shown that NuMA is an important structural MAP that works with several motor proteins in focusing MT minus ends to form and maintain the mitotic spindle poles (Compton and Cleveland, 1993; Gaglio *et al.,* 1995, 1996; Merdes *et al.,* 1996, 2000 ; Whitehead and Rattner, 1998).

n. CENP-E   CENP-E was originally identified in a screen for centromere-binding proteins. CENP-E specifically localizes to kinetochores early in mitosis and later binds MTs in the spindle mid-zone (Yen *et al.,* 1991, 1992). CENP-E contains two distinct MT-binding domains: an ATP-dependent binding domain is found in the N-terminus which is similar to those of other kinesin-like proteins (Yen *et al.,* 1992) and a second MT-binding domain is found within the C-terminus which is similar to the MT-binding domain of tau and MAP2 (Yen *et al.,* 1992). The localization pattern and presence of two MT-binding domains suggests that this protein may have several functions throughout mitosis. For example, the motor domain is required for chromosome alignment at the spindle equator (Schaar *et al.,* 1997) while cross-linking of overlapping MTs at the spindle mid-zone by the nonmotor binding domain could serve to stabilize the spindle and/or help push the spindle poles apart from each other during late anaphase (Liao *et al.,* 1994). CENP-E is also essential for the mitotic checkpoint (Abrieu *et al.,* 2000).

The *Drosophila* homolog of CENP-E, CENP-meta, does not bind spindle MTs as observed for CENP-E (Yucel *et al.,* 2000), suggesting that CENP-meta may not share a MT cross-linking function with its mammalian counterpart.

o. TPX2 This *Xenopus* MAP functions to target the plus end directed motor Xklp2 to MT minus ends during mitosis (Wittman *et al.,* 1998, 2000).

2. Destabilizers

This section surveys proteins that can destabilize MTs. Any mechanism that promotes subunit loss from the MT will destabilize the microtubule. This could include slowing subunit addition, stimulating catastrophes or inhibiting rescues. Destabilization could occur through mechanisms which: (1) remove a GTP cap at MT ends, either through severing of the MT or removing individual dimers from the MT lattice; (2) stimulate GTP hydrolysis; (3) weaken lateral interactions between protofilaments; or (4) sequester tubulin subunits. Andersen (2000) has also described molecular mechanisms that could destabilize MTs.

a. XKCM1/MCAK Family XKCM1 from *Xenopus* eggs and MCAK from mammalian cells are members of the Kin I kinesin subfamily, having the catalytic domain in the center of the protein (Walczak *et al.,* 1996; Desai *et al.,* 1999; Wordeman and Mitchison, 1995). XKCM1 increases MT catastrophes ∼4-fold in *Xenopus* extracts using an ATP-dependent mechanism (Walczak *et al.,* 1996; Desai *et al.,* 1999). XKCM1 depletion from mitotic *Xenopus* egg extracts results in long MTs and disruption of spindle assembly (Walczak *et al.,* 1996). Overexpression of MCAK or XKCM1 results in loss of MT polymer; this is observed during both mitosis and interphase (Maney *et al.,* 1998; Kline-Smith and Walczak, 2000). XKCM1 and MCAK are soluble during interphase and a fraction of these proteins also localizes to spindle poles and the centromere regions of chromosomes (Walczak *et al.,* 1996; Wordeman and Mitchison, 1995). Additional Kin I kinesins have been identified and likely have similar functions (Desai *et al.,* 1999).

b. Oncoprotein 18 (Op18)/Stathmin Op18/stathmin is a cytosolic 18-kDa phosphoprotein which was initially identified based on its increased expression in acute leukemia and its complex phosphorylation pattern in response to external stimuli (reviewed in Sobel, 1991, and Lawler, 1998). This protein was independently isolated in a functional assay to identify proteins that destabilize microtubules in *Xenopus* egg extracts (Belmont and Mitchison, 1996). Several Op18/stathmin-related proteins have been identified which are expressed in brain (Ozon *et al.,* 1997). One of these, SCG10, also destabilizes MTs (Riederer *et al.,* 1997).

Op18/stathmin is a soluble protein that does not show significant binding to MTs. Instead, Op18/stathmin binds tubulin dimers, primarily through an interaction

with α tubulin to form a complex of one Op18/stathmin and two tubulin dimers (Belmont and Mitchison, 1996; Curmi *et al.,* 1997; Jourdain *et al.,* 1997; Larsson *et al.,* 1997; Steinmetz *et al.,* 2000). The binding between Op18/stathmin and tubulin can result in tubulin sequestration and a resultant destabilization of MTs (Curmi *et al.,* 1997; Jourdain *et al.,* 1997). In addition, Op18/stathmin can function as a specific catastrophe promoter (Belmont and Mitchison, 1996; Howell *et al.,* 1999a). In *in vitro* assembly assays using purified tubulin and Op18/stathmin, the sequestering and catastrophe promoting activities can be separated by changes in pH or truncations of the Op18 protein (Howell *et al.,* 1999a). While the sequestering mechanism is clear (Curmi *et al.,* 1997; Jourdain *et al.,* 1997), the mechanism responsible for catastrophe promotion is not yet understood. Interestingly, Op18/stathmin stimulates the intrinsic GTPase activity of tubulin when Op18/stathmin is bound to two tubulin dimers (Larsson *et al.,* 1999a,b). The orientation of dimers in complex with Op18/stathmin is similar to that found along a protofilament (which provides an explanation for the stimulation of GTP hydrolysis), where Op18/stathmin favors a kinked orientation to the dimers (Steinmetz *et al.,* 2000; Gigant *et al.,* 2000).

Immunodepletion of Op18/stathmin from *Xenopus* egg extracts resulted in increased MT polymer (Belmont and Mitchison, 1996) and a 1.5- to 5-fold decrease in catastrophes (Tournebize *et al.,* 1997). Direct observation of MTs in cells with reduced Op18 protein level also showed an increase in MT polymer and an ∼3-fold decrease in catastrophes (Howell *et al.,* 1999b). Op18/stathmin may have additional functions since the change in plus end assembly dynamics was not sufficient to account for the measured increase in MT polymer (Howell *et al.,* 1999b). Thus, Op18/stathmin could influence MT polymer level by additional effects on nucleation or minus end assembly dynamics *in vivo.*

Mice lacking Op18/stathmin developed normally (Schubar *et al.,* 1996). This result was unexpected since other studies demonstrated that Op18 expression was necessary for neurite outgrowth in a PC12 model system (DiPaolo *et al.,* 1996) and that reduced expression of Op18 in K562 leukemia cells reversed many of the phenotypes characteristic of transformed cells and reduced tumor formation in an *in vivo* model system (Jeha *et al.,* 1996).

c. EMAP Echinoderm MAP (EMAP) is a 75-kDa protein and the most abundant MT-associated protein in sea urchin eggs and other echinoderms, such as starfish and sand dollars (Suprenant and Marsh, 1987). EMAP binds MTs and stimulates microtubule turnover *in vitro* through an inhibition of rescue (Hamill *et al.,* 1998). Proteins related to EMAP have been identified in humans (EMAPL and ELP-2) and *C. elegans* (Suprenant *et al.,* 2000; Eudy *et al.,* 1997). One of these proteins, EMAPL (EMAP-like), was initially isolated as the likely candidate gene mutated in Usher syndrome 1a, an autosomal recessive disease causing severe deafness and blindness (Eudy *et al.,* 1997). EMAP may also function to localize ribosomes to MTs (Suprenant *et al.,* 1993).

d. p62   This echinoderm protein was identified as a phosphorylated component of the sea urchin mitotic apparatus (Dinsmore and Sloboda, 1988), and was later shown to bind microtubules (Johnson and Sloboda, 1992). Although it is not yet clear whether this protein binds directly to MTs, p62 appears necessary for MT depolymerization at the metaphase/anaphase transition (Dinsmore and Sloboda, 1988, 1989) and likely regulates MT stability.

e. Kar3p and Kip3p   These yeast kinesins may also participate in regulating MT assembly. Kar3p is a minus-end directed yeast kinesin which also depolymerizes taxol-stabilized MTs from their minus ends *in vitro* (Endow *et al.,* 1994). In *S. cerevisiae,* deletion of KAR3 resulted in increased numbers and lengths of cytoplasmic MTs (Saunders *et al.,* 1997), consistent with a role in modifying MT assembly. It was postulated that Kar3p generated MT poleward flux during mitosis (Endow *et al.,* 1994), but flux has not been detected in *S. cerevisiae* (Maddox *et al.,* 2000), raising questions of whether Kar3p depolymerizes MTs in cells. Kip3 is also a kinesin family member that may regulate microtubule assembly since purified Kip3p can depolymerize taxol-stabilized microtubules (Smirnova and Roof, 2000). The functional significance of Kar3p or Kip3p depolymerization of MTs observed *in vitro* has not been determined.

f. Katanin   The MT-severing protein katanin (Vale, 1991; McNally and Vale, 1993; Hartman *et al.,* 1998) is composed of two subunits, p60 and p80. The p60 subunit is an ATPase that uses ATP hydrolysis to break bonds within the MT lattice, thus severing the microtubule and exposing GDP subunits at the new end (Hartman and Vale, 1999). Cutting of MTs in M-phase *Xenopus* extracts is performed solely by katanin (McNally and Thomas, 1998).

g. MINUS   This 4.7-kDa polypeptide was isolated from PC12 cells and functions to inhibit MT nucleation (Fanara *et al.,* 1999).

h. Xenopus microtubule assembly inhibitor   A partially purified activity from *Xenopus* oocytes can specifically inhibit MT plus end polymerization and raise the critical concentration for assembly (Govindan and Vale, 1999). This activity cofractionates with tubulin in a large complex and may act by binding tubulin dimers in the cytoplasm. The inhibitory activity is lost as oocytes mature into eggs (Govindan and Vale, 1999). The protein(s) responsible for the inhibitory activity have not been purified.

i. HIV-1 Rev   The viral HIV-1 Rev protein was recently shown to depolymerize MTs by stimulating formation of protofilament rings (Watts *et al.,* 2000). Microtubule depolymerization was also observed in *Xenopus* egg extracts, but at this time it is not clear whether Rev interacts with tubulin or MTs in HIV-1-infected cells

(Watts *et al.,* 2000). No mechanisms responsible for regulating the MT-destabilizing activity of Rev have been described and we will not consider this protein further.

III. Regulation of MAP Activities

A number of regulatory mechanisms are responsible for modifying MAP activities. Below we consider eight general regulatory mechanisms: (A) protein expression or protein level; (B) phosphorylation state or other modification; (C) intracellular localization; (D) cofactors or binding partners necessary for activity; (E) competition/antagonism between MAPs; (F) synergy between MAPs; (G) dimerization/ multimerization; and (H) nonenzyme regulatory proteins. Each MAP is likely regulated through a combination of the above mechanisms. The first three regulatory mechanisms have been studied in the most detail and likely reflect the three most important mechanisms regulating MAP activities. For each regulatory mechanism we summarize how or when specific MAPs are modified by this mechanism and functional consequences for MAP activity.

A. Regulation of Protein Expression or Level

A number of MAPs are regulated through changes in gene expression or the concentration of the protein in the cell. This section will include tissue- or developmental-specific expression, isoform-specific expression, cell-cycle-dependent expression, and regulated protein degradation.

1. Tissue-Specific Expression

Tissue-specific expression is most clearly demonstrated by MAP2 and tau since these MAPs are highly expressed in neuronal tissue with little or no expression in other tissues. Mechanisms responsible for regulated expression have been best studied for tau; therefore, we begin with a description of transcriptional regulation of tau expression and then summarize what is known about regulated expression of other neuronal and nonneuronal MAPs.

a. Tau   Tau protein is expressed primarily in neuronal cells (Drubin *et al.,* 1986; Andreadis *et al.,* 1992), where it is localized specifically to cell bodies and axons (see below for intracellular localization; Binder *et al.,* 1985). Using PC12 cells as a model for neuronal development, Drubin *et al.* (1988) demonstrated that tau expression is induced by nerve growth factor. This growth factor increases tau RNA level by activation of the tau promoter, an 80-nucleotide region lying -190 to -100 base pairs upstream of the tau exon 1 in rats (Sadot *et al.,* 1996). The tau

promoter is sufficient to confer neuron-specific and NGF-inducible expression of a reporter gene (Sadot *et al.,* 1996; Heicklen-Klein *et al.,* 2000; Heicklen-Klein and Ginzberg, 2000). The transcription factors Sp1 and AP-2 bind the tau promoter, as does a third, as yet unidentified protein (Heicklen-Klein and Ginzberg, 2000). All three proteins are required for neuronal-specific expression of the tau gene (Heicklen-Klein and Ginzberg, 2000), but the precise mechanism responsible for this restricted expression is still unknown since Sp1 and AP-2 are found in diverse tissues and cell types.

b. MAP1A This MAP is also highly expressed in brain but expression does not appear restricted to any specific brain region (Fink *et al.,* 1996). To our knowledge the promoter region of MAP1A has not been explored to determine mechanisms responsible for higher expression in the nervous system.

c. MAP1B MAP1B is also highly expressed in brain tissue, particularly during the axonogenesis phase of neural development (Bloom *et al.,* 1984; reviewed in Gordon-Weeks and Fischer, 2000). Neuronal expression has been examined through studies of the MAP1B gene and its promoters. MAP1B has two separate promoters with TATA boxes separated by 134 base pairs (Liu and Fischer, 1996). The downstream promoter appears to be constitutively active and is likely responsible for MAP1B expression in the adult, while the upstream promoter may allow developmentally induced expression of MAP1B (Liu and Fischer, 1996). It appears that the consitutive, downstream promoter is negatively regulated in non-neuronal tissue, resulting in higher expression in neurons (Liu and Fischer, 1997). A *Drosophila* protein, futsch has homology to MAP1B; expression of futsch during development is also enriched in the nervous system by inhibition of expression in nonneuronal cells (Hummel *et al.,* 2000).

d. MAP2 Mechanisms limiting the expression of this MAP to neuronal tissue have not been well studied to date. It appears that neuronal expression of MAP2 in early development is under control of the D1x-2 homeo-domain gene (Ding *et al.,* 1997). This result suggests that the higher level of MAP2 mRNA found in neurons (e.g., Beaman-Hall and Vallano, 1993) results from turning on the MAP2 gene, rather than a scenario where expression is repressed in nonneuronal tissues.

e. Neuron-Specific APC and EB1 Brain-specific homologs of APC and EB1 have been identified, termed APCL and EB3 (Nakagawa *et al.,* 1998, 2000). The brain-specific homologs are encoded by separate genes from their nonneuronal counterparts (Nakagawa *et al.,* 1998, 2000).

f. XMAP215/TOGp XMAP215 expression is highest in the brain of tadpole frogs (Gard and Kirschner, 1987; Becker and Gard, 2000). Similarly, TOGp is also expressed at higher amounts in human brain, although it is also expressed at

lower levels in all tissues examined (Charrasse *et al.,* 1995; our unpublished observations). TOGp is also overexpressed in colonic and hepatic tumors (Charrasse *et al.,* 1995). Mechanisms responsible for overexpression in tumors or higher expression in brain have not been studied.

g. EMAP   The major echinoderm MAP (EMAP) and related family members in humans, are expressed in a number of tissues. EMAP shows some increase in mesoderm level during sea urchin development, but the functional consequences are not known (Suprenant *et al.,* 2000). Two human proteins related to EMAP have been isolated, EMAPL (Eudy *et al.,* 1997) and ELP-2 (Lepley *et al.,* 2000). Each human EMAP is encoded by a single gene and is expressed to varying levels in different human tissues. For example, ELP-2 is expressed at relatively higher levels in pancreas, colon, thyroid, and spinal cord while EMAPL is expression is enriched in heart, skeletal muscle, small intestine, and colon (Lepley *et al.,* 2000). The mechanisms regulating tissue-specific expression have not been examined.

2. Isoform-Specific Expression

a. Tau   Tau proteins are expressed from a single gene with multiple isoforms expressed during development and adulthood through alternative splicing of the tau RNA (Himmler, 1989). A single tau isoform consisting of exons 1, 4, 5, 7, 9, and 11–13 is expressed in the fetal human brain (Goedert *et al.,* 1992). In the adult brain and central nervous system, six isoforms (48 to 67 kDa) are expressed using the same exons as above, but also include alternative splicing of exons 2, 3, and 10 (Drubin *et al.,* 1984; Himmler, 1989; Andreadis *et al.,* 1992; Goedert *et al.,* 1996, 1997a; Couchie *et al.,* 1986). In the peripheral nervous system an additional tau isoform is expressed, termed "big tau," which also results from alternative splicing, here splicing adds approximately 250 amino acids to the central region of the protein outside the MT-binding domain (Mavilia *et al.,* 1993). Isoforms lacking exon 10 contain three MT-binding repeats; inclusion of exon 10 adds a fourth MT binding repeat (Goedert *et al.,* 1989a, Kosik *et al.,* 1989; Himmler *et al.,* 1989).

The variation in MT-binding repeats between tau isoforms suggests that the isoforms could show variation in MT affinity. This idea is supported by observations that binding affinity is increased in tau containing four MT binding repeats compared to the three repeat tau (Butner and Kirschner, 1991; Gustke *et al.,* 1994). Consistent with the binding studies, the presence of four repeats also stimulates MT assembly to a greater extent than three repeat tau (Trinczek *et al.,* 1995). Tau protein also increases the flexural rigidity of MTs; proteins with fewer repeats show a reduced ability to increase MT stiffness (Felgner *et al.,* 1997).

In normal brain tissue, four repeat and three repeat tau proteins are present at approximately equal levels, suggesting that splicing is regulated to maintain

a balance between these isoforms (Hong *et al.,* 1998). Further support for the importance of splicing of tau RNA comes from the inherited disease FTDP-17 (frontotemporal dementia and parkinsonism linked to chromosome 17; Poorkaj *et al.,* 1998; reviewed in Lee and Trojanowski, 1999). Many of the point mutations identified in individuals suffering from FTDP-17 alter splicing of exon 10, changing the ratio of four-repeat to three-repeat tau and causing the formation of tau aggregates (D'Souza *et al.,* 1999; Spillantini *et al.,* 1998).

The recent identification of mutations that result in altered tau RNA splicing is helping to pinpoint mechanisms regulating splicing and splice-choice. To date it appears that the default pathway is to include exon 10 during splicing and thus isoforms lacking exon 10 must arise through inhibition of specific splice sites (Gao *et al.,* 2000), although evidence for enhancer sequences has also been presented (D'Souza and Schellenberg, 2000). The splicing inhibitors which regulate exon 10 inclusion are also highly enriched in brain, providing a potential mechanism for localized regulation of splicing within nervous tissue (Gao *et al.,* 2000). Clearly there is still plenty to learn about how tau RNA is spliced and how splicing is regulated during development and in the adult brain.

b. Other MAPs   Additional MAPs with isoforms generated by alternative splicing are listed below. Mechanisms responsible for splice choice in these RNAs have not been determined. Alternative splicing generates isoforms of (1) MAP1B (Kutschera *et al.,* 1998); (2) the high- and low-molecular-weight isoforms of MAP2 (MAP2a, -b, and -c; Kalcheva *et al.,* 1995; Garner and Matus, 1988; Chung *et al.,* 1996), including a novel splice variant expressed in oligodendrocytes from multiple sclerosis lesions (Shafit-Zagardo *et al.,* 1999); (3) the neuronal and fibroblastic STOP proteins (Bosc *et al.,* 1996; Denarier *et al.,* 1998); (4) MAP4 (Code and Olmsted, 1992; Chapin *et al.,* 1995); (5) XMAP215 (Becker and Gard, 2000); and (6) three isoforms of NuMA (Tang *et al.,* 1993; Zeng *et al.,* 1994).

Although the mechanisms responsible for MAP2 splicing are not known, expression of varying levels of MAP2 cDNA constructs *in vivo* suggest that these isoforms determine the morphology and type of neurite process through regulation of microtubule dynamics, microtubule number, and microtubule spacing (Lewis *et al.,* 1989; LeClerc *et al.,* 1993, 1996; Kalcheva *et al.,* 1998; Sharma *et al.,* 1994; Dinsmore and Solomon, 1991; Caceres *et al.,* 1992).

3. p53-Dependent Expression

The tumor suppressor protein p53 acts to either stimulate or repress transcription. It appears that transcription repression, rather than activation, is a key upstream regulator of apoptosis (Shen and Shank, 1994; Sabbatini *et al.,* 1995). Interestingly, several genes for MAPs are repressed by p53; these include MAP4 (Murphy *et al.,* 1996) and Op18/stathmin (Ahn *et al.,* 1999). The roles of the microtubule cytoskeleton and MAPs in the downstream signaling cascade leading to apoptosis

are not understood, but it appears that reduced expression of MAP4 is required for apoptosis since overexpression of MAP4 concurrent with p53 induction is sufficient to slow apoptosis (Murphy *et al.,* 1996).

4. Developmental Expression

A number of MAPs are regulated throughout development, either by regulating the of amount of protein or by expression of specific isoforms. Mechanisms responsible for changes in expression during development have not been well studied. The following section is descriptive since we can only describe when during development specific MAPs or isoforms are expressed.

a. MAP1A   MAP1a is expressed at approximately 10-fold higher levels in adult brain compared to levels in fetal brain (Fink *et al.,* 1996).

b. MAP1B   Expression of MAP1B is downregulated during development in the central nervous system (Schoenfeld *et al.,* 1989). The level of MAP1B remains at a relatively high level in the adult peripheral nervous system (Ma *et al.,* 1997). Elevated levels of MAP1B are also observed in adult dorsal root ganglions and regenerating axons following peripheral nerve damage, suggesting a role for MAP1B in neuron regeneration (Ma *et al.,* 2000).

c. MAP2   The expression of MAP2 isoforms changes during development. The smaller isoform, MAP2c is expressed in the embryonic and neonatal brain but is weakly expressed in adult brain (Garner and Matus, 1988). MAP2a and -b are not expressed during development and are then expressed in adult brain (Garner and Matus, 1988). Expression of these different isoforms is likely to be functionally significant during development since the smaller MAP2c lacks most of the projection domain found in MAP2a and -b and therefore MAP2c cannot regulate the spacing or cross-linking of microtubules (Papandrikopoulou *et al.,* 1989).

d. Tau   Of the six tau protein isoforms, only the smallest is expressed in fetal brain, while all six isoforms are expressed in adults (Goedert *et al.,* 1989a,b). The small isoform contains three microtubule binding repeats (Goedert *et al.,* 1989a,b) and has comparatively weaker binding to microtubules (Butner and Kirschner, 1991; Gustke *et al.,* 1994).

e. XMAP215   XMAP215 is expressed as two distinct isoforms which arise from alternative splicing and by the inclusion of a 36-bp insert in the longer isoform (Becker and Gard, 2000). This longer XMAP215 isoform is expressed from oogenesis through gastrulation (Becker and Gard, 2000), while the smaller isoform is expressed from gastrulation to adult. During gastrulation the abundance of XMAP215 transcripts falls by about 20-fold; this occurs concurrent with the switch from the

larger to the smaller XMAP215 isoform. As development progresses, XMAP215 expression is highest in the developing nervous system (Becker and Gard, 2000). The data suggests that the two isoforms differ in functional activities required during different developmental stages but functional differences between the isoforms have not yet been tested.

5. Cell-Cycle-Dependent Regulation of Protein Levels

Most MAPs are present at relatively constant amounts throughout the cell cycle. One exception is the yeast protein Bim1p. The transcription of this protein is not constant throughout the cell cycle. Rather, BIM1 mRNA is highest during the G1 and S phases of the cell cycle, message levels then drop off as the cell cycle approaches mitosis (Tirnauer *et al.,* 1999). This results in an approximately twofold change in Bim1p protein level during the cell cycle (Tirnauer *et al.,* 1999).

CENP-E is also expressed at different levels during the cell cycle. The mammalian CENP-E begins to accumulate late in the G2 phase of the cell cycle (Yen *et al.,* 1992). Levels of CENP-E then fall after mitosis is complete (Yen *et al.,* 1992).

6. Stress-Induced Changes in Expression

Electroconvulsive shock can generate changes in MAP2 expression in a rat model of electroconvulsive therapy. MAP2 levels rise 1.4-fold in the dendate gyrus region of the brain within hours after electric shock treatment (Pei *et al.,* 1998). Levels of tau and MAP1B are not changed in this experiment (Pei *et al.,* 1998).

Repetitive head injury can also result in damage to the cytoskeleton. While changes in MAP expression level have not been examined, tau aggregation into filaments occurs after repetitive head injury (Geddes *et al.,* 1999), which could result in further changes to the neuronal cytoskeleton.

7. Degradation

a. CENP-E The cell-cycle-dependent accumulation of CENP-E described above results primarily from changes in protein degradation rate. CENP-E is synthesized continuously throughout the cell cycle but the protein becomes much more stable during S and G2 phases, leading to protein accumulation during G2 (Brown *et al.,* 1994).

b. MAP1B MAP1B heavy and light chains are degraded at different rates in rat brains (Mei *et al.,* 2000). Since these proteins are expressed from polyproteins and later cleaved to release the light chains (Langkopf *et al.,* 1992; Fink *et al.,* 1996; Hammarback *et al.,* 1991), cells will always have an excess of LC 1 and LC 2 relative to MAP1A and MAP1B heavy chains.

c. Phosphorylation-Dependent Degradation   Phosphorylation can also mark
MAPs for degradation, suggesting that phosphorylation could have longer con-
sequences by decreasing a MAP pool. For example, phosphorylation of Op18/
stathmin enhances degradation (Melander Gradin *et al.,* 1997, 1998). In addition,
the hyperphosphorylated tau found in paired helical filaments is also ubiquinated
and targeted for destruction (Morishima-Kaswashima *et al.,* 1993). Finally, phos-
phorylation of MAP2 may serve to target it for degradation by the protease calpain
(Billger *et al.,* 1988; Springer *et al.,* 1997; Taft *et al.,* 1992). This degradation has
been correlated with brain or spinal cord injury (Springer *et al.,* 1997; Taft *et al.,*
1992), suggesting that excessive MAP2 phosphorylation and degradation could
contribute to neurodegeneration.

B. Phosphorylation/Dephosphorylation

A number of early studies clearly established that phosphorylation regulated
MAP binding to MTs with phosphorylation reducing MAP affinity for MTs (e.g.,
Jameson and Caplow, 1981; Burns *et al.,* 1984). These early studies used MAPs
isolated from neuronal tissue and generated a "rule of thumb" that phosphorylation
reduces MAP binding affinity to MTs. This rule has held up for a large number of
MAPs, but exceptions also exist where phosphorylation either does not alter MT
binding or where phosphorylation is actually required for MT binding.

Recently the MARKs (MAP/MT affinity regulating kinase) family of serine/
threonine (S/T) kinases has been identified, which specifically recognizes the
KXGS motif found within the MT binding repeats of tau, MAP2, and MAP4
(Drewes *et al.,* 1995, 1997, 1998; Illenberger *et al.,* 1996; Ebneth *et al.,* 1999). This
KXGS motif is also found in XMAP215/TOGp (Becker and Gard, 2000; Charrasse
et al., 1998; Tournbize *et al.,* 2000). The ubiquitous expression of MARKs in
mammalian tissues and the existence of homologs involved in establishing cell
polarity in lower eukaryotes (Drewes *et al.,* 1997) highlights the central role of
phosphorylation in regulating MAP functions.

The identification of phosphorylation sites at or near MT-binding domains (e.g.,
Drewes *et al.,* 1995), suggested that phosphorylation acts simply by altering bind-
ing interactions between MAPs and MTs through introduction of the negatively
charged phosphate group to the MAP. This is likely to be the case in many in-
stances, but recent experiments have suggested additional ways that phospho-
rylation can alter protein function. Many kinases phosphorylate a S/T residue
followed by a P (proline-directed kinases; e.g., MAP kinase, and Cdks). This
phosphorylated S/T–P sequence is recognized by Pin1, a peptidyl-prolyl isomerase
(Yaffee *et al.,* 1997), which can induce a conformational change in the phospho-
rylated protein and thus alter protein activity beyond what would be expected
simply from introduction of the negatively charged phosphate group (Shen *et al.,*
1998).

The activity of phosphatases is obviously critical in both reversing MAP phosphorylation and in determining the overall level of MAP phosphorylation. Although the number of different phosphatases is considerably smaller than the number of kinases, dephosphorylation of MAPs is typically accomplished by specific phosphatases (e.g., Tournebize *et al.,* 1997; Sontag *et al.,* 1996).

The localization of kinases and phosphatases can add a spatial element to MAP regulation by phosphorylation state. For example, the α subunit of Ca^{2+}/calmodulin-dependent protein kinase II is localized to dendrites (Burgen *et al.,* 1990) and although both tau and MAP are phosphorylated by this kinase (discussed below), only MAP2 should be an *in vivo* target of the kinase given their colocalization in dendrites. Cell type differences in kinase or phosphatase expression may also dictate whether a particular MAP will be regulated by phosphorylation state in a particular cell type. An example is the kinase Ca^{2+} calmodulin-dependent kinase IV/Gr, which is expressed primarily in neurons and T cells (Hanissian *et al.,* 1993). Finally, kinases and phosphatases can bind to the MT cytoskeleton, perhaps localizing enzyme activity near potential MAP substrates (Theurkauf and Vallee 1983; Morishima-Kawashima and Kosik, 1996; Sontag *et al.,* 1995; Ookata *et al.,* 1995; Andreassen *et al.,* 1998).

1. Tau

Phosphorylation of tau protein has been extensively studied since hyperphosphorylated tau was identified in the paired helical filaments found in the cytoplasm of Alzheimer's disease brain tissue (Kopke *et al.,* 1993; Ksiezak-Reding *et al.,* 1992). At this time it is not known whether hyperphosphorylation is responsible for tau aggregation or whether tau within the paired helical filaments is less accessible to phosphatases, since fetal and normal adult tau are phosphorylated on the same sites, but perhaps in a more dynamic manner (reviewed in Buee *et al.,* 2000). A total of 79 potential S or T phosphorylation sites exist in tau protein (for the longest brain isoform of 441 amino acids). Of these sites, phosphorylations at 33 sites have been identified (reviewed by Friedhoff and Mandelkow, 1991; Buee *et al.,* 2000). Many of these are S/T–P sites recognized by proline-directed kinases such as cdk5, MAP kinase, and GSK3β; these sites are localized within the regions flanking the MT-binding repeats (Drewes *et al.,* 1992; Hanger *et al.,* 1992; Paudel *et al.,* 1993; Kobayashi *et al.,* 1993). Other kinases able to phosphorylate tau include MARKs (Drewes *et al.,* 1995), PKA (Illenberger *et al.,* 1998; Andorfer and Davies, 2000), Ca^{2+} calmodulin-dependent protein kinase II (Baudier and Cole, 1987), casein kinase II (Greenwood *et al.,* 1994), and the stress activated (SAP) kinases (Goedert *et al.,* 1997b). Tau also binds to Src and Fyn, and tau can be phosphorylated on tyrosines by Fyn (Lee *et al.,* 1998).

Tau also interacts with protein phosphatases PP1 and PP2A (Sontag *et al.,* 1995; Liao *et al.,* 1998). Although both phosphatases bind tau, it appears that PP2A is the major phosphatase regulating tau phosphorylation level (Sontag *et al.,* 1996).

The role of phosphatases in regulating tau phosphorylation state is highlighted during development: tau is phosphorylated to a higher degree in fetal brain than in the adult brain (Wanatabe *et al.,* 1993) and this difference is based on a the developmental timing of phosphatase activation (Mawal-Dewan *et al.,* 1994).

Phosphorylation can modify tau function by reducing the binding affinity of tau for MTs. Phosphorylation of the flanking regions by the proline-directed kinases weakly reduces the affinity of tau for MTs (Biernat *et al.,* 1993; Drewes *et al.,* 1995). S262 of tau is critical for MT binding, phosphorylation of this residue by MARKs significantly decreases binding to MTs (Biernat *et al.,* 1993; Drewes *et al.,* 1995). Tau phosphorylated at S214 by PKA also shows significantly reduced binding to MTs (Illenberger *et al.,* 1998).

The decreases in MT binding observed after different phosphorylations are consistent with the ability of tau to stabilize MTs. In a thorough study by Trinczek *et al.* (1995), unphosphorylated tau stabilized MTs by reducing catastrophes approximately 30-fold and decreasing subunit dissociation during the elongation phase of dynamic instability, compared to the assembly dynamics of purified tubulin alone. Phosphorylation of tau by Cdk5 (a proline-directed kinase) resulted in an eight-fold decrease in catastrophes compared to tubulin alone. Thus, phosphorylation by the proline-directed kinase reduced, but did not eliminate, the ability of tau to stabilize MTs. In contrast, phosphorylation of S262 by MARKs resulted in a tau protein which did not alter assembly compared to purified tubulin alone and essentially turned off the stabilizing activity of tau (Trinczek *et al.,* 1995). S214 phosphorylation also significantly reduces the stabilizing activity of tau (Illenberger *et al.,* 1998).

When tau is expressed in dividing cells, it is heavily phosphorylated in mitosis and shows greatly reduced binding to MTs (Illenberger *et al.,* 1998). The major mitotic phosphorylation site is S214 (Illenberger *et al.,* 1998). If mitotic reentry is an early event in Alzheimer's disease (evidence discussed in Illenberger *et al.,* 1998), then the S214 phosphorylation may be an early event in disease progression. The *Drosophila* protein DMAP-85 is also inactivated by phosphorylation. This protein is phosphorylated *in vitro* by the mitotic kinase Polo, suggesting that DMAP-85 also could be released from mitotic MTs (Cambiazo *et al.,* 2000).

Phosphorylation also regulates the association of tau with the cell cortex, where dephosphorylated tau is found in association with the cortex and phosphorylated tau is not (Maas *et al.,* 2000; Arrasate *et al.,* 2000). The relevant phosphorylation sites are the S/T–P sites in the regions flanking the MT-binding domain (Maas *et al.,* 2000). These sites are also phosphorylated in Alzheimer's disease, suggesting that loss of tau from the cortex could have consequences for disease progression (Maas *et al.,* 2000).

The structure of tau is also altered by phosphorylation. In the dephosphorylated form, tau is a flexible molecule; phosphorylation by Ca^{2+} calmodulin-dependent protein kinase reduces flexibility, resulting in a longer, stiffer molecule (Hagestedt *et al.,* 1989). The functional significance of this phosphorylation-dependent change

in molecular structure is not known, nor is it known if this structure change contributes to tau aggregation into paired helical filaments.

The phosphorylation of tau at different sites is likely required for neurite outgrowth. Using tau-transfected Sf9 cells as a model for cell extensions, Biernat and Mandelkow (1999) showed that phosphorylation at the KXGS sites within the MT-binding repeats of tau are required for the extension of cellular processes. The authors suggest that a dynamic interaction between tau and MTs is necessary for process extension. The flanking regions in tau also play a role in process extension. In this case it appears that phosphorylation of S/T–P sites within these regions slows extension (Biernat and Mandelkow, 1999).

Finally, hyperphosphorylated tau is found assembled into filaments during a number of neurological diseases including Alzheimer's disease. For a review of phosphorylation and assembly of tau into these filament structures, see Buee *et al.* (2000).

2. MAP1A

Growth factor stimulation of 3T3 cells results in MAP1A phosphorylation (Erickson *et al.,* 1990). Surprisingly, no other studies have addressed MAP1A phosphorylation.

3. MAP1B

This MAP is also phosphorylated at multiple S or T residues. Two classes of phosphorylation have been recognized: mode I sites are phosphorylated by proline-directed kinases during development (and downregulated in the adult) while mode II sites are phosphorylated by casein kinase II in adult tissues expressing MAP1B (reviewed in Avila *et al.,* 1994). The major kinases responsible for mode I phosphorylation *in vivo* are likely Cdk5 and glycogen synthase kinase 3 β (GSK3β; Pigino *et al.,* 1997; Garcia-Perez *et al.,* 1998; reviewed in Gordon-Weeks and Fischer, 2000). MAP1B phosphorylated on mode I sites is found at highest concentration at growth cones and in a decreasing gradient back toward the cell body (Black *et al.,* 1994). Dephosphorylation of MAP1B is primarily accomplished by protein phosphatase 2A (Gong *et al.,* 2000).

How phosphorylation regulates MAP1B function is less clear, and it is not yet known whether the differing results reflect different sites phosphorylated by the experimental methods used. For example, phosphorylation may increase binding to MTs (Diaz-Nido *et al.,* 1988), decrease MAP1B binding to MTs (Gong *et al.,* 2000; Pedrotti *et al.,* 1996), or have no effect on binding (Goold *et al.,* 1999). One recent study has suggested that phosphorylation of MAP1B may allow MTs to remain highly dynamic while bound to the phosphorylated form of this MAP (Goold *et al.,* 1999). Overexpression of MAP1B and GSK3β in COS cells resulted in the loss of MAP1B's ability to protect MTs from nocodazole-induced depolymerization and

caused a loss of stable (detyrosinated) MTs, perhaps by preventing detyrosination (Goold *et al.,* 1999). When dephosphorylated, MAP1B also binds actin (Pedrotti and Islam, 1996), but it is not clear whether this binding is functionally significant in neuronal cells.

4. MAP2

This neuronal MAP is also phosphorylated by a variety of kinases on multiple S and T residues reaching up to 46 mol phosphate per mol MAP2 (Vallee, 1980; Tsuyama *et al.,* 1987). Kinases phosphorylating MAP2 include PKA, Ca^{2+}/calmodulin-dependent protein kinase II, PKC, ERKs, GSK3, Cdks, and MARKs (reviewed in Sanchez *et al.,* 2000). In most cases phosphorylation reduces MAP2 binding to MTs and therefore phosphorylated MAP2 is considerably less active as a MT- stabilizing protein (Hoshi *et al.,* 1992; Itoh *et al.,* 1997; Tsuyama *et al.,* 1987; Illenberger *et al.,* 1996). Loss of stabilizing activity is particularly apparent after phosphorylation within or near the MT-binding domain (Hoshi *et al.,* 1992; Illenberger *et al.,* 1996).

PKA phosphorylation also regulates the interaction of MAP2c with MTs and actin filaments. PKA phosphorylation sites reside in the KXGS motifs within the MT-binding repeats. Phosphorylation at these sites significantly reduces binding to MTs and results in MAP2c colocalization with actin filaments at the leading edge of cells (Ozer and Halpain, 2000).

MAP2 is also phosphorylated by tyrosine kinases including epidermal growth factor receptor kinase and the insulin receptor kinase (Kadowaki *et al.,* 1985; Nishida *et al.,* 1987). Tyrosine phosphorylation by epidermal growth factor receptor kinase reduced the assembly-promoting activity of MAP2 and its ability to bind actin filaments (Nishida *et al.,* 1987).

The phosphorylation of MAP2 is likely functionally important since MAP2 phosphorylation state is rapidly altered after activation of NMDA receptors (Halpain and Greengard, 1990; Quinlan and Halpain, 1996). Binding of glutamate to its receptor first results in an initial rapid increase in MAP2 phosphorylation followed by a slower dephosphorylation of MAP2, most likely mediated by the phosphatase calcineurin (Halpain and Greengard, 1990; Quinlan and Halpain, 1996).

5. MAP4

Potential phosphorylation sites for multiple kinases exist throughout the MAP4 molecule and have been demonstrated to modify MAP4 *in vitro* (Mori *et al.,* 1991; Hoshi *et al.,* 1992; Ookata *et al.,* 1995; Ebneth *et al.,* 1999). MAP4 is phosphorylated by Cdk1 *in vivo* (Ookata *et al.,* 1997) and is likely inactivated at mitosis since its rescue-promoting activity is reduced *in vitro* after phosphorylation by this kinase (Aizawa *et al.,* 1991; Ookata *et al.,* 1995). This phosphorylation does not reduce MAP4 binding to MTs, which may be important since MAP4 is at least

partially responsible for localizing Cdk1 to the MTs of the spindle (Ookata *et al.,* 1995). The critical phosphorylation site for reducing MT assembly promoting activity has been identified recently as S787 in the proline-rich region near the MT-binding domain (Kitazawa *et al.,* 2000).

Additional kinases phosphorylating MAP4 include PKC (Mori *et al.,* 1991), MAP kinase (Hoshi *et al.,* 1992), and MARKs (Illenberger *et al.,* 1996). MARKs phosphorylation of the KXGS motifs *in vitro* results in MAP4 dissociation from MTs and an increased turnover of MTs by dynamic instability (Illenberger *et al.,* 1996). Phosphorylation of MAP4 by MARKs has been demonstrated *in vivo* (Ebneth *et al.,* 1999). Here phosphorylation causes release of MAP4 from MTs and MT depolymerization (Ebneth *et al.,* 1999).

The *Xenopus* homolog of MAP4, XMAP230, is also regulated by phosphorylation during the cell cycle. This MAP is phosphorylated by Cdk1 and MAP kinase in mitotic egg extracts and *in vitro* with purified proteins (Shiina *et al.,* 1992; Andersen *et al.,* 1994). Presumably cell cycle-dependent phosphorylation turns off the stabilizing activity of XMAP230 since XMAP230 does not bind mitotic MTs in *Xenopus* egg extracts (Andersen *et al.,* 1994). Overexpression of a "phosphorylation-site deficient" mutant of XMAP230 slows chromosome movement in anaphase (Shiina and Tsukita, 1999), suggesting that release of wild-type XMAP230 from MTs is necessary for chromosome movement.

Phosphorylation may also regulate the localization of XMAP230 throughout mitosis. In a *Xenopus* cell line XMAP230 is absent from prophase spindles, becomes localized to mitotic spindles at metaphase, but does not associate with astral MTs until late anaphase/telophase (Andersen *et al.,* 1994).

6. XMAP215

This *Xenopus* MAP is also hyperphosphorylated in a cell-cycle-dependent manner, reaching highest phosphorylation level at mitosis (Gard and Kirschner, 1987). Mitotic phosphorylation does not alter the affinity of XMAP215 for MTs (Vasquez *et al.,* 1999). The purified XMAP215 protein can be phosphorylated *in vitro* with Cdk1 (Vasquez *et al.,* 1999) at up to two possible sites near the C-terminus (Becker and Gard, 2000). This Cdk1-phosphorylated XMAP215 stimulates MT elongation ~2.5-fold compared to pure tubulin (Vasquez *et al.,* 1999). Thus, phosphorylation reduces, but does not eliminate, the elongation-promoting activity of XMAP215.

The *S. pombe* protein p93[dis1] is also phosphorylated *in vivo* by Cdk1 (Nabeshima *et al.,* 1995). Phosphorylation of the other members of this MAP family has not been investigated.

7. Op18/Stathmin

Op18/stathmin is phosphorylated in response to a number of signals, including progression through the cell cycle (Larsson *et al.,* 1995; Marklund *et al.,* 1996;

Melander Gradin, 1997, 1998). In mammalian cells, overexpression of wild type or "phosphorylation site deficient" mutants of Op18/stathmin reduces interphase MT polymer (Larsson *et al.,* 1997; Marklund *et al.,* 1994a). Op18/stathmin is turned off by phosphorylation at mitosis since overexpression of "phosphorylation site deficient" Op18 causes a G2/M cell cycle block (Marklund *et al.,* 1994a). In contrast, Op18/stathmin remains active in mitotic *Xenopus* egg extracts, but it is hyperphosphorylated by an activity associated with mitotic chromatin (Andersen *et al.,* 1997), suggesting that in the larger *Xenopus* egg, Op18/stathmin activity is spatially modified during mitosis.

Mammalian Op18/stathmin contains four phosphorylation sites at serine residues (S-16, -25, -38, and -63; Beretta *et al.,* 1993; Marklund *et al.,* 1993a,b; Labdon *et al.,* 1992). The *Xenopus* homolog is lacking a S at position 63 and thus contains only three phosphorylation sites (Maucuer *et al.,* 1983). Kinases able to phosphorylate Op18/stathmin have been identified in mammalian systems: S-16 is phosphorylated by Ca^{2+} calmodulin-dependent kinase IV/Gr (Marklund *et al.,* 1994b), Ca^{2+}/calmodulin-dependent kinase II (le Gouvello *et al.,* 1998) and p65PAK (Daub *et al.,* 2000); S-16 and -63 are phosphorylated by PKA (Beretta *et al.,* 1993; Melander Gradin, 1998); S-25 and S-38 are phosphorylated by MAP kinase family members (Beretta *et al.,* 1993; Marklund *et al.,* 1993a,b) and Cdk1 and -2 (Brattsand *et al.,* 1994; Marklund *et al.,* 1996).

During progression through the cell cycle all four serine residues of Op18/stathmin must be phosphorylated to allow entry into mitosis (Larsson *et al.,* 1997). Phosphorylation occurs sequentially: S-25 and S-38 are first phosphorylated by Cdk1, allowing subsequent phosphorylation of S-16 and -63 by an unknown kinase(s) (Larsson *et al.,* 1995, 1997; Marklund *et al.,* 1996). Inactivation requires phosphorylation at S-16 and -63 (the sites dependent on prior Cdk1 phosphorylation of S-25 and -38) (Larsson *et al.,* 1997; Horowitz *et al.,* 1997; DiPaolo *et al.,* 1997). While phosphorylation of all four S residues occurs at mitosis to turn off Op18/stathmin, phosphorylations at one or two sites can also significantly reduce Op18/stathmin activity. For example, phosphorylation at S-16 and -63 by PKA turns off Op18/stathmin-mediated MT depolymerization in interphase cells (Melander Gradin *et al.,* 1998), reduces binding to tubulin (Melander Gradin *et al.,* 1998; Holmfeldt *et al.,* 2001) and inhibits both tubulin sequestering activity and specific catastrophe promotion *in vitro* (Holmfeldt *et al.,* 2001). Similarly, Ca^{2+}/calmodulin-dependent kinase IV/Gr phosphorylation of Ser-16 (Melander Gradin *et al.,* 1997) together with constitutive phosphorylation at S-38 (discussed in Melander Gradin *et al.,* 1998), turns off the MT-destabilizing activity of Op18/stathmin. Based on a number of studies, it appears that phosphorylation at S-16 and -63 cause a more potent inhibition of Op18/stathmin compared to phosphorylations at S-25 and -38 (DiPaolo *et al.,* 1997; Horowitz *et al.,* 1997; Larsson *et al.,* 1997). In addition, the multiple phosphorylations of Op18/stathmin likely serve to amplify the inhibition of this protein's activity, as demonstrated by Larsson *et al.* (1997). It is not yet known whether dual or multiple

phosphorylations of Op18/stathmin are required in order for cells to respond to extracellular signals, but the high degree and specificity of phosphorylations suggests that this is so (see Sobel, 1991, for discussion of Op18/stathmin as a signaling intermediate).

8. EMAP

Echinoderm MAP is phosphorylated during mitosis at ≥ 10 serines, presumably by Cdk1 (Brisch *et al.,* 1996). Based on sequence, EMAP has consensus phosphorylation sites for multiple kinases including PKA, PKC, casein kinase 2, and MAP kinase (Suprenant *et al.,* 2000). Progression through the cell cycle does not change the localization of EMAP to MTs (Suprenant *et al.,* 1993) and thus, the functions of possible EMAP phosphorylations are not yet known.

9. MINUS

This small polypeptide requires phosphorylation for activation as a MT nucleation inhibitor (Fanara *et al.,* 1999).

10. NuMA

The association of NuMA with MTs is regulated both by cell-cycle-dependent intracellular localization (below) and phosphorylation. Normally NuMA is present in the interphase nucleus, but when the entry of NuMA into the nucleus is blocked, it still does not bind interphase MTs (Compton *et al.,* 1992). Phosphorylation of NuMA by Cdk1 appears necessary for NuMA binding to MTs during mitosis (Sparks *et al.,* 1995; Compton and Luo, 1995). When in the nucleus, dephosphorylation of NuMA is necessary for its assembly into a "nuclear matrix-like" structure (Saredi *et al.,* 1997; Harborth *et al.,* 1999).

11. Echinoderm p62

This mitotic apparatus associated protein is phosphorylated by a calcium/calmodulin-dependent kinase, perhaps via calcium-calmodulin-dependent protein kinase II (Johnson and Sloboda, 1992). Phosporylation of p62 is necessary for MT depolymerization in the central spindle at the metaphase/anaphase transition (Dinsmore and Sloboda, 1988, 1989), which may represent activation of p62 to depolymerize MTs.

12. CENP-E

This protein is phosphorylated near its C-terminus by Cdk1 and/or MAP kinase (Liao *et al.,* 1994; Zecevic *et al.,* 1998). Phosphorylation of this domain prevents

CENP-E from cross-linking MTs (Liao *et al.,* 1994). Phosphorylation is greatly reduced at anaphase (when Cdk1 levels fall) and may allow CENP-E to cross-link MTs in the spindle midzone (Liao *et al.,* 1994).

13. CLIP170

Phosphorylation also reduces the binding of CLIP170 to MTs, with the kinase responsible for phosphorylation associated with MTs (Rickard and Kreis, 1991). The identity of this MT-associated kinase is not known. It also appears that MT assembly status can alter the phosphorylation state of CLIP170; drug-induced depolymerization of MT *in vivo* results in the rapid dephosphorylation of CLIP170 (Perez *et al.,* 1999).

14. Doublecortin

Recent studies suggest that doublecortin binding to MTs is regulated through phosphorylation, where the phosphorylated forms show reduced binding to MTs (Schaar *et al.,* 2000). It is not yet known whether phosphorylation/dephosphorylation of doublecortin functions during neuronal migration.

15. E-MAP-115/Ensconsin

Binding of this MAP to MTs is regulated during the cell cycle with E-MAP-15/ensconsin showing greatly reduced binding to spindle MTs (Masson and Kreis, 1995). Since E-MAP-115/ensconsin is also phosphorylated at this stage of the cell cycle it is likely that phosphorylation regulates its binding to spindle MTs (Masson and Kreis, 1995).

16. APC

In vitro studies have demonstrated that APC is phosphorylated by several kinases, including Cdk1 (Trzepacz *et al.,* 1997; Askham *et al.,* 2000), GSKβ3, and PKA (Rubinfeld *et al.,* 1996). Since APC appears to associate with MTs only during interphase (Nathke *et al.,* 1996; Morrison *et al.,* 1997) and APC becomes hyperphosphorylated during mitosis (Trzepacz *et al.,* 1997), modification by a cell cycle kinase is likely responsible for regulating the binding of APC to MTs.

17. Other Posttranslational Modifications

MAPs 2, 4, and tau are also modified by addition of O-linked *N*-acetylglucosamine (O-GlcNAc) to S or T residues (Ding and Vandre, 1996; Arnold *et al.,* 1996). Interestingly these S and T residues are located close to P residues, suggesting that

addition of O-GlcNAc occurs at sites also recognized by proline-directed kinases. The functional consequences of O-GlcNAc addition are not yet known.

CENP-E is modified by addition of a farnesyl group (Ashar *et al.,* 2000). Inhibition of farnesylation reduces the ability of CENP-E to bind MTs, but not kinetochores (Ashar *et al.,* 2000). It is possible that changes in farnesylation regulate CENP-E intracellular localization to either kinetochores or MTs.

C. Intracellular Localization

1. Cell-Cycle–Dependent Localizations

a. Nuclear/Cytoplasmic Localization   XMAP310 (Andersen and Karsenti, 1997), NuMA (Price and Pettijohn, 1986; Compton *et al.,* 1992; Lyderson and Pettijohn, 1980; Tousson *et al.,* 1991), TPX2 (Wittmann *et al.,* 2000), and the echinoderm protein p62 (Dinsmore and Sloboda, 1988) are present in the nucleus during interphase and are then associated with mitotic spindle MTs and spindle poles during mitosis. In each case, the MAP may be kept from binding interphase MTs by their physical localization in the nucleus. Breakdown of the nuclear envelope at the onset of mitosis gives each MAP access to the MT cytoskeleton. NuMA remains associated with spindle MTs until late in anaphase; it is then released and returns to the nucleus via nuclear import (Compton *et al.,* 1992). In contrast, p62 does not enter the nucleus through an import process; instead p62 associates with chromosomes during anaphase and is thus localized within the forming nucleus (Ye and Sloboda, 1995).

It should be noted that only the longest isoform of NuMA is localized to the nucleus during interphase (Tang *et al.,* 1994). The two lower-molecular-weight isoforms, NuMA-m and NuMA-s, differ in their C-terminal regions and are localized to the centrosome during interphase and at spindle poles during mitosis (Tang *et al.,* 1994). The *Xenopus* homolog of NuMA also does not enter the nucleus in *Xenopus* eggs, suggesting that additional regulatory mechanisms must exist to keep it from interacting with dynein/dynactin and MTs to form focused MT asters prior to mitosis (Merdes *et al.,* 2000).

APC has also been shown to shuttle between nucleus and cytoplasm and is proposed to function in each compartment. This protein contains two nuclear export signals in the N terminus (Neufeld *et al.,* 2000) and two nuclear localization signals within the C-terminus (Neufeld and White, 1997; Zhang *et al.,* 2000). Mutation of a PKA site near a nuclear localization signal reduces nuclear localization of APC (Zhang *et al.,* 2000), suggesting that nuclear import may also be regulated by phosphorylation.

b. Cell-Cycle-Dependent Microtubule Binding   Most members of the XMAP215 family show cell cycle-dependent MT localizations. For example, TOGp localizes

to the cytoplasm (our unpublished observations) or endoplasmic reticulum during interphase (Charrasse *et al.,* 1998) and then localizes to spindle poles and MTs during mitosis (Charrasse *et al.,* 1998). Similarly, ZYG9 is cytosolic during interphase and is then localized to spindle poles throughout mitosis and to spindle MTs until early anaphase (Matthews *et al.,* 1998). Stu2p and p93[dis1] are bound primarily to spindle pole bodies (Nabeshima *et al.,* 1995; Wang and Huffaker, 1997), but p93[dis1] also shows cell-cycle dependent localization to MTs, binding to cytoplasmic MTs and anaphase spindles, but not to metaphase spindles (Nabeshima *et al.,* 1995). Mechanisms restricting the binding of these proteins to spindle poles and spindle MTs are not yet understood. It should be noted that not all family members share this cell-cycle-regulated binding to MTs; XMAP215 is bound to both interphase and mitotic MTs (Tournebize *et al.,* 2000) and DdCP224 is associated with centrosomes throughout the cell cycle (Graf *et al.,* 2000).

CENP-E also shows a striking cell cycle-dependent binding to MTs. This protein first binds to the kinetochore regions of chromosomes during the early stages of mitosis and then moves to the overlapping MTs of the spindle mid-zone during anaphase (Yen *et al.,* 1992). In G2 cells, CENP-E does not appear to bind interphase MTs (Yen *et al.,* 1992), suggesting that this protein can bind to MTs only during a short window of time during mitosis.

2. Axon/Dendrite/Cell Body Localizations

a. MAP2   The subcellular targeting of MAP2 to dendrites results from several regulatory mechanisms. First, MAP2 mRNA is transported into the dendrite by a mechanism dependent upon a 640 bp sequence in the 3′UTR (Garner *et al.,* 1988; Blichenberg *et al.,* 1999), thus targeting MAP2 synthesis within the dendrite. This targeting sequence is absent from embryonic MAP2 (Papandrikopoulou *et al.,* 1989). Second, MAP2 is also synthesized in the cell body where subsequent transport into axons is suppressed (Kanai and Hirokawa, 1995). Finally, any MAP2 that finds itself in the axon is degraded (Okabe and Hirokawa, 1989). Thus, subcellular localization of MAP2 is accomplished through localized synthesis, protein transport, and regional degradation. It is not yet clear which of these mechanisms predominates *in vivo.*

Tau also shows a distinct subcellular localization in neurons and is found specifically in axons. Here targeting mechanisms have not been as well studied, but evidence has been presented for both mRNA targeting to the axon (Litman *et al.,* 1993) via a 91 bp 3′UTR (Behar *et al.,* 1995) and selective degradation of tau in dendrites (Hirokawa *et al.,* 1996).

Phosphoryation may also contribute to the subcellular localizations of MAP1b and tau. The phophorylated forms of each of these MAPs is enriched at the distal tips of dendrites and axons, respectively (Black *et al.,* 1994; Mandell and Banker, 1996; Mansfield *et al.,* 1991).

3. Growing Microtubule Ends

Within the past few years several proteins have been identified which localize specifically to MT ends. In all cases, the precise mechanism responsible for targeting these proteins to MT ends is not known. CLIP170 was the first protein shown to be localized to MT plus ends *in vivo* (Rickard and Kreis, 1990) and recent studies expressing GFP-CLIP170 fusion proteins have dramatically documented this end-specific binding (Perez *et al.,* 1999). Examination of GFP-CLIP170 at MT ends suggested that CLIP170 binds to dimers at the growing MT tip and remains associated for a short amount of time before dissociating from the MT. In this way, CLIP170 treadmills at the growing ends of MTs. CLIP170 may initially bind to MT ends together with tubulin oligomers (Diamanotopoulos *et al.,* 1999). Since CLIP170 does not show preferential binding to GTP or GDP dimers in the MT lattice, additional factors such as dimer structure within the MT lattice or phosphorylation of CLIP170 may determine when CLIP170 falls off the MT end (Diamanotopoulos *et al.,* 1999).

APC is also localized to MT plus ends and may accumulate at these ends through movement along the MT lattice in the plus end direction (Mimori-Kiyosue *et al.,* 2000a). How this movement is powered is not known. Preferential binding to MT plus ends may also localize APC to these ends directly without movement along the MT (Mimori-Kiyosue *et al.,* 2000a).

EB1 was also shown to localize at growing plus ends (Morrison *et al.,* 1998; Mimori-Kiyosue *et al.,* 2000b). Since EB1 and CLIP-170 have both been shown to bind tubulin dimers *in vitro* (Juwana *et al.,* 1999; Diamantopoulos *et al.,* 1999), EB1 may localize to plus ends similar to the copolymerization mechanism proposed for CLIP-170.

Binding to MT growing ends by the above proteins may also depend on their interactions with each other and with dynein/dynactin. For example, EB1 (Berrueta *et al.,* 1999) and CLIP-170 (Vaughan *et al.,* 1999) bind the dynein/dynactin motor complex and dynein/dynactin can also localize to MT plus ends (Vaughan *et al.,* 1999). It is not yet known how dynein/dynactin is targeted to MT plus ends, or whether this motor complex contributes to EB1 or CLIP-170 localization. APC localization to MT plus ends appears dependent on EB1 (Askham *et al.,* 2000), although it should be noted that the APC/EB1 interaction in cells is controversial (Berrueta *et al.,* 1999).

4. Stress-Induced Binding to Microtubules

a. STOPs   Cooling cells results in a striking redistribution of STOPs. These proteins are soluble in interphase but bind MTs after cells are chilled. STOPs binding to MTs stabilizes them against depolymerization by cold temperature (Denarier *et al.,* 1998). The physiological significance of STOP binding to MTs after cell chilling is not known, nor is it known how cold temperatures regulate the localization of STOPs. Denarier *et al.* (1998) hypothesized that STOPs are soluble

when phosphorylated and that cell chilling reduces kinase activity resulting in STOP dephosphorylation and association with MTs. Further experimentation is necessary to test this hypothesis.

D. Cofactors/Binding Partners Necessary for Activation or Deactivation

1. MAP1B/LC1

The heavy chain of MAP1B and its light chain LC1 each have MT-binding domains (Mann and Hammarback, 1994; Togel *et al.,* 1998; Zauner *et al.,* 1992). Most studies of MT assembly have used the complex of MAP1B/LC1 and showed that this complex acts as a relatively modest MT stabilizer *in vitro* (Vandecandelaere *et al.,* 1996) and *in vivo* (Nobel *et al.,* 1989; Takemura *et al.,* 1992). However, studies using LC1 in the absence of the heavy chain have shown that LC1 is a more effective MT stabilizer (Togel *et al.,* 1998). These results suggest that MAP1B heavy chain may downregulate the stabilizing activity of LC1 (Togel *et al.,* 1998). Since the light chain has a slower degradation rate than the heavy chain (discussed above, Mei *et al.,* 2000), it is possible that the excess LC1 functions *in vivo* to stabilize MTs.

2. Katanin

This MT-severing protein contains two subunits: p60, the ATPase responsible for severing, and p80, the noncatalytic, regulatory subunit (McNally and Vale, 1993). Transfection studies have demonstrated that p80 both enhances and inhibits the severing activity of the p60 katanin subunit (McNally *et al.,* 2000). Stimulation of severing occurs through the C-terminal region of the 80-kDa subunit; this domain also increases the binding of p60 to MTs (McNally *et al.,* 2000). In contrast, the N-terminal, WD40 domain of p80 inhibits severing by p60 (McNally *et al.,* 2000). This WD40 domain is responsible for intracellular targeting of katanin to spindle poles in mitosis (McNally *et al.,* 2000).

3. Orbit

Orbit is a recently identified *Drosophila* MAP required for mitosis (Inoue *et al.,* 2000). The orbit protein sequence contains two motifs involved in binding guanine nucleotides, including one motif similar to a guanine nucleotide binding motif found in tubulin and FtsZ (Inoue *et al.,* 2000). Guanine nucleotide binding by orbit may regulate its affinity for microtubules since *in vitro* assays demonstrated that orbit only binds MTs in the presence of GTP, but not in solutions containing GDP or GTP-γ-S. At this time it is not known whether orbit can hydrolyze GTP nor whether hydrolysis plays a role in regulating orbit binding to MTs (Inoue *et al.,* 2000).

4. STOPs

The STOP proteins can be regulated by Ca^{2+}/calmodulin where Ca^{2+}/calmodulin inhibits STOP stabilization of MTs (Job *et al.,* 1987). Since STOPs bind calmodulin (Job *et al.,* 1987), it is believed that regulation is through this direct binding interaction.

5. NuMA and TPX2

Studies over the past several years have shed light on the signaling cascade responsible for mitotic MT assembly in the vicinity of chromosomes. These studies have highlighted the role of the small GTPase Ran in its GTP bound form (Ran-GTP) in stimulating MT assembly (Carazo-Salas *et al.,* 1999; Obha *et al.,* 1999; Zhang *et al.,* 1999; Wilde and Zheng, 1999; Kalab *et al.,* 1999). Three recent papers have demonstrated that Ran-GTP acts upstream to stimulate MT assembly via the importins α and β (Gruss *et al.,* 2001; Nachury *et al.,* 2001; Wiese *et al.,* 2001). It appears that NuMA and TPX2 are bound to importin α or β (Gruss *et al.,* 2001; Nachury *et al.,* 2001; Wiese *et al.,* 2001) and since each of these MAPs is localized to the nucleus during interphase (Price and Pettijohn, 1986; Compton *et al.,* 1992; Wittmann *et al.,* 2000), binding to importin α or β may participate in their nuclear import. This binding interaction is regulated by Ran-GTP since Ran-GTP causes release of the importin α/β complex from NuMA and TPX2 by competing with the MAPs for binding to importins. Both MAPs are likely inactive when bound to the importin complex and are then activated by importin release (Gruss *et al.,* 2001; Nachury *et al.,* 2001; Wiese *et al.,* 2001). Once the nuclear envelope breaks down, release of these MAPs from the importins allows them to interact with MTs and stimulate assembly. This mechanism is localized by a proposed gradient of Ran-GTP which results from the localization of RCC1, the guanine nucleotide exchange protein which generates Ran-GTP from Ran-GDP, to chromatin (Figure 4; Carazo-Salas *et al.,* 1999; Zhang *et al.,* 1999; Wilde and Zheng, 1999; Ohba *et al.,* 1999; Kalab *et al.,* 1999; Gruss *et al.,* 2001; Nachury *et al.,* 2001; Wiese *et al.,* 2001).

Several other proteins, including XMAP215, dynein and γ tubulin, also participate in Ran-GTP stimulation of MT assembly and aster formation (Obha *et al.,* 1999; Wilde and Zheng, 1999), but how these proteins are regulated by Ran-GTP is not yet clear. In addition, Op18/stathmin is locally phosphorylated by a kinase associated with chromatin (Andersen *et al.,* 1997), but it is not whether this kinase activity is regulated by the Ran-GTP pathway.

E. Competition for Binding Sites or Competing Activities

The neuronal MAPs can compete for binding sites on the MT lattice. For example, Tokuraku *et al.* (1999b) showed that tau and MAP4 compete for MT binding. MAP2 also competes with MAP4 but to a lesser extent, suggesting the presence
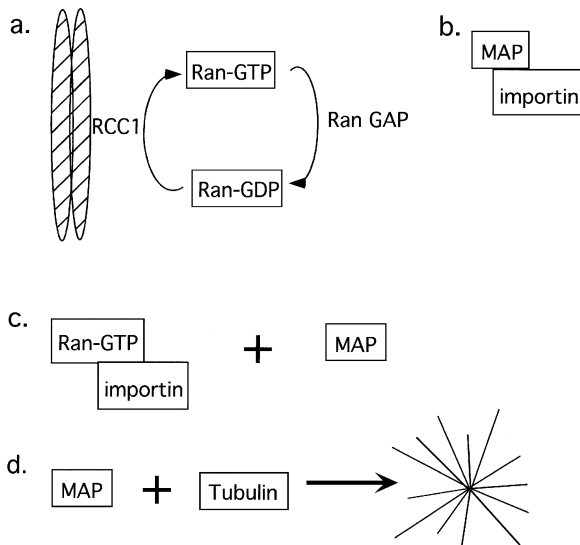
FIG. 4 Regulation of microtubule assembly by Ran-GTP. (a) Chromatin-associated RCC1 generates a local high concentration of Ran-GTP by promoting nucleotide exchange. The concentration of Ran-GTP is thought to be elevated near chromatin since Ran GAP (which stimulates hydrolysis of GTP to GDP) is a soluble protein and not localized as is RCCI. (b) The MAP is held in an inactive state by binding to importin (α or β). (c) In regions with high Ran-GTP concentration, Ran-GTP is able to compete with MAPs for binding to the importins. This releases the MAP for interaction with microtubules. (d) MAPs are then able to stimulate tubulin assembly and/or organize microtubule polymer into aster-like arrays. This scenario is based a number of recent studies summarized in the text.

of an additional MAP2 binding site on tubulin (Tokuraku *et al.,* 1999b). MAP2 and tau likely compete for binding site on MTs since these proteins share a common binding site on tubulin (Littauer *et al.,* 1986) and this competition has been demonstrated *in vitro* (Coffey and Purich, 1995). MAP1B bound to MTs can be displaced by MAP2, suggesting that these two MAPs also compete for a binding site (Pedrotti *et al.,* 1996) but conflicting results were reported recently by Tokuraku *et al.* (1999b) showing that MAP1 does not compete with MAPs 2, 4, or tau for MT binding. Finally, MAPs also compete with MT-based motors for access to the MT (Lopez and Sheetz, 1993; Koonce and Tikhonenko, 2000).

Phospholipids may compete with MTs for binding MAPs 1B and 2. Each of these MAPs binds to phospholipids: MAP1B to phosphatidylserine and MAP2 to phosphatidylinositol (Yamauchi *et al.,* 1997; Surridge and Burns, 1994). Binding of these phospholipids could determine the intracellular localization of MAP1B or MAP2 to MTs or membranes (Yamauchi *et al.,* 1997).

In frog egg extracts XMAP215 and XKCM1 compete to determine the fate of MT plus ends (Tournebize *et al.,* 2000). While XMAP215 promotes growth

and stabilizes ends (Gard and Kirschner, 1987; Vasquez *et al.,* 1994; Tournebize *et al.,* 2000), XKCM1 destabilizes ends by stimulating catastrophes (Walczak *et al.,* 1996; Tournebize *et al.,* 2000). It is easy to see how changing the activity of one of these proteins can tip the balance toward longer or shorter microtubules. Competition between MAPs and mechanisms to regulate those competitions are likely a key next step in understanding MT assembly in cells.

F. Synergy/Additive Functions

Using a cell model system for axonal growth, DiTella *et al.* (1996) showed a synergy between MAP1B and tau proteins. Suppression of MAP1B and tau expression with antisense oligonucleotides blocks axon formation, while suppression of either MAP separately results in much reduced inhibition of axon growth (DiTella *et al.,* 1996). This synergy between MAP1B and tau was shown recently in double knockout experiments in mice (Takei *et al.,* 2000). Mice null for both these MAPs die within the 4 weeks after birth. Complete deletion of the MAP1B gene results in specific defects in formation of axon tracts. This phenotype is much more severe in the double knockout (Takei *et al.,* 2000). When hippocampal neurons from these double knockout mice are cultured, the cells show defects in axon elongation, consistent with the cell model studies and showing a synergistic function of MAP1B and tau function (Takei *et al.,* 2000).

G. Dimerization/Multimerization

In order to sever MTs katanin molecules oligomerize on the MT lattice (Hartman and Vale, 1999). The p60 subunit of katanin binds the MT lattice and oligomerizes in a process dependent upon ATP hydrolysis by p60. Oligomerization is much more efficient in the presence of MTs, suggesting that the MT lattice serves as a scaffold for assembly of the p60 oligomers. ATP hydrolysis increases the affinity of p60 for MTs, which may temporarily stabilize the oligomer. Hartman and Vale (1999) propose that the release of phosphate occurs after hydrolysis and that phosphate release generates a p60 conformation favoring the monomer form, resulting in release of katanin from the MT.

H. Nonenzyme Regulatory Proteins

One protein has been identified which appears to function specifically in modulating MAP function and based on this activity has been named mapmodulin (Ulitzer *et al.,* 1997). Mapmodulin binds MAPs 2, 4, and tau and preferentially binds to soluble MAPs compared to those bound to MT, (Ulitzer *et al.,* 1997). Interestingly,

mapmodulin appears to bind MAPs at their MT-binding domains (Ulizter *et al.,* 1997) suggesting that mapmodulin could compete with the MT lattice for MAP binding and perhaps sequester MAPs from the MT cytoskeleton. It is hypothesized that mapmodulin binding to MAPs helps to clear a path along the MT lattice for cytoplasmic dynein-driven transport of membrane vesicles since the presence of mapmodulin can stimulate dynein-dependent transport to the Golgi in a lysed cell model (Ulizter *et al.,* 1997; Itin *et al.,* 1999). Whether mapmodulin additionally functions to regulate MT assembly through MAP sequestration has not been examined.

IV. Concluding Remarks

A number of mechanisms regulate the levels or activities of MAPs. These regulatory mechanisms act to control transcription, translation, posttranslational modification, and degradation of MAPs. Additional regulatory mechanisms result from synergy or competition between MAPs or by cofactors which modify MAP activities. Finally, MAP functions are also regulated through controlling intracellular localization which limits MAP activity to particular places or times. It is likely that combinations of multiple regulatory mechanisms are responsible for defining the function of each MAP *in vivo.*

Acknowledgments

References

Abrieu, A., Kahana, J. A., Wood, K. W., and Cleveland, D. W. (2000). CENP-E as an essential component of the mitotic checkpoint in vitro. *Cell* **102,** 817–826.

Adams, N. R., and Cooper, J. A. (2000). Microtubule interactions with the cell cortex causing nuclear movements in Saccharomyces cerevisiae. *J. Cell Biol.* **149,** 863–874.

Ahn, J., Murphy, M., Kratowicz, S., Wang, A., Levine, A. J., and George, D. L. (1999). Down-regulation of the stathmin/Op18 and FKBP25 genes following p53 induction. *Oncogene* **18,** 5954–8.

Aizawa, H., Emori, Y., Mirofushi, H., Kawasaki, H., Sakai, H., and Suzuki, K. (1990). Molecular cloning of a ubiquitously distributed microtubule-associated protein with Mr 190,000. *J. Biol. Chem.* **265,** 13,849–13,855.

Aizawa, H., Emori, Y., Mori, A., Mirofushi, H., Sakai, H., and Suzuki, K. (1991). Functional analysis of the domain structure of microtubule-associated protein 4 (MAPU). *J. Biol. Chem.* **266,** 9841–9846.

Allen, C., and Borisy, G. (1974). Structural polarity and directional growth of microtubules of Chlamydomonas flagella. *J. Mol. Biol.* **90,** 381–402.

Amos, L. A. (2000). Focusing-in on microtubules. *Curr. Opin. Struct. Biol.* **10,** 236–241.

Andersen, S. S. L. (2000). Spindle assembly and the art of regulating microtubule dynamics by MAPs and stathmin/Op18. *Trends Cell Biol.* **10,** 261–267.

Andersen, S. S. L., Ashford, A. J., Tournebize, R., Gavet., O., Sobel, A., Hyman, A. A., and Karsenti, E. (1997). Mitotic chromatin regulates phosphorylation of stathmin/Op18. *Nature* **389,** 640–643.

Andersen, S. S. L., Buendia, B., Dominguez, J. E., Sawyer, A., and Karsenti, E. (1994). Effect on microtubule dynamics of XMAP230, a microtubule-associated protein present in *Xenopus laevis* eggs and dividing cells. *J. Cell Biol.* **127,** 1289–1299.

Andersen, S. S. L., and Karsenti, E. (1997). XMAP310: A Xenopus rescue-promoting factor localized to the mitotic spindle. *J. Cell Biol.* **139,** 975–983.

Andorfer, C. A., and Davies, P. (2000). PKA phsophorylations on tau: Developmental studies in the mouse. *Dev. Neurosci.* **22,** 303–309.

Andreadis, A., Brown, W. M., and Kosic, K. S. (1992). Structure and novel exons of the human tau gene. *Biochemistry* **31,** 10,626–10,633.

Andreassen, P. R., Lacroix, F. B., Villa-Moruzzi, E., and Margolis, R. L. (1998). Differential subcellular localization of protein phosphatase-1α, γ1, and δ isoforms during both interphase and mitosis in mammalian cells. *J. Cell Biol.* **141,** 1207–1215.

Arnal, I., Karsenti, E., and Hyman, A. A. (2000). Structural transitions at microtubule ends correlate with their dynamic properties in Xenopus egg extracts. *J. Cell Biol.* **149,** 767–774.

Arnold, C. S., Johnson, G. V., Cole, R. N., Dong, D. L. Y., Lee, M., and Hart, G. W. (1996). The microtubule-associated protein tau is extensively modified with O-linked N-acetylglucosamine. *J. Biol. Chem.* **271,** 28741–4.

Arrasate, M., Perez, M., and Avila, J. (2000). Tau dephosphorylation at tau-1 site correlates with its association to cell membrane. *Neurochem. Res.* **25,** 43–50.

Ashar, H. R., James, L., Gray, K., Carr, D., Black, S., Armstrong, L., Bishop, W. R., and Kirschmeier., P. (2000). Farnesyl transferase inhibitors block the farnesylation of CENP-E and CENP-F and alter the association of CENP-E with the microtubules. *J Biol Chem.* **275,** 30451–7.

Askham, J. M., Moncur, P., Markham, A. F., and Morrison, E. E. (2000). Regulation and function of the interaction between the APC tumour suppressor protein and EB1. *Oncogene.* **19,** 1950–8.

Avila, J., Dominguez, J., and Diaz-Nido, J. (1994). Regulation of microtubule-associated protein expression and phosphorylation during neuronal development. *Int. J. Dev. Biol.* **38,** 13–25.

Baas, P. W., Pienkowski, T. P., and Kosik, K. S. (1991). Processes induced by tau expression in Sf9 cells have an axon-like microtubule organization. *J. Cell Biol.* **115,** 1333–1344.

Barlow, S., Gonzalez-Garay, M. L., West, R. R., Olmsted, J. B., and Cabral, F. (1994). Stable expression of heterologous microtubule-associated proteins (MAPs) in chinese hamster ovary cells: Evidence for differing roles of MAPs in microtubule organization. *J. Cell Biol.* **126,** 1017–1029.

Baudier, J., and Cole, R. D. (1987). Phosphorylation of tau proteins to a state like that in Alzheimer's brain is catalyzed by a calcium/calmodulin-dependent kinase and modulated by phospholipids. *J. Biol. Chem.* **262,** 17577–17583.

Beaman-Hall, C. M., and Vallano, M. L. (1993). Distinct mode of microtubule-associated protein 2 expression in the neuroblastoma/glioma cell line 108CC15/NG108-15. *J. Neurobiol.* **24,** 1500–1516.

Becker, B. E., and Gard, D. L. (2000). Multiple isoforms of the high molecular weight microtubule associated protein XMAP215 are expressed during development in Xenopus. *Cell Motil. Cytoskel.* **47,** 282–95.

Behar, L., Marx, R., Sadot, E., Barg, J., and Ginzberg, I. (1995). cis-Acting signals and trans-acting proteins are involved in tau mRNA targeting into neurites of differentiating neuronal cells. *Int. J. Dev. Neurosci.* **13,** 113–27.

Beinhauer, J. D., Hagan, I. M., Hegemann, J. H., and Fleig, U. (1997). Ma13, the fission yeast homolog of the human APC-interacting protein EB-1 is required for microtubule integrity and the maintenance of cell form. *J. Cell Biol.* **139,** 717–728.

Belmont, L., and Mitchison, T. (1996). Identification of a protein that interacts with tubulin dimers and increases the catastrophe rates of microtubules. *Cell.* **84,** 623–631.

Beretta, L., Dobransky, T., and Sobel, A. (1993). Multiple phosphorylation of stathmin. Identification of four sites phosphorylated in intact cells and in vitro by cyclic AMP-dependent protein kinase and p34cdc2. *J. Biol. Chem.* **268,** 20,076–20,084.

Bernhardt, R., and Matus, A. (1984). Light and electron microscopic studies of the distribution of microtubule-associated protein 2 in rat brain: A difference between dendritic and axonal cytoskeletons. *J. Comp. Neurol.* **226,** 203–221.

Berrueta, L., Kraeft, S. K., Tirnauer, J. S., Schuyler, S. C., Chen, L. B., Hill, D. E., Pellman, D., and Bierer, B. E. (1998). The adenomatous polyposis coli-binding protein EB1 is associated with cytoplasmic and spindle microtubules. *Proc. Natl. Acad. Sci. USA.* **95,** 10596–601.

Berrueta, L., Tirnauer, J. S., Schuyler, S. C., Pellman, D., and Bierer, B. E. (1999). The APC-associated protein EB1 associates with components of the dynactin complex and cytoplasmic dynein intermediate chain. *Curr. Biol.* **9,** 425–428.

Biernat, J., Gustke, N., Drewes, G., Mandelkow, E.-M., and Mandelkow, E. (1993). Phosphorylation of serine 262 strongly reduces the binding of tau protein to microtubules: Distinction between PHF-like immunoreactivity and microtubule binding. *Neuron* **11,** 153–163.

Biernat, J., and Mandelkow, E.-M. (1999). The development of cell processes induced by tau protein requires phosphorylation of serine 262 and 356 in the repeat domain and is inhibited by phosphorylation of the proline-rich domain. *Mol. Biol. Cell.* **10,** 727–740.

Billger, M., Wallin, M., and Karlsson, J. O. (1988). Proteolysis of tubulin and microtubule-associated proteins 1 and 2 by calpain I and II. Difference in sensitivity of assembled and disassembled microtubules. *Cell Calc.* **9,** 33–44.

Binder, L. I., Frankfurter, A., and Rebhun, L. I. (1985). The distribution of tau in the mammalian central nervous system. *J. Cell Biol.* **101,** 1371–1378.

Black, M. M., Slaughter, T., and Fischer, I. (1994). Microtubule-associated protein 1b (MAP1b) is concentrated in the distal region of growing axons. *J. Neurosci.* **14,** 857–70.

Black, M. M., Slaughter, T., Moshiach, S., Obrocka, M., and Fischer, I. (1996). Tau is enriched on dynamic microtubules in the distal region of growing axons. *J Neurosci.* **16,** 3601–3619.

Blichenberg, A., Schwanke, B., Rehbein, M., Garner, C. C., Richter, D., and Kindler, S. (1999). Identification of a cis-acting dendritic targeting element in MAP2 RNAs. *J. Neurosci.* **19,** 8818–8829.

Bloom, K. (2000). It's a kar9ochore to capture microtubules. *Nature Cell Biol.* **2,** E96–98.

Bloom, G. S., Luca, F. C., and Vallee, R. B. (1985). Identification of high molecular-weight microtubule-associated proteins in anterior pituitary tissue and cells using taxol-dependent purification combined with microtubule-associated protein specific antibodies. *Biochemistry* **24,** 4185–4191.

Bloom, G. S., Schoenfeld, T. A., and Vallee, R. B. (1984). Widespread distribution of the major polypeptide component of MAP1 (microtubule associated protein 1) in the nervous system. *J. Cell Biol.* **98,** 320–330.

Bosc, C., Cronk, J. D., Pirollet, F., Watterson, D. M., Haiech, J., Job, J., and Margolis, R. L. (1996). Cloning, expression, and the properties of the microtubule-stabilizing protein STOP. *Proc. Natl. Acad. Sci. USA* **93,** 2125–2130.

Boyne, L. J., Martin, K., Hockfield, S., and Fischer, I. (1995). Expression and distribution of phosphorylated MAP1B in growing axons of cultured hippocampal neurons. *J Neurosci. Res.* **40,** 439–450.

Brandt, R., Leger, J., and Lee, G. (1995). Interaction of tau with the neural plasma membrane mediated by tau's amino-terminal projection domain. *J. Cell Biol.* **131,** 1327–1340.

Brattsand, G., Marklund, U., Nylander, K., Roos, G., and Gullberg, M. (1994). Cell-cycle-regulated phosphorylation of oncoprotein 18 on Ser16, Ser25, and Ser38. *Eur. J. Biochem.* **220,** 359–68.

Bre, M. H., and Karsenti, E. (1990). Effects of brain microtubule-associated proteins on microtubule dynamics and the nucleating activity of centrosomes. *Cell Motil. Cytoskel.* **15,** 88–98.

Brenman, J. E., Topinka, J. R., Cooper, E. C., McGee, A. W., Rosen, J., Milroy, T, Ralston, H. J., and

Bredt, D. S. (1998). Localization of postsyanptic density-93 to dendritic microtubules and interaction with microtubule-associated proteins 1A. *J. Neurosci.* **18,** 8805–8813.

Brion, J. P., Guilleminot, J., Couchie, D., Flament-Durand, J., and Nunez, J. (1988). Both adult and juvenile tau microtubule-associated proteins are axon specific in the developing and adult rat cerebellum. *Neuroscience* **25,** 139–146.

Brisch, E., Daggett, M. A., and Suprenant, K. A. (1996). Cell cycle–dependent phosphorylation of the 77 kDa echinoderm microtubule-associated protein (EMAP) *in vivo* and association with the p34cdc2 kinase. *J. Cell Sci.* **109,** 2885–2893.

Brown, K. D., Coulson, R. M. R., Yen, T. J., and Cleveland, D. W. (1994). Cyclin-like accumulation and loss of the putative kinetochore motor CENP-E results from coupling continuous synthesis with specific degradation at the end of mitosis. *J. Cell Biol.* **125,** 1303–1312.

Buee, L., Bussiere, T., Buee-Scherrer, V., Delacourte, A., and Hof, P. R. (2000). Tau protein isoforms, phosphorylation and role in neurodegenerative disorders. *Brain Res. Rev.* **33,** 95–130.

Bulinski, J. C. (1994). MAP4. *In* "Microtubules" (J. S. Hymans and C. W. Lloyd, Eds.), pp. 167–182. Wiley-Liss, New York.

Bulinski, J. C., and Borisy, G. G. (1980a). Microtubule-associated proteins from cultured Hela cells. Analysis of molecular properties and effects on microtubule polymerization. *J. Biol. Chem.* **255,** 11,570–11,576.

Bulinski, J. C., and Borisy, G. G. (1980b). Widespread distribution of a 210,000 mol wt microtubule-associated protein in cells and tissues of primates. *J. Cell Biol.* **87,** 802–808.

Bulinski, J. C., McGraw, T. E., Gruber, D., Nguyen, H. L., and Sheetz, M. P. (1997). Overexpression of MAP4 inhibits organelle motility and trafficking in vivo. *J. Cell Sci.* **110,** 3055–3064.

Burgen, K. E., Waxham, M. N., Rickling, S., Westgate, S. A., Mobley, W. C., and Kelly, P. T. (1990). In situ hybridization histochemistry of Ca2+/calmodulin-dependent protein kinase in developing rat brain. *J. Neurosci.* **10,** 1788–1798.

Burns, R. G., Islam, K., and Chapman, R. (1984). The multiple phosporylation of the microtubule associated-protein MAP2 controls the MAP2:tubulin interaction. *Eur. J. Biochem.* **141,** 609–615.

Bush, M. S., Goold, R. G., Moya, F., and Gordon-Weeks, P. R. (1996). An analysis of an axonal gradient of phosphorylated MAP1B in cultured rat sensory neurons. *Eur. J. Neurosci.* **8,** 235–248.

Butner, K. A., and Kirschner, M. W. (1991). Tau protein binds to microtubules through a flexible array of distributed weak sites. *J. Cell Biol.* **115,** 717–730.

Caceres, A., and Kosik, K. S. (1990). Inhibition of neurite polarity by tau antisense oligonucleotides in primary cerebellar neurons. *Nature.* **343,** 461–463.

Caceres, A., Mautino, J., and Kosik, K. S. (1992). Suppression of MAP-2 in cultured cerebellar macroneurons inhibits minor neurite formation. *Neuron* **9,** 607–618.

Cambiazo, V., Gonzalez, M., and Maccioni, R. B. (1995). DMAP-85: A tau-like protein from Drosophila melanogaster larvae. *J. Neurochem.* **64,** 1288–1297.

Cambiazo, V., Logarinho, E., Pottstock, H., and Sunkel, C. E. (2000). Microtubule binding of the drosophila DMAP-85 protein is regulated by phosphorylation in vitro. *FEBS Lett.* **483,** 37–42.

Caplow, M., and Shanks, J. (1996). Evidence that a single monolayer tubulin-GTP cap is both necessary and sufficient to stabilize microtubules. *Mol. Biol. Cell.* **7,** 663–675.

Carazo-Salas, R. E., Guarguaglini, G., Gruss, O. J., Segref, A., Karsenti, E., and Mattaj, I. W. (1999). Generation of GTP-bound Ran by RCC1 is required for chromatin-induced mitotic spindle formation. *Nature* **400,** 178–181.

Carlier, M. F., Didry, D., and Pantaloni, D. (1987). Microtubule elongation and guanosine-5′-triphosphate hydrolysis. Role of guanine nucleotides in microtubule dynamics. *Biochemistry* **26,** 4428–4437.

Cassimeris, L., Pryer, N. K., and Salmon, E. D. (1988). Real-time observations of microtubule dynamic instability in living cells. *J. Cell Biol.* **107,** 2223–2231.

Cha, B., Cassimeris, L., and Gard, D. L. (1999). XMAP230 is required for normal spindle assembly in vivo and in vitro. *J. Cell Sci.* **112,** 4337–4346.

Chapin, S. J., and Bulinski, J. C. (1992). Microtubule stabilization by assembly-promoting microtubule-associate proteins: A repeat performance. *Cell Motil. Cytoskel.* **23,** 236–243.

Chapin, S. J., Lue, C. M., Yu, M. T., and Bulinski, J. C. (1995). Differential expression of alternatively spliced forms of MAP4: A repertoire of structurally different microtubule-binding domains. *Biochemistry* **34,** 2289–2301.

Charrasse, S., Lorca, T., Doree, M., and Larroque, C. (2000). The Xenopus XMAP215 and its human homologue TOG proteins interact with cyclin B1 to target p34cdc2 to microtubules during mitosis. *Exp. Cell Res.* **254,** 249–256.

Charrasse, S., Mazel, M., Taviaux, S., Berta, P., Chow, T., and Larroque, C. (1995). Characterization of the cDNA and pattern of expression of a new gene over-expressed in human hepatomas and colonic tumors. *Eur. J. Biochem.* **234,** 406–413.

Charrasse, S., Schroeder, M., Gauthier-Rouviere, C., Ango, F., Cassimeris, L., Gard, D. L., and Larroque, C. (1998). The TOGp protein is a new human microtubule-associated protein homologous to the *Xenopus* XMAP215. *J. Cell Sci.* **111,** 1371–1383.

Chen, J., Kanai, Y., Cowan, N. J., and Hirokawa, N. (1992). Projection domains of MAP2 and tau determine spacings between microtubules in dendrites and axons. *Nature* **360,** 674–677.

Chretien, D., Fuller, S. D., and Karsenti, E. (1995). Structure of growing microtubule ends: Two-dimensional sheets close into tubes at variable rates. *J. Cell Biol.* **129,** 1311–1328.

Chung, W. J., Kindler, S., Seidenbecher, C., and Garner, C. C. (1996). MAP2a, an alternatively spliced variant of microtubule-associated protein 2. *J. Neurochem.* **66,** 1273–1281.

Cleveland, D. W., Hwo, S. Y., and Kirschner, M. W. (1977). Physical and chemical properties of purified tau factor and the role of tau in microtubule assembly. *J. Mol. Biol.* **116,** 227–247.

Code, R. J., and Olmsted, J. B. (1992). Mouse microtubule-associated protein 4 (MAP4) transcript diversity generated by alternative polyadenylation. *Gene* **122,** 367–370.

Coffey, R. L., and Purich, D. L. (1995). Non-cooperative binding of the MAP-2 microtubule-binding region to microtubules. *J. Biol. Chem.* **270,** 1035–1040.

Compton, D. A., and Cleveland, D. W. (1993). NuMA is required for the proper completion of mitosis. *J. Cell Biol.* **120,** 947–957.

Compton, D. A., and Luo, C. (1995). Mutation of the predicted p34cdc2 phosphorylation sites in NuMA impair the assembly of the mitotic spindle and block mitosis. *J. Cell Sci.* **108,** 621–633.

Compton, D. A., Szilak, I., and Cleveland, D. W. (1992). Primary structure of NuMA, an intranuclear protein that defines a novel pathway for segregation of proteins at mitosis. *J. Cell Biol.* **116,** 1395–1408.

Couchie, D., Faivre-bauman, A., Puymirat, J., Guilleminot, J., Tixier-Vidal, A., and Nunez, J. (1986). Expression of microtubule-associated proteins during the early stages of neurite extension by brain neurons cultured in defined medium. *J. Neurochem.* **47,** 1255–1261.

Cullen, C. F., Deak, P., Glover, D. M., and Ohkura, H. (1999). Mini spindles. A gene encoding a conserved microtubule-associated protein required for the integrity of the mitotic spindle in *Drosophila*. *J. Cell Biol.* **146,** 1005–1018.

Cunningham, C. C., Leclerc, N., Flanagan, L. A., Lu, M., Janmey, P. A., and Kosik, K. S. (1997). Microtubule-associated protein 2c reorganizes both microtubules and microfilaments into distinct cytological structures in an actin-binding protein-280-deficient melanoma cell line. *J. Cell Biol.* **136,** 845–857.

Curmi, P. A., Andersen, S. S. L., Lachkar, S., Gavet, O., Karsenti, E., Knossow, M., and Sobel, A. (1997). The Stathmin/Tubulin Interaction *in vitro*. *J. Biol. Chem.* **272,** 25,029–25,036.

Daub, H., Gevaert, K., Vandekerckhove, J., Sobel, A., and Hall, A. (2000). Rac/Cdc42 and p65PAK regulate the microtubule-destabilizing protein stathmin through phosphorylation at serine 16. *J. Biol. Chem.* **276,** 1677–1680.

DeFranco, C., Chicurel, M. E., and Potter, H. (1998). A general RNA-binding protein complex that includes the cytoskeleton-associated protein MAP1A. *Mol. Biol. Cell.* **9,** 1695–1708.

Deka, J., Kuhlmann, J., and Muller, O. (1998). A domain within the tumor suppressor protein APC

shows very similar biochemical properties as the microtubule-associated protein tau. *Eur. J. Biochem.* **253,** 591–597.

Denarier, E., Fourest-Lieuvin, A., Bosc, C., Pirollet, F., Chapel, A., Margolis, R. L., and Job, D. (1998). Nonneuronal isoforms of STOP protein are responsible for microtubule cold stability in mammalian fibroblasts. *Proc. Natl. Acad. Sci. USA* **95,** 6055–6060.

Desai, A., Verma, S., Mitchison, T. J., and Walczak, C. E. (1999). Kin I kinesins are microtubule-destabilizing enzymes. *Cell* **96,** 69–78.

Dhamodharan, A., and Wadsworth, P. (1995). Modulation of microtubule dynamic instability in vivo by brain microtubule associated proteins. *J. Cell Sci.* **108,** 1679–1689.

Diamantopoulos, G. S., Perez, F., Goodson, H. V., Batelier, G., Melki, R., Kreis, T. E., and Richard, J. E. (1999). Dynamic localization of CLIP-170 to microtubule plus ends is coupled to microtubule assembly. *J. Cell Biol.* **144,** 99–112.

Diaz-Nido, J., Serrano, L., and Avila, J. (1988). A casein-kinase II-related activity is involved in phosphorylation of microtubule-associated protein MAP1B during neuroblastoma cell differentiation. *J. Cell Biol.* **106,** 2057–2065.

Ding, M., Robel, L., James, A. J., Eisenstat, D. D., Leckman, J. F., Rubenstein, J. L., and Vaccarino, F. M. (1997). D1x-2 homeobox gene controls neuronal differentiation in primary cultures of developing basal ganglia. *J. Mol. Neurosci.* **8,** 93–113.

Ding, M., and Vandre, D. D. (1996). High molecular weight microtubule-associated proteins contain O-linked-N-acetylglucosamine. *J. Biol. Chem.* **271,** 12,555–12,561.

Dinsmore, J. H., and Sloboda, R. D. (1988). Calcium and calmodulin-dependent phosphorylation of a 62 kD protein induces microtubule depolymerization in sea urchin mitotic apparatuses. *Cell.* **53,** 769–780.

Dinsmore, J. H., and Sloboda, R. D. (1989). Microinjection of antibodies to a 62 kD mitotic apparatus protein arrests mitosis in dividing sea urchin embryos. *Cell.* **57,** 127–134.

Dinsmore, J. H., and Solomon, F. (1991). Inhibition of MAP-2 expression affects both morphological and cell division phenotypes of neuronal differentiation. *Cell.* **64,** 817–826.

Dionne, M. A., Howard, L., and Compton, D. A. (1999). NuMA is a component of an insoluble matrix at mitotic spindle poles. *Cell Motil. Cytoskel.* **42,** 189–203.

Dionne, M. A., Sanchez, A., and Compton, D. A. (2000). ch-TOGp is required for microtubule aster formation in a mammalian mitotic extract. *J. Biol. Chem.* **275,** 12,346–12,352.

DiPaolo, G., Antonsson, B., Kassel, D., Riederer, B. M., and Grenningloh, G. (1997). Phosphorylation regulates the microtubule-destabilizing activity of stathmin and its interaction with tubulin. *FEBS Lett.* **416,** 149–152.

DiTella, M. C., Feiguin, F., Carri, N., Kosik, K. S., and Caceres, A. (1996). MAP-1B/tau function redundancy during laminin-enhanced axonal growth. *J. Cell Sci.* **109,** 467–477.

Drechsel, D. N., Hyman, A. A., Cobb, M. H., and Kirschner, M. W. (1992). Modulation of the dynamic instability of tubulin assembly by the microtubule-associated protein tau. *Mol. Biol. Cell.* **3,** 1141–1154.

Drechsel, D. N., and Kirschner, M. W. (1994). The minimum GTP cap required to stabilize microtubules. *Curr. Biol.* **4,** 1053–1061.

Drewes, G., Ebneth, A., and Mandelkow, E. (1998). MAPs, MARKs and microtubule dynamics. *Trends Biochem. Sci.* **23,** 307–311.

Drewes, G., Ebneth, A., Preuss, U., Mandelkow, E. M., and Mandelkow, E. (1997). MARK, a novel family of protein kinases that phosphorylate microtubule-associated proteins and trigger microtubule disruption. *Cell.* **89,** 297–308.

Drewes, G., Lichtenberg-Kraag, B., Doring, F., Mandelkow, E. M., Biernat, J., Goris, J., Doree, M., and Mandelkow, E. (1992). Mitogen-activated protein (MAP) kinase transforms tau protein into an Alzheimer's-like state. *EMBO J.* **11,** 2131–2138.

Drewes, G., Trinczek, B., Illenberger, S., Biernat, J., Schmitt-Ulms, G., Meyer, H. E., Mandelkow, E. M., and Mandelkow, E. (1995). MAP/microtubule affinity regulating kinase 9p110/MARK): A

novel protein kinase that regulates tau-microtubule interactions and dynamic instability by phospho-rylation at the Alzheimer-specific site serine 262. *J. Biol. Chem.* **270,** 7679–7688.

Drubin, D. G., Caput, D., and Kirschner, M. W. (1984). Studies on the expression of the microtubule-associated protein tau during mouse brain development with newly isolated cDNA probes. *J. Cell Biol.* **98,** 1090–1097.

Drubin, D. G., Feinstein, S. C., Shooter, E. M., and Kirschner, M. W. (1985). Nerve growth factor-induced neurite outgrowth in PC12 cells involves the coordinate induction of microtubule assembly and assembly-promoting factors. *J. Cell Biol.* **101,** 1799–1807.

Drubin, D., and Kirschner, M. W. (1986). Tau protein function in living cells. *J. Cell Biol.* **103,** 2739–2746.

Drubin, D. G., Kobayashi, S., Kellogg, S., and Kirschner, M. W. (1988). Regulation of microtubule protein levels during cellular morphogenesis in nerve growth factor-treated PC12 cells. *J. Cell Biol.* **106,** 1583–1591.

Drubin, D., Kobayashi, S., and Kirschner, M. (1986). Association of tau proteins with microtubules in living cells. *Ann. NY Acad. Sci.* **466,** 257–286.

Dhamodharan, R., and Wadsworth, P. (1995). Modulation of microtubule dynamic instability in vivo by brain microtubule associated proteins. *J. Cell Sci.* **108,** 1679–1689.

D'Souza, I., Poorkaj, P., Hong, M., Nochlin, D., Lee, V. M., Bird, T. D., and Schellenberg, G. D. (1999). Missense and silent tau gene mutations cause frontotemporal dementia with parkinsonism-chromosome 17 type, by affecting multiple alternative RNA splicing regulatory elements. *Proc. Natl. Acad. Sci. USA* **96,** 5598–603.

D'Souza, I., and Schellenberg, G. D. (2000). Determinants of 4-repeat tau expression. *J. Biol. Chem.* **275,** 17,700–17,709.

Duesbery, N. S., Choi, T., Brown, K. D., Wood, K. W., Resau, J., Fukasawa, K., Cleveland, D. W., and Vande Woude, G. F. (2000). CENP-E is an essential kinetochore motor in maturing oocytes and is masked during mos-dependent, cell cycle arrest at metaphase II. *Proc. Natl. Acad. Sci. USA* **94,** 9165–9170.

Dye, R. B., Fink, S. P., and Williams, R. C., Jr. (1993). Taxol-induced flexibility of microtubules and its reversal by MAP-2 and tau. *J. Biol. Chem.* **268,** 6847–6850.

Ebneth, A., Drewes, G., Mandelkow, E. M., and Mandelkow, E. (1999). Phosphorylation of MAP2c and MAP4 by MARK kinases leads to the destabilization of microtubules in cells. *Cell Motil. Cytoskel.* **44,** 209–224.

Edelmann, W., Zervas, M., Costello, P., Roback, L., Fischer, I., Hammarback, J. A., Cowan, N., Davies, P., Wainer, B., and Kucherlapati, R. (1996). Neuronal abnormalities in microtubule-associated protein 1B mutant mice. *Proc. Natl. Acad. Sci. USA* **93,** 1270–1275.

Endow, S. A., Kang, S. J., Satterwhite, L. L., Rose, M. D., Skeen, V. P., and Salmon, E. D. (1994). Yeast Kar3 is a minus-end microtubule motor protein that destabilizes microtubules preferentially at the minus end. *EMBO J.* **13,** 2708–2713.

Ennulat, D. J., Liem, R. K., Hashim, G. A., and Shelanski, M. L. (1989). Two separate 18-amino acid domains of tau promote the polymerization of tubulin. *J. Biol. Chem.* **264,** 5327–5330.

Erickson, A. K., Ray, L. B., and Sturgill, T. W. (1990). Microtubule-associated protein 1A is the fibroblast HMW MAP undergoing mitogen-stimulated serine phosphorylation. *Biochem. Biophys. Res. Commun.* **166,** 827–832.

Esmaeli-Azad, B., McCarty, J. H., and Feinstein, S. C. (1994). Sense and anti-sense transfection analysis of tau function: Tau influences net microtubule assembly, neurite outgrowth and neuritic stability. *J. Cell Sci.* **107,** 869–879.

Eudy, J. D., Ma-Edmonds, M., Yao, S. F., Talmadge, C. B., Kelley, P. M., Weston, MD., Kimberling, W. J., and Sumegi, J. (1997). Isolation of a novel human homologue of the gene coding for echinoderm microtubule associated protein (EMAP) from the Usher syndrome type 1a locus at 14*q*32. *Genomics* **43,** 104–106.

Faire, K., Waterman-Storer, C. M., Gruber, D., Masson, D., Salmon, E. D., and Bulinski, J. C. (1999).

E-MAP-115 (ensconsin) associates dynamically with microtubules *in vivo* and is not a physiological modulator of microtubule dynamics. *J. Cell Sci.* **112,** 4243–4255.

Fanara, P., Oback, B., Ashman, K., Podtelejnikov, A., and Brandt, R. (1999). Identification of MINUS, a small polypeptide that functions as a microtubule nucleation suppressor. *EMBO J.* **18,** 565–577.

Faulkner, N. E., Dujardin, D. L., Tai, C. Y., Vaughan, K. T., O'Connell, C. B., Wang, Y., and Vallee, R. B. (2000). A role for the lissencephaly gene LIS1 in mitosis and cytoplasmic dynein function. *Nat. Cell Biol.* **2,** 784–791.

Feany, M. B., and Dickson, D. W. (1995). Widespread cytoskeletal pathology characterizes corticobasal degeneration. *Am. J. Pathol.* **146,** 1388–1396.

Feany, M. B., Mattiace, L. A., and Dickson, D. W. (1996). Neuropathologic overlap of progressive supranuclear palsy, Pick's disease and corticobasal degeneration. *J. Neuropathol. Exp. Neurol.* **55,** 53–67.

Felgner, H., Frank, R., Biernat, J., Mandelkow, E. M., Mandelkow, E., Ludin, B., Matus, A., and Schliwa, M. (1997). Domains of neuronal microtubule-associated proteins and flexural rigidity of microtubules. *J. Cell Biol.* **138,** 1067–1075.

Fink, J. K., Jones, S. M., Esposito, C., and Wilkowski, J. (1996). Human microtubule-associated protein 1a (MAP1A) gene: Genomic organization, cDNA sequence, and developmental- and tissue-specific expression. *Genomics* **35,** 577–585.

Flament, S., Delacourte, A., and Mann, D. M. (1990). Phosphorylation of tau proteins: a major event in the process of neurofibrillary degeneration. A comparative study between Alzheimer's disease and Down's syndrome. *Brain Res.* **516,** 15–19.

Francis, F., Koulakoff, A., Boucher, D., Chafey, P., Schaar, B., Vinet, M. C., Friocourt, G., McDonnell, N., Reiner, O., Kahn, A., McConnell, S. K., Berwald-Netter, Y., Denoulet, P., and Chelly, J. (1999). Doublecortin is a developmentally regulated, microtubule-associated protein expressed in migrating and differentiating neurons. *Neuron* **23,** 247–256.

Friedhoff, P., and Mandelkow, E. (1999). Tau protein. *In* "Guidebook to Cytoskeletal and Motor Proteins" (T. Kries and R. Vale Eds.), pp. 230–236. Oxford University Press, Oxford.

Frohli Hoier, E., Mohler, W. A., Kim, S. K., and Hajnal, A. (2000). The *Caenorhabditis elegans* APC-related gene apr-1 is required for epithelial cell migration and *Hox* gene expression. *Genes Develop.* **14,** 874–886.

Gaglio, T., Saredi, A., Bingham, J. B., Hasbani, M. J., Gill, S. R., Schroer, T. A., and Compton, D. A. (1996). Opposing motor activities are required for the organization of the mammalian mitotic spindle pole. *J. Cell Biol.* **135,** 399–414.

Gaglio, T., Saredi, A., and Compton, D. A. (1995). NuMA is required for the organization of microtubules into aster-like mitotic arrays. *J. Cell Biol.* **131,** 693–708.

Gamblin, T. C., Nachmanoff, K., Halpain, S., and Williams, R. C. Jr. (1996). Recombinant microtubule-associated protein 2c reduces the dynamic instability of individual microtubules. *Biochemistry* **35,** 12,576–12,586.

Gao, Q. S., Memmott, J., Lafyatis, R., Stamm, S., Screaton, G., and Andreadis, A. (2000). Complex regulation of tau exon 10, whose missplicing causes frontotemporal dementia. *J. Neurochem.* **74,** 490–500.

Garcia-Perez, J., Avila, J., and Diaz-Nido, J. (1998). Implication of cyclin-dependent kinases and glycogen synthase kinase 3 in the phosphorylation of microtubule-associated protein 1B in developing neuronal cells. *J. Neurosci. Res.* **52,** 445–452.

Gard, D. L., and Kirschner, M. W. (1987). A microtubule-associated protein from Xenopus eggs that specifically promotes assembly at the plus-end. *J. Cell. Biol.* **105,** 2203–2215.

Garner, C. C., Garner, A., Huber, G., Kozak, C., and Matus, A. (1990). Molecular cloning of microtubule-associated protein 1 (MAP1A) and microtubule-associated protein 5 (MAP1B): Identification of distinct genes and their differential expression in developing brain. *J. Neurochem.* **55,** 146–154.

Garner, C. C., and Matus, A. (1988). Different forms of microtubule-associated protein 2 are encoded by separate mRNA transcripts. *J. Cell Biol.* **106,** 779–783.

Garner, C. C., Tucker, R. P., and Matus, A. (1988). Selective localization of messenger RNA for cytoskeletal protein MAP2 in dendrites. *Nature (London)* **336,** 674–677.

Geddes, J. F., Vowels, G. H., Nicoll, J. A., and Revesz, T. (1999). Neuronal cytoskeletal changes are an early consequence of repetitive head injury. *Acta Neuropathol. (Berlin)* **98,** 171–178.

Gigant, B., Curmi, P. A., Martin-Barbey, C., Charbaut, E., Lachkar, S., Lebeau, L., Siavoshian, S., Sobel, A., and Knossow, M. (2000). The 4 A X-ray structure of a tubulin:stathmin-like domain complex. *Cell.* **102,** 809–16.

Gleeson, J. G., Lin, P. T., Flanagan, L. A., and Walsh, C. A. (1999). Doublecortin is a microtubule-associated protein and is expressed widely by migrating neurons. *Neuron* **23,** 257–271.

Goedert, M., Hasegawa, M., Jakes, R., Lawler, S., Cuenda, A., and Cohen, P. (1997b). Phosphorylation of microtubule-associated protein tau by stress-activated protein kinases. *FEBS Lett.* **409,** 57–62.

Goedert, M, Spillanitini, M. G., and Crowther, R. A. (1992). Cloning of a big tau microtubule-associated protein characteristic of the peripheral nervous system. *Proc. Natl. Acad Sci. USA* **89,** 1983–1987.

Goedert, M, Spillanitini, M. G., Hasegawa, M., Jakes, R., Crowther, R. A., and Klug, A. (1996). *Cold Spring Harbor Symp. Quant. Biol.* **61,** 565–573.

Goedert, M., Spillantini, M. G., Jakes, R., Rutherford, D., and Crowther, R. A. (1989b). Multiple isoforms of human microtubule-associated protein tau: Sequences and localization in neurofibrillary tangles of Alzheimer's disease. *Neuron* **3,** 519–26.

Goedert, M., Spillantini, M. G., Potier, M. C., Ulrich, J., and Crowther, R. A. (1989a). Cloning and sequencing of the DNA encoding an isoform of microtubule-associated protein tau containing four tandem repeats: Differential expression of tau protein mRNAs in human brain. *EMBO J.* **8,** 393–400.

Goedert, M., Trojanowski, J. Q., and Lee., V. M. W. (1997a). The neurofibrillary pathology of Alzhemier's Disease. *In* "The Molecular and Genetic Basis of Neurological Diseases (S. B. Prusiner, R. N. Rosenberg, S. DiMauro, and R. L. Barchi, Eds.), pp. 613–627. Butterworth Heineman, Boston.

Gong, C. X., Wegiel, J., Lidsky, T., Zuck, L., Avila, J., Wisniewski, H. M., Grundke-Iqbal, I., and Iqbal, K. (2000). Regulation of phosphorylation of neuronal microtubule-associated proteins MAP1b and MAP2 by protein phosphatase-2A and -2B in rat brain. *Brain Res.* **853,** 299–309.

Goode, B. L., Denis, P. E., Panda, D., Radeke, M. J., Miller, H. P., Wilson, L., and Feinstein, S. C. (1997). Functional interactions between the proline-rich and repeat regions of tau enhance microtubule binding and assembly. *Mol. Biol. Cell.* **8,** 353–365.

Goode, B. L., and Feinstein, S. C. (1994). Identification of a novel microtubule binding and assembly domain in the developmentally regulated inter-repeat region of tau. *J. Cell Biol.* **124,** 769–782.

Goold, R. G., Owen, R., and Gordon-Weeks, P. R. (1999). Glycogen synthase kinase 3beta phosphory-lation of microtubule-associated protein 1B regulates the stability of microtubules in growth cones. *J. Cell Sci.* **112,** 3373–3384.

Gordon-Weeks, P. R., and Fischer, I. (2000). MAP1B expression and microtubule stability in growing and regenerating axons. *Microsc. Res. Tech.* **48,** 63–74.

Govindan, B., and Vale, R. D. (2000). Characterization of a microtubule assembly inhibitor from Xenopus oocytes. *Cell Motil. Cytoskeleton* **45,** 51–57.

Graf, R., Daunderer, C., and Schliwa, M. (2000). Dictyostelium DdCP224 is a microtubule-associated protein and a permanent centrosomal resident involved in centrosome duplication. *J. Cell Sci.* **113,** 1747–1758.

Greenwood, J. A., Scott, C. W., Spreen, R. C., Caputo, C. B., and Johnson, G. V. (1994). Casein kinase II preferentially phosphorylates human tau isoforms containing an amino terminal insert. Identification of threonine 39 as the primary phosphate acceptor. *J.Biol. Chem.* **269,** 4373–4380.

Grover, A., Houlden, H., Baker, M., Adamson, J., Lewis, J., Prihar, G., Pickering-Brown, S., Duff, K., and Hutton, M. (1999). 5′ Splice site mutations in tau associated with the inherited dementiaFTDP-17 affect a stem-loop structure that regulates alternative splicingof exon 10. *J. Biol. Chem.* **274,** 15,134–15,143.

Gruss, O. J., Carazo-Salas, R. E., Schatz, C. A., Guarguaglini, G., Kast, J., Wilm, M., LeBot, N., Vernos, I., Karsenti, E., and Mattaj, I. W. (2001). Ran induces spindle assembly by reversing the inhibitory effect of importin alpha on TPX2 activity. *Cell* **104,** 83–93.

Gueth-Hallonet, C., Wang, J., Harborth, J., Weber, K., and Osborn, M. (1998). Induction of a regular nuclear lattice by overexpression of NuMA. *Exp. Cell Res.* **243,** 434–452.

Gueth-Hallonet, C., Weber, K., and Osborn, M. (1996). NuMA: A bipartite nuclear localization signal and other functional properties of the tail domain. *Exp. Cell Res.* **225,** 207–218.

Gustke, N., Trinczek, B., Biernat, J., Mandelkow, E. M., and Mandelkow, E. (1994). Domains of tau protein and interactions with microtubules. *Biochemistry* **33,** 9511–9522.

Hagestedt, T., Lichtenberg, B., Wille, H., Mandelkow, E. M., and Mandelkow, E. (1989). Tau protein becomes long and stiff upon phosphorylation: Correlation between paracrystalline structure and degree of phosphorylation. *J. Cell Biol.* **109,** 1643–1651.

Halpain, S., and Greengard, P. (1990). Activation of NMDA receptors induces rapid dephosphorylation of the cytoskeletal protein MAP2. *Neuron* **5,** 237–246.

Hamill, D. R., Howell, B., Cassimeris, L., and Suprenant, K. (1998). Purification of a WD-repeat protein, EMAP, that promotes microtubule dynamics through an inhibition of rescue. *J. Biol. Chem.* **273,** 9285–9291.

Hammarback, J. A., Obar, R. A., Hughes, S. M., and Vallee, R. B. (1991). MAP1B is encoded as a polyprotein that is processed to form a complex N-terminal microtubule-binding domain. *Neuron* **7,** 129–139.

Hanger, D., Hughes, K., Woodgett, J., Brion, J., and Anderton, B. (1992). Glycogen synthase kinase-3 induces Alzheimer's disease-like phosphorylation of tau: Generation of paired helical filament epitopes and neuronal localization of the kinase. *Neurosci. Lett.* **147,** 58–62.

Hanissian, S. H., Grangakis, M., Bland, M. M., Jawahar, S., and Chatila., T. A. (1993). Expression of a Ca2+/calmodulin-dependent kinase, CaM kinase-IV/Gr, in human T lymphocytes. Regulation of kinase activity by T cell receptor signalling. *J.Biol. Chem.* **268,** 20,055–20,063.

Hanley, J. G., Koulen, P., Bedford, F., Gordon-Weeks, P. R., and Moss, S. J. (1999). The protein MAP1B links GABAc receptors to the cytoskeleton at retinal synapses. *Nature* **397,** 66–69.

Harada, A., Oguchi, K., Okabe, S., Kuno, J., Terada, S., Ohshima, T., Sato-Yoshitake, R., Takel, Y., Noda, T., and Hirokawa, N. (1994). Altered microtubule organization in small-caliber axons of mice lacking tau protein. *Nature* **369,** 488–491.

Harborth, J., and Osborn, M. (1999). Does NuMA have a scaffold function in the interphase nucleus? *Crit. Rev. Eukaryot. Gene Expr.* **9,** 319–328.

Harborth, J., Wang, J., Gueth-Hallonet, C., Weber, K., and Osborn, M. (1999). Self assembly of NuMA: Multiarm oligomers as structural units of a nuclear lattice. *EMBO J.* **18,** 1689–1700.

Hartman, J. J., Mahr, J., McNally, K., Okawa, K., Iwamatsu, A., Thomas, S., Cheeman, S., Heuser, J., Vale, R. D., and McNally, F. J. (1998). Katanin, a microtubule-severing protein, is a novel AAA ATPase that targets to the centrosome using a WD40-containing subunit. *Cell* **93,** 277–287.

Hartman, J. J., and Vale, R. D. (1999). Microtubule disassembly by ATP-dependent oligomerization of the AAA enzyme katanin. *Science* **286,** 782–785.

Heicklen-Klein, A., Aronov, S., and Ginzberg, I. (2000). Tau promoter activity in neuronally differentiated P19 cells. *Brain Res.* **874,** 1–9.

Himmler, A. (1989). Structure of the bovine tau gene: Alternatively spliced transcripts generate a protein family. *Mol. Cell Biol.* **9,** 1389–1396.

Himmler, A., Drechsel, D., Kirschner, M. W., and Martin, D. W., Jr. (1989). Tau consists of a set of proteins with repeated C-terminal microtubule-binding domains and variable N-terminal domains. *Mol Cell Biol.* **9,** 1381–1388.

Hinck, L., Nathke, I. S., Papkoff, J., and Nelson, W. J. (1994). Beta-catenin: A common target for the regulation of cell adhesion by Wnt-1 and Src signaling pathways. *Trends Biochem. Sci.* **19,** 538–542.

Hirokawa, N. (1994). Microtubule organization and dynamics dependent on microtubule-associated proteins. *Curr. Opin. Cell Biol.* **94,** 425–443.

Hirokawa, N., Funakoshi, T., Sato-Harada, R., and Kanai, Y. (1996). Selective stabilization of tau in axons and microtubule-associated protein 2C in cell bodies and dendrites contributes to polarized localization of cytoskeletal proteins in mature neurons. *J. Cell Biol.* **132,** 667–679.

Hof, P. R., Delacourte, A., and Bouras, C. (1992). Distribution of cortical neurofibrillary tangles in progressive supranuclear palsy: A quantitative analysis of six cases. *Acta Neuropathol.* **84,** 45–51.

Holmfeldt, P., Larsson, N., Segerman, B., Howell, B., Morabito, J., Cassimeris, L., and Gullberg, M. (2001). The catastrophe-promoting activity of ectopic oncoprotein 18/stathmin is required for disruption of the mitotic spindle. *Mol. Biol. Cell.,* in press.

Hong, M., Zhukareva, V., Vogelsberg-Ragaglia, V., Wszolek, Z., Reed, L., Miller, B. I., Geschwind, D. H., Bird, T. D., McKeel, D., Goate, A., Morris, J. C., Wilhelmsen, K. C., Schellenberg, G. D., Trojanowski, J. Q., and Lee, V. M. (1998). Mutation-specific functional impairments in distinct tau isoforms of hereditary FTDP-17. *Science* **282,** 1914–1917.

Hoogenraad, C. C., Akhmanova, A., Grosveld, F., DeZeeuw, C. I., and Galjart, N. (2000). Functional analysis of CLIP-115 and its binding to microtubules. *J. Cell Sci.* **113,** 2285–2297.

Horesh, D., Sapir, T., Francis, F., Wolf, S. G., Caspi, M., Elbaum, M., Chelly, J., and Reiner, O. (1999). Doublecortin, a stabilizer of microtubules. *Hum. Mol. Genet.* **8,** 1599–610.

Horio, T., and Hotani, H. (1986). Visualization of the dynamic instability of individual microtubules by dark-field microscopy. *Nature* **321,** 605–607.

Horowitz, S. B., Shen, H.-J., He, L., Dittmar, P., Neef, R., Chen, J., and Schubart, U. K. (1997). The microtubule-destabilizing activity of metablastin (p19) is controlled by phosphorylation. *J. Biol. Chem.* **272,** 8129–8132.

Hoshi, M., Ohta, K., Gotoh, Y., Mori, A., Murofushi, H., Sakai, H., and Nishida, E. (1992). Mitogen-activated-protein-kinase-catalyzed phosphorylation of microtubule-associated proteins, microtubule-associated protein 2 and microtubule-associated protein 4, induces an alteration in their function. *Eur. J. Biochem.* **203,** 43–52.

Hotani, H., and Horio, T. (1988). Dynamics of microtubules visualized by darkfield microscopy: Treadmilling and dynamic instability. *Cell Motil. Cytoskeleton* **10,** 229–236.

Howell, B., Larsson, N., Gullberg, M., and Cassimeris, L. (1999a). Dissociation of the tubulin-sequestering and microtubule catastrophe-promoting activities of oncoprotein 18/stathmin. *Mol. Biol. Cell* **10,** 105–118.

Howell, B. J., Deacon, H., and Cassimeris, L. (1999b). Decreasing oncoprotein 18 levels reduces microtubule catastrophes and increases microtubule polymer in vivo. *J. Cell Sci.* **112,** 3713–3722.

Hummel, T., Krukkert, K., Roos, J., Davis, G., and Klambt, C. (2000). Drosophilia futsch/22C10 is a MAP1b-like protein required for dendritic development and axonal development. *Neuron* **26,** 357–370.

Hunter, A. W., and Wordeman, L. (2000). How motor proteins influence microtubule polymerization dynamics. *J. Cell Sci.* **113,** 4379–4389.

Hyman, A. A., and Karsenti, E. (1996). Morphogenic properties of microtubules and mitotic spindles. *Cell* **84,** 401–411.

Hyman, A. A., Salser, S., Drechsel, D. N., Unwin, N., and Mitchison, T. J. (1992). Role of GTP hydrolysis in microtubule dynamics: Information from a slowly hydrolyzable analogue, GMPCPP. *Mol. Biol. Cell* **3,** 1155–1167.

Illenberger, S., Drewes, G., Trinczek, B., Biernat, J., Meyer, H. E., Olmsted, J. B., Mandelkow, E. M., and Mandelkow, E. (1996). Phosphorylation of microtubule-associated proteins MAP2 and MAP4 by the protein kinase p110 mark. Phosphorylation sites and regulation of microtubule dynamics. *J. Biol. Chem.* **271,** 10,834–10,843.

Illenberger, S., Zheng-Fischhofer, Q., Preuss, U., Stamer, K., Baumann, K., Trinczek, B., Biernat, J., Godemann, R., Mandelkow, E. M., and Mandelkow, E. (1998). The endogenous and cell cycle-dependent phosphorylation of tau protein in living cells: Implications for Alzheimer's disease. *Mol. Biol. Cell* **9,** 1495–1512.

Inoue, Y. H., do Carmo Avides, M., Shiraki, M., Deak, P., Yamaguchi, M., Nishimoto, Y., Matsukage, A.,

and Glover, D. M. (2000). Orbit, a novel microtubule associated protein essential for mitosis in *Drosophila melangaster. J. Cell Biol.* **149,** 153–165.

Itin, C., Ulitzer, N., Muhlbauer, B., and Pfeffer, S. R. (1999). Mapmodulin, cytoplasmic dynein, and microtubules enhance transport of mannose 6-phosphate receptors from endosomes to the trans-golgi network. *Mol. Biol. Cell* **10,** 2191–2197.

Itoh, T., Hisanaga, S., Hosoi, T., Kishimoto, T., and Hotani, H. (1997). Phosphorylation states of microtubule-associated protein 2 (MAP2) determine the regulatory role of MAP2 in microtubule dynamics. *Eur. J. Biochem.* **36,** 12,574–12,582.

Itoh, T. J., and Hotani, H. (1994). Microtubule-stabilizing activity of microtubule-associated proteins (MAPs) is due to increase in frequency of rescue in dynamic instability: Shortening length decreases with binding of MAPs onto microtubules. *Cell Struct. Funct.* **19,** 279–290.

Jameson, L., and Caplow, M. (1981). Modification of microtubule steady-state dynamics by phosphorylation of the microtubule-associated proteins. *Proc. Natl. Acad. Sci. USA* **78,** 3413–3417.

Jeha, S., Luo, X. N., Beran, M., Kantarjian, H., and Atweh, G. F. (1996). Antisense RNA inhibition of phosphoprotein p18 expression abrogates the transformed phenotype of leukemic cells. *Cancer Res.* **56,** 1445–1450.

Job, D., Rauch, C. T., and Margolis, R. L. (1987). High concentrations of STOP protein induce a microtubule super-stable state. *Biochem. Biophys. Res. Commun.* **148,** 429–434.

Johnson, J. A., and Sloboda, R. D. (1992). A 62-kD protein required for mitotic progression is associated with the mitotic apparatus during M-phase and with the nucleus during interphase. *J. Cell Biol.* **119,** 843–854.

Joly, J. C., Flynn, G., and Purich, D. L. (1989). The microtubule-binding fragment of micotubule-associated protein-2: Location of the protease-accessible site and identification of an assembly-promoting peptide. *J. Cell Biol.* **109,** 2289–2294.

Jordan, M. A., Thrower, D., and Wilson, L. (1992). Effects of vinblastine, podophyllotoxin and nocodazole on mitotic spindles: Implications for the role of microtubule dynamics in mitosis. *J. Cell Sci.* **102,** 401–416.

Jourdain, L., Curmi, P., Sobel, A., Pantaloni, D., and Carlier, M.-F. (1997). Stathmin: A tubulin-sequestering protein which forms a ternary T2S complex with two tubulin molecules. *Biochemistry.* **36,** 10,817–10,821.

Juwana, J. P., Henderikx, P., Mischo, A., Wadle, A., Fadle, N., Gerlach, K., Arends, J. W., Hoogenboom, H., Pfreundschuh, M., and Renner, C. (1999). EB/RP gene family encodes tubulin binding proteins. *Int. J. Canc.* **81,** 275–284.

Kadowaki, T., Fujita-Yamaguchi, Y., Nishida, E., Takaku, F., Akiyama, T., Kathuria, S., Akanuma, Y., and Kasuga, M. (1985). Phosphorylation of tubulin and microtubule-associated proteins by the purified insulin receptor kinase. *J. Biol. Chem.* **260,** 4016–4020.

Kalab, P., Pu, R. T., and Dasso, M. (1999). The ran GTPase regulates mitotic spindle assembly. *Curr. Biol.* **9,** 481–484.

Kalcheva, N., Albala, J., O'Guin, K., Rubino, H., Garner, C., and Shafit-Zagardo, B. (1995). Genomic structure of human microtubule-associated protein 2 (MAP-2) and characterization of additional MAP-2 isoforms. *Proc. Natl. Acad. Sci. USA* **92,** 10,894–10,898.

Kalcheva, N., Rockwood, J. M., Kress, Y., Steiner, A., and Shafit-Zagardo, B. (1998). Molecular and functional characteristics of MAP-2a: Ability of MAP-2a versus MAP-2b to induce stable microtubules in COS cells. *Cell Motil. Cytoskeleton* **40,** 272–285.

Kallajoki, M., Weber, K., and Osborn, M. (1991). A 210 kDa nuclear matrix protein is a functional part of the mitotic spindle: A microinjection study using SPN monoclonal antibodies. *EMBO J.* **10,** 3351–3362.

Kallajoki, M., Weber, K., and Osborn, M. (1992). Ability to organize microtubules in taxol-treated mitotic PtK2 cells goes with the SPN antigen and not with the centrosome. *J. Cell Sci.* **102,** 91–102.

Kanai, Y., Chen, J., and Hirokawa, N. (1992). Microtubule bundling by tau proteins in vivo: analysis of functional domains. *EMBO J.* **11,** 3953–3961.

Kanai, Y., and Hirokawa, N. (1995). Sorting mechanisms of tau and MAP2 in neuron: Suppressed axonal transit of of MAP2 and locally regulated microtubule bindings. *Neuron* **14,** 421–432.

Kanai, Y., Takemura, R., Oshima, T., Mori, H., Ihara, Y., Yanagisawa, M., Masaki, T., and Hirokawa, N. (1989). Expression of multiple tau isoforms and microtubule bundle formation in fibroblasts trans-fected with a single tau cDNA. *J. Cell Biol.* **109,** 1173–1184.

Kindler, S., Schulz, B., Goedert, M., and Garner, C. C. (1990). Molecular structure of microtubule-associated protein 2b and 2c from rat brain. *J. Biol. Chem.* **265,** 19,679–19,684.

Kintzer, K. W., and Vogelstein, B. (1996). Lessons from hereditary colorectal cancer. *Cell* **87,** 159–170.

Kitazawa, H., Iida, J., Uchida, A., Haino-Fukushima, K., Itoh, T. J., Hotani, H., Ookata, K., Murofushi, H., Bulinski, J. C., Kishimoto, T., and Hisanaga, S. (2000). Ser787 in the proline-rich region of human MAP4 is a critical phosphorylation site that reduces its activity to promote tubulin polymerization. *Cell Struct. Funct.* **25,** 33–39.

Kline-Smith, S. L., and Walczak, C. E. (2000). XKCM1 destabilizes microtubules in cells. *M. Biol. Cell.* **11,** 358a.

Knops, J., Kosik, K. S., Lee, G., Pardee, J. D., Cohen-Gould, L., and McConlogue, L. (1991). Overex-pression of tau in a nonneuronal cell induces long cellular processes. *J. Cell Biol.* **114,** 725–733.

Kobayashi, S., Ishiguro, K., Omori, A., Takamatsu, M., Arioka, M., Imahori, K., and Uchida, T. (1993). A cdc2-related kinase PSSALRE/cdk5 is homologous with the 30-kDa subunit of tau pro-tein kinase ii, a proline-directed protein-kinase associated with microtubule. *FEBS Lett.* **335,** 171–175.

Komada, M., McLean, D. J., Griswold, M. D., Russell, L. D., and Soriano, P. (2000). E-MAP-115, encoding a microtubule-associated protein, is a retinoic acid–inducible gene required for spermato-genesis. *Genes Dev.* **14,** 1332–1342.

Koonce, M. P., and Tikhonenko, I. (2000). Functional elements within the dynein microtubule-binding domain. *Mol. Biol. Cell.* **11,** 523–529.

Kopke, E., Tung, Y. C., Shaikh, S., Alonso, A. C., Iqbal, K., and Grundke-Iqbal, I. (1993). Microtubule-associated protein tau: Abnormal phosphorylation of a non-paired helical filament pool in Alzheimer's disease. *J. Biol. Chem.* **268,** 24,374–24,384.

Korinek, W. S, Copeland, M. J., Chaudhuri, A., and Chant, J. (2000). Molecular linkage underlying microtubule orientation toward cortical sites in yeast. *Science* **287,** 2257–2259.

Kosik, K. S., and Caceres, A. (1991). Tau protein and the establishment of an axonal morphology. *J. Cell Sci. Suppl.* **15,** 69–74.

Kosik, K. S., and Greenberg, S. M. (1994). Tau protein and Alzheimer's disease. *In* "Alzheimer Disease (R. Terry, R. Katzman, and K. Bick, Eds.), pp. 335–344. Raven Press, New York.

Kosik, K. S., Orechhio, L. D., Bakalis, S., and Neve, R. L. (1989). Developmentally regulated expression of specific tau sequences. *Neuron* **2,** 1389–1397.

Kowalski, R. J., and Williams, R. C., Jr. (1993). Microtubule-associated protein 2 alters the dynamic properties of microtubule assembly and disassembly. *J. Biol. Chem.* **268,** 9847–9855.

Ksiezak-Reding, H., Liu, W. K., and Yen, S. H. (1992). Phosphate analysis and dephosphorylation of modified tau associated with paired helical filaments. *Brain Res.* **597,** 209–219.

Kutschera, W., Zauner, W., Wiche, G., and Propst, F. (1998). The mouse and rat MAP1B genes: Genomic organization and alternative transcription. *Genomics* **49,** 430–436.

Labdon, J. E., Nieves, E., and Schubart, U. K. (1992). Analysis of phosphoprotein p19 by liquid chromatography/mass spectrometry. Identification of two proline-directed serine phosphorylation sites and a blocked amino terminus. *J. Biol. Chem.* **267,** 3506–3513.

Langkopf, A., Hammarback, J. A., Muller, R., Vallee, R. B., and Garner, C. C. (1992). Microtubule-associated proteins 1A and LC2. Two proteins encoded in one messenger RNA. *J. Biol. Chem.* **267,** 16,561–16,566.

Lantz, V. A., and Miller, K. G. (1998). A class VI unconventional myosin is associated with a homologue of a microtubule-binding protein, cytoplasmic linker protein-170, in neurons and at the posterior pole of Drosophila embryos. *J. Cell Biol.* **140,** 897–910.

Larsson, N., Marklund, U., Melander Gradin, H., Brattsand, G., and Gullberg, M. (1997). Control of microtubule dynamics by oncoprotein 18: Dissection of the regulatory role of multisite phosphorylation during mitosis. *Mol. Cell Biol.* **17,** 5530–5539.

Larsson, N., Melander, H., Marklund, U., Osterman, O., and Gullberg, M. (1995). G2/M transition requires multisite phosphorylation of oncoprotein 18 by two distinct protein kinase systems. *J. Biol. Chem.* **270,** 14,175–14,183.

Larsson, N., Segerman, B., Gradin, H. M., Wandzioch, E., Cassimeris, L., and Gullberg, M. (1999a). Mutations of oncoprotein 18/stathmin identify tubulin-directed regulatory activities distinct from tubulin association. *Mol. Cell Biol.* **19,** 2242–2250.

Larsson, N., Segerman, B., Howell, B., Fridell, K., Cassimeris, L., and Gullberg, M. (1999b). Op18/stathmin mediates multiple region-specific tubulin and microtubule-regulating activities. *J. Cell Biol.* **146,** 1289–1302.

Lawler, S. (1998). Microtubule dynamics: If you need a shrink try stathmin/Op18. *Curr. Biol.* **8,** R212–R214.

LeClerc, N., Baas, P. W., Garner, C. C., and Kosik, K. S. (1996). Juvenile and mature MAP2 isoforms induce distinct patterns of process outgrowth. *Mol. Biol. Cell* **7,** 443–455.

LeClerc, N., Kosik, K. S., Cowan, N., Pienkowski, T. P., and Baas, P. W. (1993). Process formation in Sf9 cells induced by the expression of a microtubule-associated protein 2C-like construct. *Proc. Natl. Acad. Sci. USA* **90,** 6223–6227.

Lee, G., Neve, R. L., and Kosik, K. S. (1989). The microtubule binding domain of tau protein. *Neuron* **6,** 1615–1624.

Lee, G., Newman, S. T., Gard, D. L., Band, H., and Panchamoorthy, G. (1998). Tau interacts with src-family non-receptor tyrosine kinases. *J. Cell Sci.* **111,** 3167–3177.

Lee, G., and Rook, S. L. (1992). Expression of tau protein in non-neuronal cells: Microtubule binding and stabilization. *J. Cell Sci.* **102** (Pt 2), 227–237.

Lee, L., Tirnauer, J. S., Li, J., Schuyler, S. C., Liu, J. Y., and Pellman, D. (2000). Positioning of the mitotic spindle by a cortical-microtubule capture mechanism. *Science* **287,** 2260–2262.

Lee, V. M., and Trojanowski, J. Q. (1999). Neurodegenerative tauopathies: Human disease and transgenic mouse models. *Neuron* **24,** 507–510.

le Gouvello, S., Manceau, V., and Sobel, A. (1998). Serine 16 of stathmin as a cytosolic target for Ca2+/calmodulin-dependent kinase II after CD2 triggering of human T lymphocytes. *J. Immunol.* **161,** 1113–1122.

Lepley, D. M., Palange, J. M., and Suprenant, K. A. (1999). Sequence and expression patterns of a human EMAP-related protein-2 (HuEMAP-2). *Gene* **237,** 343–349.

Lewis, S. A., Ivanov, I. E., Lee, G.-H., and Cowan, N. J. (1989). Organization of microtubles in dendrites and axons is determined by a short hydrophobic zipper in microtubule-associated proteins MAP2 and tau. *Nature* **342,** 498–505.

Liao, H., Li, G., and Yen, T. J. (1994). Mitotic regulation of microtubule cross-linking activity of CENP-E kinetochore protein. *Science* **265,** 394–398.

Liao, H., Li, Y., Brautigan, D. L., and Gundersen, G. G. (1998). Protein phosphatase 1 is targeted to microtubules by the microtubule-associated protein tau. *J. Biol. Chem.* **273,** 21,901–21,908.

Lim, R. M., and Halpain, S. (2000). Regulated association of microtubule-associated protein 2 (MAP2) with Src and Grb2: Evidence for MAP2 as a scaffolding protein. *J. Biol. Chem.* **275,** 20,578–20,587.

Litman, P., Bard, J., Rindzooski, L., and Ginzberg, I. (1993). Subcellular localization of tau mRNA in differentiating neuronal cell culture: Implications for neuronal polarity. *Neuron* **10,** 627–638.

Littauer, U. Z., Giveon, D., Thierauf, M., Ginzburg, I., and Ponstingl, H. (1986). Common and distinct tubulin binding sites for microtubule-associated proteins. *Proc. Natl. Acad. Sci., USA* **83,** 7162–7166.

Liu, C. W., Lee, G., and Jay, D. G. (1999). Tau is required for neurite outgrowth and growth cone motility of chick sensory neurons. *Cell Motil. Cytoskeleton* **43,** 232–242.

Liu, D., and Fischer, I. (1996). Two alternative promoters direct neuron-specific expression of the rat microtubule-associated protein 1B gene. *J. Neurosci.* **16,** 5026–5036.

Liu, D., and Fischer, I. (1997). Structural analysis of the proximal region of the microtubule-associated protein 1B promoter. *J. Neurochem.* **69,** 910–919.

Lopez, L. A., and Sheetz, M. P. (1993). Steric inhibition of cytoplasmic dynein and kinesin motility by MAP2. *Cell Motil. Cytoskeleton* **24,** 1–16.

Ludin, B., Ashbridge, K., Funfschilling, U., and Matus, A. (1996). Functional analysis of the MAP2 repeat domain. *J. Cell Sci.* **109,** 91–99.

Luduena, R.F. (1998). Multiple forms of tubulin: Different gene products and covalent modifications. *Int. Rev. Cytol.* **178,** 207–275.

Lydersen, B., and Pettijohn, D. (1980). Human-specific nuclear protein that associates with the polar regions of the mitotic apparatus: Distribution in a human/hamster hybrid cell. *Cell* **22,** 489–499.

Ma, D., Connors, T., Nothias, F., and Fischer, I. (2000). Regulation of the expression and phosphorylation of microtubule-associated protein 1B during regeneration of adult dorsal root ganglion neurons. *Neuroscience* **99,** 157–170.

Ma, D., Nothias, F., Boyne, L. J., and Fischer, I. (1997). Differential regulation of microtubule-associated protein 1B (MAP1B) in rat CNS and PNS during development. *J. Neurosci. Res.* **49,** 319–332.

Maas, T., Eidenmuller, J., and Brandt., R. (2000). Interaction of tau with the neural membrane cortex is regulated by phosphorylation at sites that are modified in paired helical filaments. *J. Biol. Chem.* **275,** 15,733–15,740.

Maddox, P. S., Bloom, K. S., and Salmon, E. D. (2000). The polarity and dynamics of microtubule assembly in the budding yeast Saccharomyces cerevisiae. *Nat. Cell Biol.* **2,** 36–41.

Maekawa, T., and Kuriyama, R. (1993). Primary structure and microtubule-interacting domain of the SP-H antigen: A mitotic MAP located at the spindle pole and characterized as a homologous protein to NuMA. *J. Cell Sci.* **105,** 589–600.

Maekawa, T., Leslie, R., and Kuriyama, R. (1991). Identification of a minus end-specific microtubule-associated protein located at the mitotic poles in cultured mammalian cells. *Eur. J. Cell Biol.* **54,** 255–267.

Mahmoud, N. N., Boolbol, S. K., Bilinski, R. T., Martucci, C., Chadburn, A., and Bertagnolli, M. M. (1997). Apc gene mutation is associated with a dominant-negative effect upon intestinal cell migration. *Canc. Res.* **57,** 5045–5050.

Mandelkow, E. M., Mandelkow, E., and Milligan, R. A. (1991). Microtubule dynamics and microtubule caps: A time-resolved cryo-electron microscopy study. *J. Cell Biol.* **114,** 977–991.

Mandell, J. W., and Banker, G. A. (1996). A spatial gradient of tau protein phosphorylation in nascent axons. *J. Neurosci.* **16,** 5727–5740.

Maney, T., Hunter, A. W., Wagenbach, M., and Wordeman, L. (1998). Mitotic centromere-associated kinesin is important for anaphase chromosome segregation. *J. Cell Biol.* **142,** 787–801.

Mangan, M. E., and Olmsted, J. B. (1996). A muscle-specific variant of microtubule-associated protein 4 (MAP4) is required in myogenesis. *Development* **122,** 771–781.

Mann, S. S., and Hammarback, J. A. (1994). Molecular characterization of light chain 3. A microtubule binding subunit of MAP1A and MAP1B. *J. Biol. Chem.* **269,** 11,492–11,497.

Mansfield, S. G., Diaz-Nido, J., Gordon-Weeks, P. R., and Avila, J. (1991). The distribution and phosphorylation of the microtubule-associated protein MAP1B in growth cones. *J. Neurocytol.* **20,** 1007–1022.

Margolis, R. L., and Job, D. (1999). STOPs. *In* "Guidebook to the Cytoskeletal Proteins" (T. Kreis and R. Vale, Eds.), 2nd ed., pp. 227–229. Oxford University Press, Oxford.

Margolis, R. L., Rauch, C. T., Pirollet, F., and Job, D. (1990). Specific association of STOP protein with microtubules in vitro and with stable microtubules in mitotic spindles of cultured cells. *EMBO J.* **9,** 4095–4102.

Margolis, R. L., and Wilson, L. (1981). Microtubule treadmills—Possible molecular machinery. *Nature* **293,** 705–711.

Marklund, U., Brattsand, G., Osterman, O., Ohlsson, P. I., and Gullberg, M. (1993b). Multiple signal transduction pathways induce phosphorylation of serines 16, 25 and 38 of oncoprotein 18 in T lymphocytes. *J. Biol. Chem.* **268,** 25,671–25,680.

Marklund, U., Brattsand, G., Shingler, V., and Gullberg, M. (1993a). Serine 25 on oncoprotein 18 is a major cytosolic target for the mitogen-activated protein kinase. *J. Biol. Chem.* **268,** 15,039–15,047.

Marklund, U., Larsson, N., Brattsand, G., Osterman, O., Chatila, T. A., and Gullberg, M. (1994b). Serine 16 of oncoprotein 18 is a major cytosolic target for the Ca2+/calmodulin-dependent protein kinase-Gr. *Eur. J. Biochem.* **225,** 53–60.

Marklund, U., Larsson, N., Melander Gradin, H., Brattsand, G., and Gullberg, M. (1996). Oncoprotein 18 is a phosphorylation-responsive regulator of microtubule dynamics. *EMBO J.* **15,** 5290–5298.

Marklund, U., Osterman, O., Melander, H., Bergh, A., and Gullberg, M. (1994a). The phenotype of a "Cdc2 kinase target site-deficient" mutant of oncoprotein 18 reveals a role of this protein in cell cycle control. *J. Biol. Chem.* **269,** 30,626–30,635.

Masson, D., and Kreis, T. E. (1993). Identification and molecular characterization of E-MAP-115, a novel microtubule-associated protein predominately expressed in epithelial cells. *J. Cell Biol.* **123,** 357–371.

Masson, D., and Kreis, T. E. (1995). Binding of E-MAP-115 to microtubules is regulated by cell cycle dependent phosphorylation. *J. Cell Biol.* **131,** 1015–1024.

Matsumine, A., Ogai, A., Senda, T., Okumura, N., Satoh, K., Baeg, G. H., Kawahara, T., Kobayashi, S., Okada, M., Toyoshima, K., and Akiyama, T. (1996). Binding of APC to the human homolog of the *Drosophila* discs large tumor suppressor protein. *Science* **272,** 1020–1023.

Matthews, L. R., Carter, P., Thierry-Mieg, D., and Kemphues, K. (1998). ZYG-9, A *Caenorhabditis elegans* protein required for microtubule organization and function, is a component of meitotic and mitotic spindle poles. *J. Cell Biol.* **141,** 1159–1168.

Maucuer, A., Moreau, J., Mechali, M., and Sobel, A. (1983). Stathmin gene family: Phylogenic conservation and developmental regulation in *Xenopus. J. Biol. Chem.* **268,** 16,420–16,429.

Mavilia, C., Couchie, D., Mattei, M. G., Nivez, M. P., and Nunez, J. (1993). High and low molecular weight tau proteins are differentially expressed from a single gene. *J. Neurochem.* **61,** 1073–1081.

Mawal-Dewan, M., Henley, J., Van de Voorde, A., Trojanowski, J. Q., and Lee, V. M. (1994). The phosphorylation state of tau in the developing rat brain is regulated by phosphoprotein phosphatases. *J. Biol. Chem.* **269,** 30,981–30,987.

McCartney, B. M., and Peifer, M. (2000). Teaching tumour suppressors new tricks. *Nat. Cell Biol.* **2,** E58–E60.

McNally, F. J., and Thomas, S. (1998). Katinin is responsible for the M-phase microtubule severing activity in *Xenopus eggs. Mol. Biol. Cell* **9,** 1847–1861.

McNally, F. J., and Vale, R. D. (1993). Identification of katanin, an ATPase that severs and disassembles stable microtubules. *Cell* **75,** 419–429.

McNally, K. P., Bazirgan, O. A., and McNally, F. J. (2000). Two domains of p80 katanin regulate microtubule severing and spindle pole targeting by p60 katanin. *J. Cell Sci.* **113,** 1623–1633.

Mei, X., Sweatt, A. J., and Hammarback, J. A. (2000). Regulation of microtubule-associated protein 1B (MAP1B) subunit composition. *J. Neurosci. Res.* **62,** 56–64.

Meixner, A., Haverkamp, S., Wassle, H., Fuhrer, S., Thalhammer, J., Kropf, N., Bittner, R. E., Lassmann, H., Wiche, G., and Propst, F. (2000). MAP1B is required for axon guidance and is involved in the development of the central and peripheral nervous system. *J. Cell Biol.* **151,** 1169–1178.

Melander Gradin, H., Larsson, N., Marklund, U., and Gullberg, M. (1998). Regulation of microtubule dynamics by extracellular signals: cAMP-dependent protein kinase switches off the activity of oncoprotein 18 in intact cells. *J. Cell Biol.* **140,** 131–141.

Melander Gradin, H., Marklund, U., Larsson, N., Chatila, T. A., and Gullberg, M. (1997). Regulation of microtubule dynamics by Ca2+/calmodulin-dependent kinase IV/Gr-dependent phosphorylation of oncoprotein 18. *Mol. Cell Biol.* **17,** 3459–3467.

Merdes, A., Heald, R., Samejima, K., Earnshaw, W. C., and Cleveland, D. W. (2000). Formation of spindle poles by dynein/dynactin-dependent transport of NuMA. *J. Cell Biol.* **149,** 851–861.

Merdes, A., Ramyar, K., Vechio, J. D., and Cleveland, D. W. (1996). A complex of NuMA and cytoplasmic dynein is essential for mitotic spindle assembly. *Cell* **87,** 447–458.

Mitchison, T., and Kirschner, M. W. (1984). Dynamic instability of microtubule growth. *Nature* **312,** 237–242.

Michison, T., and Kirschner, M. (1988). Cytoskeletal dynamics and nerve growth. *Neuron* **1,** 761–772.

Mimori-Kiyosue, Y., Shiina, N., and Tsukita, S. (2000a). Adenomatous polyposis coli (APC) protein moves along microtubules and concentrates at their growing ends in epithelial cells. *J. Cell Biol.* **148,** 505–518.

Mimori-Kiyosue, Y., Shiina, N., and Tsukita, S. (2000b). The dynamic behavior of the APC-binding protein EB1 on the distal ends of microtubules. *Curr. Biol.* **10,** 865–868.

Miyata, Y., Hoshi, M., Nishida, E., Minami, Y., and Sakai, H. (1986). Binding of microtubule-associated protein 2 and tau to the intermediate filament reassembled from neurofilament 70-kDa subunit protein. *J. Biol. Chem.* **261,** 13,026–13,030.

Mori, A., Aizawa, H., Saido, T. C., Kawasaki, H., Mizuno, K., Murofushi, H., Suzuki, K., and Sakai, H. (1991). Site-specific phosphorylation by protein kinase C inhibits assembly-promoting activity of microtubule-associated protein 4. *Biochemistry* **30,** 9341–9346.

Morishima-Kawashima, M., Hasegawa, M., Takio, K., Suzuki, M., Titani, K., and Ihara, Y. (1993). Ubiquitin is conjugated with amino-terminally processed tau in paired helical filaments. *Neuron* **10,** 1151–1160.

Morishima-Kawashima, M., and Kosik, K. S. (1996). The pool of MAP kinase associated with microtubules is small but constitutively active. *Mol. Biol. Cell* **7,** 893–905.

Morrison, E. E., Askham, J. M., Clissold, P., Markham, A. F., and Meredith, D. M. (1997). The cellular distribution of the adenomatous polyposis coli tumour suppressor protein in neuroblastoma cells is regulated by microtubule dynamics. *Neuroscience* **81,** 553–563.

Morrison, E. E., Wardleworth, B. N., Askham, J. M., Markham, A. F., and Meredith, D. M. (1998). EB1, a protein which interacts with the APC tumour suppressor, is associated with the microtubule cytoskeleton throughout the cell cycle. *Oncogene* **17,** 3471–7.

Muhua, L., Adames, N. R., Murphy, M. D., Shields, C. R., and Cooper, J. A. (1998). A cytokinesis checkpoint requiring the yeast homolog of an APC-binding protein. *Nature.* **393,** 487–491.

Muller, R., Kindler, S., and Garner, C. C. (1994). The MAP1 Family. *In* "Microtubules" (J. S. Hyams and C. W. Lloyd, Eds), pp. 141–154. Wiley-Liss, New York.

Munesitsu, S., Albert, I., Souza, B., Rubinfeld, B., and Polakis, P. (1995). Regulation of intracellular β-catenin levels by the adenomatous polyposis coli (APC) tumor suppressor protein. *Proc. Natl. Acad. Sci. USA* **92,** 3046–3050.

Munemitsu, S., Souza, B., Muller, O., Albert, I., Rubinfeld, B., and Polakis, P. (1994). The APC gene product associates with microtubules in vivo and promotes their assembly in vivo. *Cancer Res.* **54,** 3676–3681.

Murphy, M., Ahn, J., Walker, K. K., Hoffman, W. H., Evans, R. M., Levine, A. J., and George, D. L. (1999). Transcriptional repression by wild-type p53 utilizes histone deacetylases, mediated by interaction with mSin3a. *Genes Dev.* **13,** 2490–2501.

Murphy, M., Hinman, A., and Levine, A. J. (1996). Wild-type p53 negatively regulates the expression of a microtubule-associated protein. *Genes Dev.* **10,** 2971–80.

Murphy, D. B., Johnson, K. A., and Borisy, G. G. (1977). Role of tubulin-associated proteins in microtubule nucleation and elongation. *J. Mol. Biol.* **117,** 33–52.

Nabeshima, K., Kurooka, H., Takeuchi, M., Kinoshita, K., Nakaseko, Y., and Yanagida, M. (1995). p93$^{\text{disl}}$, which is required for sister chromatid separation, is a novel microtubule and spindle pole body-associating protein phosphorylated at the cdc2 target sites. *Genes Dev.* **9,** 1572–1585.

Nachury, M. V., Maresca, T. J., Salmon, W. C., Waterman-Storer, C. M., Heald, R., and Weis, K. (2001). Importin beta is a mitotic target of the small GTPase Ran in spindle assembly. *Cell* **104,** 95–106.

Nagawaa, H., Koyama, K., Murata, Y., Morito, M., Akiyama, T., and Nakamura, Y. (2000). EB3,

a novel member of the EB1 family preferentially expressed in the central nervous system, binds to a CNS-specific APC homologue. *Oncogene* **19,** 210–216.

Nagawaa, H., Murata, Y., Koyama, K., Fujiyama, A., Miyoshi, Y., Nonden, M., Akiyama, T., and Nakamura, Y. (1998). Identification of a brain-specific APC homologue, APCL, and its interaction with beta-catenin. *Cancer Res.* **15,** 5176–5181.

Nakaseko, Y., Nabeshima, K., Kinoshita, K., and Yanagida, M. (1996). Dissection of fission yeast microtubule associating protein p93Dis1: Regions implicated in regulated localization and microtubule interaction. *Genes Cells.* **1,** 633–644.

Nathke, I. S. (1999). The adenomatous polyposis coli protein. *Mol. Pathol.* **52,** 169–173.

Nathke, I. S., Adams, C. L., Polakis, P., Sellin, J. H., and Nelson, W. J. (1996). The adenomatous polyposis coli tumor suppressor protein localizes to plasma membrane sites involved in active cell migration. *J. Cell Biol.* **134,** 165–179.

Neve, R. L., Harris, P., Kosik, K. S., Kurnit, D. M., and Donion, T. A. (1986). Identification of cDNA clones for the human microtubule-associated protein tau and chromosomal localization of the genes for tau and microtubule-associated protein 2. *Brain Res.* **387,** 271–280.

Neufeld, K. L., Nix, D. A., Bogerd, H., Kang, Y., Beckerle, M. C., Cullen, B. R., and White, R. L. (2000). Adenomatous polyposis coli protein contains two nuclear export signals and shuttles between the nucleus and cytoplasm. *Proc. Natl. Acad. Sci. USA* **97,** 12,085–12,090.

Nguyen, H.-L., Chari, S., Gruber, D., Lue, C.-M., Chapin, S. J., and Bulinski, J. C. (1997). Overexpression of full- or partial-length MAP4 stabilizes microtubules and alters cell growth. *J. Cell Sci.* **110,** 281–294.

Nguyen, H. L., Gruber, D., and Bulinski, J. C. (1999). Microtubule-associated protein 4 (MAP4) regulates assembly, protomer–polymer partitioning and synthesis of tubulin in cultured cells. *J. Cell Sci.* **112,** 1813–1824.

Nishida, E., Hoshi, M., Miyata, Y., Sakai, H., Kadowaki, T., Kasuga, M., Saijo, S., Ogawara, H., and Akiyama, T. (1987). Tyrosine phosphorylation by the epidermal growth factor receptor kinase induces functional alterations in microtubule-associated protein 2. *J. Biol. Chem.* **262,** 16,200–16,204.

Noble, M., Lewis, S. A., and Cowan, N. J. (1989). The microtubule binding domain of microtubule-associated protein MAP1B contains a repeated sequence motif unrelated to that of MAP2 and tau. *J. Cell Biol.* **109,** 3367–3376.

Nogales, E., Whittaker, M., Milligan, R. A., and Downing, K. H. (1999). High-resolution model of the microtubule. *Cell* **96,** 79–88.

Nogales, E., Wolf, S. G., and Downing, K. (1998). Structure of the $\alpha\beta$ tubulin dimer by electron crystallography. *Nature* **391,** 199–203.

Ohba, T., Nakamura, M., Nishitani, H., and Nishimoto, T. (1999). Self-organization of microtubule asters induced in *Xenopus* egg extracts by GTP-bound Ran. *Science* **284,** 1356–8.

Okabe, S., and Hirokawa, N. (1989). Rapid turnover of microtubule-associated protein MAP2 in the axon revealed by microinjection of biotinylated MAP2 into cultured neurons. *Proc. Natl. Acad. Sci. USA* **86,** 4127–4131.

Olson, K. R., McIntosh, J. R., and Olmsted, J. B. (1995). Analysis of MAP 4 function in living cells using green fluorescent protein (GFP) chimeras. *J. Cell Biol.* **130,** 639–650.

Ookata, K., Hisanaga, S., Bulinski, J. C., Murofushi, H., Aizawa, H. T., Itoh, J., Hotani, H., Okumura, E., Tachibana, K., and Kishimoto, T. (1995). Cyclin B interaction with microtubule-associated protein 4 (MAP4) targets p34^{cdc2} kinase to microtubules and is a potential regulator of M-phase microtubule dynamics. *J. Cell Biol.* **128,** 849–862.

Ookata, K., Hisanaga, S., Sugita, M., Okuyama, A., Murofushi, H., Kitazawa, H., Chari, S., Bulinski, J. C., and Kishimoto, T. (1997). MAP4 is the in vivo substrate for CDC2 kinase in HeLa cells: Identification of an M-phase specific and a cell cycle-independent phosphorylation site in MAP4. *Biochemistry* **36,** 15,873–15,883.

Ozer, R. S., and Halpain, S. (2000). Phosphorylation-dependent localization of microtubule-associated protein MAP2c to the actin cytoskeleton. *Mol. Biol. Cell* **11,** 3573–3587.

Ozon, S., Maucuer, A., and Sobel, A. (1997). The stathmin family. *Eur. J. Biochem.* **248,** 794–806.

Panda, D., Miller, H. P., Banerjee, A., Luduena, R. F., and Wilson, L. (1994). Microtubule dynamics in vitro are regulated by the tubulin isotype composition. *Proc. Natl. Acad. Sci. USA* **91,** 11,358–11,362.

Panda, D., Miller, H. P., and Wilson, L. (1999). Rapid treadmilling of brain microtubules free of microtubule-associated proteins in vitro and its suppression by tau. *Proc. Natl. Acad. Sci. USA* **96,** 12,459–12,464.

Papandrikopoulous, A., Doll, T., Tucker, R. P., Garner, C. C., and Matus, A. (1989). Embryonic MAP2 lacks the cross-linking sidearm sequences and dendritic targeting signal of adult MAP2. *Nature* **340,** 650–652.

Parysek, L. M., Wolosewick, J. J., and Olmstead, J. B. (1984). MAP4: A microtubule-associated protein specific for a subset of tissue microtubules. *J. Cell Biol.* **99,** 2287–2296.

Parsons, S. F., and Salmon, E. D. (1997). Microtubule assembly in clarified *Xenopus* egg extracts. *Cell Motil. Cytoskeleton* **36,** 1–11.

Pattnaik, B., Jellali, A., Sahel, J., Dreyfus, H., and Picaud, S. (2000). GABAc receptors are localized with the microtubule-associated protein 1B in mammalian cone photoreceptors. *J. Neurosci.* **20,** 6789–6796.

Paudel, H., Lew, J., Ali, Z., and Wang, J. (1993). Brain proline-directed protein kinase phosphorylates tau on sites that are abnormally phosphorylated in tau associated with Alzheimer's paired helical filaments. *J. Biol. Chem.* **268,** 23,512–23,518.

Pedrotti, B., Colombo, R., and Islam, K. (1994). Microtubule associated protein MAP1A is an actin-binding and crosslinking protein. *Cell Motil. Cytoskeleton* **29,** 110–116.

Pedrotti, B., Francolini, M., Cotelli, F., and Islam, K. (1996). Modulation of microtubule shape in vitro by high molecular weight microtubule associated proteins MAP1A, MAP1B and MAP2. *FEBS Lett.* **384,** 147–150.

Pedrotti, B., and Islam, K. (1994). Purified native microtubule associated protein MAP1A: Kinetics of microtubule assembly and MAP1A/tubulin stoichiometry. *Biochemistry* **33,** 12,463–12,470.

Pedrotti, B., and Islam, K. (1996). Dephosphorylated but not phosphorylated microtubule associated protein MAP1B binds to microfilaments. *FEBS Lett.* **388,** 131–133.

Pei, Q., Burnet, P. J., and Zetterstrom, T.S. (1998). Changes in mRNA abundance of microtubule-associated proteins in the rat brain following electroconvulsive shock. *Neuroreport* **9,** 391–394.

Peifer, M. (1996). Regulating cell proliferation: As easy as APC. *Science* **272,** 974–975.

Peifer, M., and Polakis, P. (2000). Wnt signaling in oncogenesis and embryogenesis—a look outside the nucleus. *Science* **287,** 1606–1609.

Perez, F., Diamantopoulos, G. S., Stalder, R., and Kreis, T. E. (1999). CLIP-170 highlights growing microtubule ends *in vivo. Cell* **96,** 517–527.

Pierre, P., Sheel, J., Rickard, J. E., and Kreis, T. E. (1992). CLIP-170 links endocytic vesicles to microtubules. *Cell* **70,** 887–900.

Pigino, G., Paglini, G., Ulloa, L., Avila, J., and Caceres, A. (1997). Analysis of the expression, distribution and function of cyclin dependent kinase 5 (cdk5) in developing cerebellar macroneurons. *J. Cell Sci.* **110** (Pt.2), 257–270.

Polakis, P. (1997). The adenomatous polyposis coli (APC) tumor suppressor. *Biochim. Biophys. Acta* **1332,** F127–F147.

Pollack, A. L., Barth, A. I. M., Altschuler, Y., Nelson, W. J., and Mostov, K. E. (1997). Dynamics of beta-catenin interactions with APC protein regulate epithelial tubulogenesis. *J. Cell Biol.* **137,** 1651–1662.

Poorkaj, P., Bird, T. D., Wijsman, E., Nemens, E., Garruto, R. M., Anderson, L., Andreadis, A., Wiederholt, W. C., Raskind, M., and Schellenberg, G.D. (1998). Tau is a candidate gene for chromosome 17 frontotemporal dementia. *Ann. Neurol.* **43,** 815–825.

Preuss, U., Biernat, J., Mandelkow, E. M., and Mandelkow, E. (1997). The "jaws" model of tau-microtubule interaction examined in CHO cells. *J. Cell Sci.* **110,** 789–800.

Price, C. M., and Pettijohn, D. E. (1986). Redistribution of the nuclear mitotic apparatus protein (NuMA) during mitosis and nuclear assembly. *Exp. Cell Res.* **166,** 295–311.

Pryer, N. K., Walker, R. A., Skeen, V. P., Bourns, B. D., Soboeiro, M. F., and Salmon, E. D. (1992). Brain microtubule-associated proteins modulate microtubule dynamic instability *in vitro*. Real-time observations using video microscopy. *J. Cell Sci.* **103,** 965–976.

Quarmby, L. (2000). Cellular samurai: Katanin and the severing of microtubules. *J. Cell Sci.* **113,** 2821–2827.

Quinlan, E. M., and Halpain, S. (1996). Postsynaptic mechanisms for bidirectional control of MAP2 phosphorylation by glutamate receptors. *Neuron* **16,** 357–368.

Riederer, B., and Matus, A. (1985). Differential expression of distinct microtubule- associated proteins during brain development. *Proc. Natl. Acad. Sci. USA* **82,** 6006–6009.

Riederer, B. M., Pellier, V., Antonsson, B., Di Paolo, G., Stimpson, S.A., Lutjens, R., Catsicas, S., and Grenningloh, G. (1997). Regulation of microtubule dynamics by the neuronal growth-associated protein SCG10. *Proc. Natl. Acad. Sci. USA* **94,** 741–745.

Rickard, J. E., (1999). CLIP-170. *In* "Guidebook to Cytoskeletal Proteins" (T. Kreis and R. Vale, Eds.), 2nd ed., pp. 199–202. Oxford University Press, Oxford.

Rickard, J. E., and Kreis, T. E. (1991). Binding of pp170 to microtubules is regulated by phosphorylation. *J. Biol. Chem.* **266,** 17,597–17,605.

Rodionov, V. I., and Borisy, G. G. (1997). Microtubule treadmilling *in vivo. Science* **275,** 215–218.

Rubinfeld, B., Albert, I., Porfiri, E., Fiol, C., Munemitsu, S., and Polakis, P. (1996). Binding of GSK3β to the APC-β-catenin complex and regulation of complex assembly. *Science* **272,** 1023–1026.

Rubinfeld, B., Souza, B., Albert, I., Muller, O., Chamberlain, S. H., Masiarz, F. R., Munemitsu, S., and Polakis, P. (1993). Association of the APC gene product with β-catenin. *Science* **262,** 1731–1734.

Rubinfeld, B., Souza, B., Albert, I., Munemitsu, S., and Polakis, P. (1995). The APC protein and E-cadherin form similar but independent complexes with alpha-catenin, β-catenin, and plakoglobin. *J. Biol. Chem.* **270,** 5549–5555.

Sabbatini, P., Chiou, S. K., Rao, L., and White, E. (1995). Modulation of p53-mediated transcriptional repression and apoptosis by the adenovirus E1B-19K protein. *Mol. Cell Biol.* **15,** 1060–1070.

Sadot, E., Heicklen-Klein, A., Barg, J., Lazarovici, P., and Ginzberg, I. (1996). Identification of a tau promoter region mediating tissue-specific-regulated expression in PC12 cells. *J. Mol. Biol.* **256,** 805–812.

Sammak, P. J., and Borisy, G. G. (1988). Direct observation of microtubule dynamics in living cells. *Nature* **332,** 724–726.

Sanchez, C., Diaz-Nido, J., and Avila, J. (2000). Phosphorylation of microtubule-associated protein 2 (MAP2) and its relevance for the regulation of the neuronal cytoskeleton function. *Prog. Neurobiol.* **61,** 133–168.

Sapir, T., Elbaum, M., and Reiner, O. (1997). Reduction of microtubule catastrophe events by LIS1, platelet-activating factor acetylhydrolase subunit. *EMBO J.* **16,** 6977–6984.

Saredi, A., Howard, L., and Compton, D. A. (1997). Phosphorylation regulates the assembly of NuMA in a mammalian mitotic extract. *J. Cell Sci.* **110,** 1287–1297.

Sato-Yoshitake, R., Shiomura, Y., Miyasaka, H., and Hirokawa, N. (1989). Microtubule-associated protein 1B: Molecular structure, localization, and phosphorylation-dependent expression in developing neurons. *Neuron* **3,** 229–238.

Saunders, W., Hornack, D., Lengyel, V., and Deng, C. (1997). The *Saccharomyces cerevisiae* kinesin-related motor kar3p acts at preanaphase spindle poles to limit the number and length of cytoplasmic microtubules. *J. Cell. Biol.* **137,** 417–431.

Saxton, W. M., Stemple, D. L., Leslie, R. J., Salmon, E. D., Zavortink, M., and McIntosh, J. R. (1984). Tubulin dynamics in cultured mammalian cells. *J. Cell. Biol.* **99,** 2175–2186.

Schaar, B. T., Chan, G. K. T., Maddox, P., Salmon, E. D., and Yen, T. J. (1997). CENP-E function at kinetochores is essential for chromosome alignment. *J. Cell. Biol.* **139,** 1373–1382.

Schaar, B. T., Kinoshita, K., Hyman, A., and McConnell, S. (2000). Regulation of the microtubule binding protein, doublecortin. *Mol. Biol. Cell.* **11,** 199a.

Schwartz, K., Richards, K., and Botstein, D. (1997). Bim1 encodes a microtubule-binding protein in yeast. *Mol. Biol. Cell* **8,** 2677–2691.

Shiina, N., and Tsukita, S. (1999). Mutations at phosphorylation sites of Xenopus microtubule-associated protein 4 affect its microtubule-binding ability and chromosome movement during mitosis. *Mol. Biol. Cell.* **10,** 597–608.

Schoenfeld, T. A., McKerracher, L., Obar, R., and Vallee, R. (1989). MAP1A and MAP1B are structurally related microtubule associated proteins with distinct developmental patterns in the CNS. *J. Neurosci.* **9,** 1712–1730.

Schubart, U. K., Yu, J., Amat, J. A., Wang, Z., Hoffman, M. K., and Edelmann, W. (1996). Normal development of mice lacking metablastin (P19), a phosphoprotein implicated in cell cycle regulation. *J. Biol. Chem.* **271,** 14,062–14,066.

Schulze, E., and Kirschner, M. (1988). New features of microtubule dynamic instability behavior observed *in vivo*. *Nature* **334,** 356–359.

Seldon, S. C., and Pollard, T. D. (1983). Phosphorylation of microtubule-associated proteins regulates their interaction with actin filaments. *J. Biol. Chem.* **258,** 7064–7071.

Shafit-Zagardo, B., and Kalcheva, N. (1998). Making sense of the multiple MAP-2 transcripts and their role in the neuron. *Mol. Neurobiol.* **16,** 149–162.

Shafit-Zagardo, B., Kress, Y., Zhao, M. L., and Lee, S. C. (1999). A novel microtubule-associated protein-2 expressed in oligodendrocytes in multiple sclerosis lesions. *J. Neurochem.* **73,** 2531–2537.

Sharma, N., Kress, Y., and Shafit-Zargado, B. (1994). Antisense MAP-2 oligonucleotides induce changes in microtubule assembly and neuritic elongation in pre-existing neurites of rat cortical neurons. *Cell Motil. Cytoskeleton* **27,** 234–247.

Shen, M., Stukenberg, P. T., Kirschner, M. W., and Lu, K.P. (1998). The essential mitotic peptidyl-prolyl isomerase Pin1 binds and regulates mitosis-specific phosphoproteins. *Genes Dev.* **12,** 706–720.

Shen, Y., and Shenk, T. (1994). Relief of p53-mediated transcriptional repression by the adenovirus E1B 19 kDa protein or the cellular bcl-2 protein. *Proc. Natl. Acad. Sci. USA* **89,** 8940–8944.

Shiina, N., Moriguchi, T., Ohta, K., Gotoh, Y., and Nishida, E. (1992). Regulation of a major microtubule-associated protein by MPF and MAP kinase. *EMBO J.* **11,** 3977–3984.

Shiina, N., and Tsukita, S. (1999). Mutations at phosphorylation sites of *Xenopus* microtubule-associated protein 4 affect its microtubule-binding ability and chromosome movement during mitosis. *Mol. Biol Cell.* **10,** 597–608.

Simon, J. R., and Salmon, E.D. (1990). The structure of microtubule ends during the elongation and shortening phases of dynamic instability examined by negative-stain electron microscopy. *J. Cell Sci.* **96,** 571–582.

Smertenko, A., Saleh, N., Igarashi, H., Mori, H., Hauser-Hahn, I., Jiang, C. J., Sonobe, S., Lloyd, C. W., and Hussey, P. J. (2000). A new class of microtubule-associated proteins in plants. *Nat. Cell Biol.* **2,** 750–753.

Smirnova, O. A., and Roof, D.M. (2000). The kinesin Kip3p of Saccaromyces cerevisiae depolymerizes microtubules in vitro. *Mol. Biol. Cell* **11,** 358a.

Smith, K. J., Levy, D. B., Maupin, P., Pollard, T.D., Vogelstein, B., and Kinzler, K. W. (1994). Wild-type but not mutant APC associates with the microtubule cytoskeleton. *Cancer Res.* **54,** 3672–3675.

Sobel, A. (1991). Stathmin: A relay phosphoprotein for multiple signal transduction? *Trends Biochem. Sci.* **16,** 301–305.

Solomon, F., Magendantz, M., and Salzman, A. (1979). Identification with cellular microtubules of one of the co-assembling microtubule-associated proteins. *Cell* **18,** 431–438.

Sontag, E., Nunbhakdi-Craig., V., Bloom, G. S., and Mumby., M. C. (1995). A novel pool of protein phosphatase 2A is associated with microtubules and is regulated during the cell cycle. *J. Cell Biol.* **128,** 1131–1144.

Sontag, E., Nunbhakdi-Craig, V., Lee, G., Bloom, G. S., and Mumby, M. C. (1996). Regulation of the phosphorylation state and microtubule-binding activity of tau by protein phosphatase 2A. *Neuron* **17,** 1201–1207.

Sparks, C. A., Fey, E. G., Vidair, C. A., and Doxey, S. J. (1995). Phosphorylation of NuMA occurs during nuclear envelope breakdown and not mitotic spindle assembly. *J. Cell Sci.* **108,** 3389–3396.

Spillantini, M. G., Murrell, J. R., Goedert, M., Farlow, M. R., Klug, A., and Ghetti, B. (1998). Mutation in the tau gene in familial multiple system tauopathy with presenile dementia. *Proc. Natl. Acad. Sci. USA* **95,** 7737–7741.

Spittle, C., Charrasse, S., Larroque, C., and Cassimeris, L. (2000). The Interaction of TOGp with microtubules and tubulin. *J. Biol. Chem.* **275,** 20,748–20,753.

Springer, J. E., Azbill, R. D., Kennedy, S. E., George, J., and Geddes, J. W. (1997). Rapid calpain I activation and cytoskeletal protein degradation following traumatic spinal cord injury: Attenuation with riluzole pretreatment. *J. Neurochem.* **69,** 1592–1600.

Stebbings, H., and Hyams, J. S. (1979). "Cell Motility," pp. 45–48. Longman Group, London.

Steinmetz, M. O., Kammerer, R. A., Jahnke, W., Goldie, K. N., Lustig, A., and van Oostrum, J. (2000). Op18/stathmin caps a kinked protofilament-like tubulin tetramer. *EMBO J.* **19,** 572–580.

Su, L. K., Burrell, M., Hill, D. E., Gyuris, J., Brent, R., Wiltshire, R., Trent, J., Vogelstein, B., and Kinzler, K. W. (1995). APC binds to the novel protein EB1. *Cancer Res.* **55,** 2972–2977.

Suprenant, K. A., Dean, K., McKee, J., and Hake, S. (1993). EMAP, an echinoderm microtubule-associated protein found in microtubule-ribosome complexes. *J. Cell Sci.* **104,** 445–450.

Suprenant, K. A., and Marsh, J. C. (1987). Temperature and pH govern the self-assembly of microtubules from unfertilized sea-urchin egg extracts. *J. Cell Sci.* **87,** 71–84.

Suprenant, K. A., Tuxhorn, J. A., Daggett, M. A. F., Ahrens, D. P., Hostetler, A., Palange, J. M., VanWinkle, C. E., and Livingstone, B. T. (2000). Conservation of the WD-repeat, microtubule-binding protein, EMAP, in sea urchins, humans, and the nematode *C. elegans*. *Dev. Genes Evol.* **210,** 2–10.

Surridge, C. D., and Burns, R. G. (1994). The difference in the binding of phosphatidylinositol distinguishes MAP2 from MAP2C and Tau. *Biochemistry* **33,** 8051–8057.

Taft, W. C., Yang, K., Dixon, C. E., and Hayes, R. L. (1992). Microtubule-associated protein 2 levels decrease in hippocampus following traumatic brain injury. *J. Neurotrauma* **9,** 281–290.

Takei, Y., Kondo, S., Harada, A., Inomata, S., Noda, T., and Hirokawa, N. (1997). Delayed development of nervous system in mice homozygous for disrupted microtubule-associated protein 1B (MAP1B) gene. *J. Cell Biol.* **137,** 1615–1626.

Takei, Y., Teng, J., Harada, A., and Hirokawa, N. (2000). Defects in axonal elongation and neuronal migration in mice with disrupted tau and map1b genes. *J. Cell Biol.* **150,** 989–1000.

Takemura, R., Okabe, S., Umeyama, T., Kanai, Y., Cowan, N. J., and Hirokawa, N. (1992). Increased microtubule stability and alpha tubulin acetylation in cells transfected with microtubule-associated proteins MAP1B, MAP2 or tau. *J. Cell Sci.* **103,** 953–964.

Tang, T. K., Tang, C. J., Chen, Y. L., and Wu, C. W. (1993). Nuclear proteins of the bovine esophageal epithelium. II. The NuMA gene gives rise to multiple mRNAs and gene products reactive with monoclonal antibody W1. *J. Cell Sci.* **104,** 249–260.

Tang, T. K., Tang, C. C., Chao, Y. J., and Wu, C. W. (1994). Nuclear mitotic apparatus protein (NuMA): Spindle association, nuclear targeting, and differential subcellular localization of various NuMA isoforms. *J. Cell Sci.* **107,** 1389–1402.

Taylor, K. R., Holzer, A. K., Bazan, J. F., Walsh, G. A., and Gleeson, J. G. (2000). Patient mutations in doublecortin define a repeated tubulin-binding domain. *J. Biol. Chem.* **275,** 34,442–34,450.

Theurkauf, W. E., and Vallee, R. B. (1983). Extensive cAMP-dependent and cAMP-independent phosphorylation of microtubule-associated protein 2. *J. Biol. Chem.* **258,** 7883–7886.

Tirnauer, J. S., and Bierer, B. E. (2000). EB1 proteins regulate microtubule dynamics, cell polarity, and chromosome stability. *J. Cell Biol.* **149,** 761–766.

Tirnauer, J. S., O'Toole, E., Berrueta, L., Bierer, B., and Pellman, D. (1999). Yeast Bim1p promotes G1-specific dynamics of microtubules. *J. Cell Biol.* **145,** 993–1007.

Togel, M., Wiche, G., and Propst, F. (1998). Novel features of the light chain of microtubule-associated

protein MAP1B: Microtubule stabilization, self interaction, actin filament binding, and regulation by the heavy chain. *J. Cell Biol.* **143,** 695–707.

Tokuraku, K., Katsuki, M., Matui, T., Kuroya, T., and Kotani, S. (1999b). Microtubule-binding property of microtubule-associated protein 2 differs from that of microtubule-associated protein 4 and tau. *J. Biochem.* **264,** 996–1001.

Tokuraku, K., Katsuiki, M., Nakagawa, H., and Kotani, S. (1999). A new model for microtubule-associated protein (MAP)-induced microtubule assembly. *Eur. J. Biochem.* **259,** 158–166.

Tournebize, R., Andersen, S. S. L., Verde, F., Doree, M., Karsenti, E., and Hyman, A. (1997). Distinct roles of PP1 and PP2A-like phosphatases in control of microtubule dynamics during mitosis. *EMBO J.* **16,** 5537–5549.

Tournebize, R., Popov, A., Kinoshita, K., Ashford, A. J., Rybina, S., Pozniakovsky, A., Mayer, T. U., Walczak, C. E., Karsenti, E., and Hyman, A. A. (2000). Control of microtubule dynamics by the antagonistic activities of XMAP215 and XKCM1 in *Xenopus* egg extracts. *Nat. Cell Biol.* **2,** 13–19.

Tousson, A., Zeng, C., Brinkley, B. R., and Valdivia, M. M. (1991). Centrophilin: A novel mitotic spindle protein involved in microtubule nucleation. *J. Cell Biol.* **112,** 427–440.

Trinczek, B., Biernat, J., Baumann, K., Mandlekow, E.-M., and Mandelkow, E. (1995). Domains of tau protein, differential phosphorylation, and dynamic instability of microtubules. *Mol. Biol. Cell.* **6,** 1887–1902.

Trzepacz, C., Lowy, A. M., Kordich, J. J., and Groden, J. (1997). Phosphorylation of the tumor suppressor adenomatous polyposis coli (APC) by the cyclin-dependent kinase p34. *J. Biol. Chem.* **272,** 21,681–21,684.

Tsuyama, S., Terayama, Y., and Matsuyama, S. (1987). Numerous phosphates of microtubule associated protein 2 in living rat brain. *J. Biol. Chem.* **262,** 10,886–10,892.

Ulitzur, N., Humbert, M., and Pfeffer, S. R. (1997). Mapmodulin: A possible modulator of the interaction of microtubule-associated proteins with microtubules. *Proc. Natl. Acad. Sci. USA* **94,** 5084–5089.

Vaillant, A. R., and Brown, D. L., (1995). Accumulation of microtubule-associated protein 1A (MAP1A) in differentiating P19 embryonal carcinoma cells. *Biochem. Cell Biol.* **73,** 695–702.

Vaillant, A. R., Muller, R., Langkopf, A., and Brown, D. L. (1998). Characterization of the microtubule-binding domain of microtubule-associated protein 1A and its effects on microtubule dynamics. *J. Biol. Chem.* **273,** 13,973–13,981.

Vale, R. D. (1991). Severing of stable microtubules by a mitotically activated protein in Xenopus egg extracts. *Cell* **64,** 827–839.

Vallee, R. (1980). Structure and phosphorylation of microtubule-associated protein 2 (MAP2). *Proc. Natl. Acad. Sci. USA* **77,** 3206–3210.

Vandecandelaere, A., Pedrott, B., Utton, M. A., Calvert, R. A., and Bayley, P. M. (1996). Differences in the regulation of microtubule dynamics by microtubule-associated proteins MAP1B and MAP2. *Cell Motil. Cytoskel.* **35,** 134–146.

Vasquez, R. J., Gard, D. L., and Cassimeris, L. (1994). XMAP from *Xenopus* eggs promote rapid plus end assembly of microtubules and rapid microtubule polymer turnover. *J. Cell Biol.* **127,** 985–993.

Vasquez, R. J., Gard, D. L., and Cassimeris, L. (1999). Phosphorylation by CDK1 regulates XMAP215 function in vitro. *Cell Motil. Cytoskel.* **43,** 310–321.

Vaughan, K. T., Tynan, S. H., Faulkner, N. E., Echeverri, C. J., and Vallee, R. B. (1999). Colocalization of cytoplasmic dynein with dynactin and CLIP-170 at microtubule distal ends. *J. Cell Sci.* **112,** 1437–1447.

Vleminckx, K., Wong, E., Guger, K., Rubinfeld, B., Polakis, P., and Gumbiner, B. M. (1997). Adenomatous polyposis coli tumor suppressor protein has signaling activity in *Xenopus laevis* embryos resulting in the induction of an ectopic dorsoanterior axis. *J. Cell Biol.* **136,** 411–420.

Walczak, C. E., Mitchison, T. J., and Desai, A. (1996). XKCM1: A *Xenopus* kinesin-related protein that regulates microtubule dynamics during mitotic spindle assembly. *Cell.* **84,** 37–47.

Walker, R. A., O'Brien, E. T., Pryer, N. K., Soboeiro, M. F., Voter, W. A., Erickson, H. P., and Salmon, E. D. (1988). Dynamic instability of individual, MAP-free microtubules analyzed by video light microscopy: Rate constants and transition frequencies. *J. Cell Biol.* **107,** 1437–1448.

Wang, P. J., and Huffaker, T. C. (1997). Stu2p: A microtubule-binding protein that is an essential component of the yeast spindle pole body. *J. Cell Biol.* **139,** 1271–1280.

Wang, X. M., Peloquin, J. G., Zhai, Y., Bulinski, J. C., and Borisy, G. G. (1996). Removal of MAP4 from microtubules in vivo produces no discernable phenotype at the cellular level. *J. Cell Biol.* **132,** 349–358.

Watanabe, A., Hasegawa, M., Suzuki, M., Takio, K., Morishima-Kawashima, M., Titani, K., Arai, T., Kosik, K. S., and Ihara, Y. (1993). In vivo phosphorylation sites in fetal and adult rat tau. *J. Biol. Chem.* **268,** 25,712–25,717.

Waterman-Storer, C. M., and Salmon, E. D. (1997). Actomyosin-based retrograde flow of microtubules in the lamella of migrating epithelial cells influences microtubule dynamic instability and turnover and is associated with microtubule breakage and treadmilling. *J. Cell Biol.* **139,** 417–434.

Watts, N. R., Sackett, D. L., Ward, R. D., Miller, M. W., Wingfield, P. T., Stahl, S. S., and Stevens, A. C. (2000). HIV-1 Rev depolymerizes microtubules to form stable bilayered rings. *J. Cell Biol.* **150,** 349–360.

Weingarten, M. D., Lockwood, A. H., Hwo, S. Y., and Kirschner, M. W. (1975). A protein factor essential for microtubule assembly. *Proc. Natl. Acad. Sci. USA* **72,** 1858–1862.

West, R. R., Tenbarge, K. M., and Olmsted, J. B. (1991). A model for microtubule-associated protein 4 structure. *J. Biol. Chem.* **266,** 21,886–21,896.

Whitehead, C. M., and Rattner, J. B. (1998). Expanding the role of HsEg5 within the mitotic and post-mitotic phases of the cell cycle. *J. Cell Sci.* **111,** 2551–2561.

Wick, S. (2000). Plant microtubules meet their MAPs and mimics. *Nat. Cell Biol.* **11,** E204.

Wiese, C., Wilde, A., Moore, M. S., Adam, S. A., Merdes, A., and Zheng., Y. (2001). Role of Importin-{beta} in Coupling Ran to Downstream Targets in Microtubule Assembly. *Science* **291,** 653–656.

Wilde, A., and Zheng, Y. (1999). Stimulation of microtubule aster formation and spindle assembly by the small GTPase Ran. *Science* **284,** 1359–62.

Wittmann, T., Boleti, H., Antony, C., Karsenti, E., and Vernos, I. (1998). Localization of the kinesin-like protein Xklp2 to spindle poles requires a leucine zipper, a microtubule-associated protein, and dynein. *J. Cell Biol.* **143,** 673–685.

Wittmann, T., Wilm, M., Karsenti, E., and Vernos, I. (2000). TPX2, a novel Xenopus MAP involved in spindle pole organization. *J. Cell Biol.* **149,** 1405–1418.

Wong, M. H., Hermiston, M. L., Syder, A. J., and Gordon, J. I. (1996). Forced expression of the tumor suppressor adenomatosis polyposis coli protein induces disordered cell migration in the intestinal epithelium. *Proc. Natl. Acad. Sci. USA* **93,** 9588–9593.

Wordeman, L., and Mitchison, T. (1995). Identification and partial characterization of mitotic centromere-associated kinesin, a kinesin-related protein that associates with centromeres during mitosis. *J. Cell Biol.* **128,** 95–105.

Xia, L., Hai, B., Burnette, D., Thazhath, R., Duan, J., Bre, M. H., Levilliers, N., Gorovsky, M., and Gaertig, J. (2000). Polyglycylation of tubulin is essential and affects cell motility and division in *Tetrahymena thermophila. J. Cell Biol.* **149,** 1097–1106.

Yaffe, M. B., Schutkowskim, M., Shen, M., Zhou, X. Z., Stukenberg, P. T., Rahfeld, J. U., Xu, J., Kuang, J., Kirschner, M. W., Fischer, G., Cantley, L. C., and Lu, K. P. (1997). Sequence-specific and phosphorylation-dependent proline isomerization: A potential mitotic regulatory mechanism. *Science* **278,** 1957–1960.

Yamauchi, E., Titani, K., and Taniguchi, H. (1997). Specific binding of acidic phospholipids to microtubule-associated protein MAP1B regulates its interaction with tubulin. *J. Biol. Chem.* **272,** 22,948–22,953.

Yang, C. H., Lambie, E. J., and Snyder, M. (1992). NuMA: An unusually long coiled-coil related protein in the mammalian nucleus. *J. Cell Biol.* **116,** 1303–1317.

Ye, X., and Sloboda, R. D. (1995). A 62-kDa mitotic apparatus protein required for mitotic progression is sequestered to the interphase nucleus by associating with the chromosomes during anaphase. *Cell Motil. Cytoskel.* **30,** 310–323.

Yeh, E., Skibbens, R. V., Cheng, J. W., Salmon, E. D., and Bloom, K. (1995). Spindle dynamics and cell cycle regulation of dynein in the budding yeast, *Saccharomyces cerevisiae. J. Cell Biol.* **130,** 687–700.

Yen, T. J., Compton, D. A., Wise, D., Zinkowski, R. P., Brinkley, B. R., Earnshaw, W. C., and Cleveland, D. W. (1991). CENP-E, a novel human centromere-associated protein required for progression from metaphase to anaphase. *EMBO J.* **10,** 1245–1254.

Yen, T. J., Li, G., Schaar, B. T., Szilak, I., and Cleveland, D. W. (1992). CENP-E is a putative kinetochore motor that accumulates just before mitosis. *Nature* **359,** 536–539.

Yoshida, T., Imanaka-Yoshida, K., Murofushi, H., Tanaka, J., Ito, H., and Inagak, i M. (1996). Microinjection of intact MAP4 and fragments induces changes of the cytoskeleton in PtK2 cells. *Cell Motil. Cytoskeleton* **33,** 252–262.

Yucel, J. K., Marszalek, J. D., McIntosh, J. R., Goldstein, L. S. B., Cleveland, D. W., and Philp, A. V. (2000). CENP-meta, an essential kinetochore kinesin required for the maintenance of metaphase chromosome alignment in Drosophila. *J. Cell Biol.* **150,** 1–11.

Zauner, W., Kratz, J., Staunton, J., Feick, P., and Wiche, G. (1992). Identification of two distinct microtubule binding domains on recombinant rat MAP 1B. *Eur. J. Cell Biol.* **57,** 66–74.

Zecevic, M., Catling, A. D., Eblen, S. T., Renzi, L., Hittle, J. C., Yen, T. J., Gorbsky, G. J., and Weber, M. J. (1998). Active MAP kinase in mitosis: localization at kinetochores and association with the motor protein CENP-E. *J. Cell Biol.* **142,** 1547–1558.

Zeng, C., He, D., and Brinkley, B. R. (1994). Localization of NuMA protein isoforms in the nuclear matrix of mammalian cells. *Cell Motil. Cytoskel.* **29,** 167–176.

Zhang., C., Hughes, M., and Clarke, P. R. (1999). Ran-GTP stabilises microtubule asters and inhibits nuclear assembly in Xenopus egg extracts. *J. Cell Sci.* **112,** 2453–2461.

Zhang, F., White, R. L., and Neufeld, K. L. (2000). Phosphorylation near nuclear localization signal regulates nuclear import of adenomatous polyposis coli protein. *Proc. Natl. Acad. Sci. USA* **97,** 12,577–12,582.

Zhang, C. C., Yang, J. M., White, E., Murphy, M., Levine, A., and Hait, W. N. (1998). The role of MAP4 expression in the sensitivity to paclitaxel and resistance to vinca alkaloids in p53 mutant cells. *Oncogene* **16,** 1617–1624.

Dynein Motors of the *Chlamydomonas* Flagellum

Linda M. DiBella and Stephen M. King

Department of Biochemistry,University of Connecticut Health Center,
Farmington, Connecticut 06032

Chlamydomonas is a biflagellate unicellular green alga that has proven especially amenable for the analysis of microtubule (MT)-based molecular motors, notably dyneins. These enzymes form the inner and outer arms of the flagellum and are also required for intraflagellar transport. Dyneins have masses of ~1–2 MDa and consist of up to 15 different polypeptides. Nucleotide binding/hydrolysis and MT motor activity are associated with the heavy chains, and we detail here our current model for the substructural organization of these ~520-kDa proteins. The remaining polypeptides play a variety of roles in dynein function, including attachment of the motor to cargo, regulation of motor activity in response to specific inputs, and their necessity for the assembly and/or stability of the entire complex. The combination of genetic, physiological, structural, and biochemical approaches has made the *Chlamydomonas* flagellum a very powerful model system in which to dissect the function of these fascinating molecular motors.

KEY WORDS: Axoneme, *Chlamydomonas*, Dynein, Flagellum, Microtubule, Motility.   © 2001 Academic Press.

I. Introduction

Chlamydomonas is a unicellular green alga that has proven of great utility as a model system for the analysis of many cellular activities. This organism is motile and has two flagella (~12 μm in length) that protrude from one end of the cell. *Chlamydomonas* may be grown in large quantities and the flagella detached, isolated, and used as the starting material for the purification and biochemical analysis of individual flagellar components. In addition to biochemical studies,

Chlamydomonas has facile genetics that has proven of immense use in the dissection of complex cellular pathways, and there now exist many mutant strains that exhibit defects in specific cellular systems. More recently molecular as well as classical genetics has become possible in this model system, allowing for the detailed dissection of specific cellular activities. For example, it is now feasible to rescue mutations by incorporation of wildtype genes and to analyze designed mutant proteins in both wildtype and null genetic backgrounds. Furthermore, *Chlamydomonas* cells exhibit complex swimming behaviors in response to various light stimuli allowing for the analysis of flagellar regulatory pathways. Together, these features have made *Chlamydomonas* an excellent model system in which to dissect the structure and function of the eukaryotic flagellum.

In this review, we describe the dynein microtubule (MT) motors that make up the inner and outer arms of the *Chlamydomonas* flagellum. These enzymes are permanently attached to the A-tubule of one outer doublet MT and transiently interact with the B-tubule of the adjacent doublet to provide the motive force for *Chlamydomonas* flagellar motility. We also discuss a recently identified dynein motor that is required for assembly of the eukaryotic flagellum. In addition, we point out how advances in understanding dyneins in this unicellular model organism have led to intriguing insight into many other dynein-mediated events in both the cilia/flagella and cytoplasm of multicellular organisms, including humans.

II. Genetic Analysis of Flagellar Motility

The isolation of *Chlamydomonas* mutants that exhibit alterations in swimming behavior has allowed the identification of numerous genetic loci essential for assembly and function of the inner and outer arm dyneins within the axoneme. Most of these mutants have been named after the complex with which they associate. Thus, the *oda* mutants (outer dynein arm) affect the outer dynein arms, whereas the *ida* (inner dynein arm) strains are defective for one or more classes of inner arm. There are also several mutations that have received either *pf* (paralyzed flagella) or *fla* (flagellar assembly) designations; several of these have pleiotropic effects on multiple axonemal systems including one or more dyneins. Finally, one dynein (DHC1b) required for retrograde intraflagellar transport (IFT), and thus for flagellar assembly, is encoded at a locus designated *DHC1b*.

A. Outer Arms

In general, the *oda* and *ida* mutations result in loss of an entire dynein structure, although there are some very intriguing exceptions to this (see below). Consequently, analysis of flagellar motility in these strains has revealed clues as to the contribution of different dynein subtypes to the overall motion of the flagellum.

For instance, most of the *oda* mutants completely lack outer arms. As a consequence, flagella from these strains beat at a much lower frequency than wildtype (Kamiya and Okamoto, 1985; Mitchell and Rosenbaum, 1985). Moreover, the *oda* cells swim at greatly reduced velocity in a characteristic jerky manner. Screens for slow swimming strains combined with complementation analysis to two previously identified outer arm mutants (*pf13* and *pf22*) (Huang *et al.,* 1979) identified 10 additional *oda* genes responsible for the assembly of outer dynein arms (Kamiya, 1988). More recently, additional *oda* mutations have been identified, some of which show less severe swimming phenotypes and do not severely affect arm assembly (Pazour and Witman, 2000; Sakakibara *et al.,* 1991, 1993).

Mutations that impinge on various aspects of outer arm function are listed in Table I. The defects caused by these mutations fall into several distinct classes with discrete phenotypic consequences. Many mutants fail to assemble the entire outer arm structure and as a result swim slowly. This implies that the proteins encoded by these genes including the β and γ, heavy chains (HCs), both intermediate chains (ICs), and light chains (LCs), LC2, LC7, and LC8 are essential for the assembly of the entire structure (Mitchell and Brown, 1994; Mitchell and Kang, 1991; Pazour *et al.,* 1998, 1999b; Pazour and Witman, 2000; Wilkerson *et al.,* 1994, 1995). It is quite remarkable that the lack of subunits as small as 10–20 kDa can have such a dramatic effect on the $\sim$2 MDa arm. Analysis of the *fla14* mutant revealed that LC8 is required not only for outer arm assembly but also for the integrity of the inner arms, radial spokes, and retrograde intraflagellar transport (Pazour *et al.,* 1998). As a consequence, the *fla14* mutant assembles very short flagella. Three mutants (*oda1, oda3,* and *oda14*) do not encode components of the outer arm per se, but rather define the docking complex that acts as an adaptor required for attachment of the outer arm to its correct site within the axonemal superstructure (Casey *et al.,* 1998; Koutoulis *et al.,* 1997; Takada and Kamiya, 1994; Takada *et al.,* 2001).

Several mutant loci (*oda5, oda7, oda8,* and *oda10*) that result in the slow swimming phenotype do not encode structural components of the outer arm. These proteins may be essential for expression of dynein genes, or required for assembly and/or transport of the dynein particle within the cell body prior to its export into the flagellum. None of these gene products have yet been cloned. Both the *pf13* and the *pf22* mutations result in short flagella, a lack of outer arms (and some inner arms in the case of *pf22*), and complete flagellar paralysis (Huang *et al.,* 1979; Luck and Piperno, 1989). This suggests that the encoded proteins affect a specific assembly process.

Two mutations that occur in dynein structural genes do not lead to complete loss of the outer arm. The *ODA11* gene encodes the α HC and, remarkably, lack of this entire $\sim$520-kDa motor unit and its associated LC does not affect assembly of the remaining components (Sakakibara *et al.,* 1991). This is in sharp contrast to the β and γ HCs, which are both absolutely essential. Null mutants lacking LC6 also exhibit only a minor swimming defect (Pazour and Witman, 2000).

TABLE I

Mutations That Affect the Outer Dynein Arm

Gene	Protein[a]	Mutant phenotype	References
ODA1	DC2	Required for assembly, slow swimming	Kamiya, 1988; Takada *et al.,* 2001
ODA2	γ HC	Required for assembly, slow swimming	Mitchell and Rosenbaum, 1985
(PF28)		Suppressor mutation *sup2* is allelic with *oda2*	Kamiya, 1988; Rupp *et al.,* 1996
ODA3	DC1	Required for assembly, slow swimming	Kamiya, 1988; Koutoulis *et al.,* 1997
ODA4	β HC	Required for assembly, slow swimming; suppressor mutations *sup1-1* and *sup1-2* are allelic with *oda4* and have small deletions in the microtubule-binding region, the *oda4-s7* allele expresses a truncated version of the β HC with no motor domain	Kamiya, 1988; Sakakibara *et al.,* 1993; Porter *et al.,* 1994
ODA5	Unknown	Required for assembly, slow swimming	Kamiya, 1988
ODA6	IC2[b]	Required for assembly, slow swimming	Kamiya, 1988
ODA7	Unknown	Required for assembly, slow swimming	Kamiya, 1988
ODA8	Unknown	Required for assembly, slow swimming	Kamiya, 1988
ODA9	IC1[c]	Required for assembly, slow swimming	Kamiya, 1988
ODA10	Unknown	Required for assembly, slow swimming	Kamiya, 1988
ODA11	α HC	Not required for assembly of other outer arm proteins except LC5. Swims slightly slower than wildtype	Sakakibara *et al.,* 1991
ODA12	LC2	Required for assembly, slow swimming	Pazour *et al.,* 1999b
ODA13	LC6	Minor swimming defect	Pazour and Witman, 2000
ODA14	DC3	Required for assembly, slow swimming	Casey *et al.,* 1998
ODA15	LC7	Required for assembly, slow swimming	Pazour and Witman, 2000
FLA14	LC8	Required for assembly, very short flagella	Pazour *et al.,* 1998
PF13	Unknown	Required for assembly, short flagella	Huang *et al.,* 1979
PF22	Unknown	Required for assembly, short flagella, affects inner arms also	Huang *et al.,* 1979

[a] DC, docking complex; HC, heavy chain; IC, intermediate chain; LC, light chain.

[b] a.k.a. IC69 or IC70.

[c] a.k.a. IC78 or IC80.

Several alleles of *ODA4,* which encode mutant versions of the β HC, have been identified that have a less severe defect than the complete null. The *oda4-s7* mutant forms a truncated β HC, which lacks all but the 160-kDa, N-terminal stem of the polypeptide (Sakakibara *et al.,* 1993). This truncated HC allows for incorporation of the arm into the axoneme, indicating that this region is necessary and sufficient for dynein assembly but not for β HC-related motor functions. Also several *oda4* alleles (*supl-1* and *supl-2*) have been identified as extragenic suppressors of paralyzed flagella mutants lacking either radial spokes or the central pair MT complex (Huang *et al.,* 1982). The *sup* mutants were originally given the designation *sup-pf* (suppressor of paralyzed flagella), which was later contracted to *sup* in accordance with the three-letter standard adopted for designation of *Chlamydomonas* genes. At least one of these genes has been referred to by the alternate contraction, *spf*. Intriguingly, these mutations lead to small deletions near the MT-binding site of the β HC, suggesting that the motor domain of the β HC is the target of a regulatory signaling pathway (Porter *et al.,* 1994). An additional suppressor mutation (*sup2*) has been identified within the structural gene for the γ HC, supporting the idea that signals from the radial spoke and central pair complex are propagated through the outer arm system (Rupp *et al.,* 1996).

B. Inner Arms and the Dynein Regulatory Complex

While the outer dynein arms are necessary for generating normal flagellar beat frequency, the inner arms are responsible for efficient propagation of the waveform; mutants in this dynein system exhibit reduced shear amplitude (Brokaw and Kamiya, 1987). Composition and arrangement of the inner arm system is extremely complex and varies at different points along the length of the flagellar axoneme, presumably as a consequence of different functional requirements. There are two general classes of inner arm and two distinct nomenclatures. The class containing two HCs is termed I1 or subspecies f, whereas dyneins containing single HCs are designated subspecies a, b, c, d, e, and g; these enzymes are also collectively known as I2 and I3 (Kagami and Kamiya, 1992; Kagami *et al.,* 1990; Piperno *et al.,* 1990).

Mutant analysis combined with sophisticated biochemistry (described in a following section) has been essential in defining the composition and arrangement of the inner arm motor system (Table II). For example, the *pf9* mutant is deficient in four polypeptides that form inner arm I1 (1α and 1β HCs and ICs of 110 and 140 kDa) (Mastronarde *et al.,* 1992; Myster *et al.,* 1997; Porter *et al.,* 1992); it is likely that these mutants also are missing several LCs. The lack of these I1 subunits results in an aberrant waveform that decreases forward swimming speeds (Kamiya *et al.,* 1989). Interestingly, inner arm defects do not result in the jerky swimming phenotype characteristic of outer-arm-deficient mutants (Kamiya *et al.,* 1989). A subset of inner arms collectively known as I2/3 are missing in

TABLE II

Mutations Affecting the Inner Arm System and Dynein Regulatory Complex

Gene	Protein	Phenotype	References
IDA1 (PF9)	1α HC	Lacks arm I1, slow swimming	Kamiya *et al.,* 1991; Myster *et al.,* 1997; Porter *et al.,* 1992
IDA2	1β HC	Lacks arm I1, slow swimming	Kamiya *et al.,* 1991; Perrone *et al.,* 2000
IDA3	Unknown	Lacks arm I1, slow swimming	Kamiya *et al.,* 1991
IDA4	p28	Lacks inner arm subtypes a, c, and d	Kamiya *et al.,* 1991
IDA5	Actin	Lacks inner arm subtypes a, c, d, and e	Kato *et al.,* 1993
IDA6	Unknown	Lacks inner arm subtype e	Kato *et al.,* 1993
IDA7	IC140	Lacks arm I1; slow swimming	R. Kamiya, pers. commun.; Perrone *et al.,* 1998
IDA8	Unknown	Slow swimming, structural defect in inner arm region	M. Porter, pers. commun.
IDA9	Unknown	Lacks inner arm subtype c	R. Kamiya, pers. commun.
PF2	Unknown	Reduced levels of inner arms, *pf* suppressor	Gardner *et al.,* 1994
PF3	Unknown	Reduced levels of inner arms, *pf* suppressor	Gardner *et al.,* 1994
SUP3	Unknown	Reduced levels of inner arms, *pf* suppressor	Gardner *et al.,* 1994
SUP5	Unknown	Missing DRC components, *pf*	Piperno *et al.,* 1992
BOP2	Unknown	Slow swimming, abnormal waveform	King *et al.,* 1994
VFL2	Centrin	Mis-sense mutations only; variable length flagella but no effect on inner arm assembly	Piperno *et al.,* 1990; Taillon *et al.,* 1992

mutants defective at the *ida4* locus that encodes the p28 dynein LC (Kamiya *et al.,* 1991; LeDizet and Piperno, 1995a). The three extant alleles, *ida4-1* to *ida4-3,* each encode single nucleotide substitutions that prevent correct intron splicing. These mutants all lack the p28-associated HCs, which implies that p28 is necessary for incorporation of these subunits into the axoneme (LeDizet and Piperno, 1995b).

Genetic studies also have revealed the presence of a regulatory system that is integrated with the dynein arms in the axonemal superstructure and serves to control dynein activity during flagellar beating. Mutant flagella lacking the radial spoke or central pair apparatus are completely paralyzed (Luck, 1984). This inhibition of motility may be bypassed if the strain also carries one or more extragenic suppressor mutations that can restore flagellar motility within the central pair/radial spoke defective background (Huang *et al.,* 1982). These

additional deficiencies occur within the inner and outer arm systems, implying that a complex regulatory pathway exists within the axoneme linking the central pair/radial spokes to the dynein motor units (Piperno *et al.,* 1992; Porter *et al.,* 1994; Rupp *et al.,* 1996).

Studies of I2- and I3-deficient inner arm mutants and suppressors of flagellar paralysis identified six axoneme-associated polypeptides that serve to suppress flagellar paralysis in mutants that lack radial spokes (Piperno *et al.,* 1992). This group of axonemal polypeptides which act as extragenic suppressors has been collectively termed the dynein regulatory complex (DRC). High-resolution electron microscopic imaging has located at least part of the DRC in close association with the inner dynein arms at the base of the second radial spoke in a position to interact with inner arm I2 (Gardner *et al.,* 1994). Consistent with these findings, three DRC mutants *pf3, pf2,* and *sup3,* carry reduced numbers of inner arm structures such as one distinct isoform of inner arm I2 (Gardner *et al.,* 1994; Piperno *et al.,* 1992). Furthermore, some DRC mutants may be defective in the phosphorylation of inner arm subunits (Luck and Piperno, 1989). In the *pf2* mutant, electron microscopy (EM) imaging experiments have revealed the lack of a crescent-shaped structure normally located above the second radial spoke, presumed to be the DRC, while quantitative electrophoresis has indicated partial loss of I2/I3 inner arm subunits (Piperno *et al.,* 1994). This work provided the initial indication of how signals transduced by the radial spoke/central pair system serve to regulate dynein activity (Porter and Sale, 2000).

III. Structural Organization of Flagellar Dyneins

To date, 16 different HCs have been identified in *Chlamydomonas* using the polymerase chain reaction (Porter *et al.,* 1996). Of these, 14 are axonemal; the other two share characteristics with cytoplasmic dyneins even though at least one of these (Dhc1b) also occurs in the flagellum and is required for assembly of this organelle (see section VI). However, only 12 HCs so far have been identified at the biochemical level including 3 from the outer arm, 2 from inner arm I1, 6-monomeric inner arm species, and the Dhc1b cytoplasmic dynein (Kagami and Kamiya, 1992; Pfister *et al.,* 1982; Piperno and Luck, 1979); there is also a clear homolog of the major mammalian (Dhc1a) cytoplasmic dynein isoform. The origin of the remaining HCs is unknown, but is most likely the complex inner arm system.

The dynein MT motor is assembled around a backbone of one or more heavy chains ($\sim$530 kDa) that serve as the motor units for these massive complexes. In the *Chlamydomonas* flagellum, dyneins containing one (many inner arm subspecies), two (inner arm I1) or three (outer arm) HCs have been identified (Kagami and Kamiya, 1992; Pfister *et al.,* 1982; Piperno and Luck, 1979). When extracted from the flagellar axoneme, dyneins adopt a spread-out conformation that must undergo

TABLE III

Composition of Outer Arm Dynein from *Chlamydomonas* Flagella

Protein	Stoichiometry	Mass (kDa)	Properties
α HC	1	504	ATPase and MT motor
β HC	1	520	ATPase and MT motor
γ HC	1	513	ATPase and MT motor
IC1	1	76	WD-repeat protein, binds α-tubulin
IC2	1	63	WD-repeat protein, regulatory
LC1	2	22	Leucine-rich repeat protein, binds γ HC motor domain
LC2	1	16	Tctex2 homolog
LC3	1	17	Thioredoxin homolog
LC4	1	18	Ca^{2+}-binding EF hand protein
LC5	1	14	Thioredoxin homolog
LC6	2	14	LC8 homolog
LC7	1	12	Roadblock/bithoraxoid homolog
LC8	4	10	Highly conserved, not dynein-specific
DC1	ND	83	Docking complex, coiled coil protein
DC2	ND	62.5	Docking complex, coiled coil protein
DC3	ND	21	Docking complex, potential Ca^{2+}-binding protein

considerable folding to fit within the confines dictated by the spacing of flagellar doublet MTs. In compositional terms, there is a clear demarcation between dyneins with multiple HCs and those with only a single catalytic subunit. The composition of dyneins from the outer and inner arms is detailed in Tables III and IV. Very little is yet known about the subunit composition of cytoplasmic dynein 1b that is involved in IFT. The arrangement of the inner and outer arms *in situ* and the current understanding of protein–protein associations within the outer arm are shown in Figs. 1a and 1b (see color insert), respectively.

Each dynein particle consists of a series of large globular head domains—~12 nm in diameter (see below for the substructure of this section)—interconnected by stalks to a common base (Goodenough and Heuser, 1984; Johnson and Wall, 1983; Sale *et al.,* 1985; Witman *et al.,* 1983). The number of heads is dictated by the HC content of each dynein. The N-terminal stalk region of the HC is involved in HC–HC interactions and also serves as the assembly site for an additional subcomplex consisting of several ICs and LCs. This HC segment varies considerably between different isoforms, suggesting that it plays a gene-specific role in dynein function. There is also a stem— ~10 nm in length—that extends from the opposite side of each head and terminates in a discrete globular subdomain

TABLE IV

Composition of *Chlamydomonas* Inner Dynein Arms

Dynein	Protein	Mass (kDa)[a]	Properties
I1 (f)	1α HC	523	ATPase and microtubule motor
	1β HC	511	ATPase and microtubule motor
	IC140	110	WD-repeat protein; N-terminus is not essential
	IC138	138	Regulation of motor in response to phosphorylation
	IC110	110	—
	Unknown	22	—
	Tctex1	13	Dimeric protein; potential cargo binding activity; also found in cytoplasmic dynein (the related Tctex2 protein is found in outer arm dynein)
	LC8	10	Highly conserved dimeric protein, potential cargo binding activity; also found in cytoplasmic and outer arm dyneins
(a, c, d)	a, c, or d HC	ND	ATPase and microtubule motor—monomeric
	Actin	42	Cytoskeletal protein—essential for assembly
	p28	29	Essential for assembly
(b, e, g)	b, e, or g HC	ND	ATPase and microtubule motor—monomeric
	Actin	42	Cytoskeletal protein—essential for assembly of subtype e, but not subtypes b and g
	Centrin	19	Ca^{2+}-binding EF-hand protein
	NAP	35	Novel actin-related protein, upregulated in *ida5*—allows for assembly of subtypes b and g in the *ida5* mutant lacking actin

[a] Mass values for IC138, IC110, and the ∼22-kDa LC were estimated by gel electrophoresis. All other values derive directly from sequence.

that acts as the MT-binding site. Quick freeze/deep etch micrographs revealed additional subdomains arranged along and at the base of the interconnecting stems (Goodenough and Heuser, 1984). These likely represent the association of IC and/or LC components although the precise location of individual proteins remains unclear.

Within the flagellum, the outer arms are arranged along the doublet MTs with a spacing of 24 nm. When viewed in cross section, the outer arm appears as a crescent-shaped structure with three large lobes in position to interact with the adjacent MT (Fig. 1a). EM analysis of various outer arm mutants has revealed that these lobes correspond to the motor domains of the three HCs, with the γ HC innermost and the α HC at the axonemal periphery (Sakakibara *et al.,* 1991, 1993). These complexes are organized such that the head domain of one arm overlaps the basal region of the adjacent dynein (Avolio *et al.,* 1984; Witman and Minervini, 1982). In contrast, the organization of the inner arm dyneins is considerably more complex (Porter, 1996). These arms are organized in a triplet pattern with a 96-nm repeat length. The two-headed I1 species is the first component of the triplet

and is found along the entire axonemal length. This is followed by two of the six distinct single-headed motors. Moreover, different single-headed species are found in the region of the flagellum proximal to the cell body compared to more distal segments, suggesting that propagation of an efficient waveform requires an alteration in motor function within these different axonemal domains (Piperno and Ramanis, 1991).

IV. Biochemistry of Dynein Components

A. Heavy Chains

The HCs are each ~520 kDa in mass and form the backbone of the dynein particle. To date, at least 16 different HCs have now been identified in *Chlamydomonas* by sequence analysis, implying a wide diversity of function. Here we will first describe the basic properties of dynein HCs and then detail the distinct attributes as far as they are known.

   All dynein HCs are built to the same basic plan. This involves an N-terminal stem domain of ~160 kDa followed by a globular head containing the ATPase site(s). A short stalk also emanates from the head and terminates in the MT-binding domain. A map of the outer arm γ HC indicating the location of the various subdomains is shown in Fig. 1c. The properties of each of these functional domains are addressed below.

1. The N-terminal Stem

The N-terminal stem of one HC associates with the equivalent region of other HCs and with the IC/LC complex and is thus essential for integrity of the dynein particle (Sakakibara *et al.,* 1993). Deletion studies of *Dictyostelium* cytoplasmic dynein have revealed small overlapping regions, centered on a 150-residue segment of this HC domain, that are sufficient to mediate both HC–HC and HC–IC interactions (Habura *et al.,* 1999). Similar, although not identical, regions can be identified in *Chlamydomonas* flagellar dyneins, suggesting that the overall mechanisms involved in HC dimerization and interaction with the IC/LC complex are conserved (King, 2000). When viewed by EM, this region of the HC is often splayed out, although it must adopt a much more folded conformation *in situ*. Clearly, this region is very distinct from the coiled coil structures associated with the catalytic domains of other cytoskeletal motors such as myosin and kinesin. When the N-terminal domain of the β HC from sea urchin sperm flagella was analyzed by circular dichroism spectroscopy it was found to have low (~26%) α-helical content (Mocz and Gibbons, 1990). However, secondary structure predictions using PHD suggest a high level of helix (>60%) with

excellent reliability scores (S. M. King, unpublished). It is unclear at present how these two observations may be reconciled although one possibility is that they represent different conformational states. Alternatively, this region of the HC may adopt a novel structural fold that is not accounted for by current prediction algorithms.

2. The Motor Domain

The remaining C-terminal $\sim$350 kDa of the HC forms the globular head and MT-binding domain. The initial sequence analysis of this region identified four putative nucleotide binding or P-loop motifs (termed P1–P4) within the central 100 kDa of the motor (Gibbons *et al.,* 1991; Koonce *et al.,* 1992; Mitchell and Brown, 1994; Ogawa, 1991; Wilkerson *et al.,* 1994). Only the P1 consensus sequence G-P-A-G-T-G-K-T is completely conserved among both flagellar and cytoplasmic dyneins and is the site of adenosine triphosphate (ATP) hydrolysis. When dynein HCs are irradiated with UV light in the presence of ATP and low-micromolar levels of vanadate, the peptide backbone is cleaved at the nucleotide hydrolytic site (termed V1), completely abolishing ATPase activity (Gibbons *et al.,* 1987, King and Witman, 1987; Lee-Eiford *et al.,* 1986). In this situation, the monomeric vanadate is bound as the $Mg \cdot ADP \cdot V_i$ complex and acts as the chromophore for the reaction. Interestingly, both the *Chlamydomonas* α and γ HCs, but not the β HC, may be cleaved in the presence of vanadate alone, implying that there are significant differences in the ATP binding sites of these motor units (King and Witman, 1987; 1988). Irradiation of dynein HCs in the presence of millimolar concentrations of vanadate and Mn^{2+} (presence of this cation suppresses cleavage at the V1 site) leads to cleavage of the protein at one or more additional sites that likely correspond to other P-loop motifs (King and Witman, 1987; Tang and Gibbons, 1987). These additional sites are termed V2. These two cleavage procedures have proven very useful for mapping various sites within the dynein HCs.

The question of how many P-loop motifs are involved in nucleotide binding has proven surprisingly difficult to answer definitively. Initial studies using phase partition analysis of sea urchin sperm dynein suggested the presence of four nucleotide-binding sites per HC (Mocz and Gibbons, 1996). However, further analysis using fluorescence anisotropy to assess binding of a methylanthraniloyl nucleotide analog provided evidence for only two nucleotide-binding sites with association constants in the physiological range of 10^{-4}–10^{-5} M^{-1} (Mocz *et al.,* 1998). This latter experiment is in agreement with MT gliding experiments which indicate that the γ HC of *Chlamydomonas* outer arm dynein has both high- and low-affinity nucleotide binding sites with K_d of 8 and 80 μM, respectively (Wilkerson and Witman, 1995). Photolabeling of both *Chlamydomonas* and sea urchin HCs using azido-ATP analogs also can be interpreted in terms of a two-site model (King *et al.,* 1989; Mocz *et al.,* 1988).

Negative stain EM images of *Tetrahymena* dynein identified a pit or hole in the center of the HC head domain that accumulated stain (Marchese-Ragona *et al.,* 1988). More recent high-resolution imaging of *Dictyostelium* cytoplasmic dynein revealed that the dynein head contains seven distinct globular subdomains arranged in a ring surrounding an apparently empty central cavity (Samso *et al.,* 1998). How does the structure, determined by EM, correspond to the amino acid sequence of this HC region? Detailed sequence analysis has defined dynein as a member of the ancient AAA (ATPases associated with cellular activities) family (Neuwald *et al.,* 1999). AAA domains have been identified in an array of protein complexes that function through energy-dependent conformational changes. For example, within the eukaryotic 26S proteosome, AAA modules serve as regulatory subunits in the proteolysis of ubiquinated proteins (Baumeister and Lupas, 1997). Protein complexes involved in DNA replication and recombination also contain AAA domains, such as the *Escherischia coli* polymerase III δ' clamp loader, which binds and hydrolyzes ATP to induce conformational changes that enable it to load PCNA onto a DNA strand (Stillman, 1994). The hexameric AAA protein RuvB functions with RuvA in guiding DNA through its ring structure to elicit branch migration during resolution of Holiday junctions (Rice *et al.,* 1997; West, 1997).

The dynein motor domain contains six AAA domains (Fig. 1c) (King, 2000; Neuwald *et al.,* 1999). The first four domains (AAA 1–4) are centered on the P1–P4 loops identified previously (Gibbons *et al.,* 1991; Ogawa, 1991). The latter two AAA units (AAA 5 and AAA 6) were not originally detected as they lack intact consensus P-loops. The microtubule-binding domain and stalk (discussed in more detail below) are located between AAA 4 and AAA 5. Following the last AAA domain, there is a C-terminal segment of ∼40 kDa that is apparently completely unrelated to the AAA domain consensus.

Each AAA domain contains a series of conserved motifs that correspond to defined elements of secondary structure (Fig. 2a; see color insert). For example, the Walker A box consists of a helix, loop, and strand, and contains the glycine-rich P- loop that encircles the triphosphate tail of ATP. All of the consensus AAA domain motifs indicated in Fig. 2a may be identified in each of the six AAA units within dynein HCs (King, 2000; Neuwald *et al.,* 1999).

Recently, we proposed a model that combined the AAA domain structure of the HC with the heptameric toroidal organization determined by EM (King, 2000) (Fig. 2b; see color insert). In this arrangement, each AAA domain corresponds to one of the globular subdomains observed by EM, with the heptameric ring being closed by the unrelated C-terminal domain. This model would place the N-terminal stem domain and the MT-binding stalk structure on opposite sides of the ring as is observed by EM. A somewhat different model has been proposed by Vale (Vale, 2000) which suggests that the MT-binding stalk corresponds to one of the globular subdomains. However, this HC region is only large enough to form a coiled coil segment of ∼12 nm (which is slightly larger than the length of the protruding stalk) and does not have sufficient mass to also represent a globular subdomain of a size similar to an

entire AAA domain. Furthermore, this model does not account for the C-terminal 40-kDa segment of the HC, which is predicted to fold as a globular domain.

The model we propose incorporates clear structural parallels with *N*-ethyl maleimide-sensitive vesicle fusion protein (NSF) (Lenzen *et al.,* 1998; Yu *et al.,* 1998) and RuvB (Yu *et al.,* 1997). Both NSF and RuvB exist as annular hexameric complexes. This organization is echoed at the EM level by the presence of six globular subdomains. In these proteins, nucleotide is bound by all AAA units and furthermore, at least in NSF, there is clear evidence for the interaction between these units in a manner likely to affect the ATPase properties. For example, in NSF one Lys residue involved in coordination of the ATP γ-phosphate within each AAA domain in fact derives from the adjacent AAA domain in the ring (Fig. 2c; see color insert). The side chain of this residue takes the place of the water molecule normally required for hydrolysis. Thus, movement of this residue is required to allow for hydrolysis to occur and provides a mechanism to coordinate nucleotide hydrolysis throughout the ring. In the *Chlamydomonas* outer arm γ HC, a basic residue occurs at this location only in AAA 5 and is thus in an appropriate position to interact with AAA 4 to inhibit hydrolysis of nucleotide bound to this domain. This hypothesis predicts that mutation of K3515 in the γ HC sequence will have profound effects on dynein enzymology.

As mentioned above, the available evidence supports a maximum of two nucleotide-binding sites on dynein with only one (AAA 1) acting in a hydrolytic capacity. However, there is clear evidence that other dynein AAA domains affect mechanochemical force transduction. For example, a single base pair change in murine left–right dynein (involved in setting up left–right asymmetry in the developing mammalian embryo) leads to mutation of a conserved Glu residue to a Lys (Supp *et al.,* 1997, 1999). This alteration occurs in AAA 2 and results in motor dysfunction, immotile nodal cilia, and random organ placement. This Glu residue is in the region that connects the sensor 1 and box VII motifs, which strongly suggests a functional requirement for this region of AAA 2.

In what conformation is ATP bound to the dynein HC? Structural studies indicate that when bound to NSF, ATP is in the *syn* conformation, i.e., with the adenine base stacked above the ribose ring (Yu *et al.,* 1998). In contrast, although precise structural details are not yet available for dynein, experiments using various nucleotide analogs indicate that this enzyme preferentially hydrolyzes compounds that adopt the alternate or *anti* conformation with the base away from the sugar moiety (King *et al.,* 1989; Omoto and Nakamaye, 1989). In NSF, the adenine base is bound in a hydrophobic pocket within the protein making few specific contacts. Thus, if this relatively nonspecific binding of the nucleotide base proves to be a general feature of the AAA domain, it may be that a preference for a particular nucleotide conformation is not a conserved feature. In sharp contrast, structural analysis indicates that the NSF AAA domain makes a series of very specific contacts with the triphosphate tail of the nucleotide and with the coordinating Mg^{2+} ion. Importantly, all the NSF residues involved in these interactions are

completely conserved in AAA 1 of dynein, suggesting that this region of the ATP molecule is bound in a very similar fashion by the two enzymes.

3. Microtubule-Binding Region

The MT-binding region of the HC is located at the tip of an elongated structure that emanates from the globular head domain (Gee *et al.,* 1997; Koonce, 1997). This section of the HC is formed from a region located between AAA 4 and AAA 5 that consists of two segments with high probability of forming a coiled coil, sandwiching a region of ~125 residues that forms the globular MT-binding tip. It is presumed that the two flanking regions come together to form an antiparallel coiled coil. In the *Chlamydomonas* γ HC, each of these regions contains ~85 residues and so could form an extended α helix of ~12 nm once the superhelical twist necessary to form a coiled coil is taken into account (G. F. King and S. M. King, unpublished). This value agrees well with the actual 9- to 10-nm length measured by EM, assuming that a small amount of this region is buried within the globular subdomains in which the coiled coil originates and terminates. The intervening region between the coiled coil sections is intriguing because although it binds MTs, which is a conserved function, there is only very poor conservation at the sequence level between various dynein subtypes (only 25–30% sequence identity) (Koonce and Tikhonenko, 2000). One possibility is that minor alterations in this segment reflect the different MT-binding and translocation properties of distinct dynein species. For example, although most dyneins release from the MT in the presence of ATP, one inner arm subspecies has recently been found to remain loosely attached for most or all of the mechanochemical cycle (Sakakibara *et al.,* 1999).

4. Phosphorylation

In vivo labeling experiments have revealed that several flagellar HCs are phosphorylated, including members of the I2/3 class of monomeric HCs and the α HC from the outer arm (King and Witman, 1994; Piperno and Luck, 1981). Both types of HC were phosphorylated following labeling to steady state and also after pulse labeling, suggesting that there is significant turnover at the modified sites. Furthermore, these HCs became phosphorylated upon treatment of isolated axonemes with ATP, indicating that the kinases and probably also the phosphatases involved in this cyclic modification are integral components of the axonemal superstructure. The α HC contains at least six phosphorylation sites. Mapping studies located sites immediately N-terminal to the first AAA domain and within the C-terminal ~90 kDa of the protein that corresponds to AAA 6 and the C-terminal domain (King and Witman, 1994). Intriguingly, the current model for HC organization (King, 2000) brings this C-terminal region into close apposition with AAA 1, suggesting that all the α HC phosphorylation sites may be located close to the ATP hydrolytic domain.

B. Intermediate Chains

All dyneins with two or more HCs contain a subcomplex formed of several (usually two) ICs and several LCs (Witman *et al.,* 1991) that is located at the base of the soluble dynein particle (King and Witman, 1990; Sale *et al.,* 1995). This domain has been implicated in the attachment of both cytoplasmic and flagellar dyneins to the appropriate cargo either directly or indirectly via an adaptor complex (Karki and Holzbaur, 1995; King *et al.,* 1991). Most of the IC proteins cloned to date, including those from cytoplasmic dynein, are members of the WD-repeat protein family [(Neer *et al.,* 1994): each WD-repeat is an ∼40-residue motif containing an almost invariant Trp–Asp dipeptide; Fig. 3a] (Mitchell and Kang, 1991; Paschal *et al.,* 1992; Wilkerson *et al.,* 1995; Yang and Sale, 1998). However, one intriguing exception to this has been identified in the outer arm of sea urchin sperm flagella (Ogawa *et al.,* 1996). It also seems possible that additional novel IC proteins are present in the *Chlamydomonas* inner arm I1.

1. WD-Repeat Proteins

At the structural level, the dynein ICs can be subdivided into two distinct domains—a conserved C-terminal section and a highly variable N-terminal segment (Fig. 3a; see color insert). The C-terminal region consists of five to seven WD-repeats and short intervening regions. Multiple copies of the WD-repeat are found in a wide variety of cellular proteins, many of which are involved in cell signaling (Neer *et al.,* 1994). The three-dimensional structure of several of these proteins has now been solved and it is clear that they fold to form a toroidal arrangement—the so-called β-propeller—with four-stranded twisted anti-parallel β sheets forming the blades (Sondek *et al.,* 1996). In this structure, each WD repeat contributes the innermost three strands of one blade and the outermost strand of the adjacent blade. This unusual arrangement is stabilized by a hydrogen bond network formed between a Ser, His, Asp structural triad and the conserved Trp residue (Fig. 3b; see color insert).

While most of the obvious similarity between ICs occurs in this WD-repeat region, the N-terminal portions of the molecules are very distinct and clearly play a major role in defining IC activity (Fig. 3a). In the *Chlamydomonas* outer arm, IC1 and IC2 are encoded at the ODA9 and ODA6 genes, respectively. Although both proteins are essential for dynein assembly (Mitchell and Kang, 1991; Wilkerson *et al.,* 1995), they appear to play very different roles *in vivo*. Cross-linking studies using the carbodiimide reagent EDC revealed that IC1 is in direct contact with α-tubulin *in situ* (King *et al.,* 1991). Furthermore, *in vitro* analysis uncovered two regions within the N-terminal portion of IC1 that are required for this binding activity (King *et al.,* 1995). These experiments provided the first evidence for a role of ICs in the attachment of the dynein motor to its specific cargo. However, it has now become clear that the IC1–α-tubulin interaction is not sufficient for the

correct placement of the outer arm within the axonemal superstructure (Takada and Kamiya, 1994). This precise targeting function requires a trimeric docking complex that appears functionally analogous to dynactin that mediates the attachment of cytoplasmic dynein to membrane-bound vesicles.

In contrast, *Chlamydomonas* IC2 appears to play a regulatory role in outer arm function. Evidence for this derives from attempts to rescue the *oda6* mutation using wildtype and mutant versions of the IC2 gene (Mitchell and Kang, 1993). Both outer arm assembly and the consequent swimming defect are rescued by incorporation of the wildtype gene into the *oda6* background. However, a mutant form of IC2 containing a small deletion in the N-terminal region was able to rescue assembly, but still resulted in the aberrant motility characterstic of *oda* mutants.

Within inner arm I1, the 140-kDa IC is encoded at the *ida7* locus and also is absolutely required for assembly of that complex (Perrone *et al.,* 1998). This protein consists of a C-terminal domain containing seven copies of the WD-repeat motif and a gene-specific N-terminal section (Yang and Sale, 1998). However, in this case deletion of the first four exons that encode 283 residues results in a protein that is still able to rescue both the assembly and the motility defects observed in the *ida7* mutant (Perrone *et al.,* 1998). Thus, the role of this N-terminal segment in I1 function remains to be determined. At the very C-terminus of IC140 is a small segment that is predicted to adopt a coiled coil structure; a similar motif is present C-terminal to the WD-repeats within IC2 of the outer arm.

2. IC138 and Regulation of Inner Arm Function

Generation of a flagellar waveform demands the precise regulation of dynein activation/deactivation along the axoneme. Numerous studies support the hypothesis that this regulatory requirement is achieved by modulating the phosphorylation state of axonemal components (Porter and Sale, 2000). A regulatory pathway that extends from the central pair complex thorugh the radial spokes to the dynein arms has been defined genetically through the identification of mutants that suppress the paralyzed phenotype of central pair and radial spoke-deficient mutants (see section IIb). Direct support for this idea comes from the observation that the velocity of microtubule sliding is significantly diminished in axonemes from radial spoke mutants and is restored in reconstitution experiments that provide radial spokes or dynein derived from radial spoke-containing axonemes (Fig. 4a) (Smith and Sale, 1992). The addition of inhibitors that target cAMP-dependent protein kinase also can relieve paralysis (Hasagawa *et al.,* 1987; Howard *et al.,* 1994). This effect is reversed upon addition of cAMP that presumably stimulates kinase activity.

Reconstitution experiments in which various inner arm fractions were added to dynein-depleted axonemes revealed that inner arm I1 is an essential component in the regulation of MT sliding (Habermacher and Sale, 1996, 1997). Kinase activity and phosphatase inhibitors decreased MT-sliding rates, whereas increases were observed in the presence of kinase inhibitors. Biochemical analysis revealed that
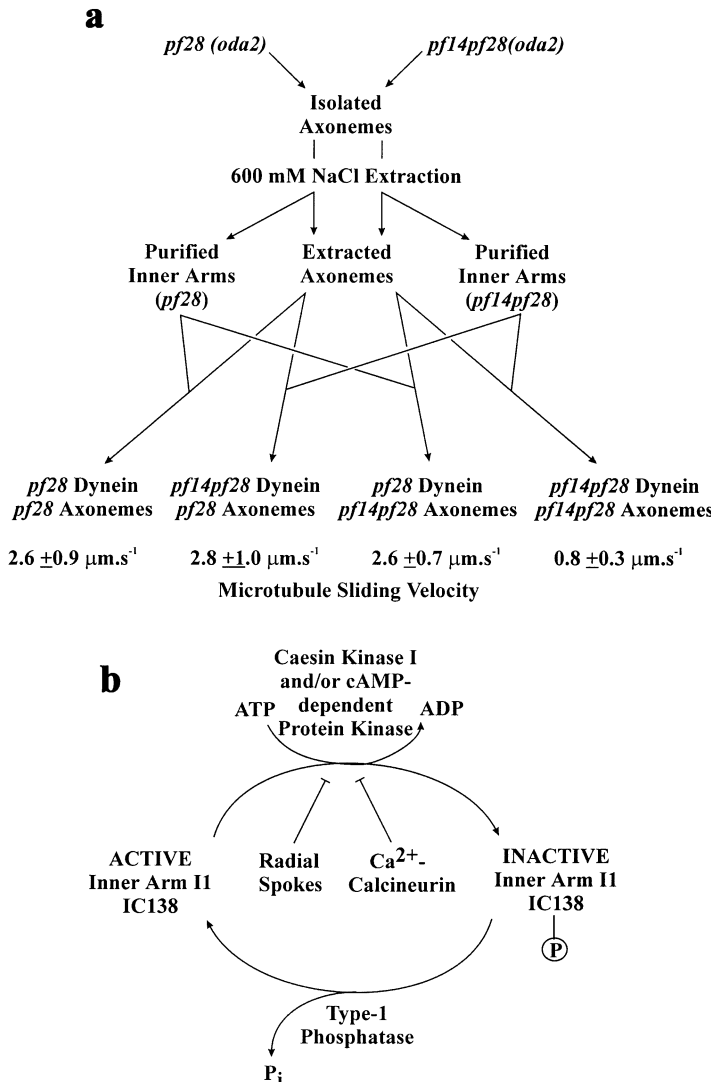
FIG. 4   Regulation of inner dynein arm function. (a) Diagram of the experiment performed by Smith and Sale (1992), demonstrating the involvement of radial spokes in control of inner arm function. These studies made use of dynein and dynein-depleted axonemes from the mutant *pf28(oda2)* that lacks outer arms and *pf14pf28(oda2)* that is missing both outer arms and radial spokes. In these reconstitution experiments, the presence of radial spokes (or dynein isolated from radial spoke-containing cells) leads to rapid microtubule sliding, whereas the lack of spokes results in a very significant reduction in rate. (b) Activation of inner arm I1 is controlled through the phosphorylation of the IC138 component by cAMP-dependent protein kinase and/or casein kinase I and dephosphorylation by a type-1 phosphatase. Signals from both the radial spokes and a Ca^{2+}- calcineurin signaling pathway reduce the level of IC138 phosphorylation and lead to active motility.

IC138 is the only phosphorylated component of inner arm I1, indicating that this IC plays a key role in regulating dynein function (Habermacher and Sale, 1997). This protein has not yet been cloned and so a more detailed understanding of its properties is lacking at present. However, several mutants that exhibit defects in phototaxis have been found to contain altered phosphorylated forms of IC138 (King *et al.,* 1994).

Recent studies have located a cAMP-dependent protein kinase anchoring protein (AKAP) at the base of the radial spokes in close proximity to inner arm I1, suggesting that the kinase is targeted to the appropriate location within the axonemal superstructure (Roush-Gaillard and Sale, 2000). Furthermore, a novel calmodulin-binding kinase has recently been identified within the radial spoke system (Yang *et al.,* 2000). There is also strong evidence that calcineurin, a Ca^{2+}/calmodulin-dependent type 2b phosphatase affects inner arm I1 function (King and Dutcher, 1997), suggesting that cAMP and Ca^{2+} signaling pathways are integrated in the control of flagellar activity (Fig. 4b).

Although inhibitors of cAMP-dependent protein kinase restore the activity of axonemes from mutants lacking radial spokes to wild type levels, they do not completely block the phosphorylation of IC138 (Yang and Sale, 2000). This suggests that additional kinases also may act on this protein. Recent studies have implicated casein kinase 1, which is an integral component of the flagellar axoneme, in this activity. Inhibition of casein kinase 1 activity restores dynein-mediated MT sliding activity and blocks the phosphorylation of IC138 (Yang *et al.,* 2000).

C. Light Chains

Light chains associated with *Chlamydomonas* flagellar dyneins represent a diverse group of proteins with homologs found in the cilia, flagella, and cytoplasm of many organisms. Within the outer arm there are two general classes of LC. The first group includes a series of proteins that interact directly with the HCs and whose properties suggest that they act to transduce regulatory input signals. The second general LC class includes three distinct LC types that associate with the ICs at the base of the particle. All members of this second group are essential for assembly of the dynein particle into the flagellum. In inner arm I1, the two LCs identified so far belong to this second class. The remaining inner arm dynein species (i.e., those with only a single HC) have a completely distinct set of LCs that includes p28, centrin, and actin. In this section, we will describe the properties and possible roles of each LC family.

1. Ca^{2+}-Binding LCs

Two *Chlamydomonas* dynein LCs capable of binding Ca^{2+} have been identified. These include centrin (*a.k.a.* caltractin), which is associated with several subtypes

of monomeric inner arms (Piperno *et al.*, 1992), and the LC4 protein, which is bound to the γ HC of outer arm dynein (King and Patel-King, 1995a). Both polypeptides are members of the EF-hand family of Ca^{2+}-binding proteins and consist of four helix–loop–helix motifs—two at each end of an intervening predicted α helical segment. In centrin, all four motifs conform to the EF-hand consensus for Ca^{2+}-binding loops (Taillon *et al.*, 1992) and indeed, this protein binds two Ca^{2+} with high affinity ($K_{Ca} = 1.2 \times 10^{-6}$ M) and two with low affinity ($K_{Ca} = 1.6 \times 10^{-4}$ M) (Weber *et al.*, 1994). In contrast, only the two N-terminal helix–loop–helix motifs in LC4 fit this consensus (Fig. 5a) and Ca^{2+}-binding experiments using a maltose-binding protein/LC4 fusion suggest that LC4 binds only a single Ca^{2+} with a K_{Ca} of $\sim 10^{-5}$ M (King and Patel-King, 1995a). The DC3 component of the outer arm docking complex also contains EF-hands that likely form metal-binding sites, although it has not yet been demonstrated to bind Ca^{2+} specifically (Casey *et al.*, 1998).

What role might these proteins play in the flagellum? *Chlamydomonas* cells move toward or away from a light source in a process called phototaxis (Fig. 5b) (Witman, 1993). In order to achieve alteration in swimming direction, the two flagella beat differentially in response to small changes in intraflagellar Ca^{2+} concentration in the submicromolar range (Kamiya and Witman, 1984). This alteration occurs in the absence of the outer arms and it is possible, although certainly not yet proven, that centrin might act as a sensor to detect the imposed change in metal concentration and transduce the effect to the inner arm system. In contrast, photoshock is an avoidance response that is mediated by an increase in intraflagellar Ca^{2+} levels from 10^{-6} to 10^{-4} M (Fig. 5b) (Bessen *et al.*, 1980). Isolated flagellar axonemes beat with a ciliary waveform at 10^{-6} M Ca^{2+}, become quiescent at 10^{-5} M and beat with a symmetric waveform at 10^{-4} M. The Ca^{2+}-binding properties of LC4 and the lower affinity sites of centrin make these proteins excellent candidates to act as flagellar sensors for this response. However, two analyses of the photoshock response in mutants lacking the outer arms have yielded different phenotypes. One study found that the response was merely aberrant (Mitchell and Rosenbaum, 1985), whereas another reported that photoshock did not occur in the absence of the outer arms (Kamiya and Okamoto, 1985). The difference between these studies has not yet been satisfactorily explained, although it might derive from the fact that different *oda* mutants were examined. Recently, a Ca^{2+}-dependent alteration in the MT-binding properties of the outer arm γ HC has been reported (Sakato and King, 2000), providing further support for the hypothesis that LC4 (the only Ca^{2+}-binding protein in the outer arm) may indeed control mechanochemical properties.

2. Thioredoxin-Related LCs

Both the α and the β HCs of the *Chlamydomonas* outer dynein arm are associated with single LCs (LC5 and LC3, respectively) (Pfister *et al.*, 1982; Pfister

a

b   Phototaxis

Differential Response to Ca^{2+}
changes in the 10^{-6}-10^{-9} M range

Occurs in *oda* mutants

Photoshock

Ca^{2+} increase from
10^{-6} to 10^{-4} M

Aberrant or missing
in *oda* mutants
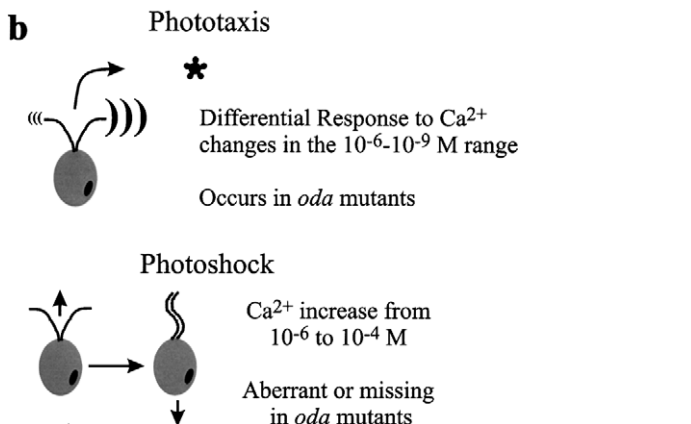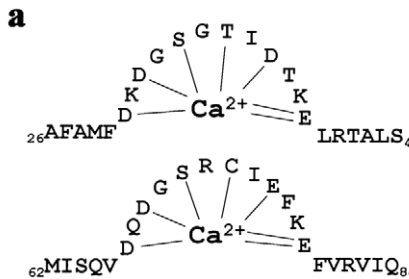
FIG. 5 Ca^{2+}-binding sites of LC4 and Ca^{2+}-mediated flagellar responses. (a) The two EF-hands within LC4 from the outer arm that are predicted to bind Ca^{2+} are shown. *In vitro* measurement of Ca^{2+} binding activity using a fusion protein revealed only one Ca^{2+} bound per protein. From King and Patel-King (1995a). (b) Diagram illustrating the two Ca^{2+}-dependent responses of *Chlamydomonas* flagella. Phototaxis is the movement toward or away from a light source (*) and is achieved by differential regulation of beat frequency. The two flagella respond differently to the Ca^{2+} stimulus. Photoshock is an avoidance response that causes a change in flagellar waveform and leads to the transient reversal of swimming direction.

and Witman, 1984). LC3 is bound to the N-terminal 160 kDa of the β HC derived from the mutant *oda4-s7* which implies that this LC binds the stem domain rather than the globular motor unit (Sakakibara *et al.,* 1993). A mutant lacking the entire α HC (*oda11*) remains capable of assembling an intact outer arm that functions relatively well. However, this dynein lacks not only the α HC but also the associated LC5 protein (Sakakibara *et al.,* 1991). Molecular analysis of the LCs associated with the α and β HCs of outer arm dynein revealed that both contain perfect copies of the redox active site motif (W-C-G-P-C-K) of thioredoxin (Patel-King *et al.,* 1996). This sequence contains two cystine residues that are

arranged such that the side chain thiols are vicinal (in close apposition). In thioredoxin, the dithiol motif can convert a vicinal dithiol on a different protein to a disulfide bond. These observations imply that both LC proteins are sulfhydryl oxidoreductases. Interestingly, molecular modeling suggests that LC3 contains a second vicinal dithiol motif and therefore may play a novel role (Patel-King *et al.,* 1996). *In vitro,* both LCs will bind to phenylarsine oxide resin through the formation of a covalent dithioarsine ring structure that may be reduced by the monothiol β-mercaptoethanol. Furthermore, attempts to purify flagellar dynein from a crude extract based on phenylarsine oxide chromatography revealed that the outer arm, but not inner arms, could be obtained in this manner. As no redox-active inner arm components have been identified, this latter result strongly suggests that the predicted vicinal dithiols indeed occur within the native outer arm (Patel-King *et al.,* 1996).

A thioredoxin also has been identified within the outer arm from sea urchin sperm flagella, although in this case it exists as part of a modular IC (with a triplet repeat of nucleoside diphosphokinase) rather than as individual LCs (Ogawa *et al.,* 1996). This observation implies that sensing redox state is of significance for flagellar motility in general and is not *Chlamydomonas*-specific. Indeed, a redox-controlled cAMP-dependent tyrosine phosphorylation cascade has been suggested to control the capacitation (i.e., the acquisition of the ability to swim) of human spermatozoa (Aitken *et al.,* 1997). It is unclear at present what role these LC proteins play in *Chlamydomonas,* however, they may allow the outer arm to monitor, and potentially react to, global changes in the cytoplasmic levels of reducing equivalents. For example, a thioredoxin is required for the light-regulated translation of chloroplast mRNA in *Chlamydomonas* (Danon and Mayfield, 1994). In this situation, the LCs may modify the redox state of thiols present on their respective HCs or, they may form part of a redox-activated cascade with one LC acting upon the other. Alternatively, these thioredoxins may play a purely structural role as has been observed in T7 DNA polymerase, where the viral enzyme co-opts the host thioredoxin for use as a subunit necessary for high fidelity and processivity. In this situation, the thioredoxin does not play a redox-active role (Kunkel *et al.,* 1994).

3. Motor Domain-Associated LC

The largest LC in the outer arm (LC1) is associated with the γ HC; this interaction is stable under conditions of high ionic strength and appears hydrophobic in nature (Pfister *et al.,* 1982). Stoichiometry measurements suggest that there are two copies of this protein per dynein particle. LC1 is a member of the leucine-rich repeat (LRR) family of proteins (Benashski *et al.,* 1999). It is most closely related to an outer arm LC from sea urchin sperm flagella (50% sequence identity) and to the SDS22 protein that acts as a modulator of type-1 phosphatase activity at the metaphase/anaphase transition in *Schizosaccharomyces pombe* (32% identity) (Ohkura and Yanagida, 1991). Cross-linking of purified dynein using

the amine-selective reagent dimethylpimelimidate attached this LC directly to the γ HC. Combining cross-linking with vanadate-mediated photocleavage at two distinct sites within the HC allowed the association site to be mapped to a region encompassing the first two AAA domains within the globular motor unit (Fig. 6a; see color insert). To date, LC1 remains the only LC known to bind directly to a dynein motor domain. Furthermore, additional cross-linking experiments performed *in situ* identified an association between LC1 and a putative MT-binding protein (p45) (Benashski *et al.,* 1999). This ionic interaction is disrupted when the outer arm is removed from the axoneme by treatment with high salt buffer.

The solution structure of LC1 has been solved by NMR spectroscopy (Wu *et al.,* 1999, 2000). This protein consists of an N-terminal helix which caps one end of a barrel formed from six $\beta\beta\alpha$ motifs (the LRRs) followed by a C-terminal helical domain that protrudes from the main protein axis (Fig. 6b; see color insert). Structural comparisons revealed that LC1 is a close structural homolog of the U2A′ protein from the human spliceosome (3.7 Å rms deviation), even though these two proteins share only 22% sequence identity over the structurally aligned regions. This analysis has allowed functional domains of LC1 to be predicted. For example, the region involved in binding the γ HC is most likely centered on the single hydrophobic patch on the LC1 surface that derives from the large β sheet face (Fig. 6c; see color insert)—the equivalent region of U2A′ binds a single helix from a second spliceosome component U2B″. Furthermore, comparison of this U2B″ helix with the γ HC identified a remarkable similarity within the Box VII motif of the first AAA domain that may represent the LC1 attachment site (Fig. 6d; see color insert). The opposite face of LC1 contains patches of both positive and negative charge that could be involved in ionic interactions with p45.

The helical C-terminal domain of LC1 is oriented such that it will protrude into the globular head of the HC (Fig. 6e; see color insert). This domain contains several basic residues that may make ionic contacts either with HC residues or potentially with nucleotide. In the U2A′ crystal structure, the equivalent region has basic residues that bind the phosphate backbone of small nuclear RNA (Price *et al.,* 1998).

4. The LC8 Family

The LC8 protein and its homolog LC6 were first identified from the *Chlamydomonas* outer arm (King and Patel-King, 1995b). Examination of the sequence databases identified homologs with an astonishing level of sequence identity in many organisms—some of which do not have cilia or flagella at any life cycle stage. For example, the human and algal forms of the ~10-kDa LC8 protein share ~90% sequence identity with many of the nonidentical positions occupied by conservative replacements (Figs. 7a and 7b; see color insert).

Biochemical studies have subsequently determined that LC8 is not a dynein-specific protein. Rather, it is an integral component of many essential cellular

enzyme systems. In addition to both outer and inner arm flagellar dyneins and cytoplasmic dynein (Harrison *et al.,* 1998; King *et al.,* 1996a; King and Patel-King, 1995b), LC8 has also been found associated with the neuronal isoform of nitric oxide synthase (Jaffrey and Snyder, 1996), the unconventional actin motor myosin V (Espindola *et al.,* 2000), and IκBα (Hiscott *et al.,* 1997). Furthermore, this protein appears to mediate the association of a variety of polypeptides, such as the proapoptotic factor Bim (Puthalakath *et al.,* 1999) and *Drosophila* swallow (Schnorrer *et al.,* 2000), viruses (e.g., rabies (Raux *et al.,* 2000)), and mRNAs (Epstein *et al.,* 2000) with motor enzymes. In the flagellum, LC8 is also a component of the radial spokes (Yang *et al.,* 2000) and is required for intraflagellar transport (IFT) (Pazour *et al.,* 1998).

Mutants defective for LC8 function have been identified in a number of organisms. In *Drosophila,* partial loss-of-function results in a variety of developmental defects in bristle and wings, female sterility, and alterations in neuronal development. Total loss-of-function mutations lead to induction of apoptosis and embryonic lethality presumably when maternally derived stores of LC8 have been depleted (Dick *et al.,* 1996a; Phillis *et al.,* 1996). The *Aspergillus* form of LC8 is encoded at *nudG,* and mutations at this locus result in defects in the migration of nuclei along the fungal hyphae (Beckwith *et al.,* 1998). In unicellular organisms, loss of LC8 is not lethal. Indeed, no obvious phenotype was observed in strains of *Saccharomyces cerevisiae* that completely lack this protein (Dick *et al.,* 1996b). In *Chlamydomonas,* the LC8-null mutant (*fla14*) is able to grow at wild type rates but is unable to construct flagella due to defects in IFT as well as in axonemal dynein and radial spoke assembly (see section IV) (Pazour *et al.,* 1998).

In both the outer arm and cytoplasmic dynein, LC8 associates with the intermediate chains at the base of the protein complex (Gatti *et al.,* 1989; King *et al.,* 1998; Tang *et al.,* 1982). Indeed, one role for this protein appears to be as a molecular glue required for stable assembly of large macromolecular complexes. There are multiple copies of this protein in each complex: the most recent stoichiometry estimates suggest two copies within cytoplasmic dynein and four within the outer dynein arm. LC8 exists as a dimer in solution and *in situ* (Benashski *et al.,* 1997), and both NMR and X-ray structures are now available (Liang *et al.,* 1999; Tochio *et al.,* 1998). These structural studies confirmed the dimeric nature of LC8 and have revealed many details of how it binds to specific cellular proteins (Figs. 7c and 7d; see color insert). Each LC8 protein in the functional dimeric unit consists of two N-terminal helices arranged orthogonally and one N-terminal and four C-terminal β strands. Each monomer contains a single five-stranded β sheet, although interestingly, one strand from each monomer (β3) is looped out and hydrogen bonds with strands forming the β sheet of the second monomer (Liang *et al.,* 1999). Two identical binding surfaces for target peptides are formed from the clefts between the monomers (Fig. 7c). Peptide binding studies have revealed that several LC8-binding proteins interact with the functional dimer via a K/R-X-T-Q-T pentapeptide motif (Lo *et al.,* 2001). All residues contribute to binding although

some positions such as the penultimate Gln residue appear particularly important. This motif is present in a number of proteins that interact with LC8 (either *in vivo* or in a yeast two-hybrid screen) such as the N-terminal domain of the cytoplasmic dynein IC, *Drosophila* swallow, and the proapoptotic factor Bim_L isoform. However, other proteins including neuronal nitric oxide synthase and myosin V do not contain obvious versions of this motif even though all have been demonstrated to directly associate with the LC8 dimer. The IC1 component of the outer arm has a distantly related sequence ($_{184}$RETFT$_{188}$) that may interact with LC8.

Outer arm dynein is unusual in that it also contains a second member of the LC8 family termed LC6; these proteins share ~40% sequence identity (King and Patel-King, 1995b; Pfister *et al.,* 1982). As shown in Fig. 7b, the LC6 protein contains three insertions compared to LC8. Two of these additions occur N- and C-terminal to the secondary structure elements that form the LC8 core fold; the third insertion is located between helix $\alpha2$ and the $\beta2$ strand and may well have consequences for peptide binding specificity. In contrast, to LC8, however, LC6 null mutants show only a minor swimming defect (Pazour and Witman, 2000). Cross-linking experiments indicate that LC6 is in close, or possibly direct, contact with another LC (termed LC2 or Tctex2—see below) (DiBella *et al.,* 2001). However, the functional significance of this interaction is unknown at present.

5. The Tctex1/Tctex2 Family

The Tctex1 and Tctex2 proteins were first cloned from the murine *t* complex—an ~40-Mb region of chromosome 17 (Huw *et al.,* 1995; Lader *et al.,* 1989). Variant forms of the *t* complex (termed *t* haplotypes) exist in wild mouse populations. They are characterized by a series of inversions that serve to suppress recombination with the wild type version of the chromosome [reviewed in (Olds-Clarke, 1997; Silver, 1993)]. As a result, the *t* haplotypes are normally transmitted as an intact unit. Male mice heterozygous for a *t* haplotype ($+/t$) pass the *t* version of the chromosome on to ~95% of their progeny through a phenomenon termed transmission ratio distortion or meiotic drive. Male mice homozygous for complementing *t* haplotypes are sterile. This process is thought to derive from changes in spermiogenesis that lead to sperm carrying the wildtype chromosome having defective motility. The biological basis for this effect is apparently mediated through the action of a *t* mutant "responder" and a series of mutant "distorter" proteins. The wildtype responder is now known to be a sperm motility kinase (Smok), whereas the *t* haplotypes encode a mutant version known as Tcr. Tctex1 and Tctex2 were initially of interest as they map close to two distorter loci (Huw *et al.,* 1995; Lader *et al.,* 1989; O'Neill and Artzt, 1995).

At the biochemical level, Tctex1 was identified as a LC of mammalian cytoplasmic dynein (King *et al.,* 1996b). However, this protein was also found in isolated sperm, suggesting that it plays an additional role (Harrison *et al.,* 1998; O'Neill and Artzt, 1995). Subsequent studies in *Chlamydomonas* allowed for genetic dissection

of the axoneme and determined that Tctex1 is specifically missing only in mutants that lack inner arm I1. Furthermore, this protein was extracted from the axoneme by high salt and copurified with I1 dynein on sucrose gradients, confirming that it is indeed a component of this inner dynein arm (Harrison *et al.,* 1998).

Although not originally thought to be related, Tctex1 and Tctex2 actually define two major branches of a diverse protein family (DiBella *et al.,* 2001; Patel-King *et al.,* 1997). Tctex2 was initially described as a sperm membrane-associated protein (Huw *et al.,* 1995). However, molecular cloning of LC2 from the *Chlamydomonas outer* arm revealed that it was the *Chlamydomonas* form of Tctex2, implying that mammalian Tctex2 is actually a dynein LC (Patel-King *et al.,* 1997). LC2 is tightly associated with the ICs, LC7 and LC8 at the base of the soluble dynein particle [reviewed in (Witman *et al.,* 1991)]; a similar location was determined for Tctex1 in cytoplasmic dynein (King *et al.,* 1998). Genetic analysis in *Chlamydomonas* has determined that LC2 (Tctex2) is encoded at *ODA12* (Pazour *et al.,* 1999b). Null mutants at this locus are completely unable to assemble outer arms indicating that this protein is essential for dynein assembly. More recently, Tctex2 has also been found associated with mammalian cytoplasmic dynein (DiBella *et al.,* 2001). These observations provided the first clue that dynein dysfunction might provide the underlying biological basis for meiotic drive. Since then, it has become clear that the strongest distorter gene within the *t* complex encodes an axonemal dynein HC (Dnahc8), which further supports this hypothesis (Fossella *et al.,* 2000).

There is now good evidence that Tctex1 in cytoplasmic dynein is involved in attachment of specific cellular cargoes such as rhodopsin (Tai *et al.,* 1999), Doc-2 (Nagano *et al.,* 1998) and Fyn kinase (Kai *et al.,* 1997; Mou *et al.,* 1998) to the motor. Indeed, mutations in the C-terminal tail of rhodopsin that disrupt this interaction lead to retinitis pigmentosa in humans. Tctex1 maps at or near the human retinal cone dystrophy-1 locus supporting an important role for this protein in maintenance of retinal integrity (Watanabe *et al.,* 1996). Intriguingly, a variety of differentially expressed Tctex1 and Tctex2 homologs are present in mammalian tissues, suggesting that dyneins from these tissues vary at least with respect to LC content (DiBella *et al.,* 2001; King *et al.,* 1998). This has given rise to the hypothesis that one mechanism for regulating dynein–cargo interactions within the cytoplasm is through transcriptional control of LC expression.

Secondary structural predictions and circular dichroism spectroscopy suggest that Tctex1 consists of an N-terminal section containing two helices followed by several β strands (DiBella *et al.,* 2001). This arrangement of secondary structural elements has been confirmed by NMR analysis (Mok *et al.,* 2001; Wu *et al.,* 2001) and is remarkably similar to the highly conserved LC8 protein (Liang *et al.,* 1999; Tochio *et al.,* 1998) that also associates with the dynein ICs (Witman *et al.,* 1991), although these LC classes are apparently unrelated by primary sequence (King *et al.,* 1996b; King and Patel-King, 1995b). This structural similarity extends to the quaternary structural level, as Tctex1, like LC8 (Benashski *et al.,* 1997), also is dimeric (DiBella *et al.,* 2001). Furthermore, the dimer structure is not disrupted

even at high dilution, which suggests a very high affinity for the interaction between monomers as has been observed for LC8. In LC8, two identical protein attachment sites are formed from clefts at the interface between the two monomers in the functional unit. The interface itself involves an unusual strand switching, with a β strand from one monomer hydrogen bonding to the β sheet of the second monomer yielding a high-affinity association (Liang *et al.,* 1999). It will be of great interest to determine whether the similarities between these protein classes extend both to strand switching and formation of the cargo-binding sites.

Stoichiometry measurements indicate that there are two copies of Tctex1 per cytoplasmic dynein particle (King *et al.,* 1996b), whereas there is only a single copy of LC2 (Tctex2) in the *Chlamydomonas* outer arm (Benashski *et al.,* 1999). These estimates are completely consistent with the observation that Tctex1 is dimeric while the related proteins Tctex2 and LC2 are not (DiBella *et al.,* 2001). Binding studies using peptides derived from the IC of cytoplasmic dynein have located the Tctex1 binding site in that protein within the N-terminal domain just upstream of the LC8-interaction motif (Mok *et al.,* 2001). Further evidence for a functional distinction between Tctex1 and LC2 (Tctex2) derived from cross-linking experiments, which indicate that LC2 interacts directly with LC6 (a homolog of the highly conserved LC8 protein). In contrast, no evidence for association of Tctex1 and LC8 has been obtained (DiBella *et al.,* 2001) [and see (Benashski *et al.,* 1997)]. The difference in stoichiometry and oligomerization status for these two proteins raises intriguing questions about dynein organization and the roles played by these polypeptides.

6. The LC7/Roadblock Family

Molecular cloning of the LC7 protein from the *Chlamydomonas* outer arm identified a third class of LCs associated with the ICs at the base of the dynein particle (Bowman *et al.,* 1999). These proteins are missing from the axonemes of *oda* mutants, and recent evidence suggests that they also are required for dynein assembly (Pazour and Witman, 2000). Genetic screens for *Drosophila* larvae only able to crawl slowly (a characteristic phenotype for molecular motor defects) identified the closely related *roadblock* (*robl*) protein (Bowman *et al.,* 1999). These strains show a wide variety of phenotypes including the absence of imaginal tissue, possibly through a defect in mitosis, and a posterior, sluggish motility in larvae that progresses to complete paralysis of the posterior. This is consistent with severe aberrations in retrograde axonal transport that lead to the accumulation of cargo proteins and ultimately to axonal degeneration observed in these strains. Null mutations in *roadblock* result in pupal lethality. Intriguingly, the EMS-induced allele *robl*[z] exhibits an even stronger phenotype yielding a larval (rather than pupal) lethal defect. Moreover, this phenotype cannot be rescued even by insertion of two copies of the wild type gene, suggesting that *robl*[z], which has an internal deletion of 54 residues replaced by 12 residues from an intron, acts as a poison product.

The *robl* and LC7 proteins are 97 and 105 residues in length, respectively, and share 57% sequence identity (70% similarity). Examination of the sequence databases has identified many members of this protein family including seven in *Drosophila* and two in *Chlamydomonas* (Bowman *et al.,* 1999; S. M. King, unpublished) Mammals also contain multiple LC7/*robl* polypeptides. This LC family includes *Drosophila* bithoraxoid (bxd) which is encoded within the homeotic *Ultrabithorax* domain. Bxd is expressed only in the abdomen at the late larval to adult stages and has been implicated in the correct development of posterior thoracic and abdominal parasegments (Hogness *et al.,* 1985; Lipshitz *et al.,* 1987). It will be of considerable interest to determine whether the bithoraxoid protein is a dynein component. More recent sequence analysis has revealed that the LC7/*robl* proteins form part of a large ancient superfamily of proteins including members of both bacterial and archaeal origin (Koonin and Aravind, 2000). Several of the bacterial proteins have been implicated in the regulation of Ras/Rab/Rho family GTPases.

7. Actin

The six subspecies of inner arms that are built around single HCs all contain actin although the role played by this conserved protein in dynein function remains unknown (Kagami and Kamiya, 1992; Kagami *et al.,* 1990; Piperno *et al.,* 1990). There is a single actin gene in *Chlamydomonas* (Sugase *et al.,* 1996). Mutation at this locus (*IDA5*) results in the loss of all actin protein and leads to the failure of some actin-requiring activities (Kato-Minoura *et al.,* 1997). For example, the *ida5* mutant is unable to produce the fertilization tubule—an actin-based cell extension formed by male gametes—and thus shows a very low mating efficiency. This defect is rescued by reintroduction of the wildtype actin gene (Ohara *et al.,* 1998). Furthermore, these mutants swim slowly as they lack a subset of the inner arms with monomeric HCs. Two subspecies of monomeric inner arms (b and g) remain competent to assemble into the flagellum (Kato-Minoura *et al.,* 1997). Surprisingly, this ability does not reflect the inessential nature of actin in the assembly process, but rather the dramatic upregulation of a novel actin-like protein (termed NAP) that can functionally replace actin in these two dynein subspecies of the *ida5* mutant (Kato-Minoura *et al.,* 1998). NAP is closely related to actin and shares 64% sequence identity with both rabbit skeletal muscle and *Chlamydomonas* actin proteins (Lee *et al.,* 1997). As NAP has only been found in the *ida5* mutant, the role this protein plays in wildtype cells remains enigmatic.

8. p28

The p28 LC is found along the length of the axoneme associated with a subset of monomeric inner arms (Kagami and Kamiya, 1992; LeDizet and Piperno, 1995b; Piperno and Ramanis, 1991; Piperno *et al.,* 1990). The p28 protein is encoded at the

IDA4 locus (Kamiya *et al.,* 1991). To date, three mutant alleles of *IDA4* that affect the intron/exon splice sites within the gene have been identified. These mutations prevent the expression of wildtype p28 protein (LeDizet and Piperno, 1995a). Deficiencies in p28 lead to the failure of inner arm assembly and consequent alterations in flagellar waveform. At present, there is no further information on other roles played by p28 or on the protein–protein associations in which this essential polypeptide is involved.

D. Outer Arm Docking Complex

A combination of *in situ* cross-linking experiments and *in vitro* binding assays revealed that ICl of the outer arm interacts directly with, and is capable of binding to, α-tubulin (King *et al.,* 1995, 1991). These observations gave rise to the hypothesis that dynein ICs are involved in attaching the motor to its specific cargo. This idea has been largely confirmed in cytoplasmic dynein where there is now good evidence to support the interaction of IC74 with dynactin (Karki and Holzbaur, 1995). However, although IC1 may be involved in cargo attachment in the axoneme (i.e., association with the A-tubule of the flagellar doublet), it is not sufficient either for binding or for dictating where attachment occurs. Evidence for the requirement of an additional complex came from experiments aimed at rebinding purified dynein onto dynein-depleted axonemes (Takada *et al.,* 1992). These studies revealed that addition of purified dynein was not sufficient for reassociation and that an additional 7S complex (the docking complex or DC) was also required. This complex is composed of three polypeptides of 83 (DC1), 62.5 (DC2), and 21 (DC3) kDa, although there remains uncertainty over the precise stoichiometry. All three DC components are required for assembly of the arm; lack of any one of these protein results in an outer-arm-less phenotype (Casey *et al.,* 1998; Koutoulis *et al.,* 1997; Takada *et al.,* 2001). Electron microscopic analysis of the *oda1* and *oda3* mutants has revealed the absence of a small projection associated with the outer arm-binding site on the doublet MTs that is present in the other *oda* strains. This projection is thought to correspond to the docking complex. Both DC1 and DC2 are coiled coil proteins (Koutoulis *et al.,* 1997; Takada *et al.,* 2001), whereas DC3 contains EF hands and may bind Ca^{2+} (Casey *et al.,* 1998).

V. Dynein Motor Properties

Analysis of the swimming behavior of *Chlamydomonas* mutants and *in vitro* study of MT translocation activity have revealed that different axonemal dynein HCs display distinct motor activities. For example, while the three HCs within the *Chlamydomonas* outer arm are able to translocate MTs in an ATP-dependent

manner following adsorption to a glass surface (Sakakibara and Nakayama, 1998), the rates at which they each induce movement are quite different. Particles containing the α and β HCs moved MTs with a velocity of 4.6 μm s^{-1} in the presence of 1 mM ATP. Removal of the α HC had a dramatic effect, reducing the translocation rate to 0.7 μm s^{-1}. Furthermore, in order to measure activity of the β HC alone it was necessary to add methylcellulose to reduce Brownian motion of the MTs, implying that the β HC has low affinity for MTs and/or is highly nonprocessive. In contrast, the isolated γ HC moved MTs at a rate of 3.8 μm s^{-1} and did not require the presence of methylcellulose to keep the MT in contact with the motor. These differences are mirrored by *in vivo* measurements of swimming velocity of mutant cells lacking either the entire α HC (*oda11*) or the motor domain of the β HC (*oda4-s7*). Wildtype cells swim at a rate of $\sim$194 μm s^{-1}, whereas cells completely lacking outer arms (such as *oda4*) have a maximal velocity of only $\sim$62 μm s^{-1} (Kamiya and Okamoto, 1985; Mitchell and Rosenbaum, 1985). Removal of only the α HC (and its associated LC) yields an intermediate swimming phenotype of 119 μm s^{-1} (Sakakibara *et al.*, 1991), whereas lack of the β HC motor domain (in the *oda4-s7* allele) results in a velocity essentially indistinguishable from that of the outer-arm-less mutant (Sakakibara *et al.*, 1993). The γ HC appears to be essential for assembly of the entire structure, as mutants assembling dynein that lacks only this HC have not been obtained.

Microtubule-binding assays have also revealed distinctions between individual motors of the outer arm (Sakato and King, 2000). Wildtype outer arms (containing $\alpha\beta\gamma$ HCs) and dynein lacking the β HC motor (α-γ HCs; *oda4-s7*) bind MTs in the absence of ATP; most of this bound dynein is released by nucleotide addition in a Ca^{2+}-independent manner. In contrast, significant amounts of $\beta\gamma$ and γ HC particles (from *oda11* and the *oda4-s7 oda11* double mutant) do not bind MTs under low Ca^{2+} conditions, but associate in an ATP-dependent manner at high Ca^{2+}. Together, these results support the hypothesis that different HCs have distinct motor properties (Moss *et al.*, 1992a,b; Sakakibara and Nakayama, 1998). *In vivo*, the β HC appears to be responsible for most of the power output of the outer arm under normal swimming conditions (Sakakibara *et al.*, 1993), whereas a Ca^{2+}-dependent activity of the γ HC is unmasked *in vitro* only in the absence of the α HC (Sakato and King, 2000).

In vitro MT translocation assays of purified inner arm dyneins has reinforced the idea that different motors have distinct properties. The dimeric inner arm I1 (subspecies f) moved MTs only at very slow rates ($\sim$0.7 μm s^{-1}) (Smith and Sale, 1991). In contrast, the monomeric inner arm HC species translocate MTs with rates ranging from 2 to 12 μm s^{-1}, and all have a K_m apparent for ATP between 10 and 100 μM. Furthermore, these monomeric HCs (except b) impart torque, leading to the rotation of the MT during translocation (Kagami and Kamiya, 1992). Additional evidence for torque generation by dynein derived from analysis of the motility properties of *Tetrahymena* dynein, both in a standard motility assay (Vale and Toyoshima, 1988), and in a system where the MT end was attached

to the glass surface (Mimori and Miki-Noumura, 1995). In this latter system, incubation with dynein resulted in migration of the free portion of the MT toward the fixed terminus. This movement caused the MT to bend and eventually form a multiturn helix where the number of gyres was a function of the distance the motile MT end slid toward the fixed terminus. Dyneins do not track along single MT protofilaments, as does kinesin (Gelles *et al.,* 1988); rather they wander over the MT surface apparently at random (Wang *et al.,* 1995). Thus, torque generation may be the result of a directional bias in the off-axis motion of individual dynein motors. The functional significance of these intriguing observations on dynein-driven MT rotation for axonemal beating remains unclear at present.

Examination of reactivated flagellar beating in detergent-extracted cell models and *in vitro* translocation assays indicate that the presence of adenosine diphosphate (ADP) has a positive effect on dynein activity. For example, the velocity of MT movement by most inner arm species in the presence of 0.1 mM ATP and 0.1 mM ADP is enhanced over that observed with 0.1 mM ATP alone (Yagi *et al.,* 1994; Yagi, 2000). This observation suggests that in addition to the ATP hydrolytic site, dyneins also bind ADP at one of the other AAA domains within the head. This suggestion is consistent with experiments on outer arm dyneins that support the presence of two nucleotide binding sites with differing dissociation constants within the γ HC (Wilkerson and Witman, 1995). Furthermore, paralyzed axonemes from mutants lacking radial spokes or the central pair MTs can be induced to beat in the presence of low concentrations of both ATP and ADP (Omoto *et al.,* 1996). These observations suggest that the radial spokes/central pair may release the inhibition of dynein-based motility observed in the presence of ATP alone.

A recent study has revealed that single molecules of inner arm subspecies c can move a MT at least 1 μm at a rate of 0.7 μm s^{-1}; in the presence of multiple motors this rate increases to 5.1 μm s^{-1} (Sakakibara *et al.,* 1999). These data indicate that inner arm c is a processive motor (i.e., a single molecule can translocate a long distance along the MT without releasing it). However, in contrast to other processive motors such as kinesin, inner arm c has a low duty ratio and thus spends most of the mechanochemical cycle in a loosely bound or detached state. Using optical trap nanometry, it was observed that inner arm c has a step size of 8 nm (the length of the tubulin dimer) but slips backward when placed under high load. This raises the possibility that the action of inner arm c under high load conditions is responsible for the high-frequency ($\sim$300 Hz) vibration detected in quiescent axonemes (Kamimura and Kamiya, 1989).

VI. Intraflagellar Transport

In addition to dynein-driven axonemal beating, a second MT motor-mediated activity has been discovered in the flagellum (Kozminski *et al.,* 1993). The flagellum is

in a constant state of flux with the addition of new axonemal components occurring at the end distal to the cell body. This ordered assembly requires the directed transport of new components to the assembly site, a process referred to as intraflagellar transport (IFT), and is necessary for maintenance of flagellar integrity.

During IFT, raft-like structures located between the flagellar membrane and the outer doublet MTs are transported distally by a heterotrimeric kinesin encoded at the *FLA10* locus and recycled proximally by a dynein (Cole *et al.,* 1998; Pazour *et al.,* 1998; Piperno *et al.,* 1998; Porter *et al.,* 1999). In the *Chlamydomonas* flagellum, these structures travel to the flagellar tip at a rate of 2 μm s^{-1} and return to the cell body at 3.5 μm s^{-1}. The rafts consist of a series of scaffolding proteins that presumably associate with axonemal components to allow their transport to the flagellar tip. The raft scaffold is compositionally complex, consisting of 15 or more polypeptides that dissociate into two distinct particles during purification (Cole *et al.,* 1998). Not all these raft proteins have yet been characterized completely, although several are highly conserved between *Chlamydomonas,* nematodes, and mammals. Genetic analysis has revealed that some raft proteins are essential for IFT; for example, lack of the p88 raft component results in the complete failure of IFT (Pazour *et al.,* 2000). In mice, mutations in the p88 homolog Tg737 lead to shorter than normal primary cilia in the kidney. These mice suffer from polycystic kidney disease and die soon after birth. IFT is also thought to play a major role in the transport of rhodopsin in photoreceptors through the connecting cilium to the membrane stacks of the outer segment (Rosenbaum *et al.,* 1999).

The current model for IFT envisages that once the new axoneme components have been offloaded at the flagellar tip, the raft scaffold is then returned to the cell body by retrograde transport. This return movement is disrupted by mutations at two loci that lead to a massive accumulation of raft material within the flagellum and very short flagella. One defect occurs at the *FLA14* locus that encodes the LC8 protein. However, loss of LC8 results in pleiotropic effects as this protein is present in many flagellar enzyme systems including inner and outer arms and the radial spokes. The other defect occurs in the structural gene for the Dhc1b HC (Pazour *et al.,* 1999a; Porter *et al.,* 1999); similar defects in IFT due to Dhc1b disruption have been observed in *C. elegans* (Signor *et al.,* 1999). This is an intriguing dynein species as it exhibits attributes expected of both axonemal and cytoplasmic motors. Sequence analysis reveals that Dhc1b is most closely related to the cytoplasmic dynein motor. However, expression of Dhc1b is upregulated in response to deflagellation as expected for an axonemal motor. A similar upregulation has been observed following deciliation in sea urchin embryos (Gibbons *et al.,* 1994) and during ciliogenesis in rat tracheal epithelial cells (Criswell *et al.,* 1996). In contrast, expression studies in other tissues revealed that the DHC1b mRNA is present in a variety of cell types (e.g., HeLa and Cos cells) and tissues lacking motile cilia, such as liver and heart. Dhc1b (*a.k.a.* DHC2) in HeLa and Cos cells is localized mainly to the Golgi apparatus, and microinjection of specific antibody against Dhc1b caused the Golgi to disperse (Vaisberg *et al.,*

1996). This is unlike the situation with rat axonemal dynein HC genes whose expression is restricted to tissues that produce cilia or flagella (Criswell *et al.,* 1996).

   The IFT rafts and associated motors do not remain tightly associated with the axoneme following removal of the flagellar membrane; rather, they are found in the detergent-extracted matrix fraction. Sucrose gradient centrifugation has revealed that the mammalian Dhc2 dynein sediments at ∼15 S which is a value intermediate between that observed for the monomeric HCs, which sediment at 10–12 S, and the dimeric/trimeric HCs with associated ICs and LCs that migrate at 18–21 S. Further attempts to purify Dhc1b or DHC2 have not yet met with a great deal of success due mostly to the very small quantities of protein present in the extracts. Thus, there is no information available at present concerning the other components of this intriguing dynein motor enzyme, although the phenotype of the *fla14* mutant clearly suggests that it may contain LC8.

VII. Concluding Remarks

The combination of genetic, structural, and biochemical techniques has made *Chlamydomonas* flagellar dyneins some of the best-characterized enzymes in this class of MT-based molecular motor. Genetic approaches have been especially powerful in uncovering regulatory pathways that ultimately impinge on motor activity and in dissecting the complexities of the inner and outer arm systems. *In vitro* analysis has allowed many details of these pathways and enzymes to be defined at the biochemical level. Furthermore, study of *Chlamydomonas* flagellar outer arm dyneins has led to detailed understanding of dynein architecture and function, and to the identification of many features/components of the related cytoplasmic isozymes. These enzymes are required for many activities including mitosis and vesicular transport, and consequently, analysis of *Chlamydomonas* dyneins has had implications that extend beyond flagellar function per se. A recent example is the initial discovery of IFT in the *Chlamydomonas* flagellum. Subsequent analysis has revealed that very similar bidirectional transport processes, mediated by heterotrimeric kinesins and the 1b class of cytoplasmic dynein, are involved in the function of certain sensory neurons and in the transport of visual pigment within the retina. With all these advantages, it is clear that the *Chlamydomonas* model system has a bright future in ongoing efforts to define the complexities of dynein biology.

Acknowledgments

References

Aitken, R. J., Harkiss, D., Knox, W., Paterson, M., and Irvine, D. S. (1997). A novel signal transduction cascade in capacitating human spermatozoa characterised by a redox-regulated, cAMP-mediated induction of tyrosine phosphorylation. *J. Cell Sci.* **111,** 645–656.

Avolio, J., Lebduska, S., and Satir, P. (1984). Dynein arm substructure and the orientation of arm-microtubule attachments. *J. Mol. Biol.* **173,** 389–401.

Baumeister, W., and Lupas, A. (1997). The proteasome. *Curr. Opin. Struct. Biol.* **7,** 273–278.

Beckwith, S. M., Roghi, C. H., Liu, B., and Ronald Morris, N. (1998). The "8-kD" cytoplasmic dynein light chain is required for nuclear migration and for dynein heavy chain localization in *Aspergillus nidulans. J. Cell.Biol.* **143,** 1239–1247.

Benashski, S. E., Harrison, A., Patel-King, R. S., and King, S. M. (1997). Dimerization of the highly conserved light chain shared by dynein and myosin V. *J. Biol. Chem.* **272,** 20,929–20,935.

Benashski, S. E., Patel-King, R. S., and King, S. M. (1999). Light chain 1 from the *Chlamydomonas* outer dynein arm is a leucine-rich repeat protein associated with the motor domain of the γ heavy chain. *Biochemistry* **38,** 7253–7264.

Bessen, M., Fay, R. B., and Witman, G. B. (1980). Calcium control of waveform in isolated flagellar axonemes of *Chlamydomonas. J. Cell Biol.* **86,** 446–455.

Bowman, A. B., Patel-King, R. S., Benashski, S. E., McCaffery, J. M., Goldstein, L. S., and King, S. M. (1999). *Drosophila roadblock* and *Chlamydomonas* LC7: A conserved family of dynein-associated proteins involved in axonal transport, flagellar motility, and mitosis. *J. Cell Biol.* **146,** 165–180.

Brokaw, C. J., and Kamiya, R. (1987). Bending patterns of *Chlamydomonas* flagella: IV. Mutants with defects in inner and outer dynein arms indicate differences in dynein arm function. *Cell Motil. Cytoskel.* **8,** 68–75.

Casey, D. M., Pazour, G. J., Wilkerson, C. G., Inaba, K., Koutoulis, A., Takada, S., Kamiya, R., and Witman, G. B. (1998). Identification and insertional mutagenesis of a new *Chlamydomonas reinhardtii* gene, *ODA14,* that encodes the 25-kDa subunit of the outer dynein arm docking complex (ODA-DC). *Mol. Biol. Cell* **9,** 155a.

Cole, D. G., Diener, D. R., Himelblau, A. L., Beech, P. L., Fuster, J. C., and Rosenbaum, J. L. (1998). *Chlamydomonas* kinesin-II-dependent intraflagellar transport (IFT): IFT particles contain proteins required for ciliary assembly in *Caenorhabditis elegans* sensory neurons. *J. Cell Biol.* **141,** 993–1008.

Criswell, P. S., Ostrowski, L. E., and Asai, D. J. (1996). A novel cytoplasmic dynein heavy chain: Expression of DHC1b in mammalian ciliated epithelial cells. *J. Cell Sci.* **109,** 1891–1898.

Danon, A., and Mayfield, S. P. (1994). Light-regulated translation of chloroplast messenger RNAs through redox potential. *Science* **266,** 1717–1719.

DiBella, L. M., Benashski, S. E., Tedford, H. W., Harrison, A., Patel-King, R. S., and King, S. M. (2001). The Tctex1/Tctex2 class of dynein light chains: Dimerization, differential expression and interaction with the LC8 protein family. *J. Biol. Chem.* **276,** 14366–14373.

Dick, T., Ray, K., Salz, H. K., and Chia, W. (1996a). Cytoplasmic dynein (ddlc1) mutations cause morphogenetic defects and apoptotic cell death in *Drosophila melanogaster. Mol. Cell Biol.* **16,** 1966–1977.

Dick, T., Surana, U., and Chia, W. (1996b). Molecular and genetic characterization of SLC1, a putative *Saccharomyces cerevisiae* homolog of the metazoan cytoplasmic dynein light chain 1. *Mol. Gen. Genet.* **251,** 38–43.

Epstein, E., Sela-Brown, A., Ringel, I., Kilav, R., King, S. M., Benashski, S. E., Yisraeli, J. K., Silver, J., and Naveh-Many, T. (2000). Dynein light chain binding to a 3′-untranslated sequence mediates parathyroid hormone mRNA association with microtubules. *J. Clin. Invest.* **105,** 505–512.

Espindola, F. S., Suter, D. M., Partata, L. B., Cao, T., Wolenski, J. S., Cheney, R. E., King, S. M., and Mooseker, M. S. (2000). The light chain composition of chicken brain myosin-Va: Calmodulin, myosin-II essential light chains, and 8-kDa dynein light chain/PIN. *Cell Motil. Cytoskel.* **47,** 269–281.

Fossella, J., Samant, S. A., Silver, L. M., King, S. M., Vaughan, K. T., Olds-Clarke, P., Johnson, K. A., Mikami, A., Vallee, R. B., and Pilder, S. H. (2000). An axonemal dynein at the *Hybrid Sterility 6* locus: Implications for *t* haplotype-specific male sterility and the evolution of species barriers. *Mamm. Genome* **11,** 8–15.

Gardner, L. C., O'Toole, E., Perrone, C. A., Giddings, T., and Porter, M. E. (1994). Components of a "dynein regulatory complex" are located at the junction between the radial spokes and the dynein arms in *Chlamydomonas* flagella. *J. Cell Biol.* **127,** 1311–1325.

Gatti, J.-L., King, S. M., Moss, A. G., and Witman, G. B. (1989). Outer arm dynein from trout spermatozoa. Purification, polypeptide composition, and enzymatic properties. *J. Biol. Chem.* **260,** 11,450–11,457.

Gee, M. A., Heuser, J. E., and Vallee, R. B. (1997). An extended microtubule-binding structure within the dynein motor domain. *Nature* **390,** 636–639.

Gelles, J., Schnapp, B. J., and Sheetz, M. P. (1988). Tracking kinesin-driven movements with nanometre-scale precision. *Nature* **331,** 450–453.

Gibbons, B. H., Asai, D. J., Tang, W. J., Hays, T. S., and Gibbons, I. R. (1994). Phylogeny and expression of axonemal and cytoplasmic dynein genes in sea urchins. *Mol. Biol. Cell* **5,** 57–70.

Gibbons, I. R., Gibbons, B. H., Mocz, G., and Asai, D. J. (1991). Multiple nucleotide-binding sites in the sequence of dynein *β* heavy chain. *Nature* **352,** 640–643.

Gibbons, I. R., Lee-Eiford, A., Mocz, G., Phillipson, C. A., Tang, W. J., and Gibbons, B. H. (1987). Photosensitized cleavage of dynein heavy chains. Cleavage at the "V1 site" by irradiation at 365 nm in the presence of ATP and vanadate. *J. Biol. Chem.* **262,** 2780–2786.

Goodenough, U., and Heuser, J. (1984). Structural comparison of purified dynein proteins with *in situ* dynein arms. *J. Mol. Biol.* **180,** 1083–1118.

Habermacher, G., and Sale, W. S. (1996). Regulation of flagellar dynein by an axonemal type-1 phosphatase in *Chlamydomonas*. *J. Cell Sci.* **109,** 1899–1907.

Habermacher, G., and Sale, W. S. (1997). Regulation of flagellar dynein by phosphorylation of a 138-kD inner arm dynein intermediate chain. *J. Cell Biol.* **136,** 167–176.

Habura, A., Tikhonenko, I., Chisholm, R. L., and Koonce, M. P. (1999). Interaction mapping of a dynein heavy chain. Identification of dimerization and intermediate chain-binding domains. *J. Biol. Chem.* **274,** 15,447–15,453.

Harrison, A., and King, S. M. (2000). The molecular anatomy of dynein. *In* "Essays *in* Biochemistry" (G. Banting and S. J. Higgins, Eds.), Vol. 35, pp. 75–87. Portland Press, London.

Harrison, A., Olds-Clarke, P., and King, S. M. (1998). Identification of the *t* complex-encoded cytoplasmic dynein light chain Tctex1 in inner arm I1 supports the involvement of flagellar dyneins in meiotic drive. *J. Cell Biol.* **140,** 1137–1147.

Hasagawa, E., Hayashi, H., Asakura, S., and Kamiya, R. (1987). Stimulation of *in vitro* motility of *Chlamydomonas* axonemes by inhibition of cAMP-dependent phosphorylation. *Cell Motil.* **8,** 302–311.

Hiscott, J., Beauparlant, P., Crepieux, P., DeLuca, C., Kwon, H., Lin, R., and Petropoulos, L. (1997). Cellular and viral protein interactions regulating IκBα activity during human retrovirus infection. *J. Leukocyte Biol.* **62,** 82–92.

Hogness, D. S., Lipshitz, H. D., Beachy, P. A., Peattie, D. A., Saint, R. B., Goldschmidt-Clermont, M., Harte, P. J., Gavis, E. R., and Helfand, S. L. (1985). Regulation and products of the Ubx domain of the Bithorax complex. *Cold Spring Harbor Symp. Quant. Biol.* **50,** 181–194.

Howard, D. R., Habermacher, G., Glass, D. B., Smith, E. F., and Sale, W. S. (1994). Regulation of *Chlamydomonas* flagellar dynein by an axonemal protein kinase. *J. Cell Biol.* **127,** 1683–1692.

Huang, B., Piperno, G., and Luck, D. J. L. (1979). Paralyzed flagellar mutants of *Chlamydomonas reinhardtii* defective for axonemal doublet microtubule arms. *J. Biol. Chem.* **254,** 3091–3099.

Huang, B., Ramanis, Z., and Luck, D. J. (1982). Suppressor mutations in *Chlamydomonas* reveal a regulatory mechanism for flagellar function. *Cell* **28,** 115–124.

Huw, L. Y., Goldsborough, A. S., Willison, K., and Artzt, K. (1995). Tctex2: A sperm tail surface protein mapping to the *t*-complex. *Dev. Biol.* **170,** 183–194.

Jaffrey, S. R., and Snyder, S. H. (1996). PIN: An associated protein inhibitor of neuronal nitric oxide synthase. *Science* **274,** 774–777.

Johnson, K. A., and Wall, J. S. (1983). Structure and molecular weight of the dynein ATPase. *J. Cell Biol.* **96,** 669–678.

Kagami, O., and Kamiya, R. (1992). Translocation and rotation of microtubules caused by multiple species of *Chlamydomonas* inner-arm dynein. *J. Cell Sci.* **103,** 653–664.

Kagami, O., Takada, S., and Kamiya, R. (1990). Microtubule translocation caused by three subspecies of inner-arm dynein from *Chlamydomonas* flagella. *FEBS Lett.* **264,** 179–182.

Kai, N., Mishina, M., and Yagi, T. (1997). Molecular cloning of Fyn-associated molecules in the mouse central nervous system. *J. Neurosci. Res.* **48,** 407–424.

Kamimura, S., and Kamiya, R. (1989). High-frequency nanometre-scale vibration in 'quiescent' flagellar axonemes. *Nature* **340,** 476–478.

Kamiya, R. (1988). Mutations at twelve independent loci result in absence of outer dynein arms in *Chlamydomonas reinhardtii*. *J. Cell Biol.* **107,** 2253–2258.

Kamiya, R., Kurimoto, E., and Muto, E. (1991). Two types of *Chlamydomonas* flagellar mutants missing different components of inner-arm dynein. *J. Cell Biol,* **112,** 441–447.

Kamiya, R., Kurimoto, E., Sakakibara, H., and Okagaki, T. (1989). A genetic approach to the function of inner and outer arm dynein. *In* "Cell Movement: The Dynein ATPases" (F. D. Warner, P. Satir, and I. R. Gibbons, Eds.), Vol. 1, pp. 209–218. A. R. Liss, New York.

Kamiya, R., and Okamoto, M. (1985). A mutant of *Chlamydomonas reinhardtii* that lacks the flagellar outer dynein arm but can swim. *J. Cell Sci.* **74,** 181–191.

Kamiya, R., and Witman, G. B. (1984). Submicromolar levels of calcium control the balance of beating between the two flagella in demembranated models of *Chlamydomonas*. *J. Cell Biol.* **98,** 97–107.

Karki, S., and Holzbaur, E. L. (1995). Affinity chromatography demonstrates a direct binding between cytoplasmic dynein and the dynactin complex. *J. Biol. Chem.* **270,** 28,806–28,811.

Kato, T., Kagami, O., Yagi, T., and Kamiya, R. (1993). Isolation of two species of *Chlamydomonas reinhardtii* flagellar mutants, *ida5* and *ida6,* that lack a newly identified heavy chain of the inner dynein arm. *Cell Struct. Funct.* **18,** 371–377.

Kato-Minoura, T., Hirono, M., and Kamiya, R. (1997). *Chlamydomonas* inner-arm dynein mutant, *ida5,* has a mutation in an actin-encoding gene. *J. Cell Biol.* **137,** 649–656.

Kato-Minoura, T., Uryu, S., Hirono, M., and Kamiya, R. (1998). Highly divergent actin expressed in a *Chlamydomonas* mutant lacking the conventional actin gene. *Biochem. Biophys. Res. Commun.* **251,** 71–76.

King, S. J., and Dutcher, S. K. (1997). Phosphoregulation of an inner dynein arm complex in *Chlamydomonas reinhardtii* is altered in phototactic mutant strains. *J. Cell Biol.* **136,** 177–191.

King, S. J., Inwood, W. B., O'Toole, E. T., Power, J., and Dutcher, S. K. (1994). The *bop2-1* mutation reveals radial asymmetry in the inner dynein arm region of *Chlamydomonas reinhardtii*. *J. Cell Biol.* **126,** 1255–1266.

King, S. M. (2000). AAA domains and organization of the dynein motor unit. *J. Cell Sci.* **113,** 2521–2526.

King, S. M., Barbarese, E., Dillman, J. F. III, Benashski, S. E., Do, K. T., Patel-King, R. S., and Pfister, K. K. (1998). Cytoplasmic dynein contains a family of differentially expressed light chains. *Biochemistry* **37,** 15,033–15,041.

King, S. M., Barbarese, E., Dillman, J. F. III, Patel-King, R. S., Carson, J. H., and Pfister, K. K. (1996a). Brain cytoplasmic and flagellar outer arm dyneins share a highly conserved M_r 8,000 light chain. *J. Biol. Chem.* **271,** 19,358–19,366.

King, S. M., Dillman, J. F. III, Benashski, S. E., Lye, R. J., Patel-King, R. S., and Pfister, K. K. (1996b). The mouse *t*-complex-encoded protein Tctex-1 is a light chain of brain cytoplasmic dynein. *J. Biol. Chem.* **271,** 32,281–32,287.

King, S. M., Haley, B. E., and Witman, G. B. (1989). Structure of the α and β heavy chains of the outer arm dynein from *Chlamydomonas* flagella. Nucleotide binding sites. *J. Biol. Chem.* **264,** 10,210–10,218.

King, S. M., and Patel-King, R. S. (1995a). Identification of a Ca^{2+}-binding light chain within *Chlamydomonas* outer arm dynein. *J. Cell Sci.* **108,** 3757–3764.

King, S. M., and Patel-King, R. S. (1995b). The $M_{(r)} = 8,000$ and 11,000 outer arm dynein light chains from *Chlamydomonas* flagella have cytoplasmic homologues. *J. Biol. Chem.* **270,** 11,445–11,452.

King, S. M., Patel-King, R. S., Wilkerson, C. G., and Witman, G. B. (1995). The 78,000-$M_{(r)}$ intermediate chain of *Chlamydomonas* outer arm dynein is a microtubule-binding protein. *J. Cell Biol.* **131,** 399–409.

King, S. M., Wilkerson, C. G., and Witman, G. B. (1991). The M_r78,000 intermediate chain of *Chlamydomonas* outer arm dynein interacts with α-tubulin *in situ*. *J. Biol. Chem.* **266,** 8401–8407.

King, S. M., and Witman, G. B. (1987). Structure of the α and β heavy chains of the outer arm dynein from *Chlamydomonas* flagella. Masses of chains and sites of ultraviolet-induced vanadate-dependent cleavage. *J. Biol. Chem.* **262,** 17596–17604.

King, S. M., and Witman, G. B. (1988). Structure of the γ heavy chain of the outer arm dynein from *Chlamydomonas* flagella. *J. Cell Biol.* **107,** 1799–1808.

King, S. M., and Witman, G. B. (1990). Localization of an intermediate chain of outer arm dynein by immunoelectron microscopy. *J. Biol. Chem.* **265,** 19,807–19,811.

King, S. M., and Witman, G. B. (1994). Multiple sites of phosphorylation within the α heavy chain of *Chlamydomonas* outer arm dynein. *J. Biol. Chem.* **269,** 5452–5457.

Koonce, M. P. (1997). Identification of a microtubule-binding domain in a cytoplasmic dynein heavy chain. *J. Biol. Chem.* **272,** 19,714–19,718.

Koonce, M. P., Grissom, P. M., and McIntosh, J. R. (1992). Dynein from *Dictyostelium:* Primary structure comparisons between a cytoplasmic motor enzyme and flagellar dynein. *J. Cell Biol.* **119,** 1597–1604.

Koonce, M. P., and Tikhonenko, I. (2000). Functional elements within the dynein microtubule-binding domain. *Mol. Biol. Cell* **11,** 523–529.

Koonin, E. V., and Aravind, L. (2000). Dynein light chains of the Roadblock/LC7 group belong to an ancient protein superfamily implicated in NTPase regulation. *Curr. Biol.* **10,** R774–R776.

Koutoulis, A., Pazour, G. J., Wilkerson, C. G., Inaba, K., Sheng, H., Takada, S., and Witman, G. B. (1997). The *Chlamydomonas reinhardtii ODA3* gene encodes a protein of the outer dynein arm docking complex. *J. Cell Biol.* **137,** 1069–1080.

Kozminski, K. G., Johnson, K. A., Forscher, P., and Rosenbaum, J. L. (1993). A motility in the eukaryotic flagellum unrelated to flagellar beating. *Proc. Natl. Acad. Sci. USA* **90,** 5519–5523.

Kunkel, T. A., Patel, S. M., and Johnson, K. A. (1994). Error-prone replication of repeated DNA sequences by T7 DNA polymerase in the absence of its processivity subunit. *Proc. Natl. Acad. Sci. USA* **91,** 6830–3834.

Lader, E., Ha, H. S., O'Neill, M., Artzt, K., and Bennett, D. (1989). *tctex-1:* A candidate gene family for a mouse *t* complex sterility locus. *Cell* **58,** 969–979.

LeDizet, M., and Piperno, G. (1995a). *ida4-1, ida4-2,* and *ida4-3* are intron splicing mutations affecting the locus encoding p28, a light chain of *Chlamydomonas* axonemal inner dynein arms. *Mol. Biol. Cell* **6,** 713–723.

LeDizet, M., and Piperno, G. (1995b). The light chain p28 associates with a subset of inner dynein arm heavy chains in *Chlamydomonas* axonemes. *Mol. Biol. Cell* **6,** 697–711.

Lee, V. D., Finstad, S. L., and Huang, B. (1997). Cloning and characterization of a gene encoding an actin-related protein in *Chlamydomonas*. *Gene* **197,** 153–159.

Lee-Eiford, A., Ow, R. A., and Gibbons, I. R. (1986). Specific cleavage of dynein heavy chains by ultraviolet irradiation in the presence of ATP and vanadate. *J. Biol. Chem.* **261,** 2337–2342.

Lenzen, C. U., Steinmann, D., Whiteheart, S. W., and Weiss, W. I. (1998). Crystal structure of the hexamerization domain of N-ethylmaleimide-sensitive fusion protein. *Cell* **94,** 525–536.

Liang, J., Jaffrey, S. R., Guo, W., Snyder, S. H., and Clardy, J. (1999). Structure of the PIN/LC8 dimer with a bound peptide. *Nat. Struct. Biol.* **6,** 735–740.

Lipshitz, H. D., Peattie, D. A., and Hogness, D. S. (1987). Novel transcripts from the Ultrabithorax domain of the Bithorax complex. *Genes Dev.* **1,** 307–322.

Lo, K. W.- H., Naisbitt, S., Fan, J.-S., Sheng, M., and Zhang, M. (2001). The 8 kDa dynein light chain binds to its targets via a conserved "K/R-X-T-Q-T" motif. *J. Biol. Chem.,* **276,** 14059–14066.

Luck, D. J. (1984). Genetic and biochemical dissection of the eucaryotic flagellum. *J. Cell Biol.* **98,** 789–794.

Luck, D. J. L., and Piperno, G. (1989). Dynein arm mutants of *Chlamydomonas*. *In* "Cell Movement: The Dynein ATPase" (F. D. Warner, P. Satir, and I. R. Gibbons, Eds.), Vol. 1, pp. 49–60. A. R. Liss, New York.

Marchese-Ragona, S. P., Wall, J. S., and Johnson, K. A. (1988). Structure and mass analysis of 14S dynein obtained from *Tetrahymena* cilia. *J. Cell Biol.* **106,** 127–132.

Mastronarde, D. N., O'Toole, E. T., McDonald, K. L., McIntosh, J. R., and Porter, M. E. (1992). Arrangement of inner dynein arms in wild-type and mutant flagella of *Chlamydomonas*. *J. Cell Biol.* **118,** 1145–1162.

Mimori, Y., and Miki-Noumura, T. (1995). Extrusion of rotating microtubules on the dynein-track from a microtubule-dynein γ-complex. *Cell Motil. Cytoskeleton* **30,** 17–25.

Mitchell, D. R., and Brown, K. S. (1994). Sequence analysis of the *Chlamydomonas* α and β dynein heavy chain genes. *J. Cell Sci.* **107,** 635–644.

Mitchell, D. R., and Kang, Y. (1991). Identification of *oda6* as a *Chlamydomonas* dynein mutant by rescue with the wild-type gene. *J. Cell Biol.* **113,** 835–842.

Mitchell, D. R., and Kang, Y. (1993). Reversion analysis of dynein intermediate chain function. *J. Cell Sci.* **105,** 1069–1078.

Mitchell, D. R., and Rosenbaum, J. L. (1985). A motile *Chlamydomonas* flagellar mutant that lacks outer dynein arms. *J. Cell Biol.* **100,** 1228–1234.

Mocz, G., and Gibbons, I. R. (1990). A circular dichroic study of helical structure in flagellar dynein. *Biochemistry* **29,** 4839–4843.

Mocz, G., and Gibbons, I. R. (1996). Phase partition analysis of nucleotide binding to axonemal dynein. *Biochemistry* **35,** 9204–9211.

Mocz, G., Helms, M. K., Jameson, D. M., and Gibbons, I. R. (1998). Probing the nucleotide binding sites of axonemal dynein with the fluorescent nucleotide analogue 2′(3′)-O-(-N- Methylanthraniloyl)-adenosine 5′-triphosphate. *Biochemistry* **37,** 9862–9869.

Mocz, G., Tang, W. J., and Gibbons, I. R. (1988). A map of photolytic and tryptic cleavage sites on the β heavy chain of dynein ATPase from sea urchin sperm flagella. *J. Cell Biol.* **106,** 1607–1614.

Mok, Y.-K., Lo, K. W.-H., and Zhang, M. (2001). Structure of Tctex-1 and its interaction with cytoplasmic dynein intermediate chain. *J. Biol. Chem.,* **276,** 14067–14074.

Moss, A. G., Gatti, J. L., and Witman, G. B. (1992a). The motile β/IC1 subunit of sea urchin sperm outer arm dynein does not form a rigor bond. *J.Cell Biol.* **118,** 1177–1188.

Moss, A. G., Sale, W. S., Fox, L. A., and Witman, G. B. (1992b). The α subunit of sea urchin sperm outer arm dynein mediates structural and rigor binding to microtubules. *J. Cell Biol.* **118,** 1189–1200.

Mou, T., Kraas, J. R., Fung, E. T., and Swope, S. L. (1998). Identification of a dynein molecular motor component in *Torpedo* electroplax: Binding and phosphorylation of Tctex-1 by Fyn. *FEBS Lett.* **435,** 275–281.

Myster, S. H., Knott, J. A., O'Toole, E., and Porter, M. E. (1997). The *Chlamydomonas* Dhc1 gene encodes a dynein heavy chain subunit required for assembly of the I1 inner arm complex. *Mol. Biol. Cell* **8,** 607–620.

Nagano, F., Orita, S., Sasaki, T., Naito, A., Sakaguchi, G., Maeda, M., Watanabe, T., Kominami, E., Uchiyama, Y., and Takai, Y. (1998). Interaction of Doc2 with tctex-1, a light chain of cytoplasmic dynein. Implication in dynein-dependent vesicle transport. *J. Biol. Chem.* **273,** 30,065–30,068.

Neer, E. J., Schmidt, C. J., Nambudripad, R., and Smith, T. F. (1994). The ancient regulatory protein family of WD-repeat proteins. *Nature* **371,** 297–300.

Neuwald, A. F., Aravind, L., Spouge, J. L., and Koonin, E. V. (1999). AAA+: A class of chaperone-like ATPases associated with the assembly, operation, and disassembly of protein complexes. *Genome Res.* **9,** 27–43.

Ogawa, K. (1991). Four ATP-binding sites in the midregion of the β heavy chain of dynein. *Nature* **352,** 643–645.

Ogawa, K., Takai, H., Ogiwara, A., Yokota, E., Shimizu, T., Inaba, K., and Mohri, H. (1996). Is outer arm dynein intermediate chain 1 multifunctional? *Mol. Biol. Cell* **7,** 1895–1907.

Ohara, A., Kato-Minoura, T., Kamiya, R., and Hirono, M. (1998). Recovery of flagellar inner-arm dynein and the fertilization tubule in *Chlamydomonas ida5* mutant by transformation with actin genes. *Cell Struct. Funct.* **23,** 273–281.

Ohkura, H., and Yanagida, M. (1991). *S.pombe* gene sds22+ essential for a midmitotic transition encodes a leucine-rich repeat protein that positively modulates protein phosphatase-1. *Cell* **64,** 149–157.

Olds-Clarke, P. (1997). Models for male infertility: the *t* haplotypes. *Rev. Reprod.* **2,** 157–164.

Omoto, C. K., and Nakamaye, K. (1989). ATP analogs substituted on the 2-position as substrates for dynein ATPase activity. *Biochim. Biophys. Acta* **999,** 221–224.

Omoto, C. K., Yagi, T., Kurimoto, E., and Kamiya, R. (1996). Ability of paralyzed flagellar mutants of *Chlamydomonas* to move. *Cell Motil. Cytoskeleton* **33,** 88–94.

O'Neill, M. J., and Artzt, K. (1995). Identification of a germ-cell-specific transcriptional repressor in the promoter of Tctex-1. *Development* **121,** 561–568.

Paschal, B. M., Mikami, A., Pfister, K. K., and Vallee, R. B. (1992). Homology of the 74-kD cytoplasmic dynein subunit with a flagellar dynein polypeptide suggests an intracellular targeting function. *J. Cell Biol.* **118,** 1133–1143.

Patel-King, R. S., Benashski, S. E., Harrison, A., and King, S. M. (1996). Two functional thioredoxins containing redox-sensitive vicinal dithiols from the *Chlamydomonas* outer dynein arm. *J. Biol. Chem.* **271,** 6283–6291.

Patel-King, R. S., Benashski, S. E., Harrison, A., and King, S. M. (1997). A *Chlamydomonas* homologue of the putative murine *t* complex distorter Tctex-2 is an outer arm dynein light chain. *J.Cell Biol.* **137,** 1081–1090.

Pazour, G. J., Dickert, B. L., Vucca, Y., Seeley, E. S., Rosenbaum, J. L., Witman, G. B., and Cole, D. G. (2000). *Chlamydomonas* IFT88 and its mouse homologue, polycystic kidney disease gene Tg737, are required for assembly of cilia and flagella. *J. Cell Biol.* **151,** 709–718.

Pazour, G. J., Dickert, B. L., and Witman, G. B. (1999a). The DHC1b (DHC2) isoform of cytoplasmic dynein is required for flagellar assembly. *J. Cell Biol.* **144,** 473–481.

Pazour, G. J., Koutoulis, A., Benashski, S. E., Dickert, B. L., Sheng, H., Patel-King, R. S., King, S. M., and Witman, G. B. (1999b). LC2, the *Chlamydomonas* homologue of the *t* complex-encoded protein Tctex2, is essential for outer dynein arm assembly. *Mol. Biol. Cell* **10,** 3507–3520.

Pazour, G. J., Wilkerson, C. G., and Witman, G. B. (1998). A dynein light chain is essential for the retrograde particle movement of intralagellar transport (IFT). *J. Cell Biol.* **141,** 979–992.

Pazour, G. J., and Witman, G. B. (2000). Forward and reverse genetic analysis of microtubule motors in *Chlamydomonas*. *Methods* **22,** 285–298.

Perrone, C. A., Myster, S. H., Bower, R., O'Toole, E. T., and Porter, M. E. (2000). Insights into the structural organization of the I1 inner arm dynein from a domain analysis of the 1β dynein heavy chain. *Mol. Biol. Cell* **11,** 2297–2313.

Perrone, C. A., Yang, P., O'Toole, E., Sale, W. S., and Porter, M. E. (1998). The *Chlamydomonas IDA7* locus encodes a 140-kDa dynein intermediate chain required to assemble the I1 inner arm complex. *Mol. Biol. Cell* **9,** 3351–3365.

Pfister, K. K., Fay, R. B., and Witman, G. B. (1982). Purification and polypeptide composition of dynein ATPases from *Chlamydomonas* flagella. *Cell Motil.* **2,** 525–547.

Pfister, K. K., and Witman, G. B. (1984). Subfractionation of *Chlamydomonas* 18 S dynein into two unique subunits containing ATPase activity. *J. Biol. Chem.* **259,** 12,072–12,080.

Phillis, R., Statton, D., Caruccio, P., and Murphey, R. K. (1996). Mutations in the 8 kDa dynein light chain gene disrupt sensory axon projections in the *Drosophila* imaginal CNS. *Development* **122,** 2955–2963.

Piperno, G., and Luck, D. J. (1979). Axonemal adenosine triphosphatases from flagella of *Chlamydomonas reinhardtii*. Purification of two dyneins. *J. Biol. Chem.* **254,** 3084–3090.

Piperno, G., and Luck, D. J. (1981). Inner arm dyneins from flagella of *Chlamydomonas reinhardtii*. *Cell* **27,** 331–340.

Piperno, G., Mead, K., LeDizet, M., and Moscatelli, A. (1994). Mutations in the "dynein regulatory complex" alter the ATP-insensitive binding sites for inner arm dyneins in *Chlamydomonas* axonemes. *J. Cell Biol.* **125,** 1109–1117.

Piperno, G., Mead, K., and Shestak, W. (1992). The inner dynein arms I2 interact with a "dynein regulatory complex" in *Chlamydomonas* flagella. *J. Cell Biol.* **118,** 1455–1463.

Piperno, G., and Ramanis, Z. (1991). The proximal portion of *Chlamydomonas* flagella contains a distinct set of inner dynein arms. *J. Cell Biol.* **112,** 701–709.

Piperno, G., Ramanis, Z., Smith, E. F., and Sale, W. S. (1990). Three distinct inner dynein arms in *Chlamydomonas* flagella: Molecular composition and location in the axoneme. *J. Cell Biol.* **110,** 379–389.

Piperno, G., Siuda, E., Henderson, S., Segil, M., Vaananen, H., and Sassaroli, M. (1998). Distinct mutants of retrograde intraflagellar transport (IFT) share similar morphological and molecular defects. *J. Cell Biol.* **143,** 1591–1601.

Porter, M. E. (1996). Axonemal dyneins: Assembly, organization, and regulation. *Curr. Opin. Cell Biol.* **8,** 10–17.

Porter, M. E., Bower, R., Knott, J. A., Byrd, P., and Dentler, W. (1999). Cytoplasmic dynein heavy chain 1b is required for flagellar assembly in *Chlamydomonas*. *Mol. Biol. Cell* **10,** 693–712.

Porter, M. E., Knott, J. A., Gardner, L. C., Mitchell, D. R., and Dutcher, S. K. (1994). Mutations in the *SUP-PF-1* locus of *Chlamydomonas reinhardtii* identify a regulatory domain in the β-dynein heavy chain. *J. Cell Biol.* **126,** 1495–1507.

Porter, M. E., Knott, J. A., Myster, S. H., and Farlow, S. J. (1996). The dynein gene family in *Chlamydomonas reinhardtii*. *Genetics* **144,** 569–585.

Porter, M. E., Power, J., and Dutcher, S. K. (1992). Extragenic suppressors of paralyzed flagellar mutations in *Chlamydomonas reinhardtii* identify loci that alter the inner dynein arms. *J. Cell Biol.* **118,** 1163–1176.

Porter, M. E., and Sale, W. S. (2000). The 9 + 2 axoneme anchors multiple inner arm dyneins and a network of kinases and phosphatases that control motility. *J. Cell Biol.* **151,** F37–F42.

Price, S. R., Euans, P. R., and Nagai, K. (1998). Crystal structure of the spliceosomal U2B″-U2A′ protein complex bound to a fragment of U2 small nuclear RNA. *Nature* **394,** 645–650.

Puthalakath, H., Huang, D. C., O'Reilly, L. A., King, S. M., and Strasser, A. (1999). The proapoptotic activity of the Bc1-2 family member Bim is regulated by interaction with the dynein motor complex. *Mol. Cell* **3,** 287–296.

Raux, H., Flamand, A., and Blondel, D. (2000). Interaction of the rabies virus P protein with the LC8 dynein light chain. *J. Virol.* **74,** 10,212–10,216.

Rice, D. W., Rafferty, J. B., Artymiuk, P. J., and Lloyd, R. G. (1997). Insights into the mechanism of homologous recombination from the structure of RuvA. *Curr. Opin. Struct. Biol.* **7,** 798–803.

Rosenbaum, J. L., Cole, D. G., and Diener, D. R. (1999). Intraflagellar transport: The eyes have it. *J. Cell Biol.* **144,** 385–388.

Roush-Gaillard, A., and Sale, W. S. (2000). Identification of the RII binding site in radial spoke protein 3, a *Chlamydomonas* axonemal AKAP. *Mol. Biol. Cell* **11,** 431a.

Rupp, G., O'Toole, E., Gardner, L. C., Mitchell, B. F., and Porter, M. E. (1996). The *suppf-2* mutations of *Chlamydomonas* alter the activity of the outer dynein arms by modification of the γ-dynein heavy chain. *J. Cell Biol.* **135,** 1853–1865.

Sakakibara, H., Kojima, H., Sakai, Y., Katayama, E., and Oiwa, K. (1999). Inner-arm dynein c of *Chlamydomonas* flagella is a single-headed processive motor. *Nature* **400,** 586–590.

Sakakibara, H., Mitchell, D. R., and Kamiya, R. (1991). A *Chlamydomonas* outer arm dynein mutant missing the α heavy chain. *J. Cell Biol.* **113,** 615–622.

Sakakibara, H., and Nakayama, H. (1998). Translocation of microtubules caused by the $\alpha\beta$, β and γ outer arm dynein subparticles of *Chlamydomonas*. *J. Cell Sci.* **111,** 1155–1164.

Sakakibara, H., Takada, S., King, S. M., Witman, G. B., and Kamiya, R. (1993). A *Chlamydomonas* outer arm dynein mutant with a truncated β heavy chain. *J. Cell Biol.* **122,** 653–661.

Sakato, M., and King, S. M. (2000). Ca^{2+} modulates the microtubule-binding activity of the $\beta\gamma$ and γ heavy chain subparticles of *Chlamydomonas* outer arm dynein. *Mol. Biol. Cell* **11,** 194a.

Sale, W. S., Goodenough, U. W., and Heuser, J. E. (1985). The substructure of isolated and *in situ* outer dynein arms of sea urchin sperm flagella. *J. Cell Biol.* **101,** 1400–1412.

Samso, M., Radermacher, M., Frank, J., and Koonce, M. P. (1998). Structural characterization of a dynein motor domain. *J. Mol. Biol.* **276,** 927–937.

Schnorrer, F., Bohmann, K., and Nusslein-Volhard, C. (2000). The molecular motor dynein is involved in targeting swallow and bicoid RNA to the anterior pole of Drosophila oocytes. *Nat. Cell Biol.* **2,** 185–190.

Signor, D., Wedaman, K. P., Orozco, J. T., Dwyer, N. D., Bargmann, C. I., Rose, L. S., and Scholey, J. M. (1999). Role of a class DHC1b dynein in retrograde transport of IFT motors and IFT raft particles along cilia, but not dendrites, in chemosensory neurons of living *Caenorhabditis elegans*. *J. Cell Biol.* **147,** 519–530.

Silver, L. M. (1993). The peculiar journey of a selfish chromosome. *Trends Genet.* **9,** 250–254.

Smith, E. F., and Sale, W. S. (1991). Microtubule binding and translocation by inner dynein arm subtype I1. *Cell Motil. Cytoskel.* **18,** 258–268.

Smith, E. F., and Sale, W. S. (1992). Regulation of dynein-driven microtubule sliding by the radial spokes in flagella. *Science* **257,** 1557–1559.

Sondek, J., Bohm, A., Lambright, D. G., Hamm, H. E., and Sigler, P. B. (1996). Crystal structure of a G-protein β/γ dimer at 2.1 Å resolution. *Nature* **379,** 369–374.

Stillman, B. (1994). Smart machines at the replication fork. *Cell* **78,** 725–728.

Sugase, Y., Hirono, M., Kindle, K. L., and Kamiya, R. (1996). Cloning and characterization of the actin-encoding gene of *Chlamydomonas reinhardtii*. *Gene* **168,** 117–121.

Supp, D. M., Brueckner, M., Kuehn, M. R., Witte, D. P., Lowe, L. A., McGrath, J., Corrales, J., and Potter, S. S. (1999). Targeted deletion of the ATP binding domain of left–right dynein confirms its role in specifying development of left-right asymmetries. *Development* **126,** 5495–5504.

Supp, D. M., Witte, D. P., Potter, S. S., and Brueckner, M. (1997). Mutation of an axonemal dynein affects left-right asymmetry in inversus viscerum mice. *Nature* **389,** 963–966.

Tai, A. W., Chuang, J. Z., Bode, C., Wolfrum, U., and Sung, C. H. (1999). Rhodopsin's carboxy-terminal cytoplasmic tail acts as a membrane receptor for cytoplasmic dynein by binding to the dynein light chain Tctex-1. *Cell* **97,** 877–887.

Taillon, B. E., Adler, S. A., Suhan, J. P., and Jarvik, J. W. (1992). Mutational analysis of centrin: An EF-hand protein associated with three distinct contractile fibers in the basal body apparatus of *Chlamydomonas*. *J. Cell Biol.* **119,** 1613–1624.

Takada, S., and Kamiya, R. (1994). Functional reconstitution of *Chlamydomonas* outer dynein arms from α- β and γ subunits: Requirement of a third factor. *J. Cell Biol.* **126,** 737–745.

Takada, S., Sakakibara, H., and Kamiya, R. (1992). Three-headed outer arm dynein from *Chlamydomonas* that can functionally combine with outer-arm-missing axonemes. *J. Biochem. (Tokyo)* **111,** 758–762.

Takada, S., Wilkerson, C. G., Kamiya, R., and Witman, G. B. (2001). The *Chlamydomonas* ODA1 gene encodes a 62-kD component necessary for docking of outer dynein arms on the doublet microtubules of flagella. In preparation.

Tang, W.-J., Bell, C. W., Sale, W. S., and Gibbons, I. R. (1982). Structure of the dynein-1 outer arm in sea urchin sperm flagella. I. Analysis by separation of subunits. *J. Biol. Chem.* **257,** 508–515.

Tang, W. Y., and Gibbons, I. R. (1987). Photosensitized cleavage of dynein heavy chains. Cleavage at the V2 site by irradiation at 365 nm in the presence of oligovanadate. *J. Biol. Chem.* **262,** 17,728–17,734.

Tochio, H., Ohki, S., Zhang, Q., Li, M., and Zhang, M. (1998). Solution structure of a protein inhibitor of neuronal nitric oxide synthase. *Nat. Struct. Biol.* **5,** 965–969.

Vaisberg, E. A., Grissom, P. M., and McIntosh, J. R. (1996). Mammalian cells express three distinct dynein heavy chains that are localized to different cytoplasmic organelles. *J. Cell Biol.* **133,** 831–842.

Vale, R. D. (2000). AAA proteins. Lords of the ring. *J. Cell Biol.* **150,** F13–F19.

Vale, R. D., and Toyoshima, Y. Y. (1988). Rotation and translocation of microtubules *in vitro* induced by dyneins from *Tetrahymena* cilia. *Cell* **52,** 459–469.

Wang, Z., Khan, S., and Sheetz, M. P. (1995). Single cytoplasmic dynein molecule movements: Characterization and comparison with kinesin. *Biophys. J.* **69,** 2011–2023.

Watanabe, T. K., Fujiwara, T., Shimizu, F., Okuno, S., Suzuki, M., Takahashi, E., Nakamura, Y., and Hirai, Y. (1996). Cloning, expression and mapping of TCTEL1, a putative human homolog of murine Tctel, to 6q. *Cytogenet. Cell Genet.* **73,** 153–156.

Weber, C., Lee, V. D., Chazin, W. J., and Huang, B. (1994). High level expression in *Escherichia coli* and characterization of the EF-hand calcium-binding protein caltractin. *J. Biol. Chem.* **269,** 15,795–15,802.

West, S. C. (1997). Processing of recombination intermediates by the Ruv ABC proteins. *Annu. Rev. Genet.* **31,** 213–244.

Wilkerson, C. G., King, S. M., Koutoulis, A., Pazour, G. J., and Witman, G. B. (1995). The 78,000 $M_{(r)}$ intermediate chain of *Chlamydomonas* outer arm dynein is a WD-repeat protein required for arm assembly. *J. Cell Biol.* **129,** 169–178.

Wilkerson, C. G., King, S. M., and Witman, G. B. (1994). Molecular analysis of the γ heavy chain of *Chlamydomonas* flagellar outer-arm dynein. *J. Cell Sci.* **107,** 497–506.

Wilkerson, C. G., and Witman, G. B. (1995). Dynein heavy chains have at least two functional ATP-binding sites. *Mol. Biol. Cell* **6,** 33a.

Witman, G. B. (1993). *Chlamydomonas* phototaxis. *Trends Cell Biol.* **3,** 403–408.

Witman, G. B., Johnson, K. A., Pfister, K. K., and Wall, J. S. (1983). Fine structure and molecular weight of the outer arm dyneins of *Chlamydomonas*. *J. Submicrosc. Cytol.* **15,** 193–197.

Witman, G. B., King, S. M., Moss, A. G., and Wilkerson, C. G. (1991). The intermediate chain/light chain complex: An important structural entity of outer arm dynein. *In* "Comparative Spermatology 20 Years After" (B. Baccetti, Eds.), pp. 439–443. Raven Press, New York.

Witman, G. B., and Minervini, N. (1982). Dynein arm conformation and mechano-chemical transduction in the eukaryotic flagellum. *Symp. Soc. Exp. Biol.* **35,** 203–223.

Wu, H., Maciejewski, M. W., Benashski, S. E., Mullen, G. P., and King, S. M. (1999). [1]H, ^{15}N and ^{13}C resonance assignments for the 22 kDa LC1 light chain from *Chlamydomonas* outer arm dynein. *J. Biomol. Nucl. Magn. Reson.* **13,** 309–310.

Wu, H., Maciejewski, M. W., Benashski, S. E., Mullen, G. P., and King, S. M. (2001). The ^{1}H, ^{15}N and ^{13}C resonance assignments for the Tctex1 dynein light chain from *Chlamydomonas* flagella. *J. Biomol. Nucl. Magn. Reson.* **20,** 89–90.

Wu, H., Maciejewski, M. W., Marintchev, A., Benashski, S. E., Mullen, G. P., and King, S. M. (2000). Solution structure of a dynein motor domain associated light chain. *Nat. Struct. Biol.* **7,** 575–579.

Yagi, T. (2000). ADP-dependent microtubule translocation by flagellar inner-arm dyneins. *Cell Struct. Funct.* **25,** 263–267.

Yagi, T., Kamimura, S., and Kamiya, R. (1994). Nanometer scale vibration in mutant axonemes of *Chlamydomonas*. *Cell Motil. Cytoskel.* **29,** 177–185.

Yang, P., Bodiwala, R., and Sale, W. S. (2000). Structural interaction of calmodulin, dynein light chain LC8 amd radial spoke protein 2 in the flagellar radial spoke. *Mol. Biol. Cell* **11,** 538a.

Yang, P., and Sale, W. S. (1998). The M_r140,000 intermediate chain of *Chlamydomonas* flagellar inner arm dynein is a WD-repeat protein implicated in dynein arm anchoring. *Mol. Biol. Cell* **9,** 3335–2249.

Yang, P., and Sale, W. S. (2000). Casein kinase I is anchored on axonemal doublet microtubules and regulates flagellar dynein phosphorylation and activity. *J. Biol. Chem.* **275,** 18,905–18,912.

Yu, X., West, S. C., and Egelman, E. H. (1997). Structure and subunit composition of the RuvAB-Holliday junction complex. *J. Mol. Biol.* **266,** 217–222.

Yu, X., West, S. C., Jahn, R., and Brunger, A. T. (1998). Structure of the ATP-dependent oligomerization domain of N-ethylmaleimide sensitive factor complexed with ATP. *Nat. Struct. Biol.* **5,** 803–811.

INDEX